Foods and Raw Materials. 2027;15(2)
ISSN 2310-9599 (Print)
ISSN 2308-4057 (Online)
Available online at https://jfrm.ru/en/
DOI: https://doi.org/10.21603/2308-4057-2027-2

CONTENTS

Petropavlovskiy Maxim V., Donnik Irina M., Krivonogova Anna S., Isaeva Albina G., Badretdinova Alisa S., Martynov Nikolay A. Genetic heterogeneity and pathogenetic mechanisms of bovine leukemia virus 257

Omoike Bright A., Okieimen Felix E., Imoisi Chinyere, Josiah James G. Starch as a sustainable alternative for bioplastic packaging: A review 270

El-Sayed Eatemad M., Elsebaie Essam M., El-Farsy Marwa F. A., Shehata Rehab A., Hozifa Shaymaa A., El-Mesiry Dalia M., Elmeslamy Soher A.-E. Beef tripe as an innovative and alternative protein source in meat products 285

Evdokimova Svetlana A., Karetkin Boris A., Guseva Elena V., Demkin Kirill M., Shevchenko Alla T., Khromova Natalya Yu., Panfilov Victor I., Gradova Nina B. Effects of sea buckthorn and black currant extracts on the growth, acid production, and antagonism of bifidobacteria 296

Alim Md. Abdul, Hossain Iqbal, Yesmin Tamanna, Islam Md. Tarakul, Zaman Rukaiya, Khan Md. Momin Valorisation of dragon fruit peel in functional squash 311

Phuong Do Viet, Thuan Nguyen Ngoc *Cassia fistula* L. fruit: Optimal conditions for total polyphenol extraction 324

Budianto, Arumsar Alif G., Yusup Abdul, Gumintang Muhammad, Rosidin Zahra S. Correlation patterns of biochemical compounds in single-clove and multi-clove garlic varieties 333

Sherstyukov Andrey G., Andreeva Oksana I., Tarasov Vasily E., Shorstkii Ivan A. Recent advances in cold plasma treatment for essential oil extraction 344

Adingra Kouassi M.-D., Gnahe Hermann D., Soro Soguimondenin, Kouadio N'guessan J. P., Tan Kablan Clarification of cashew apple juice with pectinases extracted from the epicarp of papaya cv. Solo 8 358

Vivas Lorena C., Mendoza Anthony D., Casado Moraiza J., Pérez Neyo C., Brazón Marlon F., Coll David S., Quintero Alberto J. Potential of *Sargassum* sp. in broiler chicken feed 370

Kumar Ankit, Gehlot Rakesh, Phogat Rekha, Kumar Abhishek, Chaudhary Kautilya, Kumar Ramesh Elemental profile and hydrochloric acid extractability of minerals in two indigenous *Carissa carandas* types 379

Sattayakhom Apsorn, Koomhin Phanit, Matan Narumol Prospects for developing sleep-related functional foods: Use of electroencephalography for objective sleep measurement 392

Barkovskaya Irina A., Koroleva Polina I., Turovskaya Svetlana N., Illarionova Elena E., Kondratenko Vladimir V., Bliadze Vladimir G., Yaryshev Vladislav Yu., Petrov Andrey N. Milk protein and peptide profiles under different heat loads: Molecular analysis 411

Nakisoz Henriettah, Ogwok Patrick, Mugampoza Diriisa Pulp and by-products of indigenous and non-indigenous mangoes in Uganda: Physicochemical properties 425

Nandana R, Radhalakshmi V, Linu M Salim, Jismy K J, Anooja Thomas, Jisha M S, Sajad Rehman Hybrid meat: A comprehensive review of composition, processing, and consumer acceptance 437

Maduagwu Nkechi U., Ikebunwa Obinna A., Maduagwu Chukwuebuka R., Ajunwa Marachi S., Stephen Kelechi V., Nnubia Nnamdi H., Ebiringa Stephen C., Amugo Chigoziri A., Chibuzo Christiana N., Kalu Ndukwe C., Nasralla Mariam F. Sh., Ugwuoke Precious C., Chukwueze Prince O., Igboeli Ujunwa G., Ejimofor Esther, Yakubu Cynthia, Ezenagu Kelechi I., Mbiamnozie Chigozie C., Igwe Cynthia A., Momoh Ellis E., Onah Chinecherem S., Ikpo Amazing Antioxidative and anticataractogenic effects of *Annona muricata* leaf extracts on sodium selenite-induced cataract in rat pups 449

Faskhutdinova Elizaveta R., Fotina Natalya V., Shevel Arina A., Gordienko Andrey V., Tupikin Alexey E., Mudgal Gaurav, Aksenova Larisa M., Asyakina Lyudmila K. Genomic characterization of the *Pantoea allii* strain for biotechnological applications 460

Frolova Anna S., Vesnina Anna D., Fedorova Anastasiya M., Ostapova Elena V., Yustratov Vladimir P., Milentyeva Irina S. The probiotic potential of microorganism strains: A comprehensive study 474

Foods and Raw Materials. 2027;15(2)

ISSN 2308-4057 (Print)
ISSN 2310-9599 (Online)

Research Article
Open Access

Available online at http://jfrm.ru/en
https://doi.org/10.21603/2308-4057-2027-2-707
https://elibrary.ru/QNXKHD

Genetic heterogeneity and pathogenetic mechanisms of bovine leukemia virus

Maxim V. Petropavlovskiy[1,*], Irina M. Donnik[1], Anna S. Krivonogova[2], Albina G. Isaeva[1], Alisa S. Badretdinova[1], Nikolay A. Martynov[1]

[1] Ural Federal Agrarian Scientific Research Centre, Ural Branch of the Russian Academy of Sciences, Yekaterinburg, Russia
[2] Ural State Agrarian University, Yekaterinburg, Russia

* e-mail: petropavlovsky_m@mail.ru

Received 20.11.2025; Revised 01.12.2025; Accepted 08.12.2025; Published online 05.06.2026

Abstract:
Bovine leukemia virus is an RNA virus of the *Retrovivridae* family. It causes a chronic infectious disease in farm animals that poses a serious threat to global cattle farming. According to phylogenetic studies, the pathogen is classified into 12 genotypes.
This comprehensive bioinformatic analysis featured new bovine leukemia virus isolates (n = 57) sampled from various regions of the Russian Federation with different epizootic situations. The analysis featured both new sequences and old samples from Russia available in the National Center for Biotechnology Information. This large-scale approach made it possible to cover all known genotypes.
G4 genotype was associated with major amino acid substitutions in gp51 (T47A, A73P, R121H in epitope G; S56F in epitope H; I144T in ND2; D166G in $CD8^+$). These substitutions provide a selective advantage through immune evasion mechanisms, including escape from humoral immunity, impaired T-cell recognition, and increased receptor affinity. G4 also correlated with rapid progression.
The rapid replacement of G7 by G4 in the Tyumen Region and the general dominance of G4 in Russia were due to a more aggressive course of infection resulting from the genetic ability of the pathogen to adapt to the host immune system. The obtained data underscore the necessity of developing genotype-specific diagnostic systems and implementing routine molecular-genetic monitoring to control the spread of bovine leukemia virus. New data on genetic variability and its impact on genotype-phenotype correlations may help curb the infection.

Keywords: Bovine leukemia virus, bioinformatic analysis, genotype G4, gp51, amino acid substitutions, *env* gene, epitope, epizootiology, virus evolution, diagnostics

Funding: The study was supported by the Russian Science Foundation, project No. 23-16-00103, https://rscf.ru/project/23-16-00103/

Please cite this article in press as: Petropavlovskiy MV, Donnik IM, Krivonogova AS, Isaeva AG, Badretdinova AS, *et al.* Genetic heterogeneity and pathogenetic mechanisms of bovine leukemia virus. Foods and Raw Materials. 2027;15(2):257–269. https://doi.org/10.21603/2308-4057-2027-2-707

INTRODUCTION

Bovine leukemia virus (BLV) belongs to the *Deltaretrovirus* genus of the *Retroviridae* family. It causes enzootic bovine leukemia (EBL) [1–4]. The infection has a prolonged latent stage with the virus triggering polyclonal expansion of infected B-lymphocytes that express the phenotypic markers $CD5^+$ and IgM^+. This proliferation clinically manifests as persistent lymphocytosis which progresses to malignant B-cell lymphoma or leukemia in the terminal stage [5–7].

The surface glycoprotein gp51 (SU) is crucial for BLV pathogenesis. It is encoded by the *env* gene. The receptor binding domain (RBD, 1–173 amino acids) interacts with the CAT-1 receptor of B-cells [8, 9]. Neutralizing domains ND1 (97–106 amino acids), ND2 (131–150), and ND3 (210–225) are targets for antibodies that block the infection [10, 11]. T-cell epitopes (gp51N5, gp51N11, gp51N12) induce the $CD4^+/CD8^+$ cytotoxic response [12].

The pathogenic adaptation of *env* is driven by its genetic variability, particularly in the N-terminal region [13] of gp51 (1–155 amino acids). Substitutions in the neutralizing domains disrupt the conformation of ND1 epitopes, thus reducing the affinity of neutralizing anti-

Copyright © 2026, Petropavlovskiy *et al.* This is an open access article distributed under the terms of the Creative Commons Attribution 4.0 International License (https://creativecommons.org/licenses/by/4.0/), allowing third parties to copy and redistribute the material in any medium or format and to remix, transform, and build upon the material for any purpose, even commercially, provided the original work is properly cited and states its license.

bodies [14, 15]. N-glycosylation mutations enhance the fusion of viral and cellular membranes, increasing the infectivity [13]. Recombination between G4/G7 genotypes in the *env* region may result in chimeric strains [16]. Apart from affecting laboratory diagnostics, such quasispecies with their altered pathogenicity pose risks of interspecies transmission [17–19].

Mutations in *env* can alter the infectivity, replicative capacity, and pathogenicity of BLV. Studying them is important for new diagnostic and preventive strategies [15, 20–22].

In industrial cattle farming, effective diagnostic and preventive measures depend on the severity and the rate of pathological and clinical symptoms. These two factors are important from a practical perspective [1, 2, 23, 24]. Faulty laboratory control data to correlate with the genetic variability of individual pathogen isolates. Genetic variability in the ND of gp51 directly compromises the accuracy of standard serological tests, e.g., ELISA (enzyme-linked immunosorbent assay) or AGID (agar gel immunodiffusion) kits. It happens as a result of a mismatch between the epitopes of the test system and the circulating strain. For some BLV genotypes, the sensitivity of AGID drops by 15–30% [1, 20, 25]. For natural epizootic, the polymerase chain reaction (PCR)-based identification often fails due to the genetic variability of the pathogen mutations in the target sites of primers.

Early studies of the *env* gene were limited to 444 base pairs, failing to detect many recombinations of the glycoprotein gp51 and quasispecies. Current strategies include a larger fragment when assessing important amino acid substitutions in the BLV glycoprotein gp51 (SU). The whole-genome sequencing covers 8,714 base pairs with subsequent classification into phylogroups (A, B-1, B-2, C) [26]. The deep sequencing includes 970 base pairs. It amplifies the region that encompasses all functional domains of gp51 (RBD, ND1-ND3, T-epitopes) [20, 25, 27–29]. Currently, researchers continue to accumulate more data on nucleotide substitutions in the *env* regions associated with BLV infectivity, replication, and pathogenesis [15, 20].

Our study featured the genetic heterogeneity and pathogenetic mechanisms of BLV. It relied on the molecular genetic determinants (amino acid substitutions in the gp51 glycoprotein of the *env* gene) from samples obtained across Russia.

The EBL epidemic safety differs from region to region. Our research is the first all-Russian comprehensive genetic analysis of BLV. For G4 strains, we established the range of specific amino acid substitutions in the domains of the gp51 glycoprotein that determined its antigenic properties (T47A, A73P, R121H in the G epitope; S56F in H; I144T in ND2; D166G in $CD8^+$). As a result, we modelled a molecular mechanism that explains the selective advantage and increased virulence of the G4 genotype. The identified substitutions cause a complex impairment of the immune response. Modified G and H epitopes were the primary drivers of the evasion of humoral immunity while the changes in the $CD8^+$ domain resulted in impaired T-cell recognition. We established a direct correlation between the circulation of genotype G4 and unfavorable epizootic indicators, including the prompt clinical manifestations. This fact confirms that G4 is more virulent than G7. The new fundamental data substantiate the need to improve the diagnostic and monitoring system for BLV. Genotype-specific diagnostic systems and regular molecular genetic monitoring may track the genetic changes in BLV and curb the spread of EBL.

STUDY OBJECTS AND METHODS

The study was conducted at the Ural Scientific Research Veterinary Institute – structural subdivision of the Ural Federal Agrarian Scientific Research Centre, Ural Branch of the Russian Academy of Sciences (Yekaterinburg, Russia). The clinical trials took place on agricultural premises in the regions of Sverdlovsk, Tyumen, and Krasnodar. The subjects included local cattle of various age and sex, as well as experimental sheep.

The animal studies followed the primary International Guiding Principles for Biomedical Research Involving Animals (Council for International Scientific Organizations, Geneva, 1985); the European Convention for the Protection of Vertebrate Animals used for Experimental and Other Scientific Purposes (Strasbourg, 1986); the Position on the Ethics of Animal Use in Research (Russian Science Foundation). The animal experiment protocol was approved by the Ethics Committee of the Ural Scientific Research Veterinary Institute – structural subdivision of the Ural Federal Agrarian Scientific Research Centre, Ural Branch of the Russian Academy of Sciences (Yekaterinburg, Russia). All experiments followed the procedures for virological bioassays (Gulyukin, 2008). All animal manipulations were performed by qualified veterinarians. Animal housing and nutrition followed standard physiological and veterinary-sanitary guidelines.

The serological screening relied on a solid-phase enzyme-linked immunosorbent assay (ELISA) using the ID Screen® bovine leukemia virus (BLV) Competition reagent kit (Vet Factor LLC, Russia). The results were recorded using an iMark TM photometer (Bio-RAD, USA).

The hematological studies involved an Abacus Junior Vet hematology analyzer (Diatron, Hungary) and a Micros MCX100 microscope (Micros Austria, Austria).

The immunological parameters in animals were determined by assessing the content of T- and B-lymphocytes in a spontaneous e-rosette test with sheep erythrocytes for T-lymphocytes (E-ROL), T-helper lymphocytes ($CD4^+$), and T-suppressor lymphocytes ($CD8^+$), as well as with murine erythrocytes for B-lymphocytes (M-ROL).

The phagocytic activity and neutrophil index were obtained by the opsonophagocytic reaction using latex phagocytosis as proposed in Smirnov's methodologies.

The circulating immune complexes were described by selective precipitation with polyethylene glycol on a Bio-Rad iMark microplate photometer (Bio-Rad Laboratories, USA).

The blood microscopy was imaged with a microscope equipped with an Axiocam 208 digital camera (Carl Zeiss, Germany).

The DNA extraction and quality control involved a commercial AmpliPrime RIBO-prep VET kit (Nekst-Bio LLC, Russia).

The DNA concentration was measured using a Qubit4 Fluorometer (Thermo Fisher Scientific, USA) with a Qu-Dye dsDNA HS reagent kit (200×; Lumiprobe, Russia).

The molecular genetic screening relied on a realtime PCR using the commercial Ampli Sens Leukosis reagent kits (InterLabServis LLC, Russia) and a CFX96 Touch thermal cycler (Bio-Rad, USA).

The procedure of targeted amplification was as follows. We amplified 970 base pairs of *env* using a modified semi-nested PCR method. The mix consisted of 100 mM Tris-HCl (pH 8.5 at 25°C); 100 mM KCl; 0.4 mM of each dNTP; 4 mM $MgCl_2$; 0.06 units/μL Taq DNA polymerase, 0.2% Tween 20; and HS-Taq DNA polymerase stabilizers, 0.35 μM of each primer.

The primers and amplification conditions were replicated from a study of Pluta *et al.* [27] with minor modifications. Round 1 involved AP_4762 and ZM2_5786 at the following temperature conditions: 95°C – 5 min; 40 cycles: 95°C – 25 s, 62°C – 25 s, 72°C – 50 s, 72°C – 10 min. Round 2 featured AP_4762 and ZM5_5733 at the same temperature conditions, except for the higher annealing temperature (66°C).

The Sanger sequencing was performed on an Applied Biosystems 3500 Genetic Analyzer in two directions, using forward (AP_4762) and reverse (ZM5_5733) primers. This test provided sequences up to 900 nucleotide pairs. The bioinformatics analysis included such software as FinchTV, SeqScape 3.0, and megax 10.0.5, as well as the BLAST web service. The analysis started with a primary alignment to the BLV reference whole-genome sequence from the National Center for Biotechnology Information (NC_001414.1) followed by manual editing (Fig. 1).

The analysis included a fetal lamb kidney (FLK) BLV sample obtained from a virus-producing cell line that was prepared and cryopreserved in the laboratory in advance.

RESULTS AND DISCUSSION

The molecular-genetic studies featured biological material of bovine leukemia virus (BLV)-seropositive animals from three Russian regions. According to routine serological and hematological studies as of early 2023, these regions had the following enzootic bovine leukemia (EBL) situations. Krasnodar Region: 823 clusters, 472 animals with hematological stage; Tyumen Region: 282 clusters, 152 animals with hematological stage; Sverdlovsk Region: 26 clusters, no animals with hematological stage [30].

Previously, the following BLV genotypes were reported in these areas. Krasnodar Region: G4 (Belgian) and G7 (Australian), with G4 predominating; Sverdlovsk Region: G7; Tyumen Region: G4 in all samples, with G7 predominating in 2010. These results indicated a shift in the BLV genotype circulating in these cattle populations.

Based on clinical and immunological studies, subleukemic (leukocyte concentration 25.1–40.0×10^9/L) and leukemic stages (≥ 40.0×10^9/L) were more frequent in the regions with G4 genotype. Subleukemic cows exhibited severe endogenous intoxication with an active inflammation, stressed hematopoietic system, and imbalanced reactions in the cellular and humoral parts of the immune system. They also had varying degrees of deviations in the T-cell and B-cell mediated immunity. This fact indicated a persistent epizootic situation in the region and a severe course of the disease.

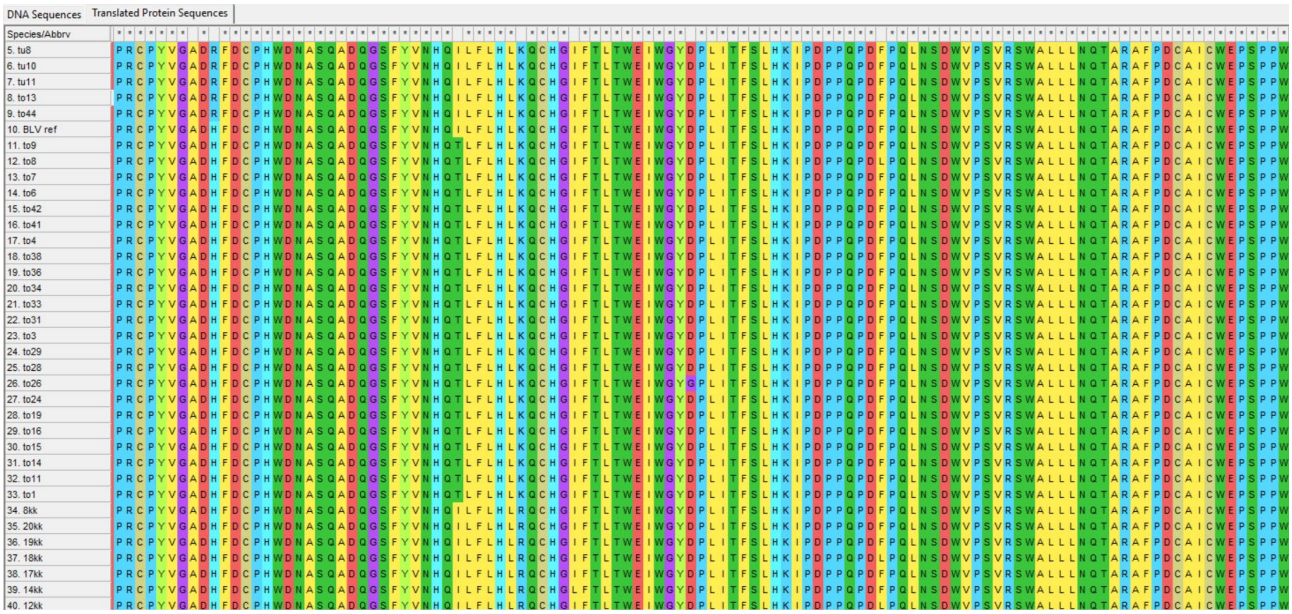


Figure 1 Aligning amino acid sequences of bovine leukemia virus glycoprotein gp 51 from different Russian regions in megax 10.0.5

We studied the pathogenetic characteristics by infecting laboratory sheep with biomaterial from cattle with different BLV genotypes.

The sheep (7–8 months; n = 6) were injected abdominally with virus-containing leukocyte material from whole bovine blood. Group 1 received G4, Group 2 received G7, and Group 3 remained intact. The sheep stayed under clinical observation for 70 days. Samples were first collected on day 1 for baseline values, and then on days 10, 30, 40, and 70 after infection. The test parameters included: peripheral blood, relative and absolute counts of T-lymphocytes and B-lymphocytes, phagocytic activity of neutrophil cells, and circulating immune complexes. On days 1 and 2, the experimental animals revealed no immediate or delayed hyperimmune reactions to the virus-containing leukocyte material.

Enzyme-linked immunosorbent assay (ELISA) and polymerase chain reaction (PCR) tests were used to diagnose BLV infection in sheep from both experimental groups on days 14–27, i.e., the interspecies barrier was overcome during parenteral inoculation of infected biological material. The T-cell and B-cell immunity demonstrated a higher count of T-lymphocytes in both experimental groups on day 10. The count of T-lymphocytes increased by a factor of 1.2–1.3 (3.48–3.77×10^9/L), compared to the background values (2.90 ± 0.13×10^9/L). The increase was quite natural, associated with antibody response to the antigen. On day 30, we observed an almost identical increase in the count of B-cells: in was 2.01–2.34×10^9/L in the infected animals, with background values of 1.81 ± 0.09×10^9/L. These results confirmed the adequacy of the immune response to BLV antigens in the experimental animals.

The Group 1 sheep infected with BLV genotype G4 developed a more severe pathological process.

The semi-nested PCR method [27] yielded 57 amplicons of various origins.

To determine the BLV genotype, the amplicons were aligned with isolates from the NCBI GenBank database. The isolates were of different geographic origins. According to phylogenetic analysis, they belonged to genotypes G1 to G12. The analysis involved sequences from other regions of Russia (including old data). The total number of isolates in the multiple alignment and subsequent bioinformatics analysis was 166 (Table 1).

A separate stage of the bioinformatic research was the study of amino acid substitutions in the epitopes or functional domains of gp51 (SU) using the megax software package (Fig. 2–4).

Figure 2 shows the differences from the reference sequence FLK-BLV M35242.1 (G1), which, together with NC_001414.1/BLV ref (isolate G4), served as a control. Sequence numbers are on the left. The colored horizontal bands above the alignment show the antigenic determinants in the structure of the surface glycoprotein gp51: Signal peptide (pink), conformational epitopes F (orange), G (blue), H (purple), ND1 – neutralization domain (light green), and $CD4^+$ and $CD8^+$ T-cell epitopes (green).

Figure 3 illustrates the differences from reference sequence FLK-BLV M35242.1 (G1). It was sequenced together with other isolates and included in the multiple alignment data as a control together with NC_001414.1/BLV ref (isolate G4). Sequence numbers are on the left. The colored horizontal bands above the alignment show the antigenic determinants in the structure of the surface glycoprotein gp51: Conformational epitope G (blue), linear epitopes E, E' (gray), ND 1,2 – neutralization domains (light green), and $CD4^+$ and $CD8^+$ T-cell epitopes (green). The zinc-binding peptide region is marked with light blue, and the hinge region of GYDP is yellow.

Figure 4 shows the differences from reference sequence FLK-BLV M35242.1 (G1). It was sequenced with the isolates to serve as a control together with reference NC_001414.1/BLV ref (isolate G4). Sequence numbers are on the left. The colored horizontal bands above the alignment show the antigenic determinants in the structure of the surface glycoprotein gp51: Linear epitopes A, B, B' and D, D' (gray), ND 3 (light green), and transmembrane hydrophobic region (TMHR) (red).

The major amino acid substitutions were localized in an N-terminal part of gp51 (SU) polyprotein: T47A, A73P, A119T, and R121H in epitope G; S56F in epitope H; D81N, N84D; ND2 in epitope of $CD8^+$ T-cells (N5); I144T, L149V, K150R, L155I in epitope of $CD8^+$ T-cells (N11 and N12), in the zinc-binding region of the peptide; and D166G in $CD8^+$ epitope, in the hinge region β-turn structural motif of GYPD (Table 2).

Some of the identified amino acid substitutions were reported in [25, 27, 31–35], but some were unique in Russia (T47A, A119T, D81N, N84D, L155I, D166G), maybe, even random.

For the first time, we identified samples of genotype G4 with H121R substitution, which are more typical of G7 isolates (samples kk1, kk7).

The highest number of amino acid substitutions belonged to G4 isolates. However, sequences of genotype G7 were more conservative.

The nucleotide substitutions in the glycoprotein gp51 (SU) are responsible for infectivity, replication, and pathogenesis, i.e., they may lead to a more malignant course of EBL.

Major amino acid substitutions and their functional impact. ***Epitope G (T47A, P73A, A119T, R121H).*** Epitope G (48, 73, 74, 82, 121 amino acids) is the key immunodominant B-cell determinant of gp51 (SU) [11].

Antibodies that target this glycoprotein domain actively neutralize viral particles. Epitopes F, G, and H of gp51 (SU) are conformational, thus the shape of the macromolecule depends on disulfide bonds and glycosylation [36].

T47A is a region near G epitope. We detected its substitution in G4 samples from the Tyumen Region (to3-to41). Threonine at position 47 can form hydrogen bonds due to its hydroxyl group. Substituting it with alanine (a hydrophobic amino acid) can disrupt the local hydrophilicity and lead to the loss of the glycosylation site, disrupting protein folding and stability.

Table 1 Bovine leukemia virus isolates in multiple alignment and amino acid substitution analysis of glycoprotein gp51 (n = 166)

Region of origin	Genotype	Name/ NCBI code	Number
Sverdlovsk Region (this study)	G7	tu3, tu5, tu6, tu8, tu9, tu10, tu11	7
Tyumen Region (this study)	G4	to1, to3, to4, to5, to6, to7, to8, to9, to11, to14, to15, to16, to17, to19, to21, to24, to26, to28, to29, to31, to32, to33, to34, to36, to38, to39, to41, to42	28
	G7	to10, to13, to18, to44	4
Krasnodar Region (this study)	G4	1kk, 2kk, 3kk, 4kk, 6kk, 7kk, 8kk, 9kk, 10kk, 11kk, 12kk, 13kk, 14kk, 16kk, 17kk, 18kk, 19kk, 20kk	18
Bashkortostan Republic, 2021	G4	bash3, bash11, bash16, bash18, bash20, bash27	6
Tyumen Region, 2020	G4	OK283585.1/1CH, OK283599.1/2CH, OK283602.1/3CH, OK283614.1/9CH, OK283570.1/10CH, OK283580.1/17CH, OK283582.1/18CH, OK283588.1/21CH, OK283591.1/23CH, OK283595.1/25CH, OK283598.1/28CH, OK283586.1/1F, OK283587.1/20F	13
	G7	OK283612.1/8CH	1
Historical samples, 2010	G4	1.Russia (Krasnodar), 2.Russia (Krasnodar), 2k.Russia (Kurgan), 6T.Russia (Tyumen), JF720358.2/10C (Chelyabinsk), 4Z.Russia (Chelyabinsk), 5Z.Russia (Chelyabinsk)	7
	G7	3k.Russia (Kurgan), 4k.Russia (Kurgan), 5T.Russia (Tyumen), 5T.Russia (Tyumen), JQ353633.1/1S-c6 (Tyumen), JF720350.2/2S (Tyumen), JF720351.2/3S (Tyumen), JF720352.2/4S (Tyumen), 4_Russia (Sverdlovsk), 5_Russia (Sverdlovsk Region), HM563749.3/5_ (Sverdlovsk Region), HM563750.2/2 (Sverdlovsk), HM563760.2/3-3 (Sverdlovsk Region)	13
Novosibirsk Region	G4	OP850751.1/Tatarsk58, ON799104.1/57_Bol, OL660389.1/51_Koch, OP850795.1/Toguchin55, OL660248.1/75_Razd	5
	G7	OL660401.1/53_Koch, OL660358.1/49m_Koch_, JQ686119.1/NK13	3
Elsewhere in Russia	G4	JQ686091.1/MC45 (Moscow Region)	1
	G7	JN695879.1/9V (Vologda Region)	1
	G8	JQ675760.1/MKC3511 (Moscow Region)	1
Foreign references	G1	flk, M35242.1/FLK-BLV, D00647.1/pBLV-A1 (Australia), EU266063.1/ Tehran (Iran)	4
	G2	AF257515.1 (Argentina), LC080654.1/lima40 (Peru)	2
	G3	AF033818.1/G4 (USA), KP201465.1/GBGS-12 (Korea)	2
	G4	MG204552.1/IR-Esfehan (Iran), EF065648.1/USCA-2 (USA), U87872.1/3 (Germany), MN966688.1/K1170 (SAR), M35240.1/LB285 (Belgium), M35238.1/LB59 (France), LC498580.1/DZ1.4 (Egypt), LC193462.1/ Zambia01-2016 (Zambia), LC060795/1_4 (Mongolia), KF801459.2/8MD (Moldova), HQ902258.1/1 (Belarus), HM563781.2/4-2 (Ukraine), HM563778.2/70 (Poland), HM563774.3/68 (Poland), EU262575.2/301 (Poland), S83530.1/I2 (Italy), AY515273.1/96 (Chili), FJ808596.1/LS-SFB (Argentina), MK820044.1/B3008 (China), OK945989.1/26AT (Kazakhstan), OK945958.1/K5 (Kazakhstan), OK945979.1/8D_BKO (Kazakhstan), (Kazakhstan), OK945972.1/50K_CKO (Kazakhstan), OK945959.1/K8 (Kazakhstan), OK631885.1/1PZ (Kazakhstan), NC_001414.1/BLV ref	26
	G5	EF065645.1/CRAG-1 (Costa-Rika), EF065643.1/CRLV (Costa-Rika)	2
	G6	FJ808582.1/PL-1238 (Argentina), AY185360.2/151 (Brazil), LC080656.1/ par62_PAR (Paraguay)	3
	G7	LC060801/1_10 (Mongolia), KF801467.2/1MD (Moldova), KF801464.2/14MD (Moldova), KF801457.1/13MD (Moldova), HM563763.2/160 (Poland), EU262555.2/151 (Poland), OK945983.1/11be (Kazakhstan), OK631887.1/12PP (Kazakhstan), OK945970.1/12K_CKO (Kazakhstan)	9
	G8	HM563764.3/4-6 (Ukraine)	1
	G9	LC080659.1/mon1_BOL (Bolivia), LC080668.1/por28_BOL (Bolivia)	2
	G10	LC154064.1/L2 (Myanmar), KU233561.1/Sa8-H1 (Thailand)	2
	G11	KU764747.1/E102 (China), KU764746.1/E101 (China)	2
	G12	OK945975.1/9S_BKO (Kazakhstan), OK945974.1/7S_BKO (Kazakhstan), OK945977.1/15D_BKO (Kazakhstan)	3

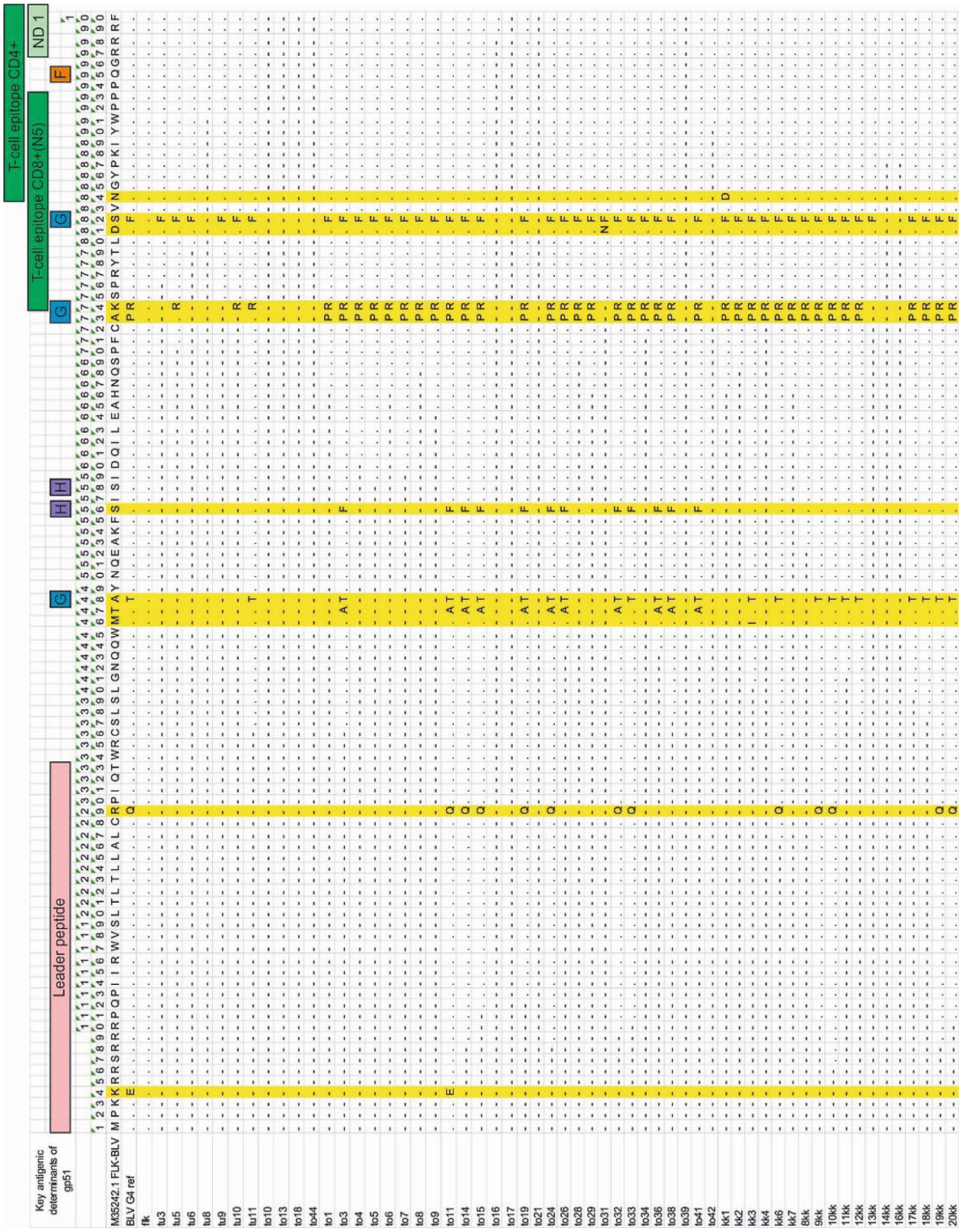


Figure 2 Aligned amino acid sequences (1–100 amino acids) of bovine leukemia virus glycoprotein gp51 (n = 57).

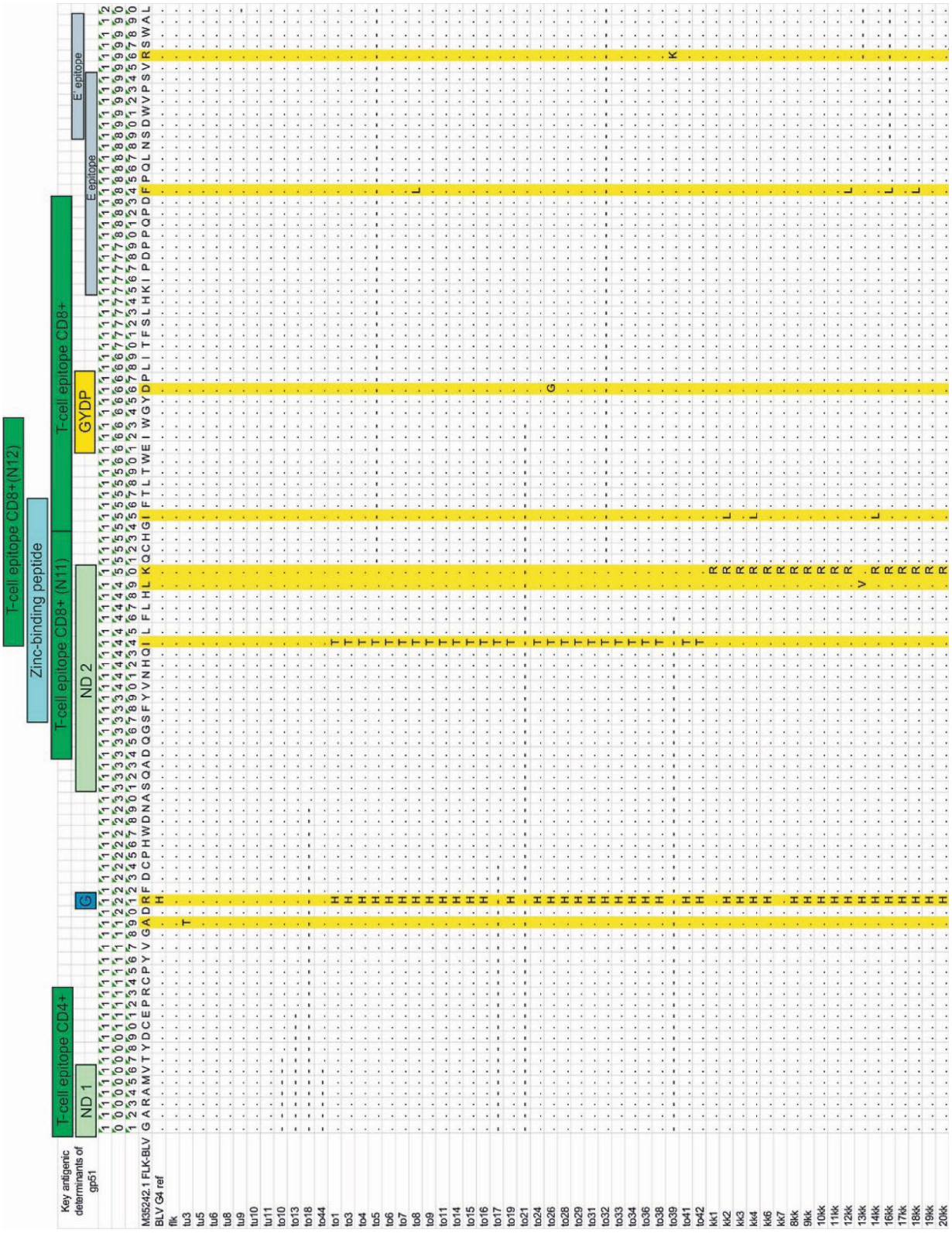


Figure 3 Aligned amino acid sequences (101–200 amino acids) of bovine leukemia virus glycoprotein gp51 (SU) (n = 57)

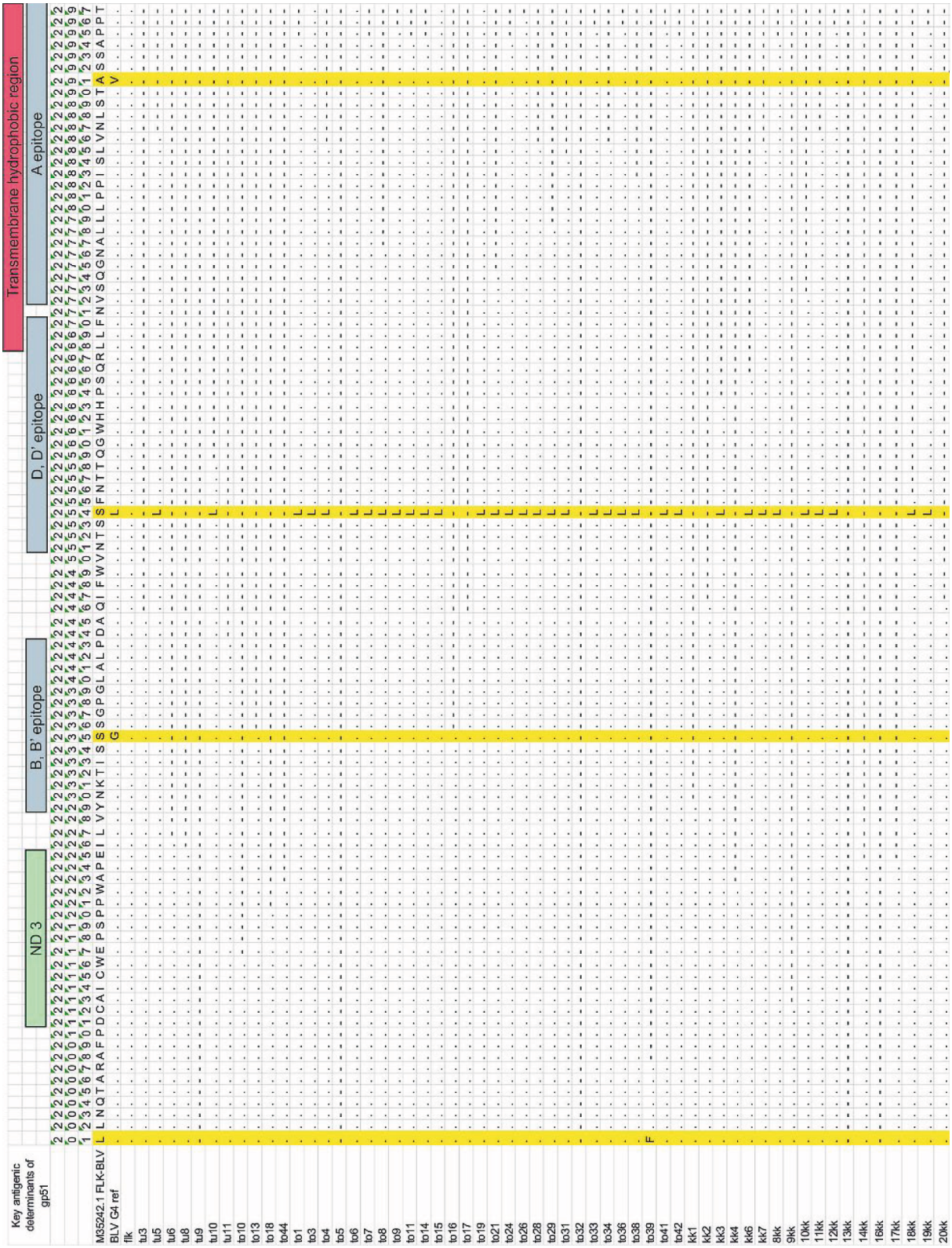


Figure 4 Aligned amino acid sequences (201–297 amino acids) of bovine leukemia virus glycoprotein gp51 (SU) (n = 57)

Table 2 Amino acid substitutions in bovine leukemia virus glycoprotein gp51 (SU) (n = 57)

Epitope or region	Mutation	Biochemical changes	Possible structural effects	Possible immune effects	Genotype
G	T47A	–OH group lost (Thr → Ala)	Hydrogen bond disrupted	Lower antibody affinity	G4
	A73P	More rigid (Ala →Pro)	*β*-hinge changed	Poor recognition of conformational epitopes	G4
	A119T	–OH group added (Ala → Thr)	Possible glycosylation	Epitope masking	G4, G7
	R121H	Different charge (Arg → His)	Hydrogen bonds with other amino acids disrupted	Poor recognition of epitopes; poor neutralization; bonds with cellular receptors disrupted	G4, G7
H	S56F	Hydrophobization (Ser → Phe)	Immersion in lipid bilayer	Loss of antibody affinity	G4
$CD8^+$ T-cell N5	D81N	Negative charge lost (Asp → Asn)	TCR bonds disrupted	Low CTL activation (↓ proliferation)	G4
	N84D	Negative charge added (Asn → Asp)	Orientation in MHC-I changed	Impaired recognition of TCR (↓ IFN-*γ*)	G4
ND 2, $CD8^+$ T-cell (N11, N12), zinc finger	I144T	Hydrophobe → polar (Ile → Thr)	Hydrophobic core disrupted; zinc finger destabilized	Poor neutralization of antibodies	G4
	L149V	Smaller size (Leu → Val)	Denser structure; zinc finger destabilized	Low antibody avidity	G4
	K150R	Longer chain (Lys → Arg)	Stronger ionic interactions; zinc finger destabilized	Resistance to antibodies	G4
$CD8^+$, zinc finger	L155I	Neutral change (Leu → Ile)	Minor local compactions of protein structure; zinc finger destabilized	–	G4
$CD8^+$ (GYPD hinge)	D166G	COO^- group lost (Asp → Gly)	Hinge disrupted; conformation changed	Poor recognition	G4

The A73P substitution was detected in all isolates of G4 genotype. Alanine at position 73 imparts flexibility to the local polypeptide chain. Proline has a cyclic structure (pyrrolidine ring). Substitution with proline can increase chain rigidity by affecting its shape or hinge, which potentially correlate with the conformational dynamics of the entire region.

We detected the A119T substitution in the G7 isolate from the Sverdlovsk Region (tu3). This substitution was not random, as it had been detected in the same region in 2020 (3CH, 17CH, 23CH, 1F, 20F), but it was identified for G4 genotype. Alanine at position 119 is a hydrophobic amino acid whereas threonine is polar. This substitution may increase the hydrophilicity of this region of the N-terminal region of gp51 (SU). An extra potential glycosylation site may affect protein folding and stability, which correlates with antibody interaction.

The R121H substitution is typical of all BLV G4 samples. However, we registered its reverse variant, H121R, in two BLV G4 isolates from the Krasnodar Region (kk1, kk7). H121R is typical of G7 (in this study as well). As with A119T, this phenomenon indicates cross-recombination between the G4/G7 genotypes of BLV. Arginine has a positively charged guanidine group while histidine has a variable charge, i.e., it can be neutral or positive, depending on the environment pH. This substitution can significantly alter the electrostatic properties of this glycoprotein region, thus disrupting salt bridges or hydrogen bonds with other amino acids. Changes in the electrostatic potential affect the binding to cellular receptors and recognition by neutralizing antibodies due to the changes in epitope conformation.

Epitope H is a crucial neutralizing epitope. We identified the amino acid substitution substitution of S56F in the G4 samples from the Tyumen Region (TO3, TO11, TO14, TO15, TO19, TO24, TO26, TO32, TO33, TO36, TO38, TO41). It was previously reported in Novosibirsk, Moldova, Kazakhstan, and France. A small polar amino acid (serine) is replaced with a large hydrophobic aromatic amino acid (phenylalanine), which can cause steric obstacles and significant changes in protein conformation. The S56F substitution must alter the antigenic architecture of this epitope, which allows the virus to evade recognition by existing antibodies. Mamoun *et al.* [37] proved that the amino acid substitution of S56F in the H epitope altered the recognition of the monoclonal antibody to this immunogenic region by replacing a small serine residue with a large hydrophobic phenylalanine residue [25].

The N-terminal region of gp51 (SU) contains conformational epitopes F, G, and H, which are critical for recognition by neutralizing antibodies [38]. It contains (1–173 amino acids) the receptor-binding domain (RBD), which mediates binding to the cellular receptor (CAT1/SLC7A1) and triggers membrane fusion [9]. Johnston *et al.* [8] reported systematic single amino acid substitutions in 23 BLV *env* gene variants. The substitutions in the N-terminal region (SU) often retained the

ability to induce syncytia. The substitutions sometimes exhibited signs of misfolding, which reduced the binding of monoclonal antibodies to conformational epitopes.

Callebaut *et al.* [10] built a structural model of the N-terminal region of BLV gp51SU 1 based on alignment with the RBD of the ecotropic murine leukemia virus (Friend, F-MuLV). Most of the residues with substitutions that determine the antigenic properties of the leukemia virus (including region 73) were exposed on the surface of the molecule. This fact means that they were accessible for direct contact with antibodies and immune cell receptors. Therefore, a substitution at one of these positions, e.g., A73P, can directly alter the efficiency of immune recognition of the virus.

The substitutions of D81N and N84D (T-cell epitope N5) were random: we detected them in one sample from the Krasnodar Region (kk1) and one from the Tyumen Region (to31). The D81N polymorphism from negatively charged aspartic acid to neutral asparagine can eliminate the negative charge at position 81. This result potentially disrupts the electrostatic interactions with positively charged regions of the T-cell receptor (TCR), e.g., in CDR3. N84D is the reverse substitution: it adds a negative charge, which can lead to a new electrostatic repulsion or attraction with the TCR.

The D81N and N84D substitutions in antigenic BLV peptides may represent a mechanism for T-cell evasion. This mechanism is due to the modification of the charged residues that are critical for electrostatic interaction with the TCR. This effect alters recognition of the peptide-MHC-I complex, which is consistent with the mechanisms of immune evasion reported for other viruses, e.g., HIV-1. In these viruses, such substitutions directly reduce the TCR binding affinity and the efficiency of T-cell activation [39]. However, in the case of BLV, this mechanism remains hypothetical and requires experimental confirmation.

Substitutions in the zinc-binding motif (137–156 amino acids) of gp51 (SU) belonged to ND2 and $CD8^+$ epitope (N11, N12). Mutations of I144T were found in most isolates from the Tyumen Region (to1, to3-to9, to11, to14-to17, to19, to24, to26, to28, to29, to31-to34, to36, to38). This amino acid substitution was previously identified in some historical samples from Chelyabinsk (G4), Tyumen (G4), Novosibirsk (G4), Krasnodar (G4) (2010, 2020), Moldova (G4), Kazakhstan (G4), Mongolia (G4), France (G4), South Africa (G4), Zambia (G4), Iran (G4), China (G11), Thailand (G10), Myanmar (G10), Brazil (G6), and Bolivia (G9). Substitutions of L149V (13kk) and K150R (kk1-kk4, kk6-12kk, 14kk, 16kk, 18kk-20kk) were previously reported for isolates from Bashkortostan and Kazakhstan. Substitutions of L155I (kk2, kk4, kk14) were found in the Krasnodar Region.

The zinc-binding region is critical for protein stability and structure. Substitution of the hydrophobic isoleucine with the polar, hydrophilic threonine at position 144 may disrupt the hydrophobic core. Altered hydrophobicity may compromise the stability of the zinc-binding motif or alter the conformation of the ND2 and $CD8^+$ epitopes, potentially reducing antibody recognition. Leucine at position 149 has a larger side chain (isobutyl group). Its substitution with valine (isopropyl group) may lead to minor changes in the compaction of the hydrophobic core and flexibility of the protein chain. Arginine at position 150 has a longer and more rigid guanidine group in the side chain than lysine (amino group). This substitution maintains a positive charge. This fact is important for interactions with negatively charged cellular receptors or other molecules but may alter steric parameters and hydrogen bonding. Leucine and isoleucine at position 155 are stereoisomers with very similar sizes and hydrophobic properties. The only difference is the position of the methyl group: it is branched in leucine, and it is linear in isoleucine. This substitution is conservative (neutral) and has a slight effect on the local compaction of the gp51 structure (SU).

A substitution in the $CD8^+$ epitope occurs in the GYPD motif region (D166G) [11]. The GYPD motif is conserved and typical of other retroviruses. It is presumably involved in the formation of a hinge in the structure of the gp51 glycoprotein (SU) [40]. The D166G substitution may disrupt this hinge, altering the conformation of the region.

As described by de Brogniez *et al.* [15], gp51 SU (137–156 amino acids) contains residues (H150, D153) that coordinate a zinc ion (Zn^{2+}) and forms part of a conformational epitope. Zn^{2+} binding is crucial for stabilizing the tertiary structure of the protein, which, in turn, is necessary to develop a neutralizing epitope [15]. The functional importance of this region is confirmed by monoclonal antibody-based assays, e.g., mAbs 3C8 or 1H1. Binding to this epitope entirely depends on the presence of a Zn^{2+} and the native conformation of the protein [41].

Biophysical studies of ion mobility and mass spectrometry demonstrate that amino acid substitutions in zinc-binding motifs can significantly affect zinc affinity and structural conformations of peptides [42]. Extrapolating these data to the current study, we may conclude that amino acid substitutions or combinations in ND2 (I144T, L149V, K150R, L155I) can disrupt Zn^{2+} coordination and destroy the zinc-binding site. It partially or completely destabilizes the conformational epitope, making it unrecognizable to neutralizing antibodies. This mechanism is crucial for the formation of BLV resistance to neutralization, as confirmed by other studies.

Furthermore, substitutions in $CD8^+$ T-cell epitopes (N11, N12) can disrupt the processing and presentation of peptides by histocompatibility complex class I (MHC I) molecules. This, in turn, inhibits the activity of virus-specific cytotoxic T-lymphocytes (CTLs). This means weak cytotoxic T-cell response and a weak key mechanism for the elimination of virus-infected cells [12].

CONCLUSION

Amino acid substitutions in glycoprotein gp51 of bovine leukemia virus (BLV) proved to concentrate in the key functional domains that interact with the host

immune system. Being a mechanism of immune evasion for the virus, these substitutions are often associated with high pathogenicity.

Genotype G4 possesses a selective advantage over G7 due to the cumulative effect of specific amino acid substitutions (in epitopes G, H, zinc motif of ND2, etc.) and their combinations in crucial neutralizing epitopes of the glycoprotein gp51 (SU).

We identified sequences with up to five simultaneous different amino acid substitutions, e.g., in the G4 isolates from the Tyumen Region. For example, isolate to26 from this region had six substitutions, i.e., T47A, A73P, R121H (G epitope); S56F (H epitope); I144T (ND2), and D166G ($CD8^+$ T-cell epitope). In the same region, we identified a shift in the genetic landscape from G7 to G4.

Substitutions in the N-terminal region of gp51(SU) lead to antigenic drift, and the combined effects of weakening both the cellular (CTL) and humoral (antibody) immune responses allow the virus to evade immune control. The poor immune recognition ultimately leads to viral persistence in the host. The combined effect of high viral infectivity may also be achieved through improved receptor binding and accelerated membrane fusion, as indicated by substitutions in the receptor binding domain polypeptide region. Mutations are markers of virulence. Mechanisms and their cascades associated with impaired immune control allow the virus to replicate freely. They correlate with the development rate of clinical symptoms, persistent lymphocytosis, and the development of B-cell lymphomas in susceptible animals. Enzootic bovine leukemia induced by G4 BLV in cattle with an average age of 3.5 years was most often described in the subleukemic and leukemic stages [43]. The rate of pathological development is an important indicator in leukemia. An increase in the proviral load mediates the spread of the pathogen in the population [44]. This thesis is confirmed by compared results of epizootic, molecular-genetic, and clinical immunological analysis across Russia. The lowest infection rate belonged to the G7 genotype while medium infection could be caused by both G7 and G4, and high infection rate was associated with G4.

Changes in the antigenic structure of the glycoprotein may reduce the effectiveness of enzyme-linked immunosorbent assay and polymerase chain reaction diagnostics, thus leading to false-negative results.

Monitoring the antigenic landscape of the leukemia pathogen proved to be a relevant research issue, as did the studies of the epizootiology and immunobiology of its genetic variants in various Russian regions. They may contribute to more effective diagnostic strategies and disease control measures. New genotype-specific diagnostic tests and innovative vaccines should take into account the antigenic characteristics of the particular strain.

Further scientific research requires whole genome sequencing to monitor the genetic variability of BLV. It will help predict risks using molecular modeling, immunochemical analysis, and interreceptor interactions.

CONTRIBUTION

M.V. Petropavlovskiy and I.M. Donnik developed the research concept and supervised the project; A.S. Krivonogova and A.G. Isaeva were responsible for the validation; M.V. Petropavlovskiy and N.A. Martynov provided formal analysis, methodology, and research; A.G. Isaeva and A.S. Badretdinova performed the data curation and proofread the article. The authors have reviewed and approved of the final version of manuscript.

CONFLICT OF INTEREST

The authors declared to conflict of interest regarding the publication of this article.

REFERENCES

1. Brujeni GN, Houshmand P, Soufizadeh P. Bovine leukemia virus: A perspective insight into the infection and immunity. Iranian Journal of Veterinary Research. 2023;24(4):290–300. https://doi.org/10.22099/IJVR.2023.48236.7023
2. Kuczewski A, Mason S, Orsel K, van der Meer F. Pilot implementation of a newly developed bovine leukemia virus control program on 11 Alberta dairy farms. Journal of Dairy Science. 2021;104(4):4549–4560. https://doi.org/10.3168/jds.2020-19251
3. Lv G, Wang J, Lian S, Wang H, Wu R. The global epidemiology of bovine leukemia virus: Current trends and future implications. Animals. 2024;14(2):297. https://doi.org/10.3390/ani14020297
4. Pereira JG, Silva CA, Silva LD, Lima CAA, do Rosário CJRM, *et al*. Diagnosis and phylogenetic analysis of bovine leukemia virus in dairy cattle in northeastern Brazil. Frontiers in Veterinary Science. 2022;9:1080994. https://doi.org/10.3389/fvets.2022.1080994
5. Zhao Y, Wang J, Chen J, Chen Y, Huet C, *et al*. Bovine leukemia virus: Origin, prevalence, phylogenetic diversity, risk factors, and strategies for control. Animals. 2025;15(9):1344. https://doi.org/10.3390/ani15091344
6. Poryvaeva AP, Pechura EV, Petrova OG, Bezborodova NA, Lysova YaYu, *et al*. The effectiveness of scientifically based monitoring programs and therapeutic and preventive measures for controlled infectious diseases of animals. International Journal of Veterinary Medicine. 2023;(4):96–110. (In Russ.) https://doi.org/10.52419/issn2072-2419.2023.4.96
7. Shrestha S, Orsel K, Barkema HW, Martins L, Shrestha S, *et al*. Effects of bovine leukemia virus seropositivity and proviral load on milk, fat, and protein production of dairy cows. Journal of Dairy Science. 2024;107(1):530–539. https://doi.org/10.3168/jds.2023-23695

8. Johnston ER, Albritton LM, Radke K. Envelope proteins containing single amino acid substitutions support a structural model of the receptor-binding domain of bovine leukemia virus surface protein. Journal of Virology. 2002;76(21):10861–10872. https://doi.org/10.1128/jvi.76.21.10861-10872.2002
9. Tomé-Poderti L, Olivero-Deibe N, Carrión F, Portela MM, Obal G, *et al*. Characterization and application of recombinant bovine leukemia virus *env* protein. International Journal of Scientific Reports. 2024;14:12190. https://doi.org/10.1038/s41598-024-62811-8
10. Callebaut I, Voneche V, Mager A, Fumière O, Krchnak V, *et al*. Mapping of B-neutralizing and T-helper cell epitopes on the bovine leukemia virus external glycoprotein gp51. Journal of Virology. 1993;67(9):5321–5327. https://doi.org/10.1128/JVI.67.9.5321-5327.1993
11. Zhao X, Buehring GC. Natural genetic variations in bovine leukemia virus *envelope* gene: Possible effects of selection and escape. Virology. 2007;366(1):150–165. https://doi.org/10.1016/j.virol.2007.03.058
12. Bai L, Takeshima S, Isogai E, Kohara J, Aida Y. Novel $CD8^+$ cytotoxic T cell epitopes in bovine leukemia virus with cattle. Vaccine. 2015;33(51):7194–7202. https://doi.org/10.1016/j.vaccine.2015.10.128
13. de Brogniez A, Bouzar AB, Jacques JR, Cosse JP, Gillet N, *et al*. Mutation of a single envelope N-Linked glycosylation site enhances the pathogenicity of bovine leukemia virus. Journal of Virology. 2015;89(17):8945–8956. https://doi.org/10.1128/JVI.00261-15
14. Murakami H, Uchiyama J, Suzuki C, Nikaido S, Shibuya K, *et al*. Variations in the viral genome and biological properties of bovine leukemia virus wild-type strains. Virus Research. 2018;253:103–111. https://doi.org/10.1016/j.virusres.2018.06.005
15. de Brogniez A, Mast J, Willems L. Determinants of the bovine leukemia virus envelope glycoproteins involved in infectivity, replication and pathogenesis. Viruses. 2016;8(4):88. https://doi.org/10.3390/v8040088
16. Pluta A, Rola-Łuszczak M, Hoffmann FG, Donnik I, Petropavlovskiy M, *et al*. Genetic variability of bovine leukemia virus: Evidence of dual infection, recombination and quasi-species. Pathogens. 2024;13(2):178. https://doi.org/10.3390/pathogens13020178
17. Olaya-Galán NN, Corredor-Figueroa AP, Velandia-Álvarez S, Vargas-Bermudez DS, Fonseca-Ahumada N, *et al*. Evidence of bovine leukemia virus circulating in sheep and buffaloes in Colombia: Insights into multispecies infection. Archives of Virology. 2022;167:807–817. https://doi.org/10.1007/s00705-021-05285-7
18. Blanco R, Quezada-Romegialli C, Muñoz JP. Bovine leukemia virus and human breast cancer: A review of clinical and molecular evidence. Viruses. 2025;17(3):324. https://doi.org/10.3390/v17030324
19. Khan Z, Abubakar M, Arshed MJ, Aslam R, Sattar S, *et al*. Molecular investigation of possible relationships concerning bovine leukemia virus and breast cancer. Scientific Reports. 2022;12:4161. https://doi.org/10.1038/s41598-022-08181-5
20. Polat M, Takeshima SN, Aida Y. Epidemiology and genetic diversity of bovine leukemia virus. Journal of Virology. 2017;14:209. https://doi.org/10.1186/s12985-017-0876-4
21. Bai L, Soya M, Ichikawa M, Matsuura R, Arimura Y, *et al*. Antigenicity of subregions of recombinant bovine leukemia virus (BLV) glycoprotein gp51 for antibody detection. Journal of Virological Methods. 2023;311;114644. https://doi.org/10.1016/j.jviromet.2022.114644
22. Ramalho GC, Silva MLCR, Falcão BMR, Limeira CH, Nogueira DB, *et al*. High herd-level seroprevalence and associated factors for bovine leukemia virus in the semi-arid Paraíba state, Northeast Region of Brazil. Preventive Veterinary Medicine. 2021;190:105324. https://doi.org/10.1016/j.prevetmed.2021.105324
23. Donnik IM, Gulyukin MI, Busol VA, Kovalenko LV, Kovalenko AM Bovine leukemia virus infection – diagnostics, eradication, and anthropozoonotic potential (background) (review). Agricultural Biology. 2021;56(2):230–244. (In Russ.) https://doi.org/10.15389/agrobiology.2021.2.230eng
24. Marawan MA, Alouffi A, Tokhy SE, Badawy S, Shirani I, *et al*. Bovine leukaemia virus: Current epidemiological circumstance and future prospective. Viruses. 2021;13(11):2167. https://doi.org/10.3390/v13112167
25. Suzuki A, Chapman R, Douglass N, Carulei O, van Rensburg J, et al. Phylogenetic analysis of South African bovine leukaemia virus (BLV) isolates. Viruses. 2020;12(8):898. https://doi.org/10.3390/v12080898
26. Maezawa M, Fujii Y, Akagami M, Kawakami J, Inokuma H, *et al*. Phylogenetic analysis based on whole genome sequence of bovine leukemia virus in cattle under 3 years old with enzootic bovine leukosis. PLoS One. 2023;18(1):e0279756. https://doi.org/10.1371/journal.pone.0279756
27. Pluta A, Rola-Luszczak M, Kubis P, Balov S, Moskalik R, *et al*. Molecular characterization of bovine leukemia virus from Moldovan dairy cattle. Archives of Virology. 2017;162(6):1563–1576. https://doi.org/10.1007/s00705-017-3241-4

28. Rola-Łuszczak M, Sakhawat A, Pluta A, Ryło A, Bomba A, *et al*. Molecular characterization of the *env* gene of bovine leukemia virus in cattle from Pakistan with NGS-Based evidence of virus heterogeneity. Pathogens. 2021;10(7):910. https://doi.org/10.3390/pathogens10070910

29. Baboshko DA, Gashnikova NM, Totmenin AV, Nefedova AA, Osipova IP, *et al*. Genetic diversity of BLV, common in the territory of the Kochenevsky district of the Novosibirsk region. Veterinariya i kormleniye. 2022;2:17–19. (In Russ.) https://doi.org/10.30917/ATT-VK-1814-9588-2022-2-4

30. Donnik IM, Petropavlovsky MV, Makutina VA, Gulyukin MI, Barsukov YuI. The current bovine leukemia spread situation in the Russian Federation. Veterinariya. 2024;(11):18–22. (In Russ.) https://doi.org/10.30896/0042-4846.2024.27.11.18-22

31. Sultanov A, Rola-Łuszczak M, Mamanova S, Ryło A, Osiński Z, *et al*. Molecular characterization of bovine leukemia virus with the evidence of a new genotype circulating in cattle from Kazakhstan. Pathogens. 2022;11(2):180. https://doi.org/10.3390/pathogens11020180

32. Lee E, Kim EJ, Joung HK, Kim BH, Song JY, *et al*. Sequencing and phylogenetic analysis of the gp51 gene from Korean bovine leukemia virus isolates. Journal of Virology. 2015;12:64. https://doi.org/10.1186/s12985-015-0286-4

33. Úsuga-Monroy C, Díaz FJ, González-Herrera LG, Echeverry-Zuluaga JJ, López-Herrera A. Phylogenetic analysis of the partial sequences of the *env* and *tax* BLV genes reveals the presence of genotypes 1 and 3 in dairy herds of Antioquia, Colombia. VirusDisease. 2023;34:483–497. https://doi.org/10.1007/s13337-023-00836-9

34. Yang Y, Chen L, Dong M, Huang W, Hao X, *et al*. Molecular characterization of bovine leukemia virus reveals existence of genotype 4 in Chinese dairy cattle. Journal of Virology. 2019;16(1):108. https://doi.org/10.1186/s12985-019-1207-8

35. Rola-Łuszczak M, Pluta A, Olech M, Donnik I, Petropavlovskiy M, *et al*. The molecular characterization of bovine leukaemia virus isolates from Eastern Europe and Siberia and its impact on phylogeny. PLoS One. 2013;8(3):e58705. https://doi.org/10.1371/journal.pone.0058705

36. Bruck C, Rensonnet N, Portetelle D, Cleuter Y, Mammerickx M, *et al*. Biologically active epitopes of bovine leukemia virus glycoprotein gp51: Their dependence on protein glycosylation and genetic variability. Virology. 1984;136(1):20–31. https://doi.org/10.1016/0042-6822(84)90244-7

37. Mamoun RZ, Morisson M, Rebeyrotte N, Busetta B, Couez D, *et al*. Sequence variability of bovine leukemia virus *env* gene and its relevance to the structure and antigenicity of the glycoproteins. Journal of Virology. 1990;64(9):4180–4188. https://doi.org/10.1128/jvi.64.9.4180-4188.1990

38. Rola-Łuszczak M, Grabowska A, Szewczyk B, Kuźmak J. Baculovirus expression and potential diagnostic application of the gp51 envelope glycoprotein of genetic mutants of the bovine leukaemia virus. Journal of Veterinary Research. 2019;63(1):1–6. https://doi.org/10.2478/jvetres-2019-0020

39. Wu X, Li T, Jiang R, Yang X, Guo H, *et al*. Targeting MHC-I molecules for cancer: Function, mechanism, and therapeutic prospects. Molecular Cancer. 2023;22:194. https://doi.org/10.1186/s12943-023-01899-4

40. Moratorio G, Fischer S, Bianchi S, Tomé L, Rama G, *et al*. A detailed molecular analysis of complete bovine leukemia virus genomes isolated from B-cell lymphosarcomas. Veterinary Research. 2013;44:19. https://doi.org/10.1186/1297-9716-44-19

41. Gatot JS, Callebaut I, van Lint C, Demonté D, Kerkhofs P, *et al*. Bovine leukemia virus SU protein interacts with zinc, and mutations within two interacting regions differently affect viral fusion and infectivity *in vivo*. Journal of Virology. 2002;76(16):7956–7967. https://doi.org/10.1128/jvi.76.16.7956-7967.2002

42. Adomako RA, Owusu MB, Oberdick RK, Senyah K, Asare P, *et al*. Zn (II) affinity and structural conformations of 2His-2Cys zinc finger-like motif peptide determined by ion mobility-mass spectrometry and PM6 molecular modeling. Journal of Mass Spectrometry. 2025;60(3):e5113. https://doi.org/10.1002/jms.5113

43. Donnik IM, Petropavlovsky MV. Cattle leukosis: Modern approach. Dairy cattle breeding. 2022;S2:57–59. (In Russ.) https://doi.org/10.25701/ZZR.2022.03.03.011

44. Petersen MI, Suarez Archilla G, Miretti MM, Trono KG, Carignano HA Whole-transcriptome analysis of BLV-infected cows reveals downregulation of immune response genes in high proviral loads cows. Frontiers in Veterinary Science. 2025;12:1550646. https://doi.org/10.3389/fvets.2025.1550646

Additional information about the authors

Maksim V. Petropavlovskiy ORCID 0000-0002-9892-6092; eLIBRARY SPIN 7603-9476
Irina M. Donnik ORCID 0000-0001-8349-3004; eLIBRARY SPIN 2610-5633
Anna S. Krivonogova ORCID 0000-0003-1918-3030; eLIBRARY SPIN 8427-7651
Albina G. Isaeva ORCID 0000-0001-8395-1247; eLIBRARY SPIN 7308-9644
Alisa S. Badretdinova ORCID 0000-0003-0189-2963; eLIBRARY SPIN 9488-1815
Nikolay A. Martynov ORCID 0000-0001-9251-0056; eLIBRARY SPIN 7332-1403

Foods and Raw Materials. 2027;15(2)

ISSN 2308-4057 (Print)
ISSN 2310-9599 (Online)

Review Article
Open Access

Available online at http://jfrm.ru/en
https://doi.org/10.21603/2308-4057-2027-2-708
https://elibrary.ru/SQVBQP

Starch as a sustainable alternative for bioplastic packaging: A review

Bright A. Omoike[1,*], Felix E. Okieimen[2], Chinyere Imoisi[1], James G. Josiah[1]

[1] Mewar International University, Masaka, Nigeria
[2] University of Benin, Benin City, Nigeria

* e-mail: brightomoike@yahoo.com

Received 14.12.2024; Revised 18.04.2025; Accepted 08.12.2025; Published online 05.06.2026

Abstract:
The escalating environmental concerns associated with traditional plastic packaging materials have prompted a paradigm shift towards sustainable and eco-friendly alternatives. Starch, a naturally abundant and renewable polysaccharide, has emerged as a promising raw material source for the development of biodegradable plastic packaging films. This review aimed to provide a comprehensive overview of the current state of starch-based bioplastics, highlighting their potential as a sustainable alternative to conventional plastics.

A comprehensive search of peer-reviewed articles and reviews was conducted in the period of 2022–2024 using Google scholar. We examined the latest research on starch-based bioplastics focusing on the starch structure, extraction, modification, and processing, as well as applications, challenges, and future directions. The data were systematically gathered, evaluated, and organized into logical sections. We also discussed the processing methods employed to fabricate starch-based films, including casting, extrusion, and blown film extrusion.

We explored the structural and functional properties of starch, its modification techniques, and its blending with other biopolymers to enhance performance. Furthermore, we examined the physical, mechanical, and barrier properties of starch-based films, as well as their biodegradability and compostability. The challenges and limitations associated with starch-based packaging films include moisture sensitivity and poor mechanical properties. Finally, starch-based packaging films have potential applications in the food, pharmaceutical, and cosmetic industries.

By providing a comprehensive analysis of starch-based bioplastics, this review stimulates further research and development in this field, contributing to a more sustainable and environmentally friendly packaging industry.

Keywords: Starch, bioplastics, biofilms, sustainability, packaging, biodegradability, renewability

Please cite this article in press as: Omoike BA, Okieimen FE, Imoisi C, Josiah JG. Starch as a sustainable alternative for bioplastic packaging: A review. Foods and Raw Materials. 2027;15(2):270–284. https://doi.org/10.21603/2308-4057-2027-2-708

INTRODUCTION

The packaging industry is a significant contributor to global plastic production, with millions of tons of plastic packaging materials being produced annually [1]. However, the environmental impact of these traditional materials has become a major concern, as they are primarily derived from non-renewable fossil fuels and contribute to plastic waste accumulation in landfills and oceans [2]. The urgent need for sustainable and eco-friendly packaging solutions has led to the exploration of alternative raw materials, such as starch, for the development of biodegradable plastic packaging films [3–5]. Starch, a naturally abundant and renewable polysaccharide, is the second most abundant biomass resource on Earth after cellulose. Its unique properties, such as biodegradability, non-toxicity, and renewability, make it an attractive raw material for the development of sustainable packaging films [5, 6]. Starch-based packaging films have the potential to replace traditional plastic packaging materials in various applications, including food, pharmaceutical, and cosmetic packaging [5, 7].

Recent studies have focused on improving the properties of starch-based packaging films through various modification techniques, such as chemical modification [8, 9], blending with other biopolymers [5, 10], and nanocomposite formation [11, 12]. These advancements have enhanced the mechanical, barrier, and thermal properties of starch-based packaging films, making them more competitive with traditional plastic packaging materials [9].

Despite these advancements, starch-based packaging films still face several challenges, including moisture sensitivity, poor mechanical properties, and limited scalability [9, 13]. Therefore, extensive research and

Copyright © 2026, Omoike *et al.* This is an open access article distributed under the terms of the Creative Commons Attribution 4.0 International License (https://creativecommons.org/licenses/by/4.0/), allowing third parties to copy and redistribute the material in any medium or format and to remix, transform, and build upon the material for any purpose, even commercially, provided the original work is properly cited and states its license.

development efforts are necessary to overcome these limitations and fully exploit the potential of starch as a sustainable raw material for plastic packaging films.

This review aimed to provide a comprehensive overview of the current state of starch-based packaging films, discussing their development, properties, and applications. We also examined the challenges and limitations associated with starch-based packaging films and explored future perspectives and potential solutions to overcome these challenges.

STUDY OBJECTS AND METHODS

We examined the latest research on starch-based bioplastics focusing on the starch structure, extraction, modification, and processing, as well as applications, challenges, and future directions. The data were systematically gathered, evaluated, and organized into logical sections.

Starch was defined as a natural polysaccharide consisting of amylose and amylopectin repeat units, which are linked together by α-1,4 and α-1,6 glycosidic bonds.

Bioplastic was defined as a type of plastic that is made from renewable biomass sources such as plants, animals, micro-organisms or agricultural waste rather than traditional fossil fuels. It has the advantage of being biodegradable unlike petroleum-based plastics.

Packaging was defined as a material used to enclose, protect, and prepare a product for distribution, storage, and safety.

A comprehensive search of peer-reviewed articles and reviews was conducted in the period of 2022–2024 using Google scholar. The following keywords were used in the search: starch, bioplastics, packaging. Our aim was to gather and evaluate relevant publications in the reputable journals.

RESULTS AND DISCUSSION

Recent studies on starch-based bioplastic packaging. Starch-based bioplastic packaging has gained significant attention in recent years due to its biodegradable and renewable nature. Researchers have focused on improving the properties of starch-based bioplastics through various modification techniques, blending with other biopolymers, and nanocomposite formation (Fig. 1).

Among the various modification techniques, chemical modification of starch has been widely explored to enhance its properties. For example, Altuna *et al.* [14] reported that modifying starch with octenyl succinic anhydride improves its paste properties such as viscosity, while lowering its gelatinization temperature for pharmaceutical applications. Similarly, Chen *et al.* [15] modified tapioca starch by crosslinking it with citric acid, which resulted in enhanced thermal stability and tensile mechanical properties. The crosslinking process created a network of starch molecules that are held more closely together, providing better resistance to thermal energy and tensile stretching. Furthermore, Choi *et al.* [16] developed sweet potato starch-based edible films through the chemical modification of starch for improved water solubility in vegetable and dairy products packaging.

Blending starch with other biopolymers has also been investigated to improve its properties. In a recent study, Gao *et al.* [17] investigated the effect of blending on the physiochemical properties of polylactic acid (PLA)/modified starch blend. Their findings demonstrated that PLA/modified starch blend exhibited improved thermal and mechanical properties, as well as substantial biodegradability, when compared to native starch. In another study, Omoike *et al.* [5] developed a cassava starch/polyvinyl alcohol (PVA) blend with potential applications in food and pharmaceutical packaging. The focus was on determining the optimal blend ratio to achieve superior properties, including tensile mechanical strength, barrier properties, and thermal stability. The study revealed that the optimal blend ratio of 40% cassava starch and 60% PVA exhibited the best balance of properties. Furthermore, researchers have explored the potential of using crosslinking agents to enhance the properties of biopolymer blends. In a notable study, Wu *et al.* [18] utilized citric acid as a crosslinking agent in a potato starch-chitosan blend. This significantly improved the water resistance, mechanical properties, and antimicrobial activity of the blend,

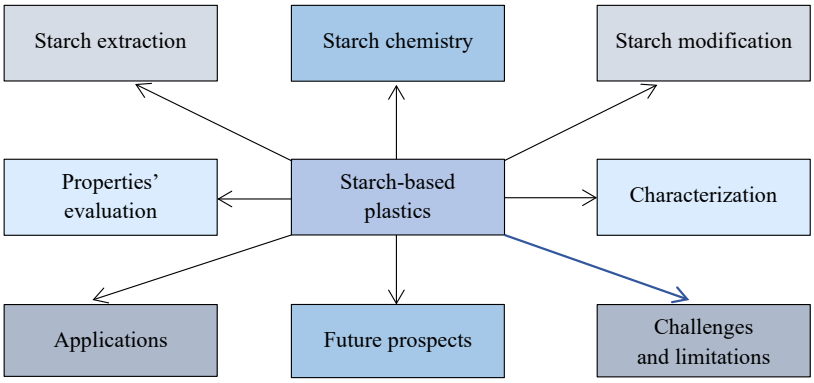


Figure 1 Graphical overview of starch as a source for bioplastics

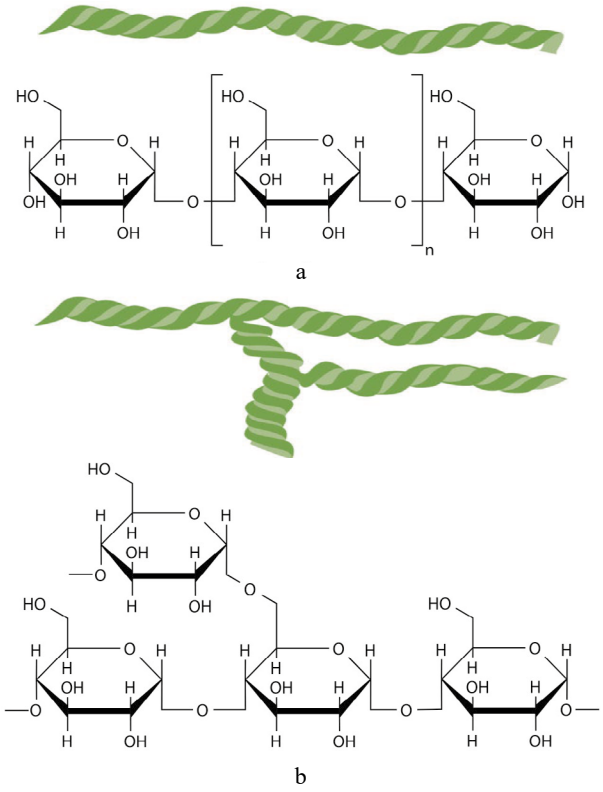


Figure 2 Structure of amylose (a) and amylopectin (b)[1]

demonstrating the effectiveness of crosslinking agents in optimizing biopolymer blend performance.

Nanocomposite formation has also been explored to enhance the properties of starch-based bioplastics. Coelho *et al.* [19] successfully developed starch-based nanocomposite films reinforced with cellulose nanocrystals extracted from grape pomace. The incorporation of cellulose nanocrystals increased the tensile strength and lowered the water vapor permeability of the starch-based nanocomposites, which are important parameters in packaging. Furthermore, Wang *et al.* [20] developed starch-based nanocomposites with graphene oxide to enhance their thermal stability and barrier properties.

Starch chemistry. Structurally, starch is a polysaccharide consisting of *α*-D-glucopyranose repeat units, which are linked together by α-1,4 and α-1,6 glycosidic bonds [21, 22]. These bonds are formed through the condensation reaction of neighboring *α*-D glucose molecules, resulting in the release of water molecules. The polymerization of glucose units leads to the formation of two main polysaccharide fractions: linear amylose and branched amylopectin. Amylose is primarily a linear fraction with few branches, consisting of long chains of *α*-D-glucopyranose residues connected by *α*-1,4-glycosidic bonds [23]. In contrast, amylopectin is a highly branched fraction with a complex molecular structure, comprising short and long chains [23]. The branched architecture of amylopectin with its intricate network of branching points enables the formation of a more extensive and complex branched structure. This significantly influences the rheological properties of starch solutions, particularly their viscosity and texture [15]. The branching points in amylopectin are classified into three types: A-chains (short, unbranched chains), B-chains (branched chains), and C-chains (long chains with branching points) [24]. The structure and properties of starch are influenced by various factors, including genetic conditions, plant species and varieties, cultivation conditions, and non-polysaccharide components [25]. These factors contribute to the diversity of starch grains and their physical and chemical properties (Fig. 2).

Native starch is insoluble in cold water and most organic solvents due to the presence of the amylose fraction, which is insoluble or sparingly soluble. However, starch grains can absorb water through reversible swelling, increasing their volume by up to 30% [26]. This swelling is an exothermic process where water molecules are absorbed into the amorphous zone and bonded to free hydroxyl groups of glucose units in polymer chains through hydrogen bonds [27].

Starch gelatinization. When starch is heated above a certain temperature, its granules undergo gelatinization, a thermal transition characterized by spherical swelling and amorphization leading to the formation of a more viscous structure [28]. The gelatinization temperature varies depending on the botanical starch type and is a range rather than a single value, as it depends on the grain size. For example, potato starch gelatinizes

[1]Structure and Function of Carbohydrates. Biology for Majors I. [cited 2024 Sept 10]. Available from: https://courses.lumenlearning.com/wm-biology1/chapter/reading-types-of-carbohydrates/

at 50–70°C [29]. Gelatinization is accompanied by loss of birefringence, which is the ability of starch granules to split light into two beams with different polarizations and velocities [30]. This property is due to the ordered arrangement of starch molecules in the granule. When starch granules are heated during gelatinization, the ordered arrangement of molecules is disrupted, leading to a loss of birefringence [30]. During starch gelatinization, the viscosity of the starch suspension increases significantly due to the following factors: starch granule swelling, breakdown of crystalline structure leading to more disordered and random arrangement of starch molecules, uncoiling of starch molecules, and increased molecular interactions via new hydrogen bonding [31, 32].

Furthermore, gelatinization increases the electrical conductivity of starch due to the hydration of starch molecules, formation of more conductive pathways, and increased ionic mobility. Gelatinization increases the mobility of ions within the starch matrix enabling them to carry electrical charge more efficiently [33].

Starch retrogradation. Starch retrogradation is a process where gelatinized starch molecules re-associate and re-crystallize, leading to a more ordered and rigid structure [32]. This process occurs over time, often resulting in a loss of flexibility and an increase in brittleness. During retrogradation, the starch molecules that were previously uncoiled and hydrated during gelatinization start to re-form their crystalline structure. This re-association is driven by hydrogen bonding between the starch molecules, leading to a more rigid and inflexible network [32].

Starch extraction. Starch extraction is a process of isolating starch from plant sources, such as corn, potatoes, and cassava [34]. This process is crucial for various industries, including food, pharmaceuticals, and paper production, as starch is a versatile ingredient with numerous applications.

The first step in starch extraction is harvesting, where the plant material is collected from its source and washed to remove dirt, soil, and other impurities. It is then pulverized into a milky mash and suspended in water to soften the tissues and remove the starch granules. This pulverization process is typically done using a mill or grinder, and the resulting mash is mixed with water to create a starch suspension. The starch suspension is then centrifuged or sieved to separate the starch from the other plant components. The centrifuge spins the mixture at high speeds, causing the starch to settle at the bottom of the centrifuge, while the supernatant is removed. The starch is then washed with water to remove any remaining impurities and dried to remove excess moisture [34–36].

There are different methods of starch extraction, including wet milling (Fig. 3), dry milling, enzymatic extraction, and alkaline extraction. Wet milling is the most common method, which involves grinding the plant material in water. Dry milling, on the other hand, involves grinding the plant material without water and is used for plants with a low moisture content. Wet milling generally yields higher purity starch compared to dry milling due to its superior ability to separate starch from proteins, lipids, and fibers. This is because wet milling uses water to hydrate and swell the starch granules, making them more easily separable from the other components. In contrast, dry milling relies solely on the mechanical force to break down the starch granules, which can lead to a higher likelihood of contamination with proteins, lipids, and fibers [37]. Enzymatic extraction uses enzymes to break down the plant cell walls and release the starch, while alkaline extraction uses an alkaline solution to achieve the same result.

The efficiency of starch extraction depends on various factors, including plant variety, moisture content, grinding method, water quality, and temperature. Different plant varieties have different starch contents and properties, which affect the extraction process. The moisture content in the plant material also plays a crucial role, as excessive moisture can lead to poor starch yields. The grinding method can also impact the release of starch from the plant cells, and the quality of water can affect the purity of the extracted starch.

Starch extraction has numerous applications in various industries. In the food industry, starch is used as a thickening agent, stabilizer, and emulsifier in food products

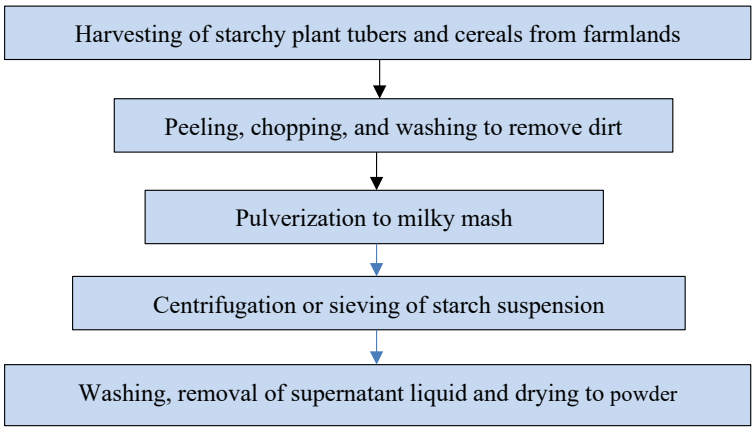


Figure 3 Flowchart for the extraction of starch from plant sources (wet method)

such as soups, sauces, and baked goods. In the pharmaceutical industry, starch is employed as an excipient in tablets, capsules, and ointments. In the paper industry, starch is used as a sizing agent to improve the strength and durability of paper. It is also used as a sizing agent in the textile industry and as a sustainable alternative to synthetic polymers in biodegradable packaging [9].

Starch modification. Starch modification is a process of altering the properties of starch to enhance its functionality and performance in various applications [38]. Starch is a versatile carbohydrate that can be modified in various ways to suit specific requirements.

Chemical modification. One common method of starch modification is chemical modification, which involves treating starch with chemicals to alter its structure and properties. This can include reactions such as etherification, esterification, and cross-linking, which can improve starch stability, solubility, and resistance to degradation. Chemical modification can also be used to introduce new functional groups, such as hydroxyl or carboxyl groups, which can enhance starch reactivity and versatility [39, 40].

Physical modification. Physical modification involves treating starch with physical agents such as heat, light, or radiation to alter its structure and properties [41]. This can include processes such as heat treatment, mechanical treatment, high pressure application, moisture treatment, and electrical treatment. These methods can improve starch solubility, gelatinization, viscosity, crystallinity, and stability for various industrial applications. Physical modification can also be used to create new starch-based materials, such as nanocrystals and nanoparticles, which have unique properties and applications [42].

Enzymatic modification. Enzymatic modification is another method of starch modification, which involves using enzymes to break down or modify starch molecules. This can include processes such as hydrolysis, which can break down starch into simpler sugars, and transglycosylation, which can create new glycosidic bonds and modify the starch structure and properties. Enzymatic modification can be used to improve digestibility, solubility, and stability of starch, as well as to create new starch-based products with specific properties and applications.

Genetic modification. Genetic modification of starch refers to the use of biotechnology techniques to alter the genetic code of plants to produce starch with desired properties [43]. This is achieved through the introduction of specific genes or changes to existing genes that regulate starch biosynthesis, structure, and functionality [44]. One approach is to enhance the starch content and yield in plants, allowing for increased production and efficiency. This can be done by introducing genes that regulate starch biosynthesis, such as those involved in the production of the enzymes ADP-glucose pyrophosphorylase or starch synthase. Alternatively, genes that limit starch production can be suppressed to increase yields [45].

Another strategy is to modify the starch structure and properties (e.g., increase its amylose content) to improve its suitability for specific applications. This can be achieved by introducing genes that encode enzymes involved in starch biosynthesis, such as granule-bound starch synthase, or by modifying the existing genes to alter their activity [46, 47]. For example, RNA interference technology can be used to silence the genes responsible for amylose degradation, resulting in a higher amylose content. Genetic modification can also be used to introduce new functional properties into starch, such as improved thermal stability, biodegradability, or resistance to degradation [43]. This can be achieved by introducing genes from other organisms, such as bacteria or fungi that encode enzymes with desired activities. For example, introducing a gene that encodes a heat-stable enzyme can improve the thermal stability of starch.

Starch-based bioplastic processing techniques. Starch-based bioplastics are a sustainable alternative to traditional plastics and are made from renewable resources such as corn starch, potato starch, or tapioca starch. Their processing involves various methods to convert starch into a plastic-like material.

One common technique is extrusion, where starch is mixed with other biodegradable polymers and additives, and then fed into an extruder. The extruder converts the mixture to a flowable viscous melt by heating. The viscous melt is then homogenized and forced through a die by means of a rotating screw where it is shaped into a desired form [47]. This process can produce a wide range of products, including packaging materials, disposable cutlery, and bags (Fig. 4).

Another technique is injection molding, which involves melting starch-based pellets in an extruder and injecting the molten plastic into a mold cavity of specific shapes and designs. As the molten plastic cools and solidifies in the mold, it takes the shape of the mold cavity. The final solidified product is ejected from the mold [49]. This process is often used for producing high-precision items with fast production rates and quality.

Blown film extrusion is another method used to produce starch-based bioplastics, particularly for packaging materials like bags and wraps. This process involves extruding starch-based pellets through a die to create a tube, which is then blown up like a balloon and cooled to form a thin film [50]. Thermoforming is also used to process starch-based bioplastics, where a sheet of starch-based material is heated to a pliable and flexible form and molded into a specific shape by cooling in a mold [49]. This process is often used for producing trays, containers, and other packaging materials.

Solvent casting is a technique used to produce starch-based bioplastics with specific properties, such as transparency and flexibility. This process involves dissolving starch and other additives in a solvent (usually water), heating, and stirring for the viscous solution to gelatinize and homogenize. This is followed by casting it into a thin film, and then evaporating the solvent to create a solid material (Fig. 5) [5, 51].

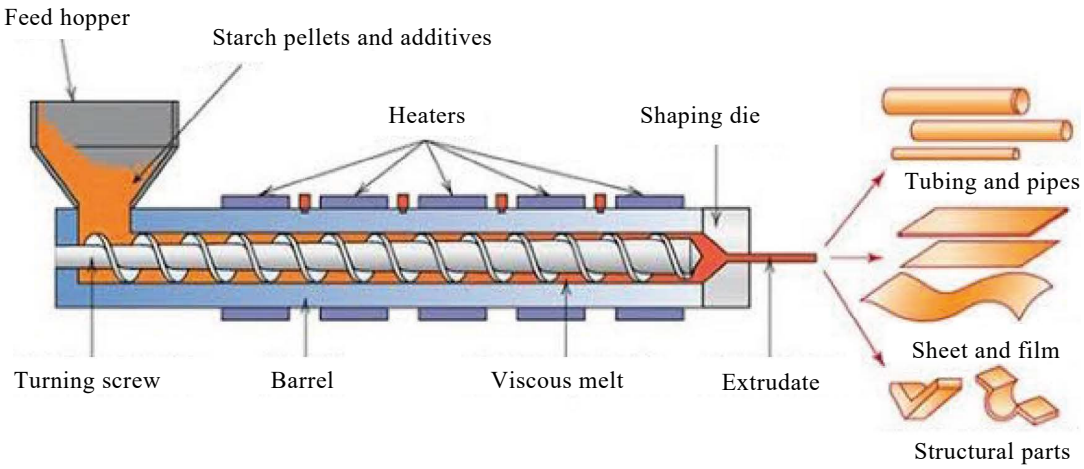


Figure 4 Extrusion of starch-based bioplastics using a single screw extruder (adapted from Bacalhau *et al.* [48])

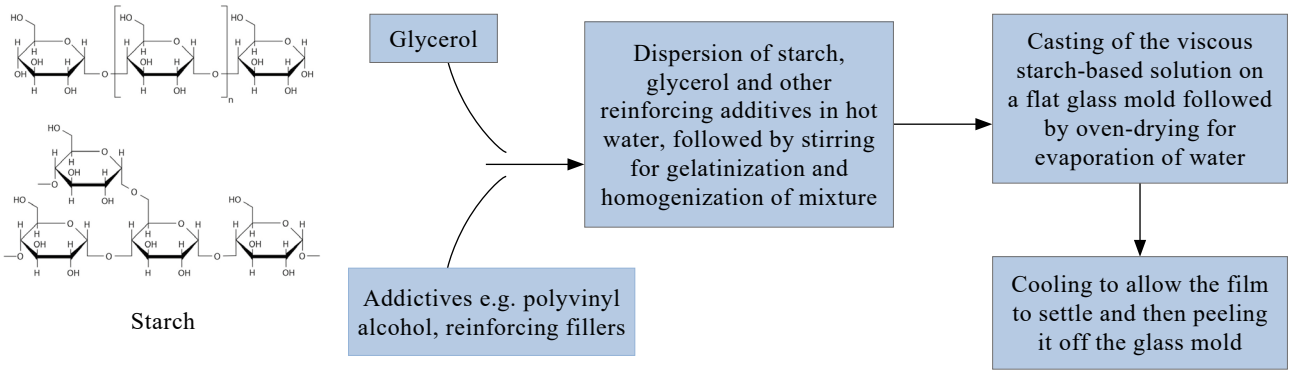


Figure 5 Preparation of starch-based plastics using solvent casting techniques

Three-dimensional printing is also being explored as a processing technique for starch-based bioplastics, allowing for the creation of complex shapes and designs with high precision and accuracy [52]. It involves layer-by-layer deposition of starch-based filaments to create a physical object. Here, a starch-based plastic filament is fed through a heated extruder, which melts and deposits the material on a build platform or substrate. The deposited material is then cooled and solidified thereby bonding to the previous layer. This process is repeated until the entire object is printed (Fig. 6) [52].

The advantages of starch-based bioplastic processing techniques include the use of renewable resources, biodegradability, and reduced greenhouse gas emissions. However, challenges still exist, such as high production costs, limited scalability, and the need for improved material properties. Research and development is ongoing to overcome these challenges and improve the processing techniques for starch-based bioplastics. This includes the development of new starch-based materials with improved properties, the optimization of processing conditions, and the scale-up of production processes.

Scanning electron microscopy characterization of starch-based bioplastics. Scanning Electron Microscopy (SEM) characterization of starch-based bioplastic packaging provides valuable insights into the material's

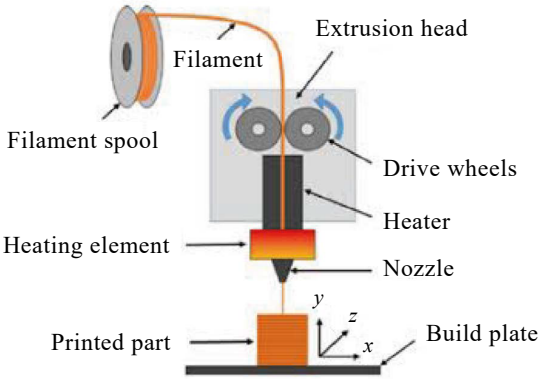


Figure 6 Three-dimensional printing of bioplastic coating on objects (adapted from Andanje *et al.* [53])

surface morphology, structure, and properties. The SEM analysis reveals the texture, porosity, and topography of the bioplastic surface, which is essential for understanding its performance and functionality [5, 54].

The SEM images of starch-based bioplastic packaging typically show a smooth and continuous surface with no visible pores or cracks. This morphology is attributed to the well gelatinization of starch granules and good compatibility with other biopolymers and suitable

additives [5, 55–57]. The surface morphology can affect the bioplastic's barrier properties, mechanical strength, and biodegradability.

The SEM analysis also reveals the presence of starch granules, their size and distribution, and the extent of gelatinization. The degree of gelatinization affects the bioplastic's properties, such as its solubility, swelling behavior, and enzymatic digestibility. In addition, SEM can detect the presence of additives, such as plasticizers, fillers, or reinforcing materials, and their distribution within the bioplastic matrix.

The SEM characterization of starch-based bioplastic packaging can be used to study the effect of processing conditions on the bioplastic's microstructure and properties. It can also analyze the bioplastic's degradation behavior under different environmental conditions, as well as compare the properties of starch-based bioplastics with those of conventional plastics. In summary, SEM is a powerful tool for understanding the microstructure and properties of starch-based bioplastic packaging, enabling the development of high-performance, sustainable packaging materials.

X-ray diffraction. X-ray diffraction (XRD) analysis reveals the crystal structure, degree of crystallinity, molecular arrangement, and lattice spacing, which are essential for understanding the bioplastic's properties and behavior [58]. The XRD patterns of starch-based bioplastic packaging typically show a semi-crystalline structure, with both amorphous and crystalline regions [5, 57, 59]. The crystalline regions are attributed to the ordered arrangement of starch molecules, while the amorphous regions are due to the disordered structure. The degree of crystallinity affects the bioplastic's mechanical strength, thermal stability, and barrier properties [5].

The XRD analysis can also detect the presence of different polymorphs, such as A, B, or C, which are related to the starch source and processing conditions. The polymorphs have different crystal structures and properties that influence the bioplastic's behavior [60]. Furthermore, XRD can monitor changes in the crystal structure and crystallinity during processing, aging, or degradation, providing valuable information on the bioplastic's stability and durability [58].

Thermogravimetric analysis. Thermogravimetric analysis (TGA) is a powerful analytical technique used to characterize the thermal properties of starch-based bioplastic packaging. The TGA instrument measures the weight loss of the bioplastic as a function of temperature, providing valuable insights into its thermal stability, decomposition behavior, and moisture content [61]. The TGA curves of starch-based bioplastic packaging typically exhibit a multi-step decomposition process. The first step involves the loss of moisture, which occurs at temperatures below 150°C [5, 62]. The second step corresponds to the decomposition of starch molecules, which takes place between 200 and 300°C [63]. The final step involves the degradation of the bioplastic matrix, which occurs at temperatures above 300°C [5, 57].

TGA provides important information on the bioplastic's thermal stability, which is essential for its processing and application. The decomposition temperature and weight loss associated with each step provide insights into the bioplastic's degradation mechanism and volatile content, which can affect its performance and shelf life. Additionally, TGA can detect the presence of additives, such as plasticizers or fillers, which can affect the bioplastic's thermal behavior.

Tensile mechanical properties of starch-based bioplastics. Starch-based bioplastics are biodegradable polymers derived from renewable resources such as corn starch, potato starch, or tapioca starch. The mechanical properties of starch-based bioplastics are crucial in determining their suitability for various applications. Their tensile mechanical properties, such as tensile strength, percentage elongation at break, and tensile modulus, can be evaluated using tensile testing machines.

The tensile strength is the maximum stress a material can withstand when subjected to tensile force. For starch-based bioplastics, the tensile strength ranges from 1 to 100 MPa, depending on the type of starch and processing conditions [64]. This is lower than the tensile strength of traditional plastics such as polyethylene (20–30 MPa) and polypropylene (30–40 MPa) [65]. Studies have shown that the greater the strength of molecular interaction between polymer constituents, the higher the tensile strength [5, 57]. The tensile strength of starch-based bioplastics can be improved through incorporation of biopolymers such as PVA or chitosan [5], as well as through reinforcement with nanofillers such as clay, carbon black, and fibers [9].

The percentage elongation at break is a measure of the flexibility and extensibility of a polymer material, indicating its ability to stretch and deform without rupturing. In starch-based bioplastics, while high tensile strength is desirable, a substantial level of flexibility is equally important to meet packaging requirements. In particular, flexibility ensures that the material can withstand handling, storage, and transportation without cracking or breaking. The incorporation of plasticizers into starch film matrices can provide higher molecular mobility and increased flexibility, allowing the bioplastic film to become more pliable and less brittle [66, 67]. The elongation at break for starch-based bioplastics ranges from 10 to 50%, depending on the type of starch and processing conditions. This is lower than the range for traditional plastics such as polyethylene (50–100%) or polypropylene (100–200%) [68].

The tensile modulus is defined as a ratio of stress to strain within the proportionality limit of a material, indicating its stiffness and resistance to deformation. For starch-based bioplastics, the tensile modulus ranges from 100 to 500 MPa, which is lower than the range for traditional plastics such as polyethylene (1000–1500 MPa) or polypropylene (1,500–2,000 MPa) [69].

Water vapor barrier properties. Starch-based bioplastics have barrier properties that are essential for various applications, including packaging and dispos-

able products. The barrier properties of starch-based bioplastics refer to their ability to prevent the passage of gases, vapors, and liquids through the material [6].

One of the critical barrier properties of starch-based bioplastics is their water vapor transmission rate. Starch-based bioplastics have a higher water vapor transmission rate compared to that of traditional plastics, which can be a limitation for applications requiring high moisture barrier properties [5, 51, 70].

Starch-based bioplastics also have a relatively high oxygen transmission rate, which can affect their ability to protect products from oxidation [71]. This can be a concern for applications such as food packaging, where oxygen can cause spoilage or degradation. However, some starch-based bioplastics have been developed with improved oxygen transmission rate properties, making them suitable for specific applications.

The carbon dioxide transmission rate (CO_2TR) of starch-based bioplastics is another essential barrier property. Starch-based bioplastics have a higher CO_2TR compared to traditional plastics, which can affect their ability to maintain pressure and prevent carbonation loss in applications such as beverage packaging.

The barrier properties of starch-based bioplastics can be improved through various techniques, such as adding barrier coatings or layers, using nanoclay or other reinforcing materials, optimizing processing conditions, and blending with other biodegradable polymers [9]. Some starch-based bioplastics have been developed with improved barrier properties, making them suitable for food packaging, pharmaceutical packaging, and cosmetic packaging.

Biodegradability assessment. Starch-based bioplastics are biodegradable, meaning they can break down naturally in the environment through microbial action, enzymatic degradation, or chemical hydrolysis. The biodegradability of these bioplastics is influenced by various factors, including the type of starch used, processing conditions, and the presence of additives or coatings [57, 72].

The biodegradability of starch-based bioplastics can be assessed through various tests, such as ASTM D6400, ASTM D6868, and ISO 14855 [73]. These tests evaluate the biodegradability of plastics in different environments, including composting, soil, and water. The biodegradability of starch-based bioplastics is affected by several factors including crystallinity, molecular weight, and hydrophilicity [57, 74]. Bioplastics with lower crystallinity, molecular weight, and higher hydrophilicity are more biodegradable. Additionally, the presence of additives or coatings can also impact the biodegradability of starch-based bioplastics. Biodegradability offers several benefits, including reduced plastic waste, lower carbon footprint, and improved sustainability.

Applications of starch-based bioplastics. Starch-based bioplastics have a wide range of applications across various industries, including packaging, disposable cutlery and tableware, agricultural films, medical devices, and three-dimensional printing.

Food packaging. Starch-based bioplastics are used in food packaging as a biodegradable and renewable alternative to traditional plastics. They are applied in various forms, such as flexible packaging films, rigid containers, disposable cutlery, and edible packaging materials. Starch-based bioplastics have been successfully utilized in packaging various food products, including baked goods, fresh produce, dairy products, and beverages [75]. These bioplastics can enhance food safety, quality, and shelf life, as well as improve packaging performance, by providing a barrier against moisture, oxygen, and other external factors [76]. Furthermore, several studies have shown that starch-based bioplastics can be engineered to possess antimicrobial and antioxidant properties to further extend the shelf life of packaged food products [57, 77, 78]. Additionally, starch-based bioplastics are compostable and therefore they reduce food waste and environmental impact. They can also be customized to meet specific packaging requirements, making them an attractive solution for sustainable food packaging.

The development of starch-based bioplastics has also led to the creation of innovative, smart packaging materials that can monitor food freshness and quality. For instance, starch-based bioplastics infused with natural extracts, such as anthocyanins, can change color in response to changes in pH levels, indicating spoilage or contamination [79]. Additionally, starch-based bioplastics can be designed to release preservatives or nutrients in a controlled manner, enhancing food quality and safety [5]. With ongoing advancements in nanotechnology, electrospinning, and three-dimensional printing, the potential applications of starch-based bioplastics in food packaging are vast and promising, offering a sustainable and environmentally-friendly alternative to traditional plastic packaging materials.

Medicine and pharmaceutical industry. In medicine, starch-based bioplastics offer useful applications as biodegradable and biocompatible medical implants, such as bone screws and plates that can dissolve over time, eliminating the need for surgical removal [75]. The breakthroughs in biodegradable starch materials have paved the way for innovative biomedical applications, including the creation of advanced drug delivery systems such as capsules and tablets, which can release medication in a controlled manner [80]. Starch-based bioplastics are also used in wound dressing materials, surgical meshes, and tissue engineering scaffolds that promote tissue growth and regeneration [80]. For instance, the study by Kiran *et al.* [81] shows the potential of starch-based bioplastics obtained from banana peel to be used as material for intravenous tubes for medical operations, thereby reducing the application of single use plastics which could constitute environmental waste. Furthermore, starch-based bioplastics are used in pharmaceutical packaging, such as compostable blister packs and containers, also reducing environmental waste. In a recent study, Omoike *et al.* [5] developed a starch/PVA blend to be used as a coating in food and

pharmaceuticals applications. This innovative blend combines the biodegradable and renewable properties of starch with the flexibility and strength of PVA, making it a viable material in sustainable drug packaging.

Agriculture and agro-allied industry. Agricultural films made from starch-based bioplastics are used as mulch films, greenhouse covers, and soil conditioning materials [82]. These bioplastics improve soil health and reduce water consumption. They are also used in controlled-release fertilizer coatings, seed coatings, and plant growth promoters that enhance crop yields and reduce environmental impact [83]. Additionally, they are applied in biodegradable planting pots, trays, and containers, which eliminates the need for plastic waste disposal. Furthermore, starch-based bioplastics are used in animal feed packaging, agricultural packaging materials, and bio-based composites for agricultural equipment. Overall, starch-based bioplastics offer a versatile and biodegradable solution for various agricultural and agro-allied applications, reducing plastic waste and promoting sustainability.

Cosmetological industry. Starch-based bioplastic are used in the cosmetological industry as a biodegradable and renewable material for various applications. They are used to create edible skin-care, hair products, and edible packaging for cosmetics and personal care products, thereby enhancing human well-being and sustainability [84]. Starch-based bioplastics offer a sustainable alternative in the production of disposable makeup remover wipes, facial masks, and exfoliating scrubs that are gentle on the skin and the environment. Additionally, they find promising application in biodegradable microbeads for skin care products, replacing traditional plastic microbeads that harm the environment [85]. Overall, starch-based bioplastics provide a sustainable and eco-friendly solution for the cosmetological industry, reducing plastic waste and promoting environmental responsibility.

Future prospects of starch-based bioplastics. Starch-based bioplastics have promising prospects, with potential growth and expansion in various industries.

Increasing demand. The demand for starch-based bioplastics is expected to rise significantly due to the growing concerns about plastic pollution, climate change, and sustainability [86]. Governments, consumers, and businesses are increasingly seeking eco-friendly alternatives to traditional plastics, driving the demand for biodegradable plastics. This trend is expected to continue, with starch-based bioplastics playing a crucial role in reducing plastic waste and promoting sustainable practices.

Technological advancements. Ongoing research and development in the field of starch-based bioplastics is expected to improve their performance, scalability, and cost-effectiveness. New technologies will enhance their mechanical properties, barrier properties, and processing capabilities, making them more competitive with traditional plastics [87]. These advancements will also enable the production of starch-based bioplastics with tailored properties for specific applications.

Expanded applications. Starch-based bioplastics will find new applications in various industries, including textiles, automotive, and construction. They will be used in a wider range of products, such as biodegradable fibers, composites, and building materials [49]. This expansion will be driven by the growing demand for sustainable materials and the need to reduce plastic waste.

Sustainable agriculture. Starch-based bioplastics will promote sustainable agriculture practices by utilizing waste biomass and reducing synthetic fertilizer use. This will contribute to a circular economy and reduce environmental impacts [88]. The use of starch-based bioplastics will also provide new revenue streams for farmers and rural communities.

Biodegradable plastics. Starch-based bioplastics will play a crucial role in replacing traditional plastics in packaging, disposable products, and single-use items [89]. They will help reduce plastic waste and marine pollution, which are major environmental concerns. The use of biodegradable plastics will also reduce greenhouse gas emissions and mitigate climate change.

Global market growth. The global starch-based bioplastic market is expected to grow significantly, driven by the increasing demand, technological advancements, and expanding applications [90]. The market growth will also be fueled by government policies, regulations, and incentives that promote the use of biodegradable plastics. This will also create new business opportunities and jobs in the sustainable materials sector.

Current challenges and limitations of starch-based bioplastics. While starch-based bioplastics offer tremendous potential for driving eco-friendly innovations, their adoption is hindered by several key challenges and limitations. Recognizing and addressing these constraints is essential for successfully harnessing their benefits.

Lower strength and durability. One of the significant challenges hindering the widespread adoption of starch-based bioplastics is their lower strength and durability [72]. The incorporation of starch, a natural component, can compromise the structural integrity and mechanical properties of the resulting polymer blend. This can make it unsuitable for applications that require robustness and long-term durability, such as packaging and durable goods manufacturing. This limitation underscores the need for further research and development to enhance the mechanical strength and durability of starch-based bioplastics, thereby expanding their potential applications and promoting their adoption as a sustainable alternative to traditional plastics.

Moisture sensitivity. High moisture sensitivity poses a significant challenge to the use of starch-based bioplastics. These materials are prone to water absorption, which can trigger degradation and compromise their performance and shelf life [72]. This sensitivity to environmental moisture can be particularly problematic in humid climates or in applications where exposure to water is unavoidable, such as packaging for food or beverages. As a result, moisture sensitivity of starch-based

bioplastics can limit their utility and reliability, emphasizing the need for further research and development to enhance their water resistance and durability.

Limited shelf life. The limited shelf life of starch-based bioplastics is a significant concern, as these materials tend to degrade more rapidly than traditional plastics. Their shorter shelf life can lead to a decline in their mechanical properties, such as strength and flexibility, ultimately affecting their performance and integrity over time [91]. As a result, starch-based bioplastics may become brittle, crack, or break down, which renders them unsuitable for long-term applications. Moreover, the degradation process can also lead to the release of volatile compounds, potentially impacting the quality and safety of packaged products. This highlights the need for improved formulations and preservation methods to extend the shelf life of these biodegradable materials.

Limited scalability. The limited scalability of starch-based bioplastics is a significant hurdle to their widespread adoption, primarily due to their higher production costs compared to traditional plastics. The expense of starch-based bioplastics can be attributed to various factors, including the cost of raw materials, processing, and manufacturing. Consequently, large-scale production of starch-based bioplastics becomes challenging, making it difficult for manufacturers to achieve economies of scale and reduce costs. This scalability limitation can hinder the ability of starch-based bioplastics to compete with traditional plastics in terms of price. This can restrict their market penetration and adoption in various industries, such as packaging, textiles, and automotive.

Limited availability of raw materials. Starch-rich crops such as corn, potatoes, and tapioca are the primary feedstocks for starch-based bioplastics, but their availability can be regionally constrained. This limited availability can lead to fluctuations in raw material prices, affecting the overall cost of production and making it difficult for manufacturers to maintain a stable supply chain [50]. Furthermore, reliance on specific geographic regions for raw material sourcing can also create logistical challenges and increase transportation costs. This can exacerbate the environmental impact of production, ultimately hindering the growth and development of the starch-based bioplastics industry.

Lack of standardization. There is a lack of standardization in the production and processing of starch-based bioplastics, which can affect their quality, performance, and overall reliability.

Without standardized manufacturing protocols, the resulting bioplastics can exhibit varying levels of mechanical strength, thermal stability, and biodegradability, making it difficult for manufacturers to ensure consistency and predictability in their products. This lack of standardization can also hinder regulatory frameworks and industry-wide quality control measures.

Limited compatibility with existing infrastructure. The limited compatibility of starch-based bioplastics with the existing packaging infrastructure poses a significant barrier to their widespread adoption. Many conventional packaging facilities and equipment designed to handle traditional plastics may not be suitable for processing starch-based bioplastics, which can have different melting points, viscosity, and other physical properties. This incompatibility can lead to difficulties in manufacturing, filling, and sealing, ultimately increasing costs and reducing efficiency. This highlights the need for specialized infrastructure and equipment to support the production and use of starch-based bioplastics.

Public perception and awareness. Limited public awareness and understanding of starch-based bioplastics can hinder their adoption and use. Consumers may be skeptical or uninformed about the benefits and characteristics of these biodegradable materials. Without adequate education and awareness, consumers may not recognize the environmental advantages of starch-based bioplastics, such as their renewable sourcing, biodegradability, and reduced carbon footprint. There is therefore a need for targeted educational campaigns and outreach initiatives to promote awareness and acceptance of these sustainable materials.

CONCLUSION

This review provided an exhaustive examination of the production process, properties, applications, challenges, and future directions of starch-based bioplastic packaging, demonstrating its potential to transform the packaging industry. The merits of starch-based bioplastics are multifaceted, including biodegradability, compostability, renewability, and reduced greenhouse gas emissions. These benefits make them an attractive solution to the environmental and sustainability concerns associated with traditional plastics. The versatility of starch-based bioplastics has been demonstrated through their successful application in various packaging sectors, including food, beverage, and cosmetic packaging.

While challenges persist, ongoing research and development is addressing the limitations of starch-based bioplastics, such as high production costs, limited scalability, and inferior mechanical properties. The future directions for starch-based bioplastics are promising, with potential applications in edible, smart, and nanotechnology-enhanced packaging. Policy support and public awareness are crucial in promoting the adoption of starch-based bioplastic packaging, so encouraging regulations and education will drive the growth of the bioplastic industry. The development of starch-based bioplastics has the potential to revolutionize the packaging industry, mitigating plastic waste and reducing environmental pollution.

In summary, this review comprehensively demonstrated that starch-based bioplastic packaging is a sustainable alternative to conventional plastics, offering improved environmental and sustainability benefits. Our findings have significant implications for the packaging industry, policymakers, and consumers, highlighting the need for a shift towards sustainable and biodegradable

packaging solutions. Overall, this review lays a foundation for further research and development in starch-based bioplastic packaging, driving innovation and sustainability in packaging technologies.

CONTRIBUTION

All the authors contributed equally and substantially to this research work. Each author was involved in the conception, design, implementation, and interpretation of the research findings, as well as in the writing of this manuscript.

CONFLICT OF INTEREST

The authors declare that there is no conflict of interest, financial or personal, that could bias the work reported in this paper.

REFERENCES

1. Pilapitiya PGCNT, Ratnayake AS. The world of plastic waste: A review. Cleaner Materials. 2024;11:100220. https://doi.org/10.1016/j.clema.2024.100220
2. Atiwesh G, Mikhael A, Parrish CC, Banoub J, Le TAT. Environmental impact of bioplastic use: A review. Heliyon. 2021;7(9):e07918. https://doi.org/10.1016/j.heliyon.2021.e07918
3. Ibrahim ID, Hamam Y, Sadiku ER, Ndambuki JM, Kupolati WK, *et al*. Need for sustainable packaging: An overview. Polymers. 2022;14(20):4430. https://doi.org/10.3390/polym14204430
4. Eremeeva NB. Nanoparticles of metals and their compounds in films and coatings: A review. Foods and Raw Materials. 2024;12(1):60–79. https://doi.org/10.21603/2308-4057-2024-1-588
5. Omoike BA, Okieimen FE, Imoisi C, Abubakar MA. Characterization and evaluation of properties of cassava starch/poly(vinyl alcohol) films for food and pharmaceutical packaging applications. Singapore Journal of Scientific Research. 2024;14(1):34–42. https://doi.org/10.3923/sjsr.2024.34.42
6. Singh P, Pandey VK, Singh R, Singh K, Dash KK, *et al*. Unveiling the potential of starch-blended biodegradable polymers for substantializing the eco-friendly innovations. Journal of Agriculture and Food Research. 2024;15:101065. https://doi.org/10.1016/j.jafr.2024.101065
7. Onyeaka H, Obileke K, Makaka G, Nwokolo N. Current research and applications of starch-based biodegradable films for food packaging. Polymers. 2022;14(6):1126. https://doi.org/10.3390/polym14061126
8. Xu H, Cheng H, McClements DJ, Chen L, Long J, *et al*. Enhancing the physicochemical properties and functional performance of starch-based films using inorganic carbon materials: A review. Carbohydrate Polymers. 2022;295:119743. https://doi.org/10.1016/j.carbpol.2022.119743
9. Omoike BA, Okieimen FE, Imoisi C. Design and optimization of eco-friendly biocomposite films for packaging applications using response surface methodology. Tanzania Journal of Science. 2024;50(5):961–974.
10. Halley PJ, Avérous L. Chapter 5 – Starch modification to develop novel starch-biopolymer blends. Starch Polymers. Amsterdam: Academic Press; 2014, pp. 105–143. https://doi.org/10.1016/B978-0-444-53730-0.00022-1
11. Li C, Guo Y, Chen M, Wang S, Gong H, *et al*. Recent preparation, modification and application progress of starch nanocrystals: A review. International Journal of Biological Macromolecules. 2023;250:126122. https://doi.org/10.1016/j.ijbiomac.2023.126122
12. Prasad J, Dixit A, Sharma SP, Mwakosya AW, Petkoska AT, *et al.* Nanoemulsion-based active packaging for food products. Foods and Raw Materials. 2024;12(1):22–36. https://doi.org/10.21603/2308-4057-2024-1-585
13. Henning FG, Ito VC, Demiate IM, Lacerda LG. Non-conventional starches for biodegradable films: A review focussing on characterisation and recent applications in food packaging. Carbohydrate Polymer Technologies and Applications. 2022;4:100157. https://doi.org/10.1016/j.carpta.2021.100157
14. Altuna L, Herrera ML, Foresti ML. Synthesis and characterization of octenyl succinic anhydride modified starches for food applications. A review of recent literature. Food Hydrocolloids. 2018;80:97–110. https://doi.org/10.1016/j.foodhyd.2018.01.032
15. Chen WC, Judah SNMSM, Ghazai SK, Munthoub DI, Alias H, *et al*. The effects of citric acid on thermal and mechanical properties of crosslinked starch film. Chemica Engineerng Transactions. 2021;83:199–204. https://doi.org/10.3303/CET2183034
16. Choi I, Shin D, Lyu JS, Lee JS, Song HG, *et al*. Physicochemical properties and solubility of sweet potato starch-based edible films. Food Packaging and Shelf Life. 2022;33:100867. https://doi.org/10.1016/j.fpsl.2022.100867
17. Gao H, Hu S, Su F, Zhang J, Tang G. Mechanical, thermal, and biodegradability properties of PLA/modified starch blends. Polymer composites. 2011;32(12):2093–2100. https://doi.org/10.1002/pc.21241
18. Wu H, Lei Y, Lu J, Zhu R, Xiao D, *et al*. Effect of citric acid induced crosslinking on the structure and properties of potato starch/chitosan composite films. Food Hydrocolloids. 2019;97:105208. https://doi.org/10.1016/j.foodhyd.2019.105208

19. Coelho CCS, Silva RBS, Carvalho CWP, Rossi AL, Teixeira JA, *et al*. Cellulose nanocrystals from grape pomace and their use for the development of starch-based nanocomposite films. International Journal of Biological Macromolecules. 2020;159:1048–1061. https://doi.org/10.1016/j.ijbiomac.2020.05.046
20. Wang P, Tang SW, Sheng F, Cai J, Fei P, *et al*. Crystallization, thermal stability, barrier property, and aging resistance application of multi-functionalized graphene oxide/poly (lactide)/starch nanocomposites. International Journal of Biological Macromolecules. 2019;132:1208–1220. https://doi.org/10.1016/j.ijbiomac.2019.03.183
21. Chaudhary S, Jain VP, Jaiswar G. Chapter 4 – The composition of polysaccharides: Monosaccharides and binding, group decorating, polysaccharides chains. Innovation in Nano-Polysaccharides for Eco-sustainability. Amsterdam: Academic Press; 2022, pp. 83–118. https://doi.org/10.1016/B978-0-12-823439-6.00005-2
22. Boahemaa LV, Dzandu B, Amissah JGN, Akonor PT, Saalia FK. Physico-chemical and functional characterization of flour and starch of taro (*Colocasia esculenta*) for food applications. Food and Humanity. 2024;2:100245. https://doi.org/10.1016/j.foohum.2024.100245
23. Xie F, Pollet E, Halley PJ, Averous L. Starch-based nano-biocomposites. Progress in Polymer Science. 2013;38(10–11):1590–1628. https://doi.org/10.1016/j.progpolymsci.2013.05.002
24. Martens BMJ, Gerrits WJJ, Bruininx EMAM, Schols HA. Amylopectin structure and crystallinity explains variation in digestion kinetics of starches across botanic sources in an in vitro pig model. Journal of Animal Science and Biotechnology. 2018;9:91. https://doi.org/10.1186/s40104-018-0303-8
25. Zou J, Li Y, Wang F, Su X, Li Q. Relationship between structure and functional properties of starch from different cassava (*Manihot esculenta* Crantz) and yam (*Dioscorea opposita* Thunb) cultivars used for food and industrial processing. LWT. 2023;173:114261. https://doi.org/10.1016/j.lwt.2022.114261
26. Donald AM. 5 – Understanding starch structure and functionality. Starch in Food. Cambridge, MA: Woodhead Publishing; 2004, pp. 156–184. https://doi.org/10.1533/9781855739093.1.156
27. Zarski A, Bajer K, Kapuśniak J. Review of the most important methods of improving the processing properties of starch toward non-food applications. Polymers. 2021;13(5):832. https://doi.org/10.3390/polym13050832
28. Jane J, Chen YY, Lee LF, Mcpherson AE, Wong KS, *et al*. Effects of amylopectin branch chain length and amylose content on the gelatinization and pasting properties of starch. Cereal Chemistry. 1999;76(5):629–637. https://doi.org/10.1094/CCHEM.1999.76.5.629
29. Chakraborty I, Pooja N, Mal SS, Paul UC, Rahman MH, *et al*. An insight into the gelatinization properties influencing the modified starches used in food industry: A review. Food and Bioprocess Technology. 2022;15:1195–1223. https://doi.org/10.1007/s11947-022-02761-z
30. Rittenauer M, Gladis S, Gastl M, Becker T. Gelatinization or pasting? The impact of different temperature levels on the saccharification efficiency of barley malt starch. Foods. 2021;10(8):1733. https://doi.org/10.3390/foods10081733
31. Waigh TA, Gidley MJ, Komanshek BU, Donald AM. The phase transformations in starch during gelatinisation: A liquid crystalline approach. Carbohydrate Research. 2000;328(2):165–176. https://elibrary.ru/AIBWPX
32. Wang S, Li C, Copeland L, Niu Q, Wang S. Starch retrogradation: A comprehensive review. Comprehensive Reviews in Food Science and Food Safety. 2015;14(5):568–585. https://doi.org/10.1111/1541-4337.12143
33. Xie F. Natural polymer starch-based materials for flexible electronic sensor development: A review of recent progress. Carbohydrate Polymers. 2024;337:122116. https://doi.org/10.1016/j.carbpol.2024.122116
34. Rashwan AK, Younis HA, Abdelshafy AM, Osman AI, Eletmany MR, *et al*. Plant starch extraction, modification, and green applications: A review. Environmental Chemistry Letters. 2024;22:2483–2530. https://doi.org/10.1007/s10311-024-01753-z
35. Ghoshal G, Kaur M. Optimization of extraction of starch from sweet potato and its application in making edible film. Food Chemistry Advances. 2023;3:100356. https://doi.org/10.1016/j.focha.2023.100356
36. Liu Z, Zhao Y, Zheng J, Wang Z, Yan X, *et al*. Influence of enzymatic extraction on the properties of corn starch. Food Bioscience. 2024;58:103775. https://doi.org/10.1016/j.fbio.2024.103775
37. da Silva LR, de Carvalho CWP, Velasco JI, Fakhouri FM. Extraction and characterization of starches from pigmented rice. International Journal of Biological Macromolecules. 2020;156:485–493. https://doi.org/10.1016/j.ijbiomac.2020.04.034
38. Amaraweera SM, Gunathilake C, Gunawardene OHP, Fernando NML, Wanninayaka DB, *et al*. Development of starch-based materials using current modification techniques and their applications: A review. Molecules. 2021;26(22):6880. https://doi.org/10.3390/molecules26226880
39. Masina N, Choonara YE, Kumar P, du Toit LC, Govender M, *et al*. A review of the chemical modification techniques of starch. Carbohydrate Polymers. 2017;157:1226–1236. https://doi.org/10.1016/j.carbpol.2016.09.094

40. Shrestha AK, Halley PJ. Chapter 5 – Starch modification to develop novel starch-biopolymer blends: State of art and perspectives. Starch Polymers: From Genetic Engineering to Green Applications. Amsterdam: Elsevier; 2014, pp. 105–143. https://doi.org/10.1016/B978-0-444-53730-0.00022-1
41. Golachowski A, Zięba T, Kapelko-Żeberska M, Drożdż W, Gryszkin A, *et al*. Current research addressing starch acetylation. Food Chemistry. 2015;176:350–356. https://doi.org/10.1016/j.foodchem.2014.12.060
42. Velásquez-Castillo LE, Leite MA, Tisnado VJA, Ditchfield C, Sobral PJA, *et al*. Cassava starch films containing quinoa starch nanocrystals: Physical and surface properties. Foods. 2023;12(3):576. https://doi.org/10.3390/foods12030576
43. Vega-Álvarez E, Pineda-Hidalgo KV, Salazar-Salas NY, Soto-López OA, Canizalez-Román VA, *et al*. Genetic and molecular analysis of starch physicochemical properties and its relationship with endosperm modification in quality protein maize. BIOtecnia. 2022;24(3):140–149. https://doi.org/10.18633/biotecnia.v24i3.1725
44. Ansah EO, Chen G, Xiong F, Wu Y, Endosperm starch in rice: What influences its structure, properties, and biosynthesis. Acta Physiologiae Plantarum. 2023;45:121. https://doi.org/10.1007/s11738-023-03599-4
45. Upadhyaya CP, Bagri DS, Upadhyaya DC. Genetically modified potato as a source of novel carbohydrates. In: Yildiz M. Potato – from incas to all over the world. London: IntechOpen; 2018, pp. 19–35. https://doi.org/10.5772/intechopen.71079
46. Gaenssle ALO, van der Maarel MJEC, Jurak E. The influence of amylose content on the modification of starches by glycogen branching enzymes. Food Chemistry. 2022;393:133294. https://doi.org/10.1016/j.foodchem.2022.133294
47. Zhai C, Yu Y, Zhu Y, Zhang J, Zhong Y, *et al*. The impact of foaming effect on the physical and mechanical properties of foam glasses with molecular-level insights. Molecules. 2022;27(3):876. https://doi.org/10.3390/molecules27030876
48. Bacalhau JB, Cunha TM, Afonso CRM. Effect of Ni content on the hardenability of a bainitic steel for plastics processing. 24th ABCM International Conference of Mechanical Engineering: Conference paper. Curitiba, 2017. https://doi.org/10.26678/ABCM.COBEM2017.COB17-1174
49. Hossain MT, Shahid MD, Akter S, Ferdous J, Afroz K, *et al*. Cellulose and starch-based bioplastics: A review of advances and challenges for sustainability. Polymer-Plastics Technology and Materials. 2024;63(10):1329–1349. https://doi.org/10.1080/257
50. Zibaei R, Ebrahimi B, Rouhi M, Hashami Z, Roshandel Z, *et al*. Development of packaging based on PLA/POE/SeNPs nanocomposites by blown film extrusion method: Physicochemical, structural, morphological and antioxidant properties. Food Packaging and Shelf Life. 2023;38:101104. https://doi.org/10.1016/j.fpsl.2023.101104
51. Omoike BA, Okieimen FE, Imoisi C. Water vapour transport properties of cassava starch/poly(vinyl alcohol) films via experimental and Fickian methods. Trends in Applied. Sciences Research. 2024;19(1):225–232. https://doi.org/10.3923/tasr.2024.225.232
52. Subramani R, Mustafa MA, Ghadir KG, Al-Tmimi HM. Exploring the use of biodegradable polymer materials in sustainable 3D printing. Applied Chemical Engineering. 2024;7(2):3870. https://doi.org/10.59429/ace.v7i2.3870
53. Andanje MN, Mwangi JM, Mose BR, Carrara S. Biocompatible and biodegradable 3D printing from bioplastics: A review. Polymers. 2023;15(10):2355. https://doi.org/10.3390/polym15102355
54. Amin MR, Chowdhury MA, Kowser MA. Characterization and performance analysis of composite bioplastics synthesized using titanium dioxide nanoparticles with corn starch. Heliyon. 2019;5(8):e02009. https://doi.org/10.1016/j.heliyon.2019.e02009
55. Iheanacho BC, Ajoge HN, Ismail U, Zoum FA, Ifeanyi-Nze FO, *et al*. A comprehensive study on the production and characterization of eco-friendly biodegradable plastic films from dent corn starch. Archives of Advanced Engineering Science. 2025;3(3):178–187. https://doi.org/10.47852/bonviewAAES42022946
56. Su CY, Li D, Wang LJ, Wang Y. Biodegradation behavior and digestive properties of starch-based film for food packaging – A review. Critical Reviews in Food Science and Nutrition. 2023;63(24):6923–6945. https://doi.org/10.1080/10408398.2022.2036097
57. Omoike BA, Okieimen FE, Imoisi C. Development of lemongrass oil-based starch/PVA/kaolin films: Antimicrobial properties and biodegradability. Science International. 2025;13(1):1–12. https://doi.org/10.17311/sciintl.2025.01.12
58. Sangian HF, Maneking E, Tongkukut SHJ, Mosey HIR, Suoth V, *et al*. Study of SEM, XRD, TGA, and DSC of cassava bioplastics catalyzed by ethanol. IOP Conference Series: Material Science and Engineering. 2021;1115(1):012052. https://doi.org/10.1088/1757-899x/1115/1/012052
59. Rao LS, Naidu CD, Tiwari S. Investigation on synthesis, structure and degradability of starch based bioplastics. Materials Today: Proceedings. 2022;49(Part 2):257–261. https://doi.org/10.1016/j.matpr.2021.01.917
60. Chandrasekar CM, Krishnamachari H, Farris S, Romano D. Development and characterization of starch-based bioactive thermoplastic packaging films derived from banana peels. Carbohydrate Polymer Technologies and Applications. 2023;5:100328. https://doi.org/10.1016/j.carpta.2023.100328

61. Ruggero F, Carretti E, Gori R, Lotti T, Lubello C. Monitoring of degradation of starch-based biopolymer film under different composting conditions, using TGA, FTIR and SEM analysis. Chemosphere. 2020;246:125770. https://doi.org/10.1016/j.chemosphere.2019.125770

62. Yadav M, Chiu FC. Cellulose nanocrystals reinforced κ-carrageenan based UV resistant transparent bionanocomposite films for sustainable packaging applications. Carbohydrate Polymers. 2019;211:181–194. https://doi.org/10.1016/j.carbpol.2019.01.114

63. Kaczmarska K, Żymankowska-Kumon S, Grabowska B, Bobrowski A, Cukrowicz S. Study of thermal degradation of starch-based binder by TG-DTG-DSC, Py-GC/MS and DRIFTS. Archives of Foundry Engineering. 2019;19(4):21–26. https://doi.org/10.24425/afe.2019.129624

64. Abe MM, Martins JR, Macedo JV, Brienzo M, Sanvezzo PB, *et al*. Advantages and disadvantages of bioplastics production from starch and lignocellulosic components. Polymers. 2021;13(15):2484. https://doi.org/10.3390/polym13152484

65. Safitri A, Sinaga PSD, Nasution H, Harahap H, Masyithah Z, *et al*. The role of various plastisizers and fillers additions in improving tensile strength of starch-based bioplastics: A mini review. IOP Conference Series: Earth and Environmental Science. 2022;1115(1):012076. https://doi.org/10.1088/1755-1315/1115/1/012076

66. Ballesteros-Mártinez L, Pérez-Cervera C, Andrade-Pizarro R. Effect of glycerol and sorbitol concentrations on mechanical, optical, and barrier properties of sweet potato starch film. NFS journal. 2020;20:1–9. https://doi.org/10.1016/j.nfs.2020.06.002

67. Narváez-Gómez G, Figueroa-Flórez J, Salcedo-Mendoza J, Pérez-Cervera C, Andrade-Pizarro R. Development and characterization of dual-modified yam (*Dioscorea rotundata*) starch-based films. Heliyon. 2021;7(4):e06644. https://doi.org/10.1016/j.heliyon.2021.e06644

68. Yang J, Ching YC, Julai JS, Chuah CH, Nguyen DH, *et al*. Comparative study on the properties of starch-based bioplastics incorporated with palm oil and epoxidized palm oil. Polymers and Polymer Composites. 2022;30:1–11. https://doi.org/10.1177/09673911221087595

69. Navasingh RJH, Gurunathan MK, Nikolova MP, Królczyk JB. Sustainable bioplastics for food packaging produced from renewable natural sources. Polymers. 2023;15(18):3760. https://doi.org/10.3390/polym15183760

70. Agarwal S, Singhal S, Godiya CB, Kumar S. Prospects and applications of starch based biopolymers. International Journal of Environmental Analytical Chemistry. 2023;103(18):6907–6926. https://doi.org/10.1080/03067319.2021.1963717

71. Jayarathna S, Andersson M, Andersson R. Recent advances in starch-based blends and composites for bioplastics applications. Polymers. 2022;14(21):4557. https://doi.org/10.3390/polym14214557

72. Attallah OA, Mojicevic M, Garcia EL, Azeem M, Chen Y, *et al*. Macro and micro routes to high performance bioplastics: Bioplastic biodegradability and mechanical and barrier properties. Polymers. 2021;13(13):2155. https://doi.org/10.3390/polym13132155

73. Folino A, Pangallo D, Calabrò PS. Assessing bioplastics biodegradability by standard and research methods: Current trends and open issues. Journal of Environmental Chemical Engineering. 2023;11(2):109424. https://doi.org/10.1016/j.jece.2023.109424

74. Zoungranan Y, Lynda E, Dobi-Brice KK, Tchirioua E, Bakary C, *et al*. Influence of natural factors on the biodegradation of simple and composite bioplastics based on cassava starch and corn starch. Journal of Environmental Chemical Engineering. 2020;8(5):104396. https://doi.org/10.1016/j.jece.2020.104396

75. Samsudin H, Hani NM. Chapter 8 – Use of starch in food packaging. Starch-based materials in food packaging. NY: Academic Press; 2017, pp. 229–256. https://doi.org/10.1016/B978-0-12-809439-6.00008-X

76. Diah SBM, Abdullah SHYS, Seok YB, Fatah IYA, Rahman NIA, *et al*. Towards sustainable food packaging: A review of thermoplastic starch (TPS) as a promising bioplastic material, its limitations, and improvement strategies with bio-fillers and essential oils. Journal of Advanced Research in Fluid Mechanics and Thermal Sciences. 2024;119(1):80–104. https://doi.org/10.37934/arfmts.119.1.80104

77. deAraújo GKP, deSouza SJ, daSilva MV, Yamashita F, Gonçalves OH, *et al.* Physical, antimicrobial and antioxidant properties of starch-based film containing ethanolic propolis extract. International Journal of Food Science and Technology. 2015;50(9):2080–2087. https://doi.org/10.1111/ijfs.12869

78. Bharti SK, Pathak V, Alam T, Arya A, Singh VK, *et al.* Starch bio-based composite active edible film functionalized with *Carum carvi* L. essential oil: Antimicrobial, rheological, physic-mechanical and optical attributes. Journal of Food Science and Technology. 2022;59:456–466. https://doi.org/10.1007/s13197-021-05028-1

79. D'Almeida AP, de Albuquerque TL. Innovations in food packaging: From bio-based materials to smart packaging systems. Processes. 2024;12(10):2085. https://doi.org/10.3390/pr12102085

80. Narancic T, Cerrone F, Beagan N, O'Connor KE. Recent advances in bioplastics: Application and biodegradation. Polymers. 2020;12(4):920. https://doi.org/10.3390/polym12040920

81. Kiran V, Kavi Varsha A, Vijayalaksmi M, Vishnuvarthanan G, Anisha M, *et al*. Synthesis and characterization of banana peel starch-based bioplastic for intravenous tubes preparation. Materials Today Communications. 2022; 33:104464. https://doi.org/10.1016/j.mtcomm.2022.104464

82. Merino D, Mansilla AY, Casalongué CA, Alvarez VA. Performance of bio-based polymeric agricultural mulch films. In: Gutiérrez T, editor. Polymers for Agri-Food Applications. Cham: Springer; 2019, pp. 215–240. https://doi.org/10.1007/978-3-030-19416-1_12

83. Pirzada T, de Farias BV, Mathew R, Guenther RH, Byrd MV, *et al*. Recent advances in biodegradable matrices for active ingredient release in crop protection: Towards attaining sustainability in agriculture. Current Opinion in Colloid & Interface Science. 2020;48:121–136. https://doi.org/10.1016/j.cocis.2020.05.002

84. Dini I. "Edible beauty": The evolution of environmentally friendly cosmetics and packaging. Antioxidants. 2024;13(6):742. https://doi.org/10.3390/antiox13060742

85. Bikiaris N, Nikolaidis NF, Barmpalexis P. Microplastics (MPs) in cosmetics: A review on their presence in personal-care, cosmetic, and cleaning products (pccps) and sustainable alternatives from biobased and biodegradable polymers. Cosmetics. 2024;11(5):145. https://doi.org/10.3390/cosmetics11050145

86. Forfora N, Azuaje I, Kanipe T, Gonzalez JA, Lendewig M, *et al*. Are starch-based materials more eco-friendly than fossil-based? A critical assessment. Cleaner Environmental Systems. 2024;13:100177. https://doi.org/10.1016/j.cesys.2024.100177

87. Yu X, Chen L, Jin Z, Jiao A. Research progress of starch-based biodegradable materials: A review. Journal of Materials Science. 2021;56:11187–11208. https://doi.org/10.1007/s10853-021-06063-1

88. Gamage A, Liyanapathiranage A, Manamperi A, Gunathilake C, Mani S, *et al*. Applications of starch biopolymers for a sustainable modern agriculture. Sustainability. 2022;14(10):6085. https://doi.org/10.3390/su14106085

89. Rahardiyan D, Moko EM, Tan JS, Lee CK. Thermoplastic starch (TPS) bioplastic, the green solution for single-use petroleum plastic food packaging – A review. Enzyme and microbial technology. 2023;168:110260. https://doi.org/10.1016/j.enzmictec.2023.110260

90. Laycock BG, Halley PJ. Chapter 14 – Starch applications: State of market and new trends. Starch polymers. Amsterdam: Elsevier; 2014, pp. 381–419. https://doi.org/10.1016/B978-0-444-53730-0.00026-9

91. Rahman R, Sood M, Gupta N, Bandral JD, Hameed F, *et al*. Bioplastics for food packaging: A review. International Journal of Current Microbiology and Applied Sciences. 2019;8(3):2311–2321. https://doi.org/10.20546/ijcmas.2019.803.274

Additional information about the authors

Bright A. Omoike ORCID 0009-0009-7812-2626
Chinyere Imoisi ORCID 0000-0001-9680-1635
James G. Josiah ORCID 0000-0001-6983-0043

Foods and Raw Materials. 2027;15(2)

ISSN 2308-4057 (Print)
ISSN 2310-9599 (Online)

Research Article
Open Access

Available online at http://jfrm.ru/en
https://doi.org/10.21603/2308-4057-2027-2-709
https://elibrary.ru/TAUZPA

Beef tripe as an innovative and alternative protein source in meat products

Eatemad M. El-Sayed[1], Essam M. Elsebaie[2,*], Marwa F. A. El-Farsy[1], Rehab A. Shehata[3], Shaymaa A. Hozifa[1], Dalia M. El-Mesiry[1], Soher A.-E. Elmeslamy[1]

[1] Al-Azhar University, Cairo, Egypt
[2] Kafrelsheikh University, Kafr-El-Shiekh, Egypt
[3] University of Bisha, Bisha, Saudi Arabia

* e-mail: Essam.ahmed@agr.kfs.edu.eg

Received 14.06.2025; Revised 25.08.2025; Accepted 08.12.2025; Published online 09.07.2026

Abstract:
Tripe has a high protein level, which could serve as a functional ingredient in the meat industry.
Raw and boiled beef tripe and frozen beef meat were examined for proximate composition, mineral and amino acid content, fatty acid profile, protein quality indices, microbiological safety, and functional parameters. Tripe was incorporated into corned beef and sausage formulations, which were analyzed for their nutritional quality, microbial stability, and consumer acceptability.
The raw tripe exhibited a favorable pH (6.83 ± 0.08), moderate water holding capacity (58.86%), and acceptable cooking yield (64.88%), indicating functional suitability. The boiled tripe demonstrated a superior protein content (24.15%) and energy value (146.71 kcal/100 g), compared to the raw tripe and frozen beef meat. Mineral analysis showed significantly higher levels of calcium (up to 112.5 mg/100 g), iron (4.19 mg/100 g), and copper (0.28 mg/100 g) in the raw tripe. The boiled tripe had a well-balanced amino acid profile, with its essential amino acid content (37.98%) exceeding the FAO/WHO standards. It also showed improved protein quality indices, namely the computed protein efficiency ratio of 2.38 and the biological value of 74.19%. Boiling also enhanced the lipid quality by increasing unsaturated fatty acids. Microbial analysis confirmed the safety of the boiled tripe, with pathogen counts below permissible limits. The tripe-based corned beef and sausage showed higher fat, ash, and energy contents than their beef counterparts, while maintaining acceptable protein levels and sensory qualities. Sensory evaluation revealed that the overall acceptability of tripe-based products was comparable to that of traditional meat products.
These findings highlight that boiled beef tripe is a safe, nutrient-rich, and sensory-acceptable ingredient. They also support its use as a sustainable, cost-effective ingredient in value-added meat products such as sausages and canned meats.

Keywords: Meat by-products, rumen, sausage, corned beef, amino acids, microbiology, functional products

Please cite this article in press as: El-Sayed EM, Elsebaie EM, El-Farsy MFA, Shehata RA, Hozifa SA, *et al.* Beef tripe as an innovative and alternative protein source in meat products. Foods and Raw Materials. 2027;15(2):285–295. https://doi.org/10.21603/2308-4057-2027-2-709

INTRODUCTION

Ensuring global food security remains one of the most critical challenges, particularly with the increasing population and rising food prices [1]. Meat, comprising muscle and organ tissues, has long been recognized as a vital component of the human diet due to its high-quality protein and essential mineral contents [2]. However, economic constraints and changing consumer preferences have intensified the search for alternative, cost-effective protein sources, including edible bovine by-products [3].

Bovine by-products such as liver, kidney, heart, tripe, and lungs are traditionally consumed in many cultures and offer considerable nutritional value [4]. Tripe, derived from the stomach chambers of cattle, represents a significant portion of slaughter by-products but remains underutilized due to its unfavorable microbiological profile and sensory characteristics [5]. Despite these challenges, tripe is recognized for its rich protein content and could serve as a functional ingredient in food systems [6].

Tripe, also referred to as rumen meat or "potti", accounts for approximately 1.3% of the animal's live weight, with an average mass of 4.36 to 5.45 kg per animal [5]. Different sections of tripe include the rumen (blanket or smooth tripe), reticulum (honeycomb or pocket tripe),

Copyright © 2026, El-Sayed *et al.* This is an open access article distributed under the terms of the Creative Commons Attribution 4.0 International License (https://creativecommons.org/licenses/by/4.0/), allowing third parties to copy and redistribute the material in any medium or format and to remix, transform, and build upon the material for any purpose, even commercially, provided the original work is properly cited and states its license.

and omasum (book or leaf tripe), all of which have culinary uses, especially in soups and sausages [7].

The inherent toughness of tripe due to its collagen content, combined with its poor sensory attributes and limited shelf life, has constrained its industrial application. However, with appropriate processing to improve palatability and safety, tripe can be transformed into a high-value component of meat products [6]. In Egypt and several other countries, including India, tripe remains underutilized despite its nutritional potential.

Beef sausage is among the most traditional processed meat products in Egypt and widely accepted across all age groups. It is typically composed of beef, fat, rusk, salt, and spices [8]. Corned beef, a shelf-stable product with historical roots in the British Empire, is valued for its high protein and mineral contents (especially sodium and zinc) and a long shelf life of 2 to 4 years [9].

In this context, we aimed to assess the nutritional quality and microbiological profile of underutilized beef tripe. Additionally, we explored its potential application as an alternative animal protein source in the industrial production of traditional comminuted meat products such as sausage and corned beef tripe.

STUDY OBJECTS AND METHODS

Fresh beef tripe was procured from the municipal slaughterhouse in Tanta, Egypt. All the media (plate count agar, potatoes dextrose agar, sulfite polymyxin sulfadiazine agar, skim milk agar, Tributyrin agar, Baird-Parker agar with egg yolk tellurite, violet red bile agar, xylose lysine deoxycholate agar, and salmonella-shigella agar) used in the microbial examination were purchased from Oxoid, UK. All the analytical-grade chemicals utilized in this study were sourced from El-Gomhoria Company.

Beef tripe processing. The beef tripe was initially rinsed under tap water, followed by brief immersion in boiling water to facilitate cleaning. Subsequent scalding with a sharp knife was performed until the tripe attained a white coloration. The cleaned tripe was divided into two portions: one underwent cooking for 40 min, while the other remained uncooked. Each portion was individually minced and homogenized using an industrial food blender (Moulinex, France) to achieve uniform consistency. The homogenized samples were then packaged and stored at −18°C until further analysis. All the samples were analyzed in triplicate to ensure reproducibility.

Preparation of tripe-based products. ***Tripe sausage formulation.*** Sausage formulations were prepared as detailed in Table 1, following the methodology described by Evanuarini *et al.* [10]. Each formulation was emulsified using a bowl cutter (Nr-963009, Scharfen-Witten, Germany), incorporating chilled water and homogenizing for 2 min. The resulting batter was stuffed into natural sheep casings, with links formed at approximately 15 cm intervals. The sausages were then grilled briefly to evaluate color and texture attributes.

Corned beef preparation. Corned beef was prepared according to the protocol outlined by Silalahi *et al.* [11], with formulations presented in Table 1. Both beef meat (control) and boiled beef tripe were subjected to wet curing in a pickle solution containing salt, black pepper, cardamom, coriander, and bay leaves for 48 h at 4 ± 1°C. After curing, the samples were drained, boiled for 30 min, and then mixed thoroughly with wheat flour, salt, corn oil, gelatin, a spice mixture, onion powder, and garlic powder. The mixture was ground through a 3-mm plate, filled into glass containers while warm, partially sealed, and exhausted in steam to achieve an internal temperature of 77°C. The containers were then sealed and autoclaved at 121°C for 20 min, followed by cooling with water.

Physical properties of tripe products. ***Cooking loss*****, %,** ***and yield*****, %.** Cooking loss was determined by measuring the weight difference of the samples before and after frying, conducted in triplicate. The calculations were as follows:

$$\text{Cooking loss} = \left[\frac{W_i - W_f}{W_i}\right] \times 100 \quad (1)$$

where W_i is the weight of the samples before frying, g; W_f is the weight of the samples after frying, g.

$$\text{Cooking yield} = 100 - \text{Cooking loss} \quad (2)$$

Water holding capacity. The water holding capacity (WHC, %) was assessed using the method described by Elsebaie *et al.* [12]. The percentage of bound water was calculated based on the area, representing the WHC, using the conversion factor of 8.4 mg of free water per cm^2.

$$\text{WHC} = \left[\frac{M - \left(\frac{A \times 8.4 \times 100}{0.3 \times 1000}\right)}{M}\right] \times 100 \quad (3)$$

where M is the moisture, %; A is the area, cm^2.

pH measurement. A 10 g sample was homogenized in 100 mL of distilled water, and the pH was measured using a calibrated pH meter (Model JENCO 608, USA), following the procedure by Abdelhakam *et al.* [13].

Table 1 Beef and tripe meat products formulations

Ingredient, g/100 g	Corned beef		Beef sausage	
	Meat	Tripe	Meat	Tripe
Frozen beef meat	80.0	–	75.0	–
Boiled beef tripe	–	80.0	–	75.0
Fat	8.0	8.0	12.0	12.0
Starch	–	–	3.0	–
Wheat flour	2.5	2.5	–	3.0
Salt	1.5	1.5	1.5	1.5
Spice mixture	1.5	1.5	1.5	1.5
Garlic powder	0.3	0.3	1.0	1.0
Chilled water	–	–	6.0	6.0
Onion powder	0.3	0.3	–	–
Gelatin powder	2.0	2.0	–	–

Chemical analyses. ***Proximate composition.*** Moisture, protein, ether extract, ash, and crude fiber contents were determined according to the AOAC methods[1]. The carbohydrate content was calculated by difference.

Mineral content. The samples were ashed and digested with concentrated nitric acid. Mineral concentrations (Ca, Mg, Na, K, Zn, and Fe) were quantified using an atomic absorption spectrophotometer (PerkinElmer Model 4100 ZL), as per the AOAC guidelines[2].

Amino acid composition and protein quality. *Amino acid analysis*. Approximately 100 mg of a dried, ground sample was hydrolyzed with 10 mL of 6N HCl containing 0.1% mercaptoethanol at 110°C for 24 h. After the hydrolysis, the sample was filtered, diluted to 25 mL, and 5 mL of aliquot was evaporated under vacuum. The residue was reconstituted in 1 mL of sodium citrate buffer (pH 2.2) and analyzed using a Beckman amino acid analyzer (Model 119 CL), following the protocol by Ali *et al*. [14].

Chemical score calculation. The chemical scores were computed by comparing the amino acid profile of the sample to the FAO/WHO/UNU reference pattern, identifying the limiting amino acid as per Ali *et al*. [14].

The computed protein efficiency ratio (C-PER) was calculated using Eq. (4):

$$\text{C-PER} = -0.468 + 0.454 \times \\ \times \text{Leucine content} - 0.105 \times \text{Tyrosine content} \quad (4)$$

The biological value (BV) was determined using the formula, as described by Metwaly *et al*. [15]:

$$\text{BV} = 49.09 + 10.53 \times \text{C-PER} \quad (5)$$

Fatty acid composition. Lipids were extracted from 10 g samples using a 2:1 (v/v) chloroform/methanol mixture, following the method of Li *et al*. [16]. The extracts were filtered, washed with 0.72% KCl solution, and the organic phase was concentrated using a rotary evaporator. Fatty acid methyl esters were prepared and analyzed via gas chromatography (Hewlett Packard 6890) equipped with an HP-5 column (30 m × 0.32 mm, 0.25 µm film thickness). The operating conditions included an initial oven temperature of 150°C (held for 2 min), injector temperature of 220°C, detector temperature of 250°C, and nitrogen as the carrier gas at a flow rate of 1 mL/min. Fatty acid percentages were calculated accordingly.

Microbiological analyses. Microbial assessments included total plate counts, molds and yeasts, and psychrophilic bacteria, following the protocols outlined by de Souza *et al*. [17]. Spore-forming, proteolytic, and lipolytic bacteria were enumerated as per Liu *et al*. [18]. *Staphylococcus* spp. were identified according to Economou *et al*. [19], coliforms were detected as described by Medhat *et al*. [20], and *Salmonella* and *Shigella* spp. were assessed following Ahmed *et al*. [21] procedures.

Sensory evaluation. A panel of ten trained individuals from the Department of Food Science and Technology, Faculty of Agriculture for Girls, Al-Azhar University, conducted sensory evaluations of the prepared beef and tripe products. The assessments were based on a 10-point hedonic scale evaluating taste, flavor, color, texture, and overall acceptability, with 1 indicating a strong dislike and 10 indicating a strong like, as described by Essa & Elsebaie [22].

Statistical analysis. The data were analyzed using analysis of variance (ANOVA) via the SPSS software. Duncan's multiple range test was employed to determine significant differences among the means at a significance level of $p \leq 0.05$.

RESULTS AND DISCUSSION

Physical properties of raw beef tripe. The physical properties of the raw beef tripe under study (Table 2) indicated its promising potential for application in processed meat products. The recorded pH value of 6.83 ± 0.08 fell within the typical range for bovine offal and suggests a favorable environment for protein solubility and microbial stability, both of which are critical in meat product formulation [23]. The water holding capacity was measured at 58.86 ± 0.06%, reflecting the material's moderate ability to retain moisture, which is essential for maintaining juiciness and improving yield during thermal processing [24]. The cooking loss and cooking yield amounted to 35.12 ± 0.04 and 64.88 ± 0.05%, respectively. These values were consistent with those observed in other studies involving cooked tripe and edible by-products [25, 26]. The relatively high cooking loss might be due to the elevated collagen content in tripe. However, the yield remained within the acceptable limits for comminuted meat products. Collectively, these findings support the use of beef tripe as a viable alternative protein source in the development of value-added meat products such as sausages and canned meats, particularly when formulated with suitable fat, binders, and water-retaining agents to optimize their texture and stability.

Gross chemical composition of main raw materials. The proximate chemical composition of the main raw materials revealed significant differences among the frozen beef meat, raw beef tripe, and boiled beef tripe (Table 3), providing insight into their nutritional value and processing potential. The boiled beef tripe exhibited the highest crude protein content (24.15 ± 0.12%), surpassing both raw tripe (15.39 ± 0.05%) and frozen beef meat (19.79 ± 0.04%). This increase is primarily attributed

Table 2 Physical properties of raw beef tripe

Parameter	Value
pH	6.83 ± 0.08
Water holding capacity, %	58.86 ± 0.06
Cooking loss, %	35.12 ± 0.04
Cooking yield, %	64.88 ± 0.05

[1] Latimer GW. The official methods of analysis of AOAC international (22nd Edition). Gaithersburg, MD: AOAC International; 2023. https://doi.org/10.1093/9780197610145.001.0001

[2] The same.

Table 3 Gross chemical composition and mineral contents of main raw materials

Parameter	Frozen beef meat	Raw beef tripe	Boiled beef tripe
Moisture, % ww	74.38 ± 0.10[b]	77.14 ± 0.03[a]	67.83 ± 0.06[c]
Crude protein, % ww	19.79 ± 0.04[b]	15.39 ± 0.05[c]	24.15 ± 0.12[a]
Ether extract, % ww	2.99 ± 0.09[c]	5.12 ± 0.04[a]	4.03 ± 0.07[b]
Crude ash, % ww	0.82 ± 0.06[a]	0.46 ± 0.11[b]	0.53 ± 0.03[b]
Nitrogen free extract, % ww	2.02 ± 0.03[b]	1.89 ± 0.06[c]	3.46 ± 0.08[a]
Energy, kcal/100 g	114.15 ± 0.08[b]	105.20 ± 0.04[c]	146.71 ± 0.03[a]
Mineral contents, mg/100 g			
Ca	5.40 ± 0.24[c]	112.50 ± 1.21[a]	92.11 ± 0.98[b]
Na	66.30 ± 0.72[a]	37.50 ± 0.93[b]	20.70 ± 0.51[c]
K	324.00 ± 2.13[a]	120.94 ± 1.82[b]	95.81 ± 0.70[c]
P	268.00 ± 2.78[a]	97.33 ± 0.98[c]	128.01 ± 1.65[b]
Zn	4.10 ± 0.69[a]	1.80 ± 0.54[b]	1.10 ± 0.38[c]
Fe	2.40 ± 0.33[c]	4.19 ± 0.66[a]	2.67 ± 0.49[b]
Cu	0.10 ± 0.06[c]	0.28 ± 0.09[b]	0.69 ± 0.12[a]
Mg	12.15 ± 0.95[b]	15.84 ± 1.06[a]	12.96 ± 0.82[b]

The values are means ± standard deviation of triplicate trails. The values with the same superscript letters in a row are not significantly different at $p \leq 0.05$

(19.79 ± 0.04%). This increase is primarily attributed to moisture reduction during cooking, which concentrates the protein fraction, a phenomenon commonly observed in thermally treated animal tissues [23]. The elevated protein levels in the boiled tripe suggest its suitability as a protein-dense ingredient in value-added meat products. Conversely, the raw tripe had the highest moisture content (77.14 ± 0.03%), which can negatively affect its texture and yield during processing unless properly managed through formulation strategies [24]. Regarding the fat content, the raw tripe revealed the highest ether extract (5.12 ± 0.04%), followed by the boiled tripe (4.03 ± 0.07%) and the frozen beef meat (2.99 ± 0.09%). These findings are consistent with previous reports indicating that visceral tissues often contain higher fat levels than skeletal muscle [27]. While fat enhances the flavor and mouthfeel, its presence must be balanced with processing goals and product type. In terms of ash, the frozen beef meat had a significantly higher value (0.82 ± 0.06%) compared to both the tripe forms, which could reflect differences in bone or connective tissue residues. Nitrogen-free extract, representing the carbohydrate fraction, was the highest in the boiled tripe (3.46 ± 0.08%), possibly due to concentration effects or incorporation of glycogen derivatives during processing.

Lastly, the energy content was the highest in the boiled tripe (146.71 ± 0.03 kcal/100 g), significantly exceeding that of the raw tripe (105.20 ± 0.04 kcal/100 g) and frozen beef (114.15 ± 0.08 kcal/100 g). This aligns with its higher protein and fat contents, offering a calorically dense option for meat product development.

In summary, the boiled beef tripe demonstrated superior nutritional attributes compared to both the raw tripe and traditional frozen beef meat, particularly in terms of protein and energy contents. These findings support its incorporation into protein-rich processed meat products. The results also suggest its potential to partially or fully replace conventional beef meat in formulations such as sausages or canned meats, with minimal compromise in nutritional quality.

Mineral contents. Table 3 presents a comparative analysis of the mineral composition in the raw and boiled beef tripe versus the frozen beef meat, revealing the nutritional superiority of tripe in several key micronutrients. The calcium content was significantly higher in raw tripe (112.5 mg/100 g) and boiled tripe (92.11 mg/100 g) compared to frozen beef meat (5.4 mg/100 g). This is particularly relevant given the role of calcium in bone health and metabolic functions. This finding aligns with other studies that classify organ meats as excellent natural sources of minerals [28]. Similarly, iron, which is essential for hemoglobin synthesis, was more abundant in the raw tripe (4.19 mg/100 g) and boiled tripe (2.67 mg/100 g) than in the beef meat (2.4 mg/100 g), indicating that tripe can be an important dietary component to combat iron-deficiency anemia[3] [2].

In terms of phosphorus, the beef meat showed the highest level (268 mg/100 g), followed by the boiled tripe (128.01 mg/100 g) and raw tripe (97.33 mg/100 g). Despite a slight reduction due to boiling, the levels in the tripe remain adequate to contribute to bone development and energy metabolism. Magnesium levels were also favorable in the raw (15.84 mg/100 g) and boiled tripe (12.96 mg/100 g) compared to the beef (12.15 mg/100 g). Zinc, which is essential for immune function and enzyme activity, was present at 1.8 mg/100 g in the raw tripe, 1.1 mg/100 g in the boiled tripe, and 4.1 mg/100 g in the beef meat. Copper, a trace mineral involved in iron metabolism and antioxidant defense, was notably higher in the tripe samples (0.28 and 0.69 mg/100 g for raw and boiled, respectively) compared to the beef

[3] FAO/WHO/UNU. Protein and amino acid requirements in human nutrition: Joint FAO/WHO/UNU expert consultation. WHO Technical Report Series No. 935. 2007. World Health Organization. [cited 2025 Feb 10]. Available from: http://apps.who.int/iris/bitstream/10665/43411/1/WHO_TRS_935_eng.pdf?ua=1

Table 4 Amino acid composition of beef tripe

Amino acid content, %	Raw beef tripe	Boiled beef tripe	FAO/WHO (2007)	
			School children	Adult
Essential amino acids				
Methionine	2.10	2.43	2.30	1.60
Leucine	6.92	6.94	6.00	5.90
Isoleucine	3.60	4.42	3.00	3.00
Lysine	5.83	5.87	4.80	4.50
Phenylalanine	5.78	5.81	4.10	3.80
Threonine	3.81	3.57	2.50	2.30
Histidine	2.04	2.64	1.60	1.50
Valine	5.45	5.29	2.90	3.90
Tryptophan	1.12	1.01	0.60	0.60
Total essential amino acids	36.65	37.98	28.20	27.50
Non-essential amino acids				
Cystine	4.60	4.20	–	–
Glutamic acid	14.70	15.38	–	–
Aspartic acid	9.71	10.30	–	–
Arginine	5.32	5.20	–	–
Tyrosine	3.48	2.85	–	–
Alanine	6.60	6.62	–	–
Glycine	5.70	5.02	–	–
Serine	4.85	4.41	–	–
Proline	7.72	7.14	–	–
Total non-essential amino acids	62.68	61.12	–	–
Total amino acids	99.33	99.10	–	–
Essential/non-essential amino acids ratio	0.585	0.621	–	–
Ammonia	0.67	0.90	–	–

(0.10 mg/100 g). This reinforces the idea that tripe is a rich source of trace elements [2]. On the other hand, sodium and potassium were higher in the frozen beef meat (72.2 and 270.5 mg/100 g, respectively), which may enhance palatability but raises concerns regarding dietary sodium intake[4].

Collectively, these results suggest that beef tripe, particularly after boiling, retains considerable mineral contents, including iron, calcium, magnesium, and copper. This supports its use in food formulations aimed at improving micronutrient intake. In addition, beef tripe can be applied in functional or fortified meat products, offering a sustainable and nutritionally valuable alternative to skeletal muscle meat.

Amino acid composition of beef tripe. Table 4 provides a comparative analysis of the amino acid compositions of the raw and boiled beef tripe samples, highlighting their value as potential alternative protein sources in food applications.

Both beef tripe samples demonstrated a well-balanced amino acid profile with a favorable distribution of essential and non-essential amino acids, supporting their classification as complete protein sources. According to Table 4, the boiled beef tripe exhibited a slightly higher total essential amino acid (EAA) content (37.98%) compared to the raw tripe (36.65%). This enhancement can be attributed to moisture reduction during boiling, which concentrates the dry matter and thus the protein fraction. The EAA contents in both forms exceeded the FAO/WHO/UNU[5] requirements both for adults (27.5%) and children (28.2%), indicating that beef tripe can provide adequate dietary protein for human nutrition. Among the essential amino acids, leucine and lysine were dominant, with values in the boiled tripe reaching 6.94 and 5.87%, respectively. These values are well above the FAO/WHO references, suggesting a strong potential for growth and tissue repair support[6]. Methionine, however, was identified as the first limiting amino acid in both raw and boiled tripes (2.1 and 2.43%, respectively), although its concentration still exceeded adult requirements (1.6%), making it nutritionally acceptable.

Regarding non-essential amino acids, glutamic acid, aspartic acid, and glycine were notably abundant in both samples, with the boiled tripe showing slightly higher concentrations. These amino acids are known to contribute to the umami taste and functional properties such as water-binding and gelation, which are valuable in meat product development [29]. Additionally, the ratio of essential to total amino acids improved marginally from 39.90% in the raw tripe to 38.32% in the boiled tripe, further confirming the favorable nutritional quality of the cooked product.

[4] Guideline: Sodium intake for adults and children. 2021. World Health Organization. [cited 2025 Feb 10]. Available from: https://who.int/publications/i/item/9789241504836

[5] FAO/WHO/UNU. Protein and amino…

[6] The same.

Table 5 Amino acid scores computed protein efficiency ratio, and biological value of beef tripe

Essential amino acid	Amino acid scores, %			
	Raw beef tripe		Boiled beef tripe	
	School children	Adult	School children	Adult
Methionine	91.30*	131.25	105.65*	151.87
Leucine	115.33**	117.29*	115.67**	117.63*
Isoleucine	120.00	120.00**	147.33	147.33
Lysine	121.46	129.56	122.29	130.44**
Phenylalanine	140.98	154.47	141.71	152.89
Threonine	152.40	165.65	142.80	155.22
Histidine	127.50	136.00	165.00	176.00
Valine	187.93	139.74	182.41	135.64
Tryptophan	186.67	186.67	168.33	168.33
Computed protein efficiency ratio	2.31		2.38	
Biological value, %	73.40		74.19	

* – first limiting amino acid; ** – second limiting amino acid. Compiled based on the source data: FAO/WHO (2007)

These amino acid composition data align with previous studies that emphasize a high nutritional value of edible offal and underutilized meat by-products when properly processed [30, 31]. Therefore, boiled beef tripe, with its concentrated EAA profile and increased digestibility, presents a viable protein source for incorporation into functional meat products such as sausages, meat patties, and canned meats.

Amino acid scores, computed protein efficiency ratio, and biological value of beef tripe. Table 5 presents the protein quality indices of raw and boiled beef tripes, indicating an overall improvement in nutritional value after thermal processing. The boiled tripe exhibited a higher computed protein efficiency ratio of 2.38 compared to 2.31 in the raw tripe, suggesting enhanced biological utilization of protein upon cooking. This aligns with previous findings that heat treatment can improve protein digestibility and availability by denaturing antinutritional factors and unfolding protein structures, thereby enhancing enzymatic hydrolysis [29]. Similarly, the biological value increased from 73.40% in raw tripe to 74.19% in boiled tripe, reflecting a higher proportion of absorbed nitrogen in the body. The chemical score, which is based on the most limiting amino acid relative to FAO/WHO/UNU[7] requirements, rose slightly from 66.53 to 68.26% in boiled tripe, with methionine identified as the limiting amino acid in both cases, although its concentration still exceeded the adult requirement. Furthermore, the amino acid index, which represents the overall balance of essential amino acids relative to an ideal reference protein, improved from 82.25 in raw tripe to 84.62 in boiled tripe. These enhancements confirm that boiling not only increases amino acid availability but also improves the overall quality of beef tripe protein, making it a nutritionally viable alternative for use in functional meat products and protein-enriched diets[8] [16].

Table 6 presents the fatty acid composition of raw and boiled beef tripes, revealing a nutritionally balanced profile with significant proportions of saturated, monounsaturated, and polyunsaturated fatty acids, as well as showing a favorable shift after boiling. In particular, boiling resulted in a slight decrease in total saturated fatty acids (from 45.18 to 46.13%) and a corresponding increase in total unsaturated fatty acids (from 46.23 to 49.83%), indicating an improved lipid profile. Oleic acid ($C_{18:1}$), a heart-healthy monounsaturated fatty acid known to reduce low-density lipoprotein cholesterol,

Table 6 Fatty acid composition of beef tripe, %

Fatty acid	Raw beef tripe	Boiled beef tripe
Saturated fatty acid		
Capric acid ($C_{10:0}$)	0.02	0.03
Lauric acid ($C_{12:0}$)	0.01	0.10
Myristic acid ($C_{14:0}$)	2.95	3.11
Palmitic acid ($C_{16:0}$)	22.73	18.60
Margaric acid ($C_{17:0}$)	2.10	2.00
Stearic acid ($C_{18:0}$)	17.12	22.03
Arachidic acid ($C_{20:0}$)	0.25	0.26
Total saturated fatty acid	45.18	46.13
Monounsaturated fatty acid		
Lauroleic acid ($C_{12:1}$)	0.07	0.11
Tetradecenoic ($C_{14:1}$)	0.46	0.50
Palmitoleic acid ($C_{16:1}$)	0.08	2.10
Heptadecenoic acid ($C_{17:1}$)	0.12	0.23
Oleic acid ($C_{18:1}$)	34.90	37.01
Ecosenoic acid ($C_{20:1}$)	2.53	2.57
Total Monounsaturated fatty acid	38.16	42.52
Polyunsaturated fatty acid		
Linoleic acid ($C_{18:2}$)	5.61	4.15
Linolenic acid ($C_{18:3}$)	1.33	0.98
Arachidonic acid ($C_{20:4}$)	1.11	2.17
Ecosapentanoic acid ($C_{20:5}$)	0.02	0.01
Total polyunsaturated fatty acids	8.07	7.31
Total unsaturated fatty acids	46.23	49.83
Unknown	8.59	4.04
Unsaturated/Saturated fatty acid ratio	1.023	1.080

[7] FAO/WHO/UNU. Protein and amino…

[8] The same.

was predominant in both raw (34.90%) and boiled (37.01%) tripes, consistent with reports on organ meats and ruminant fats [2, 32].

As also shown in Table 6, palmitic acid ($C_{16:0}$) was predominant among saturated fatty acids, followed by stearic acid ($C_{18:0}$) in both raw (22.73 and 18.60%) and boiled (17.12 and 22.03%) tripes, respectively. The unsaturated/saturated fatty acid ratio also dereased slightly (from 1.023 to 1.080), which is a favorable indicator associated with reduced cardiovascular disease risk [33]. Additionally, essential polyunsaturated fatty acids such as linoleic ($C_{18:2}$) and linolenic ($C_{18:3}$) acids were present in appreciable amounts, particularly in boiled tripe, contributing to essential fatty acid intake for functions such as inflammatory regulation and cell membrane integrity [34]. These findings suggest that beef tripe, especially when boiled, offers a health-beneficial lipid profile, supporting its potential application in functional and value-added meat products.

Microbiological quality attributes of beef tripe. Table 7 illustrates the microbiological profile of the raw and boiled beef tripes, emphasizing the substantial reduction in microbial load achieved through thermal processing. The raw tripe exhibited elevated counts of total viable bacteria (5.10 $\log_{10}$ CFU/g), molds and yeasts (3.54 $\log_{10}$ CFU/g), and coliforms (2.95 $\log_{10}$ CFU/g). The samples also contained foodborne pathogens such as Salmonella and Shigella, which are indicative of contamination due to inadequate hygiene during slaughtering and handling [35]. In contrast, boiling significantly decreased microbial counts across all tested groups, with a total bacterial load reduced to 3.87 $\log_{10}$ CFU/g. The pathogens Salmonella and Shigella were completely eliminated, confirming the effectiveness of heat treatment in ensuring food safety.

Also the data in Table 7 indicate a notable reduction in *Staphylococci* counts after boiling, from 3.41 $\log_{10}$ CFU/g in the raw tripe to 1.78 $\log_{10}$ CFU/g in the boiled tripe. This significant decline highlights the effectiveness of thermal processing in eliminating potential enterotoxin-producing bacteria commonly associated with post-slaughter contamination. These results align with established findings that cooking above 70°C inactivates most vegetative pathogens [36]. Furthermore, the boiled tripe showed microbial levels comparable to, or lower than, the frozen beef in some cases, reinforcing its microbiological stability and suitability for use in value-added meat products such as sausages and canned meats.

Importantly, all microbiological counts in the boiled tripe samples remained within the acceptable limits for meat and meat products established by the Egyptian Organization for Standardization and Quality, supporting its safety for human consumption [37]. The complete absence of coliforms, molds, and psychrotrophs in boiled tripe further supports its potential as a safe and hygienic meat ingredient, provided that proper handling and processing protocols are observed [19].

Gross chemical composition of beef products. Table 8 provides a comparative analysis of the proximate composition of corned beef and sausage products formulated with either beef meat or beef tripe, revealing key nutritional and functional differences. In the corned beef, the moisture content was slightly higher in the meat-based product (57.95%) than in the tripe-based sample (57.03%). This was likely due to the superior water-binding capacity of muscle fibers compared to the collagen-rich tripe tissue. Similarly, crude protein was

Table 7 Microbiological attributes of main raw materials, $\log_{10}$ CFU/g

Microbial count	Frozen beef meat	Raw tripe	Boiled tripe
Total plate count	4.01 ± 0.11^{b}	5.10 ± 0.18^{a}	3.87 ± 0.10^{c}
Mould and yeast	2.67 ± 0.14^{b}	3.54 ± 0.21^{a}	1.47 ± 0.15^{c}
Coliform group	1.30 ± 0.22^{b}	2.95 ± 0.30^{a}	0
Staphylococcus aureus	2.10 ± 0.10^{b}	3.41 ± 0.15^{a}	1.78 ± 0.15^{c}
Salmonella & *Shigella*	0	1.12 ± 0.17^{a}	0

The values with the same superscript letters in a row are not significantly different at $p \leq 0.05$. The values are means ± standard deviation of triplicate trails

Table 8 Gross chemical composition of prepared beef products

Parameter	Corned beef		Beef sausage	
	Meat (control)	Tripe	Meat (control)	Tripe
Moisture, % ww t	57.95 ± 0.07^{b}	57.03 ± 0.08^{b}	58.62 ± 0.06^{a}	55.98 ± 0.06^{c}
Crude protein, % ww	22.12 ± 0.11^{b}	22.78 ± 0.06^{a}	21.18 ± 0.04^{c}	21.83 ± 0.04^{c}
Ether extract, % ww	10.69 ± 0.06^{c}	11.99 ± 0.03^{b}	13.25 ± 0.07^{a}	13.92 ± 0.12^{a}
Crude ash, % ww	2.52 ± 0.08^{b}	2.14 ± 0.10^{c}	2.73 ± 0.03^{a}	2.46 ± 0.03^{b}
Nitrogen-free extract, % ww	6.72 ± 0.14^{a}	6.06 ± 0.08^{b}	4.22 ± 0.09^{d}	5.81 ± 0.06^{c}
Energy, kcal/100 g	215.57 ± 0.09^{c}	235.27 ± 0.07^{a}	224.85 ± 0.11^{b}	239.84 ± 0.03^{a}

The values with the same superscript letters in a row are not significantly different at $p \leq 0.05$. The values are means ± standard deviation of triplicate trails

marginally lower in the corned beef meat (22.12%) than in the beef tripe (22.78%), consistent with the structural protein concentration in skeletal versus smooth muscle tissues [38]. Conversely, the tripe-based corned beef had a higher fat content (11.99%) compared to the meat-based one (10.69%), which may result from the fat entrapment properties of tripe's fibrous matrix [39]. Conversely, the tripe-based products also showed lower ash contents (2.14 vs. 2.52%), reflecting their richer mineral composition, which was in agreement with previous mineral analyses (Table 3). The nitrogen-free extract, which includes available carbohydrates, was lower in the tripe-based corned beef (6.06%) compared to the meat-based formulation (6.72%) due to a lower starch content or higher fiber levels. This shiftin macronutrient balance contributed to higher energy values for the tripe-based corned beef (235.27 kcal/100 g) compared to meat-based one (215.57 kcal/100 g), positioning tripe as a favorable ingredient in high-calorie, nutrient-rich canned products [29].

A similar pattern was observed in sausage formulations. The beef sausage exhibited slightly higher moisture (58.62%) and lower protein (21.18%) levels than the tripe sausage (55.98 and 21.83%, respectively). This was due to muscle tissue's superior hydration and protein density. The tripe sausage had a greater fat content (13.92%) compared to the beef sausage (13.25%), which contributed to its higher energy value of 239.84 kcal/100 g versus 224.85 kcal/100 g in the beef sausage. This fat-retaining quality may enhance both the flavor and caloric density, making tripe-based sausages particularly suitable for consumers with elevated energy needs. The ash content was lower in the tripe sausage (2.46%) than in its meat-based counterpart (2.73%), reaffirming the enhanced mineral contribution of organ meats [39]. The nitrogen-free extract was slightly higher in the tripe sausage (5.81%), compared to the beef sausage (4.22%), this minor difference does not significantly affect the nutritional profile. These findings collectively support the incorporation of tripe as a cost-effective, nutritionally rich, and functionally suitable alternative to traditional meat in both sausages and canned meat products.

Microbiological attributes of prepared beef products. Table 9 outlines the microbiological profiles of corned beef and sausage products prepared from both beef meat and beef tripe, revealing strong evidence of safety across all formulations. In the corned beef, none of the tested microbial groups (total viable count, molds and yeasts, coliforms, *Staphylococcus aureus*, *Salmonella* & *Shigella*) were detected in either beef meat or tripe-based products. This complete absence of contamination highlights the effectiveness of the thermal processing methods used, including boiling, curing, and autoclaving at 121°C for 20 min. These procedures align with established food safety standards, as cooking at core temperatures above 70°C is known to inactivate most vegetative pathogens [36]. The absence of spoilage organisms further supports the microbiological stability of tripe-based canned products, indicating that when properly processed, tripe is microbiologically as safe as conventional meat [19, 21]. These findings endorse the inclusion of beef tripe as a viable, shelf-stable ingredient in value-added meat products without compromising food safety.

Similarly, the microbiological analysis of the beef and tripe sausages demonstrated acceptable hygiene and safety levels, with all the values falling within the permissible limits for cooked meat products. The total viable count was slightly higher in the beef meat sausage (3.62 $\log_{10}$ CFU/g) compared to the tripe sausage (3.51 $\log_{10}$ CFU/g), but both values were well within the safe ranges. Notably, coliforms were not detected in tripe sausage, whereas they were present at a low level (1.12 $\log_{10}$ CFU/g) in the beef sausage, indicating possibly better hygiene or thermal treatment in the tripe sample. Both sausage types were free from *Salmonella* and *Shigella*, confirming effective pathogen control. The presence of *Staphylococcus aureus* was minimal and similar in both the samples (1.39 $\log_{10}$ CFU/g in beef vs. 1.38 in tripe). Their levels were far below the critical thresholds, indicating proper post-cooking handling. Additionally, no molds or yeasts were detected in either sample, reinforcing their microbial stability. Overall, the data support the safe use of beef tripe in cooked meat products such as sausages, aligning with the growing body of research that promotes the hygienic and sustainable utilization of edible meat by-products [29].

Table 9 Microbiological attributes of prepared beef products, $\log_{10}$ CFU/g

Microbial count	Corned Beef		Beef sausage	
	Meat (control)	Tripe	Meat (control)	Tripe
Total plate count	0	0	3.62 ± 0.11^{a}	3.51 ± 0.15^{b}
Mould and yeast	0	0	1.88 ± 0.23^{a}	1.56 ± 0.18^{b}
Coliform group	0	0	1.12 ± 0.18^{a}	0
Staphylococcus aureus	0	0	1.39 ± 0.18^{a}	1.18 ± 0.18^{b}
Salmonella & Shigella	0	0	0	0
Total spore-forming bacterial counts	0	0	n.d.	n.d.
Protolytic bacteria	0	0	n.d.	n.d.
Lipolytic bacteria	0	0	n.d.	n.d.

The values with the same superscript letters in a row are not significantly different at $p \leq 0.05$. The values are means ± standard deviation of triplicate trails. n.d. – not detected

Table 10 Sensory evaluation of prepared beef products

Sample	Taste	Odor	Color	Texture	Appearance	Overall acceptability
Beef meat sausage (control)	8.00 ± 0.82[a]	8.20 ± 0.63[a]	8.10 ± 0.57[b]	8.90 ± 0.57[a]	8.20 ± 0.63[a]	8.08 ± 0.46[a]
Beef tripe sausage	7.60 ± 0.52[c]	7.70 ± 0.67[c]	8.10 ± 0.74[b]	8.00 ± 0.67[b]	8.10 ± 0.74[a]	7.90 ± 0.27[b]
Corned beef meat (control)	8.05 ± 0.60[a]	8.10 ± 0.70[b]	8.30 ± 0.67[a]	8.10 ± 0.32[b]	8.15 ± 0.47[a]	8.14 ± 0.20[a]
Corned beef tripe	7.85 ± 0.53[b]	8.40 ± 0.52[a]	7.95 ± 0.69[c]	7.90 ± 0.52[c]	7.90 ± 0.52[b]	8.01 ± 0.38[a]

The values with the same superscript letters in a column are not significantly different at $p \leq 0.05$.

Sensory evaluation of prepared beef products. Table 10 presents the sensory evaluation results for both corned beef and sausage products formulated from beef meat and beef tripe, demonstrating high overall acceptability across all the parameters. The corned beef meat (control) achieved the highest overall acceptability score of 8.14 ± 0.20, while the tripe-based corned beef followed closely with 8.01 ± 0.38, indicating that the inclusion of tripe did not significantly compromise the consumer appeal. While the taste score was marginally higher for the corned meat-based product (8.05 ± 0.60) compared to the tripe-based one (7.85 ± 0.53), the odor rating was notably higher in the tripe sample (8.40 ± 0.52) compared to the meat sample (8.10 ± 0.70). This was possibly due to the distinctive aroma of organ meats after curing. Other sensory parameters such as color, texture, and appearance remained largely comparable, with their values ranging from 7.90 to 7.95 in the ripe products and 8.10 to 8.30 in the meat-based ones. These results suggest that tripe can be incorporated into canned meat formulations with minimal impact on sensory characteristics, offering a nutritionally beneficial and cost-effective alternative to traditional muscle-based products.

Similarly, sensory scores for the sausage products under study indicated a high level of consumer acceptance for both formulations. The beef sausage received an overall acceptability score of 8.08 ± 0.28, while the tripe sausage scored 7.90 ± 0.18, reflecting only a slight preference for the conventional version. The taste and odor ratings were nearly equivalent between the two. The color ratings were nearly equivalent between the two, and although the appearance of beef sausage was rated slightly higher (8.20 ± 0.63) than that of tripe sausage (8.10 ± 0.74), the difference was not substantial. Taste, odor and texture also remained within acceptable ranges, with beef sausage scoring 8.00 ± 0.82, 8.20 ± 0.63, and 8.90 ± 0.57, compared to 7.60 ± 0.52, 7.70 ± 0.67, and 8.00 ± 0.67 in tripe sausage, respectively. These closely aligned results indicate that tripe does not adversely affect the product's quality. This is due to the functional properties of collagen that enhance binding and mouthfeel [29]. The overall findings are consistent with previous literature supporting the use of edible by-products in meat formulations. They reinforce the potential of tripe as a sustainable, affordable, and sensory-acceptable ingredient in value-added meat products [40, 41].

Similarly, sensory scores for sausage products indicated a high level of consumer acceptance for both formulations. Beef sausage received an overall acceptability score of 8.08 ± 0.28, while tripe sausage scored 7.90 ± 0.18, reflecting only a slight preference for the conventional version. These closely aligned results indicate that tripe's inclusion does not adversely affect product quality, likely due to the functional properties of collagen that enhance binding and mouthfeel [29]. The overall findings are consistent with previous literature supporting the use of edible by-products in meat formulations, reinforcing tripe's potential as a sustainable, affordable, and sensory-acceptable ingredient in value-added meat products [40, 41].

CONCLUSION

Results indicate that beef tripe, as a meat by-product, is an alternative and economical source of high-quality protein. It can also serve as a functional ingredient for household applications in combined meat products, such as corned tripe and tripe sausage. Incorporating beef tripe can therefore reduce the cost of meat products and optimize their nutritional balance. These findings could be beneficial for the future development of value-added meat products from beef tripe, which is considered to be an unutilized and widely available meat by-product.

CONTRIBUTION

E.M. El-Sayed collected the data, conceived and designed the analysis, and wrote the paper. E.M. Elsebaie performed the analysis and wrote the paper. M.F.A. El-Farsy conceived and designed the analysis. R.A. Shehata collected the data and wrote the paper. S.A. Hozifa conceived and designed the analysis. D.M. El-Mesiry contributed the data and analysis tools. S.A. Elmeslamy preformed the analysis.

CONFLICT OF INTEREST

The authors declare no conflict of interest regarding this article.

AI DECLARATION

ChatGPT (OpenAI, version 4.0) was used at the manuscript preparation stage to improve grammar, enhance clarity, and assist with text organization. All the outputs generated by the tool were carefully reviewed, edited, and verified by the authors to ensure accuracy, integrity, and scientific validity. The impact on the conclusions was negligible, as all the data interpretation, experimental results, and scientific insights were developed independently by the authors.

REFERENCES

1. Pandey DK, Mishra R. Towards sustainable agriculture: Harnessing AI for global food security. Artificial Intelligence in Agriculture. 2024;12:72–84. https://doi.org/10.1016/j.aiia.2024.04.003
2. Shehu AA, Mohammed MI, Baba SA. Proximate composition of offal of selected ruminant animals slaughtered at Kano Central Abattoir, Kano state, Nigeria. Bayero Journal of Pure and Applied Sciences. 2024;15(1):65–71.
3. Luo W, Zhang J, Ahmmed MK, Sakai K, Shahidi F, *et al*. Valorization of animal by-product enzymes: Advancing sustainable food processing through innovative extraction, purification, and application strategies. Trends in Food Science & Technology. 2025;156:104870. https://doi.org/10.1016/j.tifs.2025.104870
4. Fuerniss HF, Gifford CL, Mortensen EG, Belk KE, Engle TE, *et al*. Nutrient analysis of raw united states beef offal items. Nutrients. 2024;16(18):3104. https://doi.org/10.3390/nu16183104
5. Sedykh TA, Subhankulov NR, Presnyakova AK, Gizatullin RS, Kosilov VI. Slaughter qualities and by-product yield in Limousin bull calves of different genotypes. E3S Web of Conferences: Intern. Sci. Conf. "Fundamental and Applied Scientific Research in the Development of Agriculture in the Far East" (AFE-2023), 2023;462:01005. https://doi.org/10.1051/e3sconf/202346201005
6. Du M, Zhang Y, Zhao Y, Fang Ya. Agarose/konjac glucomannan double network hydrogels to mimic the texture of beef tripe. Food Hydrocolloids. 2023;135:108173. https://doi.org/10.1016/j.foodhyd.2022.108173
7. Zou Q, Liu Y, Luo L, Chen Y, Zheng Y, *et al*. Screening of optimal konjac glucomannan–protein composite gel formulations to mimic the texture and appearance of tripe. Gels. 2024;10(8):528. https://doi.org/10.3390/gels10080528
8. Xiong Y, Zhang P, Warner RD, Hossain MN, Leonard W, *et al*. Effect of sorghum bran incorporation on the physicochemical and microbial properties of beef sausage during cold storage. Food Control. 2022;132:108544. https://doi.org/10.1016/j.foodcont.2021.108544
9. Molina JRG, Frías-Celayeta JM, Bolton DJ, Botinestean C. A comprehensive review of cured meat products in the Irish market: Opportunities for reformulation and processing. Foods. 2024;13(5):746. https://doi.org/10.3390/foods13050746
10. Evanuarini H, Susilo A, Rahayu PP. Enhancing the quality of beef sausage by using papaya peel flour as a filler. Proceedings of the 5th Intern. Conf. on Environmentally Sustainable Animal Industry (ICESAI 2024), 2024:95–102. https://doi.org/10.2991/978-94-6463-670-3_10
11. Silalahi TJ, Suryani A, Suryani A. Analysis of nitrite and nitrate in the corned beef and smoked beef by using visible spectrophotometry method. IOP Conference Series Earth and Environmental Science. 2018;205(1):012039. https://doi.org/10.1088/1755-1315/205/1/012039
12. Elsebaie EM, Elmahdy A, El-Gezawy ES, Badr MR, Asker GA, *et al*. Effects of faba bean hull nanoparticles on physical properties, protein and lipid oxidation, colour degradation, and microbiological stability of burgers under refrigerated storage. Antioxidants. 2022;11(5):938. https://doi.org/10.3390/antiox11050938
13. Abdelhakam O, Elsebaie E, Ghazi A, Gouda M. Quality characteristics of beef hamburger enriched with red grape pomace powder during freezing storage. Slovenian Veterinary Research. 2019:56(22-Suppl):333–340. https://doi.org/10.26873/SVR-772-2019
14. Ali AM, Essa RY, Zein RI, Salama AA. Preparation and evaluation of functional corn snacks using *Spirulina* protein isolate. Egyptian Journal of Chemistry. 2024;67(5):641–650.
15. Metwaly HR, El-Sayed AEKB, Amin HF. Chemical and biochemical properties of marine algae *Ulva lactuca* and *Nannocholoropsis oculata*. Egyptian Journal of Aquatic Biology & Fisheries. 2023;27(3):19–34 https://doi.org/10.21608/EJABF.2023.298840
16. Li G, Ma L, Yan Z, Zhu Q, Cai J, *et al*. Extraction of oils and phytochemicals from *Camellia oleifera* seeds: Trends, challenges, and innovations. Processes. 2022;10(8):1489. https://doi.org/10.3390/pr10081489
17. de Souza AC, Simões LA, Schwan RF, Dias DR. Enumerating yeast in foods and water using the spread plating technique. Detection and Enumeration of Bacteria, Yeast, Viruses, and Protozoan in Foods and Freshwater. NY: Springer; 2021, pp. 93–110. https://doi.org/10.1007/978-1-0716-1932-2_10
18. Liu Y, Gao X, Zang M, Sun B, Zhang S, *et al*. Insights into Microbial community and its enzymatic profiles in commercial dry-aged beef. Foods. 2025;14(3):529. https://doi.org/10.3390/foods14030529
19. Economou V, Tsitsos A, Theodoridis A, Ambrosiadis I, Arsenos G. Effects of chitosan coatings on controlling *Listeria monocytogenes* and methicillin-resistant *Staphylococcus aureus* in beef and mutton cuts. Applied Sciences. 2022;12(22):11345. https://doi.org/10.3390/app122211345
20. Medhat M, Khalafalla FA, Mohamed FH, Mohamed OA, Hassan AHA. Prevalence, virulence and antibiotic resistance of *Escherichia coli* isolated from fresh, chilled and frozen retail marketed beef in Egypt. Egyptian Journal of Veterinary Sciences. 2024:1–10. https://doi.org/10.21608/ejvs.2024.294487.2142

21. Ahmed FS, Abdo JM, Jakhsi NSA. Detection of *Salmonella* Spp. in meat and meat products by culture, biochemical and molecular characterization in duhok city. Egyptian Journal of Veterinary Sciences. 2024;55(3):661–669. https://doi.org/10.21608/ejvs.2023.230031.1569

22. Essa RY, Elsebaie EM. New fat replacement agent comprised of gelatin and soluble dietary fibers derived from date seed powder in beef burger preparation. LWT. 2022;156:113051. https://doi.org/10.1016/j.lwt.2021.113051

23. Toldrá F. Chapter 9 – The storage and preservation of meat. III – Meat processing. Lawrie's meat science. Soston: Woodhead Publishing; 2023, pp. 281–314. https://doi.org/10.1016/B978-0-323-85408-5.00002-9

24. Pearce KL, Rosenvold K, Andersen HJ, Hopkins DL. Water distribution and mobility in meat during the conversion of muscle to meat and ageing and the impacts on fresh meat quality attributes – A review. Meat Science. 2011;89(2):111–124. https://doi.org/10.1016/j.meatsci.2011.04.007

25. Anandh MA, Radha K, Lakshmanan V, Mendiratta SK. Development and quality evaluation of cooked buffalo tripe rolls. Meat Science. 2008:80(4):1194–1199. https://doi.org/10.1016/j.meatsci.2008.05.014

26. Wazir AA, Hussain MA, Shah QA, Ahmad S, Kakar I, *et al*. Evaluation of physico-chemical characteristics of meat and edible offals of cattle. Pak-Euro Journal of Medical and Life Sciences. 2021:4(4):235–244.

27. Hamad HI, Sulieman AME, Mustafa WA, Osman OA. Impact of Season on the chemical composition and pH of Beef meat and offal's samples collected from Wad-Medani Market, Central Sudan. University of Bakht Alruda Journal. 2020:(32):152–159.

28. Latoch A, Stasiak DM, Siczek P. Edible offal as a valuable source of nutrients in the diet – A review. Nutrients. 2024:16(11):1609. https://doi.org/10.3390/nu16111609

29. Toldrá F, Aristoy MC, Mora L, Reig M. Innovations in value-addition of edible meat by-products. Meat science. 2012:92(3):290–296. https://doi.org/10.1016/j.meatsci.2012.04.004

30. Zarkadas GC, Karatzas CD, Zarkadas CG. Assessing the myofibrillar and connective tissue protein contents and protein quality of beef tripe. Journal of Agricultural and Food Chemistry. 1996:44(9):2563–2572. https://doi.org/10.1021/jf950262y

31. Morshdy AEM, Ahmed AMG, Thaewat AE, Darwish WS. A review of the nutritive value and microbial quality of animal edible offal. Assiut Veterinary Medical Journal. 2026:72:77–89. https://doi.org/10.21608/avmj.2025.395053.1763

32. Wood JD. Meat composition and nutritional value. Lawrie´s Meat Science. Soston: Woodhead Publishing; 2017, pp. 635–659. https://doi.org/10.1016/B978-0-08-100694-8.00020-0

33. Kim Y, Je Y, Giovannucci EL. Association between dietary fat intake and mortality from all-causes, cardiovascular disease, and cancer: A systematic review and meta-analysis of prospective cohort studies. Clinical Nutrition. 2021;40(3):1060–1070.

34. Kapoor B, Kapoor D, Gautam S, Singh R, Bhardwaj S. Dietary polyunsaturated fatty acids (PUFAs): Uses and potential health benefits. Current Nutrition Reports. 2021;10:232–242. https://doi.org/10.1007/s13668-021-00363-3

35. Khalil AM, Mousa MM, El-Bahy EF. Sanitary Condition of some raw edible beef offal. Alexandria Journal of Veterinary Sciences. 2018:59(2):165–172. https://doi.org/10.5455/ajvs.234694

36. Bensink JC, Dobrenov B, Mulenga MP, Bensink ZS, McKee JJ. The microbiological quality of beef tripe using different processing techniques. Meat science. 2002:62(1):85–92. https://doi.org/10.1016/s0309-1740(01)00232-7

37. Amin HF, El-Sayed AEKB, Elsebaie EM, Metwaly HR. Quality of catfish luncheon supplemented with marine algae (*Ulva lactuca* and *Nannocholoropsis oculata*) during frozen storage. The Annals of the University Dunarea de Jos of Galati. Fascicle VI-Food Technology. 2024;48(2):27–44.

38. Baldi G, Soglia F, Petracci M. Chapter 21 – Valorization of meat by-products. Food waste recovery. NY: Academic Press; 2021, pp. 419–443. https://doi.org/10.1016/B978-0-12-820563-1.00017-2

39. Anandh MA. Quality of cooked goat meat sausages incorporated with goat tripe. Asian Journal of Dairy and Food Research. 2017;36(4):349–352. https://doi.org/10.18805/ajdfr.DR-1222

40. Karibe WG, Kunyanga CN, Imungi JK. Microbiological status of ready to eat (RTE) bovine tripe rolls under different storage conditions. Food Science and Quality Management. 2018;78:7–16.

41. Shukurlu Y, Salmanova A, Sharifova M. Biotechnological aspects of the modification of secondary collagen-containing raw materials – tripe for the production of cost-effective functional meat products. Food Science and Technology. 2022;42:e85521. https://doi.org/10.1590/fst.85521

Additional information about the authors

Eatemad M. El-Sayed ORCID 0000-0002-9462-3123
Essam M. Elsebaie ORCID 0000-0002-8507-0694
Marwa F. A. El-Farsy ORCID 0000-0002-9329-9034
Rehab A. Shehata ORCID 0009-0001-9092-9889
Shaymaa A. Hozifa ORCID 0000-0002-2963-5451
Dalia M. El-Mesiry ORCID 0000-0002-5520-3118
Soher A.-E. Elmeslamy ORCID 0009-0001-5352-5164

Foods and Raw Materials. 2027;15(2)

ISSN 2308-4057 (Print)
ISSN 2310-9599 (Online)

Research Article
Open Access

Available online at http://jfrm.ru/en
https://doi.org/10.21603/2308-4057-2027-2-711
https://elibrary.ru/TODILQ

Effects of sea buckthorn and black currant extracts on the growth, acid production, and antagonism of bifidobacteria

Svetlana A. Evdokimova, Boris A. Karetkin*, Elena V. Guseva, Kirill M. Demkin, Alla T. Shevchenko, Natalya Yu. Khromova, Victor I. Panfilov, Nina B. Gradova

Mendeleev University of Chemical Technology, Moscow, Russia

* e-mail: karetkin.b.a@muctr.ru

Received 20.11.2025; Revised 05.12.2025; Accepted 08.12.2025; Published online 09.07.2026

Abstract:
Plant polyphenols have recently been recognized as promising new-generation prebiotics. However, the concentrations and profiles of polyphenols vary significantly among different plants, so the effects of their extracts on probiotic strains are also highly variable. This study assessed the effects of ethanol and supercritical fluid extracts of black currant and sea buckthorn on the growth of bifidobacteria and their antagonism against intestinal pathogens.

Extracts of black currant and sea buckthorn were obtained using reflux ethanol extraction or supercritical fluid extraction. Total phenols in the extracts were determined by the Folin-Ciocalteu colorimetric method. Individual phenolic compounds were identified by UV-Vis spectroscopy. Effects of the extracts on bifidobacteria and the intestinal pathogens *Bacillus cereus* and *Staphylococcus aureus* were evaluated in monoculture. Antagonism of bifidobacteria against the pathogens was evaluated in co-culture in the media with various ethanol extracts. Concentrations of organic acids were determined using HPLC.

Phenolic components of the berries had stimulated, neutral, or negative effects on probiotic growth and organic acid production, depending on the type of raw material and the extraction method. *Bifidobacterium adolescentis* and *Bifidobacterium longum* were the most sensitive to, and strongly inhibited by, the extracts, while no pronounced growth-stimulating effect was observed for any of the studied bifidobacteria strains. Additionally, the effect of total phenolic concentrations in the extracts on the strain growth was evaluated by diluting the native extracts. Minimum inhibitory concentrations in the ethanol extracts for bifidobacteria ranged from 30 to 140 μg GAE/mL, while those in the supercritical fluid extracts were lower (13–32 μg GAE/mL). The sea buckthorn supercritical fluid extract stimulated *Bifidobacterium bifidum* growth, while the ethanol extract of sea buckthorn and the supercritical fluid extract of black currant stimulated the growth of *Bifidobacterium breve* and *B. longum* subsp. *infantis*. *B. cereus* was not sensitive to changes in total phenolic concentrations. The minimum inhibitory concentration of total phenols for *S. aureus* was the lowest (7 μg GAE/mL) in the supercritical fluid extract of sea buckthorn. The extracts had mostly neutral or positive effects on lactic and acetic acids production by bifidobacteria. The greatest increase in acid concentrations was observed for *B. breve* in the medium with black currant ethanol extract. The greatest suppression of pathogen growth was achieved by a combination of *B. breve* with either of the ethanol extracts.

The results demonstrate that black currant and sea buckthorn extracts are highly selective prebiotics that exert different effects on the antagonism of bifidobacteria against pathogens. The study revealed the most effective combination of the bifidobacteria and berry extracts against the pathogens, as well as the most effective symbiotic composition.

Keywords: Bifidobacteria, sea buckthorn, black currant, supercritical fluid extraction, ethanol extraction, flavonoids, antagonism, synbiotics

Funding: The research was supported by the Russian Science Foundation, grant No. 24-19-00298, https://rscf.ru/project/24-19-00298/

Please cite this article in press as: Evdokimova SA, Karetkin BA, Guseva EV, Demkin KM, Shevchenko AT, *et al.* Effects of sea buckthorn and black currant extracts on the growth, acid production, and antagonism of bifidobacteria. Foods and Raw Materials. 2027;15(2):296–310. https://doi.org/10.21603/2308-4057-2027-2-711

INTRODUCTION

In recent decades, interest in natural plant-based bioactive compounds has significantly increased due to their potential health benefits, such as antioxidant, anti-inflammatory, antimicrobial, and prebiotic properties [1]. Special attention has been paid to flavonoids, a class of polyphenolic compounds. These compounds are widespread in plants and possess a variety of biological activities [2]. Flavonoids are secondary plant metabolites that play a key role in protecting against ultraviolet radiation, pathogens, and other stress factors [3]. Their chemical structure is based on a C6-C3-C6 skeleton,

Copyright © 2026, Evdokimova *et al.* This is an open access article distributed under the terms of the Creative Commons Attribution 4.0 International License (https://creativecommons.org/licenses/by/4.0/), allowing third parties to copy and redistribute the material in any medium or format and to remix, transform, and build upon the material for any purpose, even commercially, provided the original work is properly cited and states its license.

consisting of two aromatic rings linked by a three-carbon bridge that can form a heterocyclic ring (pyran or pyrone) [4]. Depending on the degree of oxidation and substitution in the skeleton, flavonoids are divided into several classes, including flavonols (e.g., quercetin and kaempferol), flavones (apigenin and luteolin), flavanones (naringenin and hesperidin), isoflavones (genistein and daidzein), anthocyanidins (cyanidin and pelargonidin), and catechins (epicatechin and epigallocatechin) [5]. Flavonoids are widely distributed in plants. Their main sources include fruits, vegetables, cereals, tea, wine, and medicinal plants [6]. However, berry crops such as sea buckthorn, black currant, shadberry, and blackberry occupy a special place due to their high flavonoid content and diversity [7, 8]. For example, sea buckthorn is rich in quercetin and isorhamnetin, while black currant is rich in anthocyanidins [9–12]. These berries are not only valuable raw materials for the isolation of flavonoids but they also contain other substances with pronounced biological activity. Thus, these materials have enormous potential in functional foods and pharmaceuticals [10, 11].

Besides their important role in plant protection, flavonoids have a positive effect on human health. They exhibit antioxidant properties by neutralizing free radicals and preventing oxidative stress, which is associated with the development of cancer, cardiovascular diseases, and neurodegenerative disorders [13]. In addition, flavonoids show anti-inflammatory activity by inhibiting key enzymes such as cyclooxygenase and lipoxygenase, and also modulate signaling pathways associated with inflammation [14]. Their ability to interact with the intestinal microbiota makes them promising candidates for use as prebiotics [15].

The intestinal microbiota is a complex ecosystem consisting of trillions of microorganisms that play a key role in maintaining the host's homeostasis. Bifidobacteria and lactobacilli are among the most important representatives of the intestinal microbiota. They help strengthen the immune system, synthesize vitamins, and suppress the growth of pathogenic microorganisms [16, 17]. An imbalance in the composition of the microbiota, known as dysbiosis, can lead to the development of various diseases, including inflammatory bowel disease, obesity, and even neurodegenerative disorders [18]. This explains the current scientific interest in natural compounds that stimulate the growth of beneficial bacteria and suppress pathogens.

Recent studies have shown that flavonoids can have a significant impact on the composition and function of the intestinal microbiota. For example, quercetin and kaempferol promote the growth of bifidobacteria and lactobacilli while inhibiting the growth of pathogens such as *Escherichia coli* and *Salmonella typhimurium* [19]. Anthocyanidins contained in berries also exhibit prebiotic properties, increasing the number of beneficial bacteria and reducing the level of intestinal inflammation [20]. The mechanisms behind this effect include the modulation of bacterial metabolic activity, changes in the pH of the medium, and stimulation of the production of short-chain fatty acids (acetic, propionic, butyric, etc.), which play an important role in maintaining intestinal health [21].

Berries such as sea buckthorn, black currant, shadberry, and blackberry are rich in flavonoids, vitamins, and other bioactive substances [22]. They are traditionally used in folk medicine to treat various diseases, with their extracts demonstrating pronounced antioxidant and antimicrobial activity [23]. For example, sea buckthorn has strong antioxidant and anti-inflammatory properties due to high concentrations of quercetin and isorhamnetin [24]. Black currant has a protective effect on the cardiovascular system due to a high content of anthocyanidins that give the berries their characteristic color [25]. Shadberry and blackberry stimulate the immune system and improve digestion due to significant amounts of flavonoids such as catechins and flavonols [26, 27].

Supercritical fluid extraction and alcohol (ethanol or methanol) extraction are the most effective methods for isolating bioactive compounds from raw plant materials [28]. Supercritical fluid extraction is a technological process in which a supercritical fluid is used as a solvent [29]. A supercritical fluid is a specific state of matter with no distinction between liquid and gas. Supercritical fluid extraction, in particular, produces high-purity extracts without the use of toxic solvents, making it an ecologically safe alternative to traditional extraction methods [30]. Alcohol extraction is widely used to isolate flavonoids due to its high efficiency and availability [31]. Thus, each method has both advantages and limitations [32].

The aim of this study was to evaluate the effect of ethanol and supercritical fluid extracts of black currant and sea buckthorn on the growth of bifidobacteria and their antagonism against the test strains of intestinal pathogens. We examined the prebiotic potential of the extracts depending on the species of bifidobacteria. Applying co-culture, we identified the strongest combination of bifidobacteria strain and berry extract against the pathogens, as well as their most effective symbiotic composition.

STUDY OBJECTS AND METHODS

Study objects. The fruits of sea buckthorn (*Hippophae rhamnoides* L.) and black currant (*Ribes nigrum* L.) produced by Moroshka (Russia) were used as raw materials for the isolation of flavonoids. The berries were supplied frozen and stored at –18°C.

The prebiotic potential of the isolated polyphenolic components (flavonoids) was assessed by using the following bifidobacteria strains: *Bifidobacterium adolescentis* VKPM AC1662 (ATCC 15703), *Bifidobacterium longum* subsp. *longum* VKPM AC1665 (ATCC 15707), *Bifidobacterium bifidum* VKPM AC1666 (ATCC 29521), *Bifidobacterium breve* VKPM AC1911 (ATCC 15698), and *B. longum* subsp. *infantis* VKPM AC1912 (DSM 20218). Their antagonistic activity was measured against the test strains of intestinal pathogens and food contaminants, *Bacillus cereus* VKPM B8076 (ATCC 11778) and *Staphylococcus aureus* ATCC 43300. The *S. aureus*

strain was purchased from the American Type Culture Collection, while the other strains were obtained from the National Bioresource Center's All-Russian Collection of Industrial Microorganisms.

Methods of berry extraction. Just before reflux ethanol extraction, the berries were milled using an immersion blender. A sample of the milled raw material was weighed on an analytical balance and an extractant (70% (v/v) ethanol) was added at a solid dry matter-to-solvent ratio of 1:12. The extraction was carried out in flasks placed in a water bath with a reflux condenser at gentle boiling. The extraction time was 30 min from the start of boiling.

For supercritical fluid extraction, the berries were first freeze-dried. Milled dry berries (40 g) were loaded into a high-pressure extractor with a total volume of 250 mL. A co-solvent (10% w/w ethanol relative to the mass of carbon dioxide in static mode; see below) was added before sealing the chamber. The pressure in the sealed extractor was then increased to 200 bar, and supercritical carbon dioxide was introduced at 40°C. Once the target temperature and pressure were reached, extraction was carried out in static mode for 30 min. During this stage, supercritical carbon dioxide penetrates the structure of the raw material, facilitating the dissolution of bioactive substances. After static extraction, dynamic extraction was performed at a supercritical carbon dioxide flow rate of 1 kg/h for 20 min. In this stage, the extract is continuously removed from the raw material and collected in an extract collector. After dynamic extraction, the supply of carbon dioxide was stopped, and the system pressure was gradually reduced over 15 min to prevent potential equipment damage or extractor freezing due to adiabatic cooling. The extracts were stored at 5°C and used no later than 12 h after extraction.

Nutrient media. Mono- and co-cultivation of bifidobacteria was carried out in half-media according to Rossi *et al.* [33], with some modifications. The medium containing, mg/mL: 5 of casein tryptone (Dia-M); 3.8 yeast extract (Dia-M); 2.5 meat extract (Panreac); 0.5 ascorbic acid (AppliChem); 5 glucose; 0.5 sodium acetate; 2.5 $(NH_4)_2SO_4$; 1 urea; 0.1 $MgSO_4 \times 7H_2O$; 0.005 $FeSO_4 \times 7H_2O$; 0.0035 $MnSO_4 \times 7H_2O$; 0.005 NaCl; 0.5 Tween-80; and 0.25 cysteine. The pH was adjusted to 7.0. Carbohydrate-free media (in 80% of the total water volume) and glucose solution (in 10% of the total water volume) were autoclaved separately for 30 min at 115°C and aseptically mixed before inoculation.

The berry extracts obtained by ethanol and supercritical fluid extractions were diluted with an ethanol–water mixture to an ethanol concentration of 70% (v/v). These extracts were then further diluted with distilled water (1:1) to facilitate the transition of extracted substances into the aqueous phase of the nutrient media. The diluted extracts were autoclaved for 30 min at 115°C. The treated extracts were added to the nutrient media at a final concentration of 10% (v/v). Before inoculation, the complete nutrient media were incubated at 37°C for 12–15 h with stirring at 180–200 rpm to detect any microbial contamination and to allow additional ethanol evaporation. Control media were prepared in the same manner, replacing the extracts with 35% (v/v) ethanol. Just before inoculation, the pH of the nutrient media was adjusted to 7.0 under sterile conditions using a sterile 10% (w/v) NaOH solution in saline. The initial ethanol concentration in the media before inoculation did not exceed 6 mg/mL, as determined by high-performance liquid chromatography.

In monoculture experiments, viable bifidobacteria cells were counted in a bifidum medium containing, mg/mL: 10 of casein tryptone (Dia-M); 5 yeast extract (Dia-M); 7.5 glucose; 2.5 lactose; 0.5 cysteine; 2.5 NaCl; 0.5 $MgSO_4 \times 7H_2O$; 0.5 ascorbic acid (AppliChem); 0.3 sodium acetate; and 1.75 (pH 6.8–7.0) agar. To enumerate bifidobacteria cells in co-culture experiments, 4 mL/L of propionic acid was added to the bifidum medium before analysis, adjusting the pH to approximately 5.0 to suppress the growth of the test strains.

The test strains (*B. cereus*, *S. aureus*) were counted on Petri dishes with LB agar containing, mg/mL: 20 of glucose; 10 casein tryptone (Difco Laboratories); 5 yeast extract; and 2 (pH 7.2) NaCl. Growth of bifidobacteria on these Petri dishes was excluded due to aerobic incubation conditions.

Quantification of organic acids and ethanol. The concentrations of lactic acid, acetic acid, and ethanol were determined by high-performance liquid chromatography according to established methods [34, 35], with some modifications. The samples were analyzed refractometrically using an Agilent 1220 Infinity chromatograph (Agilent, USA) equipped with an Agilent Hi-Plex H column (250×4.6 mm). The supernatant of the samples, which was obtained by centrifugation at 12,000 rpm for 15 min, was additionally filtered through a cellulose acetate membrane (HAWP, MF-Millipore) with a pore size of 0.45 μm. The analysis was performed at 50°C, with a flow rate of 0.3 mL/min, using 0.002 M H_2SO_4 as the mobile phase. The injection volume was 3 μL.

Assessment of the extract effect on bifidobacterial. The cultivations were carried out in a CO_2 incubator CB-210 (Binder, Germany) with shaking (170 rpm) under anaerobic conditions (2% CO_2, 98% N_2) at 37°C for 10 h. The cultivation time corresponded to the final exponential growth phase. The inoculates were prepared under similar conditions in nutrient media without extracts for 17 h. Bifidobacteria cells were pre-washed by centrifugation (6,000 rpm, 4 min) and resuspended in sterile phosphate-buffered saline to a standard optical density (OD = 0.5). The prepared samples for monoculture fermentations were inoculated at 1% (v/v). Samples were taken at the initial and final time points of cultivation.

To assess the effect of extract phenolic concentrations on the growth of bifidobacteria and test-strain bacteria, serial two-fold dilutions of the preliminarily treated extracts were applied. Specifically, the extracts and a 70% (v/v) ethanol–water solution were mixed with distilled water in a 1:1 ratio and autoclaved as described above.

A series of two-fold dilutions, ranging from 2× to 32×, was prepared using the treated solutions. These extracts (corresponding to the maximum total phenolic concentration) and their dilutions were added to the nutrient medium. Inoculation and cultivation were performed as described above. Viable cells were counted at the initial and final (after 10 h) time points of cultivation.

The inoculates of the test strains (*B. cereus* and *S. aureus*) for both monoculture (negative control) and co-culture experiments were prepared, pre-washed, and resuspended to a standard optical density (OD = 0.5) under the same conditions as for bifidobacteria. Then, 0.2% (v/v) of the standardized cell suspensions was inoculated. The experimental conditions were identical to those used for bifidobacteria monoculture. Samples were taken at the initial and final time points of cultivation. The concentrations of lactic acid, acetic acid, and ethanol were determined by high-performance liquid chromatography. Cell enumeration was performed using the ten-fold serial dilution method.

Enumeration of bacteria. Ten-fold dilutions in sterile phosphate-buffered saline were plated on the appropriate media. Incubation was carried out under selective conditions to allow for the separate enumeration of bifidobacteria and the test strains. The dilutions were plated onto a bifidum medium and incubated at 37°C for 48 h for bifidobacteria enumeration. For the test strains, the dilutions were plated on LB agar and incubated aerobically at 37°C for 24 h. All measurements were performed in triplicate.

Evaluation of bifidobacteria antagonism against the test strains. The antagonistic activity of bifidobacteria against the test strains was evaluated using a previously proposed approach involving the synbiotic factor [36]. This method is based on the co-cultivation of the test strain with probiotics and the assessment of the antagonistic effect resulting from the production of lactic and acetic acids (metabolites of bifidobacteria). The synbiotic factor was calculated according to Eq. (1), using experimental data and previously determined inhibition constants:

$$SF = \frac{K_{iL}}{L + K_{iL}} \times \frac{K_{iA}}{A + K_{iA}} \quad (1)$$

where L, A are the concentrations of lactic and acetic acids, respectively, mg/mL; K_{iL}, K_{iA} are the inhibition constants for lactic and acetic acids, respectively, mg/mL; SF is the synbiotic factor indicating how many times the specific growth rate of the test strain will decrease due to inhibition by probiotic metabolites. The values of the inhibition constants for *B. cereus* and *S. aureus* were obtained from previous studies [37].

Determination of total phenols and identification of phenolic compounds. Total phenols in the extracts were determined using the Folin-Ciocalteu colorimetric method. Briefly, the Folin-Ciocalteu reagent (Central Drug House Ltd., India) was diluted ten-fold with bidistilled water. A sample of the extract (0.25 mL) was mixed with the diluted reagent (1.25 mL) and thoroughly shaken. After 3 min, a 7.5% (w/v) solution of Na_2CO_3 (Central Drug House (P) Ltd., India) was added. The mixture was shaken again and incubated in the dark for 2 h. Measurements were carried out using an SF-104 spectrophotometer (JSC Aquilon, Russia) at 765 nm. The results were presented as μg-equivalents of gallic acid per mL (μg GAE/mL).

UV-Vis spectroscopy (190–600 nm) was used to identify individual phenolic compounds, employing an SF-104 spectrophotometer (JSC Aquilon, Russia) with UV-WIN software for data processing. The baseline was measured using a 70% (v/v) ethanol–water solution. Each peak was identified by comparison with literature data according to the wavelength value [38–51].

Statistical analysis. All measurements were performed in triplicate with three biological replicates, and the results were expressed as the mean standard deviation (± SD). The data were analyzed using one-way ANOVA followed by Tukey's HSD post hoc test in Statistica 10 software. Statistical significance was set at $p = 0.05$.

RESULTS AND DISCUSSION

Effect of extracts on the growth of bifidobacterial. All the extracts were analyzed for total phenolic concentrations both before and after the treatment (Table 1). The concentrations decreased slightly, despite a preliminary two-fold dilution with water, presumably due to ethanol evaporation during autoclaving. Individual phenolic compounds in the extracts were identified using UV-Vis spectroscopy (Table 1). The compositions varied not only between the different berries but also between the extraction methods. In general, the sea buckthorn extracts were more diverse than the black currant extracts, and the supercritical fluid extracts were more diverse than the ethanol extracts. Catechin, epigallocatechin, quercetin, and rutin were detected in all the extracts.

The results of bifidobacteria monoculture fermentations in the media supplemented with ethanol and supercritical fluid extracts of black currant and sea buckthorn showed that flavonoids influenced the final probiotic cell count. The initial bacterial count in all the variants was 6.5 ± 0.1 log CFU/mL. We observed both positive and negative effects of the extracts on the final bacterial counts, relative to the control medium (Table 2).

All the extracts had a negative effect on the growth of *Bifidobacterium adolescentis* compared to the blank experiments. The strongest inhibitory effect was observed with the ethanol extract of black currant, where the final count was 1.30 log CFU/mL lower than in the blank experiment. The weakest effect was from the supercritical fluid extract of black currant, which resulted in a reduction of 0.77 log CFU/mL compared to the control medium. In the media with sea buckthorn extracts, the final viable cell count was approximately 1 log CFU/mL lower than in the blank experiments.

However, the influence of the extracts on *Bifidobacterium longum* was also negative. The ethanol extract of black currant exhibited the greatest suppressive effect

Table 1 Total phenols and phenolic compounds in the extracts

Extract	Total phenols, μg GAE/mL	Total phenols in treated extract, μg GAE/mL	Phenolic compounds
Black currant ethanol extract	2451.82 ± 36.18	2233.16 ± 26.11	Catechin, epicatechin, epigallocatechin, tannins, quercetin, rutin, anthocyanins, resveratrol
Black currant supercritical fluid extract	1342.71 ± 42.13	1264.72 ± 30.07	Catechin, epigallocatechin, tannins, ellagitannins, gallotannins, dihydroquercetin, resveratrol, quercetin, rutin
Sea buckthorn ethanol extract	5724.15 ± 27.31	5551.24 ± 34.54	Catechin, epigallocatechin, luteolin, quercetin, isorhamnetin, apigenin, *p*-coumaric acid, resveratrol, rutin
Sea buckthorn supercritical fluid extract	1183.92 ± 19.02	1042.24 ± 18.03	Catechin, epigallocatechin, tannins, isorhamnetin, luteolin, apigenin, quercetin, *p*-coumaric acid, naringenin, hesperetin, rutin

Table 2 Bifidobacteria final counts in the monocultures

Bifidobacteria species	Final count of bifidobacteria[1], log CFU/mL, in a medium[2] with				
	Ethanol (blank)	Ethanol extracts		Supercritical fluid extracts	
		Black currant	Sea buckthorn	Black currant	Sea buckthorn
Bifidobacterium adolescentis	7.88 ± 0.03[a]	6.58 ± 0.03*	6.95 ± 0.05*	7.11 ± 0.04*	6.83 ± 0.02*
Bifidobacterium longum	7.82 ± 0.04[a]	6.32 ± 0.02*	7.46 ± 0.09*	7.29 ± 0.05[b]	7.23 ± 0.03[b]
Bifidobacterium bifidum	8.49 ± 0.04[c]	8.18 ± 0.07[d,e]	8.51 ± 0.03[c]	8.11 ± 0.04[d,f]	8.86 ± 0.02[g]
Bifidobacterium breve	8.54 ± 0.07[c]	8.39 ± 0.05*	8.88 ± 0.06[g]	8.81 ± 0.03[g]	8.04 ± 0.04[f]
Bifidobacterium infantis	7.26 ± 0.02[b]	7.23 ± 0.04[b]	8.28 ± 0.03[e]	8.10 ± 0.04[d,f]	6.72 ± 0.02*

[1] – the values are mean ± SD of three measurements in triplicate. No significant difference ($p \leq 0.05$) was found among the values with the same letter, according to Tukey's HSD test. The values subscribed with an asterisk (*) significantly differ from all the other values. [2] – the procedure of introducing the extracts and a 70% (v/v) ethanol–water solution into the nutrient medium was the same

(1.56 log CFU/mL lower than the control), while the ethanol extract of sea buckthorn had the weakest suppressive effect (0.36 log CFU/mL lower than in the blank experiment). The final cell counts in all the media with the supercritical extracts did not differ significantly from one another ($p < 0.05$) and were approximately 0.56 log CFU/mL lower than in the blank experiment.

For *Bifidobacterium bifidum*, the supercritical fluid sea buckthorn extract had a positive effect, while the ethanol extract of sea buckthorn showed a neutral effect (no significant difference at $p < 0.05$). Both black currant extracts had a negative effect compared to the control group. However, this effect was relatively weak, with the final count being only 0.37 log CFU/mL lower than in the blank experiment. Notably, *B. bifidum* demonstrated one of the highest final counts (8.86 log CFU/mL) among the studied strains when grown in medium with the supercritical fluid extract of sea buckthorn.

The growth of *Bifidobacterium breve* was equally stimulated by the ethanol extract of sea buckthorn and the supercritical fluid extract of black currant, with increases of approximately 0.30 log CFU/mL over the blank experiment. The weakest negative effect on *B. breve* growth was observed in the medium with the ethanol extract of black currant, while the strongest negative effect was seen with the supercritical fluid extract of sea buckthorn, showing reductions of 0.16 and 0.50 log CFU/mL, respectively, compared to the control.

B. longum subsp. *infantis* showed the weakest growth (7.26 log CFU/mL) in the control medium among the studied strains. However, the effect of the extract components on its growth was similar to that observed for *B. breve*. The ethanol extract of sea buckthorn and the supercritical fluid extract of black currant significantly stimulated the growth of *B. infantis*, with the final counts 1.02 and 0.85 log CFU/mL higher than the blank value, respectively. In contrast, the supercritical fluid extract of sea buckthorn decreased the final count by 0.54 log CFU/mL. No significant difference ($p < 0.05$) was observed between the final counts in the control medium and in the medium containing the ethanol extract of black currant.

Thus, *B. adolescentis* and *B. longum* were the most sensitive to the suppression effect of black currant and sea buckthorn extracts, while the extraction method had a weak effect. The effect of the extracts on the growth of *B. bifidum* and *B. breve* was mainly moderate, and the growth of *B. infantis* was highly dependent on both the type of berries and the extraction method.

The effect of the extract concentration was evaluated for all bifidobacteria strains using serial two-fold dilutions. The final viable cell counts at various concentrations of total phenols (considered the principal active components of the extracts) are presented in Tables 3–6. Significant changes in bacterial growth, both inhibitory and stimulatory, were observed when total phenol concentrations ranged from about 26 to 57 μg GAE/mL.

Further increases up to the highest studied concentrations of total phenols (i.e., in non-diluted extracts) showed no substantial changes in final bifidobacteria

Table 3 Final cell counts for bifidobacteria and test strains in the monocultures at various concentrations of black currant ethanol extract

Bifidobacteria species	Concentration of total phenols from extract in medium, μg GAE/mL						
	223	121	57	30	13	7	0
Bifidobacteria, log CFU/mL							
Bifidobacterium adolescentis	6.58 ± 0.03	6.62 ± 0.02	6.68 ± 0.02	6.82 ± 0.05	7.15 ± 0.04	7.43 ± 0.02	7.88 ± 0.03
Bifidobacterium longum	6.32 ± 0.02	6.47 ± 0.04	6.64 ± 0.03	6.82 ± 0.02	6.98 ± 0.03	7.37 ± 0.01	7.82 ± 0.04
Bifidobacterium bifidum	8.18 ± 0.07	8.19 ± 0.03	8.25 ± 0.07	8.30 ± 0.05	8.38 ± 0.04	8.41 ± 0.06	8.49 ± 0.04
Bifidobacterium breve	8.39 ± 0.05	8.38 ± 0.05	8.41 ± 0.03	8.45 ± 0.05	8.48 ± 0.06	8.53 ± 0.04	8.54 ± 0.07
Bifidobacterium infantis	7.23 ± 0.04	7.20 ± 0.07	7.18 ± 0.03	7.21 ± 0.06	7.19 ± 0.03	7.31 ± 0.03	7.26 ± 0.02
Test strains, log CFU/mL							
Bacillus cereus	7.35 ± 0.05	7.35 ± 0.06	7.36 ± 0.09	7.35 ± 0.12	7.40 ± 0.14	7.42 ± 0.08	7.50 ± 0.07
Staphylococcus aureus	7.92 ± 0.04	7.93 ± 0.08	7.99 ± 0.09	8.07 ± 0.04	8.12 ± 0.11	8.25 ± 0.13	8.57 ± 0.25

Table 4 Final cell counts for bifidobacteria and test strains in the mono-cultures at various concentrations of the extracts

Bifidobacteria species	Concentration of total phenols from extract in medium, μg GAE/mL						
	555	278	139	69	35	17	0
Bifidobacteria, log CFU/mL							
Bifidobacterium adolescentis	6.95 ± 0.05	7.01 ± 0.05	7.03 ± 0.05	7.14 ± 0.05	7.39 ± 0.05	7.61 ± 0.05	7.88 ± 0.03
Bifidobacterium longum	7.46 ± 0.09	7.51 ± 0.06	7.59 ± 0.05	7.61 ± 0.07	7.63 ± 0.03	7.75 ± 0.05	7.82 ± 0.04
Bifidobacterium bifidum	8.51 ± 0.03	8.49 ± 0.06	8.50 ± 0.05	8.52 ± 0.06	8.49 ± 0.03	8.47 ± 0.05	8.49 ± 0.04
Bifidobacterium breve	8.88 ± 0.06	8.85 ± 0.06	8.81 ± 0.06	8.82 ± 0.06	8.72 ± 0.06	8.62 ± 0.06	8.54 ± 0.07
Bifidobacterium infantis	8.28 ± 0.03	8.13 ± 0.06	8.01 ± 0.02	7.82 ± 0.05	7.64 ± 0.04	7.42 ± 0.05	7.26 ± 0.02
Test strains, log CFU/mL							
Bacillus cereus	7.64 ± 0.08	7.63 ± 0.07	7.62 ± 0.07	7.60 ± 0.07	7.61 ± 0.07	7.55 ± 0.07	7.50 ± 0.07
Staphylococcus aureus	7.37 ± 0.13	7.40 ± 0.08	7.58 ± 0.11	7.66 ± 0.08	7.95 ± 0.01	8.12 ± 0.09	8.57 ± 0.25

Table 5 Final cell counts for bifidobacteria and test strains in the mono-cultures at various concentrations of black currant supercritical fluid extract

Bifidobacteria species	Concentration of total phenols from extract in medium, μg GAE/mL						
	126	63	32	16	8	4	0
Bifidobacteria, log CFU/mL							
Bifidobacterium adolescentis	7.11 ± 0.04	7.23 ± 0.07	7.27 ± 0.05	7.41 ± 0.06	7.52 ± 0.04	7.74 ± 0.06	7.88 ± 0.03
Bifidobacterium longum	7.29 ± 0.05	7.32 ± 0.07	7.41 ± 0.02	7.49 ± 0.05	7.58 ± 0.06	7.65 ± 0.07	7.82 ± 0.04
Bifidobacterium bifidum	8.11 ± 0.04	8.10 ± 0.02	8.12 ± 0.04	8.14 ± 0.01	8.25 ± 0.07	8.39 ± 0.08	8.49 ± 0.04
Bifidobacterium breve	8.81 ± 0.03	8.79 ± 0.07	8.80 ± 0.08	8.72 ± 0.03	8.63 ± 0.04	8.59 ± 0.08	8.54 ± 0.07
Bifidobacterium infantis	8.10 ± 0.04	7.94 ± 0.05	7.86 ± 0.08	7.79 ± 0.07	7.57 ± 0.06	7.38 ± 0.05	7.26 ± 0.02
Test strains, log CFU/mL							
Bacillus cereus	7.33 ± 0.06	7.31 ± 0.07	7.35 ± 0.05	7.39 ± 0.07	7.41 ± 0.07	7.48 ± 0.04	7.50 ± 0.07
Staphylococcus aureus	8.42 ± 0.11	8.40 ± 0.08	8.39 ± 0.09	8.43 ± 0.12	8.50 ± 0.18	8.51 ± 0.21	8.57 ± 0.25

Table 6 Final cells count for bifidobacteria and test strains in the mono-cultures at various concentrations of the extracts

Bifidobacteria species	Concentration of total phenols from extract in medium, μg GAE/mL						
	104	52	26	13	7	3	0
Bifidobacteria, log CFU/mL							
Bifidobacterium adolescentis	6.83 ± 0.02	6.87 ± 0.07	6.91 ± 0.05	7.02 ± 0.04	7.33 ± 0.06	7.61 ± 0.08	7.88 ± 0.03
Bifidobacterium longum	7.23 ± 0.03	7.25 ± 0.07	7.27 ± 0.02	7.33 ± 0.05	7.42 ± 0.07	7.59 ± 0.08	7.82 ± 0.04
Bifidobacterium bifidum	8.86 ± 0.02	8.84 ± 0.09	8.86 ± 0.06	8.81 ± 0.04	8.74 ± 0.06	8.62 ± 0.05	8.49 ± 0.04
Bifidobacterium breve	8.04 ± 0.04	8.05 ± 0.08	8.09 ± 0.11	8.12 ± 0.02	8.23 ± 0.01	8.36 ± 0.08	8.54 ± 0.07
Bifidobacterium infantis	6.72 ± 0.02	6.71 ± 0.03	6.74 ± 0.07	6.81 ± 0.03	6.92 ± 0.07	7.01 ± 0.09	7.26 ± 0.02
Test strains, log CFU/mL							
Bacillus cereus	7.26 ± 0.05	7.25 ± 0.07	7.25 ± 0.04	7.28 ± 0.09	7.31 ± 0.09	7.39 ± 0.07	7.50 ± 0.07
Staphylococcus aureus	8.19 ± 0.08	8.19 ± 0.08	8.21 ± 0.12	8.25 ± 0.08	8.31 ± 0.13	8.43 ± 0.06	8.57 ± 0.24

counts. Therefore, for cases with growth inhibition, these concentrations can be considered as the minimum inhibitory concentrations (Table 7). Exceptions were observed for *B. bifidum* with the ethanol extract of sea buckthorn and *B. infantis* with the ethanol extract of black currant, where the effect of total phenols remained neutral at all the studied concentrations. Growth stimulation was observed for *B. infantis* and *B. breve* with the ethanol extract of sea buckthorn and the supercritical fluid extract of black currant, as well as for *B. bifidum* with the supercritical fluid extract of sea buckthorn.

Gwiazdowska *et al*. [52] showed that the effect of phenolic compounds, particularly flavonoids, on the growth of bifidobacteria depends on the concentration, specific compound, and microorganism species involved, which is consistent with our results. The effect can be stimulating, neutral, or suppressive [53]. Therefore, the differences in bacterial growth observed in our study are likely due to variations in the qualitative composition of the extracts. Supercritical fluid extraction predominantly yields non-polar flavonoids (such as flavanols and flavanones), while the total polyphenol yield is often lower. In contrast, reflux thermal extraction using organic solvents typically results in a higher polyphenol yield due to the extraction of polar compounds, including anthocyanins and phenolic acids [54]. In the ethanolic gemmotherapy extract of black currant, about 80 flavonoids have been identified. The most abundant non-glycosidic flavonoids are luteolin, quercetin, and apigenin, which together account for 91.7% of the total flavonoid content, while the presence of kaempferol is relatively minor [53]. The polyphenolic composition of sea buckthorn berries includes gallic acid, catechin, epicatechin, *p*-coumaric acid, caffeic acid, ferulic acid, rutin, quercetin, resveratrol, myricetin, and others [55]. Among these, the most polar compounds, rutin, myricetin, and quercetin, are likely to predominate in alcoholic extracts.

Gwiazdowska *et al*. [52] also reported an inhibitory effect of quercetin and hesperidin on the growth of *B. adolescentis* NCFB 2004 and *B. bifidum* NCFB 2235. This effect was dose-dependent, with changes in concentration causing significant differences in bacterial growth rates. Another study found that galangin inhibited the growth of *B. adolescentis* JCM 1275T by 30–70%, while quercetin and fisetin caused only minor inhibition (~ 20%) [56]. These findings indicate that the effects of flavonoids are not only species-specific but also strain-specific. Thus, the qualitative composition of berry extracts plays a critical role in determining their biological activity. Further analysis of extract composition is needed to more accurately understand its influence on different *Bifidobacterium* strains, which will be addressed in future studies.

Effect of extracts on the production of lactic and acetic acids by bifidobacterial. The presence of black currant and sea buckthorn extracts in the nutrient media had a weak effect on lactic acid production by *B. adolescentis* (Table 8). The effect of the supercritical fluid sea buckthorn extract was statistically insignificant compared to the blank experiment ($p < 0.05$).

For *B. longum*, a slight stimulation of lactic acid production was observed (an increase of 0.12 to 0.19 mg/mL) in the media with all the extracts, except for the ethanol extract of sea buckthorn, which showed a neutral effect.

Lactic acid production by *B. bifidum* was not affected by the sea buckthorn ethanol extract or the black currant supercritical fluid extract ($p < 0.05$). However, the ethanol extract of black currant and the supercritical fluid extract of sea buckthorn increased lactic acid production by 0.22 and 0.48 mg/mL, respectively.

The ethanol extracts stimulated lactic acid production by *B. breve* relative to the control medium, with increases of 0.54 mg/mL (black currant) and 0.31 mg/mL (sea buckthorn). The supercritical fluid extract of black currant had no effect on *B. breve*, while the supercritical fluid extract of sea buckthorn reduced lactic acid production by 0.11 mg/mL compared to the control.

A similar pattern was observed for *B. infantis*. Lactic acid production in the media with the supercritical fluid extracts did not differ significantly ($p < 0.05$), but greater stimulation was observed with the sea buckthorn ethanol extract, which increased lactic acid levels by 0.27 mg/mL compared to the blank.

A similar pattern was observed for acetic acid production (Table 9). None of the extracts significantly affected acetic acid production by *B. adolescentis* compared

Table 7 The minimum inhibitory concentration of total phenols, μg GAE/mL, for bifidobacteria and test strains

Cultures	Ethanol extract		Supercritical fluid extract	
	Black currant	Sea buckthorn	Black currant	Sea buckthorn
Bifidobacteria				
Bifidobacterium adolescentis	57.0 ± 0.5	140.0 ± 0.5	32.0 ± 0.5	26.0 ± 0.5
Bifidobacterium longum	30.0 ± 0.5	35.0 ± 0.5	32.0 ± 0.5	13.0 ± 0.5
Bifidobacterium bifidum	57.0 ± 0.5	n.a.	17.0 ± 0.5	26.0 ± 0.5*
Bifidobacterium breve	57.0 ± 0.5	70.0 ± 0.5*	32.0 ± 0.5*	13.0 ± 0.5
Bifidobacterium infantis	n.a.	140.0 ± 0.5*	17.0 ± 0.5*	26.0 ± 0.5
Test strains				
Bacillus cereus	n.a.	n.a.	n.a.	n.a.
Staphylococcus aureus	13.0 ± 0.5	140.0 ± 0.5	n.a.	7.0 ± 0.5

n.a. – not affected; * – shows maximum growth stimulation

Table 8 Lactic acid production by bifidobacteria monocultures

Bifidobacteria species	Lactic acid production[1], mg/mL, in a medium[2] with				
	Ethanol (blank)	Ethanol extract		Supercritical fluid extract	
		Black currant	Sea buckthorn	Black currant	Sea buckthorn
Bifidobacterium adolescentis	0.53 ± 0.02[a]	0.57 ± 0.02[b]	0.60 ± 0.02[b]	0.59 ± 0.02[b]	0.56 ± 0.02[a,b]
Bifidobacterium longum	0.90 ± 0.04[c]	1.02 ± 0.05[d]	0.94 ± 0.04[c]	1.09 ± 0.05[e]	1.03 ± 0.05[d]
Bifidobacterium bifidum	0.65 ± 0.03[f]	0.87 ± 0.04[c]	0.62 ± 0.02[b,f]	0.66 ± 0.03[f]	1.13 ± 0.05*
Bifidobacterium breve	0.76 ± 0.03[g]	1.30 ± 0.06*	1.07 ± 0.05*	0.72 ± 0.03[g]	0.65 ± 0.03[f]
Bifidobacterium infantis	0.60 ± 0.02[b]	0.65 ± 0.02[f]	0.87 ± 0.04[c]	0.61 ± 0.02[b,e]	0.61 ± 0.02[b]

[1] – the values are mean ± SD of three measurements in triplicate. No significant difference ($p \leq 0.05$) was found among the values with the same letter, according to Tukey's HSD test. The values subscribed with an asterisk (*) significantly differ from all other values. [2] – the procedure of introducing the extracts and a 70% (v/v) ethanol–water solution into the nutrient medium was the same

Table 9 Acetic acid production by bifidobacteria monocultures

Bifidobacteria species	Acetic acid production[1], mg/mL, in a medium[2] with				
	Ethanol (blank)	Ethanol extract		Supercritical fluid extract	
		Black currant	Sea buckthorn	Black currant	Sea buckthorn
Bifidobacterium adolescentis	0.72 ± 0.03[a]	0.71 ± 0.03[a]	0.80 ± 0.03[b]	0.76 ± 0.03[a,b]	0.77 ± 0.03[a,b]
Bifidobacterium longum	1.19 ± 0.05[e]	1.16 ± 0.05[c,d]	1.23 ± 0.05[e]	1.37 ± 0.06[e]	1.24 ± 0.05[e,f]
Bifidobacterium bifidum	0.99 ± 0.04[g]	1.29 ± 0.05[f]	1.03 ± 0.04[g]	1.13 ± 0.05[d]	1.81 ± 0.08*
Bifidobacterium breve	1.10 ± 0.05[d]	2.07 ± 0.09*	1.62 ± 0.07*	1.40 ± 0.06[e]	1.13 ± 0.05[d]
Bifidobacterium infantis	0.73 ± 0.03[a]	0.74 ± 0.03[a,b]	1.49 ± 0.06*	1.01 ± 0.04[g]	0.79 ± 0.04[b]

[1] – the values are mean ± SD of three measurements in triplicate. No significant difference ($p \leq 0.05$) was found among the values with the same letter, according to Tukey's HSD test. The values subscribed with an asterisk (*) significantly differ from all other values. [2] – the procedure of introducing the extracts and a 70% (v/v) ethanol–water solution into the nutrient medium was the same

to the blank experiment ($p < 0.05$), except for the sea buckthorn ethanol extract, which weakly stimulated the synthesis.

For *B. longum*, acetic acid production in the media with the extracts did not differ significantly from the blank ($p < 0.05$). The exception was the supercritical fluid extract of black currant, which increased the acetic acid concentration by 0.18 mg/mL compared to the control.

When *B. bifidum* was cultivated in the medium with the sea buckthorn ethanol extract, acetic acid levels were comparable to the control ($p < 0.05$). However, stimulation was observed with all the other extracts. The strongest effect (0.82 mg/mL increase compared to the control) was observed with the supercritical fluid extract of sea buckthorn, while the weakest effect (0.14 mg/mL increase) was noted with the supercritical fluid extract of black currant.

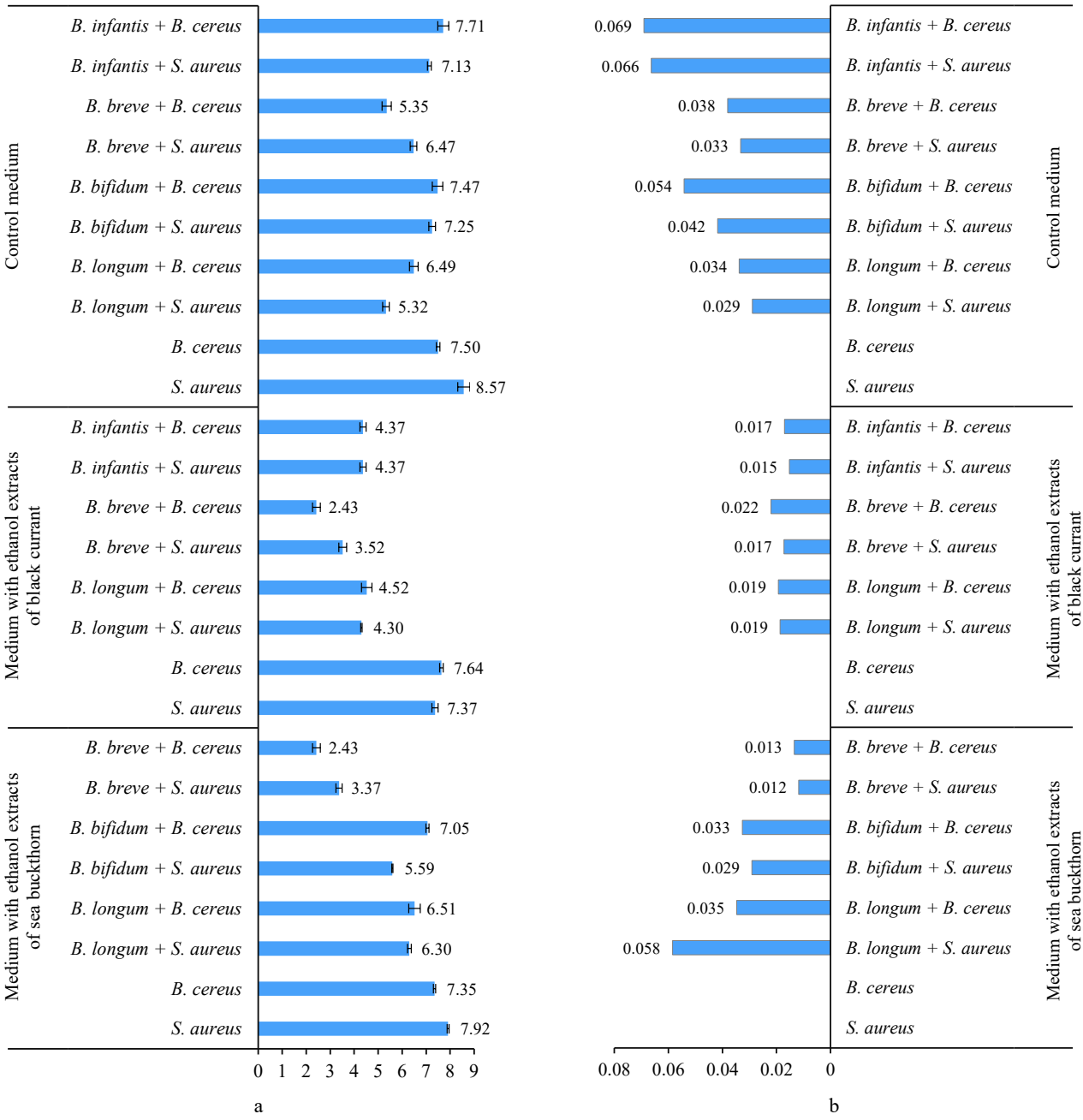
Stimulation of acetic acid production by *B. breve* was observed in the media with most extracts. The ethanol extract of black currant produced the strongest effect, increasing acetic acid levels by 0.97 mg/mL over the control, whereas the supercritical fluid extract of sea buckthorn had no significant effect.

For *B. infantis*, the supercritical fluid extract of sea buckthorn and the ethanol extract of black currant had no significant effect on acetic acid synthesis ($p < 0.05$). In contrast, the ethanol extract of sea buckthorn and the supercritical fluid extract of black currant stimulated the production, increasing its levels by 0.76 and 0.28 mg/mL, respectively, compared to the blank experiment.

The data on the stimulation or suppression of lactic and acetic acid production by bifidobacteria in the presence of flavonoids are relatively limited. In an *in vitro* batch colonic fermentation study, the addition of polyphenol-enriched extracts from three Chilean boiled beans (extracted with a ethanol–water solution, 7:3) did not influence acetate production, with acetate levels not being significantly different from those in the negative control [57]. In another study, polyphenols, particularly gallic acid, were shown to reduce short-chain fatty acid synthesis in the gut microbiota of mice *in vivo*, while simultaneously increasing polysaccharide and bile acid metabolism [58]. In contrast, our study found neutral or positive effects of the extracts on organic acid production by bifidobacteria. Particularly, significant stimulation of acid production was observed for *B. bifidum* with the supercritical fluid extract of sea buckthorn, for *B. breve* with the black currant ethanol extract, and for *B. infantis* with the sea buckthorn ethanol extract. These results suggest that flavonoids may stimulate the catabolic activity of bifidobacteria, leading to increased production of lactic and acetic acids [59]. In our study, the effect was clearly species-specific, highlighting the importance of selecting compatible components when designing synbiotic compositions. Since organic acids are the key factors in the inhibition of intestinal pathogens and food contaminants by probiotics, their enhanced production can be exploited to develop targeted synbiotic formulations aimed at suppressing pathogen growth.

Antagonism of bifidobacteria against test strains in co-culture studies. The suppression of pathogen growth by probiotics is known to be mediated by the production of several substances, including organic acids. In addition, prebiotics can enhance their antagonistic activity.

To study the antagonistic effect of synbiotic compositions (bifidobacteria + berry extract) against the test strains of intestinal pathogens, we selected three bifidobacteria strains (*B. longum*, *B. bifidum*, and *B. breve*) based on their highest accumulation of organic acids in the respective nutrient media variants. Since acid production by the bifidobacteria monocultures was higher in the media with ethanol extracts, supercritical fluid extracts were excluded from this part of analysis. The final counts of the test strains (Fig. 1a) co-cultured with the bifidobacteria in the media with black currant or sea buckthorn extracts were compared with those for the co-cultures in the control extract-free medium (blank) and the test strain monocultures (negative blank). As an additional measure of synbiotic antagonism, the previously proposed synbiotic factor was applied (Fig. 1b). The synbiotic factor indicates how many times the specific growth rate of the test strain is reduced as a result of inhibition by probiotic metabolites (lactic and acetic acids) [36]. A lower synbiotic factor value corresponds to a lower specific growth rate of the test strain and, consequently, a lower final bacterial count.



Antagonism is expressed through the growth of test strain cells (final count) in the co-cultures with bifidobacteria in the media with the extracts or in the control medium (blank), and th rough the synbiotic factor based on the final concentrations of lactic and acetic acids. Data on test strain growth in all the media are also included to demonstrate the solo effects of the extracts (negative control)

Figure 1 Effect of black currant and sea buckthorn ethanol extracts on the antagonistic activity of bifidobacteria against *Bacillus cereus* and *Staphylococcus aureus*: (a) final count of test-strain cells, log CFU/mL; (b) synbiotic factor

Antagonism is expressed through the growth of test strain cells (final count) in the co-cultures with bifidobacteria in the media with the extracts or in the control medium (blank), and through the synbiotic factor based on the final concentrations of lactic and acetic acids. Data on test strain growth in all the media are also included to demonstrate the solo effects of the extracts (negative control)

Both black currant and sea buckthorn extracts had a weak effect on the growth of *Bacillus cereus* in the monoculture. In the control medium (without extracts), the test strain's count reached 7.5 log CFU/mL. In the medium with sea buckthorn extract, the count was 0.14 log CFU/mL higher, whereas in the medium with black currant extract, it was 0.15 log CFU/mL lower. The suppression of *Staphylococcus aureus* growth by the extracts in the monoculture showed more variation. In the control medium, the test strain reached 8.57 log CFU/mL at the end of fermentation. In the presence of sea buckthorn and black currant extracts, the final counts were 7.37 log CFU/mL and 7.92 log CFU/mL, respectively. Thus, sea buckthorn extract showed the strongest suppression of *S. aureus* growth in the absence of probiotics. Additionally, we determined the minimum inhibitory concentrations of total phenols for each extract (Table 7).

In the co-culture experiments in the control medium (without extracts), different bifidobacteria strains showed varying levels of antagonism against *B. cereus*. No suppression was observed in the co-culture with *B. infantis* or *B. bifidum* (final counts were 7.71 and 7.47 log CFU/mL, respectively). *B. longum* decreased the final count of *B. cereus* by 0.99 log CFU/mL compared to the monoculture, while *B. breve* showed the greatest antagonistic effect, reducing the test strain's count by 2.15 log CFU/mL. For *S. aureus*, the co-culture with any bifidobacteria strain in the control medium resulted in a lower final count compared to the monoculture. *B. infantis* and *B. bifidum* had moderate antagonistic effects, reducing the count by 1.44 and 1.32 log CFU/mL, respectively. The strongest suppression was observed with *B. longum*, which decreased the final count of *S. aureus* by 3.25 log CFU/mL compared to the monoculture.

In the co-cultures (test strains + bifidobacteria) in the media containing black currant extract, *B. breve* had the most pronounced antagonistic effect, reducing the final counts of *S. aureus* and *B. cereus* by 4.5 and 4.9 log CFU/mL, respectively, compared to their monocultures. The antagonistic effects of *B. longum* and *B. bifidum* in combination with black currant extract were significantly lower than those of *B. breve*. These results are consistent with the levels of organic acid production observed in the monocultures, suggesting a species-specific interaction with the extract components. The highest total organic acid production was recorded in the combination of *B. breve* with the ethanol extract of black currant. Notably, this extract significantly enhanced the antagonistic activity of *B. breve* against both test strains. It also increased the antagonism of *B. longum* and *B. bifidum* against *S. aureus* when compared to the co-cultures in the control medium. When co-cultured with *S. aureus,* the two bifidobacteria had an additive antagonistic effect, likely resulting from the combined effects of their metabolites and the extract components. In contrast, the combination of *B. breve* with black currant extract demonstrated a clear synergistic effect, as the observed suppression exceeded the sum of the individual effects. This is further supported by the lowest synbiotic factor values, calculated as 0.013 for *B. cereus* and 0.012 for *S. aureus* co-cultured with *B. breve*. In comparison, the co-culture of *B. longum* with *S. aureus* produced the highest synbiotic factor value (0.058), indicating the lowest efficiency of this synbiotic combination against the test strain.

In the co-cultures (test strains + bifidobacteria) in the media containing sea buckthorn extract, the greatest antagonistic effect against both test strains was again demonstrated by *B. breve*. In this medium, the final counts of *S. aureus* and *B. cereus* were reduced by 3.8 and 5.2 log CFU/mL, respectively, compared to their respective monocultures. *B. longum* and *B. infantis* also actively suppressed the growth of the pathogens in the presence of sea buckthorn extract, each reducing the final count by approximately 3 log CFU/mL relative to the monocultures. Notably, in all the co-culture variants, antagonistic activity was higher in the presence of extract components than in the control medium (without extracts). The synbiotic factor values were also lower for all combinations with sea buckthorn extract compared to the control medium, confirming increased inhibitory efficiency. The most pronounced difference in the synbiotic factor values was observed in the co-cultures with *B. infantis*, which showed weak suppression of pathogen growth in the absence of the extracts. In contrast, when sea buckthorn extract was present, the differences in final test strain counts between the monocultures and the co-cultures were substantial, indicating a clear synergistic effect.

The antimicrobial activity of plant polyphenolic compounds, including flavonoids, against pathogens has been demonstrated in several studies. Suppressive effects on bacterial growth have been reported for both individual flavonoids and whole plant extracts, which typically contain a complex mixture of active compounds [60]. Antimicrobial activity against various strains of *S. aureus* has been shown for alcoholic extracts of rosemary [61], ethanol extracts of sage (containing limonene, among other compounds) [62], *Heliotropium europaeum* L. ethanol extracts [63], and ethanol extracts of thyme and sage (which include caffeic acid) [64]. Among individual flavonoids, quercetin, morin, naringenin, and kaempferol have demonstrated inhibitory effects on staphylococcal growth [65]. The growth of *B. cereus* was also inhibited by ethanol extracts of thyme and sage [64], whereas many other plant extracts had no significant effect on this species [60].

While the influence of flavonoids on the growth of bifidobacteria and the production of organic acids is

relatively well studied, data on their ability to activate antagonistic activity are limited. Nonetheless, several studies have examined the effect of prebiotics on the antagonistic activity of probiotics against various pathogens in co-culture *in vitro* experiments. For example, the suppression of *Clostridioides difficile* by *B. infantis* JCM 1222 was stronger in a medium containing the next-generation prebiotic galactosyl-*β*1,4-L-rhamnose compared to a glucose-containing medium [66]. *Lactiplantibacillus plantarum* and *Lacticaseibacillus rhamnosus* inhibited the growth of *Salmonella* and *Shigella* strains when cultured in the media supplemented with oligosaccharide extracts from various plant sources [67]. Similarly, the antimicrobial activity of *Lactobacillus* strains against *Klebsiella oxytoca* was demonstrated in co-culture with commercial prebiotic fructans [68]. The formulation of synbiotic preparations has also been supported by a series of *in vitro* experiments, where the use of commercial prebiotics as carbon sources enhanced the antagonistic activity of *Lactobacillus* strains against *Salmonella* spp. and *Listeria monocytogenes* [69]. Bifidobacteria combined with fructans extracted from burdock root or Jerusalem artichoke tubers (precipitated with 20% ethanol) exhibited enhanced antagonistic activity against *S. aureus* ATCC 43300 when applied as synbiotics [70]. In our study, we employed a similar approach to investigate the influence of black currant and sea buckthorn extracts on the antagonistic activity of *Bifidobacterium* strains against *B. cereus* and *S. aureus*. The results revealed a promising synergistic synbiotic composition involving *B. breve* and both black currant and sea buckthorn ethanol extracts.

CONCLUSION

We studied the effects of ethanol and supercritical fluid extracts of black currant and sea buckthorn on the growth of five *Bifidobacterium* species currently accepted as probiotics. The phenolic components of the berries demonstrated stimulating, neutral, or suppressive effects on probiotic growth and organic acid production, depending on both the type of raw material and the extraction method. In addition, we evaluated the synergistic potential of the *Bifidobacterium* strains and the ethanol extracts based on their ability to suppress the growth of intestinal pathogens in co-culture. The results revealed that black currant and sea buckthorn polyphenols may act as highly selective and strain-specific prebiotics. Among the tested combinations, synbiotic compositions involving *B. breve* and either extract were the most promising, with strong antagonistic effects against *Bacillus cereus* and *Staphylococcus aureus*. Future research will focus on a more detailed characterization of polyphenol composition to better understand the mechanisms underlying these effects. Additionally, there is a need for optimizing supercritical fluid extraction techniques based on the biological activity of the resulting extracts.

CONTRIBUTION

Conceptualization, V.I. Panfilov and B.A. Karetkin; methodology, E.V. Guseva and S.A. Evdokimova; validation, S.A. Evdokimova and N.Yu. Khromova; formal analysis, S.A. Evdokimova, A.T. Shevchenko and K.M. Demkin; investigation, S.A. Evdokimova, A.T. Shevchenko and K.M. Demkin; data curation, S.A. Evdokimova and A.T. Shevchenko; writing – original draft preparation, S.A. Evdokimova; writing – review and editing, S.A Evdokimova, B.A. Karetkin and E.V. Guseva; visualization, B.A. Karetkin; supervision, N.B. Gradova and V.I. Panfilov; project administration, V.I. Panfilov; funding acquisition, V.I. Panfilov. All the authors have read and approved the final version of the manuscript.

CONFLICT OF INTEREST

The authors declare that there are no competing interest regarding this publication.

REFERENCES

1. Stachelska MA, Karpiński P, Kruszewski B. A comprehensive review of biological properties of flavonoids and their role in the prevention of metabolic, cancer and neurodegenerative diseases. Applied Sciences. 2025;15(19):10840. https://doi.org/10.3390/app151910840
2. Williams RJ, Spencer JPE, Rice-Evans C. Flavonoids: Antioxidants or signalling molecules? Free Radical Biology and Medicine. 2004;36(7):838–849. https://doi.org/10.1016/j.freeradbiomed.2004.01.001
3. Winkel-Shirley B. Flavonoid biosynthesis. A colorful model for genetics, biochemistry, cell biology, and biotechnology. Plant Physiology. 2001;126(2):485–493. https://doi.org/10.1104/pp.126.2.485
4. Serafini M, Peluso I, Raguzzini A. Flavonoids as anti-inflammatory agents. Proceedings of the Nutrition Society. 2010;69(3):273–278. https://doi.org/10.1017/S002966511000162X
5. Kumar S, Pandey AK. Chemistry and biological activities of flavonoids: An overview. The Scientific World Journal. 2013;2013(1):162750. https://doi.org/10.1155/2013/162750
6. Manach C, Scalbert A, Morand C, Rémésy C, Jiménez L. Polyphenols: Food sources and bioavailability. The American Journal of Clinical Nutrition. 2004;79(5):727–747. https://doi.org/10.1093/ajcn/79.5.727
7. Kähkönen MP, Hopia AI, Heinonen M. Berry phenolics and their antioxidant activity. Journal of Agricultural and Food Chemistry. 2001;49(8):4076–4082. https://doi.org/10.1021/jf010152t

8. Guseva EV, Khromova NYu, Karetkin BA, Artemiev AI, Demkin KM, *et al*. Biological value of berry polyphenols and prospects for supercritical extraction application for their isolation: A review. Foods and Raw Materials. 2026;14(1): 1–13. https://doi.org/10.21603/2308-4057-2026-1-653
9. Skrovankova S, Sumczynski D, Mlcek J, Jurikova T, Sochor J. Bioactive compounds and antioxidant activity in different types of berries. International Journal of Molecular Sciences. 2015;16(10):24673–24706. https://doi.org/10.3390/ijms161024673
10. Määttä K, Kamal-Eldin A, Törrönen R. Phenolic compounds in berries of black, red, green, and white currants (*Ribes* sp.). Antioxidants & Redox Signaling. 2001;3(6):981–993. https://doi.org/10.1089/152308601317203521
11. Tang J, Zhang H, Wu R, Liu H, He K, *et al*. Sea buckthorn: A potential prebiotic and promising functional ingredient for fermented dairy products. Journal of Future Foods. 2026;6(3):348–360. https://doi.org/10.1016/j.jfutfo.2025.04.006
12. Kodentsova VM, Risnik DV, Serba EM, Abramova IM, Sokolova EN, *et al*. Prospects for integrated processing of black currant. Food Processing: Techniques and Technology. 2024;54(3):621–632. (In Russ.) https://doi.org/10.21603/2074-9414-2024-3-2525
13. Pietta PG. Flavonoids as antioxidants. Journal of Natural Products. 2000;63(7):1035–1042. https://doi.org/10.1021/np9904509
14. García-Lafuente A, Guillamón E, Villares A, Rostagno MA, Martínez JA. Flavonoids as anti-inflammatory agents: Implications in cancer and cardiovascular disease. Inflammation Research. 2009;58:537–552. https://doi.org/10.1007/s00011-009-0037-3
15. Murota K, Nakamura Y, Uehara M. Flavonoid metabolism: The interaction of metabolites and gut microbiota. Bioscience, Biotechnology & Biochemistry. 2018;82(4):600–610. https://doi.org/10.1080/09168451.2018.1444467
16. Yadav MK, Kumari I, Singh B, Sharma KK, Tiwari SK. Probiotics, prebiotics and synbiotics: Safe options for next-generation therapeutics. Applied Microbiology and Biotechnology. 2022;106:505–521. https://doi.org/10.1007/s00253-021-11646-8
17. Vesnina A D, Frolova A S, Chekushkina DYu, Milentyeva IS, Luzyanin SL, *et al*. Gut microbiota and its role in development of chronic disease and aging. Foods and Raw Materials. 2026;14(1):174–197. https://doi.org/10.21603/2308-4057-2026-1-668
18. Levy M, Kolodziejczyk AA, Thaiss CA, Elinav E. Dysbiosis and the immune system. Nature Reviews Immunology. 2017;17:219–232. https://doi.org/10.1038/nri.2017.7
19. Ruiz de la Bastida A, Peirotén Á, Langa S, Álvarez I, Arqués JL, *et al*. Metabolism of flavonoids and lignans by lactobacilli and bifidobacteria strains improves the nutritional properties of flaxseed-enriched beverages. Food Research International. 2021;147:110488. https://doi.org/10.1016/j.foodres.2021.110488
20. Liang A, Leonard W, Beasley JT, Fang Z, Zhang P, *et al*. Anthocyanins-gut microbiota-health axis: A review. Critical Reviews in Food Science and Nutrition. 2024;64(21):7563–7588. https://doi.org/10.1080/10408398.2023.2187212
21. Louis P, Hold GL, Flint HJ. The gut microbiota, bacterial metabolites and colorectal cancer. Nature Reviews Microbiology. 2014;12:661–672. https://doi.org/10.1038/nrmicro3344
22. Kähkönen MP, Hopia AI, Heinonen M. Berry phenolics and their antioxidant activity. Journal of Agricultural and Food Chemistry. 2001;49(8):4076–4082. https://doi.org/10.1021/jf010152t
23. Heinonen M. Antioxidant activity and antimicrobial effect of berry phenolics – A Finnish perspective. Molecular Nutrition & Food Research. 2007;51:684–691. https://doi.org/10.1002/mnfr.200700006
24. Zeb A. Chemical and nutritional constituents of sea buckthorn juice. Pakistan Journal of Nutrition. 2004;3(2):99–106. https://doi.org/10.3923/pjn.2004.99.106
25. Gopalan A, Reuben SC, Ahmed S, Darvesh AS, Hohmann J, *et al*. The health benefits of blackcurrants. Food & Function. 2012;3(8):795–809. https://doi.org/10.1039/c2fo30058c
26. Donno D, Cerutti AK, Mellano MG, Prgomet Z, Beccaro GL. Serviceberry, a berry fruit with growing interest of industry: Physicochemical and quali-quantitative health-related compound characterisation. Journal of Functional Foods. 2016;26:157–166. https://doi.org/10.1016/j.jff.2016.07.014
27. Solverson PM, Rumpler WV, Leger JL, Redan BW, Ferruzzi MG, *et al*. Blackberry feeding increases fat oxidation and improves insulin sensitivity in overweight and obese males. Nutrients. 2018;10(8):1048. https://doi.org/10.3390/nu10081048
28. Wrona O, Rafińska K, Możeński C, Buszewski B. Supercritical fluid extraction of bioactive compounds from plant materials. Journal of AOAC International. 2017;100(6):1624–1635. https://doi.org/10.5740/jaoacint.17-0232
29. Williams JR, Clifford AA, Al-Saidi SH. Supercritical fluids and their applications in biotechnology and related areas. Molecular Biotechnology. 2002;22:263–286. https://doi.org/10.1385/MB:22:3:263

30. Singh S, Verma DK, Thakur M, Tripathy S, Patel AR, *et al*. Supercritical fluid extraction (SCFE) as green extraction technology for high-value metabolites of algae, its potential trends in food and human health. Food Research International. 2021;150(Part A):110746. https://doi.org/10.1016/j.foodres.2021.110746
31. Azmir J, Zaidul ISM, Rahman MM, Sharif KM, Mohamed A, *et al*. Techniques for extraction of bioactive compounds from plant materials: A review. Journal of Food Engineering. 2013;117(4):426–436. https://doi.org/10.1016/j.jfoodeng.2013.01.014
32. Frolova AS, Fokina AD, Milentyeva IS, Asyakina LK, Proskuryakova LA, *et al*. The biological active substances of *Taraxacum officinale* and *Arctium lappa* from the Siberian Federal District. International Journal of Molecular Sciences. 2024;25(6):3263. https://doi.org/10.3390/ijms25063263
33. Rossi M, Corradini C, Amaretti A, Nicolini M, Pompei A, *et al*. Fermentation of fructooligosaccharides and inulin by bifidobacteria: A comparative study of pure and fecal cultures. Applied and Environmental Microbiology. 2005;71(10):6150–6158. https://doi.org/10.1128/AEM.71.10.6150-6158.2005
34. Scherer R, Rybka ACP, Ballus CA, Meinhart AD, Filho JT, *et al*. Validation of a HPLC method for simultaneous determination of main organic acids in fruits and juices. Food Chemistry. 2012;135(3):150–154. https://doi.org/10.1016/j.foodchem.2012.03.111
35. Zaky AS, Pensupa N, Andrade-Eiroa Á, Tucker GA, Du C. A new HPLC method for simultaneously measuring chloride, sugars, organic acids and alcohols in food samples. Journal of Food Composition and Analysis. 2017;56:25–33. https://doi.org/10.1016/j.jfca.2016.12.010
36. Karetkin BA, Guseva EV, Evdokimova SA, Mishchenko AS, Khabibulina NV, *et al*. A quantitative model of *Bacillus cereus* ATCC 9634 growth inhibition by bifidobacteria for synbiotic effect evaluation. World Journal of Microbiology and Biotechnology. 2019;35:89. https://doi.org/10.1007/s11274-019-2665-2
37. Evdokimova S, Karetkin B, Nokhaeva V, Guseva E, Shakir I. Minimum inhibitory concentrations of organic acids against foodborne opportunistic microbial pathogens. In: Proceedings of the 21st Intern. Multidisciplinary Sci. GeoConf. SGEM. Albena, 2021:193–200. https://doi.org/10.5593/sgem2021/6.1/s25.25
38. Yilmaz Y, Toledo RT. Major flavonoids in grape seeds and skins: Antioxidant capacity of catechin, epicatechin, and gallic acid. Journal of Agricultural and Food Chemistry. 2004;52(2):255–260. https://doi.org/10.1021/jf030117h
39. Fu M, Zhang L, Killeen R, Onugwu KE, McCarrick RM, *et al*. Green tea polyphenol epigallocatechin gallate interactions with copper-serum albumin. Molecules. 2025;30(2):320. https://doi.org/10.3390/molecules30020320
40. Elgailani IEH, Ishak CY. Methods for extraction and characterization of tannins from some acacia species of Sudan. Pakistan Journal of Analytical & Environmental Chemistry. 2016;17(1):43–49. https://doi.org/10.21743/pjaec/2016.06.007
41. Pawlak-Lemanska K, Szymusiak H, Tyrakowska B, Zielinski R, Soffers AEMF, *et al*. The influence of pH on antioxidant properties and the mechanism of antioxidant action of hydroxyflavones. Free Radical Biology and Medicine. 2001;31(7):869–881. https://doi.org/10.1016/S0891-5849(01)00638-4
42. Giusti MM, Wrolstad RE. Characterization and measurement with UV-Visible spectroscopy. Current Protocols in Food Analytical Chemistry. Hoboken: John Wiley & Sons; 2001, pp. F1.2.1–F1.2.13. https://doi.org/10.1002/0471142913.faf0102s00
43. Frémont L. Biological effects of resveratrol. Life Sciences. 2000;66(8):663–673. https://doi.org/10.1016/S0024-3205(99)00410-5
44. Quideau S, Feldman KS. Ellagitannin chemistry. Chemical Reviews. 1996;96(1):475–504. https://doi.org/10.1021/cr940716a
45. Niemetz R, Gross GG. Enzymology of gallotannin and ellagitannin biosynthesis. Phytochemistry. 2005;66(17):2001–2011. https://doi.org/10.1016/j.phytochem.2005.01.009
46. Zhang Y, Yu J, Dong XD, Ji HY. Research on characteristics, antioxidant and antitumor activities of dihydroquercetin and its complexes. Molecules. 2018;23(1):20. https://doi.org/10.3390/molecules23010020
47. Hopia A, Heinonen M. Antioxidant activity of flavonol aglycones and their glycosides in methyl linoleate. Journal of the American Oil Chemists' Society. 1999;76:139–144. https://doi.org/10.1007/s11746-999-0060-0
48. Kahraman N, Karadag R. Characterization of sixteenth to nineteenth century ottoman silk brocades by scanning electron microscopy – energy dispersive X-ray spectroscopy and high-performance liquid chromatography. Analytical Letters. 2017;50(10):1553–1567. https://doi.org/10.1080/00032719.2016.1236264
49. De Souza LA, Soeiro MM, De Almeida WB. A DFT study of molecular structure and ^{1}H NMR, IR, and UV-Vis spectrum of Zn(II)-kaempferol complexes: A metal-flavonoid complex showing enhanced anticancer activity. International Journal of Quantum Chemistry. 2018;118:e25773. https://doi.org/10.1002/qua.25773

50. Robbins RJ. Phenolic acids in foods: An overview of analytical methodology. Journal of Agricultural and Food Chemistry. 2003;51(10):2866–2887. https://doi.org/10.1021/jf026182t

51. Gil-Izquierdo A, Gil MI, Ferreres F, Tomás-Barberán FA. *In vitro* availability of flavonoids and other phenols in orange juice. Journal of Agricultural and Food Chemistry. 2001;49(2):1035–1041. https://doi.org/10.1021/jf0000528

52. Gwiazdowska D, Juś K, Jasnowska-Małecka J, Kluczyńska K. The impact of polyphenols on *Bifidobacterium* growth. Acta Biochimica Polonica. 2015;62(4):895–901. https://doi.org/10.18388/abp.2015_1154

53. Téglás T, Mihok E, Cziáky Z, Oláh NK, Nyakas C, *et al*. The flavonoid rich black currant (*Ribes nigrum*) ethanolic gemmotherapy extract elicits neuroprotective effect by preventing microglial body swelling in hippocampus and reduces serum TNF-*α* level: Pilot study. Molecules. 2023;28(8):3571. https://doi.org/10.3390/molecules28083571

54. Pereira P, Cebola MJ, Oliveira MC, Bernardo-Gil MG. Supercritical fluid extraction vs conventional extraction of myrtle leaves and berries: Comparison of antioxidant activity and identification of bioactive compounds. The Journal of Supercritical Fluids. 2016;113:1–9. https://doi.org/10.1016/j.supflu.2015.09.006

55. Attri S, Sharma K, Raigond P, Goel G. Colonic fermentation of polyphenolics from Sea buckthorn (*Hippophae rhamnoides*) berries: Assessment of effects on microbial diversity by principal component analysis. Food Research International. 2018;105:324–332. https://doi.org/10.1016/j.foodres.2017.11.032

56. Kawabata K, Sugiyama Y, Sakano T, Ohigashi H. Flavonols enhanced production of anti-inflammatory substance(s) by *Bifidobacterium adolescentis*: Prebiotic actions of galangin, quercetin, and fisetin. Biofactors. 2013;39(4):422–429. https://doi.org/10.1002/biof.1081

57. Nina N, Bressa C, de Lucas B, Martin de la Torre I, Jiménez-Aspee F, *et al*. Polyphenol metabolism, short-chain fatty acids production, and microbiota changes during *in vitro* digestion and fermentation of Chilean beans (*Phaseolus vulogaris* L.). Food Chemistry. 2025;486:144669. https://doi.org/10.1016/j.foodchem.2025.144669

58. Yang K, Zhang L, Liao P, Xiao Z, Zhang F, *et al*. Impact of gallic acid on gut health: Focus on the gut microbiome, immune response, and mechanisms of action. Frontiers in Immunology. 2020;11:580208. https://doi.org/10.3389/fimmu.2020.580208

59. Li X, Xie E, Sun S, Shen J, Ding Y, *et al*. Flavonoids for gastrointestinal tract local and associated systemic effects: A review of clinical trials and future perspectives. Journal of Advanced Research. 2025;77:15–41. https://doi.org/10.1016/j.jare.2025.01.014

60. Makarewicz M, Drożdż I, Tarko T, Duda-Chodak A. The interactions between polyphenols and microorganisms, especially gut microbiota. Antioxidants. 2021;10(2):188. https://doi.org/10.3390/antiox10020188

61. Qabaha KI. Antimicrobial and free radical scavenging activities of five Palestinian medicinal plants. African Journal of Traditional, Complementary and Alternative Medicines. 2013;10(4):101–108. https://doi.org/10.4314/ajtcam.v10i4.17

62. Veličković DT, Randjelović NV, Ristić MS, Veličković AS, Šmelcerović AA. Chemical constituents and antimicrobial activity of the ethanol extracts obtained from the flower, leaf and stem of *Salvia officinalis* L. Journal of the Serbian Chemical Society. 2003;68(1):17–24. https://doi.org/10.2298/JSC0301017V

63. Bozyel ME, Şenturan M, Benek A, Bozyel EM, Canli K, *et al*. *In vitro* antimicrobial activity screening of *Heliotropium europaeum* against wide range of microorganisms and multi drug resistant (MDR) bacteria. European Journal of Biomedical and Pharmaceutical Sciences. 2019;6(3):113–117.

64. Al-Juraifani AA. Antimicrobial activity of some medicinal plants used in Saudi Arabia. Canadian Journal of Pure and Applied Sciences. 2011;5(2):1509–1512.

65. Rauha JP, Remes S, Heinonen M, Hopia A, Kähkönen M, *et al*. Antimicrobial effects of Finnish plant extracts containing flavonoids and other phenolic compounds. International Journal of Food Microbiology. 2000;56(1):3–12. https://doi.org/10.1016/S0168-1605(00)00218-X

66. Hirano R, Sakanaka M, Yoshimi K, Sugimoto N, Eguchi S, *et al*. Next-generation prebiotic promotes selective growth of bifidobacteria, suppressing *Clostridioides difficile*. Gut Microbes. 2021;13(1):1973835. https://doi.org/10.1080/19490976.2021.1973835

67. Alowo D, Olum S, Mukisa IM, Ongeng D. Prebiotic potential of oligosaccharides extracted from improved Ugandan varieties of millet, sesame, soybean, and sorghum: Enhancing probiotic growth and enteric pathogen inhibition. BMC Microbiology. 2025;25:307. https://doi.org/10.1186/s12866-025-04028-x

68. Higashi B, Mariano TB, de Abreu Filho BA, Gonçalves RAC, de Oliveira AJB. Effects of fructans and probiotics on the inhibition of *Klebsiella oxytoca* and the production of short-chain fatty acids assessed by NMR spectroscopy. Carbohydrate Polymers. 2020;248:116832. https://doi.org/10.1016/j.carbpol.2020.116832

69. Śliżewska K, Chlebicz-Wójcik A. The *in vitro* analysis of prebiotics to be used as a component of a synbiotic preparation. Nutrients. 2020;12(5):1272. https://doi.org/10.3390/nu12051272

70. Evdokimova SA, Nokhaeva VS, Karetkin BA, Guseva EV, Khabibulina NV, *et al*. A study on the synbiotic composition of *Bifidobacterium bifidum* and fructans from *Arctium lappa* roots and *Helianthus tuberosus* tubers against *Staphylococcus aureus*. Microorganisms. 2021;9(5):930. https://doi.org/10.3390/microorganisms9050930

Additional information about the authors

Svetlana A. Evdokimova ORCID 0000-0002-4808-5002; eLIBRARY SPIN 1614-0686
Boris A. Karetkin ORCID 0000-0002-0976-9700; eLIBRARY SPIN 2267-8881
Elena V. Guseva ORCID 0000-0002-6835-4513; eLIBRARY SPIN 7052-6117
Kirill M. Demkin ORCID 0000-0002-3299-6397; eLIBRARY SPIN 8959-0312
Alla T. Shevchenko ORCID 0009-0009-2751-9930; eLIBRARY SPIN 7406-7852
Natalya Yu. Khromova ORCID 0000-0001-9852-9401; eLIBRARY SPIN 8982-5985
Victor I. Panfilov ORCID 0000-0002-8158-7012; eLIBRARY SPIN 5437-7183
Nina B. Gradova ORCID 0000-0002-9220-0602; eLIBRARY SPIN 5992-1164

Foods and Raw Materials. 2027;15(2)

ISSN 2308-4057 (Print)
ISSN 2310-9599 (Online)

Research Article
Open Access

Available online at http://jfrm.ru/en
https://doi.org/10.21603/2308-4057-2027-2-712
https://elibrary.ru/VDEGAG

Valorisation of dragon fruit peel in functional squash

Md. Abdul Alim[1], Iqbal Hossain[1], Tamanna Yesmin[1], Md. Tarakul Islam[2], Rukaiya Zaman[2], Md. Momin Khan[2,*]

[1] Bangladesh Agricultural University, Mymensingh, Bangladesh
[2] Gopalganj Science and Technology University, Gopalganj, Bangladesh

* e-mail: mominkhan00040.fe@gstu.edu.bd

Received 28.04.2025; Revised 12.08.2025; Accepted 03.02.2026; Published online 09.07.2026

Abstract:
Dragon fruit (*Hylocereus* spp.) peel is a waste product rich in bioactive components.
This study developed and evaluated three experimental formulations of functional dragon peel squash with different acidulants, nutritional values, and sensory profiles. The acidulants were amla juice, citric acid, and lemon juice. The experimental samples were compared with the control sample and analyzed using standard methods, which included the proximate analysis, the Folin-Ciocalteu assay for phenolics, the DPPH assay for antioxidant activity, and a nine-point hedonic scale for sensory evaluation. The color degradation was evaluated over three successive one-week storage intervals.
The proximate composition (wet basis) showed that the peel consisted of 92.81% moisture, 1.49% ash, 0.528% protein, 0.20% fat, and 4.9% carbohydrates. The squash showed 40–47°Brix of total soluble solids, pH 2.32–4.83, 0.18–1.5% titratable acidity, and ≤ 108 mg/100 mL ascorbic acid. The sample with amla juice possessed the highest phenolic content (5.20 mg GAE/100 g) and the control has highest antioxidant level (IC_{50} = 0.725 mg/mL), as well as the lowest microbial load (1.3×10^3 CFU/mL) after three weeks of storage. As for the sensory assessment, the amla juice sample was preferred for color and aroma, while the sample with lemon juice received a higher score for taste. The ANOVA test (df = 2.4) showed a stable L^* over 21 days, whereas the b^* values tended to increase in all four formulations, and the a^* value increased in the sample with lemon juice ($p < 0.05$). The significant change in b^* indicated poor storage stability, which is to be improved by reformulation with color stabilizers.
In this research, dragon fruit peel was converted into a nutritious and organoleptically attractive squash. This functional beverage offers a sustainable strategy for valorizing agricultural waste.

Keywords: Squash, dragon fruit peel, pitaya, total polyphenol content, DPPH, sensory quality, storage stability

Please cite this article in press as: Alim MA, Hossain I, Yesmin T, Islam MT, Zaman R, *et al.* Valorisation of dragon fruit peel in functional squash. Foods and Raw Materials. 2027;15(2):311–323. https://doi.org/10.21603/2308-4057-2027-2-712

INTRODUCTION

Dragon fruit, also known as pitaya or pitahaya, is a delicious fruit belonging to the *Cactaceae* family and two distinct genera: *Hylocereus* and *Selenicereus* [1, 2]. The most popular commercially cultivated variants are from the *Hylocereus* genus, which consists of 16 different species [3]. They are cultivated in about 20 countries, including Bangladesh, Japan, Malaysia, the Philippines, Taiwan, Vietnam, Thailand, Indonesia, the United States, and China [2].

Dragon fruit peel is an agricultural by-product in the fruit juice processing sector. Most often, it is utilized as fertilizer. Wastes discarded mostly by the beverage industry include 25–30% of peels, followed by seeds, cores, pulp, pomace, etc. However, all these materials have a good potential as natural functional food components [4–7]. Dragon fruit peels are rich in bioactive substances. For instance, quercetin, gallic acid, and chlorogenic acid are known for anti-cancer, antihyperlipidemic, antidiabetic, and antioxidant properties. Other health-beneficial substances include phenolic compounds and betacyanins. As peel is primarily comprised of such antioxidants as pectin, betacyanin pigments, and dietary fiber, it has stronger phenolic and radical scavenging activity than pulp [8–11].

Squash is a concentrated fruit-flavored and non-alcoholic syrup prepared from fruit juice, water, and sugar or its substitute [12]. Fruit squashes, which contain around 25% of fruit juice, are gaining popularity over synthetic beverages due to their superior flavor, taste, nutritional value, and storage stability. As a result, squash has become a popular nutritious soft drink [13, 14].

Dragon fruit peel constitutes 20–22% of the whole fresh fruit, yet it is disregarded as waste, despite its

Copyright © 2026, Alim *et al.* This is an open access article distributed under the terms of the Creative Commons Attribution 4.0 International License (https://creativecommons.org/licenses/by/4.0/), allowing third parties to copy and redistribute the material in any medium or format and to remix, transform, and build upon the material for any purpose, even commercially, provided the original work is properly cited and states its license.

great health advantages. This research featured a new value-added dragon fruit squash made of underutilized peel waste and provided with detailed physiochemical, sensory, and storage profiles.

STUDY OBJECTS AND METHODS

Experimental site. The study was carried out in the laboratory of the Department of Food Engineering and Technology, Bangladesh Agricultural University (Mymensingh, Bangladesh).

Materials and equipment. The dragon fruits were purchased from a local market in Mymensingh, Bangladesh. The trays, knife, slicer, chopping board, balance, spatula, crucible, desiccator, and other tools came from the laboratory stock. The drying operation involved a cabinet dryer (Model No. 1816, Modern Laboratory Equipment, USA).

Formulation. Mature dragon fruits were washed and peeled to eliminate the scales on the outer layer. The pulp and inner peel, once separated, were finely chopped into small pieces. Seeds were extracted by pressing, followed by filtration through paper cloth. Amla juice, citric acid, or lemon juice were added to dragon fruit peel. Next, we added sugar syrup to those experimental samples and thoroughly mixed it with a spoon. The soluble solids content was adjusted to 40–50° in the concentrate resulted in a final drink with 10–15°Brix after dilution. The control sample did not include any acidifying agents. Figure 1 illustrates the method. Table 1 demonstrates the formulations of the squash under study.

Proximate analysis. The fresh dragon fruit peel was analyzed for moisture and protein (Kjeldahl method) as recommended by the Association of Official Agricultural Chemists (AOAC)[1]. The fat and ash contents were determined by Ranganna's method [15] while the carbohydrate content was calculated using Pearson's test [16].

Physicochemical analysis. The physicochemical analysis for total soluble solids in the squash involved a hand refractometer (Model No. 8987, Puji Kuki, Japan) followed by AOAC (2012)[2]. The pH, titratable acidity, and ascorbic acid were tested as recommended by AOAC (2005)[3].

Table 1 Formulations of experimental dragon fruit peel squash

Ingredient	Sample			
	Control	Peel + amla juice	Peel + citric acid	Peel + lemon juice
Peel, g	70	70	70	70
Sugar, g	200	200	200	200
Water, g	730	580	715	580
Amla juice, mL	–	150	–	–
Citric acid, g	–	–	15	–
Lemon juice, mL	–	–	–	150
Total, g/mL	1,000	1,000	1,000	1,000

[1] Official methods of analysis of AOAC International. 19th ed. In: Horwitz W, Latimer GW, editors. Rockville: AOAC International; 2012.
[2] The same.
[3] Official methods of analysis of AOAC International. 18th ed. Washington: AOAC International; 2005.

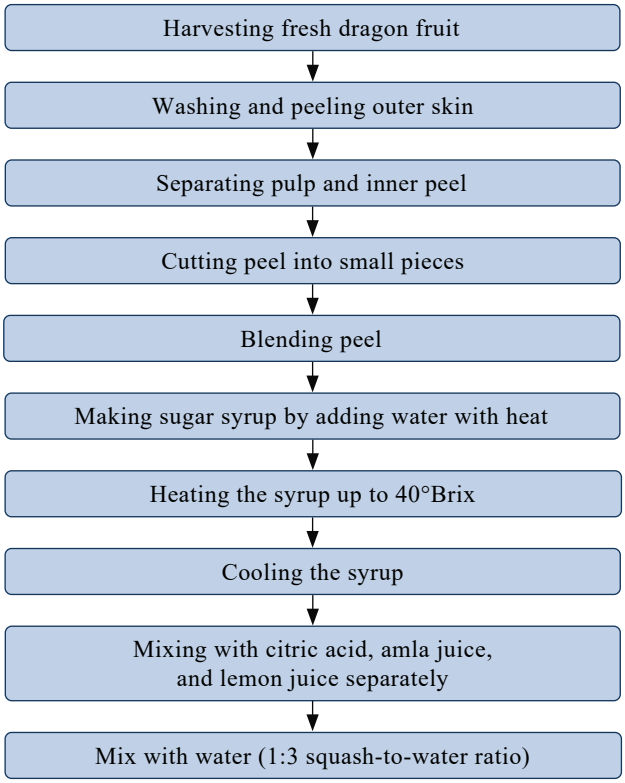


Figure 1 Scheme for preparing dragon fruit peel squash

Total phenolic content. To determine the total phenolic content, we applied the Folin-Ciocalteu reagent technique followed by Zahan *et al*. [17]. Gallic acid (GAE) served as reference during the colorimetric experiment. Briefly, we mixed 1 mL of extract solution with 5 mL of Folin-Ciocalteu's reagent for 2 min and added 4 mL of 7.5% (w/v) sodium carbonate. After a 15-s vortexing, the mix was allowed to stand for 30 min at room temperature for color development. The absorbance was measured at 765 nm with a Photolab 7600 spectrophotometer (UV-Vis, EU). Gallic acid was employed for calibration. The estimate was done in triplicate, and the findings were averaged before being expressed as GAE mg/g dry extract.

DPPH (2,2-diphenyl-1-picrylhydrazyl) radical scavenging activity. The DPPH radical is a stable free radical or oxidizing radical that is subsequently reduced by the antioxidant. It also serves as a reaction marker. We used DPPH to assess the ability of the extract to eliminate free radicals. The antioxidant activity of the powder was assessed as recommended by Nitisuk *et al*. [18]. A set of ethanol solutions with varying concentrations (60, 80, 100, 120, 140, and 160 µg/mL) were created by diluting while the control was conducted similarly but with ethanol. This experiment combined a 1 M DPPH solution with a 1 mL extract solution at various concentrations. The total volume was then adjusted to 10 mL using ethanol. After agitating the contents for 15 s, we placed the solutions in a lightless environment at an ambient temperature for 30 min to facilitate the chemical reaction. Subsequently, we measured the absorbance

at a wavelength of 517 nm using a single beam spectrophotometer (Photolab 7600, UV-Vis, EU) with a blank as reference. The capacity to scavenge DPPH radical was determined as in Eq. (1):

$$\text{DPPH radical} = \frac{A_0 - A}{A_0} \times 100 \quad (1)$$

where A_0 is the absorbance of the control solution, which contained the same reagents but no dragon fruit peel extract; A is the absorbance of the DPPH solution containing the dragon fruit peel extract. The DPPH radical scavenging activity, %, was plotted against the concentration of dragon fruit peel extract to determine the concentration necessary to decrease the DPPH radical scavenging by 50% (IC_{50}).

Storage conditions. The squash samples were stored at 4 ± 1°C in a refrigerator (RT28T3122S, Samsung Electronics, South Korea) for 21 days. Initially, the samples were evaluated immediately after preparation, and subsequent evaluations were performed at seven-day intervals.

Total plate count. To obtain the total plate count in the dragon fruit peel squash, we used the conventional plate count method[4]. The samples stored at 4 ± 1°C were aseptically collected (10 mL) on days 0, 7, 14, and 21, diluted in 90 mL of sterile 0.1% peptone water (1:10), and serially diluted (10^{-2} to 10^{-6}). Using pipette aids, we spread in triplicate 0.1 mL of each dilution onto plate count agar, incubated them at 35 ± 1°C for 48 ± 2 h, and counted colonies (25–250 per plate) to calculate the total plate count, CFU/mL, as in Eq. (2):

$$\text{Total plate count} = \frac{A_c}{D_f \times 0.1} \quad (2)$$

where A_c is the average colonies; D_f is the dilution factor.

Sensory evaluation during storage. The sensory evaluation was performed by a panel of ten faculty members, staff, and students of the Department of Food Engineering and Technology, Bangladesh Agricultural University (Mymensingh, Bangladesh). As in a study by Hasan *et al.* [19], the hedonic scale ranged from 1 to 9 and covered the color, aroma, taste, flavor, and overall acceptability of four squash samples, including the control (Fig. 2). The scale was arranged as follows: 9 – like extremely; 8 – like very much; 7 – like moderately; 6 – like slightly; 5 – neither like nor dislike; 4 – dislike slightly; 3 – dislike moderately; 2 – dislike very much; and 1 – dislike extremely.

Color parameters during storage. The color of squash powder was measured according to Khan *et al.* [20] using a CR-400/410 Chroma Meter (Konica Minolta, Japan). Using the Hunter *L*, *a*, *b* color scale, we conducted the measurements under illuminants **C* and D65. In Fig. 3, *L**, *a**, and *b** stand for greenness (−), blueness (−) or yellowness (+), and lightness (100:white, 0:black). The tests were conducted in duplicate.

[4] Zhang G, Ferguson M, Blodgett RJ. Bacteriological analytical manual. Chapter 3: Aerobic Plate Count. May 2025 ed. Silver Spring: FDA; 2025, pp. 2–13.



Figure 2 Experimental dragon fruit peel squash samples for sensory evaluation: control (a); peel + amla juice (b); peel + citric acid (c); and peel + lemon juice (d)

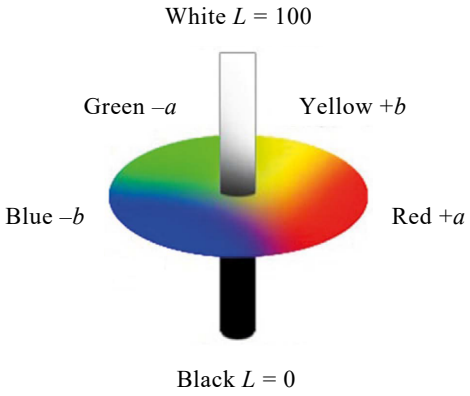


Figure 3 Hunter *L*, *a*, *b* color scale [23]

Statistical analysis. The statistical analysis was performed in Microsoft Excel 2019 and then exported into SPSS Version 27.0 software (SPSS Inc., USA), where we applied ANOVA to compare mean values among treatments. The Phyton programming (Python Software Foundation) made it possible to visualize the graph. The results were reported with 5% significance level.

RESULTS AND DISCUSSION

Proximate analysis. To determine the moisture content, ash, protein, fat, and carbohydrates in the dragon fruit peel, we applied a chemical analysis that involved both water content and dry weight (Table 2).

The peel demonstrated a high moisture content of 92.81% (wet basis). The protein content was 0.528% wet basis and 7.350% dry basis, while the fat content was relatively low at 0.20% wet basis and 2.78% dry basis. The ash contents were 1.49% wet basis and 20.72% dry basis, reflecting the presence of essential minerals. The content of carbohydrates, which contributed to the energy status of the experimental beverage, accounted for 4.90% wet basis and 68.15% dry basis. Thus, we

Table 2 Proximate composition of fresh dragon fruit peel

Parameter	Wet basis	Dry basis
Moisture content, %	92.81 ± 0.42[p]	–
Protein, %	0.528 ± 0.080[p]	7.350 ± 0.310[q]
Ash, %	1.49 ± 0.11[p]	20.72 ± 0.95p
Fat, %	0.20 ± 0.03[p]	2.78 ± 0.14[q]
Carbohydrate, %	4.90 ± 0.01[p]	68.15 ± 1.03[q]
Total phenolic content, mg GAE/100 g	3.20	–
IC_{50}, mg/mL	0.729	–

The values are presented as mean ± standard deviation. The values with same superscripts in the same row are not significantly different ($p < 0.05$)

confirmed the nutritional potential of dragon fruit peel, supporting its application in value-added food products.

In this particular research, the moisture content in dragon fruit peel was 92.81% (wet basis) (Table 2). This aligns almost perfectly with Nur *et al*. [22] and Alam *et al*. [23], who reported a moisture content of 86.95 and 92.24% (wet basis), respectively. Meanwhile, Qalbi *et al*. [24] reported a much lower water content of 9.73% in dragon fruit peel powder (dry weight). The variation might be due to the differences in the drying methods, stage of maturity, environmental effects, or post-harvest handling.

In our case, the protein content in dragon fruit peel was 0.528% wet basis and 7.350% dry basis (Table 2), which exceeded the crude protein (4.35%) in dried peel powder [25]. Nur *et al*. [22] (dragon fruit peel) and Arivalagan *et al*. [26] (dragon fruit) reported lower protein contents. Other sources give a higher protein range of 13.07 to 15.18% (dry basis), indicating that the composition depends, to some extent, on the species or sample processing method [24]. A complimentary feed of soybean and fish paste with added dragon fruit peels demonstrated a higher protein content (16.28–20.60% dry basis) [27]. However, the protein percentage was lower than the results published by Alam *et al*. [23] and Yasmin *et al*. [28].

The amount of ash in a food product is the leftover inorganic material that remains after organic matter [29]. In this research, the ash content was 1.49% wet basis and 20.72% dry basis for fresh dragon fruit peel. Our results were very close to the 15.91% reported by Chumroenvidhayakul *et al*. [30]. In Rosiana *et al*. [27], the ash content also ranged from 4.28 to 5.05%. Thus, dragon fruit peel is extremely rich in minerals. Another study, however, reported as low as 3.56% (wet basis) of ash content in dragon fruit peel [23]. These variations across the studies can be due to the differences in soil, plant variety, and processing conditions.

The fat content in this study was relatively low, measuring 0.20% wet basis and 2.78% dry basis. Our finding agreed with the value (0.76 %) in Prasad's research [31] on carrot squash drink but was much lower than in [22]. However, Rosiana *et al*. [27] detected a much higher fat content, ranging from 15.51 to 15.60% in complementary feeding from soybeans and dragon fruit peels. Due to the antioxidant effect, a lower fat content in dragon fruit peel helped keep the produce fresh for a longer period [32].

In terms of bioactive compounds and antioxidant activity, the dragon peel had 3.2 mg GAE/100 g (wet basis) of total phenolic content. Its IC_{50} value was 0.729 mg/mL (wet basis), indicating a moderate radical scavenging ability (Table 2). However, Madane *et al*. [32] reported 36–39 mg GAE/100 g in dragon fruit peel, accompanied by good radical scavenging activity. Another study showed an IC_{50} value of 0.112 mg/mL in aqueous dragon fruit extract, which was below our findings [11]. In our case, the total phenolic content was relatively low while the IC_{50} was high, which could be due to the fresh state of peel and the extraction methods.

Fruits are rich in carbohydrates, but the exact content depends on the type of fruit, ripeness, and origin. Carbohydrates in fruit juices are a crucial source of energy for recovering patients [33]. The carbohydrate contents of dragon fruit peel in this study were 4.9% wet basis and 68.15% dry basis (Table 2), which was compatible with Rosiana *et al.* [27]. Qalbi *et al*. [24] observed a comparably lower carbohydrate content in the range of 34.99 to 39.49% (dry basis) in dragon fruit peel powder, whereas Chumroenvidhayakul *et al*. [30] documented a slightly higher carbohydrate content in dragon fruit peel than in the current study. The high carbohydrate content suggests that dragon fruit peel could be a valuable source of dietary fiber and other polysaccharides.

Physicochemical analysis. Table 3 summarizes the physicochemical properties of different parts of two dragon fruit species. The physicochemical properties differed across the formulations, depending on the type of acidulants used, i.e., amla juice, lemon juice, and citric acid. The total soluble solids ranged from 40.30 to 47.00°Brix, the pH values were between 2.32 and 4.83, the titratable acidity was 0.15–1.50%, and the content of ascorbic acid (Vitamin C) ranged from 0.40 to 108.00 mg/100 mL (Table 3). The sample with amla juice showed the highest contents of total soluble solids (47.00°Brix) and ascorbic acid (108.00 mg/100 mL), indicating excellent nutritional and sensory quality. The control sample showed the highest pH (4.83) and the lowest total soluble solids (40.30°Brix) and titratable acidity (0.15%), compared to other formulations (Table 3).

Our total soluble solids were higher than those previously reported for fresh dragon fruit peels and pulp, which generally ranged between 7.03 and 10.78°Brix [22], or equaled 8.73°Brix for white flesh dragon fruit [23]. Our results also exceeded the values found in cucumber and summer squash fruits [34] but were quite comparable to squash products fortified with lime (41–45°Brix), mango (47.91°Brix), and dragon fruit (48.5°Brix) [12, 14, 35]. Apparently, the product demonstrated good sweetness and concentration.

The pH value was at its maximum in the control sample (4.83) ($p < 0.05$), but the other formulations had almost the same values (2.90, 2.32, and 2.42) (Table 3). These results coincided with the findings for various

Table 3 Physicochemical profile of experimental dragon fruit peel squash

Parameter	Sample			
	Control	Peel + amla juice	Peel + citric acid	Peel + lemon juice
Total soluble solid, °Brix	40.30 ± 0.27^{r}	47.00 ± 0.58^{p}	41.00 ± 0.32^{r}	46.00 ± 0.51^{q}
pH	4.83 ± 0.05^{p}	2.90 ± 0.02^{q}	2.32 ± 0.06^{q}	2.41 ± 0.07^{q}
Titratable acidity, %	0.15 ± 0.02^{r}	0.18 ± 0.01^{r}	1.50 ± 0.23^{p}	0.90 ± 0.11^{q}
Ascorbic acid, mg/100 mL	4.70 ± 1.25^{q}	108.00 ± 1.25^{q}	0.40 ± 0.02^{r}	9.50 ± 0.45^{p}

The values are presented as mean ± standard deviation. The values with different superscripts in the same row are significantly different ($p < 0.05$)

squash products, e.g., tamarind squash (2.60) [36] or mango and guava blended squash (2.70–2.82) [13]. However, they were comparatively lower than those reported for dragon fruit peel squash (3.40) [14], mango squash (3.30–3.45) [22], or carrot squash (6.0) [31]. Another study detected a higher pH value in a refined squash peel extract [37]. The low pH in our squash samples suggested higher acidity and potentially better microbial stability.

In terms of titratable acidity, the maximal level belonged to the combination of dragon peel with citric acid (Table 3). The titratable acidity values of the samples with citric acid and lemon juice aligned well with those in peach squash (1.52%) [31] and carrot squash (1%) [38]. This acidity level suggested better taste and preservation.

High levels of vitamin C boost antioxidant capacity [27]. For ascorbic acid, the maximal recorded value was (108.00 mg/100 mL) in the sample with amla juice, compared to the control (4.70 mg/100 mL), the sample with citric acid (0.40 mg/100 mL), and the sample with lemon juice (9.50 mg/100 mL) ($p < 0.05$), which exceeded the values reported for dragon fruit peel (9.81 mg/100 g) in [22], tamarind squash (46.75 mg/mL) [36], and mango and guava blended squash (33.05–39.30 mg/100 mL) [13]. Even carrot squash had a much lower range of ascorbic acid, which was quite comparable with the sample with citric acid [31]. The high vitamin C content in the sample with amla juice was likely due to its exceptional ascorbic acid concentration.

Total phenolic content levels. In functional foods, phenolics are responsible for antioxidant properties associated with scavenging free radicals and chelating metal ions. In humans, they react against bacteria, inflammation, and oxidation [39, 40]. In our study, the concentration vs. absorbance curve for gallic acid was as in Fig. 4, which led to the following regression Eq. (3):

$$y = 0.0011x + 0.2758 \quad (3)$$
$$R^2 = 0.9961$$

where y is the absorbance at 765 nm; x is the amount of gallic acid.

The absorbance increased proportionally with the concentration of gallic acid in dragon fruit peel (Fig. 3). The regression equation yielded a total polyphenol content of 3.20 mg GAE/100 g (Table 2).

The total phenolic content across the dragon fruit peel squash formulations in this study ranged from 2.89 to 5.20 mg GAE/100 g, with sample 1 (amla juice) exhibiting the maximum (Table 4). These values were modest but consistent with those reported for other experimental processed fruit beverages. For instance, the total phenolic contents in dragon fruit peel extracts and powders were significantly higher, e.g., 454.79 mg GAE/g powder [30] and 35.81 mg/g dry basis [41], which could be attributed to the concentrated nature of those samples.

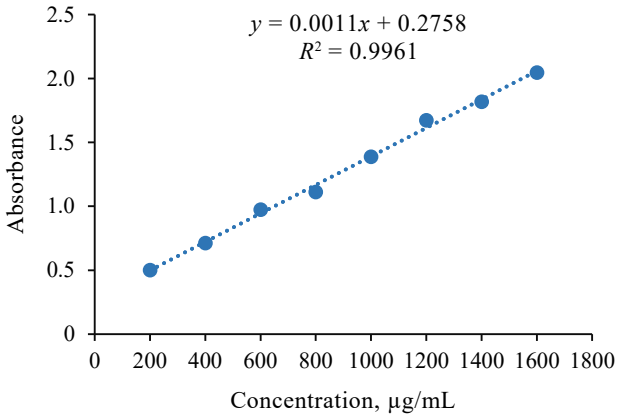


Figure 4 Concentration vs. absorbance (765 nm) curve of gallic acid in dragon fruit peel

Table 4 Total phenolic content and DPPH radical scavenging activity in experimental dragon fruit peel squash

Sample	Total phenolics, mg GAE/100 g	IC_{50}, mg/mL
Control	2.89 ± 0.10^{n}	0.725 ± 0.020^{s}
Peel + amla juice	5.20 ± 0.12^{m}	0.633 ± 0.015^{p}
Peel + citric acid	3.41 ± 0.43^{l}	0.711 ± 0.101^{q}
Peel + lemon juice	4.24 ± 0.14^{m}	0.691 ± 0.021^{r}

The values are presented as mean ± standard deviation. The values with different superscripts in the same column are significantly different ($p < 0.05$)

Other studies on dragon fruit peel and squash-like products report similar total phenolics [42]. In general, our results validated that the squash from dragon fruit peel retained its functional phenolic content, thus confirming its values as a health-beneficial beverage and a way for sustainable utilization of fruit waste.

DPPH (2,2-diphenyl-1-picrylhydrazyl) radical scavenging activity. The antioxidant capacity depends on the ability of the substance to neutralize stable organic

Table 5 Total plate count during storage

Sample	Total plate count, CFU/mL, during storage, day			
	0	7	14	21
Control	$1.8\times10^2 \pm 25^{aD}$	$5.2\times10^3 \pm 300^{aC}$	$3.1\times10^5 \pm 4{,}500^{aB}$	$8.7\times10^6 \pm 95{,}000^{aA}$
Peel + amla juice	$1.5\times10^2 \pm 20^{aC}$	$2.8\times10^2 \pm 35^{cC}$	$6.0\times10^2 \pm 80^{cB}$	$1.3\times10^3 \pm 150^{cA}$
Peel + citric acid	$2.1\times10^2 \pm 30^{aD}$	$1.1\times10^3 \pm 150^{bC}$	$4.5\times10^3 \pm 500^{bB}$	$2.2\times10^4 \pm 2{,}500^{bA}$
Peel + lemon juice	$1.9\times10^2 \pm 25^{aC}$	$3.5\times10^2 \pm 40^{cC}$	$7.8\times10^2 \pm 90^{dB}$	$1.8\times10^3 \pm 200^{cA}$

The results are given as means ± standard deviation. Lowercase letters in the same column (same storage time) indicate significant differences across samples (Tukey's HSD, $p < 0.05$). Uppercase letters in the same row (same sample) indicate significant differences across storage times (Tukey's HSD, $p < 0.05$)

free radicals. The inhibitory function or DPPH (2,2-diphenyl-1-picrylhydrazyl) scavenging activity, in our case, increased with the extract concentration (Table 4). The IC_{50} values represent the concentration needed to eliminate 50% of DPPH free radicals [43]. Greater DPPH radical scavenging percentage and lower IC_{50} value suggest higher antioxidant ability [24].

We studied the DPPH radical scavenging activity of dragon fruit peel extract at different concentrations. By plotting the absorbance of gallic acid against concentration in linear graph paper, we obtained a regression line and a regression Eq. (4):

$$y = 0.0018x + 31.708 \quad (4)$$
$$R^2 = 0.9955$$

where y is the absorbance at 765 nm; x is the concentration of gallic acid, µg/mL.

As the concentration increased, the percentage of radical scavenging activity rose from 39.86 to 76.51% (Fig. 5), highlighting a clear concentration-dependent antioxidant effect. The IC_{50} value was 0.715 mg/mL (Table 2).

The formulated squash showed IC_{50} values from 0.633 to 0.725 mg/mL, which were higher than those reported for other varieties of dragon fruit [28]. However, dragon fruit peel powders showed the highest antioxidant activity [24]. Another study on dragon fruit peel found good antioxidant activity consistent with the current results [41]. All in all, our experimental squash demonstrated powerful antioxidant activity.

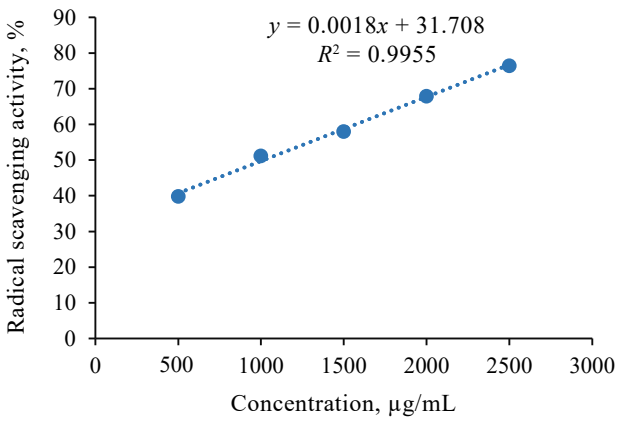


Figure 5 DPPH scavenging activity of dragon fruit peel

Total plate count during storage. Microbial safety is an essential quality factor when it comes to assessing the shelf-life and acceptability of fruit beverages [44, 45]. According to the Bangladesh Food Safety Authority, ready-to-drink fruit beverages must not exceed a total plate count of 1×10^4 CFU/mL to be considered microbiologically safe; otherwise, the beverage may cause potential health risks and spoilage[5]. In this study, the total plate count was monitored on storage days 0, 7, 14, and 21 across all formulations (Table 5).

The control sample experienced a significant increase in microbial load, jumping from 1.8×10^2 to 8.7×10^6 CFU/mL by day 21 (Table 5). This phenomenon indicated the susceptibility of untreated fruit-based beverages to microbial contamination over time, consistent with previous findings in unprocessed dragon fruit pulp and juice [46, 47]. In contrast, the sample with amla juice demonstrated the most effective microbial control, with only 1.3×10^3 CFU/mL at the end of storage (Table 5). This reduction was likely due to the natural antibacterial properties of amla juice, which contained a lot of polyphenols and ascorbic acid (Tables 3 and 4), which are known to suppress microbial growth in fortified herbal beverages [44, 48].

The sample with citric acid showed moderate microbial control, with the value rising to 2.2×10^4 CFU/mL after 21 days (Table 5). The acidic environment created by citric acid may have contributed to the microbial inhibition, aligning with other studies that reported the preservative effects of such acidulants as ascorbic and citric acid in dragon fruit products [46, 49].

The sample with lemon juice included vitamin C, which effectively limited the microbial growth from 1.9×10^2 to 1.8×10^3 CFU/mL (Table 5). Our results were comparable to the antimicrobial activities of lemon juice observed in sugarcane juice [50]. Therefore, the samples with amla and lemon juice demonstrated more acceptable microbial limits throughout the storage period, which meant a more extended shelf-life and a safer consumption than in the other samples.

Sensory evaluation. The current trends in functional beverages are towards the favor of fruit squashes over synthetic beverages. Due to their taste, flavor, nutritive value, and storage stability, squash drinks have really

[5] Food Safety (Determination and Control of microbiological contaminants) Regulations. Dhaka: Bangladesh Food Safety Authority; 2023.

Table 6 Sensory evaluation of experimental dragon fruit peel squash during storage

Sensory characteristic	Sample	Storage time, day			
		0	7	14	21
Color	Control	6.80 ± 0.15^{cA}	6.20 ± 0.13^{cB}	5.50 ± 0.19^{cC}	4.10 ± 0.21^{cD}
	Peel + amla juice	7.40 ± 0.12^{aA}	7.00 ± 0.35^{aA}	6.50 ± 0.13^{aB}	5.80 ± 0.22^{aC}
	Peel + citric acid	6.20 ± 0.20^{bA}	5.80 ± 0.11^{bB}	5.30 ± 0.22^{bC}	4.80 ± 0.21^{bD}
	Peel + lemon juice	5.30 ± 0.21^{dA}	4.80 ± 0.27^{dB}	4.20 ± 0.30^{dC}	3.60 ± 0.24^{dD}
Aroma	Control	5.80 ± 0.20^{dA}	5.30 ± 0.24^{dB}	4.90 ± 0.29^{dC}	4.00 ± 0.33^{dD}
	Peel + amla juice	7.00 ± 0.25^{aA}	6.60 ± 0.31^{aB}	6.20 ± 0.22^{aC}	5.70 ± 0.15^{aD}
	Peel + citric acid	6.50 ± 0.28^{bA}	6.10 ± 0.74^{bA}	5.60 ± 0.35^{bB}	5.10 ± 0.38^{bC}
	Peel + lemon juice	6.70 ± 0.26^{cA}	6.30 ± 0.46^{cA}	5.80 ± 0.54^{cB}	5.30 ± 0.67^{cC}
Taste	Control	5.50 ± 0.22^{cA}	5.10 ± 0.16^{dA}	4.30 ± 0.31^{dB}	3.10 ± 0.26^{dC}
	Peel + amla juice	6.70 ± 0.23^{bA}	6.30 ± 0.21^{bB}	5.80 ± 0.23^{bC}	5.30 ± 0.27^{bD}
	Peel + citric acid	6.70 ± 0.24^{bA}	6.30 ± 0.23^{bA}	5.80 ± 0.14^{bB}	5.30 ± 0.64^{bC}
	Peel + lemon juice	7.30 ± 0.33^{aA}	6.90 ± 0.42^{aA}	6.40 ± 0.38^{aB}	5.90 ± 0.13^{aC}
Flavor	Control	5.20 ± 0.30^{cA}	4.90 ± 0.26^{cB}	4.40 ± 0.31^{cC}	3.00 ± 0.27^{cD}
	Peel + amla juice	6.70 ± 0.42^{aA}	6.20 ± 0.20^{aB}	5.70 ± 0.42^{aC}	5.20 ± 0.42^{aD}
	Peel + citric acid	6.00 ± 0.50^{bA}	5.60 ± 0.34^{bB}	5.10 ± 0.65^{bC}	4.60 ± 0.52^{bD}
	Peel + lemon juice	6.00 ± 0.48^{bA}	5.50 ± 0.23^{bB}	5.00 ± 0.46^{bC}	4.50 ± 0.83^{bD}
Overall acceptability	Control	5.50 ± 0.25^{cA}	5.10 ± 0.19^{cB}	4.40 ± 0.41^{cC}	3.30 ± 0.54^{cD}
	Peel + amla juice	6.50 ± 0.21^{aA}	6.10 ± 0.24^{aB}	5.60 ± 0.61^{aC}	5.00 ± 0.29^{aD}
	Peel + citric acid	6.50 ± 0.23^{aA}	5.90 ± 0.42^{aB}	5.30 ± 0.55^{aC}	4.70 ± 0.44^{bD}
	Peel + lemon juice	6.20 ± 0.24^{bA}	5.70 ± 0.14^{bB}	5.20 ± 0.63^{bC}	4.60 ± 0.25^{bD}

The results are given as means ± standard deviation. Lowercase letters in the same column (same storage time) indicate significant differences for that sensory characteristic across samples (Tukey's HSD, $p < 0.05$). Uppercase letters in the same row (same sample) indicate significant differences across storage times for that sensory characteristic (Tukey's HSD, $p < 0.05$)

taken the market across the globe as an important nutritious drink [5, 6]. The expert panel evaluated the experimental dragon fruit peel squash in terms of color, aroma, taste, flavor, and general acceptance (Table 6).

Color. Food color is a crucial factor in establishing the first visual impression; typically, bright and striking colors have more appeal for consumers [51]. The sensory evaluation revealed a distinct ranking across the samples regarding color preferences at storage time up to 21 days. The sample with amla juice received the highest score of 7.40 ("like moderately"), followed by the control (6.80, "like slightly") and the sample with citric acid (6.20, "like slightly"). The sample with lemon juice received the lowest score (5.30), indicating the least preferred color (Table 6). The initial value in the control sample dropped to 4.10 by day 21, showing the poorest color retention, while the sample with amla juice consistently scored highest for color, starting at 7.40 (day 0) and declining to 5.80 (day 21). It maintained its visual appeal despite a significant decrease over time ($p < 0.05$). The color score in the samples with citric acid and lemon juice decreased from 6.20 and 5.30 to 4.80 and 3.60, respectively, after 21 days (Table 6). A similar color degradation pattern was reported for mango squash during eight weeks of storage [14] and dragon fruit pulp during three months [44].

The superior color retention in the sample with amla juice was likely due to the antioxidant properties of ascorbic acid in amla juice, which stabilized betacyanin pigments in dragon fruit. Ascorbic acid had a similar protective effect on betalains [52]. Color preference often collaborates with visual appeal [51]. Obiloma *et al.* [33], who also studied fruit drinks, reported similar appearance scores of 5.30–8.35, which aligned with the color score in the current study. In another study, dragon fruit squash scored higher in color and appearance, i.e., consumers tend to prefer colored products [35]. Thus, the visual appeal of the sample was positively received.

Aroma. Aroma influences consumer preference and product quality. The samples from this study scored impressively, with an aroma score ranging from 4 to 7 across samples under different storage times. In the control, the initial value of 5.80 fell to 4.00 at the end of experimental storage ($p < 0.05$). The sample with amla juice achieved the highest initial aroma score of 7.00, which declined to 5.70 by day 21 ($p < 0.05$). The samples with citric acid and lemon juice initially scored 6.50 and 6.70, respectively, dropping significantly to 5.10 and 5.30 ($p < 0.05$) (Table 6).

Our values were comparable to those detected in leh berry fruit squash, where the aroma score ranged from 6.40 to 8.20 [52]. Obiloma & Afam-Anene [33], however, provided a higher aroma score in fruit drinks. The high initial aroma score in the sample with amla juice may be attributed to the aromatic compounds in amla juice, which enhanced the sensory appeal, as seen in [44], where ascorbic acid-treated pulp maintained favorable aroma. The relatively high aroma score in the sample with lemon juice may stem from the volatile compounds in lemon juice, which provided a fresh citrus note, align-

ing with other findings for herbal beverages [53]. Overall, the experimental dragon fruit peel squash scored quite satisfactory for aroma.

Taste. Taste is often the most influential sensory attribute [51]. Following the taste evaluation, the control sample scored the lowest, falling from 5.50 to 3.10 during experimental storage (21 days), while the samples with amla juice and citric acid both exhibited similar reduction values (from 6.70 to 5.30). The sample with lemon juice scored highest at 7.30 at day 0, decreasing to 5.90 by day 21, indicating better taste retention compared to others ($p < 0.05$) (Table 6). A report on dragon fruit pulp displayed a decreasing trend with storage time up to three months [44]. Other studies also exhibited a similar decreasing behavior of consumer taste preference profile for prepared fruit squash during storage [14, 52]. The moderate taste score in the sample with amla juice was less preferred than in the sample with lemon juice. Obiloma & Afam-Anene [33] obtained similar taste scores (6.20–9.00) for other fruit drinks. However, Archana *et al*. [35] obtained a taste score of 8 for dragon fruit squash, which was slightly higher than in the current study. All in all, our samples received good taste scores with moderate sweetness, therefore supporting that carefully adjusted ratios and processing control lead to optimal taste profiles.

Flavor. Flavor is a mix of various sensations derived from foods [54]. The control sample showed the lowest score range (5.20–3.00) for flavor preference. The sample with amla juice displayed the highest score (6.70) at the initial stage, falling to 5.20 on day 21, followed by the samples with citric acid (6.00–4.60) and lemon juice (6.00–4.50) (Table 6). The poor flavor retention in the control sample aligned with [44], where untreated pulp showed significant flavor loss after three months of storage.

The present result is positively comparable with other studies. Archana *et al*. [35] reported a very similar flavor score in dragon fruit value-added products. In [14], the flavor score dropped from 5.93 to 6.78 for mango squash after eight weeks, which was in concurrence with our dragon fruit peel squash after 21 days of storage. The experts in the current research confirmed that the flavors were well-balanced and within an acceptable limit.

Overall acceptability. Overall acceptability integrates all sensory attributes. The control sample scored the lowest range (5.50–3.30), while the samples with amla juice and citric acid received the same scores (6.50) at day 0, which reduced to 5.00 and 4.70, respectively, over 21 days of storage (Table 6). The high acceptability of the sample with amla juice stemmed from its superior color and aroma, aligning with the higher acceptability range for dragon fruit juice beverages [53]. The acceptance score for leh berry fruit squash corroborated with our findings [52]. Archana *et al*. [35] revealed a higher acceptance score of 8.20 whereas mango squash and mixed fruit drinks had similar scores [14, 33].

Products featuring dragon fruit or other tropical fruits tend to gain high consumer approval due to their appealing sensory combinations [35]. For instance, an ice cream with pumpkin and dragon fruit (50:50) was also top-rated [51]. Well-balanced formulations lead to greater acceptability [42]. These observations together back up the idea that the formulation took the best route in ingredient pairing, which led to its high marks for sensory parameters, and it is degraded with prolonged storage may be due to chemical changes and microbial acceleration. All in all, the current formulated product mirrored the successful trends seen across multiple studies, and its scores ensured its position as a strong contender in consumer preference**.**

Color parameters during storage. The color attributes of dragon fruit peel squash are crucial in determining consumer acceptability and overall product quality. In the present study, the color values of the dragon fruit peel squash samples were recorded in terms of lightness (L^*), redness (a^*), and yellowness (b^*), and were evaluated during 1, 2, and 3 weeks of storage (Fig. 6–8).

Lightness (L*) reflected distinct trends across the formulations. The control showed a gradual increase in L^* from 17.01 to 17.83, likely attributable to the sedimentation of suspended particles. Thermally treated fruit juices stabilize color and cloudiness by inactivating enzymes and coagulating proteins [55]. The sample with amla juice displayed fluctuating L^* values, increasing from 17.05 to 17.33 during week 2, then dropping to 16.70 by week 3. This pattern suggested an initial stabilizing effect of ascorbic acid that diminished over time [56]. The sample with citric acid was more acidic (pH 2.32). It displayed a consistent L^* increase from 14.48 to 16.23. Citric acid was reported to stabilize anthocyanins and reduce enzymatic browning [57, 58]. The sample with lemon juice had the brightest lightness at 21.40 in week 2, but then it fell to 16.66 by week 3, indicating unstable interactions between lemon juice components and peel pigments (Fig. 6).

Archana *et al*. [35] recorded L^* value for dragon fruit squash, which stood at 20.51. In contrast, Qalbi *et al*. [24] reported L^* values for dried peel powder that ranged

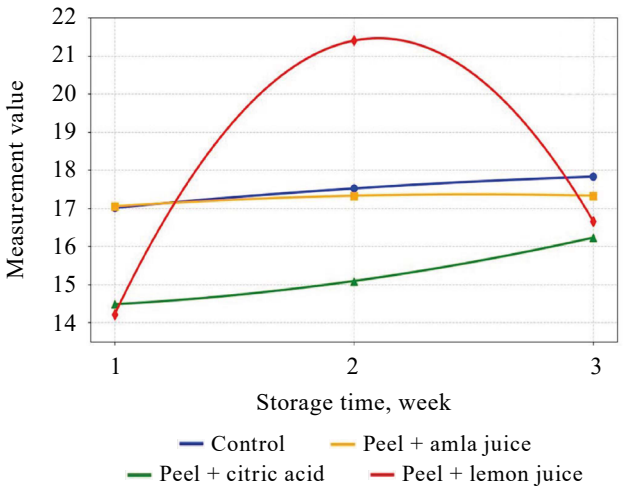


Figure 6 Lightness (L^*) in dragon fruit peel squash during storage

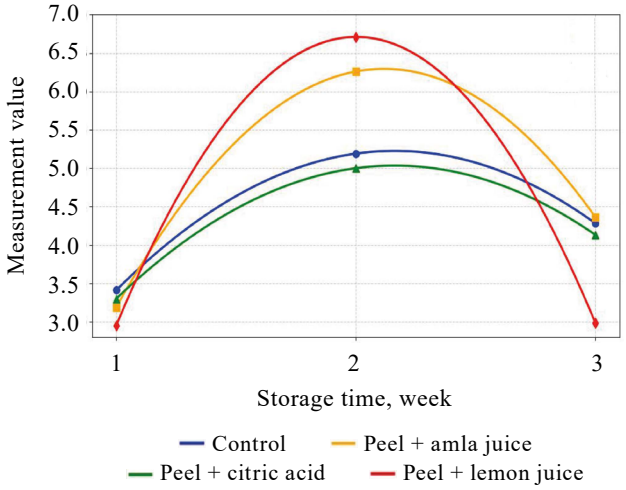


Figure 7 Redness/greenness (*a**) in dragon fruit peel squash during storage

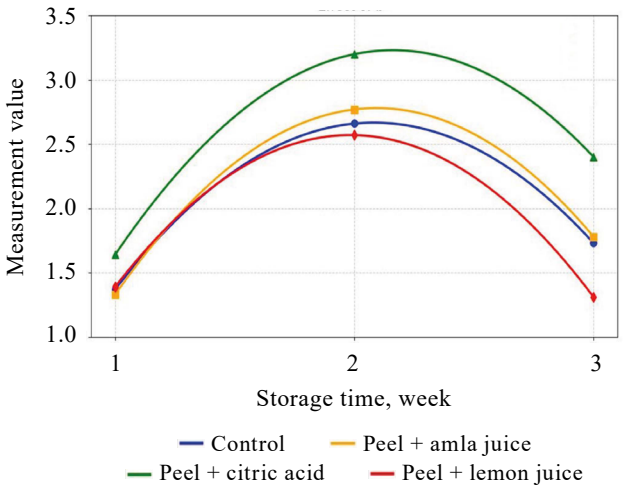


Figure 8 Yellowness/blueness (*b**) in dragon fruit peel squash during storage

Table 6 ANOVA results for color parameters during storage

Sample	Color parameter	Storage time, week			*F*-value	Significance
		1	2	3		
Control	*L**	17.01	17.52	17.83	0.073	n.s.
	*a**	3.41	5.19	4.28	1.649	n.s.
	*b**	1.37	2.66	1.73	11.823	*
Peel + amla juice	*L**	17.05	17.33	16.70	0.006	n.s.
	*a**	3.19	6.26	4.36	4.07	n.s.
	*b**	1.33	2.77	1.78	12.056	*
Peel + citric acid	*L**	14.48	15.09	16.23	0.1778	n.s.
	*a**	3.30	5.00	4.13	1.225	n.s.
	*b**	1.64	3.2	2.4	13.467	*
Peel + lemon juice	*L**	14.21	21.4	16.66	3.069	n.s.
	*a**	2.95	6.71	2.98	7.87	*
	*b**	1.39	2.57	1.31	10.989	*

n.s. – not significant ($p \geq 0.05$, $F \leq 6.944$); * – significant ($p < 0.05$; $F > 6.944$)

from 29.68 to 30.23, indicating a lighter appearance compared to the product in this study. This difference might be due to more browning reactions occurring in the current samples. Nurhadi *et al.* [59] observed a discernible pattern of betacyanin pigment in dragon fruit peel powder with storage time in dragon fruit-based beverages, which correlated with our *L** values due to the state of pigment polymerization and browning reactions. Additionally, the dragon fruit peel showed a wider range of *L** values, from 32.43 to 45.47, which were notably higher than the recent findings [42]. Interestingly, even non-red fruits, like butternut squash [60], displayed much higher lightness values with the emphasis of the darker natural pigment profile of dragon fruit peel products. The lower *L** values observed in this study could be linked to pigment degradation during storage or specific characteristics of formulations in the samples, which could reduce light reflectance.

Redness/greenness (a*). Redness (*a**) is the most critical parameter for betalains stability and visual appeal. Its value shows the range from red to green, with red being positive and green being negative of the sample [24]. In this study, it rose in all samples between week 1 and 2 and dropped during week 3. This trend indicated initial color enhancement of red pigment, perhaps, via enhanced extraction or stabilization followed by degradation. In the control sample, *a** increased from 3.41 to 5.19 and then decreased to 4.28. the sample with amla juice showed a more pronounced increase (3.19 to 6.26), maybe, because of the protective action of ascorbic acid on pigment [61], before declining to 4.36. In the sample with citric acid, the value of *a** rose from 3.30 to 5.00, then dropped to 4.13 with its low pH (2.32) by 21 days. This result closely corroborated the study where maximum betalains deteriorated in pH 2.0 [62], potentially accelerating degradation. The sample with lemon juice also peaked as 6.71 in week 2 but dropped to 2.98 by week 3, showing that lemon juice deteriorated long-term redness stability (Fig. 7).

Archana *et al.* [35] reported an *a** value of 22.18, which indicated a much stronger reddish tone compared to our experimental product. Additionally, Martínez *et al.* [60] highlighted very high *a** values in butternut squash hydrocolloids. Other investigations into dried peel prod-

ucts revealed slightly elevated redness values [24, 42]. Hence, the existing previous values showed very reddish squashes, especially when the squashes were ripe and the acidity was adjusted to maintain pigmentation. The relatively lower redness observed in the current samples (Fig. 7) could be attributed to the gradual degradation of such natural red pigments as betalains or lower initial concentrations of these pigments in the sample matrix.

Yellowness/blueness (b*). The yellowness (*b**) showed the same pattern, rising from week 1 to 2 and decreasing during week 3 across all the samples, indicating a temporary production and a breakdown of yellow pigments. This phenomenon occurs when betalains degrade into betalamic acid, which contains yellow betaxanthins [63]. In the control sample, the value of *b** rose from 1.37 to 2.66 and dropped to 1.73. The sample with amla juice was 2.77 in week 2, possibly as a result of the amla juice effect. The sample with citric acid was 3.2, likely owing to its high acidity accelerating degradation. The sample with lemon juice increased to 2.57 during week 2 before decreasing to 1.31, which indicated rapid color shifts towards yellow colors.

Our values were considerably below those documented in other publications. Qalbi *et al*. [24] observed the *b** values in dried peel powders between 15.20 and 16.53, which tended to drop as the drying time increased; yet, their results remained significantly higher than ours. Raj & Dash [42] also registered much higher *b** values (23.97–28.33) in dragon fruit peel, likely due to the color concentration through drying. Martínez *et al*. [60], who studied butternut squash peels, found even more pronounced *b** values. Therefore, the lower *b** values in the current study suggested either minimal yellow pigment presence or substantial degradation during storage. These results are expected to reflect betacyanin-rich compositions with yellows but not overly predominant.

ANOVA test for color parameters during storage. Table 6 presents the color parameter values (*L**, *a**, *b**) for dragon fruit peel squash formulations across samples during weeks 1 (7 days), 2 (14 days), and 3 (21 days), with *F*-values testing the effect of storage time within each sample. Twoway ANOVA (D_f = 2,4; critical F = 6.944) involved a common MSE (*L** = 4.3575; *a** = 0.590; *b** = 0.045). The lightness (*L**) did not vary significantly with storage time in any sample ($F < 6.944$, ns); the redness (*a**) increased significantly only in the sample with lemon juice ($F = 7.87$, $p < 0.05$), and the yellowness (*b**) changed significantly in all four formulations.

The *L** values started to alter in just over 21 days, showing good overall lightness retention; however, the values of *a** and *b** increased considerably, showing difficulty in retaining the normal red–pink color under storage conditions. Compared to [24] with *L** 29.68–30.23 in dried peel powder and *L** 32.43–45.47 in dragon fruit peel, our experimental squash showed poorer color stability, most probably as a result of the greater pigment breakdown in the aqueous matrix. For enhanced shelf life and consumer acceptability, future studies would need to investigate formulation adjustments (e.g., natural color stabilizers) and storage optimization (light-protected, antioxidant-supplemented packaging) to reduce the existing *a** and *b** drift.

CONCLUSION

This study demonstrated the feasibility of utilizing dragon fruit peel for the production of functional squash. Conventionally regarded as waste, dragon fruit peel proved to be a highly valued functional ingredient. The chemical analysis revealed 92.81% of moisture content, 1.49% ash, 0.528% protein, 0.20% fat, and 4.90% carbohydrate (wet basis). The formulated squash samples were within the acceptable microbial range and possessed favorable physicochemical properties, especially total soluble solids, which ranged from 45.00 to 47.00°Brix. The low pH and sufficient acidity guaranteed safety and palatability. The samples fortified with amla juice and citric acid tied in overall acceptability (6.50), with oversteps in color (7.40) and aroma (7.00). The sample with with lemon juice was ahead in taste (7.30). The formulation with amla juice showed a superior ascorbic acid content (108.00 mg/100 mL) and antioxidant activity (IC_{50} = 0.633 mg/mL). The ANOVA result revealed storage time effects on redness (*a**, $p < 0.05$), as well as storage time and sample type effects on yellowness (*b**, $p < 0.05$), indicating pigment breakdown after three weeks of storage. In general, the dragon fruit peel squash proved to be a healthy drink with a good commercial potential, but it requires optimized storage conditions or natural stabilizers to maintain color qualities that are significant to consumer acceptance.

CONTRIBUTION

M.A. Alim was responsible for the research concept, methodology, formal analysis, and original draft; I. Hossain wrote the original draft, performed the analysis, and worked with the software; T. Yesmin wrote the original draft, performed the analysis, and conducted the data curation; M.T. Islam was responsible for the review, proofreading, validation, software, and research concept; R. Zaman was responsible for the review, proofreading, validation, and data curation; M.M. Khan supervised the research, developed the concept, designed the methodology, wrote the review, and proofread the manuscript.

CONFLICT OF INTEREST

The authors declared no conflict of interest regarding the publication of this research.

REFERENCES

1. Arivalagan M, Karunakaran G, Roy TK, Dinsha M, Sindhu BC, *et al*. Biochemical and nutritional characterization of dragon fruit (*Hylocereus* species). Food Chemistry. 2021;353:129426. https://doi.org/10.1016/J.FOODCHEM.2021.129426

2. Jalgaonkar K, Mahawar MK, Bibwe B, Kannaujia P. Postharvest profile, processing and waste utilization of dragon fruit (*Hylocereus* spp.): A review. Food Reviews International. 2022;38(4):733–759. https://doi.org/10.1080/87559129.2020.1742152
3. Tel-Zur N. Breeding an underutilized fruit crop: A long-term program for *Hylocereus*. Horticulture Research. 2022;9:uhac078. https://doi.org/10.1093/HR/UHAC078
4. Hernawati, Setiawan NA, Shintawati R, Priyandoko D. The role of red dragon fruit peel (*Hylocereus polyrhizus*) to improvement blood lipid levels of hyperlipidaemia male mice. Journal of Physics: Conference Series. 2018;1013:012167. https://doi.org/10.1088/1742-6596/1013/1/012167
5. Nirmal NP, Khanashyam AP, Mundanat AS, Shah K, Babu KS, *et al*. Valorization of fruit waste for bioactive compounds and their applications in the food industry. Foods. 2023;12(3):556. https://doi.org/10.3390/foods12030556
6. Pérez-Marroquín XA, Estrada-Fernández AG, García-Ceja A, Aguirre-Álvarez G, León-López A. Agro-food waste as an ingredient in functional beverage processing: Sources, functionality, market and regulation. Foods. 2023;12(8):1583. https://doi.org/10.3390/foods12081583
7. Asan-Ozusaglam M, Celik I. Formulating edible films with red pitahaya extract and probiotic. Foods and Raw Materials. 2025;13(1):144–154. https://doi.org/10.21603/2308-4057-2025-1-631
8. Chumroenvidhayakul S, Thilavech T, Abeywardena M, Adisakwattana S. Dragon fruit peel waste (*Hylocereus undatus*) as a potential ingredient for reducing lipid peroxidation, dietary advanced glycation end products, and starch digestibility in cookies. Antioxidants. 2023;12(5):1002. https://doi.org/10.3390/ANTIOX12051002
9. Septiansyah MR, Wijirahayu S, Zharifa P, Barickly LRH, Agatha C, *et al*. An antioxidant potential and cholesterol-lowering effects of dragon fruit peel. Proceeding of Forum for University Scholars in Interdisciplinary Opportunities and Networking 2024;1(1):273–281.
10. Panjaitan RGP, Novitasari. Anti-diabetic activity of the red dragon fruit peel (*Hylocereus polyrhizus*) in ethanol extract against diabetic rats. Pharmacognosy Journal. 2021;13(5):1079–1085. https://doi.org/10.5530/pj.2021.13.140
11. Padmavathy K, Sivakumari K, Karthika S, Rajesh S, Ashok K. Phytochemical profiling and anticancer activity of dragon fruit *Hylocereus undatus* extracts against human hepatocellular carcinoma cancer (hepg-2) cells. International Journal of Pharmaceutical Sciences and Research. 2021;12(5):2770–2778. https://doi.org/10.13040/IJPSR.0975-8232.12(5).2770-78
12. Dasgupta R, Chakraborty C, Kakali B, Ganguly S. Development and characterization of biocolor (*Brassica oleracea var. capitata* F. *rubra*) fortified lime squash. The Pharma Innovation Journal. 2019;8(1):42–47.
13. Uddin MN, Wahab S, Muhammad A, Bilal H, Din MU, *et al*. Development and quality evaluation of mango and guava blended squash during storage. Pure and Applied Biology. 2019;8(2):1182–1190. http://doi.org/10.19045/bspab.2019.80060
14. Awais M, Sajid A, Muhammad A, Wisal S, Shabbir H, *et al*. Physicochemical and sensory evaluation of mango squash utilizing chemical preservatives during storage. Indus Journal of Bioscience Research. 2025;3(5):1–8. https://doi.org/10.70749/ijbr.v3i5.683
15. Ranganna S. Handbook of analysis and quality control for fruit and vegetable products. Noida; Tata McGraw-Hill; 1986, 1112 p.
16. Pearson D. The chemical analysis of foods. 7th ed. London: Churchill Livingstone; 1976, 575 p.
17. Zahan I, Khan MM, Rana MS, Sahabuddin M, Rasik MR, *et al*. Effect of selective preservatives on shelf-life of guava juice extracted using pectinase enzyme. Heliyon. 2024;10(18):e37596. https://doi.org/10.1016/j.heliyon.2024.e37596
18. Nitisuk P, Wanyo P, Chamsai T, Charoenjit K. Sustainable valorization of tropical fruit peels for sustainable production of natural antioxidants and functional food ingredients. Sustainable Food Technology. 2025;3(4):1189–1202. https://doi.org/10.1039/D4FB00371C
19. Hasan MM, Khan MM, Jony ME, Akter F, Alim MA. Studies on the preparation and shelf life of aloe vera juice. Asian Food Science Journal. 2023;22(9):64–73. https://doi.org/10.9734/afsj/2023/v22i9658
20. Khan M, Rana S, Rana J, Jony E, Arifin MS, *et al*. Effects of coconut flour and milk powder supple-mentation on the physicochemical properties of peanut butter. Food Processing: Techniques and Technology. 2024;54(4):701–710. https://doi.org/10.21603/2074-9414-2024-4-2537
21. Lovetskiy KP, Sevastianov LA, Nikolaev NE. Numerical modeling of color perception of optical radiation. Mathematical Modelling and Geometry. 2018;6(1):21–36. https://doi.org/10.26456/mmg/2018-612
22. Nur MA, Uddin MR, Uddin MJ, Satter MA, Amin MZ. Physiochemical and nutritional analysis of the two species of dragon fruits (*Hylocereus* sp.) cultivated in Bangladesh. South African Journal of Botany 2023;155:103–109. https://doi.org/10.1016/J.SAJB.2023.02.006

23. Alam M, Biswas M, Ahmed J, Hosain MA, Alam A, *et al*. Physico-chemical properties, antioxidant activity and bioactive compounds in edible and non-edible portions of dragon fruit cultivars native to Bangladesh. Food Research. 2023;7(4):194–203. https://doi.org/10.26656/FR.2017.7(4).243
24. Qalbi R, Giovani S, Guo Q, Adelina NM. Effect of drying time on physicochemical characteristics of dragon fruit peels powder (*Hylocereus polyrhizus*). Journal of Agri-Food Science and Technology. 2023;4(2):81–96. https://doi.org/10.12928/jafost.v4i2.9294
25. Cacatian SB, Guittap LJV. Production, proximate analysis and functional properties of dragon fruit peel powder. IAMURE International Journal of Ecology and Conservation. 2018;25(1).
26. Arivalagan M, Karunakaran G, Roy TK, Dinsha M, *et al*. Biochemical and nutritional characterization of dragon fruit (*Hylocereus species*). Food Chemistry. 2021;353:129426. https://doi.org/10.1016/J.FOODCHEM.2021.129426
27. Rosiana NM, Olivia Z, Suryana AL. Nutritional and antioxidant content in complementary feeding from soybeans and dragon fruit peel. Food Research. 2023;7(Suppl. 5):38–45. https://doi.org/10.26656/FR.2017.7(S5).11
28. Yasmin A, Sumi MJ, Akter K, Rabbi RHM, Almoallim HS, *et al*. Comparative analysis of nutrient composition and antioxidant activity in three dragon fruit cultivars. PeerJ. 2024;12:e17719. https://doi.org/10.7717/peerj.17719
29. Ismail BP. Ash content determination. Nielsen's Food Analysis Laboratory Manual. Cham: Springer; 2024, pp. 129–131. https://doi.org/10.1007/978-3-031-44970-3_14
30. Chumroenvidhayakul S, Thilavech T, Abeywardena M, Adisakwattana S. Investigating the impact of dragon fruit peel waste on starch digestibility, pasting, and thermal properties of flours used in Asia. Foods. 2022;11(14):2031. https://doi.org/10.3390/foods11142031
31. Prasad S. Development, analysis and sensory evaluation of carrot squash as a natural health drink. International Journal of Innovative Research in Technology 2021;8(3):1071–1077.
32. Madane P, Das AK, Nanda PK, Bandyopadhyay S, Jagtap P, *et al*. Dragon fruit (*Hylocereus undatus*) peel as antioxidant dietary fibre on quality and lipid oxidation of chicken nuggets. Journal of Food Science and Technology. 2020;57(4):1449–1461. https://doi.org/10.1007/s13197-019-04180-z
33. Obiloma AA, Afam-Anene O. Evaluation of chemical composition and acceptability of fruit drinks made from noni, date and jack. Tropical Journal of Engineering Science and Technology 2024;3(1):35–47.
34. Rashwan MA, Naser Alkoaik F, Morsy MI, Blanqueza Fulleros R, Nagy Ibrahim M. Influence of tomato waste compost ratios on plant growth and fruit quality of cucumber and summer squash. Journal of the Air & Waste Management Association. 2021;71(9):1067–1075. https://doi.org/10.1080/10962247.2021.1890278
35. Archana R, Rani CI, Geetha P, Amuthaselvi G, Muthuvel I, *et al*. Value addition in dragon fruit and evaluation of the products (*Hylocereus costaricensis*). Biological Forum – An International Journal. 2023;15(8a):180–186.
36. Akshayasri M, Chitra P, Sudagar IP, Amaravel M, Bagathsingh C, *et al*. Characterization and optimization of Tamarind squash formulations: Chemical and sensory attributes. Journal of Food Measurement and Characterization. 2025;19:3205–3213. https://doi.org/10.1007/s11694-025-03172-2
37. Mansour RB, Falleh H, Hammami M, Hadid FB, Barros L, *et al*. Optimizing the encapsulation of the refined extract of squash peels for functional food applications: A sustainable approach to reduce food waste. Open Life Sciences. 2025;20(1):20251124. https://doi.org/10.1515/biol-2025-1124
38. Singh N, Karimullah, Singh SN, Chandra S. Physico-chemical evaluation of the squash prepared from different varieties of peach. Biological Forum – An International Journal. 2023;15(1):28–35.
39. Kruk J, Aboul-Enein BH, Duchnik E, Marchlewicz M. Antioxidative properties of phenolic compounds and their effect on oxidative stress induced by severe physical exercise. The Journal of Physiological Sciences. 2022;72(1):19. https://doi.org/10.1186/s12576-022-00845-1
40. Rao MJ, Zheng B. The role of polyphenols in abiotic stress tolerance and their antioxidant properties to scavenge reactive oxygen species and free radicals. Antioxidants. 2025;14(1):74. https://doi.org/10.3390/antiox14010074
41. Suryaningsih S, Muslim B, Djali M. The antioxidant activity of roselle and dragon fruit peel functional drink in free radical inhibition. Journal of Physics: Conference Series. 2021;1836(1):012069. https://doi.org/10.1088/1742-6596/1836/1/012069
42. Raj GVSB, Dash KK. Development of hydrocolloids incorporated dragon fruit leather by conductive hydro drying: Characterization and sensory evaluation. Food Hydrocolloids for Health. 2022;2:100086. https://doi.org/10.1016/j.fhfh.2022.100086
43. Singh M, Yerramilli V. *In-vitro* and *in-vivo* antioxidant potential and GC-MS profile of *Argemone mexicana* L. The Journal of the Indian Botanical Society. 2023;103(02):119–126.
44. Br V, Naik KR, Gorabal K, Deepa T, Sn P. Bacteriological and sensory stability in dragon fruit (*Hylocereus polyrhizus*) pulp during storage: As influenced by chemical treatments. Journal of Pharmacognosy and Phytochemistry 2020;9(6):901–904.

45. Ahmed T, Das KK, Uddin MA. The microbiological quality of commercial fruit juices-current perspectives. Bangladesh Journal of Microbiology. 2019;35(2):128–133. https://doi.org/10.3329/bjm.v35i2.42643

46. Nithya C, Sudheer KP, Abdullah S. Impact of retort thermal pasteurization on the quality and stability of red dragon fruit (*Hylocereus polyrhizus*) juice. Journal of Tropical Agriculture. 2025;63(1&2):29–35. https://doi.org/10.63599/jta.2025.1520

47. Hafiz MS, Mudiyanselage K, Karunanayaka IU, Nugraheni K, Fernando GSN. Valorisation of dragon fruit peel in drinking yoghurt: Development, physicochemical, proximate, functional properties, and shelf-life evaluation. Czech Journal of Food Sciences. 2025;43(3):179–186. https://doi.org/10.17221/21/2025-CJFS

48. Surya N, Poornakala SJ, Kanchana S, Hemalatha G. Development of Amla (*Emblica officinalis*) ready to serve beverage fortified with dietary fiber. Emergent Life Sciences Research. 2020;06(1):06–15. https://doi.org/10.31783/elsr.2020.610615

49. Vara S, Karnena MK, Dwarapureddi BK. 6 – Natural preservatives for nonalcoholic beverages. Preservatives and Preservation Approaches in Beverages. 2019;15:The Science of Beverages:179–201. https://doi.org/10.1016/B978-0-12-816685-7.00006-9

50. Bag BB, Panigrahi C, Gupta S, Mishra HN. Efficacy of plant-based natural preservatives in extending shelf life of sugarcane juice: Formulation optimization by MOGA and correlation study by principal component analysis. Applied Food Research. 2022;2(2):100164. https://doi.org/10.1016/j.afres.2022.100164

51. Prayitno SA. The sensory evaluation on pumpkin ice cream that formulated by red dragon fruit. Food Science. 2020;2:1–7.

52. Selvamuthukumaran M, Khanum F. Stability assessment of Leh Berry fruit squash. Indian Journal of Horticulture. 2020;77(1):167–172. http://doi.org/10.5958/0974-0112.2020.00018.3

53. Kumar J, Patel KK, Goyal SK, Shankar Bunkar D, Rai JP. Process optimization for dragon fruit juice based herbal beverage fortified with stevia (*Stevia rebaudiana*) and safed musli (*Chlorophytum borivilianum*). Innovative Farming 2023;8(1):10–23. https://elibrary.ru/BKLPQI

54. Zhu Y. Emotional response to food flavor and its application in food products. Flavor-Associated Applications in Health and Wellness Food Products. Cham: Springer; 2024, pp. 347–70. https://doi.org/10.1007/978-3-031-51808-9_14

55. Genovese DB, Elustondo MP, Lozano JE. Color and cloud stabilization in cloudy apple juice by steam heating during crushing. Journal of Food Science. 1997;62:1171–1175. https://doi.org/10.1111/j.1365-2621.1997.tb12238.x

56. Benjuma AA, Salem BA, Eshkourfu RO, Hamarsheh RO, Amawi KF. Study of the effect of storage on the physicochemical characteristics of some industrial juices traded in local markets. Artificial Intelligence, Sustainable Technologies, and Business Innovation: Opportunities and Challenges of Digital Transformation. Cham: Springer; 2025, vol. 1171. pp. 331–340. https://doi.org/10.1007/978-3-031-77925-1_29

57. Moon KM, Kwon EB, Lee B, Kim CY. Recent trends in controlling the enzymatic browning of fruit and vegetable products. Molecules. 2020;25(12):2754. https://doi.org/10.3390/molecules25122754

58. Macedo MJ, Silva JDR, Júnior MRM. Stability of anthocyanins during food processing. Handbook of Analysis and Extraction Methods of Anthocyanins. Abingdon-on-Thames: Taylor & Francis Group; 2025, pp. 34–64. https://doi.org/10.1201/9781003453260-3

59. Nurhadi B, Qonit MAH, Mubarok S, Saputra RA. Enhancing betacyanin stability: Comparison of dragon fruit (*Hylocereus polyrhizus*) pulp and peel powders through encapsulation technology during storage. Food Science & Nutrition. 2024;12:3251–3264. https://doi.org/10.1002/fsn3.3992

60. Martínez SEQ, Fuentes EET, Zapateiro LAG. Food hydrocolloids from butternut squash (*Cucurbita moschata*) peel: Rheological properties and their use in *Carica papaya* Jam. ACS Omega 2021;6(18):12114–12123. https://doi.org/10.1021/acsomega.1c00822

61. Lim TW, Lim RLH, Pui LP, Tan CP, Ho CW. Red dragon fruit (*Hylocereus polyrhizus*), a superfruit rich in betacyanins pigments with antioxidative potential for hepatoprotection: A review. Future Foods. 2025;11:100562.

62. Abarna S, Joshi A, Sethi S, Tomar BS, Kumar R, *et al*. Betalains stability and antioxidant activity of beetroots: As a function of maturity stage. Sugar Tech. 2024;26:77–86. https://doi.org/10.1007/s12355-023-01321-9

63. Hernández-Aguirre OA, Muro C, Hernández-Acosta E, Alvarado Y, Díaz-Nava MDC. Extraction and stabilization of betalains from beetroot (*Beta vulgaris*) wastes using deep eutectic solvents. Molecules. 2021;26(21):6342. https://doi.org/10.3390/molecules26216342

Additional information about the authors

Md. Abdul Alim ORCID 0000-0001-6084-617X
Iqbal Hossain ORCID 0009-0005-6912-5586
Tamanna Yesmin ORCID 0009-0006-0689-2718
Md. Tarakul Islam ORCID 0009-0003-1121-0062
Rukaiya Zaman ORCID 0009-0003-1592-5735
Md. Momin Khan ORCID 0009-0002-4874-6314

Foods and Raw Materials. 2027;15(2)

ISSN 2308-4057 (Print)
ISSN 2310-9599 (Online)

Research Article
Open Access

Available online at http://jfrm.ru/en
https://doi.org/10.21603/2308-4057-2027-2-714
https://elibrary.ru/YGIZFA

Cassia fistula L. fruit: Optimal conditions for total polyphenol extraction

Do Viet Phuong, Nguyen Ngoc Thuan*

Industrial University of Ho Chi Minh City, Ho Chi Minh, Vietnam

* e-mail: nguyenngocthuan@iuh.edu.vn

Received 20.05.2025; Revised 14.07.2025; Accepted 03.02.2026; Published online 02.09.2026

Abstract:
This study optimized the polyphenol extraction conditions for *Cassia fistula* L., commonly known as the Osaka tree. Its fruit contains a complex of valuable natural compounds, which remain underexploited in Vietnam and other countries where Osaka trees grow in abundance.
Methods employed included phytochemical screening, determination of total phenolic and moisture content, preliminary factor screening, and optimization using Response Surface Methodology (RSM) with a Box-Behnken design, followed by statistical analysis using t-tests, ANOVA, and Tukey's HSD post-hoc test.
Most previous studies focused on testing and evaluating individual extraction parameters, such as temperature, solid-to-solvent ratio, and time. This study comprehensively integrated these factors into a unified optimization model. Based on the design of preliminary diagnostic experiments, the solid-to-solvent ratios ranged from 1:10 to 1:50 (w/v), the extraction temperature was 30–70°C, and the extraction time ranged from 5 to 30 min. The Box-Behnken model combined with response surface methodology made it possible to optimize multiple factors simultaneously. The total polyphenol content reached its highest value of 10.64 mg GAE/g DW under the following optimal conditions: 50°C; 21.15 min extraction time; 1:31.69 (w/v) solid-to-solvent ratio. The model demonstrated high reliability ($R^2 = 0.94$), confirming its industrial potential.
The results obtained open up new prospects for sustainable exploitation of natural polyphenols from *C. fistula* in functional foods and pharmaceuticals.

Keywords: *Cassia fistula* L., Osaka tree, bioactive compounds, extraction, optimization, response surface methodology, Box-Behnken model

Please cite this article in press as: Phuong DV, Thuan NN. *Cassia fistula* L. fruit: Optimal conditions for total polyphenol extraction. Foods and Raw Materials. 2027;15(2):324–332. https://doi.org/10.21603/2308-4057-2027-2-714

INTRODUCTION

Bioactive compounds derived from plants have been of interest in recent years because they are not only a source of food but also a valuable source of pharmaceuticals. In this context, indigenous plant species often become the focus of research due to their biodiversity and medicinal applications [1–4]. *Cassia fistula* L. is commonly known as the Osaka tree, Indian laburnum, or golden shower tree (*Fabaceae*). This plant stands out for its bright yellow inflorescences and is highly valued for its medicinal properties. It contains a cluster of bioactive compounds with antibacterial, insecticidal, and antioxidant properties [5, 6].

Cassia fistula L. fruit has a unique elongated cylindrical shape and turns dark brown when ripe. Beside its aesthetic value, the pod-like fruit has long been appreciated for its powerful laxative properties, as well as for its antibacterial, anti-inflammatory, neuroprotective, and cardioprotective effects [7]. However, its industrial use requires more scientific studies to verify its medicinal profile. Recent phytochemical studies demonstrated that Osaka fruits are rich in polyphenols, flavonoids, anthraquinones, and anthraquinone glycoside derivatives [8, 9]. These compounds exhibit strong antioxidant activity, which can protect cells from free radical damage, thus preventing such serious chronic diseases as diabetes, cancer, and neurodegenerative disorders. These findings open up many new application prospects for the functional food industry, pharmaceuticals, and cosmetics [10].

In Vietnam, Osaka trees are widely distributed in humid and tropical environments, but their medicinal potential has not been fully exploited [11]. Most applications are still limited to folk remedies. This shows a huge gap between the abundance of resources and their effective application. To maximize the exploitation pro-

Copyright © 2026, Phuong *et al.* This is an open access article distributed under the terms of the Creative Commons Attribution 4.0 International License (https://creativecommons.org/licenses/by/4.0/), allowing third parties to copy and redistribute the material in any medium or format and to remix, transform, and build upon the material for any purpose, even commercially, provided the original work is properly cited and states its license.

cess and enhance the economic value of this promising plant, scientists and affiliated companies must conduct more in-depth investigations [12]. One of the most promising directions is to optimize the extraction of bioactive compounds, especially total phenolics, which are known for their anti-inflammatory and cardioprotective effects [13].

The extraction of natural compounds from plants is a complex process because the yield depends on many factors. In this research, we combined the response surface methodology with the Box-Behnken experimental design to reduce the number of experiments, thereby reducing time and cost compared to the traditional trial and error method. In addition, this method also helps understand the multidimensional correlation between different factors in the extraction process [14]. Furthermore, advanced techniques, such as microwave-assisted extraction or ultrasound-assisted extraction can further improve the phenolic recovery [15].

This study had two main objectives:

– to evaluate the effects of such technological factors as ethanol solvent concentration, temperature, and extraction time on the total phenolic yield;

– to use the response surface methodology to develop an accurate mathematical model that would make it possible to optimize the polyphenol extraction process while minimizing time and cost.

Although extraction time is not an absolutely important factor, it was included in this study as an independent variable based on previous studies. For instance, Wei *et al.* [16] demonstrated a significant correlation between time and bioactive compound yields (triterpenes).

This study stems from the significant potential and challenges associated with maximizing the industrial value of the Osaka tree. The results not only provide important and comprehensive scientific information on the bioactive profile of *Cassia fistula* L. fruit, but also provide support for the future development of high-value application products, e.g., safe and effective natural cosmetics and functional foods. Furthermore, the sustainable use of *C. fistula* fruit is consistent with the general goals of green and sustainable production.

STUDY OBJECTS AND METHODS

Materials. The pulp of *Cassia fistula* L. fruit was obtained from trees cultivated in Ho Chi Minh City, Vietnam. After harvesting fresh fruits, the seeds and husks were manually removed to isolate the fleshy pulp for extraction and analysis (Fig. 1).

Chemicals and equipment. The Folin-Ciocalteu reagent (Merck) was used to determine total phenolic content. The key equipment comprised a UV-Vis spectrophotometer (Shimadzu UV-1800), an infrared moisture analyzer (Ohaus MB45), and a blender (Fuki).

Phytochemical screening. Exactly 5 g of *C. fistula* fruit pulp was macerated in ethanol at a 1:30 (w/v) solvent-to-sample ratio for 8 h to obtain the primary extract. The extraction process was repeated twice under identical conditions. The three extracts were then combined, concentrated under reduced pressure, and subjected to a qualitative phytochemical analysis for bioactive compounds (Table 1) [17].

Determining the total phenolic content. The total phenolic content was determined according to the method developed by Sirichan *et al.* [19], with minor modifications to adapt to the experimental conditions. Briefly, 5 g of *C. fistula* fruit pulp was macerated in 30 mL of 98% ethanol in a 250-mL Erlenmeyer flask for 24 h at room temperature, followed by filtration to obtain crude extract. The extraction process (soaking and washing) was triplicated, and the combined extracts were pooled and adjusted to a final volume of 100 mL with ethanol.

For total phenolic content quantification, the extract was diluted 10-fold and analyzed using ultraviolet-visible spectroscopy at 765 nm, with gallic acid as the standard



a b

Figure 1 *Cassia fistula* L. tree (a) and *Cassia fistula* L. fruit (b)

Table 1 Phytochemical screening of bioactive compounds [18]

Qualitative compound	Methodology	Reaction result
Polyphenols and tannin	2 mL extract + 2 mL H_2O + 2–3 drops 5% $FeCl_3$	Dark blue, brown, blue
Alkaloids	2 mL extract + 3–4 drops Wagner's reagent	Red-brown precipitate
Flavonoids	2 mL extract + 2 mL 10% lead acetate	Yellow precipitate
Saponins	2 mL extract + 10 mL distilled water (boiled 2 min)	Persistent foam formation
Terpenoids and steroid	5 mL extract + 2 mL $CHCl_3$ + 3 mL concentrated H_2SO_4	Red-brown interface ring
Coumarins	2 mL extract + 3 mL 10% NaOH	Yellow coloration

reference compound. The total phenolic content, mg GAE/g DW, was calculated using the following formula:

$$\text{Total phenolic content} = C_x \times \frac{V_{dm}}{10^3} \times \frac{100}{a \times (100 - W)} \times K \quad (1)$$

where C_x is the measured gallic acid concentration, ppm, obtained from the standard curve; V_{dm} is the final volume of the standardized extract, mL; 10^3 served as the conversion factor from μg to mg; W is the sample moisture content, %; a is the initial sample mass, g; and K is the dilution factor applied when necessary.

Determining the moisture content. The moisture content was determined by the constant-weight drying method at 105°C [20].

Preliminary factor screening. Three key extraction parameters to be investigated included:

– extraction time: 5, 10, 15, 20, 25, and 30 min (fixed at 50°C and 1:30 g/mL solid-to-water ratio);
– temperature: 30, 40, 50, 60, and 70°C (fixed at 20 min and 1:30 g/mL ratio); and
– solid-to-water ratio: 1:10, 1:20, 1:30, 1:40, and 1:50 g/mL (fixed at 20 min and 50°C).

All experiments were triplicated, with the total phenolic content determined as previously described.

Optimizing the response surface methodology. Based on the preliminary screening results, we selected the optimal ranges for key extraction parameters for further optimization using the Box-Behnken experimental design: extraction time (15–25 min), temperature (40–60°C), and solid-to-water ratio (1:20–1:40 g/mL). A 15-run experimental matrix relied on the JMP 10 software (SAS Institute) to evaluate the effects of these parameters and their interactions on total phenolic content:

$$Y = \beta_0 + \sum \beta_i X_i + \sum \beta_{ii} X_i^2 + \sum \beta_{ij} X_i X_j \quad (2)$$

where Y is the total phenolic content; X_i is the independent variables (time, temperature, ratio); β_0, β_i, β_{ii}, β_{ij} denoted regression coefficients. The model adequacy was evaluated using R^2 and p-values.

Experimental validation. The optimal conditions predicted by the response surface methodology were experimentally validated in triplicate. To compare the predicted and the actual values, we used t-tests (Statgraphics).

Statistical analysis. After developing a multivariate regression model, we designed further experiments using the Box-Behnken approach implemented in the JMP 10 software (SAS Institute, USA). This statistical tool enabled optimization of extraction conditions for *C. fistula* fruit polyphenols while excluding variables that were not statistically significant ($p > 0.05$) based on experimental results.

To validate the model and assess the medicinal effects, we applied ANOVA followed by Tukey's honestly significant difference post-hoc test using the Statgraphics Centurion XI software (Statgraphics Technologies, Inc., USA). This analysis confirmed the model's reliability and revealed statistically significant differences ($p < 0.05$) between experimental treatments, ensuring the robustness of the research findings.

RESULTS AND DISCUSSION

Qualitative analysis of bioactive compounds in *Cassia fistula* L. fruit. Table 2 illustrates the preliminary qualitative results for secondary metabolite groups in *C. fistula* fruit. This analysis demonstrated a potential diversity in the chemical composition of the plant, with marked differences in the levels of presence of each metabolite group.

Three dominant groups of compounds were phenolic compounds, tannins, and flavonoids, which exhibited high contents (+++). *C. fistula* indeed proved to be a rich source of bioactive components with therapeutic potential. For phenolic compounds, their presence at highest levels correlated with antioxidant, anti-inflammatory, and antibacterial properties [21]. Tannins are complex polyphenols with properties similar to the phenolic group, which is prominent for its strong antioxidant and antibacterial profile [22]. Flavonoids also belong to the polyphenol group, known for its cardioprotective, anti-inflammatory, and antioxidant effects [23].

The list of compounds with moderate content (++) included coumarins, terpenoids, and steroids. Coumarins and their derivatives have clinically significant anticoagulant and anti-inflammatory effects [24]. Terpenoids possess reliable antibacterial and anticancer properties. Steroids include both hormonal compounds and phytosterols, which may contribute to the overall biological activity of the plant [25].

The compounds with low content (+) included alkaloids and saponins. Alkaloids possess potent pharmacological effects, but their presence is quite low, indicating

Table 2 Qualitative identification of secondary metabolites in *Cassia fistula* L. fruit

Compound class	Test method	Detection result	Relative abundance
Polyphenols	Folin-Ciocalteu	+++	High
Tannins	Ferric chloride	+++	High
Flavonoids	Aluminum chloride	+++	High
Coumarins	NaOH test	++	Moderate
Alkaloids	Mayer's reagent	+	Low
Terpenoids	Salkowski test	++	Moderate
Steroid	Liebermann-Burchard	++	Moderate
Saponins	Foam test	+	Low

that the therapeutic effect in *C. fistula* fruit is not high. Saponins were detected in trace form. They have characteristic foaming properties and biological activity, but their presence does not indicate any therapeutic efficiency [26].

Overall, *C. fistula* fruit pulp demonstrated a remarkable chemical composition with phenolics, tannins, and flavonoids. We conducted a detailed quantitative analysis to measure the concentration of each bioactive compound, thus creating a solid basis for the exploitation and application of the Osaka tree in medicine, cosmetics, and many other fields.

Effect of extraction time on total phenolic yield. According to Zainal *et al.* [27] and Zhang *et al.* [28], extraction time is an important factor affecting total phenolic content. Longer time often facilitates better solubilization and diffusion of phenolic compounds. Figure 2 shows that the total phenolic yield increased together with extraction time. Specifically, starting from the lowest value of 9.939 mg GAE/g DW recorded after 5 min, the total phenolic content showed a significant increase at subsequent times. After 10 min, the value rose to 10.273 mg GAE/g DW, followed by a sharp increase to 11.193 mg GAE/g DW after 15 min, reaching 11.587 mg GAE/g DW after 20 min.

However, after 20 min, the increase rate slowed down significantly, indicating a tendency towards saturation or equilibrium during the extraction process. When the extraction time reached 25 min, the total phenolic content only increased slightly to 11.598 mg GAE/g DW, showing an insignificant difference compared to the 20-min value. At the peak of the survey (30 min), the total phenolic content peaked at 11.699 mg GAE/g DW but showed no significant difference compared to the samples obtained at 20 and 25 min.

The total phenolic content tended to increase over time, but the pattern was not linear. Most of the rapidly soluble and diffusible phenolic compounds entered the solvent during the initial extraction stage [29]. As extraction time increased, the remaining phenolics were located deep within the cell structure or became more tightly bound. This phenomenon required either increasing the extraction kinetics or extending the time. In addition, the equilibrium established between the solid and liquid phases further slowed down the extraction process [30].

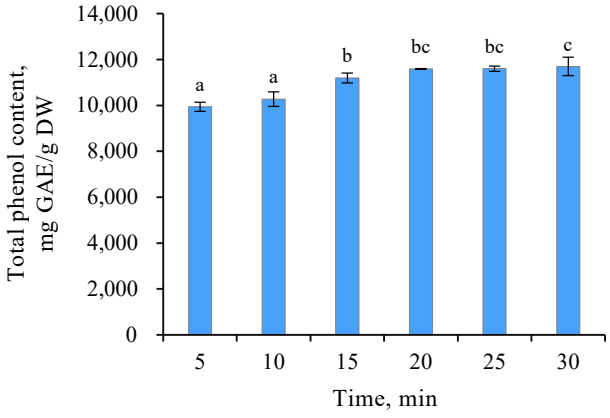
Thus, the extraction time had a significant effect on the phenolic recovery, especially in the early stages of the process. Extending the extraction time can help increase the total phenolic content, but not significantly. Therefore, determining the optimal extraction time is very important to balance the extraction efficiency and cost. In this study, 20 min was the best choice to recover most phenolics.

Effect of temperature on total phenolic yield. Figure 3 shows a complex correlation between the extraction temperature and the total phenolic content. In the range of 30–50°C, the phenolic extraction efficiency increased significantly, going from 9.27 to 11.02 mg GAE/g DW. This phenomenon could be explained by an increase in molecular kinetic energy and a decrease in solvent viscosity, which improved the diffusion and solubility of polyphenols into the extract. However, when the temperature exceeded 50°C (≤ 70°C), the total phenolic content dropped to 9.62 mg GAE/g DW, possibly due to the degradation of some thermosensitive polyphenols with increasing temperature. In addition, high temperatures might destroy their chemical structures or cause undesirable reactions [31].

Our results were similar to those reported by Vuong *et al.* [32], who examined the changes in the total phenolic content for *Carica papaya* L. In their case, the initial total phenolic content increased together with temperature, but as the temperature continued to increase, the total phenolic content decreased due to thermal decomposition.

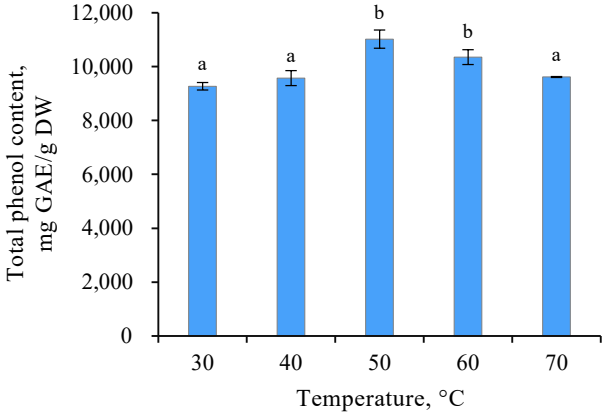
Based on experimental data, 50°C proved to be the optimal temperature to maximize the total phenolic yield from *C. fistula* This temperature balanced the enhancing mass transfer and the minimizing polyphenol degradation. For systematic optimization in further studies, the temperature range should be 40–60°C.

Effect of *C. fistula* fruit pulp/water ratio on total phenolic content. The raw material/solvent ratio is as



Different lowercase letters (a, b, c) indicate statistically significant differences at ($\rho < 0.05$)

Figure 2 Effect of time on total phenolic content



Different lowercase letters (a, b, c) indicate statistically significant differences at ($\rho < 0.05$)

Figure 3 Effect of temperature on total phenolic content

important for phenolic extraction as time or temperature. In [16], the optimal raw material/solvent ratio ranged from 1:10 to 1:50 (w/v), and the extraction process required heating.

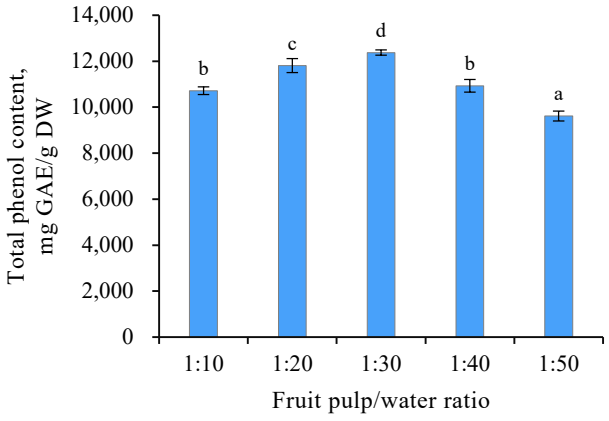
In this research, the raw material/solvent ratio between 1:10 and 1:30 (w/v) increased the total phenolic content significantly, from 10.72 mg GAE/g DW to a peak value of 12.38 mg GAE/g DW (Fig. 4). This phenomenon could be explained by the enhanced solubility and diffusion of phenolic compounds in larger solvent volumes [33]. A larger solvent ratio increased the contact surface area between the raw material and the solvent, thereby improving the mass transfer and maximizing the phenolic release into the extract [34].

If the ratio continued to increase beyond 1:30, the total phenolic content decreased significantly, dropping to 9.62 mg GAE/g DW at the ratio of 1:50. This decrease might be due to either the dilution effect of phenolic concentration [34] or the decreased solvent selectivity, meaning that when the solvent ratio went up, the viscosity of the solution went down, thereby reducing the solubility of phenolic compounds [35].

Sulaiman *et al*. [36] obtained similar results for phenolic extraction and reported the suitable solvent ratio as 1:40. Similarly, Myo & Khat-Udomkiri [37] observed that the solid/solvent ratio below 1:10 was not effective in extracting phenolic compounds, possibly because the solvent volume was not enough to dissolve the compounds.

The raw material/solvent ratio proved to be an important factor in achieving the highest phenolic yield. Based on the experimental data, we chose the ratio of 1:30 as the basis for the solvent ratio optimization experiment. The raw material/solvent ratio between 1:20 (lower limit) and 1:40 (upper limit) was selected to establish the optimal range.

Optimizing the extraction conditions. ***Optimal eximental modeling.*** In this study, we selected three optimization parameters, i.e., time, temperature, and solvent ratio. Table 3 presents the variation range for these factors.



Different lowercase letters (a, b, c) indicate statistically significant differences at ($\rho < 0.05$)

Figure 4 Effect of *Cassia fistula* L. fruit pulp/water ratio on total phenolic content

Table 3 Levels of experimental factors to optimize the extraction process

Independent variable	Symbol	Coded level		
		–1	0	1
Time	X_1	15	20	25
Temperature	X_2	40	50	60
Fruit/water ratio	X_3	20	30	40

Optimal extraction conditions. Table 4 shows the results of applying the JMP 17 pro-optimization software and the Box-Behnken model to the experimental matrix. The total polyphenol content fluctuated quite strongly, ranging from 6.30 to 11.37 mg GAE/g DW. This fluctuation shows the significant impact of various extraction parameters on the phenolic yield. The lowest total phenolic content (6.30 mg GAE/g DW) occurred under suboptimal conditions: short time (15 min), low temperature (40°C), and low solvent ratio (1:20 w/v). The highest total phenolic content (11.37 mg GAE/g DW) was achieved under a more favorable combination of time and solvent ratio.

We used a quadratic regression model to determine the correlation between the independent variables (X_1 – time; X_2 – temperature; X_3 – solvent ratio) and the total phenolic content objective function (Y):

$$Y = 10.56 + 0.53X_1 - 0.03X_2 - 0.42X_3 - 0.38X_1X_2 + \\ + 0.85X_1X_3 + 0.56X_2X_3 - 1.50X_1^2 - 0.70X_2^2 - 1.48X_3^2$$

Table 5 shows the optimal results, corresponding to the experimental data (Table 4) and combined with the Box-Behnken prediction model. The correlation coefficient of $R^2 = 0.9429$ was quite high, meaning that the regression equation explained > 94% of the actual data collected. In addition, the p-value of > 0.05 showed that the initial selection model was consistent with the experimental data. This result was also consistent with some previous studies. For instance, Szpisják-Gulyás *et al*. [14] reported an R^2-value of 0.94, which confirmed the accuracy and reliability of our approach.

The p-value of the regression equation was ≤ 0.05, indicating that the initially selected model was significant at 5%, i.e., the independent variables of time, temperature, and solvent ratio all had an effect on the final phenolic yield.

The correction coefficient $R^2_{adj} = 0.8402$ showed that the regression model explained > 84%, demonstrating a high accuracy of agreement between the experimental values and the predicted model values. In addition, Q^2 was a parameter to evaluate the model's ability to predict the accuracy. If $Q^2 > 0.5$ and R^2-$Q^2 < 0.3$, the model had a fairly high accuracy [38]. The Q^2 value in this case (0.8115) was considered satisfactory. Therefore, the initially selected model was able to predict the data generated by such factors as solvent ratio, extraction temperature, and extraction time.

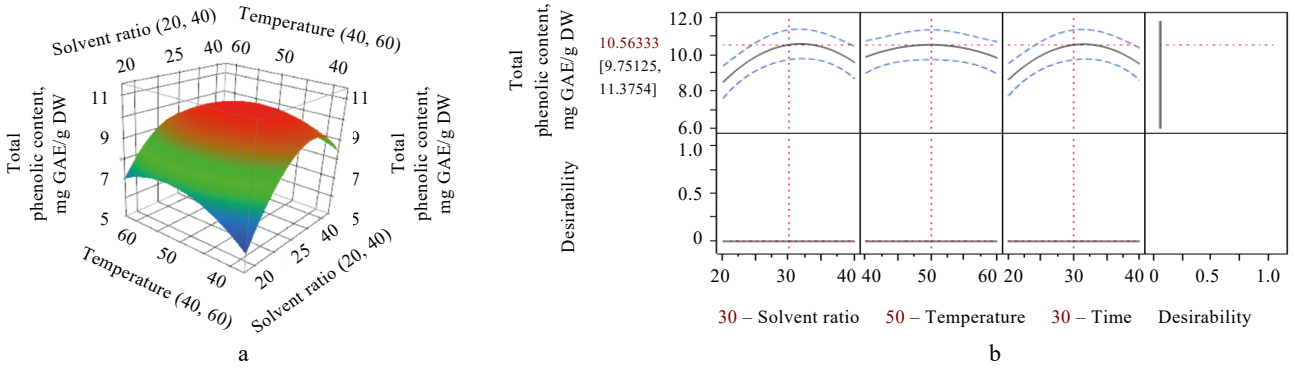
Table 4 Experimental design matrix and anticipated outcomes

Formula	Independent factor						Total phenolic content, mg GAE/g DW	
	X_1	X_2	X_3	Time, min	Temperature, °C	Fruit/water ratio, g/mL	Experimental value	Predicted value
1	0	+	+	20	60	40	9.63	9.54
2	–	0	–	15	50	30	7.67	7.35
3	0	0	0	20	50	30	10.04	10.24
4	+	0	–	25	50	30	7.11	7.25
5	0	0	0	20	50	30	10.28	10.24
6	–	+	0	15	60	40	8.17	8.14
7	+	+	0	25	60	40	8.39	8.27
8	0	–	+	20	40	20	8.45	8.48
9	–	–	0	15	40	20	7.58	7.46
10	0	+	–	20	60	40	7.21	7.25
11	0	–	–	20	40	20	8.26	8.38
12	0	0	0	20	50	30	10.37	10.24
13	–	0	+	15	50	30	6.30	6.35
14	+	0	+	25	50	30	9.20	9.26
15	+	–	0	25	50	20	9.32	9.38

"–" – low level encoding; "0" – center of variables; "+" – high level encoding

Table 5 Variance analysis and regression equation coefficients

Y	Coefficient	Standard error	p-value
Constant	10.563333	0.315916	< 0.001*
X_1	0.5375	0.193458	0.0390*
X_2	–0.02625	0.193458	0.8974
X_3	0.41625	0.193458	0.0841
X_1X_1	–0.38	0.273591	0.2235
X_2X_2	0.865	0.273591	0.0250*
X_3X_3	0.5575	0.273591	0.0972
X_1X_2	–1.507917	0.284763	0.0032*
X_1X_3	–0.690417	0.284763	0.0598
X_2X_3	–1.485417	0.284763	0.0034*
N = 20	R^2 = 0.9429	R^2_{adj} = 0.8402	Q^2 = 0.8115
Regression equation model: p-value = 0.0125*			
Lack of fit: p-value = 0.9617			



a b

Figure 5 Effects of solvent-to-material ratio, extraction temperature, and extraction time on total polyphenol content: (a) Response surface plots, (b) prediction profiler

The model yielded the following optimal extraction conditions: 21.15 min extraction time, 50°C extraction temperature, and 1:31.69 (w/v) solvent ratio. The optimal parameters given predicted the highest total phenolic content of 10.67 mg GAE/g DW (Fig. 5).

Experimental validation. The validation experiments were conducted with the predicted optimal conditions to evaluate the reliability and predictability of the optimization model. Table 6 compares the modeled total phenolic contents with those obtained by experimental extraction at the optimal conditions.

The difference between the predicted model and the experimental survey was very small (0.28%). The results demonstrated that the initially selected model was

Table 6 Total phenolic content obtained at optimal conditions

Factor	X_1, min	X_2, °C	X_3, g/mL	Total phenolic content, mg GAE/g DW
Predicted result	21.15	50	31.69	$10.67^a \pm 0.34$
Experimental result				$10.64^a \pm 0.03$

consistent with the experiment and demonstrated the high accuracy and predictive ability of the response surface methodology in determining the most effective extraction conditions for total phenolic yield from *C. fistula* fruit.

CONCLUSION

This study successfully optimized the extraction conditions for total phenolic yield from *Cassia fistula* L. (Osaka) fruit using the response surface methodology and the Box-Behnken model. The optimal results obtained from the initial selection model were as follows: the highest total phenolic content reached 10.64 mg GAE/g DW at 21.15 min extraction time, 50°C extraction temperature, and 31.69 (w/v) solvent ratio.

The optimized model was consistent with the experimental studies, providing reliable practical data for industrial scale-up of polyphenol extraction. These findings highlight the potential of *C. fistula* as an abundant natural source of such bioactive compounds as polyphenols, which can be used to develop new functional foods and pharmaceutical products.

CONTRIBUTION

D.V. Phuong and N.N. Thuan developed the research concept, designed the study, performed the experiments, collected the data, and drafted the manuscript. N.N. Thuan wrote the abstract and approved the final version.

CONFLICT OF INTEREST

The authors declared no conflict of interest regarding the publication of this article.

ACKNOWLEDGEMENTS

The authors would like to thank the Institute of Biotechnology and Food Technology, Industrial University of Ho Chi Minh City, Vietnam, and their colleagues for technical support.

AI DECLARATION

AI tools (ChatGPT (GPT-5), Grammarly (2025 version), Google Translate (2025 version), and QuillBot (2025 version)) were used to improve translation and increase readability, not to create content or change data. All manuscript content was carefully reviewed and edited by the authors after processing using AI tools.

REFERENCES

1. Alam S, Sarker MMR, Afrin S, Richi FT, Zhao C, *et al.* Traditional herbal medicines, bioactive metabolites, and plant products against COVID-19: Update on clinical trials and mechanism of actions. Frontiers in Pharmacology. 2021;12:671498. https://doi.org/10.3389/fphar.2021.671498
2. Pushpakaran AMK, Singh J, Rasane P, Kaur S, Kaur J, Kaur J, *et al.* Immunomodulatory effect of ashwagandha (*Withania somnifera* L. Dunal) and its impact on COVID-19. Foods and Raw Materials. 2025;13(1):46–57. https://doi.org/10.21603/2308-4057-2025-1-622
3. Velichkovich NS, Dunchenko NI., Stepanova AA, Kozlova OV, Faskhutdinova ER, Yustratov VP., *et al.* The phytochemical composition of Kuzbass medicinal plants. Foods and Raw Materials. 2025;13(2):219–232. https://doi.org/10.21603/2308-4057-2025-2-649
4. Vesnina AD, Milentyeva IS, Le VM, Fedorova AM, Altshuler OG, Prosekov AYu. Quercetin isolated from *Hedysarum neglectum* Ledeb. as a preventer of metabolic diseases. Foods and Raw Materials. 2025;13(1):192–201. https://doi.org/10.21603/2308-4057-2025-1-633
5. Eldemerdash MM, El-Sayed SAS, Hussein HA, Teleb SS, Shehata RS. Molecular and metabolic traits of some Egyptian species of *Cassia* L. and *Senna* Mill (Fabaceae-Caesalpinioideae). BMC Plant Biology. 2022;22:205. https://doi.org/10.1186/s12870-022-03543-7
6. Mwangi RW, Macharia JM, Wagara IN, Bence RL. The medicinal properties of *Cassia fistula* L: A review. Biomedicine & Pharmacotherapy. 2021;144:112240. https://doi.org/10.1016/j.biopha.2021.112240
7. Saeed M, Naseer S, Hussain S, Iqbal M. Phytochemical composition and pharmacological effects of *Cassia fistula.* Scientific Inquiry and Review. 2019;4(1):59–69. https://doi.org/10.32350/sir.41.05
8. Konar A, Ghosh P, Chatterjee S, Lake S, Sector V, *et al. Cassia fistula* is a miraculous medicinal plant: A brief Review. Journal of Plant and Agronomy. 2023;1(1):25–31. https://doi.org/10.5281/zenodo.8079450
9. Tabrez S, Rahman F, Ali R, Alouffi AS, Alshehri BM, *et al.* Assessment of the antileishmanial potential of *Cassia fistula* leaf extract. ACS omega. 2021;6(3):2318–2327. https://doi.org/10.1021/acsomega.0c05629

10. Nortjie E, Basitere M, Moyo D, Nyamukamba P. Extraction methods, quantitative and qualitative phytochemical screening of medicinal plants for antimicrobial textiles: A review. Plants. 2022;11(15):2011. https://doi.org/10.3390/plants11152011

11. Le Tra TT, Phuong TT, Truong PX, Khai TQ, Chi NM. Insect pests damaging *Cassia fistula* trees (Fabaceae) in Vietnam. Ecologica Montenegrina. 2025;81:108–118. https://doi.org/10.37828/em.2025.81.15

12. Singh R, Khanam H, Pandey J. The biological properties and medical importance of *Cassia fistula:* A mini review. Chemistry Proceedings. 2023;14(1):95. https://doi.org/10.3390/ecsoc-27-16149

13. Bucciantini M, Leri M, Nardiello P, Casamenti F, Stefani M. Olive polyphenols: Antioxidant and anti-inflammatory properties. Antioxidants. 2021;10(7):1044. https://doi.org/10.3390/antiox10071044

14. Szpisják-Gulyás N, Al-Tayawi AN, Horváth ZH, László ZS, Kertész SZ, *et al*. Methods for experimental design, central composite design and the Box–Behnken design, to optimise operational parameters: A review. Acta Alimentaria. 2023;52(4):521–537. https://doi.org/10.1556/066.2023.00235

15. Castañeda-Valbuena D, Ayora-Talavera T, Luján-Hidalgo C, Álvarez-Gutiérrez P, Martínez-Galero N, *et al.* Ultrasound extraction conditions effect on antioxidant capacity of mango by-product extracts. Food and Bioproducts Processing. 2021;127:212–224. https://doi.org/10.1016/j.fbp.2021.03.002

16. Wei L, Zhang W, Yin L, Yan F, Xu Y, *et al.* Extraction optimization of total triterpenoids from *Jatropha curcas* leaves using response surface methodology and evaluations of their antimicrobial and antioxidant capacities. Electronic Journal of Biotechnology. 2015;18(2):88–95. https://doi.org/10.1016/j.ejbt.2014.12.005

17. Van HT, Phan-thi DT, Nguyen NT, Lam BBP, Luu HT, *et al.* Morpho-anatomical traits, DNA barcode and phytochemical screening of Aglaonema cochinchinense. Historia naturalis bulgarica. 2024;46(12):325–337. https://doi.org/10.48027/hnb.46.122

18. Shaikh JR, Patil MK. Qualitative tests for preliminary phytochemical screening: An overview. International Journal of Chemical Studies. 2020;8(2):603–608. https://doi.org/10.22271/chemi.2020.v8.i2i.8834

19. Sirichan T, Kijpatanasilp I, Asadatorn N, Assatarakul K. Optimization of ultrasound extraction of functional compound from makiang seed by response surface methodology and antimicrobial activity of optimized extract with its application in orange juice. Ultrasonics Sonochemistry. 2022;83:105916. https://doi.org/10.1016/j.ultsonch.2022.105916

20. Zambrano MV, Dutta B, Mercer DG, MacLean HL, Touchie MF. Assessment of moisture content measurement methods of dried food products in small-scale operations in developing countries: A review. Trends in Food Science & Technology. 2019;88:484–496. https://doi.org/10.1016/j.tifs.2019.04.006

21. Zeb A. Concept, mechanism, and applications of phenolic antioxidants in foods. Journal of Food Biochemistry. 2020;44:e13394. https://doi.org/10.1111/jfbc.13394

22. Do YV, Le QNT, Nghia NH, Vu ND, Tran NTY, *et al.* Assessment of the changes in product characteristics, total ascorbic acid, total flavonoid content, total polyphenol content and antioxidant activity of dried soursop fruit tea (*Annona muricata* L.) during product storage. Food Science & Nutrition. 2024;12(4):2679–2691. https://doi.org/10.1002/fsn3.3949

23. Hazafa A, Rehman KU, Jahan N, Jabeen Z. The role of polyphenol (flavonoids) compounds in the treatment of cancer cells. Nutrition and Cancer. 2020;72(3):386–397. https://doi.org/10.1080/01635581.2019.1637006

24. Kumar A, Kumar P, Shravya H, Pai A. Coumarins as potential anticoagulant agents. Research Journal of Pharmacy and Technology. 2022;15(4):1659–1663.

25. Happi GM, Teufel R. Steroids from the Meliaceae family and their biological activities. Phytochemistry. 2024;121:114039. https://doi.org/10.1016/j.phytochem.2024.114039

26. Andersa KN, Tamiru M, Teka TA, Ali IM, Chane KT, *et al.* Proximate composition, some phytochemical constituents, potential uses, and safety of neem leaf flour: A review. Food Science & Nutrition. 2024;12(10):6929–6937. https://doi.org/10.1002/fsn3.4336

27. Zainal WNHW, Azian NAAM, Albar SS, Rusli AS. Effects of extraction method, solvent and time on the bioactive compounds and antioxidant activity of *Tetrigona apicalis* Malaysian propolis. Journal of Apicultural Research. 2022;61(2):264–270. https://doi.org/10.1080/00218839.2021.1930958

28. Zhang Y, Truzzi F, D'Amen E, Dinelli G. Effect of storage conditions and time on the polyphenol content of wheat flours. Processes. 2021;9(2):248. https://doi.org/10.3390/pr9020248

29. Zhou Y, Liu H, Zhang Y, Zhu W, Meng F, *et al.* Strong interaction between the hydrophobic deep eutectic solvent and phenol enables efficient separation of aqueous and phenol system. Process Safety and Environmental Protection. 2025;199:107247. https://doi.org/10.1016/j.psep.2025.107247

30. Sadeghi A, Rajabiyan A, Nabizade N, Nezhad NM, Zarei-Ahmady A. Seaweed-derived phenolic compounds as diverse bioactive molecules: A review on identification, application, extraction and purification strategies. International Journal of Biological Macromolecules. 2024;266(Part 1):131147. https://doi.org/10.1016/j.ijbiomac.2024.131147

31. Antony A, Farid M. Effect of temperatures on polyphenols during extraction. Applied Sciences. 2022;12(4):2107. https://doi.org/10.3390/app12042107
32. Vuong QV, Hirun S, Roach PD, Bowyer MC, Phillips PA, *et al.* Effect of extraction conditions on total phenolic compounds and antioxidant activities of *Carica papaya* leaf aqueous extracts. Journal of Herbal Medicine. 2013;3(3):104–111. https://doi.org/10.1016/j.hermed.2013.04.004
33. de Oliveira IL, Domínguez-Rodríguez G, Montero L, Viganó J, Cifuentes A, *et al.* Advanced extraction techniques combined with natural deep eutectic solvents for extracting phenolic compounds from pomegranate (*Punica granatum* L.) peels. International Journal of Molecular Sciences. 2024;25(18):9992. https://doi.org/10.3390/ijms25189992
34. Ozdemir M, Gungor V, Melikoglu M, Aydiner C. Solvent selection and effect of extraction conditions on ultrasound-assisted extraction of phenolic compounds from galangal (*Alpinia officinarum*). Journal of Applied Research on Medicinal and Aromatic Plants. 2024;38:100525. https://doi.org/10.1016/j.jarmap.2023.100525
35. Sadrmousavi-Dizaj A, Xu D, Zhang L, Gao J, Ma Y, *et al.* Removal of phenolic compounds from aqueous solution using Hydrophobic deep eutectic Solvent: Liquid-Liquid phase behavior and intermolecular interactions. Journal of Molecular Liquids. 2024;408:125385. https://doi.org/10.1016/j.molliq.2024.125385
36. Sulaiman ISC, Basri M, Masoumi HRF, Chee WJ, Ashari SE, *et al.* Effects of temperature, time, and solvent ratio on the extraction of phenolic compounds and the anti-radical activity of *Clinacanthus nutans* Lindau leaves by response surface methodology. Chemistry Central Journal. 2017;11:54. https://doi.org/10.1186/s13065-017-0285-1
37. Myo H, Khat-Udomkiri N. Optimization of ultrasound-assisted extraction of bioactive compounds from coffee pulp using propylene glycol as a solvent and their antioxidant activities. Ultrasonics Sonochemistry. 2022;89:106127. https://doi.org/10.1016/j.ultsonch.2022.106127
38. Balekundri A, Ahire ED, Shelke RU, Rishipathak DD, Kshirsagar SJ. Eco-friendly HPTLC method for Trifluridine and Tipiracil determination: Quality-by-design meets green analytical chemistry. Green Analytical Chemistry. 2025;13:100234. https://doi.org/10.1016/j.greeac.2025.100234

Additional information about the author

Do Viet Phuong ORCID 0000-0002-0081-0930
Nguyen Ngoc Thuan ORCID 0000-0002-1644-236X

Foods and Raw Materials. 2027;15(2)

ISSN 2308-4057 (Print)
ISSN 2310-9599 (Online)

Research Article
Open Access

Available online at http://jfrm.ru/en
https://doi.org/10.21603/2308-4057-2027-2-713
https://elibrary.ru/XQYITV

Correlation patterns of biochemical compounds in single-clove and multi-clove garlic varieties

Budianto*, Alif G. Arumsari, Abdul Yusup, Muhammad Gumintang, Zahra S. Rosidin

Institute of Science and Technology Al-Kamal, Jakarta, Indonesia

* e-mail: budianto_delta@yahoo.com

Received 09.02.2025; Revised 22.04.2025; Accepted 03.02.2026; Published online 09.07.2026

Abstract:
Garlic is used in traditional medicine due to its diverse bioactive components.
The study focused on three garlic varieties, namely the multi-clove Honan and Tawangmangu cultivars and the single-clove Lanang garlic. To evaluate their biochemical profiles, a comprehensive analytical approach was employed, involving LC-MS/MS and HPLC for phenolic compound quantification, GC-FID for fatty acid analysis, and HS-SPME-GC-MS for the identification of volatile organosulfur compounds, followed by PCA and ANOVA for statistical evaluation.
This study investigated the biochemical composition of a new Indonesian single-clove garlic variety (Lanang) in comparison with two multi-clove varieties (Honan and Tawangmangu) in order to assess its potential as a traditional medicinal source. A total of 23 phenolic compounds, 9 volatile organosulfur compounds, and 8 types of fatty acids were identified and quantified using UPLC-MS/MS and GC-MS analyses. Lanang garlic exhibited the highest concentration of kainic acid among the phenolic compounds (80.774 μg/g) and showed a dominant presence of such volatile compound as diallyl disulfide (86.41%). Meanwhile, Honan garlic recorded the highest concentrations of most fatty acids, particularly linoleic (27.90%) and oleic acid (17.16%). The principal component analysis revealed that Lanang garlic contributed most significantly to PC1 for volatile compounds (76.90%) and phenolic compounds (69.93%), while Honan garlic did so for fatty acids (88.24%). Tawangmangu garlic showed lower biochemical diversity compared to the other varieties.
These findings demonstrate that Lanang garlic has a unique and enriched biochemical profile, particularly in phenolic and volatile compounds, indicating its strong potential as a medicinal garlic variety.

Keywords: Bioactive components, garlic, fatty acids, phenolics, organosulfur compounds, PCA

Please cite this article in press as: Budianto, Arumsari AG, Yusup A, Gumintang M, Rosidin ZS. Correlation patterns of biochemical compounds in single-clove and multi-clove garlic varieties. Foods and Raw Materials. 2027;15(2):333–343. https://doi.org/10.21603/2308-4057-2027-2-713

INTRODUCTION

Lanang garlic, a single-clove variety, has long been used in traditional medicine and is believed to enhance immunity and promote overall health [1]. However, the scientific understanding of its bioactive components remains limited, while more common garlic varieties have been extensively studied. This creates a significant knowledge gap, where health claims related to Lanang garlic have largely not been verified through rigorous scientific investigation. The high functional potential of Lanang garlic based on its traditional use [2] calls for research into its specific biochemical components that may contribute to its health benefits.

Although Lanang garlic grows naturally in unique geographical environments [3], it is rarely compared to other garlic varieties that are more commonly used as spices, which leaves a gap in the literature. If Lanang garlic is found to contain different or higher levels of bioactive compounds than other varieties, this could open up new opportunities for its application in both healthcare and food industry.

The advantages of single-clove garlic have been well-researched, such as its soluble sugar content (which has been proven higher compared to the Taicangbaipi, Ershuizao, and Hongqixing varieties [4]), its fructan molecular weight [5], antioxidant activity, hepatoprotective effects, and phenolic [6] and organosulfur content [7]. However, significant differences have also been found between single-clove and regular garlic in terms of morphology, active components, and pharmacological properties [8]. However, correlation patterns are yet to be revealed between the biochemical compounds of Lanang garlic, as well as its position among other varieties. Visualization can be employed to show the biochemical

Copyright © 2026, Budianto, *et al.* This is an open access article distributed under the terms of the Creative Commons Attribution 4.0 International License (https://creativecommons.org/licenses/by/4.0/), allowing third parties to copy and redistribute the material in any medium or format and to remix, transform, and build upon the material for any purpose, even commercially, provided the original work is properly cited and states its license.

profiles of different varieties, demonstrating the vast and complex richness of garlic.

The use of garlic as a natural remedy in traditional medicine has been recognized for centuries, primarily due to its diverse bioactive components. Compounds such as phenolics, volatiles, and fatty acids in garlic have attracted significant research efforts due to their potential health benefits. In particular, garlic has been studied for its role in preventing various diseases, including cancer [9], cardiovascular diseases [10], and microbial infections [11]. Phenolic compounds in garlic are known for their antioxidant activity, which can protect the body from free radicals [12], while its volatile compounds are often associated with antimicrobial properties that help combat infections [13]. Fatty acids, on the other hand, play a crucial role in cardiovascular health by maintaining blood vessel elasticity and regulating blood pressure [14].

Furthermore, several studies have demonstrated the potential of garlic in cancer prevention through its organosulfur compounds, such as diallyl disulfide (DADS) and diallyl trisulfide (DATS). These compounds are associated with mechanisms that inhibit cancer cell proliferation and trigger apoptosis [15]. Garlic's role in maintaining heart health is also significant, with allicin compounds proven to have antioxidant effects and support vascular functions [16].

This study aimed to analyze the bioactive composition of different garlic varieties, highlighting their potential for promoting health, both in disease prevention and as therapeutic agents in traditional medicine. Specifically, we investigated the organosulfur compounds, phenolic acids, and fatty acids present in the single-clove variety (Lanang garlic), as well as in the multi-clove varieties (Honan and Tawangmangu). In addition, we identified correlation patterns among the biochemical compounds using the Principal Component Analysis.

STUDY OBJECTS AND METHODS

Sample preparation. Garlic samples of the multi-clove varieties (Honan and Tawangmangu) and the single clove variety (Lanang garlic) were purchased online from a supermarket in Indonesia (May 2024). The garlic samples were peeled and cut into small pieces measuring 3 mm. They were sun-dried in the shade (30°C) until a moisture content of 8–10% was achieved. The dried samples were then stored in airtight bottles and labeled for identification.

Identification and quantification of phenolic compounds by liquid chromatography-tandem mass spectrometry (LC-MS/MS). The analytical method was adapted from Kayiran *et al.* [17] and involved a LC-MS/MS system consisting of an ultra-high-performance liquid chromatographer (Thermo Scientific UltiMate 3000) and a triple quadrupole mass spectrometer (Waters Xevo TQ-XS). The liquid chromatography system included a pump, a degasser, a column oven, and an autosampler. Separation was performed on a C18 Kinetex column (100×2.1 mm, 2 µm). Ultra-pure water was used as the mobile phase A, and acetonitrile was used as the mobile phase B.

To enhance separation and ionization, 8 mM ammonium formate and 0.1% formic acid were added to the water phase. The flow rate of the mobile phase was set at 0.3 mL/min, with an injection volume of 5 µL. Electrospray ionization (ESI) operated in both negative and positive modes. The LC- ESI-MS/MS data were processed using the Empower software (Waters, USA) in the multiple reaction monitoring mode. The mass spectrometer parameters included an interface temperature of 360°C, a desolvation line temperature of 240°C, and a nebulizer gas (N2) flow rate of 2.5 L/min.

Identification and quantification of phenolic compounds by HPLC. We used 1.2 M HCl and 45% methanol to extract phenolic compounds from the Honan, Tawangmangu, and Lanang garlic varieties. The extraction process lasted for 1.5 h at 75°C. After cooling, the samples were filtered using Whatman No. 4 paper (0.45 µm). 25 µL of the filtrate was injected into an Agilent HPLC system, which consisted of a model 1260 pump and a G1314B UV detector. The detection wavelength for phenolic compounds was set at 275 nm. Chromatography was performed using an XBridge BEH C18 column (4.6×250 mm, 5 µm) with elution using 0.1% phosphoric acid (A) and acetonitrile (B) with the following gradient profile: 0 min, 10% B; 30 min, 25% B; 50 min, 10% B. The flow rate was set at 0.9 mL/min. After elution, the column was washed and stabilized for 8 min. The concentration of the compounds was reported as mg/kg based on the total weight of the dried varieties. The detection wavelength for reference compounds was set at 270–390 nm, and the standard UV spectrum was compared with the sample.

Extraction and identification of fatty acid composition by GC-FID. Our research method was based on the method of Jarukas *et al.* [18] with some modifications. For gas chromatography (GC) analysis, fatty acids in the lipids must be converted to their methyl ester derivatives. Lipids were extracted using a hexane/isopropanol mixture (3/2 v/v). The sample (5 g) was homogenized for 30 s in the hexane and isopropanol mixture. The mixture was then centrifuged at 9,000 rpm for 12 min. The supernatant was collected and placed in a sealed test tube. A total of 4 mL of 2% methanolic sulfuric acid was added and mixed well using a vortex. This mixture was left to undergo methylation in a water bath at 52°C for 10 h. Afterwards, the tube was removed from the water bath, cooled to room temperature, and 6 mL of 5% sodium chloride was added, followed by thorough mixing. The fatty acid methyl esters formed in the test tube were separated with 4 mL of hexane. The hexane phase was collected using a pipette, treated with 4 mL of 2% $KHCO_3$ solution, and allowed to stand for 3 h for phase separation. The methyl esters were then isolated and measured using gas chromatography with flame ionization detection (GC-FID) (L-Analytix GC, model 22, Malaysia) connected to GC 20 Version 2 software for data recording.

Analysis of volatile organosulfur compounds by HS-SPME and GC-MS. Volatile organosulfur compounds were analyzed by the HS-SPME (Headspace Solid Phase Microextraction) method with some modifications [19]. Garlic samples from the three varieties (Honan, Tawangmangu, and Lanang garlic) were finely ground. A total of 100 mg from each sample was placed in a 1.5-mL SPME screw-cap vial, and (Z)-3-hexenyl acetate dissolved in water was added to a final concentration of 2 µg per vial. The SPME fiber was manually inserted into the vial containing the sample and incubated at 50°C for 30 min. After incubation, the fiber was withdrawn and inserted into the injection port of the gas chromatography-mass spectrometry (GC-MS) instrument for analysis.

The GC-MS analysis was performed using a Mitra GCX 600 gas chromatograph connected to a Mitra MASS-9000 mass spectrometer (Mitra Lab Instruments, Malaysia). The system was equipped with a DB-5 capillary column (30 m×0.25 mm i.d.×0.25 µm film thickness; Supelco). The injector and interface temperatures were set at 220°C. The temperature program for volatile analysis started at 40°C for 3 min, then increased to 180°C at a rate of 12°C/min, was held for 5 min, and then further increased to 240°C at a rate of 40°C/min, and was held for 5 min. Helium was used as the carrier gas at a flow rate of 0.9 mL/min. A splitless injection mode was chosen due to the low concentration of volatiles in the samples.

To ensure complete elution of the volatile compounds, the SPME fiber was conditioned in the injector at 220°C for 2 min before each analysis. Blank tests were performed between the sample analyses. The mass spectrometer operated in the Electron Ionization (EI) mode at 70 eV with a scanning range of *m/z* 40–500.

Volatile components were identified by comparing the retention indices relative to n-alkanes (C6–C20) and matching the mass spectra with those established by the National Institute of Standards and Technology [20] and present in Wiley libraries, as well as with available reference standards. Peaks were analyzed using the AMDIS software from the National Institute of Standards and Technology before mass spectrum matching.

Statistical analysis. We employed the Principal Component Analysis (PCA) to identify patterns of variation and reduce the dimensionality of biochemical data across the three garlic varieties: Honan, Tawangmangu, and Lanang garlic. PCA was instrumental in revealing the main differences among the varieties.

To test for biochemical differences between the varieties, we performed ANOVA followed by post-hoc Tukey HSD test using SPSS version 26, with a significance level of $p < 0.05$. Data visualization was conducted using a Chord Diagram in Origin Pro to facilitate interpretation of the relationships between the biochemical components and the garlic varieties.

RESULTS AND DISCUSSION

Phenolic compounds. The parameters such as *m/z* (parent ion), LOD (limit of detection), LOQ (limit of quantification), and UCL (upper confidence limit), %, in the LC-MS/MS (liquid chromatography-tandem mass spectrometry) analysis play a critical role in ensuring the accuracy and sensitivity of the method. For instance, the *m/z* value of 578.05 for rhoifolin confirmed the identity of this compound within the samples. The LOD and LOQ were 3.20 and 4.00 µg/g, respectively, demonstrating the method's ability to detect and quantify compounds at low concentrations. The UCL of 0.0940% ensured a high level of confidence in the quantification results. Although rhoifolin was not detected in any of the three garlic varieties, these parameters affirm the reliability and precision of the employed method.

Gallic acid emerged as the dominant phenolic compound across all the samples (Table 1). Statistical comparisons revealed a significant difference ($p < 0.05$) in the gallic acid content between Lanang garlic and both Honan and Tawangmangu varieties. However, no significant difference was found between Honan and Tawangmangu garlics ($p > 0.05$). Notably, Tawangmangu exhibited the highest gallic acid concentration at 172.648 ± 1.949 µg/g. This aligns partially with the findings of Bozin *et al.* [21], who reported average total phenolic contents of 6.5 mg GAE/g in garlic samples, much lower than in our study. This discrepancy may stem from the differences in the cultivar type, extraction procedures, or environmental growth conditions.

Kainic acid was the second most abundant phenolic compound, showing significant inter-varietal variation ($p < 0.05$). Lanang garlic recorded the highest concentration at 80.774 ± 0.528 µg/g, suggesting a distinct phytochemical profile that supports its potential medicinal use. Malic acid, ranking third, was most concentrated in Tawangmangu garlic (93.992 ± 0.918 µg/g), with significant differences across all the varieties ($p < 0.05$). These results demonstrate a clear biochemical differentiation, supporting the hypothesis that single-clove garlic (Lanang) possesses a unique and more potent phenolic composition compared to its multi-clove counterparts.

Qualitatively, a total of 12 phenolic analytes were identified in Lanang garlic, while only 11 were detected in Honan and Tawangmangu. Only Lanang garlic contained 4-OH-benzoic acid and chlorogenic acid. In contrast, coumarin was present in Honan and Tawangmangu but absent in Lanang. This compositional divergence supports the Principal Component Analysis (PCA) results, which indicated that Lanang garlic had a distinctly different phenolic profile compared to that of the multi-clove varieties. Such variation may reflect genetic and environmental influences, which are common determinants in secondary metabolite biosynthesis among Allium species.

Comparative literature reports total phenolic contents in garlic ranging from 0.98 to 10.8 mg GAE/g, depending on the variety and method used [21, 22]. Our findings fall within this range but highlight a more detailed compound-specific distribution, which provides a deeper understanding of bioactive profiles. Furthermore, the absence of certain phenolics such as sinapic acid (< 0.1 mg/kg in literature) in our samples may be due

Table 1 Analytical parameters of the liquid chromatography-tandem mass spectrometry method and the phenolic profiles of garlic varieties

Code	Analyte	Retention time, min	Parent ion (*m/z*)	LOD/LOQ, µg/g	UCL, %	Quantification, µg Analyte/g		
						Honan	Tawangmangu	Lanang
1	Kainic acid	1.129	191.95	0.25/0.50	0.0081	62.136 ± 1.564[a]	73.736 ± 0.446[b]	80.774 ± 0.528[c]
2	Malic acid	1.280	132.00	2.50/3.00	0.0115	32.926 ± 1.847[a]	93.992 ± 0.918[c]	72.820 ± 0.539[b]
3	Fumaric acid	1.479	114.00	2.50/3.50	0.0123	12.378 ± 0.532[a]	21.400 ± 0.524[b]	33.940 ± 1.399[c]
4	Gallic acid	3.090	167.85	0.28/0.40	0.0281	171.408 ± 2.802[b]	172.648 ± 1.949[b]	120.860 ± 1.384[a]
5	Protocatechuic acid	4.920	153.95	8.10/9.42	0.0410	0.240 ± 0.336[a]	1.586 ± 0.389[a]	36.720 ± 1.807[b]
6	Pyrocatechol	6.477	109.20	25.60/27.50	0.0234	n.d.	n.d.	n.d.
7	4-OH-benzoic acid	7.129	135.95	0.50/0.78	0.0288	n.d.	n.d.	38.830 ± 1.626[a]
8	Chlorogenic acid	7.328	354.15	2.00/2.50	0.0070	n.d.	n.d.	8.932 ± 0.620[a]
9	Vanilic acid	8.567	167.09	4.10/5.00	0.0509	22.706 ± 0.727[a]	22.366 ± 0.904[a]	26.216 ± 0.896[b]
10	Caffeic acid	8.820	177.95	0.50/1.26	0.0353	n.d.	n.d.	n.d.
11	Syringic acid	9.120	195.95	1.20/2.30	0.0237	3.316 ± 0.352[b]	1.996 ± 0.298[a]	3.254 ± 0.439[b]
12	Vanillin	10.868	152.10	4.20/5.00	0.0279	n.d.	n.d.	n.d.
13	*p*-Coumaric acid	11.550	163.05	0.60/0.65	0.0515	3.920 ± 0.225[b]	2.856 ± 0.294[a]	9.426 ± 0.623[c]
14	Sinapinic acid	12.570	223.15	7.60/8.00	0.0280	n.d.	n.d.	n.d.
15	Hesperidin	12.590	611.20	0.50/0.55	0.0261	6.988 ± 0.658[b]	3.888 ± 0.211[a]	4.336 ± 0.434[a]
16	Ferulic acid	12.890	191.95	1.50/1.90	0.0493	4.916 ± 0.135[b]	2.696 ± 0.209[a]	2.430 ± 0.396[a]
17	Rutin	13.050	608.95	5.60/6.60	0.0158	n.d.	n.d.	n.d.
18	Isoquercitrin	13.410	463.50	5.30/6.20	0.0132	n.d.	n.d.	n.d.
19	Rosmarinic acid	14.570	357.90	6.70/8.90	0.0712	n.d.	n.d.	n.d.
20	*o*-Coumaric acid	15.470	163.95	24.30/31.00	0.0512	n.d.	n.d.	n.d.
21	Quercitrin	16.670	448.15	2.10/3.10	20.078	n.d.	n.d.	n.d.
22	Apigenin	31.530	269.95	6.80/8.50	0.0353	n.d.	n.d.	n.d.
23	Coumarin	17.380	148.05	1.30/2.30	0.0236	10.570 ± 0.361[b]	2.814 ± 0.268[a]	n.d.
24	Myricetin	18.690	318.00	1.30/1.50	0.0125	n.d.	n.d.	n.d.
25	Fisetin	19.430	285.95	4.50/6.30	0.0147	n.d.	n.d.	n.d.
26	Liquiritigenin	25.720	255.95	5.40/6.50	0.0340	n.d.	n.d.	n.d.
27	Quercetin	28.350	301.90	2.20/3.10	0.0542	n.d.	n.d.	n.d.
28	Rhoifolin	16.320	578.05	3.20/4.00	0.0940	n.d.	n.d.	n.d.
29	Hesperetin	17.300	303.95	8.20/9.40	0.0184	n.d.	n.d.	n.d.
30	Naringenin	17.980	271.95	2.40/3.20	0.0147	n.d.	n.d.	n.d.
31	Formononetin	18.820	267.30	2.20/2.60	0.0030	n.d.	n.d.	n.d.
32	Kaempferol	18.960	283.95	2.40/2.80	0.0486	n.d.	n.d.	n.d.
33	Acacetin	24.570	285.05	2.10/3.20	0.0070	n.d.	n.d.	n.d.
34	Genistein	30.680	268.95	7.90/9.50	0.0289	n.d.	n.d.	n.d.
35	Baicalein	35.630	268.85	6.80/8.90	0.0215	n.d.	n.d.	n.d.
36	Biochanin A	35.890	281.930	5.20/6.30	0.0542	n.d.	n.d.	n.d.

n.d. – not detected; LOD – limit of detection; LOQ – limit of quantification; UCL – upper confidence limit; 95% relative standard uncertainty at confidence level. The data were analyzed using ANOVA followed by post hoc Tukey's HSD test at a significance level of $p < 0.05$. The results are expressed as mean ± standard deviation. Different superscripts within the same column indicate significant differences. All analyses were performed in five replicates

to their concentrations being below the detection limits or varietal metabolic expression.

In summary, the phenolic compound profile of Lanang garlic had a larger number and a higher concentration of unique analytes, particularly kainic acid and chlorogenic acid, compared to the multi-clove varieties. These results, corroborated by robust analytical validation and significant statistical differences, demonstrate Lanang's strong potential for further development as a medicinal garlic variety.

Volatile compounds. The composition of volatile compounds in the Honan, Tawangmangu, and Lanang garlic varieties was analyzed using the gas chromatography-mass spectrometry (GC-MS) method (Table 2). The parameters such as the retention time and the retention index play a crucial role in compound identification. In particular, the retention time helps determine the time taken for a compound to reach the detector, while the retention index provides information about the polarity and volatility of the compounds. Additionally, the relative abundance percentage reveals the proportion of each compound within the total mixture.

The analysis of volatile compounds revealed diallyl disulfide as the predominant compound, with its highest concentration in Lanang garlic (86.405%), followed by Honan (56.762%) and Tawangmangu (38.889%). This result is consistent with previous reports showing that diallyl disulfide dominates in several garlic varieties, ranging from 21–26% [23]. Other studies, however, reported the dominance of diallyl trisulfide at 33.4% [24]. This indicates that Lanang garlic has a stronger aromatic potential compared to the other varieties.

Table 2 Composition of volatile compounds in Honan, Tawangmangu, and Lanang garlics according to gas chromatography-mass spectrometry (ISTA Laboratory, Jakarta, Indonesia, 2024)

Code	Analyte	Retention time, min	Retention index	Relative abundance, %		
				Honan	Tawangmangu	Lanang
S1	Diallyl sulphide	5.46	845	0.522 ± 0.030^{a}	0.814 ± 0.047^{b}	2.663 ± 0.090^{c}
S2	1-Propenyl methyl disulphide	6.92	919	5.350 ± 0.053^{b}	3.464 ± 0.131^{a}	8.803 ± 0.213^{c}
S3	Dimethyl trisulphide	7.78	952	7.402 ± 0.234^{b}	4.638 ± 0.179^{a}	9.560 ± 0.222^{c}
S4	Dimethyl trisulphide isomer	8.15	965	0.628 ± 0.171^{a}	0.520 ± 0.074^{a}	7.531 ± 0.163^{b}
S5	2-Acetylpyrrole	9.54	1,056	12.386 ± 0.193^{b}	10.430 ± 0.115^{a}	14.473 ± 0.415^{c}
S6	Diallyl disulphide	9.73	1,064	56.762 ± 0.031^{b}	38.889 ± 0.107^{a}	86.405 ± 0.400^{c}
S7	Tetramethylpyrazine	10.05	1,089	3.686 ± 0.062^{b}	5.528 ± 0.062^{c}	1.791 ± 0.125^{a}
S8	2-Propenylthioacetonitrile	10.21	1,092	3.502 ± 0.096^{b}	2.652 ± 0.037^{a}	7.328 ± 0.332^{c}
S9	Isopropyl-*α*-mercaptopropionate	10.27	1,098	9.158 ± 0.720^{b}	5.652 ± 0.181^{a}	21.663 ± 0.185^{c}
S10	Allyl methyl trisulphide	10.68	1,111	3.374 ± 0.386^{b}	1.462 ± 0.154^{a}	1.306 ± 0.532^{a}
S11	Diethanol disulphide	10.83	1,133	9.324 ± 0.221^{b}	4.424 ± 0.360^{a}	15.583 ± 0.255^{c}
S12	Methyl pentyl disulphide	11.00	1,152	18.632 ± 0.222^{b}	5.318 ± 0.192^{a}	23.695 ± 0.169^{c}
S13	*Cis*-methyl propenyl sulphide	11.09	1,163	2.156 ± 0.160^{c}	1.174 ± 0.107^{b}	0.735 ± 0.178^{a}
S14	Allyl methyl trisulphide	11.18	1,176	15.286 ± 0.142^{a}	16.454 ± 0.280^{b}	21.555 ± 0.195^{c}
S15	Geranyl nitrile	11.32	1,192	0.738 ± 0.180^{a}	0.580 ± 0.128^{a}	0.718 ± 0.128^{a}
S16	Methyl 2-methylheptanoate	11.46	1,208	n.d.	n.d.	0.363 ± 0.426^{a}
S17	3-Ethenyl-1.2-dithi-4-ene	11.65	1,210	n.d.	n.d.	n.d.
S18	Diallyl disulphide isomer	11.78	1,225	n.d.	n.d.	n.d.
S19	3-Vinyl-1.2-dithiacyclohex-5-ene	11.98	1,249	31.830 ± 1.217^{b}	29.034 ± 0.775^{a}	44.486 ± 1.107^{c}
S20	3-Ethenyl-1.2-dithi-5-ene isomer	12.08	1,262	n.d.	n.d.	n.d.
S21	Dimethyl tetrasulphide	12.15	1,272	4.344 ± 0.331^{a}	5.252 ± 0.379^{b}	11.496 ± 0.377^{c}
S22	*p*-Cuminaldehyde	12.36	1,302	n.d.	n.d.	0.776 ± 0.851^{a}
S23	3-Isopropyl benzaldehyde	12.57	1,314	n.d.	n.d.	1.825 ± 0.0.988^{a}
S24	4.7-Dimethylundecane	12.74	1,321	1.634 ± 0.597^{a}	1.418 ± 0.294^{a}	n.d.
S25	Diallyl trisulphide	13.01	1,325	17.770 ± 0.586^{b}	12.472 ± 0.385^{a}	32.370 ± 0.396^{c}
S26	(Allylsulfanyl)acetonitrile	13.23	1,331	5.848 ± 0.111^{a}	6.266 ± 0.480^{a}	12.256 ± 0.220^{b}
S27	Dipropyl trisulphide	13.78	1,341	4.180 ± 0.292^{b}	3.244 ± 0.687^{a}	7.503 ± 0.549^{c}
S28	Diallyl trisulphide isomer	14.54	1,453	5.272 ± 0.294^{b}	1.926 ± 0.160^{a}	8.698 ± 0.950^{c}
S29	4-(Methylsulfinyl)butanenitrile	14.76	1,478	n.d.	n.d.	0.433 ± 0.484^{a}
S30	Diallyl tetrasulphide	15.78	1,592	6.416±0.889^{b}	3.670 ± 0.549^{a}	3.960 ± 0.535^{a}
S31	2.4-Dimethyl-5.6-dithia-2.7-nonadienal	15.96	1,634	n.d.	n.d.	2.695 ± 0.396^{a}
S32	Ethyl dodecanoate	16.56	1,673	n.d.	n.d.	2.246 ± 0.267^{a}
S33	Diethyl phthalate	16.89	1,698	n.d.	n.d.	3.293 ± 0.411^{a}
S34	2.4-Dimethyl-5.6-dithia-2.7-nonadienal	17.00	1,789	22.534 ± 0.557^{c}	15.214 ± 0.401^{a}	16.470 ± 0.306^{b}

n.d. – not detected. The data were analyzed using ANOVA followed by post hoc Tukey's HSD test at a significance level of $p < 0.05$. The results are expressed as mean ± standard deviation. Different superscripts within the same column indicate significant differences. All analyses were performed in five replicates

Other key compounds such as 1-propenyl methyl disulfide and dimethyl trisulfide also showed significant accumulation in Lanang garlic (8.803 and 9.560%, respectively), contributing to its distinct aromatic characteristics. The presence of 2-acetylpyrrole, which contributes to roasted flavors, was also higher in Lanang garlic (14.473%) compared to the multi-clove varieties. Similarly, methyl pentyl disulfide reached 23.695% in Lanang, further enhancing its sensory appeal.

In contrast, 2.4-dimethyl-5,6-dithia-2,7-nonadienal was higher in Honan garlic (22.534%) than in Lanang (16.470%) or Tawangmangu (15.214%), showing specific variation between the varieties. The absence of three compounds across all the samples may be due to degradation or transformation during storage and analysis [25]. Overall, the volatile compound profile of Lanang garlic showed higher intensity and diversity, supporting its potential as a superior variety in terms of aroma and commercial value.

Fatty acids. The analysis of fatty acids was based on gas chromatography with flame ionization detection (GC-FID), which has high sensitivity and stability in detecting volatile compounds such as fatty acids. The use of the retention index provides greater consistency in compound identification compared to relying solely on the retention time. According to the results (Table 3), oleic acid (FA11) was the most abundant fatty acid, particularly in Lanang (28.464%) and Tawangmangu (27.476%) garlics, compared to Honan (13.340%). This was in line with previous studies reporting oleic acid, along with linoleic and palmitic acids, among the dominant fatty acids in Allium species [26].

Lauric acid (FA1) was also the highest in Lanang (0.550%) and Tawangmangu (0.535%), compared to Honan (0.085%). Conversely, myristic acid (FA2) showed a unique trend, with Honan garlic recording the highest level (1.552%). Similar patterns were observed for *cis*-10-pentadecanoic acid (FA4), which was significantly lower in Honan (3.046%) compared to Tawangmangu and Lanang (both around 8%).

Gamma-linolenic acid (FA13) was especially high in Honan (3.06%) compared to Tawangmangu (0.218%) and Lanang (0.19%), indicating unique lipid accumulation. On the other hand, palmitic (FA5) and palmitoleic

Table 3 Composition of fatty acids in Honan, Tawangmangu, and Lanang garlics according to gas chromatography with flame ionization detection

Code	Analyte	Retention time, min	Relative abundance, %		
			Honan	Tawangmangu	Lanang
FA1	Lauric acid	16.90	0.085 ± 0.004^{a}	0.535 ± 0.004^{b}	0.550 ± 0.010^{c}
FA2	Myristic acid	21.90	1.552 ± 0.175^{b}	0.725 ± 0.004^{a}	0.723 ± 0.006^{a}
FA3	Pentadecanoic acid	25.95	0.015 ± 0.003^{a}	0.860 ± 0.015^{b}	0.850 ± 0.012^{b}
FA4	*Cis*-10-pentadecanoic acid	26.96	3.046 ± 0.061^{a}	8.020 ± 0.114^{b}	7.988 ± 0.081^{b}
FA5	Palmitic acid	28.95	8.504 ± 4.226^{a}	7.746 ± 0.129^{a}	7.630 ± 0.045^{a}
FA6	Palmiteloic acid	29.40	0.034 ± 0.010^{b}	0.008 ± 0.002^{a}	0.007 ± 0.001^{a}
FA7	Heptadecanoic acid	31.20	0.601 ± 0.099^{b}	1.156 ± 0.036^{c}	0.017 ± 0.001^{a}
FA8	*Cis*-10-heptadecanoic acid	31.90	n.d.	n.d.	n.d.
FA9	Stearic acid	33.59	n.d.	n.d.	n.d.
FA10	Elaidic acid	34.60	n.d.	n.d.	n.d.
FA11	Oleic acid	34.80	13.340 ± 1.230^{a}	27.476 ± 0.886^{b}	28.464 ± 1.093^{b}
FA12	Linoleic acid	36.08	8.022 ± 1.013^{a}	19.400 ± 1.557^{b}	19.060 ± 1.281^{b}
FA13	γ-Linolenic acid	38.19	3.060 ± 0.091^{b}	0.218 ± 0.019^{a}	0.190 ± 0.015^{a}
FA14	α-Linolenic acid	38.56	7.336 ± 0.416^{b}	3.312 ± 0.465^{a}	3.438 ± 0.484^{a}
FA15	Arachidic acid	39.32	2.468 ± 0.320^{a}	4.638 ± 0.395^{b}	4.716 ± 0.451^{b}
FA16	*Cis*-11-eicosenoic acid	39.76	1.782 ± 0.214^{b}	0.682 ± 0.112^{a}	0.468 ± 0.124^{a}
FA17	Heneicosanoic acid	41.34	5.032 ± 0.141^{c}	3.180 ± 0.151^{b}	1.938 ± 0.154^{a}
FA18	*Cis*-11.14-eicosadienoic acid	41.78	1.420 ± 0.192^{b}	0.598 ± 0.110^{a}	0.634 ± 0.056^{a}
FA19	*Cis*-8.11.14-eicosatrienoic acid	42.49	1.292 ± 0.086^{b}	0.260 ± 0.023^{a}	0.278 ± 0.019^{a}
FA20	Behenic acid	42.68	0.808 ± 0.199^{b}	0.320 ± 0.130^{a}	0.200 ± 0.059^{a}
FA21	*Cis*-11.14.17-eicosatrienoic acid	42.98	1.720 ± 0.216^{b}	0.772 ± 0.090^{a}	0.708 ± 0.115^{a}
FA22	Erucic acid	43.12	5.312 ± 0.577^{b}	2.340 ± 0.207^{a}	2.416 ± 0.171^{a}
FA23	Arachidonic acid	43.67	1.988 ± 0.069^{a}	2.008 ± 0.448^{a}	0.994 ± 0.074^{a}
FA24	Tricosanoic acid	44.64	2.892 ± 0.154^{b}	0.672 ± 0.097^{a}	0.616 ± 0.168^{a}
FA25	*Cis*-13.16-docosadienoic acid	45.27	4.970 ± 0.195^{c}	1.460 ± 0.167^{a}	3.786 ± 0.398^{b}
FA26	*Cis*-5.8.11.14.17-eicosapentaenoic acid	46.34	3.068 ± 0.111^{b}	0.342 ± 0.133^{a}	0.482 ± 0.127^{a}
FA27	Lignoceric acid	47.34	6.640 ± 0.502^{b}	3.140 ± 0.219^{a}	3.124 ± 0.195^{a}
FA28	Nervonic acid	47.98	3.874 ± 0.177^{b}	1.564 ± 0.352^{a}	1.342 ± 0.267^{a}
FA 29	Unknown	48.05	4.000 ± 0.111^{b}	0.526 ± 0.063^{a}	0.536 ± 0.076^{a}

n.d. – not detected. The data were analyzed using ANOVA followed by post hoc Tukey's HSD test at a significance level of $p < 0.05$. The results are expressed as mean ± standard deviation. Different superscripts within the same column indicate significant differences. All analyses were performed in five replicates

(FA6) acids showed no significant differences among the three varieties. Differences were also observed in arachidic (FA15) and heneicosanoic (FA17) acids, with Honan garlic showing significantly different values compared to the other two varieties.

These results align with previous findings that garlic lipids consist of approximately 60% neutral lipids, 23% phospholipids, and 14% glycolipids, with oleic, linoleic, palmitic, and α-linolenic acids as dominant components [26, 27]. The fatty acid profiles highlight distinct biochemical traits among the varieties, particularly higher unsaturated fatty acid contents in Lanang and Tawangmangu.

Principal component analysis. ***Volatile compounds.*** The principal component analysis (PCA) of volatile compounds from the Lanang, Tawangmangu, and Honan garlic varieties (Fig. 1a and 1b) successfully identified

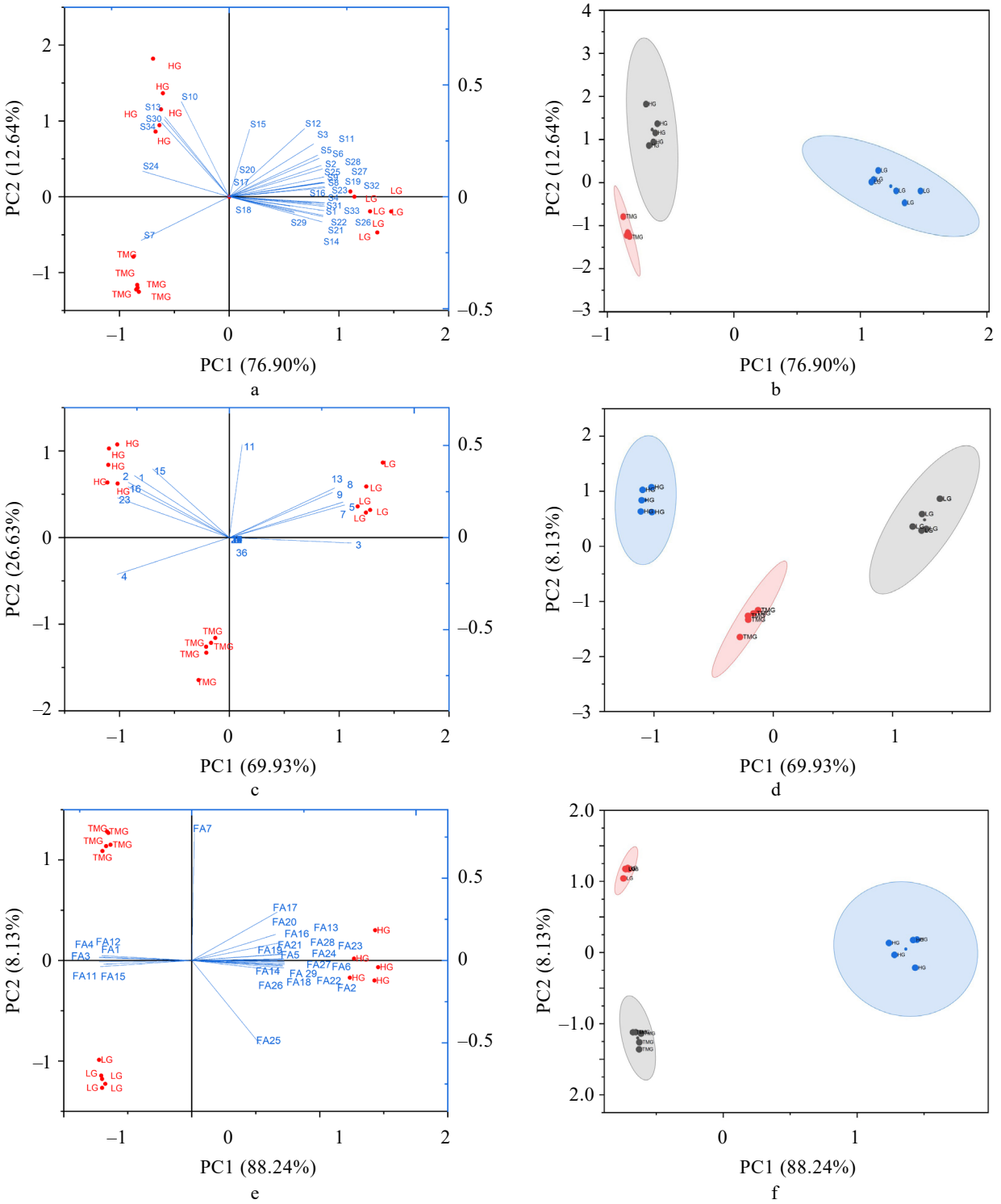


Figure 1 Principal component analysis of Lanang (LG), Tawangmangu (TMG), and Honan (HG) garlic varieties. Cluster plot of volatile compounds (a), phenolic compounds (c), and fatty acids (e). Cluster plot with confidence for volatile compounds (b), phenolic compounds (d), and fatty acids (f)

two principal components: PC1, which accounted for 76.90% of the variance, and PC2, with 12.64%. Overall, these two components capture nearly 90% of the information from the analyzed data, providing a clear overview of the differences in volatile compound profiles among the three varieties.

Lanang garlic is positioned in the upper right and lower right quadrants, indicating a positive correlation of its volatile compounds with PC1, while exhibiting variability in PC2. The position in the upper right quadrant suggests that several volatile compounds exhibit strong characteristics on both components, whereas those in the lower right quadrant are more dominant in PC1 but demonstrate a negative contribution to PC2.

In contrast, the Tawangmangu garlic variety is located in the lower left quadrant, signifying a negative correlation of its volatile compounds with both PC1 and PC2, particularly for analyte S7. This positioning indicates that this variety possesses a significantly different volatile profile compared to Lanang garlic, demonstrating an opposing pattern in relation to both principal components.

On the other hand, Honan garlic displays a more dispersed distribution, with several analytes (S24, S10, S34, S23, and S30) located in the upper left quadrant. This suggests that the volatile compounds from this garlic variety have a negative correlation with PC1 while showing a positive correlation with PC2. This illustrates a considerable difference between Honan and the other varieties, particularly regarding the characteristics explained by PC2. However, some other analytes from Honan follow a pattern more similar to Lanang garlic, indicating a resemblance in the volatile compound profiles at certain points.

Phenolic compounds. The PCA analysis of phenolic compounds from the three garlic varieties revealed that PC1 accounted for 69.93 % of the variance, while PC2 accounted for 26.36 % (Fig. 1c and 1d). The PCA diagram shows intriguing results in the distribution of the garlic varieties. Lanang garlic is located in the upper right quadrant, with identified analytes 3, 5, 7, 8, 9, 11, and 13. This position indicates that the phenolic compounds in this variety possess strong and positive characteristics, correlating with both principal components and creating a prominent profile in this analysis.

In contrast, Tawangmangu is positioned in the lower left quadrant, with analyte 4. This suggests that the phenolic compounds from this variety tend to correlate negatively with both PC1 and PC2, indicating a different and lower profile compared to Lanang garlic. This implies that the composition of phenolic compounds in Tawangmangu is less diverse or exhibits weaker characteristics than those in the other varieties.

Honan garlic occupies the upper left quadrant, with analytes 1, 2, 15, 16, and 23. This position suggests that the phenolic compounds in this variety correlate positively with PC2 but negatively with PC1. This reflects the unique characteristics of the phenolic compounds in Honan, which differ from Lanang yet share some similarities with Tawangmangu. Overall, Lanang garlic displays the richest and most diverse profile, Tawangmangu presents a simpler profile, and Honan exhibits a combination of distinct characteristics.

Fatty acids. The PCA analysis of fatty acids from the three garlic varieties (Fig. 1e and 1f) indicates that PC1 accounted for 88.24%, reflecting a significant contribution to the data variation, while PC2 accounted for only 8.13%, highlighting additional important variation.

Honan garlic stands out in both the upper right and lower right quadrants, indicating a rich diversity in fatty acids, which reflects its high potential for nutritional composition. Tawangmangu is located in the lower left quadrant, with analytes FA4, FA12, FA3, and FA1, suggesting a simpler yet stable fatty acid profile, with unique characteristics that can be further explored.

Lanang garlic is situated in the upper left quadrant, with analytes FA8, FA10, FA15, and FA11, demonstrating a specific fatty acid composition that differs from that of Tawangmangu.

Visualization of biochemical distribution. In the chord diagram illustrating the distribution of phenolic compounds (Fig. 2a), the total band width showed

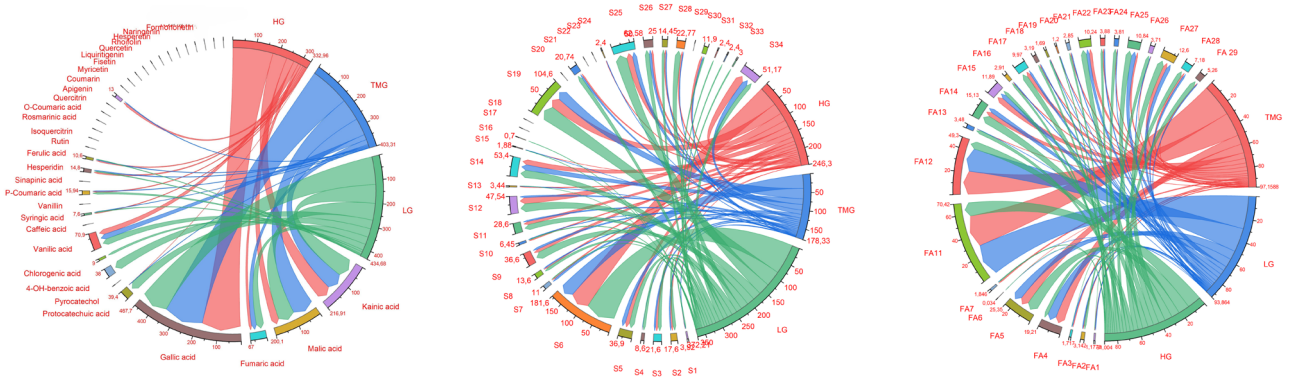


Figure 2 Chord diagram visualizing the biochemical distribution in the Lanang (LG), Tawangmangu (TMG), and Honan (HG) garlic varieties: (a) phenolic, (b) volatile, and (c) fatty acid

that Lanang garlic had the highest value at 434.68, followed by Tawangmangu at 403.31, and Honan garlic at 332.96. Gallic acid was the dominant compound across the three varieties, indicating its significant presence in each. Additionally, Lanang also showed the highest levels of other analytes such as protocatechuic acid and 4-hydroxybenzoic acid, compared to the other two varieties.

In the chord diagram illustrating volatile compound distribution (Fig. 2b), Lanang garlic had the largest total band width at 375, followed by Honan at 246.3, and Tawangmangu at 178.33. Lanang showed the highest levels of analytes such as S6, S19, S25, and S12, compared to the other two varieties. The chord diagram depicting fatty acid distribution (Fig. 2c) shows that Tawangmangu garlic had the highest total band width at 97.1588, followed by Lanang at 93.864, and Honan at 91.004. The distribution of analytes across the three varieties appeared to be relatively even, reflecting the consistency of fatty acid content among the varieties. Despite this even distribution, analytes FA11 and FA12 dominated, indicating that these fatty acids were present in higher concentrations compared to the other analytes across the three varieties.

Based on this study, Lanang garlic demonstrated significant potential in treating various diseases, particularly those related to cardiovascular disorders and cancer [28]. The richer and more diverse phenolic compound profile of this garlic compared to the other two varieties indicates its strong antioxidant potential. These phenolic compounds play a key role in preventing cellular damage caused by free radicals, which contribute to the development of chronic diseases such as cancer and heart disease [29]. The profile exhibited by Lanang garlic suggests its superior pharmacological potential in maintaining health and preventing degenerative diseases.

Garlic phenolics have been extensively studied for their ability to neutralize free radicals and provide protective effects on cells and tissues. This potent antioxidant function is critical in preventing oxidative stress, which contributes to plaque formation in arteries and cancer cell development [30]. Furthermore, phenolics possess anti-inflammatory properties that may reduce the risk of diseases such as type 2 diabetes and chronic inflammation [31]. With its stronger phenolic profile, Lanang garlic offers significant health benefits that support its traditional use in treating various diseases.

The analysis of volatile compounds in the three garlic varieties revealed significant differences in their aromatic characteristics. Lanang garlic exhibited a wider and more pronounced variety of volatile compounds, contributing to its rich and complex aroma. This may explain why Lanang is frequently used in various culinary and traditional medicinal applications, as a strong aroma is often associated with higher bioactive potential. These findings align with previous studies on organosulfur compounds in single-clove garlic [7, 8]

Volatile compounds play a crucial role in creating distinctive aromas and flavors, which not only affect the palatability of food but also provide therapeutic effects [32]. The position of Lanang garlic in the upper right quadrant suggests the presence of volatile compounds with strong characteristics, which are potentially linked to antimicrobial [33] and antioxidant activity [34]. This makes Lanang a valuable choice for enhancing nutritional and health benefits. In contrast, Tawangmangu garlic had a negatively correlated profile, which may indicate volatile compounds with lower functional potential in this regard. However, its unique characteristics could add value in certain culinary applications. Meanwhile, Honan garlic showed a more dispersed distribution, reflecting a diversity of volatile compounds. This might indicate a range of sensory properties and health benefits that need further exploration. The diversity and interactions among these compounds provide each garlic variety with distinct advantages, which can be harnessed in the development of functional foods and herbal products [35, 36].

The diverse fatty acid compounds found in Honan garlic may significantly contribute to its nutritional value, including anti-inflammatory effects, cholesterol regulation, and potential protection against cardiovascular diseases [14]. The variation in its fatty acid composition suggests the possibility of a unique combination that could be optimized for use in food formulations or health supplements. On the other hand, the simpler yet stable fatty acid profile of Tawangmangu garlic may offer consistency in the final product, which could be advantageous in the food industry. Meanwhile, Lanang garlic, with its specific fatty acid composition, shows potential for developing functional properties that could be further explored in food or pharmaceutical applications.

CONCLUSION

Our study demonstrated the dominance of Lanang garlic in terms of phenolic and volatile compound contents. The phenolic content in Lanang garlic, specifically kainic acid, was higher than in the other varieties (80.774 ± 0.528 μg/g). Gallic acid was the most abundant phenolic compound, with the highest concentration found in Tawangmangu garlic (172.648 ± 1.949 μg/g), followed by kainic acid and malic acid. Lanang garlic contained the largest number of analytes (12), including two specific compounds not present in the other varieties.

Among the volatile compounds, diallyl disulfide was dominant, with Lanang garlic recording the highest concentration (86.405%). Other variations were observed in the compounds such as 1-propenyl methyl disulfide and dimethyl trisulfide, where Lanang garlic again exhibited the highest concentrations. Meanwhile, the highest levels of oleic acid were found in Lanang (28.464%) and Tawangmangu (27.476%), compared to Honan garlic (13.340%). Honan garlic, however, had the highest concentrations of most fatty acid compounds.

The principal component analysis revealed clear differences in the chemical profiles of the three garlic

varieties. For volatile compounds, PC1 accounted for 76.90% of the variation, with Lanang garlic showing a strong positive correlation and Tawangmangu garlic correlating negatively. In the phenolic compound analysis, Lanang garlic had the richest profile, contributing 69.93% to the variation, whereas Tawangmangu displayed lower diversity. In the fatty acid analysis, PC1 accounted for 88.24%, indicating high diversity in Honan garlic and unique characteristics in both Lanang and Tawangmangu garlics. These findings indicate that each variety has a distinct chemical composition, which may influence its nutritional quality and health benefits.

CONTRIBUTION

All the authors were involved in conducting the research and writing the manuscript.

CONFLICT OF INTEREST

There is no conflict of interest between the authors regarding this article.

REFERENCES

1. Fitriana N, Ainayya AA, Pamasyah FA, Anam MA, Lestari SR. The effectiveness comparison of single bulb garlic extract for antibacterial agent *P. aeruginosa*. IOP Conference Series: Earth and Environmental Science. 2019;276: 12028. https://doi.org/10.1088/1755-1315/276/1/012028
2. Purwaditya AK, Muliana NAA, Shahrul RU, Anoraga SB. Feasibility study of black garlic's home industry in Ngestiharjo village. Journal of Agri-Food Science and Technology. 2021;2(1):75–80. https://doi.org/10.12928/jafost.v2i1.3880
3. Budianto B, Arifin MJ, Naryani N, Sukmawati E, Suwaji S, *et al*. Plant proteases and anti-bacterial substances in *Allium sativum* L. varieties. Foods and Raw Materials. 2024;12(2):240–248. https://doi.org/10.21603/2308-4057-2024-2-606
4. Chen C, Cai J, Liu SQ, Qiu GL, Wu XG, *et al*. Comparative study on the composition of four different varieties of garlic. PeerJ. 2019;7:e6442. https://doi.org/10.1021/acs.jafc.3c07898
5. Qiu Z, Li L, Du H, Chen H, Chen G, *et al*. Physicochemical, structural, and functional properties of fructans from single-clove garlic and multiclove garlic: A comparison. Journal of Agricultural and Food Chemistry. 2024;72(14): 7818–7831. https://doi.org/10.1021/acs.jafc.3c07898
6. Naji KM, Al-Shaibani ES, Alhadi FA, Al-Soudi SA, D'souza MR. Hepatoprotective and antioxidant effects of single clove garlic against CCl_4-induced hepatic damage in rabbits. BMC Complementary and Alternative Medicine. 2017;17:411. https://doi.org/10.1186/s12906-017-1916-8
7. Arifah SN, Atho'illah MF, Lukiati B, Lestari SR. Herbal medicine from single clove garlic oil extract ameliorates hepatic steatosis and oxidative status in high fat diet mice. Malaysian Journal of Medical Sciences. 2020;27(1):46–56. https://doi.org/10.21315/mjms2020.27.1.5
8. Wafaey AA, El-Hawary, SS, Abdelhameed MF, El Raey MA, Abdelrahman SS, *et al*. The chemical constituents and pharmacological effects of single-clove and multi-clove garlic: A comprehensive overview. Egyptian Journal of Chemistry. 2024;67(9):277–287. https://doi.org/10.21608/EJCHEM.2024.263815.9210
9. Zhang Y, Liu X, Ruan J, Zhuang X, Zhang X, *et al*. Phytochemicals of garlic: Promising candidates for cancer therapy. Biomedicine & Pharmacotherapy. 2020;123:109730. https://doi.org/10.1016/j.biopha.2019.109730
10. Ribeiro M, Alvarenga L, Cardozo LFMF, Chermut TR, Sequeira J, *et al*. From the distinctive smell to therapeutic effects: Garlic for cardiovascular, hepatic, gut, diabetes and chronic kidney disease. Clinical Nutrition. 2021;40(7):4807–4819. https://doi.org/10.1016/j.clnu.2021.03.005
11. Flouchi R, Fikri-Benbrahim K. Prevention of COVID 19 by aromatic and medicinal plants: A systematic review. Journal of Pharmaceutical Sciences and Research. 2020;12(8):1106–1111.
12. Wang W, Sun Y. *In vitro* and *in vivo* antioxidant activities of polyphenol extracted from black garlic. Food Science and Technology. 2017;37(4):681–685. https://doi.org/10.1590/1678-457x.30816
13. Arslaner A. The effects of adding garlic (*Allium sativum* L.) on the volatile composition and quality properties of yogurt. Food Science and Technology. 2020;40(suppl 2):582–591. https://doi.org/10.1590/fst.31019
14. Lee DB, Pyo YH. *In vitro* anti-obesity effects of raw garlic and pickled garlic. Journal of Korean Medicine for Obesity Research. 2021;21(2):69–79. https://doi.org/10.15429/jkomor.2021.21.2.69
15. Ko JW, Jeong SH, Kwon HJ, Shin NR, Seo YS, *et al*. Preventive effect of garlic oil and its organosulfur component diallyl-disulfide on cigarette smoke-induced airway inflammation in mice. Nutrients. 2018;10(11):1659. https://doi.org/10.3390/nu10111659
16. Elosta A, Slevin M, Rahman K, Ahmed N. Aged garlic has more potent antiglycation and antioxidant properties compared to fresh garlic extract *in vitro*. Scientific Reports. 2017;7(1):39613. https://doi.org/10.1038/srep39613
17. Kayiran SD, Ozkan EE, Kara EM, Yilmaz MA, Zengin G, *et al*. Comprehensive analysis of an uninvestigated wild edible medicinal garlic species from Turkey: *Allium macrochaetum* Boiss. & Hausskn. Journal of Food Biochemistry. 2019;43:e12928. https://doi.org/10.1111/jfbc.12928

18. Jarukas L, Kuraite G, Baranauskaite J, Marksa M, Bezruk I, *et al*. Optimization and validation of the GC/FID method for the quantification of fatty acids in bee products. Applied Sciences. 2020;11(1):83. https://doi.org/10.3390/app11010083
19. Yu S, Huang X, Wang L, Wang Y, Jiao X, *et al*. Characterization of the volatile flavor profiles of black garlic using nanomaterial-based colorimetric sensor array, HS-SPME-GC/MS coupled with chemometrics strategies. Food Chemistry. 2024;458:140213. https://doi.org/10.1016/j.foodchem.2024.140213
20. Stein S, Mirokhin D, Tchekhovskoi D, Mallard G. The NIST mass spectral search program for the NIST/EPA/NIH mass spectra library. Standard Reference Data Program of the National Institute of Standards and Technology. 2002.
21. Bozin B, Mimica-Dukic N, Samojlik I, Goran A, Igic R. Phenolics as antioxidants in garlic (*Allium sativum* L., Alliaceae). Food Chemistry. 2008;111(4):925–929. https://doi.org/10.1016/j.foodchem.2008.04.071
22. Beato VM, Orgaz F, Mansilla F, Montaño A. Changes in phenolic compounds in garlic (*Allium sativum* L.) owing to the cultivar and location of growth. Plant Foods for Human Nutrition. 2011;66:218–223. https://doi.org/10.1007/s11130-011-0236-2
23. Molina-Calle M, Priego-Capote F, de Castro MDL. HS–GC/MS volatile profile of different varieties of garlic and their behavior under heating. Analytical and Bioanalytical Chemistry. 2016;408:3843–3852. https://doi.org/10.1007/s00216-016-9477-0
24. Satyal P, Craft JD, Dosoky NS, Setzer WN. The chemical compositions of the volatile oils of garlic (*Allium sativum)* and wild garlic (*Allium vineale*). Foods. 2017;6(8):63. https://doi.org/10.3390/foods6080063
25. Khubber S, Hashemifesharaki R, Mohammadi M, Gharibzahedi SMT. Garlic (*Allium sativum* L.): A potential unique therapeutic food rich in organosulfur and flavonoid compounds to fight with COVID-19. Nutrition Journal. 2020;19:124.
26. Tsiaganis MC, Laskari K, Melissari E. Fatty acid composition of *Allium* species lipids. Journal of Food Composition and Analysis. 2006;19(6–7):620–627. https://doi.org/10.1016/j.jfca.2005.06.003
27. Kamanna VS, Chandrasekhara N. Fatty acid composition of garlic (*Allium sativum* Linnaeus) lipids. Journal of the American Oil Chemists' Society. 1980;57:175. https://doi.org/10.1007/BF02883781.
28. Sobenin IA, Myasoedova VA, Iltchuk MI, Zhang DW, Orekhov AN. Therapeutic effects of garlic in cardiovascular atherosclerotic disease. Chinese Journal of Natural Medicines. 2019;17(10):721–728.
29. Zong J, Martirosyan DM. Anticancer effects of garlic and garlic-derived bioactive compounds and its potential status as functional food. Bioactive Compounds in Health and Disease. 2018;1(2):16–35. https://doi.org/10.31989/bchd.v1i2.530
30. Li G, Chen P, Zhao Y, Zeng Q, Ou S, *et al*. Isolation, structural characterization and anti-oxidant activity of a novel polysaccharide from garlic bolt. Carbohydrate Polymers. 2021;267:118194. https://doi.org/10.1016/j.carbpol.2021.118194
31. Hu Q, Xiong Y, Zhu GH, Zhang YN, Zhang YW, *et al*. The SARS-CoV-2 main protease (M^{pro}): Structure, function, and emerging therapies for COVID-19. MedComm. 2022;3:e151. https://doi.org/10.1002/mco2.151
32. Srimathi R, Raja MMMK, Kathiravan MK. *In silico* screening of traditional herbal medicine derived chemical constituents for possible potential inhibition against sars-cov-2. Journal of Natural Remedies. 2020;20(2):79–88. https://doi.org/10.18311/jnr/2020/25278
33. Das R, Mehta DK. Microbial biofilm and quorum sensing inhibition: Endowment of medicinal plants to combat multidrug-resistant bacteria. Current Drug Targets. 2018;19(16):1916–1932. http://doi.org/10.2174/1389450119666180406111143
34. Yun HM, Jin P, Park KR, Hwang JR, Jeong HS, *et al*. Thiacremonone potentiates anti-oxidant effects to improve memory dysfunction in an APP/PS1 transgenic mice model. Molecular neurobiology. 2016;53:2409–2420. https://doi.org/10.1007/s12035-015-9208-0
35. Özcan MM. Bioactive properties of garlic (*Allium sativum* L.) – A review. Journal of Medicinal and Spice Plants. 2016;21(4):174–182.
36. Hacıseferoğulları H, Özcan M, Demir F, Çalışır S. Some nutritional and technological properties of garlic (*Allium sativum* L.). Journal of Food Engineering. 2005;68(4):463–469. https://doi.org/10.1016/j.jfoodeng.2004.06.024

Additional information about the authors

Budianto ORCID 0000-0002-8277-6202
Alif G. Arumsari ORCID 0000-0003-4081-444X
Abdul Yusup ORCID 0009-0002-6880-5983
Muhammad Gumintang ORCID 0009-0001-3208-5681
Zahra S. Rosidin ORCID 0009-0005-9015-9692

Foods and Raw Materials. 2027;15(2)

ISSN 2308-4057 (Print)
ISSN 2310-9599 (Online)

Review Article
Open Access

Available online at http://jfrm.ru/en
https://doi.org/10.21603/2308-4057-2027-2-710
https://elibrary.ru/XGSABI

Recent advances in cold plasma treatment for essential oil extraction

Andrey G. Sherstyukov, Oksana I. Andreeva, Vasily E. Tarasov, Ivan A. Shorstkii*

Kuban State Technological University, Krasnodar, Russia

* e-mail: i-shorstky@mail.ru

Received 25.07.2025; Revised 13.10.2025; Accepted 03.02.2026; Published online 09.07.2026

Abstract:
The substitution of imported supplements and flavorings with domestic products is the key to food security in Russia and Belarus. Essential oils are used in a variety of sectors, including medicine, cosmetics, perfumery, food, and confectionery. The depth and rate of their extraction determine the efficiency of the essential oil industry. Cold plasma treatment increases the rate of extraction by 15–20%. The use of this treatment can make Russian producers more competitive in the domestic market, as well as give them a competitive advantage internationally by ensuring high quality.

This review examines the use of cold plasma treatment in preparation for essential oil extraction, briefly describing its mechanism of action, as well as process and equipment. The scientific papers published between 2010 and 2025 were subjected to retrospective analysis.

Essential oil materials were classified and their essential oil receptacles were examined structurally to determine the type of cold plasma treatment to be used. We analyzed the surface and penetrating cold plasma effects on the morphology and microstructure of material tissues. Cold plasma generation methods were classified and their applications were presented for materials with external and internal essential oil receptacles. We described factors that affect the efficiency of essential oil extraction. Finally, potential applications were outlined for cold plasma technology in essential oil extraction and production of high-quality target products.

This review demonstrates the critical importance of developing innovative electrophysical technologies for the food and essential oil industries. Cold plasma treatment of freshly harvested essential oil materials is a promising approach to ensure high extraction efficiency and high quality of the resulting products.

Keywords: Essential oil materials, extraction, food flavoring, electrophysical technologies, cold plasma, dietary supplement

Funding: This research was supported by the Kuban Science Foundation (project No. 25-16-20114) and the Russian Science Foundation (project No. 25-16-20114), https://rscf.ru/project/25-16-20114/

Please cite this article in press as: Sherstyukov AG, Andreeva OI, Tarasov VE, Shorstkii IA. Recent advances in cold plasma treatment for essential oil extraction. Foods and Raw Materials. 2027;15(2):344–357. https://doi.org/10.21603/2308-4057-2027-2-710

INTRODUCTION

The choice of essential oil extraction method depends on the properties of plant material, the type of tissue that contains essential oil, the composition of oil and the properties of its components, as well as the nature of bond between essential oil and material. If essential oil is in a bound state, the material is fermented before or during extraction. A properly selected method for preparing and processing plant material ensures the highest yield and the best quality of the product [1]. Many plant materials are rich not only in essential oils but also in other bioactive substances. Therefore, an integrated technology should be applied to ensure the maximum extraction of all components. Essential oil can be extracted by the following physicochemical and mechanical methods [2, 3]: steam distillation; extraction with volatile organic solvents; extraction with non-volatile solvents (maceration); water extraction; extraction with liquefied gases; sorption with various sorbents (enfleurage and dynamic sorption); and mechanical pressing.

Extraction is one of the primary methods for processing essential oil materials. Its products include essential oils, fragrant resinous substances, waxes, and wax-like substances. The cosmetic industry uses mixtures of essential oil, resins, and waxes extracted with volatile hydrocarbon solvents [4]. The food industry produces hydroalcoholic, hydroalcoholic glycerin, and oil extracts from essential oil materials [5]. These extracts contain bioactive substances such as carotenoids, tocopherols, flavonoids, etc. The efficiency of the essential oil industry is determined by the depth and rate of extraction.

Copyright © 2026, Sherstyukov, *et al.* This is an open access article distributed under the terms of the Creative Commons Attribution 4.0 International License (https://creativecommons.org/licenses/by/4.0/), allowing third parties to copy and redistribute the material in any medium or format and to remix, transform, and build upon the material for any purpose, even commercially, provided the original work is properly cited and states its license.

According to the Russian Ministry of Energy, high energy intensity is a pressing issue in essential oil production, which significantly limits its competitiveness [6].

The shortage of local essential oil materials and their extracts forces the producers to spend millions of dollars annually on importing them [7, 8]. Currently, as part of import substitution policy, the industry is seeking to restore domestic essential oil production, its technology and equipment [6].

Improving essential oil extraction technology to increase extract yield and maintain extract quality is an important step in intensifying mass transfer processes. Figure 1 shows what methods of essential oil extraction are available today.

Extraction can be intensified by both thermomechanical methods (grinding, flattening, wet-heat treatment, fermentation) and modern "green" technologies [9] which make use of high-precision instruments and equipment. Today, the food industry usually uses solvents to extract target components from essential oil plant materials [10]. In solid-liquid extraction, a solid sample is immersed in a solvent, and the extracted component begins to separate due to the difference in concentrations at the phase boundary. Extraction efficiency can be increased by using external methods such as microwave heating [11, 12], ultrasound [13], intense electric fields, and discharge technologies [14, 15]. These methods offer unique advantages for extraction under specific temperatures. However, microwave heating is not widely applied in essential oil extraction due to difficulties controlling the process and possible overheating. Ultrasonic vibrations demonstrate good efficiency, but have a narrow operating range, necessitating the use of a large number of ultrasonic sensors in large-scale production.

A promising way of increasing extraction efficiency is to develop a surface structure by cold plasma treatment at atmospheric pressure. Such preparation can help predict the process's direction, which is important for its control. However, intensive extraction using cold plasma treatment is in need of scientific support, since the estimated relationships available are, in most cases, empirical and have a limited scope of application. This is primarily due to a lack of understanding of the morphological and structural changes that occur during cold plasma treatment, or the chemical reactions that take place when reactive plasma particles interact with essential oil material tissue.

Of interest are some studies that show changes in the structure of a colloidal capillary-porous body, describing the presence of additional channels formed by cold plasma treatment [16, 17]. This new continuum results from a unique relaxation transfer process caused by a change in the shape of the moisture or oil bond [18–20].

STUDY OBJECTS AND METHODS

This review examines the use of cold plasma treatment in preparation for essential oil extraction, briefly describing its mechanism of action, as well as process and equipment. The keywords "essential oil material", "cold plasma", and "assisted extraction" were used to search the Scopus, Web of Science, and eLIBRARY.RU databases. The scientific papers published between 2010 and 2025 were subjected to retrospective analysis.

Classification of essential oil materials. Essential oil-bearing plant materials can be classified by the part of a plant used industrially and by the type of interaction between essential oil components and other substances such as carbohydrates. According to the plant part, plant materials are classified into five groups [3, 21]:

– grains and fruits: coriander, anise, fennel, caraway, dill;
– leaves, stems, and branches: mint, rose geranium, patchouli, eucalyptus, sweet bay, wormwood, catnip, sweet violet, rosemary, grindelia, dill, lemon, conifers, tobacco, mock orange, fennel, anise, etc.;

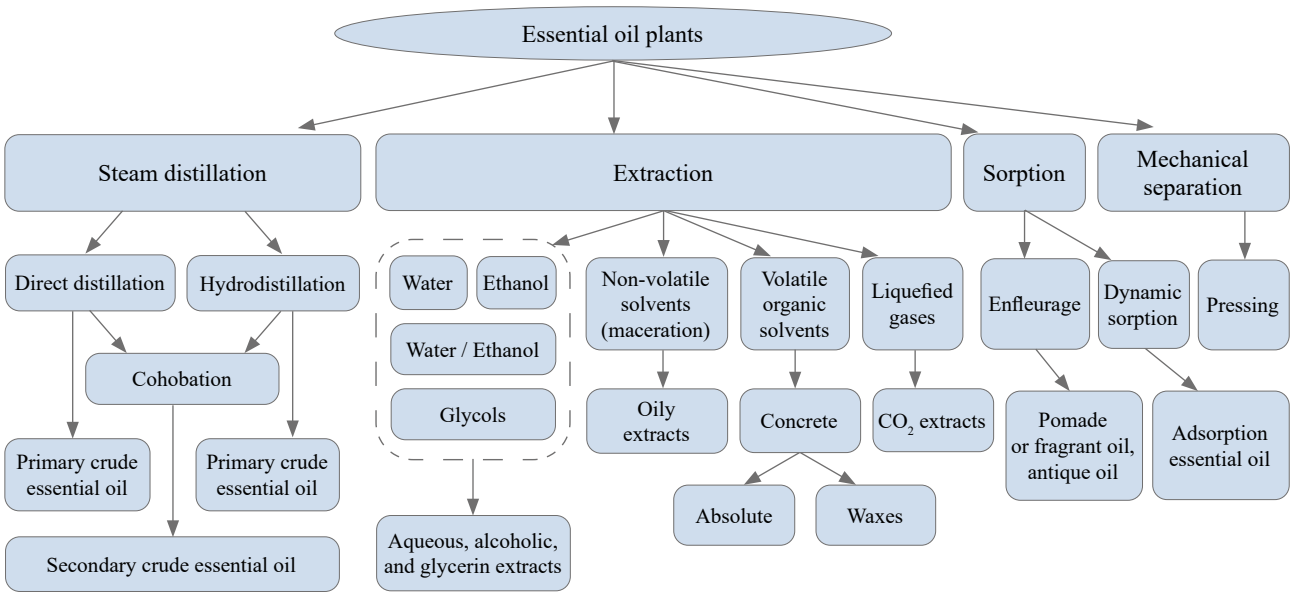


Figure 1 Methods of essential oil extraction

– flowers and flower buds: azalea, rose, clary sage, lavender, lavandin, Spanish jasmine, tobacco, white lily, regal lily, lilac, false acacia, silver-green wattle acacia, chamomile, yarrow, mock orange, iris, clove tree (buds), etc.;
– roots and rhizomes: calamus, vetiver, iris; and
– materials for obtaining fixatives: lichen – oak moss and cistus.

Each essential oil plant is usually a source of one type of material and one type of essential oil. This is typical for plants in which essential oil is found in only one organ or has similar compositions in different organs (e.g., coriander seeds, mint leaves and flowers, basil, and laurel branches). Some plants can be a source of two types of material and a single type of essential oil. Exceptions include citrus fruits, whose young branches yield petitgrain essential oil (bergamot-like aroma due to linalyl acetate), whose flowers yield neroli oil (citrus blossom aroma due to methyl anthranilate), and whose fruits yield lemon oil, orange oil, and other essential oils (characteristic aroma due to citral, limonene, and other compounds).

Essential oils in plants exist in both free and bound forms. If the oil is bound, this plant material does not have a scent characteristic of any particular essential oil, as its components are in the form of glycosides. The oil can be released only after hydrolysis or enzymatic cleavage of the glycosides.

Localization of essential oils in plant materials. Bound essential oils are usually distributed evenly throughout the plant tissues and are not strictly localized. Free essential oils and resinous substances are found in special excretory structures, or essential oil receptacles, on the surface or within plant tissues (Fig. 2).

Waxy substances can be found on the surface of all plant organs, in the cell membranes of the skin (epidermis), in the cuticle, and on its surface. In the outer walls of the epidermal cell membranes, they form cuticular layers alternating with cellulose. The cuticle, which covers the epidermis, is primarily composed of these layers. Waxes, which come in the form of small grains, thin rods, or solid crusts, form a waxy coating above the cuticle. The thickness of the cuticle and waxy coating varies among different plants, their organs and parts [22, 23].

RESULTS AND DISCUSSION

Composition and application of essential oils. Essential oils are widely used in the food industry as flavoring agents (plant extracts), as well as in the pharmaceutical and cosmetic industries (Fig. 3). An essential oil is a plant-based complex of mostly fragrant volatile

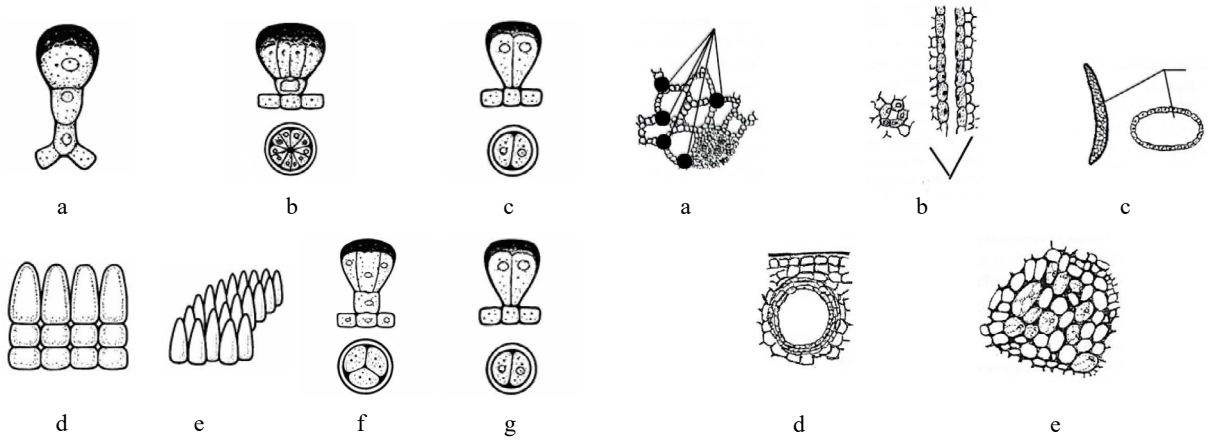


Figure 2 Essential oil receptacles
External oil receptacles (left): (a) geranium hair; (b) rosemary gland; (c) patchouli hair; (d) papillary hairs of rose petal; (e) upper epidermis of rose petal; (f) peppermint hair; and (g) eugenol basil gland;
Internal oil receptacles (right): (a) idioblasts of calamus rhizomes; (b) resin duct (channel); (c) essential oil channel of coriander fruit; (d) eucalyptus leaf gland; (e) water-bearing idioblasts of geranium with essential oil in a finely dispersed state

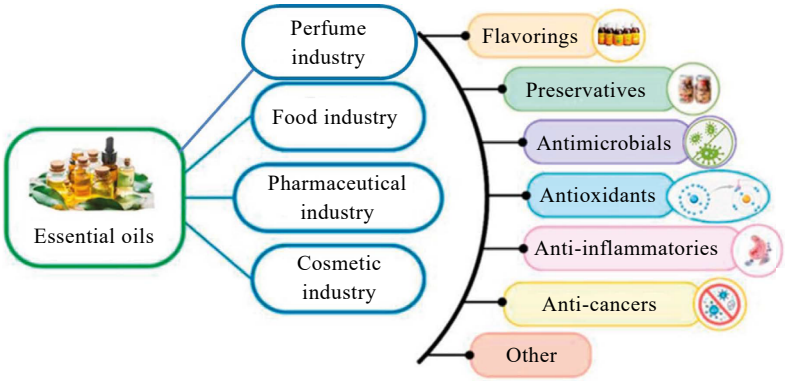


Figure 3 Essential oil applications

terpene compounds, which are responsible for the plant's scent [24]. Physicochemically, essential oils are usually transparent, or sometimes yellowish, optically active liquids. Some oils are exceptions and have rich colors: dark brown (cinnamon oil), green (bergamot oil), blue or greenish-blue (wormwood, chamomile, and yarrow oils), or red (thyme oil). Almost all essential oils have a relative density of less than 1 g/cm^3 (except for clove, basil, and cinnamon oils), as well as unique taste and aroma [25].

Terpene compounds in essential oils are primarily members of the mono- and sesquiterpene classes, as well as their oxygen-containing derivatives (ketones, alcohols, aldehydes, acids, esters, lactones, etc.) known as terpenoids. These compounds are systems of conjugated double bonds, making them extremely reactive during metabolic processes within plant cells. Terpenes are also essential components of natural balsams and resins [26]. In addition to terpenes, essential oils contain aromatic hydrocarbons, organic sulfides, amines, as well as phenolic and heterocyclic compounds. Typically, a predominant terpene or terpenoid (or a mixture of both) determines the specific scent of oil, as well as its pharmacological properties.

In the food industry, essential oils are used as flavoring agents in soft drinks (kvass), confectionery (gingerbread, lollipops, caramel, chewing gum, fruit desserts), tea, meat dishes, cheeses, and liqueurs. They are also added to enrich the flavor of various spices, seasonings, sauces, table salt, sugar, and table vinegar. Their introduction into food products in the form of food essences or flavorings is regulated by State Standard 10-237-99 "Food Flavorings. Specifications" [27]. Since essential oils mainly consist of bioactive terpene compounds, they can be used in parapharmaceutical dietary supplements. These supplements are taken as part of preventative and adjuvant therapy, as well as to support the functional activity of organs and systems within physiological limits. However, they cannot be used to correct the chemical composition of human food, unlike nutraceuticals [2].

According to some studies [28], the active components of essential oils improve digestion and normalize the cardiovascular system, as well as have powerful effects on the genitourinary system and nervous tissue. All of this provides grounds for developing dietary supplements based on essential oils. As noted in a study of Baser and Bonello, the demand for plant extracts of essential oils is expected to grow due to a global trend toward replacing synthetic components in food products with natural ones [29]. In this regard, essential oils are a natural alternative to synthetic flavors and food preservatives, and they can be used to improve food safety and extend shelf life.

Essential oils have potential as additives for increasing the shelf life of food products. Patrignani *et. al.* [30] refer to many studies that used essential oils in pure form or as part of preparations and observed a significant increase in the shelf life of food products stored in containers made of cardboard, tin, glass, polyethylene, or natural fabrics. Furthermore, one of the studies found that some components of essential oil, such as citral, citronellol, eugenol, farnesol, and nerol, can protect chili seeds and fruits from fungal infection for six months. The authors also reported that the essential oil isolated from *Ageratum conyzoides* L. increased the shelf life of mandarins by 30 days by fighting against blue mold rotting. In other studies, the essential oils of lemongrass (*Cymbopogon nardus* (L.) Rendle) and basil (*Ocimum basilicum* L.) controlled the development of anthracnose on bananas, increasing their shelf life by 21 days. Thus, essential oils are promising biocontrol agents acting against fungal and bacterial pathogens. Some researchers are exploring their use for integrating pathogens into food containers. For example, some oils can be used as fumigants in containers made of natural fabric, cardboard, and even wooden planks. They can also be introduced as fumigant sprays into the product itself [31].

Extraction of essential oils pre-treated with cold plasma. ***Cold plasma characteristics.*** The term "plasma", which was introduced by Irving Langmuir in 1927, was based on an analogy between its complex composition and that of blood plasma [32]. In the 1970s, plasma technologies were commercially used mainly in the electronics and polymer industries [33]. Over the past 5 years, however, cold plasma has been actively applied to food processes and technologies. Cold plasma is formed through the ionization of a gas by an electric discharge using various media (air, argon, oxygen, etc.). A cold plasma jet generates cations, anions, free and excited electrons, and a number of volatile atoms and molecules [34], which can be divided into reactive oxygen species and reactive nitrogen species. Its interaction with food products causes complex physical and chemical reactions to occur. Their effects include sterilization, enzyme inactivation, impact on the anatomical integrity of plant cells, and surface changes [35, 36]. The diversity of active cold plasma particles indicates high chemical activity, which is used for various purposes, including the bactericidal treatment of food products [37, 38].

As cold plasma technology developed, it began to be used to modify the surface and capillary-porous structure of food materials due to a so-called "etching" effect [39].

Cold plasma generation methods. Cold plasma can be generated in various ways (Fig. 4): a dielectric barrier discharge (two oppositely charged plates), an arc discharge [40], a microplasma jet [41], a corona discharge, and a microplasma jet supported by thermionic emission. The processes of cold plasma treatment are shown in Fig. 4.

Thermionic emission-supported cold plasma can form a thin cord of charged particles with a directed energy effect on the object treated. Furthermore, due to thermionic emission, electric field strengths are in the range of 6–8 kV/cm, compared to the typical range of 15–20 kV/cm for other cold plasma generation methods [35]. This reduces overall energy consumption and creates a controlled plasma combustion and treatment. With this type of electrophysical action, the material remains unheated, and the process can be scaled up in the flow [20, 42].

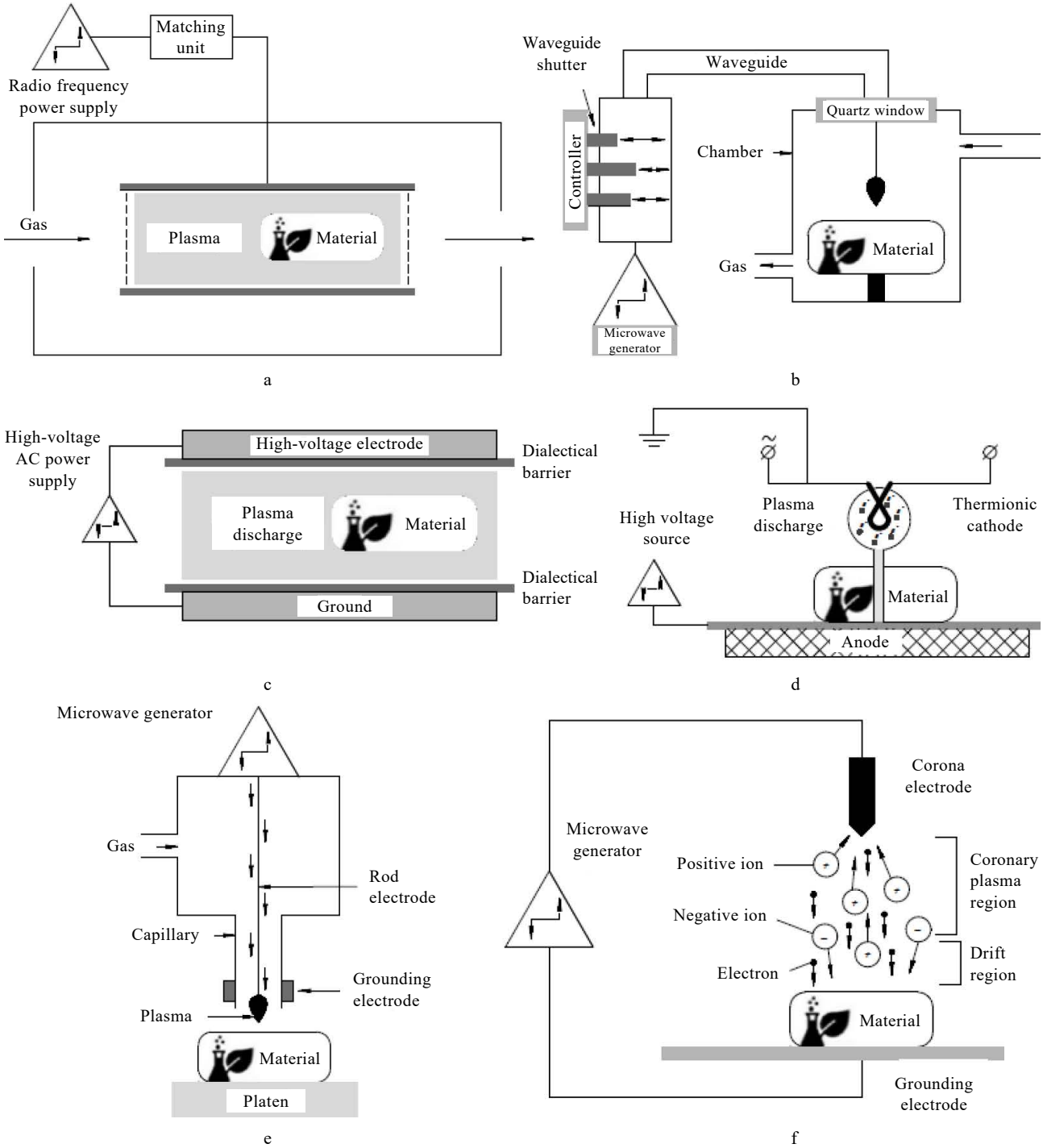


Figure 4 Cold plasma treatment schemes: (a) radio frequency discharge; (b) microwave discharge; (c) dielectric barrier discharge; (d) microplasma discharge; (e) glow discharge flow; and (f) corona discharge

With a corona discharge, cold plasma generation requires a system of point-on-plane electrodes spaced at 3–10 cm from each other. Although low energy consumption is an advantage of cold plasma, the corona discharge only has an "etching" effect on the surface of the material without penetrating its internal structure.

A cold plasma jet with pressurized gas supply is used most widely for cold plasma generation. The intensity of cold plasma treatment can be controlled by the generator power, treatment time, distance, and working gas flow rate [43]. Compared to other methods, a plasma jet is more flexible and is not limited by the space between the electrodes. Its major drawback, however, is a limited surface area and low penetration into the material structure, similarly to a corona discharge.

For a dielectric barrier discharge, the object under treatment is positioned between metal electrodes coated with a dialectic material. To cover a larger area, two plane-parallel electrodes are used, with at least one of them coated with a dielectric material [44]. To ensure

discharge stability, the distance between the two electrodes is limited to a few millimeters. A discharge at atmospheric pressure requires a sinusoidal or pulsed high-voltage power source. The main advantage is that food materials can be treated with cold plasma in dielectric packaging, such as polyethylene film. However, given the treatment area of several millimeters, this method can be used primarily for powdered materials.

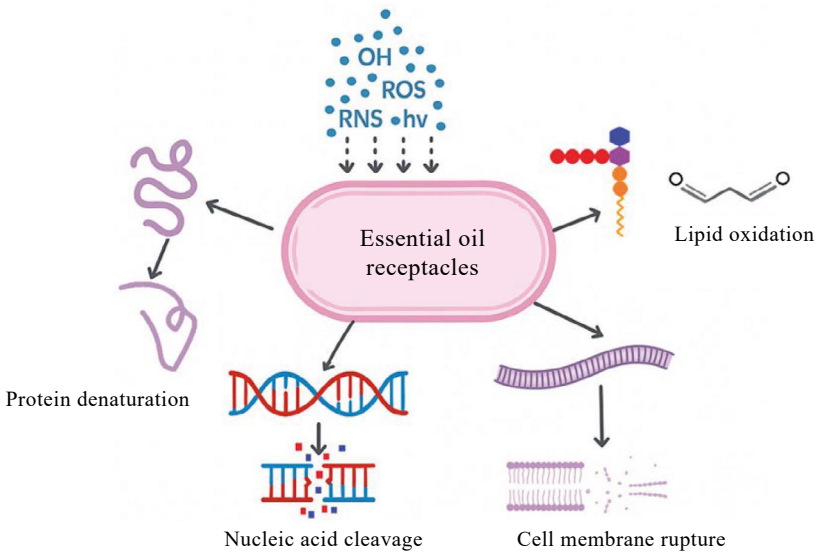
A Jacob's Ladder can be used to demonstrate an arc discharge in the air. For this, two or more electrodes are positioned perpendicularly to the plane. An arc is first ignited in the narrowest gap between the two electrodes and then slides in the direction of the injected gas, lengthening [45]. The sliding arc discharge has high energy and gas consumption, and most of the energy is used to stimulate chemical reactions rather than to heat the gas. Furthermore, compared to other plasma-generating devices, the sliding arc discharge can have a uniform effect over a large area, which enables its use in heat and mass transfer processes [40, 46].

Surface-type cold plasma treatment of essential oil materials. Figure 5 shows the principle that explains the mechanism of cold plasma action on the surface of plant materials. Particles of reactive oxygen species and reactive nitrogen species bombard and interact with the surface of the plant material in the form of a shell and a covering layer. This interaction between reactive particles and plant tissue components can be explained by lipid oxidation processes, membrane electroporation, protein denaturation, and nucleic acid cleavage [47]. Most studies describe it through the "etching" effect, which is associated with the decomposition of the wax shell [35] and the disintegration of plant cell membranes [48, 49]. Other approaches require high-precision equipment and a full spectrum of analyses, from the data on reactive plasma particles to the parameters of bioactive compounds.

Essential oil materials, with their target component in the internal structure, have a wax shell which acts a "diffusion barrier" for mass transfer [50]. Cold plasma treatment of the surface layer and the capillary-porous structure of the material reduces this barrier. Macedo *et al.* [51] studied the effect of cold plasma on the surface morphology of kapok fibers. The treatment parameters were: an electric current of 0.09–0.12 A, a voltage of 400–500 V, a sample's temperature of 72°C, an oxygen flow rate of 10 cm^3/min, and a working distance of 4.0 cm. The authors analyzed changes in fiber roughness and absorption characteristics caused by the treatment. Karunanithi *et al.* [52] reported the effect of dielectric barrier plasma on the morphology of betel leaf fibers. The authors found significant structural changes, the presence of damaged cells, and an etching effect. The impact of reactive particles on the integrity of oil globules affected the yield of subsequent extraction.

Khudyakov *et al.* [53] treated tobacco leaves (*Nicotiana tabacum* L. var. *virginia*) with cold plasma. The authors varied the discharge current and observed two main results. At low discharge currents (5 mA), the cellular structure acquired a darker color due to the interaction between reactive particles and tobacco leaf tissue. The resulting oxidation indicated the intense action of oxygen-containing reactive particles in cold plasma. Increasing the discharge current caused through holes to form on the surface of the tobacco leaf plate (Fig. 6).

The change in color can be explained by the degradation of chlorophyll. Ahmadian *et al.* [54] reported chlorophyll degradation and changes in phenolic components of peppermint, stinging nettle, and Schisandra leaves after cold plasma treatment using a dielectric barrier discharge. However, the specific mechanism of interaction between cold plasma particles and bioactive components of the plant materials remains unknown.



ROS – reactive oxygen species; RNS – reactive nitrogen species

Figure 5 Interaction between cold plasma and plant cell surface

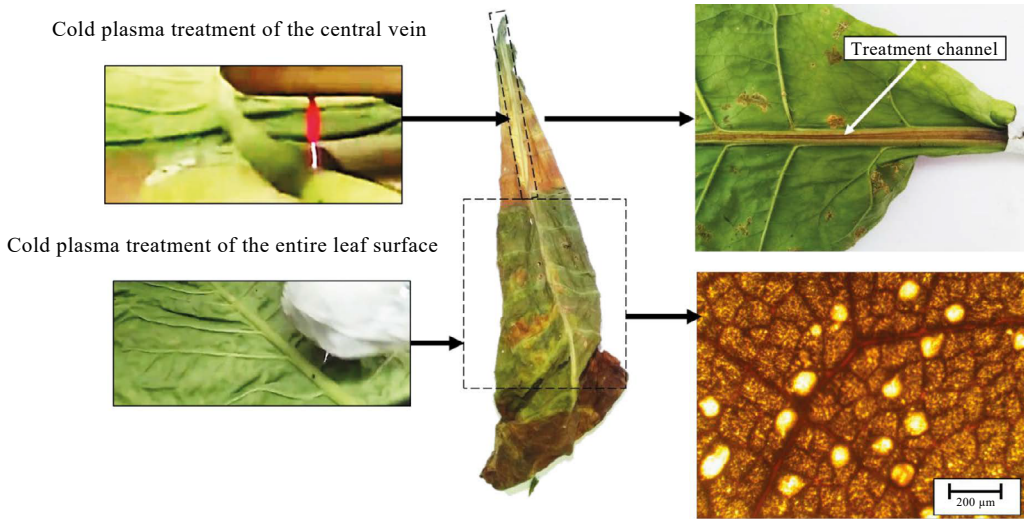


Figure 6 The effect of cold plasma on the plate and vein of a tobacco leaf

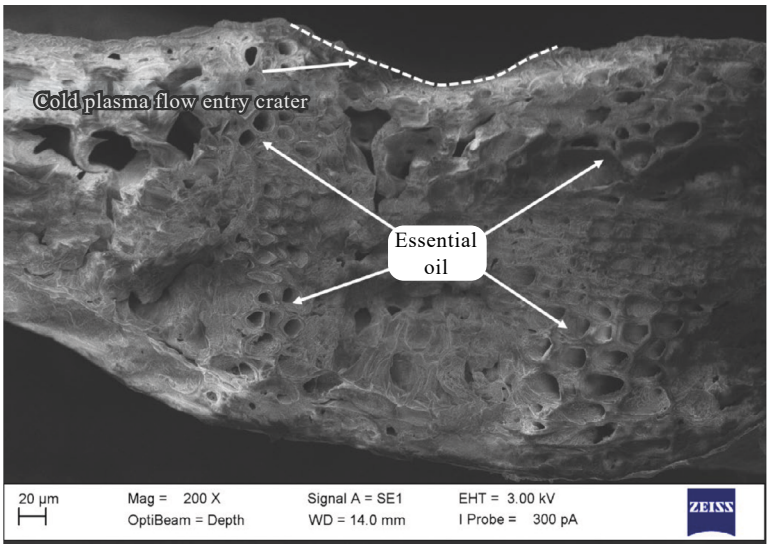


Figure 7 A section of a laurel leaf with internal essential oil receptacles (scanning electron microscope image) [57]

Noteworthily, Baser and Bonello reported that the temporary pores formed as a result of cold plasma treatment changed their size over time [29]. Pore size is known to directly affect the efficiency of extracting the target component from essential oil receptacles. Therefore, further research is needed to maximize the effect of cold plasma. In a study by Bunse *et al*. [28], an apple disc treated with cold plasma had a pore diameter of 100 µm. These electrically induced pores accelerated mass transfer by 15–20%. It should be noted that pores and channels can form on the surface of herbaceous plants as well. For example, positive effects were observed when treating the stem of hyssop (*Hyssopus officinalis* L.) with cold plasma [54, 56].

The effectiveness of the "etching" effect of cold plasma treatment depends on the thickness of the material layers and the presence of air gaps. Consequently, longer treatment and higher moisture of the material can significantly increase the number of micropores and cracks on the treated surface, which affects the duration of the drying process [20, 49].

Penetrating cold plasma treatment of essential oil materials. As noted above, the surface effects caused by cold plasma can accelerate the removal of the diffusion barrier in the material. However, cold plasma can also affect the internal structure of the material. Since essential oil receptacles can be located in its thickness, removing the diffusion barrier of the wax shell is only the first part of deep processing. The next barrier to effective mass transfer during essential oil extraction lies in plant cell membranes and internal tissue structures. It was not until recently that researchers began to examine the use of cold plasma to improve essential oil extraction by modifying the internal structure of the material. Spark discharge or thermionic emission methods (Fig. 4) are typically used for penetrating effects.

As shown in Fig. 7, essential oil receptacles are located in the thickness of a laurel (*Laurus nobilis* L.) leaf,

which requires penetrating cold plasma exposure. The discharge passed through the structure of the material, creating a developed structure on the surface of essential oil receptacles. Khudyakov *et al*. [57] observed similar effects of a low-current spark discharge on the tissues of lavender inflorescences.

Auguste *et al*. [58] reported the effects of cold plasma treatment on the physical and biochemical properties of basil leaves. The highest concentration of estragole was found in the leaves, while linalool dominated in the flowers, followed by estragole, eugenol, eucalyptol, and methyl cinnamate. Overall, cold plasma treatment increased the yield of antioxidant components in the essential oil extracts.

Cold plasma treatment had a penetrating effect on tobacco leaves, forming through holes of 40–50 μm in the leaf blade [53]. Keshavarzi *et al*. [59] studied the effects of cold plasma on the components of *Camellia sinensis* (L.) Kuntze leaves. Pectin and cellulose are the main components of a plant cell wall. Based on the data obtained by Cao *et al*. [60], we can assume that pectin molecules may be ruptured by the cleavage of the C_4–O covalent bond, resulting from oxidation caused by cold plasma exposure. Consequently, cold plasma treatment can promote the rupture of covalent bonds in the cell wall, thereby increasing the rate of water diffusion.

Despite the complexity of cold plasma impact on multicomponent food products, only the "etching" effect and the electroporation of plant cell membranes have been confirmed for most of the studied materials. However, important factors include the depth of cold plasma penetration into the material structure, the nature of its propagation in the cross-section of the material, and the size of pores and channels forming in the thickness of the material. Various research groups are working on these problems in Europe, China, America, and the Middle East [40, 61, 62].

Efficiency factors of essential oil extraction using cold plasma treatment. There has been limited research into the effects of cold plasma on essential oil extraction. This is primarily due to high demands placed on experimental design and lack of high-tech equipment. These studies mainly focus on increasing the yield of essential oil. However, their results are quite contradictory. Some studies demonstrated a negative effect of cold plasma on essential oil yield. For example, Jangi *et al*. [63] reported a decrease in the yield of essential oil from hyssop (*H. officinalis*) leaves treated with cold plasma. Similar results were observed by Ebadi *et al*. [64] for lemon verbena (*Aloysia citrodora* L.) extracts exposed to prolonged cold plasma treatment. A positive effect of cold plasma treatment was reported for betel leaves (*Piper betle* L.) [52], mint leaves (*Mentha spicata* L.) [65], thyme leaves (*Thymus vulgaris* L.) [66], black pepper (*Piper nigrum* L.) [67], and cumin seeds (*Cuminum cyminum* L.) [68]. The extraction efficiency was analyzed against such parameters as the power level and duration of cold plasma treatment, the plant type (matrix structure, type of cutting), and the use of concomitant extraction methods (Table 1).

The use of surface plasma treatment required high energy consumption and long exposure times, with a relatively small increase in essential oil yield [66]. However, the use of a combined approach (e.g., cold plasma and microwave exposure) shortened the extraction time or reduced the amount of energy consumption, increasing the yield of essential oil [52].

As noted above, cold plasma treatment improves extraction primarily by changing the microstructure of the material surface (e.g., creating micro-holes in plant cell walls), thereby accelerating mass transfer [69]. In addition, reactive plasma particles destroy non-covalent bonds in the polymer bonds that make up the cell walls, reducing their stability and promoting the formation of additional intercellular spaces and cavities [70]. Namjoo *et al*. [69] also reported changes in the physicomechanical properties of the materials. Jangi *et al.* [63] suggested that cold plasma destroys glandular trichomes –

Table 1 Parameters and efficiency of cold plasma treatment

Material and method of treatment	Treatment efficiency	Reference
Hyssop leaves (*Hyssopus officinalis* L.) Barrier discharge	Decrease in essential oil yield by 33–56%	[63]
Lemon verbena (*Aloysia citrodora* L.) Microwave plasma in a low-pressure gas environment	Decrease in essential oil yield by 36.7%	[64]
Betel leaves (*Piper betle* L.) Microwave plasma	Increase in essential oil yield by 3.33 ± 1.2%	[52]
Mint leaves (*Mentha spicata* L.) Barrier discharge	Increase in essential oil yield by 1.81%	[65]
Thyme leaves (*Thymus vulgaris* L.) Barrier discharge	Increase in essential oil yield by 20%	[66]
Lavandin inflorescences (*Lavandula hybrid* var. *grosso*) Barrier discharge	Increase in essential oil yield by 0.25% after treatment for 1 min and decrease by 0.12% after treatment for 10 min	[16]
Black peppercorns (*Piper nigrum* L.) Sliding discharge	Increase in essential oil yield by 27.6%	[67]
Cumin seeds (*Cuminum cyminum* L.) Argon plasma	Increase in essential oil yield by 44% compared to control	[68]

epidermal structures found in 30% of all plants. These structures are responsible for the production and storage of eosinophils. Low exposure to cold plasma can increase the yield of eosinophils.

Shokoohi *et al.* found that pretreatment with cold plasma can affect not only the yield of essential oil in the extract, but also its composition [66]. Although some researchers observed no such effects [66, 68], most studies emphasized the duration and intensity of plasma treatment as having the key effect on the quality of essential oil. Jangi *et al.* reported a significant decrease in the contents of major compounds in hyssop leaves treated with cold plasma for longer times at all intensity levels [63]. At high intensity and the longest treatment time, the contents of trans-pinocamphone, *β*-pinene, and *cis*-pinocamphone decreased by 17, 21.3, and 28.6%, respectively. However, at low and medium intensity and a relatively short time (1 and 5 min), cold plasma treatment had a positive effect on the composition of essential oils.

In general, oxygenated compounds are not as important for the quality of essential oils as monoterpene hydrocarbons, which have a more pronounced scent. The above studies found a direct relationship between the duration of cold plasma treatment and its intensity, as well as the contents of oxygenated compounds and monoterpene hydrocarbons. Short treatments of 1–3 min increased the conversion of monoterpene hydrocarbons over time. Longer treatments of over 3 min had the opposite effect – an increased amount of monoterpene hydrocarbons caused by the decomposition of oxygenated monoterpenes [64].

A combined use of cold plasma and ultrasound had a positive effect on the composition of essential oils [71], increasing the amount of oxygenated compounds. Combining cold plasma with microwave treatment resulted in a yield of 3.33% compared to the control at 2.87% [72]. This was because oxygenated molecules with higher dipole moments interacted vigorously with microwaves compared to monoterpene hydrocarbons with lower dipole moments, resulting in a smaller thermal and hydrolytic effect [73]. Other factors that influence the final composition of essential oils include the type of cold plasma working gas, the type of essential oil material, the location of essential oil receptacles, and the composition of bioactive components [74].

Although the studies show that cold plasma treatment is used to accelerate extraction, we still do not know how it affects the solid phase of the capillary-porous body of essential oil material. It is still unclear whether the plasma treatment modifies its structure creating new channels, or whether the essential oil undergoes a transition from a bound to a free form. To address this, we need to develop a method for evaluating extraction kinetic curves that describes the bond form of the essential oil.

Industrial application of cold plasma technology for essential oil extraction. Industrial belt-type units have been created to prepare plant materials for extraction [42]. Figure 8 shows one of such units developed by the Kuban State University of Technology in partnership with Shelris Company. This unit can treat up to one ton of material per hour, followed by its transfer for extraction or steam distillation.



Figure 8 Industrial belt-type unit for cold plasma treatment created by Kuban State University of Technology and Shelris Company

The past year saw a steady increase in the number of patents related to the use of cold plasma in the food industry. For examples, Pańka *et al.* [75] presented a pilot system based on a belt conveyor for using cold plasma to sterilize food product surfaces. This system could potentially be adapted for preparing essential oil materials for extraction.

Technological challenges of using cold plasma for essential oil extraction. The implementation of innovative solutions in the food and essential oil industries requires combined efforts of scientists from various fields, as well as manufacturers and agricultural suppliers. Cold plasma treatment offers a number of advantages. In particular, cold plasma can: reduce the diffusion barrier in the essential oil material by having an etching effect that can improve subsequent extraction; increase the yield of essential oil extraction (although quality assessment is vital at every stage); and be generated by a variety of highly efficient and scalable methods.

Below are several directions for the intensive implementation of cold plasma in essential oil extraction processes.

The current equipment for cold plasma treatment is expensive and needs to be adapted for each type of plant material. Commercial units are being developed for generating cold plasma for extraction, but mostly on a small scale. Therefore, the limited facilities that are available today have to be tried out on a wide range of plant materials, which, in turn, have to be adapted to industrial conditions. This process can be facilitated by expanding and advancing research and development in this area.

One of the limitations of cold plasma is its low penetration into thick materials. This can reduce the efficiency

of the equipment, making it inapplicable on a large scale, and lower the quality of the treatment. Therefore, better technical organization of the process and special preparation (e.g., unifying thickness and fill rate) are needed to ensure high-quality cold plasma treatment.

Promising research directions. Food Industry 5.0 requires the use of alternative, less energy-intensive approaches to extracting essential oils. This process can be made more efficient and cost-effective by incorporating modern electrophysical technologies into traditional processes and using smart systems at all stages of the food supply chain [88]. Furthermore, these technologies need to be green and ensure high quality of the resulting essential oils. Therefore, a promising direction could be a symbiosis of advanced electrophysical technologies in the overall food production chain (Fig. 9). This approach can have a multiple synergistic effect, enabling the production of high-quality essential oils in sufficient quantities.

The analysis of innovative physical methods in essential oil production revealed a number of technological barriers for cold plasma treatment. To overcome them, we need to:

– identify reactions and mechanisms of interaction between reactive plasma particles and individual components of food matrices (lipids, proteins, carbohydrates, etc.). Our systematic review of experimental studies showed a lack of data on the effects of cold plasma treatment on individual food components, including wax shells, pectin, cellulose, and others. This requires an in-depth analysis of reactive cold plasma particles and component compositions of materials under treatment;

– optimize cold plasma generation methods and ensure a continuous material flow to reduce overall energy costs. For example, atmospheric cold plasma treatment takes place under ambient conditions without the use of vacuum equipment. In addition, there is a need for a standardized methodology for calculating energy indicators of cold plasma treatment;

– analyze the effect of cold plasma treatment on the size of electrically induced pores and channels, as well as determine the effect of the pore size on the chemical composition of the resulting essential oil, which is an important quality indicator; and

– determine the electrical and dielectric characteristics of essential oil materials, essential oils, and by-products. The dielectric properties of essential oils are understudied, although the use of electrophysical treatment requires a thorough understanding of the mechanism by which electromagnetic fields affect plant materials, as well as their response.

CONCLUSION

This review presented the latest advances in the application of cold plasma treatment in essential oil extraction. Cold plasma treatment significantly increases the depth of extraction and accelerates the rate of essential oil recovery by 15–20%. Various modes of cold plasma treatment create an “etching” effect on surface tissues and cause electroporation of essential oil globule membranes. These effects contribute to a developed capillary-porous structure in essential oil materials.

One of the downsides to cold plasma treatment is insufficient penetration of reactive plasma particles into the plant material structure, limiting the disruption of essential oil globule membranes. Further research is needed to identify optimal modes of cold plasma treatment for essential oil materials with varying thickness. Localized overheating from cold plasma can affect the quality of the resulting essential oil and therefore must be avoided.

A methodology for assessing the form of essential oil binding to the capillary-porous structure needs to be developed to better understand the mechanism by which cold plasma affects essential oil extraction. This methodology will describe the physical model of essential oil transfer and lay the foundation for developing a mathematical model for extracting essential oils pre-treated with cold plasma.

The existing studies use a limited range of essential oil materials to explore the potential of cold plasma for

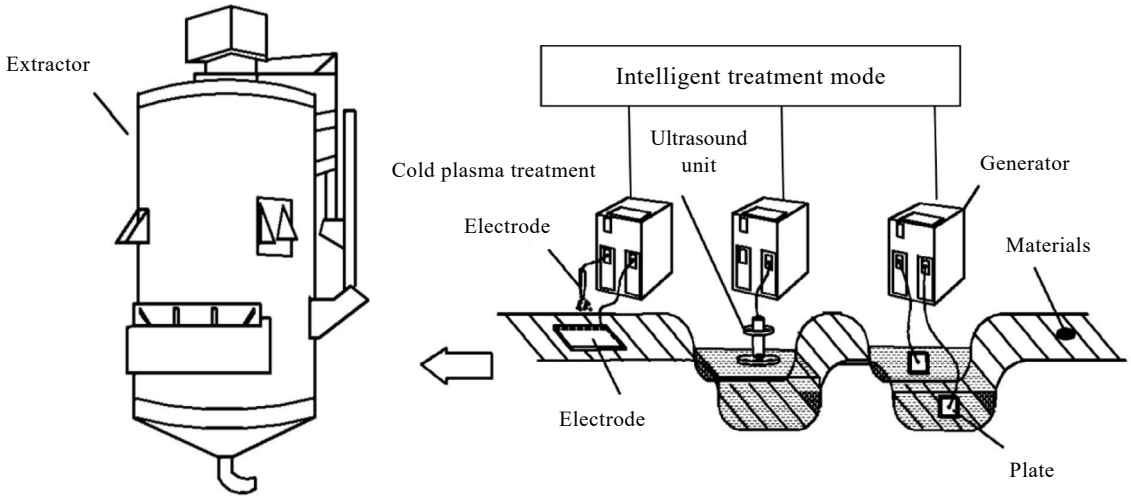


Figure 9 Preparation of food materials for extraction (based on Industry 5.0)

extraction. Therefore, the range of plant materials needs to be expanded to test the technology of cold plasma treatment and adjust it to industrial processes and scales.

CONTRIBUTION

A.G. Sherstyukov and O.I. Andreeva were responsible for information retrieval and graphic design. V.E. Tarasov and I.A. Shorstkii were involved in information retrieval and supervised the writing process.

CONFLICT OF INTEREST

The authors declared no potential conflict of interest regarding the research, authorship, and/or publication of this article.

REFERENCES

1. Midhun J, Stephi D, Muthamil Selvi K, Kameshwari Y, Swatika SK, *et al*. Effect of emerging pretreatment methods on extraction and quality of edible oils: A review. Food and Humanity. 2023;1:1511–1522. https://doi.org/10.1016/j.foohum.2023.10.018
2. Tongnuanchan P, Benjakul S. Essential oils: Extraction, bioactivities, and their uses for food preservation. Journal of Food Science. 2014;79(7):R1231–R1249. https://doi.org/10.1111/1750-3841.12492
3. Kant R, Kumar A. Review on essential oil extraction from aromatic and medicinal plants: Techniques, performance and economic analysis. Sustainable Chemistry and Pharmacy. 2022;30:100829. https://doi.org/10.1016/j.scp.2022.100829
4. Guzmán E, Lucia A. Essential oils and their individual components in cosmetic products. Cosmetics. 2021;8(4):114. https://doi.org/10.3390/cosmetics8040114
5. Saeed K, Pasha I, Chughtai MFJ, Ali Z, Bukhari H, *et al*. Application of essential oils in food industry: challenges and innovation. Journal of Essential Oil Research. 2022;34(2):97–110. https://doi.org/10.1080/10412905.2022.2029776
6. Nevkrytaya NV, Mishnev AV. Actual and contemporary directions of biochemical research of oil-bearing plants. 2018;(4):102–124. (In Russ.) https://doi.org/10.25637/TVAN2018.04.10
7. Pashtetskiy VS, Nevkrytaya NV, Mishnev AV. History, modern state and prospects of the essential oil industry development. Agrarian Bulletin of the Urals. 2017;11:37–46. (In Russ.) https://doi.org/10.25637/TVAN2018.01.02
8. Demchenko NP, Verdysh MV, Popova AA, Polyakova NUDE. Analysis of the import and export of essential oils by the Russian Federation. Scientific notes of the V.I. Vernadsky Crimean Federal University. Economics and management. 2019;5(4):28–35. (In Russ.)
9. Armenta S, Garrigues S, de la Guardia M. The role of green extraction techniques in Green Analytical Chemistry. TrAC Trends in Analytical Chemistry. 2015;71:2–8. https://doi.org/10.1016/j.trac.2014.12.011
10. Casazza AA, Aliakbarian B, Mantegna S, Cravotto G, Perego P. Extraction of phenolics from *Vitis vinifera* wastes using non-conventional techniques. Journal of Food Engineering. 2010;100(1):50–55. https://doi.org/10.1016/j.jfoodeng.2010.03.026
11. Amarni F, Kadi H. Kinetics study of microwave-assisted solvent extraction of oil from olive cake using hexane: Comparison with the conventional extraction. Innovative Food Science & Emerging Technologies. 2010;11(2):322–327. https://doi.org/10.1016/j.ifset.2010.01.002
12. Spigno G, Marinoni L, Garrido GD. 1 – State of the art in grape processing by-products. Handbook of Grape Processing By-Products. Amsterdam: Elsevier; 2017, pp. 1–27. https://doi.org/10.1016/B978-0-12-809870-7.00001-6
13. Pingret D, Fabiano-Tixier AS, Chemat F. An improved ultrasound clevenger for extraction of essential oils. Food Analytical Methods. 2014;7:9–12. https://doi.org/10.1007/s12161-013-9581-0
14. Kodama S, Thawatchaipracha B, Sekiguchi H. Enhancement of essential oil extraction for steam distillation by DBD surface treatment. Plasma Processes and Polymers. 2014;11:126–132. https://doi.org/10.1002/ppap.201300047
15. Ghazanfari N, Yazdi FT, Mortazavi SA, Mohammadi M. Using pulsed electric field pre-treatment to optimize coriander seeds essential oil extraction and evaluate antimicrobial properties, antioxidant activity, and essential oil compositions. LWT. 2023;182:114852. https://doi.org/10.1016/j.lwt.2023.114852
16. Molina R, López-Santos C, Balestrasse K, Gómez-Ramírez A, Sauló J. Enhancing essential oil extraction from lavandin grosso flowers via plasma treatment. International Journal of Molecular Sciences. 2024;25(4):2383. https://doi.org/10.3390/ijms25042383
17. Khan MA, Akram S, Naeem R, Kamal MU, Muhammad G, *et al*. Essentials and pertinence of cold plasma in essential oils, metal–organic frameworks and agriculture. Food Science & Nutrition. 2024;12(12):9928–9950. https://doi.org/10.1002/fsn3.4583
18. Moshinsky AI. The effect of pulsation motion of a liquid in a bidisperse porous medium on the propagation of matter in it. Izvestia RAN, Mekhanika Zhidkosti i Gaza. 2010;(6):109–121. (In Russ.)
19. Boonmee T, Wongthaveethong L, Sinpoo C, Disayathanoowat T, Pettis JS, *et al*. Surface modification of materials by atmospheric-pressure plasma to improve impregnation with essential oils for the control of *Tropilaelaps* Mites in Honeybees (*Apis mellifera*). Applied Sciences. 2022;12(12):5800. https://doi.org/10.3390/app12125800

20. Shorstkii I. Application of cold filamentary microplasma pretreatment assisted by thermionic emission for potato drying. Innovative Food Science & Emerging Technologies. 2020;66:102540. https://doi.org/10.1016/j.ifset.2020.102540
21. Sethunga M, Ranaweera KKDS, Gunathilake KDPP, Munaweera I. Recent advances in the extraction methods of essential oils and oleoresins from plant materials and its potential applications: A comprehensive review. Journal of Food and Bioprocess Engineering. 2022;5(2):151–167. https://doi.org/10.22059/jfabe.2022.347001.1126
22. Seow YX, Yeo CR, Chung HL, Yuk HG. Plant essential oils as active antimicrobial agents. Critical Reviews in Food Science and Nutrition. 2014;54(5):625–644. https://doi.org/10.1080/10408398.2011.599504
23. Herman RA, Ayepa E, Shittu S, Fometu SS, Wang J. Essential oils and their applications – A mini review. Advances in Nutrition & Food Science. 2019;4:1–13. https://doi.org/10.33140/ANFS.04.04.08
24. Vora LK, Gholap AD, Hatvate NT, Naren P, Khan S, *et al*. Essential oils for clinical aromatherapy: A comprehensive review. Journal of Ethnopharmacology. 2024;330:118180. https://doi.org/10.1016/j.jep.2024.118180
25. Alieva SR, Qodirova GA, Sherova ZU, Usmanova SR, Muhidinov ZK. Emulsion micro- and nanocapsules of the lactoglobulin concentrate / pectin system with essential oil of Lavandula angustifolia stabilized by ultrasound. Proceedings of Universities. Applied Chemistry and Biotechnology. 2024;14(4):482–494. (In Russ.) https://doi.org/10.21285/achb.944
26. Chindo BA, Howes MJR, Abuhamdah S, Mallam D, Micah T, *et al*. Evaluation of the anti-nociceptive profile of essential oil from *Melissa officinalis* L. (lemon balm) in acute and chronic pain models. Journal of Ethnopharmacology. 2024;321:117500. https://doi.org/10.1016/j.jep.2023.117500
27. Austriavskikh AN, Zakharenko MA, Zinovieva EN, Poznyakovsky VM. New specialized plant-based product. Bulletin of KSAU. 2022;(7):204–211. https://doi.org/10.36718/1819-4036-2022-7-204-211
28. Bunse M, Daniels R, Gründemann C, Heilmann J, Kammerer DR, *et al*. Essential oils as multicomponent mixtures and their potential for human health and well-being. Frontiers in Pharmacology. 2022;13:956541. https://doi.org/10.3389/fphar.2022.956541
29. Baser KH, Bonello JM. Global trade of essential oils. Journal of Essential Oil Research. 2025;37(2):208–214. https://doi.org/10.1080/10412905.2025.2470791
30. Patrignani F, Siroli L, Serrazanetti DI, Gardini F, Lanciotti R. Innovative strategies based on the use of essential oils and their components to improve safety, shelf-life and quality of minimally processed fruits and vegetables. Trends in Food Science & Technology. 2015;46:311–9. https://doi.org/10.1016/j.tifs.2015.03.009
31. Tu XF, Hu F, Thakur K, Li XL, Zhang YS, *et al*. Comparison of antibacterial effects and fumigant toxicity of essential oils extracted from different plants. Industrial Crops and Products. 2018;124:192–200. https://doi.org/10.1016/j.indcrop.2018.07.065
32. Tonks L, Langmuir I. A general theory of the plasma of an arc. Physical review. 1929;34:876. https://doi.org/10.1103/PhysRev.34.876
33. Wróbel AM, Kryszewski M, Rakowski W, Okoniewski M, Kubacki Z. Effect of plasma treatment on surface structure and properties of polyester fabric. Polymer. 1978;19(8):908–912. https://doi.org/10.1016/0032-3861(78)90197-0
34. Pan Y, Cheng JH, Sun DW. Cold plasma-mediated treatments for shelf life extension of fresh produce: A review of recent research developments. Comprehensive Reviews in Food Science and Food Safety. 2019;18(5):1312–1326. https://doi.org/10.1111/1541-4337.12474
35. Du Y, Yang F, Yu H, Xie Y, Yao W. Improving food drying performance by cold plasma pretreatment: A systematic review. Comprehensive Reviews in Food Science and Food Safety. 2022;21(5):4402–4421. https://doi.org/10.1111/1541-4337.13027
36. Tarasov A, Bochkova A, Muzyukin I, Chugunova O, Stozhko N. The effect of pre-treatment of arabica coffee beans with cold atmospheric plasma, microwave radiation, slow and fast freezing on antioxidant activity of aqueous coffee extract. Applied Sciences. 2022;12(12):5780. https://doi.org/10.3390/app12125780
37. Ganesan AR, Tiwari U, Ezhilarasi PN, Rajauria G. Application of cold plasma on food matrices: A review on current and future prospects. Journal of Food Processing and Preservation. 2021;45:e15070. https://doi.org/10.1111/jfpp.15070
38. Yeasmen N, Orsat V. Green extraction and characterization of leaves phenolic compounds: A comprehensive review. Critical Reviews in Food Science and Nutrition. 2023;63(21):5155–5193. https://doi.org/10.1080/10408398.2021.2013771
39. Shorstkii I, Mounassar EHA. Atmospheric microplasma treatment based on magnetically controlled Fe–Al dynamic platform for organic and biomaterials surface modification. Coatings. 2023;13(8):1362. https://doi.org/10.3390/coatings13081362
40. Niu XX, Wang QH, Zhang C, Sutar PP, Zhang FL, *et al*. Gliding arc plasma pretreatment to plum: A sustainable and environmentally friendly solution to enhance drying efficiency. Innovative Food Science & Emerging Technologies. 2025;103:104054. https://doi.org/10.1016/j.ifset.2025.104054

41. Khudyakov D, Sosnin M, Shorstkii I, Okpala COR. Cold filamentary microplasma pretreatment combined with infrared dryer: Effects on drying efficiency and quality attributes of apple slices. Journal of Food Engineering. 2022;329:111049. https://doi.org/10.1016/j.jfoodeng.2022.111049

42. Andreeva OI, Shorstkii IA. Innovative physical techniques in freeze-drying. Foods and Raw Materials. 2025;13(2): 341–354. https://doi.org/10.21603/2308-4057-2025-2-643

43. Chen YQ, Cheng JH, Sun DW. Chemical, physical and physiological quality attributes of fruit and vegetables induced by cold plasma treatment: Mechanisms and application advances. Critical Reviews in Food Science and Nutrition. 2020;60(16):2676–2690. https://doi.org/10.1080/10408398.2019.1654429

44. Jangra S, Mishra R, Mishra A, Pandey S, Prakash R. Analysis of short-term treatment effects of dielectric barrier discharge plasma to improve germination characteristics of wheat seeds. Radiation Effects and Defects in Solids. 2024;179(7–8):1023–1031. https://doi.org/10.1080/10420150.2024.2378437

45. Almazova KI, Belonogov AN, Borovkov VV, Gorelov EV, Dubinov AE, *et al*. Dynamics of gliding arc climbing in a unipolar Jacob's ladder. Technical Physics. 2020;65(7):1032–1035. (In Russ.) https://doi.org/10.21883/JTF.2020.07.49439.408-19

46. Ashtiani SHM, Rafiee M, Morad MM, Khojastehpour M, Khani MR, *et al*. Impact of gliding arc plasma pretreatment on drying efficiency and physicochemical properties of grape. Innovative Food Science and Emerging Technologies. 2020;63:102381. https://doi.org/10.1016/j.ifset.2020.102381

47. Özdemir E, Başaran P, Kartal S, Akan T. Cold plasma application to fresh green leafy vegetables: Impact on microbiology and product quality. Comprehensive Reviews in Food Science and Food Safety. 2023;22(6):4484–4515. https://doi.org/10.1111/1541-4337.13231

48. He X, Sun T, Zhang W, Yang W, Li L, *et al*. Cold plasma treatment maintains antioxidant capacity and cell membrane integrity in apricot fruit by inducing reactive oxygen species scavenging systems. Postharvest Biology and Technology. 2025;230:113815. https://doi.org/10.1016/j.postharvbio.2025.113815

49. Shorstkii I, Koshevoi E. Drying technology assisted by nonthermal pulsed filamentary microplasma treatment: Theory and practice. ChemEngineering 2019;3(4):91. https://doi.org/10.3390/chemengineering3040091

50. Feizollahi E, Misra NN, Roopesh MS. Factors influencing the antimicrobial efficacy of Dielectric Barrier Discharge (DBD) Atmospheric Cold Plasma (ACP) in food processing applications. Critical Reviews in Food Science and Nutrition. 2021;61(4):666–689. https://doi.org/10.1080/10408398.2020.1743967

51. Macedo MJP, Silva GS, Feitor MC, Costa THC, Ito EN, *et al*. Surface modification of kapok fibers by cold plasma surface treatment. Journal of Materials Research and Technology. 2020;9(2):2467–2476. https://doi.org/10.1016/j.jmrt.2019.12.077

52. Karunanithi S, Guha P, Srivastav PP. Cold plasma-assisted microwave pretreatment on essential oil extraction from betel leaves: Process optimization and its quality. Food and Bioprocess Technology. 2023;16:603–626. https://doi.org/10.1007/s11947-022-02957-3

53. Khudyakov DA, Shorstkii IA, Ulyanenko EE, Gnuchykh EV. Influences of cold atmospheric plasma pretreatment on drying kinetics, structural, fractional and chemical characteristics of tobacco leaves. Drying Technology. 2022;40(15):3285–3291. https://doi.org/10.1080/07373937.2021.2021230

54. Ahmadian S, Kenari RE, Amiri ZR, Sohbatzadeh F, Khodaparast MHH. Effect of ultrasound-assisted cold plasma pretreatment on cell wall polysaccharides distribution and extraction of phenolic compounds from hyssop (*Hyssopus officinalis* L.). International Journal of Biological Macromolecules. 2023;233:123557. https://doi.org/10.1016/j.ijbiomac.2023.123557

55. Sosnin MD, Shorstkii IA. Cold Atmospheric Gas Plasma Processing of Apple Slices. Food Processing: Techniques and Technology. 2023;53(2):368–383. (In Russ.) https://doi.org/10.21603/2074-9414-2023-2-2442

56. Popova EA. Effect of salinity on secondary metabolites and antioxidant activity in callus extracts of *Hyssopus officinalis* L. Food Processing: Techniques and Technology. 2025;55(4):767–777. (In Russ.) https://doi.org/10.21603/2074-9414-2025-4-2604

57. Sherstyukov AG, Shorstkiy IA, Khudyakov DA. Comparative characterisation of lavender essential oil distillation methods using low-current spark discharge pretreatment. Storage and Processing of Farm Products. 2025;33(3):81. (In Russ.) https://doi.org/10.36107/spfp.2025.3.665

58. Auguste S, Buonopane GJ, Tanielyan S, Guerrero DE, Lopez JL. Effects of cold plasma treatment on growth enhancement and on the chemical composition of sweet basil plants (*Ocimum basilicum*). The European Physical Journal D. 2023;77:64. https://doi.org/10.1140/epjd/s10053-023-00633-5

59. Keshavarzi M, Najafi G, Gavlighi HA, Seyfi P, Ghomi H. Enhancement of polyphenolic content extraction rate with maximal antioxidant activity from green tea leaves by cold plasma. Journal of Food Science. 2020;85(10):3415–3422. https://doi.org/10.1111/1750-3841.15448

60. Cao Y, Hua H, Yang P, Chen M, Chen W, *et al*. Investigation into the reaction mechanism underlying the atmospheric low-temperature plasma-induced oxidation of cellulose. Carbohydrate Polymers. 2020;233:115632. https://doi.org/10.1016/j.carbpol.2019.115632

61. Gao X, Zhang A, Héroux P, Sand W, Sun Z, Zhan J, *et al*. Effect of dielectric barrier discharge cold plasma on pea seed growth. Journal of Agricultural and Food Chemistry. 2019;67(39):10813–10822. https://doi.org/10.1021/acs.jafc.9b03099

62. Misra NN, Martynenko A, Chemat F, Paniwnyk L, Barba FJ, *et al*. Thermodynamics, transport phenomena, and electrochemistry of external field-assisted nonthermal food technologies. Critical Reviews in Food Science and Nutrition. 2018;58(11):1832–1863. https://doi.org/10.1080/10408398.2017.1287660

63. Jangi F, Ebadi MT, Ayyari M. Qualitative changes in hyssop (*Hyssopus officinalis* L.) as affected by cold plasma, packaging method and storage duration. Journal of Applied Research on Medicinal and Aromatic Plants. 2021;22:100289. https://doi.org/10.1016/j.jarmap.2020.100289

64. Ebadi MT, Abbasi S, Harouni A, Sefidkon F. Effect of cold plasma on essential oil content and composition of lemon verbena. Food Science & Nutrition. 2019;7(4):1166–1171. https://doi.org/10.1002/fsn3.876

65. Rezaei S, Ebadi MT, Ghobadian B, Ghomi H. Optimization of DBD-Plasma assisted hydro-distillation for essential oil extraction of fennel (*Foeniculum vulgare* Mill.) seed and spearmint (*Mentha spicata* L.) leaf. Journal of Applied Research on Medicinal and Aromatic Plants. 2021;24:100300. https://doi.org/10.1016/j.jarmap.2021.100300

66. Shokoohi F, Ebadi MT, Ghomi H, Ayyari M. Changes in qualitative characteristics of garden thyme (*Thymus vulgaris* L.) as affected by cold plasma. Journal of Applied Research on Medicinal and Aromatic Plants. 2022;31:100411. https://doi.org/10.1016/j.jarmap.2022.100411

67. Amunugoda PNRJ, de Silva ABG, Weeratunge H, Gunawardena SHP, de Alwis AAP. Low-pressure and atmospheric-pressure cold plasma treatment as a pretreatment for extracting volatile oils from black pepper (*Piper nigrum*) seeds. Journal of the Sri Lanka Association for the Advancement of Science. 2024;6(1):25–38. https://doi.org/10.5281/zenodo.11404205

68. Shokoohi F, Ebadi MT, Ghomi H, Rezaeinezhad AR, Haghani SF. Increasing the efficiency of cumin essential oil extraction using cold plasma pretreatments. Journal of the Science of Food and Agriculture. 2024;104(9):5001–9. https://doi.org/10.1002/jsfa.13290

69. Namjoo M, Moradi M, Dibagar N, Niakousari M. Cold plasma pretreatment prior to ultrasound-assisted air drying of cumin seeds. Food and Bioprocess Technology. 2022;15:2065–2083. https://doi.org/10.1007/s11947-022-02863-8

70. Shishir MRI, Karim N, Bao T, Gowd V, Ding T, *et al*. Cold plasma pretreatment – A novel approach to improve the hot air drying characteristics, kinetic parameters, and nutritional attributes of shiitake mushroom. Drying Technology. 2020;38(16):2134–2150. https://doi.org/10.1080/07373937.2019.1683860

71. Moradi-Sadr J, Ebadi MT, Ayyari M, Ghomi H. Optimization of ultrasonic Bath and cold plasma pre-treatments in the spearmint essential oil isolation process. Food Science & Nutrition. 2023;11(4):1904–1915. https://doi.org/10.1002/fsn3.3224

72. Karunanithi S, Gupta RK. Aqueous extraction of tomato seed oil using combination of ohmic heating and microwave heating as pretreatment. Food Physics. 2024;1:100018. https://doi.org/10.1016/j.foodp.2024.100018

73. Filly A, Fernandez X, Minuti M, Visinoni F, Cravotto G, *et al*. Solvent-free microwave extraction of essential oil from aromatic herbs: From laboratory to pilot and industrial scale. Food Chemistry. 2014;150:193–198. https://doi.org/10.1016/j.foodchem.2013.10.139

74. Fernandes FAN, Maia DLH, Canuto KM, de Brito ES. Aroma modulation of limonene-rich essential oil using cold plasma technology. Plasma Chemistry and Plasma Processing. 2025;45:1925–1944. https://doi.org/10.1007/s11090-025-10585-w

75. Pańka D, Jeske M, Łukanowski A, Baturo-Cieśniewska A, Prus P, *et al*. Can cold plasma be used for boosting plant growth and plant protection in sustainable plant production? Agronomy. 2022;12(7):841. https://doi.org/10.3390/agronomy12040841

76. Hassoun A, Jagtap S, Trollman H, Garcia-Garcia G, Abdullah NA, *et al*. Food processing 4.0: Current and future developments spurred by the fourth industrial revolution. Food Control. 2023;145:109507. https://doi.org/10.1016/j.foodcont.2022.109507

Additional information about the authors

Andrey G. Sherstyukov ORCID 0009-0005-6318-8797; eLIBRARY SPIN 8031-3941
Oksana I. Andreeva ORCID 0009-0008-4265-9651; eLIBRARY SPIN 8613-7201
Vasily E. Tarasov eLIBRARY SPIN 4913-2381
Ivan A. Shorstkii ORCID 0000-0001-5804-7950; eLIBRARY SPIN 8541-4857

Foods and Raw Materials. 2027;15(2)

ISSN 2308-4057 (Print)
ISSN 2310-9599 (Online)

Research Article
Open Access

Available online at http://jfrm.ru/en
https://doi.org/10.21603/2308-4057-2027-2-715
https://elibrary.ru/VSNZIB

Clarification of cashew apple juice with pectinases extracted from the epicarp of papaya cv. Solo 8

Kouassi M.-D. Adingra*, Hermann D. Gnahe, Soguimondenin Soro, N'guessan J. P. Kouadio, Kablan Tano

Nangui Abrogoua University, Abidjan, Côte d'Ivoire

* e-mail: maxadingra@gmail.com

Received 26.06.2025; Revised 06.11.2025; Accepted 03.02.2026; Published online 09.07.2026

Abstract:
Cashew apples are often discarded after nut extraction, despite their potential for juice production. This study aimed to clarify cashew apple juice using pectinases extracted from the epicarp of papaya cultivar Solo 8.
These enzymes were previously purified using ammonium sulfate precipitation followed by dialysis and isoelectric focusing. Cashew apples were sourced from a village plantation in Bondoukou, Gontougo region. Clarification tests were conducted using standard methods.
According to the results, the juice clarity improved significantly over 120 minutes: from 44.67% to 83.18% with pectin methylesterase, to 93.32% with polygalacturonase, and to 72.44% with pectin lyase. The browning index and color intensity of the raw juice decreased from 82.98 to 41.69% and from 75.86 to 26.91%, respectively. The vitamin C content declined from 327.82 to 202.94 mg/100 mL (pectin methylesterase), 280.99 mg/100 mL (polygalacturonase), and 208.70 mg/100 mL (pectin lyase). Viscosity reductions were also notable: 67% with pectin methylesterase, 72% with polygalacturonase, and 59% with pectin lyase. Among enzyme combinations, the most effective was a mix of pectin methylesterase (0.087 mg/mL) and polygalacturonase (0.264 mg/mL), which reduced the juice's viscosity by over 76% and increased its clarity by more than 50%.
These findings highlight the potential of papaya-derived pectinases in improving cashew apple juice quality and marketability.

Keywords: *Carica papaya* L., cashew apple, juice valorization, epicarp, pectinases, clarification, viscosity

Please cite this article in press as: Adingra KMD, Gnahe HD, Soro S, Kouadio NJP, Tano K. Clarification of cashew apple juice with pectinases extracted from the epicarp of papaya cv. Solo 8. Foods and Raw Materials. 2027;15(2):358–369. https://doi.org/10.21603/2308-4057-2027-2-715

INTRODUCTION

Coffee and cocoa have always been the mainstay of Ivorian agriculture. However, other crops, although considered minor, have also begun to experience significant development. These crops include the cashew tree (*Anacardium occidentale* L.). The main producers of cashew are Côte d'Ivoire, India, Vietnam, and Nigeria. The cashew tree is primarily cultivated for its nut, which is the main commercial product and represents approximately 8–12% of the total fruit weight, whereas the cashew apple accounts for the remaining 88–92% [1].

Cashew apple has a high water content (85.5 to 90%) and a low protein content. It is rich in sugars and micronutrients such as iron, phosphorus, calcium, vitamin C, flavonoids, and polyphenols [2, 3]. Its high water content makes cashew apple a highly perishable food in its fresh state, raising the importance of its transformation into stable products. In Togo, just as in Côte d'Ivoire, cashew apple valorization trials have enabled the use of cashew apple powder in animal feed [4, 5]. A study in Benin has demonstrated the use of cashew apple powder in the bread-making industry [6]. In Côte d'Ivoire, the work of Sahie *et al.* [7] highlighted the influence of processing steps on the nutritional and organoleptic quality of cashew apples, as well as on clarification, stabilization, concentration, and dehydration methods. Similarly, the study by Adou *et al.* [8] focused on the stabilization and sensory evaluation of cashew apple juices.

The processing of fruits into juice is generally considered the main method of their valorization [9–12]. However, the cashew fruit is usually harvested for the nut, with the apple being left in the fields without proper valorization [13]. Moreover, the juice extracted from cashew apple is astringent due to the presence of condensed tannins and turbid due to the high concentration of pectins [11, 14]. Pectins are complex polysaccharides

Copyright © 2026, Adingra, *et al.* This is an open access article distributed under the terms of the Creative Commons Attribution 4.0 International License (https://creativecommons.org/licenses/by/4.0/), allowing third parties to copy and redistribute the material in any medium or format and to remix, transform, and build upon the material for any purpose, even commercially, provided the original work is properly cited and states its license.

found in the cell walls of most higher plants [12]. Their high concentration in cashew apple leads to the formation of colloids [15, 16]. Cloudy juices need to be clarified since most consumers find them unacceptable [17]. Clarified cashew apple juice is clear and has a pale yellow color. Its astringent taste, which dries the mouth, is eliminated by almost 95%. Studies have shown that various enzymes are involved in the clarification of cloudy fruit juices, particularly pectinases. For example, fungal pectinases have been extensively used to clarify fruit and vegetable juices [11, 18].

Cashew apple, a by-product of the cashew tree (*A. occidentale*) has been widely used in juice production [8, 19]. However, the turbidity of cashew apple juice lowers its marketability. Some authors have used different clarification techniques to reduce its viscosity, including tangential microfiltration, membrane coupling, electroflotation, and ultrafiltration [20–22]. However, these techniques require significant financial resources, creating a need for finding more affordable ways of clarifying cashew apple juice. For example, our recent study showed that the epicarp of commercial papaya cultivar Solo 8 contained three pectinases, namely polygalacturonase (acidic and mesophilic), pectin methylesterase (alkaline and thermophilic), and pectin lyase (alkaline and mesophilic) [23]. We purified these pectinases by using three separation steps: ammonium sulfate precipitation, dialysis, and isoelectric focusing. The purification yielded specific activities of 198 U/mg of protein for pectin methylesterase, 3.62 IU/mg of protein for polygalacturonase, and 0.176 IU/mg of protein for pectin lyase. When purified, these enzymes could be used for clarifying cashew apple juice. Therefore, this study aimed to use these pectinolytic enzymes in cashew apple juice clarification trials.

STUDY OBJECTS AND METHODS

Biological material. Cashew apples (Fig. 1) were harvested from a village plantation in Mérékou on the Tanda-Assuéfry axis in the Gontougo region, located about 384 km from the Félix Houphouët-Boigny Airport in Abidjan (Côte d'Ivoire).

Cashew apple sampling. Yellow cashew apples were harvested at the mature stage in April 2016. Harvesting was done manually, and only ripe, undamaged cashew apples were picked. Once in the laboratory, the fruits were pitted, then washed and disinfected. The apples were divided into 10 kg batches to undergo a series of operations detailed in the apple juice extraction section.

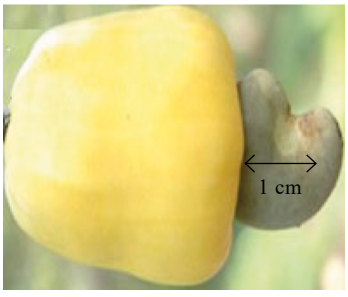


Figure 1 Cashew fruit

Juice extraction. The technique described by Abdullah *et al.* [24] was slightly modified to obtain raw cashew apple juice (Fig. 2). At the end of extraction, 2.5 L of juice was obtained from 10 kg of cashew apples.

Enzymatic clarification. To perform the clarification, the following parameters were previously determined: incubation time (15–120 min), enzyme concentration (0.008 to 0.140 mg/mL), and the concentration of each substrate (0.5–2.0%). The clarification was performed using the modified technique of Anuradha *et al.* [25]. In fact, a determined volume of each enzyme (50 µL of pectin lyase, 100 µL of polygalacturonase, and 100 µL of pectin methylesterase) was added to 100 mL of cashew apple juice. Then, the reaction mixture was incubated in a water bath at the optimal temperature for each enzyme (45°C for polygalacturonase, 50°C for pectin lyase, and 60°C for pectin methylesterase) for 120 min. At regular intervals of 15 min, an aliquot of 10 mL was taken and heated at 85 °C for 5 min to inactivate the pectinases. After cooling, the reaction medium was centrifuged at 10,000 rotations/min for 15 min and the supernatant, which constituted the clarified juice, was collected in tubes for the analyses below.

Physicochemical analyses of clarified juice. To assess the physicochemical and nutritional quality of the clarified juice, we determined its pH, titratable acidity, and vitamin C content using standard and referenced methods. The soluble solids expressed in °Brix were measured with a portable refractometer equipped with a temperature corrector (model FG103/113, Milan, Italy). Clarity, color, and browning index were determined using a

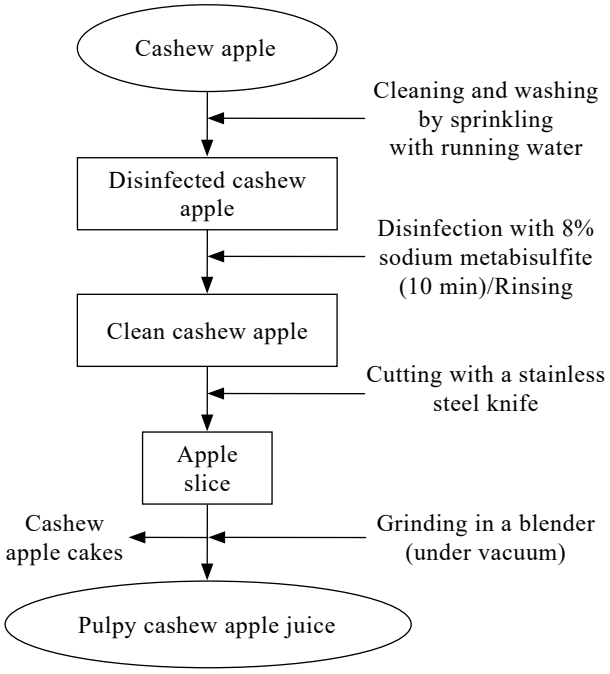


Figure 2 Flow chart of cashew apple juice extraction ([24] modified)

spectrophotometer (NanoDrop® ND-1000, Thermo Fischer Scientific) at the respective wavelengths of 660 nm, 440 nm, and 420 nm, with the use of distilled water as a control [9, 26, 27]. Viscosity was determined using a viscometer (Visco Star R, fungilab.S.A.).

Statistical analyses. All the analyses were performed in triplicate, and the data were expressed as the arithmetic mean with the corresponding statistical standard deviation. One-way analysis of variance (ANOVA) was performed on all the results to determine significant statistical differences between the calculated mean values. Significant statistical differences were demonstrated using Duncan's test at the 95% confidence level. The statistical analysis was performed using Statistica 7.1 software.

RESULTS AND DISCUSSION

This study was conducted in two stages. The first stage consisted of verifying the individual effect of each pectinase on the clarification of cashew apple juice. The second stage involved combining two most effective pectinases for the clarification of cashew apple juice.

Clarification with purified pectinases. ***Study of the minimum clarifying concentration.*** Purified pectinases isolated from the epicarp of papaya cultivar Solo 8 were used to clarify cashew apple juice. Their concentrations were 0.008 mg/mL for pectin lyase (0.176 IU/mg), 0.0348 mg/mL for pectin methylesterase (198 U/mg), and 0.0352 mg/mL for polygalacturonase (3.6 IU/mg) (Fig. 3).

Clarification of cashew apple juice with pectin methylesterase. ***Clarity, color, and browning index.*** Table 1 shows the changes in clarity, color, and browning index of cashew apple juice after the addition of pectin methylesterase. As can be seen, the clarity of cashew apple juice increased from 44.67 to 83.18% during the 120-min clarification period, stabilizing after 105 min. However, the color and browning decreased throughout clarification, reaching respective values of 43.65 and 28.18% at 120 min. Furthermore, the color intensity of cashew apple juice no longer changed after 105 min.

pH, titratable acidity, soluble solids, and vitamin C. After the addition of pectin methylesterase, the pH and titratable acidity of cashew apple juice changed very little (Table 2). In particular, the pH slightly decreased from 4.87 ± 0.03 to 4.77 ± 0.03, whereas titratable acidity slightly increased from 0.208 ± 0.030 to 0.240 ± 0.010 g/100 mL at the end of clarification. Statistical analysis revealed that there was no significant difference in the pH values after 15 min of clarification. However, it showed a significant difference in the titratable acidity of the juice clarified with pectin methylesterase between 0 and 120 min. The initial soluble dry extract of the raw juice (12°Brix) decreased during clarification to reach a value of 7.90 ± 0.01°Brix at 105 min.

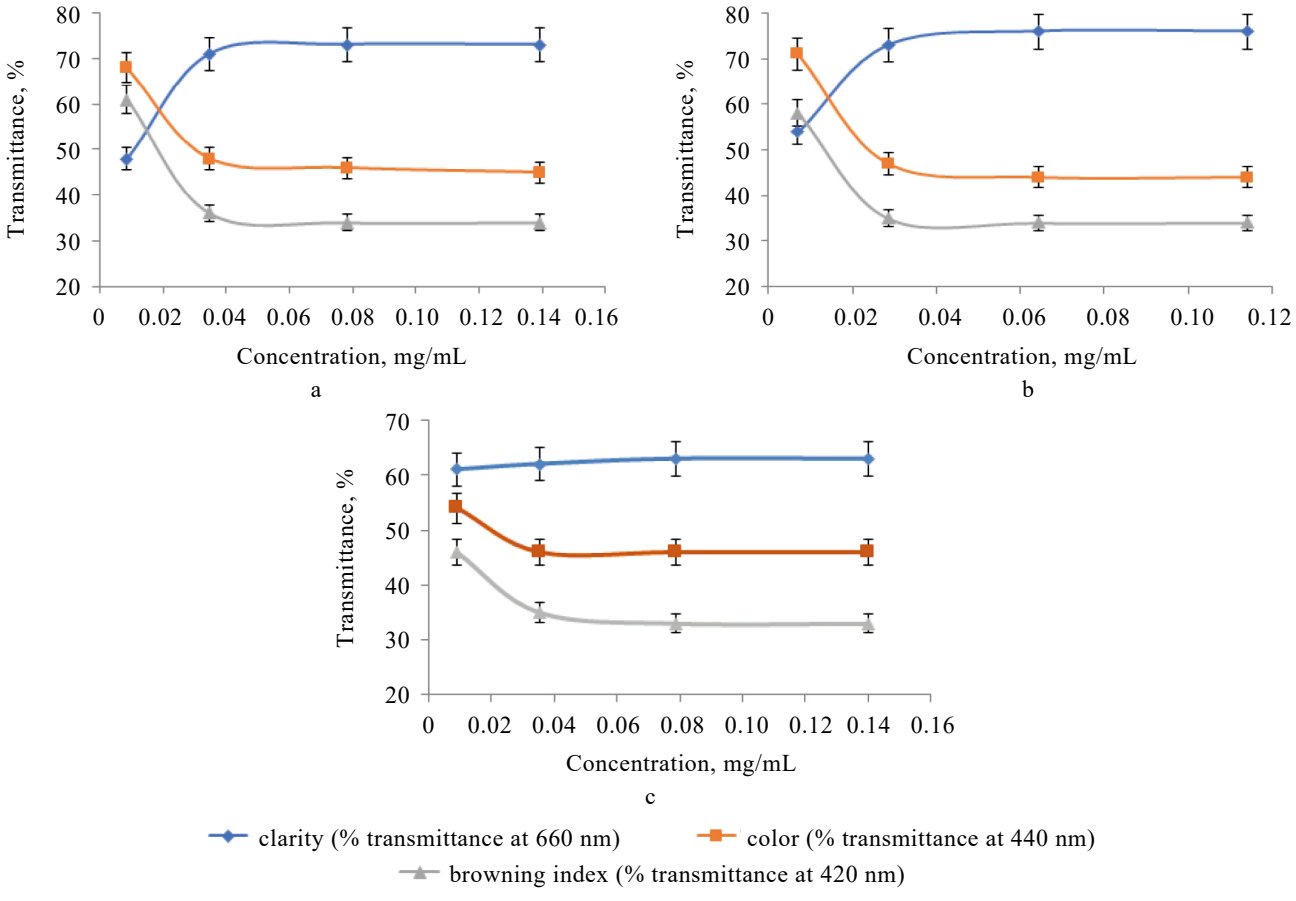


Figure 3 Influence of pectinase concentration on the appearance of cashew apple juice: (a) pectin methylesterase, PMI; (b) polygalacturonase, PG; and (c) pectin lyase, PL

Table 1 Changes in clarity, color, and browning index of cashew apple juice after addition of pectin methylesterase

Clarification time, min	Clarity (660 nm), %	Color (440 nm), %	Browning (420 nm), %
0	44.67 ± 0.01^{h}	82.98 ± 0.03^{a}	75.86 ± 0.01^{a}
15	50.12 ± 0.04^{g}	72.44 ± 0.01^{b}	58.88 ± 0.00^{b}
30	52.48 ± 0.03^{f}	56.23 ± 0.03^{c}	43.65 ± 0.01^{c}
45	63.09 ± 0.06^{e}	50.12 ± 0.01^{d}	38.02 ± 0.01^{d}
60	72.44 ± 0.01^{d}	46.77 ± 0.01^{e}	35.48 ± 0.01^{e}
75	75.86 ± 0.01^{c}	45.71 ± 0.01^{f}	33.11 ± 0.01^{f}
90	81.28 ± 0.03^{b}	44.67 ± 0.03^{g}	30.20 ± 0.03^{g}
105	83.18 ± 0.03^{a}	43.65 ± 0.01^{h}	28.84 ± 0.03^{h}
120	83.18 ± 0.01^{a}	43.65 ± 0.00^{h}	28.18 ± 0.01^{i}

Means ± standard deviations followed by the same lowercase letter in a column for a parameter are not significantly different at the 5% threshold according to Duncan's test

Table 2 Changes in pH, titratable acidity, soluble solids, and vitamin C during clarification of cashew apple juice using pectin methylesterase

Clarification time, min	Parameter			
	pH	Titratable acidity, g/100 mL	Refractometric dry extract, °Brix	Vitamin C, mg/100 mL
0	4.87 ± 0.03^{a}	0.208 ± 0.000^{c}	12.00 ± 0.00^{a}	327.82 ± 0.00^{a}
15	4.80 ± 0.03^{b}	0.212 ± 0.000^{c}	11.40 ± 0.01^{b}	304.41 ± 0.03^{b}
30	4.79 ± 0.01^{b}	0.220 ± 0.010^{b,c}	10.60 ± 0.00^{c}	280.99 ± 0.03^{c}
45	4.79 ± 0.03^{b}	0.224 ± 0.000^{a,b,c}	10.10 ± 0.03^{d}	257.56 ± 0.03^{d}
60	4.79 ± 0.01^{b}	0.224 ± 0.000^{a,b,c}	9.30 ± 0.03^{e}	249.76 ± 0.03^{e}
75	4.79 ± 0.00^{b}	0.232 ± 0.000^{a,b}	8.60 ± 0.01^{f}	234.15 ± 0.01^{f}
90	4.78 ± 0.01^{b}	0.232 ± 0.000^{a,b}	8.20 ± 0.03^{g}	218.54 ± 0.00^{g}
105	4.77 ± 0.01^{b}	0.240 ± 0.000^{a}	7.90 ± 0.01^{h}	218.54 ± 0.01^{g}
120	4.77 ± 0.03^{b}	0.240 ± 0.010^{a}	7.76 ± 0.00^{i}	202.94 ± 0.03^{h}

Means ± standard deviations followed by the same lowercase letter on a line for a parameter are not significantly different at the 5% threshold according to Duncan's test

Table 3 Changes in clarity, color, and browning index of cashew apple juice after addition of polygalacturonase

Clarification time, min	Clarity (660 nm), %	Color (440 nm), %	Browning (420 nm), %
0	44.67 ± 0.01^{h}	82.98 ± 0.03^{a}	75.86 ± 0.01^{a}
15	50.12 ± 0.03^{g}	74.13 ± 0.01^{b}	57.28 ± 0.00^{b}
30	54.95 ± 0.03^{f}	51.29 ± 0.01^{c}	48.98 ± 0.01^{c}
45	66.07 ± 0.04^{e}	46.77 ± 0.01^{d}	39.81 ± 0.01^{d}
60	75.86 ± 0.03^{d}	46.77 ± 0.00^{e}	34.67 ± 0.01^{e}
75	81.28 ± 0.03^{c}	45.71 ± 0.01^{f}	32.16 ± 0.01^{f}
90	87.09 ± 0.01^{b}	45.71 ± 0.00^{f}	30.90 ± 0.01^{g}
105	93.32 ± 0.01^{a}	44.67 ± 0.01^{g}	30.20 ± 0.01^{h}
120	93.32 ± 0.00^{a}	43.65 ± 0.01^{h}	29.51 ± 0.01^{i}

Means ± standard deviations followed by the same lowercase letter in a column for a parameter are not significantly different at the 5% threshold according to Duncan's test

Furthermore, the initial vitamin C content (327.82 ± 0.00 mg/100 mL) of cashew apple juice decreased to 218.54 ± 0.01 mg/100 mL after 90 min of clarification and remained at this level after 105 min of the treatment. Statistical analysis also showed a significant difference between the soluble dry extract and the vitamin C content of the juice clarified with pectin methylesterase.

Clarification of cashew apple juice with polygalacturonase. ***Clarity, color, and browning index.*** The addition of polygalacturonase caused an increase in clarity and a decrease in color and browning index (Table 3). In particular, the clarity of the raw juice increased significantly from 44.67 ± 0.01 to 93.32 ± 0.00% between 0 and 120 min, with no significant difference between 105 and 120 min. The color and browning index decreased to 43.65 ± 0.01 and 29.51 ± 0.01%, respectively.

pH, titratable acidity, soluble solids, and vitamin C. The treatment of cashew apple juice with polygalacturonase caused a decrease in its pH, refractometric solids, °Brix, and vitamin C, as well as an increase in its titratable acidity (Table 4). In particular, the raw juice's pH of 4.87 ± 0.03 and vitamin C content of 327.82 ± 0.00 mg/100 mL decreased to 4.77 ± 0.00 and 280.99 ± 0.03 mg/100 mL, respectively, after 120 min of clarifica-

Table 4 Changes in pH, titratable acidity, soluble solids, and vitamin C during clarification of cashew apple juice by polygalacturonase

Clarification time, min	Parameter			
	pH	Titratable acidity, g/100 mL	Refractometric dry extract, °Brix	Vitamin C, mg/100 mL
0	4.87 ± 0.03[a]	0.208 ± 0.000[c]	12.00 ± 0.00[a]	327.82 ± 0.00[a]
15	4.79 ± 0.03[b]	0.212 ± 0.000[c]	11.60 ± 0.01[b]	320.01 ± 0.03[b]
30	4.78 ± 0.01[b]	0.224 ± 0.000[b]	10.80 ± 0.03[c]	312.21 ± 0.04[c]
45	4.78 ± 0.03[b]	0.232 ± 0.000[a]	9.90 ± 0.03[d]	312.21 ± 0.01[c]
60	4.77 ± 0.00[b]	0.236 ± 0.000[a]	9.50 ± 0.03[e]	304.41 ± 0.01[d]
75	4.77 ± 0.01[b]	0.236 ± 0.000[a]	9.30 ± 0.04[f]	296.60 ± 0.01[e]
90	4.77 ± 0.03[b]	0.236 ± 0.000[a]	8.20 ± 0.03[g]	296.60 ± 0.00[e]
105	4.77 ± 0.01[b]	0.236 ± 0.000[a]	7.90 ± 0.01[h]	288.80 ± 0.01[f]
120	4.77 ± 0.00[b]	0.236± 0.000[a]	7.79 ± 0.01[i]	280.99 ± 0.03[g]

Means ± standard deviations followed by the same lowercase letter on a line for a parameter are not significantly different at the 5% threshold according to Duncan's test

Table 5 Changes in clarity, color, and browning index of cashew apple juice after addition of pectin lyase

Clarification time, min	Clarity (660 nm), %	Color (440 nm), %	Browning (420 nm), %
0	44.67 ± 0.01[g]	82.98 ± 0.03[a]	75.86 ± 0.01[a]
15	48.98 ± 0.01[f]	82.98 ± 0.00[b]	61.66 ± 0.02[b]
30	52.48 ± 0.02[e]	54.95 ± 0.01[c]	43.65 ± 0.01[c]
45	53.70 ± 0.01[d]	50.12 ± 0.01[d]	38.90 ± 0.05[d]
60	63.10 ± 0.04[c]	45.71 ± 0.02[e]	33.11 ± 0.01[e]
75	70.80 ± 0.01[b]	43.65 ± 0.01[f]	32.36 ± 0.03[f]
90	72.44 ± 0.03[a]	41.69 ± 0.01[g]	28.18 ± 0.01[g]
105	72.44 ± 0.01[a]	41.69 ± 0.00[g]	26.91 ± 0.01[h]
120	72.44 ± 0.03[a]	41.69 ± 0.01[g]	26.91 ± 0.00[h]

Means ± standard deviations followed by the same lowercase letter in a column for a parameter are not significantly different at the 5% threshold according to Duncan's test

tion. Furthermore, its soluble solids (12.00 ± 0.00°Brix) decreased to 7.79 ± 0.01°Brix in 120 min. On the other hand, the titratable acidity of the juice increased from 0.208 ± 0.000 to 0.236 ± 0.000 g /100 mL after 120 min. Statistical analysis showed no significant difference between the pH values of the clarified juice from 15 min of the treatment. It found no significant difference between the acidity values of the juice from 45 min of clarification. However, the analysis revealed a significant difference for the soluble solids and vitamin C values during the treatment.

Clarification of cashew apple juice with pectin lyase. ***Clarity, color, and browning index.*** Table 5 shows changes in the clarity, color, and browning index of cashew apple juice after adding pectin lyase. In particular, the clarity increased from 44.67 to 72.44% and no longer changed after 90 min of preincubation with pectin lyase. The color intensity decreased from 82.98 to 41.70% at the end of clarification, stabilizing after 90 min. Furthermore, the initial browning index (75.86%) of cashew apple juice decreased by half (38.90%) after 45 min of hydrolysis.

pH, titratable acidity, soluble solids, and vitamin C. The physicochemical parameters of cashew apple juice measured after the addition of pectin lyase are given in Table 6. During the clarification process, the initial pH decreased from 4.87 to 4.78 after 120 min, while the soluble solids and vitamin C decreased from 12 to 7.76°Brix and from 327.82 to 208.70 mg/100 mL, respectively, after 120 min. In contrast, the titratable acidity increased from 0.208 to 0.232 g/100 mL after 120 min. Furthermore, statistical analysis revealed no significant difference in titratable acidity during clarification. However, it indicated a significant difference in pH values after 15 min of the treatment. The analysis of soluble solids, °Brix, and vitamin C results showed significant differences during the clarification of cashew apple juice with pectin lyase.

Clarification of cashew apple juice with pectin methylesterase and polygalacturonase. ***Clarity, color, and browning index.*** Table 7 shows changes in the clarity, color, and browning index of cashew apple juice after the addition of different mixtures of pectin methylesterase and polygalacturonase, namely 0.087 + 0.264 mg/mL (mixture 1), 0.174 + 0.176 mg/mL (mixture 2), and 0.261 + 0.088 mg/mL (mixture 3), respectively. As can be seen, mixture 1 provided greater clarity than the other two mixtures during the clarification period. In particular, it increased the clarity to 83.18% after six minutes, while mixtures 2 and 3 provided a clarity of 81.28 and 79.43%, respectively, after 75 min of clarification. After 105 min of treatment with mix-

Table 6 Changes in pH, titratable acidity, soluble solids, and vitamin C during clarification of cashew apple juice by pectin lyase

Clarification time, min	Parameter			
	pH	Titratable acidity, g/100 mL	Refractometric dry extract, °Brix	Vitamin C, mg/100 mL
0	4.87 ± 0.03[a]	0.208 ± 0.000[a]	12.00 ± 0.00[a]	327.82 ± 0.00[a]
15	4.80 ± 0.00[b]	0.210 ± 0.000[a]	11.40 ± 0.04[b]	304.41 ± 0.03[b]
30	4.79 ± 0.04[b]	0.220 ± 0.000[a]	10.16 ± 0.03[c]	288.80 ± 0.01[c]
45	4.79 ± 0.03[b]	0.228 ± 0.000[a]	10.12 ± 0.03[d]	280.99 ± 0.03[d]
60	4.78 ± 0.01[b]	0.232 ± 0.000[a]	9.30 ± 0.03[e]	265.36 ± 0.03[e]
75	4.78 ± 0.01[b]	0.232 ± 0.000[a]	8.60 ± 0.04[f]	248.76 ± 0.01[f]
90	4.78 ± 0.00[b]	0.232 ± 0.000[a]	8.20 ± 0.04[g]	234.15 ± 0.01[g]
105	4.78 ± 0.03[b]	0.232 ± 0.000[a]	7.90 ± 0.05[h]	218.54 ± 0.03[h]
120	4.78 ± 0.01[b]	0.232 ± 0.000[a]	7.76 ± 0.03[i]	208.70 ± 0.01[i]

Means ± standard deviations followed by the same lowercase letter on a line for a parameter are not significantly different at the 5% threshold according to Duncan's test

Table 7 Changes in clarity, color, and browning index of cashew apple juice after addition of mixtures of pectinases (pectin methylesterase and polygalacturonase)

Clarification time, min	Enzymes concentration	Clarity (660 nm), %	Color (440 nm), %	Browning (420 nm), %
0	Mixture 1	44.67 ± 0.01	82.98 ± 0.01	75.86 ± 0.01
	Mixture 2	44.67 ± 0.01	82.98 ± 0.01	75.86 ± 0.01
	Mixture 3	44.67 ± 0.01	82.98 ± 0.01	75.86 ± 0.01
15	Mixture 1	52.48 ± 0.06	54.95 ± 0.04	51.29 ± 0.01
	Mixture 2	50.12 ± 0.01	67.61 ± 0.03	54.95 ± 0.03
	Mixture 3	50.12 ± 0.03	67.61 ± 0.03	61.66 ± 0.04
30	Mixture 1	66.07 ± 0.09	48.98 ± 0.01	46.77 ± 0.03
	Mixture 2	54.95 ± 0.06	52.48 ± 0.04	50.12 ± 0.04
	Mixture 3	54.95 ± 0.01	54.95 ± 0.03	46.77 ± 0.03
45	Mixture 1	79.43 ± 0.03	46.77 ± 0.03	35.48 ± 0.01
	Mixture 2	66.07 ± 0.06	48.98 ± 0.01	38.02 ± 0.03
	Mixture 3	67.61 ± 0.03	50.12 ± 0.01	43.65 ± 0.03
60	Mixture 1	83.18 ± 0.01	45.71 ± 0.03	35.48 ± 0.03
	Mixture 2	72.44 ± 0.01	46.77 ± 0.03	34.67 ± 0.01
	Mixture 3	74.13 ± 0.03	46.77± 0.03	39.81 ± 0.03
75	Mixture 1	91.20 ± 0.04	44.67 ± 0.03	31.62 ± 0.01
	Mixture 2	81.28 ± 0.06	46.77 ± 0.04	30.90 ± 0.04
	Mixture 3	79.43 ± 0.03	45.71 ± 0.01	33.88 ± 0.04
90	Mixture 1	93.32 ± 0.06	44.67 ± 0.01	30.20 ± 0.01
	Mixture 2	89.12 ± 0.03	45.71 ± 0.03	29.51 ± 0.03
	Mixture 3	83.18 ± 0.03	44.67 ± 0.03	31.62 ± 0.03
105	Mixture 1	95.50 ± 0.03	43.65 ± 0.03	29.51 ± 0.03
	Mixture 2	91.20 ± 0.03	43.65 ± 0.03	29.51 ± 0.01
	Mixture 3	87.10 ± 0.01	43.65 ± 0.01	29.51 ± 0.03
120	Mixture 1	95.50 ± 0.01	43.65 ± 0.01	28.84 ± 0.04
	Mixture 2	91.20 ± 0.06	43.65 ± 0.01	28.18 ± 0.03
	Mixture 3	87.10 ± 0.03	43.65 ± 0.03	28.18 ± 0.03

Mixture 1: pectin methylesterase (0.087 mg/mL) + polygalacturonase (0.264 mg/mL); Mixture 2: pectin methylesterase (0.174 mg/mL) + polygalacturonase (0.176 mg/mL); and Mixture 3: pectin methylesterase (0.261 mg/mL) + polygalacturonase (0.088 mg/mL)

ture 1, the juice showed a maximum clarity of 95.50%, compared to 91.20 and 87.10% for mixtures 2 and 3, respectively. Furthermore, the three mixtures decreased the color intensity of cashew apple juice from 82.98 to 43.65%. The color intensity stabilized after 105 min. Finally, the browning index of cashew apple juice decreased by half after 45 min of treatment with the three mixtures.

pH, titratable acidity, soluble solids, and vitamin C of cashew apple juice clarified with mixture 1. Mixture 1 (0.087 mg/mL pectin methylesterase + 0.264 mg/mL polygalacturonase) resulted in a reduction in pH, soluble solids, and vitamin C values (Table 8). Statistical analysis revealed a significant difference in soluble solids during the enzymatic clarification process ($P < 5\%$). This analysis also showed a significant difference in

Table 8 Changes in pH, titratable acidity, soluble solids, and vitamin C during clarification of cashew apple juice with mixture 1

Clarification time, min	Parameter			
	pH	Titratable acidity, g/100 mL	Refractometric dry extract, °Brix	Vitamin C, mg/100 mL
0	4.87 ± 0.03[a]	0.208 ± 0.000[c]	12.00 ± 0.00[a]	327.82 ± 0.00[a]
15	4.82 ± 0.03[b]	0.210 ± 0.000[c]	11.60 ± 0.08[a]	320.01 ± 0.03[b]
30	4.80 ± 0.01[b,c]	0.212 ± 0.000[c]	11.00 ± 0.04[b]	312.21 ± 0.03[c]
45	4.80 ± 0.00[b,c]	0.220 ± 0.000[b]	10.40 ± 0.06[c]	296.60 ± 0.01[d]
60	4.79 ± 0.01[b,c]	0.228 ± 0.000[a]	9.50 ± 0.00[d]	288.80 ± 0.03[e]
75	4.79 ± 0.00[b,c]	0.232 ± 0.000[a]	8.90 ± 0.14[e]	280.97 ± 0.03[f]
90	4.78 ± 0.00[c]	0.232 ± 0.000[a]	8.40 ± 0.00[f]	265.36 ± 0.01[g]
105	4.78 ± 0.00[c]	0.232 ± 0.000[a]	7.80 ± 0.07[g]	249.75 ± 0.03[h]
120	4.78 ± 0.00[c]	0.232 ± 0.000[a]	7.77 ± 0.01[g]	241.95 ± 0.01[i]

Means ± standard deviations followed by the same lowercase letter on a line for a parameter are not significantly different at the 5% threshold according to Duncan's test

Table 9 Changes in pH, titratable acidity, soluble solids, and vitamin C during clarification of cashew apple juice with mixture 2

Clarification time, min	Parameter			
	pH	Titratable acidity, g/100 mL	Refractometric dry extract, °Brix	Vitamin C, mg/100 mL
0	4.87 ± 0.03[a]	0.208 ± 0.000[e]	12.00 ± 0.00[a]	327.82 ± 0.00[a]
15	4.80 ± 0.03[b]	0.212 ± 0.000[d,e]	11.60 ± 0.03[b]	320.01 ± 0.03[b]
30	4.80 ± 0.01[b]	0.216 ± 0.000[d]	11.00 ± 0.03[c]	312.21 ± 0.03[c]
45	4.79 ± 0.01[b]	0.224 ± 0.000[c]	10.20 ± 0.01[d]	294.55 ± 0.01[d]
60	4.79 ± 0.00[b]	0.232 ± 0.000[b]	9.00 ± 0.03[e]	286.66 ± 0.03[e]
75	4.78 ± 0.01[b]	0.240 ± 0.000[a]	8.40 ± 0.03[f]	279.47 ± 0.01[f]
90	4.77 ± 0.00[b]	0.240 ± 0.000[a]	8.00 ± 0.00[g]	273.17 ± 0.03[g]
105	4.77 ± 0.00[b]	0.244 ± 0.000[a]	7.79 ± 0.01[h]	257.56 ± 0.01[h]
120	4.77 ± 0.00[b]	0.244 ± 0.000[a]	7.77 ± 0.00[h]	241.74 ± 0.03[i]

Means ± standard deviations followed by the same lowercase letter on a line for a parameter are not significantly different at the 5% threshold according to Duncan's test

vitamin C levels ($P < 5\%$). However, there was no significant difference in the pH values during the clarification time intervals of 30 to 75 min, or 90 to 120 min of treatment. In particular, the initial pH of 4.87 ± 0.03 decreased to the value of 4.82 ± 0.03 after 15 min of treatment. This value hardly varied, reaching 4.79 ± 0.00 after 75 min of treatment. From 90 to 120 min, the pH value stabilized at 4.78. Furthermore, the soluble solids of the raw juice varied very little during the first half hour of clarification. However, after 45 min of treatment, the soluble solids decreased from 10.4 ± 0.28 to 7.77 ± 0.01°Brix at 120 min. Finally, the vitamin C content decreased according to the clarification time. After half an hour of clarification, it decreased from 327.82 ± 0.00 to 312.21 ± 0.03 mg/100 mL. It then continued to decrease to reach 241.95 ± 0.01 mg/100 mL. On the other hand, the titratable acidity of cashew apple juice (0.208 ± 0.000 g/100 mL) increased during the treatment (Table 8) to reach 0.232 ± 0.000 g/100 mL after 75 min. This value remained stable until the end of the treatment.

pH, titratable acidity, soluble solids, and vitamin C of cashew apple juice clarified with mixture 2. Changes in the parameters of cashew apple juice clarified with mixture 2 (0.174 mg/mL pectin methylesterase + 0.176 mg/mL polygalacturonase) are presented in Table 9. As can be seen, the pH, soluble solids, and vitamin C decreased during the clarification process, while the titratable acidity increased. In particular, the initial pH of 4.87 ± 0.03 decreased to 4.77 ± 0.00 after 90 min of clarification, where it remained stable for up to 120 min. Furthermore, the vitamin C content of the raw juice (327.82 ± 0.03 mg/100 mL) decreased with the duration of the clarification treatment to reach 241.74 ± 0.03 mg/100 mL after 120 min. The soluble dry extract of the raw juice decreased from 12.00 ± 0.00 to 7.77 ± 0.00°Brix at the end of clarification. Statistical analysis revealed no significant difference between the pH values after 15 min of the treatment but it showed a significant difference between the pH values at different clarification times and the control juice. The analysis also showed a significant difference between the contents of soluble solids and vitamin C. However, no significant difference was found for titratable acidity after 75 min of clarification.

pH, titratable acidity, soluble solids, and vitamin C of cashew apple juice clarified with mixture 3 consisting of pectin methylesterase (0.261 mg/mL) and polygalacturonase (0.088 mg/mL). The clarification of cashew apple juice with mixture 3 (0.261 mg/mL pectin methylesterase + 0.088 mg/mL polygalacturonase) caused

a reduction in the initial physicochemical parameters, except for titratable acidity (Table 10). This reduction was accentuated over the clarification time. Indeed, the initial vitamin C content of 327.82 ± 0.00 mg/100 mL decreased to 312.21 ± 0.03 mg/100 mL after 15 min. It then continued to decrease reaching 234.15 ± 0.03 mg/100 mL after 120 min. The pH values decreased to stabilize at 4.77 after 75 min of clarification. Statistical analysis revealed no significant difference between the pH values after 15 min of clarification. The content of soluble solids in the juice also decreased with clarification time. At the beginning of the treatment, its variation was low but after 30 min, it became more noticeable. The titratable acidity, however, increased from 0.208 to 0.24 g/100 mL after 75 min of the treatment. This value remained stable until the end of clarification. Statistical analysis showed a significant difference between the contents of vitamin C and soluble solids during the clarification process.

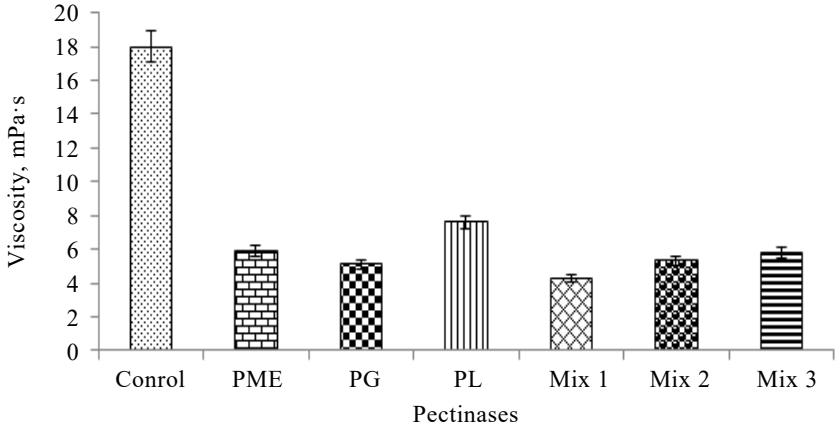
Viscosity. The raw cashew apple juice had a viscosity of 18 cP (18 mPa·s), which decreased after its clarification with the enzymes (pectin methylesterase, polygalacturonase, and pectin lyase) (Fig. 4). In particular, polygalacturonase produced a lower viscosity than the other two enzymes. Furthermore, mixture 1 (0.264 mg/mL polygalacturonase and 0.087 mg/mL pectin methylesterase) reduced the viscosity to 4.3 mPa·s. This viscosity value was lower than that produced by the other two mixtures. Indeed, the clarification treatment using this mixture resulted in a 76% reduction in the initial viscosity.

Clarification is a very important process in the juice industry as it improves the product's acceptability. In this study, we tested the effect of pectinases isolated, and partially purified, from the epicarp of papaya cultivar Solo 8 on the turbidity of cashew apple juice. We found that the use of pectin methylesterase, polygalacturonase, and pectin lyase reduced the viscosity of the juice by 67, 72, and 59%, respectively. In modern fruit juice manufacturing, enzymes (pectinases, hemicellulases, cellulases, amylases) should be used to optimize the process. The main objectives are to increase the extraction of juice from raw materials; improve the processing efficiency; and generate a final product that is clear and visually attractive to the consumer [9]. The transmittances at 660, 440, and 420, which are excellent indices of clarity, color, and browning, made it possible to conduct the enzymatic clarification of cashew apple juice [9, 26, 27].

Table 10 Changes in pH, titratable acidity, soluble solids, and vitamin C during clarification of cashew apple juice with mixture 3

Clarification time, min	Parameter			
	pH	Titratable acidity, g/100 mL	Refractometric dry extract, °Brix	Vitamin C, mg/100 mL
0	4.87 ± 0.03^{a}	0.208 ± 0.000^{e}	12.00 ± 0.00^{a}	327.82 ± 0.00^{a}
15	4.80 ± 0.03^{b}	0.212 ± 0.000^{d,e}	11.60 ± 0.03^{b}	320.01 ± 0.03^{b}
30	4.80 ± 0.01^{b}	0.216 ± 0.000^{d}	11.00 ± 0.03^{c}	312.21 ± 0.03^{c}
45	4.79 ± 0.01^{b}	0.224 ± 0.000^{c}	10.20 ± 0.01^{d}	294.55 ± 0.01^{d}
60	4.79 ± 0.00^{b}	0.232 ± 0.000^{b}	9.00 ± 0.03^{e}	286.66 ± 0.03^{e}
75	4.78 ± 0.01^{b}	0.240 ± 0.000^{a}	8.40 ± 0.03^{f}	279.47 ± 0.01^{f}
90	4.77 ± 0.00^{b}	0.240 ± 0.000^{a}	8.00 ± 0.00^{g}	273.17 ± 0.03^{g}
105	4.77 ± 0.00^{b}	0.244 ± 0.000^{a}	7.79 ± 0.01^{h}	257.56 ± 0.01^{h}
120	4.77 ± 0.00^{b}	0.244 ± 0.000^{a}	7.77 ± 0.00^{h}	241.74 ± 0.03^{i}

Means ± standard deviations followed by the same lowercase letter on a line for a parameter are not significantly different at the 5% threshold according to Duncan's test



PME – Pectin methylesterase
PG – Polygalacturonase
PL – Pectin lyase
Mix 1 – PME (0.087 mg/mL) + PG (0.264 mg/mL)
Mix 2 – PME (0.174 mg/mL) + PG (0.176 mg/mL)
Mix 3 – PME (0.261 mg/mL) + PG (0.088 mg/mL)

Figure 4 Viscosity of cashew apple juice clarified with pectinases

To obtain visual clarity, the juice needs to be completely depectinized by adding pectinases. In particular, partially purified pectin methylesterase, polygalacturonase, and pectin lyase required concentrations of 0.034, 0.028, and 0.008 mg/mL, respectively, to initiate clarification. The use of these enzymes could be explained by their reaction mechanism. Indeed, pectin lyases require a lower concentration because they act on pectins, oligomers, and polymers of galacturonic acid by catalyzing the breakage between two galacturonic acid units by a β-elimination mechanism [28]. In addition, only pectin lyases are able to degrade pectins without the prior action of other enzymes [29, 30]. This low concentration required for pectin lyase could also be due to the satisfactory purity of this enzyme compared to the other two enzymes (pectin methylesterase and polygalacturonase), which were partially purified.

The duration and temperature of heat treatments affect the clarity, color, browning index, brix, pH, titratable acidity, viscosity, and vitamin C content of the juice. The use of pectinases increases the clarity of juices during processing. Generally, pectinases are added to cashew apple juice to hydrolyze colloids. It is well known that pectin is the main cause of opalescence of the juice [31, 32]. Indeed, interactions between the negatively charged sites of demethylated pectin and divalent ions (Ca^{2+} and Mg^{2+}) lead to the formation of insoluble pectic salts.

In the clarification experiments using partially purified pectinases extracted from papaya epicarp, polygalacturonase (PG) showed a greater effect on the reduction of cashew apple juice turbidity than the other enzymatic fractions. This higher efficiency can be explained by the structural characteristics of pectic polysaccharides present in cashew apple, which are mainly composed of homogalacturonan regions susceptible to hydrolysis by polygalacturonase. Recent studies have highlighted that the degradation of pectic substances by polygalacturonase promotes the breakdown of the pectin network, facilitating the aggregation and sedimentation of suspended particles and consequently improving juice clarity [33, 34].

Furthermore, the pectinases added for clarification caused the hydrolysis of pectins, which are mainly responsible for the cloudiness of cashew apple juice. Also, we found that the clarity of the juice increased over time and stabilized thereafter. This finding is consistent with the results of Sharma *et al.* [35]. According to them, the increase in juice clarity with incubation time reflects the progressive hydrolysis of pectic polysaccharides by pectinases. As the enzyme–substrate interaction proceeds, the pectin network is disrupted, reducing colloidal stability and facilitating the sedimentation of suspended particles. Once most of the accessible pectin has been hydrolyzed, further incubation has little effect on juice clarity, resulting in a stabilization phase.

During the clarification of cashew apple juice, its color intensity decreased by almost half after 60 min. Thus, the juice was neither too pale nor too dark. To be more competitive on the market, the color of the juice must be an effective means of attracting the consumer [36]. The decrease in the yellow color intensity of cashew apple juice could be explained by the destruction of carotenoids responsible for the yellow color. Indeed, carotenoids are molecules sensitive to oxygen, light, acidity, metals, and heat [37]. However, the enzymatic clarification tests of cashew apple juice were carried out in a lit laboratory in the presence of oxygen from the air. In contrast, high-temperature processing has been widely reported to promote non-enzymatic browning in fruit juices through ascorbic acid degradation, 5-hydroxymethylfurfural (5-HMF) formation, and Maillard-type reactions, leading to increased color intensity. Therefore, the discrepancy between our findings and those reported for thermally processed cashew apple juice is most likely due to the absence of severe heat treatment in the present study [38].

The low viscosity of the juice clarified with polygalacturonase is a good indicator of this enzyme's effectiveness. This decrease in viscosity has also been highlighted by Ninga *et al.* [39] and Falcão *et al.* [40]. For these authors, the depolymerization of pectin reduces its ability to keep particles in suspension by causing their precipitation. This process causes a reduction in the viscosity of the juice [41]. However, the three enzymes used in our study showed different results in clarifying cashew apple juice. In particular, pectin methylesterase, polygalacturonase, and pectin lyase decreased the viscosity of the raw juice by 67, 72, and 59%, respectively. Although reducing viscosity, pectin methylesterase should be used with caution because its action generates methanol, which is toxic.

The decrease in pH and the increase in titratable acidity during the enzymatic clarification of cashew apple juice could be explained by the presence of organic acids in the medium. Indeed, the hydrolysis of pectin by pectinases leads to the formation of galacturonic acids. Our results corroborate those of Nguyen *et al.* [42]. These authors also showed that the pH of clarified apple juice decreases, while its acidity increases during clarification.

The decrease in soluble solids from 12 to 7.76°Brix in all the treatments was due to the loss of suspended particles. Indeed, after the action of pectinases the juice is centrifuged to remove its pellet. Our results are contrary to those of Sharma *et al.* [35], who reported an increase in soluble solids during the clarification of cloudy fruit juices. This difference could be explained by the juice extraction protocol and the state of maturity of the fruit used for juice production.

Finally, the vitamin C content also decreased during the clarification. This decrease was more pronounced with higher heating time and the loss of vitamin C was due to its thermolability. Our results were consistent with those of Nguyen *et al.* [42], who studied the clarification of apple juice by pectinases.

Of all the combinations tested, the most effective was mixture 1, consisting of pectin methylesterase (0.087 mg/mL) and polygalacturonase (0.264 mg/mL). It re-

duced the viscosity of raw cashew apple juice (18 mPa·s) by more than 76%, while increasing its clarity by more than half. This performance of mixture 1 could be explained by the synergistic action of the two enzymes on natural pectins. Indeed, pectin methylesterase creates demethoxylated sequences allowing hydrolysis by polygalacturonase. Our findings agree with those Flores-Fernández *et al.* [43], Padma *et al*. [44] and Lhamo *et al*. [45]. However, the use of pectin methylesterase in this combination could be a limiting factor for its application because its action generates methanol, which is a toxic product.

CONCLUSION

The partially purified pectinases from the crude epicarp extract of papaya cultivar Solo 8 were effective in reducing the viscosity of cashew apple juice. Of the three enzymes, polygalacturonase resulted in the greatest reduction of the juice's viscosity (72%). The combination of pectin methylesterase (0.087 mg/mL) and polygalacturonase (0.264 mg/mL) led to an even greater viscosity reduction of 76%, while also increasing the clarity of cloudy juice by half. Thus, these pectinases can be used to clarify local cloudy juices.

Our results open up new research avenues for a better use of papaya and cashew nuts, which are widely produced in Côte d'Ivoire. The scientific rigor of this study could be strengthened by measuring the residual concentration of sulfur dioxide and quantifying protopectin before and after enzymatic treatment. A preliminary mechanical clarification would also help optimize enzymatic efficiency and enhance the clarity of the results.

CONTRIBUTION

K.M.-D. Adingra and K. Tano participated in the original research and writing of the manuscript. N.J.P. Kouadio and K.M.-D. Adingra conducted the clarification tests. H.D. Gnahe and S. Soro performed the physicochemical evaluation. All the authors were involved in editing, revising, and proofreading of the manuscript. All the authors have read and approved the final version of the manuscript.

CONFLICT OF INTEREST

The authors declare that they have no conflict of interest which could hinder the publication of this article.

ACKNOWLEDGEMENTS

The authors thank the Romanian government for funding part of the research through the Eugen Ionescu scholarship.

REFERENCES

1. Gutiérrez-Paz C, Rodríguez-Moreno M-C, Hernández-Gómez M-S, Fernández-Trujillo JP. The cashew pseudofruit (Anacardium occidentale): Composition, processing effects on bioactive compounds and potential benefits for human health. Foods. 2024;13(2357):1–19. https://doi.org/10.3390/foods13152357
2. Ndiaye L, Charahabil MM, Niang L, Diouf A, Ayessou NC. Nutritional and energy value of cashew apples (*Anacardium occidental* L.) from Casamance (Senegal). Afrique Science Revue Internationale des Sciences et Technologie. 2022; 21(2):13–24. (In French)
3. Njoku OG, Babarinde GO, Ogunlakin GO, Ameen OA. Quality evaluation of cashew apple varieties using different drying methods. Asian Journal of Food Research and Nutrition. 2025;4(2):314–324. https://doi.org/10.9734/ajfrn/2025/v4i2247
4. Dansou X, Ouadja B, Baba G. Production and characterization of cashew apple powder. Asian Journal of Dairy and Food Research. 2023;42(3):392–397. https://doi.org/10.18805/ajdfr.DRF-316
5. Hamian EL, Kadji BRL, Kakou KE, Soro D, Abo K, *et al*. Production and physicochemical, biochemical profile of cashew apple powder from Côte d'Ivoire. World Journal of Advanced Research and Reviews. 2025;26(01): 1557–1565. https://doi.org/10.30574/wjarr.2025.26.1.0927
6. Gnagne A, Soro D, Ouattara YA, Koui EW, Koffi E. A literature review of cashew apple processing. African Journal of Food, Agriculture, Nutrition and Development. 2023;23(2):22452–22469. https://doi.org/10.18697/ajfand.117.20705
7. Sahie LBC, Soro D, Kone KY, Assidjo NE, Yao KB. Some processing steps and uses of cashew apples: a review. Food and Nutrition Sciences. 2023;14: 38-57. https://doi.org/10.4236/fns.2023.141004
8. Adou M, Tetchi FA, Adjouman YD, Amani N. Stabilization and sensory evaluation of cashew apple juice (*Anacardium occidentale* L.) from the northeast region in Côte d'Ivoire. Journal of Food Science and Nutrition Research. 2019; 2(2):108–127. https://doi.org/10.26502/jfsnr.2642-11000013
9. Danilov I, Vlajkov V, Šumić Z, Milić A, Horecki AT, *et al*. Valorization of strawberry juice production wastewater: Possibilities for polyphenols recovery and plant biostimulant production. Foods. 2024;13(3224):1–18. https://doi.org/10.3390/foods13203224
10. Pinto T, Vilela A, Cosme F. Chemical and sensory characteristics of fruit juice and fruit fermented beverages and their consumer acceptance. Beverages. 2022;8(2):33. https://doi.org/10.3390/beverages8020033
11. Detoni B, Sanches ACC, Maller A. Use of pectinases in juice clarification processes: A scoping review. Novel Techniques in Nutrition & Food Science. 2025;8(2):816–826. https://doi.org/10.31031/NTNF.2025.08.000685

12. Cosgrove DJ. Structure and growth of plant cell walls. Nature Reviews Molecular Cell Biology. 2024;25:340–358. https://doi.org/10.1038/s41580-023-00691-y

13. Aluko A, Makule E, Kassim N. Underutilized cashew apple fruit: Its utility and development as a source of nutrients and value added products in Tanzania. Current Research in Nutrition and Food Science. 2023;11(2):719–734. https://doi.org/10.12944/crnfsj.11.2.22

14. Ghinea C, Prisacaru AE, Leahu A. Physico-chemical and sensory quality of pasteurized apple juices extracted by blender and cold pressing juicer. Ovidius University Annals of Chemistry. 2022;33(1):84–93. https://doi.org/10.2478/auoc-2022-0012

15. Wang H, Yuan J, Chen L, Ban Z, Zheng Y, *et al*. Effects of fruit storage temperature and time on cloud stability of not-from-concentrated apple juice. Foods. 2022;11(17):2568. https://doi.org/10.3390/foods11172568

16. Molaee PM, Khorshidian N, Yousefi M, Zendeboodi F, Mirsaeedghazi H. Effect of membrane clarification on the physicochemical properties of fruit juices: A review. Iranian Journal of Chemistry and Chemical Engineering. 2022;41(10):3377–3390. https://doi.org/10.30492/IJCCE.2021.533304.4818

17. Kowalska M, Konopska J, Feszterová M, Zbikowska A, Kowalska B. Quality assessment of natural juices and consumer preferences in the range of citrus fruit juices. Applied Sciences. 2023;13(2):765. https://doi.org/10.3390/app13020765

18. Amin F, Mohsin A, Bhatti HN, Bilal M. Production, thermodynamic characterization and fruit juice quality improvement characteristics of an Exo-polygalacturonase from *Penicillium janczewskii*. Biochimica et Biophysica Acta – Proteins and Proteomics. 2020;1868(5):140379. https://doi.org/10.1016/j.bbapap.2020.140379

19. Adou M, Adjouman YD, Kouadio KO, Tetchi AF, Amani, N.G. Improvement of cashew apple juice (*Anacardium occidentale* L.) by association with passion fruit juice (*Passiflora edulis*). Food and Nutrition Sciences. 2021;12(7):787–804. https://doi.org/10.4236/fns.2021.127059

20. Satyannarayana KVV, Sandhya RSL, Vinoth KR. Clarification of citrus fruit juices using microfiltration technique equipped with indigenously developed novel ceramic membrane. Journal of Food Science and Technology. 2023;60:2001–2011. https://doi.org/10.1007/s13197-023-05734-y

21. Abdullah S, Karmakar S, Mishra S, Pradhan RC. Ultrafiltration of cashew apple juice using hollow fibers for shelf life extension: Process optimization, flux modelling and storage study. Journal of Food Measurement and Characterization. 2023;17:2182–2192. https://doi.org/10.1007/s11694-022-01790-8

22. Arikrishnan D, Keshav A. Pineapple juice clarification by continuous dead-end microfiltration using a low-cost ceramic membrane. Journal of Food Measurement and Characterization. 2023;17:863–881. https://doi.org/10.1007/s11694-022-01634-5

23. Adingra KMD, Hubert KK, Parfait KEJ, Constant YJ, Tano K. Partial purification and Characterization of two pectinases (Polygalacturonase and Pectin lyase) from Papaya Pericarp (*Carica papaya* cv. solo 8). International Journal of Current Microbiology and Applied Sciences. 2017;6(6):2729–2739. https://doi.org/10.20546/ijcmas.2017.606.326

24. Abdullah S, Pradhan R, Mishra S. Effect of cellulase and tannase on yield, ascorbic acid and other physicochemical properties of cashew apple juice. Fruits. 76(2):51–60. https://doi.org/10.17660/th2021/76.2.1

25. Anuradha K, Naga PP, Venkateshwar S, Reddy G. Mango juice clarification with polygalacturonase produced by *Aspergillus awamori* MTCC 9166-Optimization of conditions. International Food Research Journal. 2016;23(1):147–151.

26. Aponso MMW, Marapana RAUJ, Manawaduge R. Physicochemical analysis of grape juice from Israel blue (*Vitis vinifera* L.) grape cultivar under different processing conditions and a comparison with Red Globe and Michele Palieri grape varieties. Journal of Pharmacognosy and Phytochemistry. 2017;6(3):381–385.

27. Demircan B, Velioglu YS. Control of browning, enzyme activity, and quality in stored fresh-cut fruit salads through chitosan coating enriched with bergamot juice powder. Foods 2024;13(147):1–21. https://doi.org/10.3390/foods13010147

28. Zheng L, Xu Y, Li Q, Zhu B. Pectinolytic lyases: a comprehensive review of sources, category, property, structure, and catalytic mechanism of pectate lyases and pectin lyases. Bioresources Bioprocessing. 2021;8(1):79. https://doi.org/10.1186/s40643-021-00432-z

29. Yadav K, Dwivedi S, Gupta S, Tanveer A, Yadav S *et al*. Recent insights into microbial pectin lyases: A review. Process Biochemistry. 2023;134(1):199–217.

30. Suberkropp K. Pectin-degrading enzymes: polygalacturonase and pectin lyase. In: Bärlocher F, Gessner M, Graça M, editors. Methods to Study Litter Decomposition. Springer, Cham. 2020;419–424. https://doi.org/10.1007/978-3-030-30515-4_45

31. Aghajanzadeh S, Ziaiifar AM. A review of pectin methylesterase inactivation in citrus juice during pasteurization, Trends in Food Science & Technology. 2018;71:1–12. https://doi.org/10.1016/j.procbio.2023.10.008

32. Amobonye A, t Bhagwat P, Ruzengwe FM, Singh S, Pillai S. Pear juice clarification using polygalacturonase from *Beauveria bassiana*: Effects on rheological, antioxidant and quality properties. Polish Journal of Food and Nutrition Sciences. 2022;72(1): 57–67. https://doi.org/10.31883/pjfns/145704

33. Pui LP, Saleena LAK. Enzyme-aided treatment of fruit juice: A review. Food Processing: Techniques and Technology. 2023;53(1):38–48. https://doi.org/10.21603/2074-9414-2023-1-2413

34. Nighojkar A, Patidar MK, Nighojkar S. Pectinases: Production and applications for fruit juice beverages. Processing and Sustainability of Beverages. 2019;2:235–273. https://doi.org/10.1016/B978-0-12-815259-1.00008-2

35. Sharma HP, Patel H, Sugandha. Enzymatic added extraction and clarification of fruit juices–A review. Critical Reviews in Food Science and Nutrition. 2017;57(6), 1215–1227. https://doi.org/10.1080/10408398.2014.977434

36. Dey S, Nagababu BH. Applications of food color and bio-preservatives in the food and its effect on the human health. Food Chemistry Advances. 2022;1:100019. https://doi.org/10.1016/j.focha.2022.100019

37. González-Peña MA, Ortega-Regules AE, Anaya de Parrodi C, Lozada-Ramírez JD. Chemistry, occurrence, properties, applications, and encapsulation of carotenoids-A Review. Plants. 2023;12(313):1-23. https://doi.org/10.3390/plants 12020313

38. D. Buvé C, Pham HTT, Hendrickx M, Grauwet T, Van Loey A. Reaction pathways and factors influencing non-enzymatic browning in shelf-stable fruit juices during storage. Comprehensive Reviews in Food Science and Food Safety. 2021;20:5698–5721.https://doi.org/10.1111/1541-4337.12850

39. Ninga KA, Carly Desobgo ZS, De S, Nso EJ. Pectinase hydrolysis of guava pulp: Effect on the physicochemical characteristics of its juice. Heliyon. 2021;7(10):e08141. https://doi.org/10.1016/j.heliyon.2021.e08141

40. Falcão LdS, Monteiro TEdA, do Amaral TS, Azevedo SCM, Batista BN, *et al.* Optimized production of fungal polygalacturonase using Cupuaçu (*Theobroma grandiflorum*) peel as substrate and its effect on clarification of Cupuaçu juice. Beverages. 2025;11(6):1–16. https://doi.org/10.3390/beverages11010006

41. Patel VB, Chatterjee S, Dhoble AS. A review on pectinase properties, application in juice clarification, and membranes as immobilization support. Journal of Food Science. 2022;87(8):3338–3354. https://doi.org/10.1111/1750-3841.16233

42. Nguyen TH, Nguyen T, Nguyen TMA, Nguyen TH, Nguyen VH, *et al*. Effect of pretreatment methods on juice extraction yield and nutritional composition of cashew apple (*Anacardium Occidentale* L.) harvested from Binh Phuoc (Vietnam). Current Research in Nutrition and Food Science. 2024;12(1):115–124. https://doi.org/10.12944/ crnfsj.12.1.09

43. Flores-Fernández CN, Cárdenas-Fernández M, Lye GJ, Ward JM. Synergistic action of thermophilic pectinases for pectin bioconversion into D-galacturonic acid. Enzyme and Microbial Technology. 2022;160(110071):1–10. https:// doi.org/10.1016/j.enzmictec.2022.110071

44. Padma PN, Sravani P, Mishra P, Sneha N, Anuradha K. Synergistic effect of multiple enzymes on apple juice clarification. Indian Journal of Science and Technology. 2017;10(10):1–5. https://doi.org/10.17485/ijst/2017/v10i10/107716

45. Lhamo S, Tobgay S, Maya D, Deki D. Study on Clarification of Apple Juice using Enzymes. Bhutanese Journal of Agriculture. 2022;5(1):183–195. https://doi.org/10.55925/btagr.22.5115

Additional information about the authors

Kouassi M.-D. Adingra ORCID 0009-0006-5614-1795
Hermann D. Gnahe ORCID 0009-0009-4332-8309
Soguimondenin Soro ORCID 0009-0005-3026-7771
N'guessan J. P. Kouadio ORCID 0000-0003-0512-0135
Kablan Tano ORCID 0000-0003-0198-3638

Foods and Raw Materials. 2027;15(2)

ISSN 2308-4057 (Print)
ISSN 2310-9599 (Online)

Research Article
Open Access

Available online at http://jfrm.ru/en
https://doi.org/10.21603/2308-4057-2027-2-721
https://elibrary.ru/ASFEMU

Potential of *Sargassum* sp. in broiler chicken feed

Lorena C. Vivas, Anthony D. Mendoza, Moraiza J. Casado, Neyo C. Pérez, Marlon F. Brazón, David S. Coll, Alberto J. Quintero*

Venezuelan Institute for Scientific Research, San Antonio de Los Altos, Venezuela

* e-mail: albertojosequinteroaraque@gmail.com

Received 26.08.2025; Revised 20.11.2025; Accepted 03.02.2026; Published online 02.09.2026

Abstract:
This study investigated the impact of the diet of broiler chickens 10% *Sargassum* sp. on their productive performance, gut health, and immune status.
The study was conducted in Maracay, Venezuela, and involved 264 Ross broilers distributed between two treatments (control and 10% *Sargassum* sp.) over three phases (Pre-starter, Starter, and Finisher). A one-way Analysis of Variance design was used, with three replicates of 44 birds.
The inclusion of *Sargassum* sp. did not significantly affect the final body weight ($p > 0.05$) (2759.34 vs. 2743.88 g for the control). However, the *Sargassum* sp. diet demonstrated two noteworthy benefits: it drastically improved the feed conversion ratio in all the phases (e.g., 1.07 vs. 1.53 in the Finisher) and considerably reduced mortality in the Pre-starter phase (6.82 vs. 20.25% for the control). The blood analysis demonstrated a positive hypocholesterolemic effect, with the *Sargassum* sp. treatment normalizing cholesterol levels and potentially reducing total lipids. However, the drinking water analysis revealed some quality issues (no residual chlorine, high nitrate levels), suggesting a high-stress environment and its possible influence on the overall health and performance results.
The inclusion of 10% *Sargassum* sp. in the broiler diet improved feed efficiency and early viability in broilers, although its growth-promoting effects may be limited by antinutritional factors (high ash) at this inclusion level.

Keywords: *Sargassum* sp., broilers, productivity, hematology, blood biochemistry, macroalgae, water

Funding: The research was supported by the National Fund for Science, Technology and Innovation (Fonacit) (No. 249053).

Please cite this article in press as: Vivas LC, Mendoza AD, Casado MJ, Pérez NC, Brazón MF, *et al.* Potential of *Sargassum* sp. in broiler chicken feed. Foods and Raw Materials. 2027;15(2):370–378. https://doi.org/10.21603/2308-4057-2027-2-721

INTRODUCTION

The global poultry industry faces a constant challenge in balancing the quality and cost of feed rations, which typically account for 60 to 70% of total operating expenses [1]. These formulations are dominated by traditional ingredients, primarily soybean meal and corn, as well as fishmeal. However, reliance on these products makes farmers vulnerable to price volatility and competition for resources on the global market. Furthermore, there is growing concern about the sustainability of these ingredients, linked to deforestation (soybeans) and overfishing (fishmeal).

At the same time, the poultry industry is undergoing a health transformation. The ban on, and growing public concern about, the use of antibiotic growth promoters in animal feed to increase bacterial resistance have created an urgent need for alternatives. This has spurred research into functional additives (eubiotics) that not only provide nutrients but also actively promote gut health and immunity in poultry. In this context, marine resources, specifically macroalgae, have emerged as a promising and sustainable alternative [1–4].

Macroalgae as a sustainable functional resource. Macroalgae, commonly known as seaweed, are a naturally abundant biomass. They are taxonomically classified into *Phaeophyceae* (brown), *Chlorophyceae* (green), and *Rhodophyceae* (red) [1]. The genus *Sargassum* (brown algae) is particularly interesting. These algae are rich in protein, minerals, vitamins, polysaccharides, and polyphenols [3]. The use of locally available natural resources such as macroalgae contributes significantly to food security and the sustainability of production systems [2]. In addition to their nutritional potential, macroalgae play a critical role in carbon dioxide capture and nutrient cycling in the marine ecosystem.

Brown seaweed and its derivatives are used as structural modifiers, antioxidants, preservatives, moisture-retaining agents, and sources of vitamins and minerals

Copyright © 2026, Vivas *et al.* This is an open access article distributed under the terms of the Creative Commons Attribution 4.0 International License (https://creativecommons.org/licenses/by/4.0/), allowing third parties to copy and redistribute the material in any medium or format and to remix, transform, and build upon the material for any purpose, even commercially, provided the original work is properly cited and states its license.

in the development of functional and preventive food products. They are also used as ingredients in meat, dairy, bakery and flour products, as well as in food additives and beverages, to provide potential health benefits and essential nutrients. Studies have proven the functional effectiveness of food products containing brown seaweed and its derivatives. The incorporation of seaweed components into functional foods could contribute to global food security [5].

The species of the genus *Sargassum*, which inhabit a wide range of habitats, can form large floating mats adrift in the open ocean. The massive recurrence of *Sargassum* in the Atlantic has generated a significant environmental and socioeconomic challenge. This challenge spurs efforts to transform this excessive biomass into an opportunity for various sectors, including animal feed. These algae utilize carbon dioxide and other nutrients, such as nitrogen and phosphorus, for their growth. Furthermore, they possess the capacity to absorb various pollutants from the aquatic environment.

Nutritional and biochemical profile of *Sargassum* sp. Seaweed is a complex and concentrated source of crucial nutrients, including proteins, minerals, vitamins, and carbohydrates [1]. Chemical analysis reveals that the crude protein content in seaweed can vary widely (from 9.07 to 63.63%), suggesting that it can partially replace imported protein sources in poultry feed [6].

A comparative analysis of the nutritional composition of different macroalgae has revealed specific characteristics for *Sargassum*. For example, *Sargassum wightii* Greville ex J. Agardh has a comparatively higher content of crude fiber, ether extract, acid-insoluble ash, and calcium, compared to *Gracilaria corticata* (J. Agardh) J. Agardh, 1852 and *Ulva lactuca* Linnaeus, 1753. In contrast, species such as *G. corticata* tend to have a higher content of crude protein and gross energy [7].

Furthermore, *Sargassum* species are notably rich in beta-carotene and various vitamins. Supplementing the base feed with *Sargassum* powder (at levels of 1 to 4%) has been shown to provide a greater amount of essential amino acids, long-chain fatty acids, and minerals necessary for poultry growth, compared to the diet without supplementation [8]. The lipid profile of algae includes fatty acid derivatives, terpenoids, and aliphatic hydrocarbons, many of which have a functional impact on animal physiology [7].

Functional effects and modulation of health. Scientific interest in applying biotechnology to nutrition focuses on the potential of macroalgae to act as nutraceuticals or functional additives. This functionality stems from the presence of bioactive molecules that exhibit antioxidant, anti-inflammatory, antifungal, and antimicrobial properties. These bioactive components possess remarkable medicinal properties, including anti-inflammatory, cholesterol-lowering, and hepatoprotective effects [7].

The dietary inclusion of brown algae has been shown to improve the health and physiological state of broilers, namely:

– immune response. Supplementation with algae such as *Sargassum* sp., *Spirulina* sp., or *Gracilaria* sp. can positively modulate the immune status of broiler chickens [9]. Specifically, supplementation with 0.13% of brown algae (*S. wightii*) has been shown to significantly improve cell-mediated immune response and increase the weight of lymphoid organs (thymus and spleen), the key elements in the body defense [3]. A study with *Sargassum siliquastrum* (Mertens ex Turner) C. Agardh 1820 in Japanese quail also reported a significant improvement in immune response [10];
– lipid metabolism (a positive cholesterol-lowering effect). In specific trials, dietary supplementation with *Sargassum muticum* extract has been shown to significantly reduce total cholesterol in broiler chickens [11, 12].

Zootechnical challenges and antinutritional factors. Despite the clear immunological and metabolic potential of macroalgae, their incorporation into monogastric diets presents significant challenges, mainly due to the presence of antinutritional factors. The main of such factors in the brown algae *Sargassum* sp. is their high alginate content [13]. Alginates are polysaccharides that can increase the viscosity of intestinal contents, hindering the digestion and absorption of nutrients and binding to them, which can potentially reduce feed efficiency.

This challenge highlights the need to optimize the inclusion and processing of macroalgae to ensure maximum nutrient assimilation. For example, processing methods were investigated to reduce the alginate content in *Sargassum binderi* Sonder ex J. Agardh, 1848 for use in laying hen feed [13]. Similarly, other authors reduced the salt content in *Sargassum crassifolium* J. Agardh, 1848 meal by immersion, achieving an inclusion rate of up to 18% without adverse effects on internal organs [14].

Environmental and food safety risk. A crucial aspect of food traceability and safety is the ability of algae to absorb and concentrate contaminants from the aquatic environment. The main concern is the bioaccumulation of heavy metals (such as arsenic) and, to a lesser extent, organic contaminants. Furthermore, the presence of naturally occurring radioactive elements such as lead and polonium has been reported in algae [2]. Although *Sargassum* has been considered as antinutrient-free in some contexts, the risk of heavy metal contamination is a critical consideration that requires strict quality control and monitoring of the harvesting source. The occurrence of harmful algal blooms also poses a risk to the safety of using algae in animal feed [2].

Evidence of productive performance. Scientific literature presents a mixed picture of using algae at different inclusion levels. A systematic review and meta-analysis confirmed the strong interest in using seaweed as a functional ingredient in poultry feed [15]. Regarding production outcomes, there is conflicting evidence, although the immunological and lipid metabolism benefits are well documented. For example, in a trial with broiler chickens, supplementation with 0.13% of brown algae (*S. wightii*) resulted in greater weight gain and a better feed conversion ratio [3]. In another study, *Sargassum*'s growth-promoting ability reached its maximum

effect at 2% inclusion, achieving a significantly greater weight gain compared to the control group [8]. The inclusion of up to 18% *S. crassifolium* or up to 2% (20 g/kg) algae mixtures, respectively, did not significantly affect the chickens' growth performance (daily weight gain and feed conversion ratio) or live weight, although the supplementation had a positive effect on their gastrointestinal ecology [14, 16].

Therefore, we aimed to evaluate the inclusion of 10% *Sargassum* sp. in the formulation of a balanced feed for broiler chickens, focusing on productive variables and blood parameters.

STUDY OBJECTS AND METHODS

Location and environmental conditions. The study was conducted at the Nicolino Ierrobueno agricultural production unit (Maracay, Aragua State, Venezuela). The average temperature at the study site was 30.3°C and the humidity was 57.5%.

Experimental design and bird management. A one-way Analysis of Variance (ANOVA) design was used, with two treatments, each consisting of 132 one-day-old Ross chicks divided into three replicates of 44 broilers, across three stages: Pre-starter (1–10 days), Starter (11–22 days), and Finisher (23–42 days). The chicks were raised in pens measuring 4.84 m² with rice husk bedding, as shown in Fig. 1. They were provided with water and feed ad libitum. During the Pre-starter stage, the broilers had heat lamps all day and in the Starter phase, only at night.

Dietary treatments. The control group received commercial feed, and the experimental group received commercial feed with 10% of the macroalgae *Sargassum* sp.

Feed and water analysis. The bromatological analysis of the raw materials and feed was carried out according to the official methods of analysis developed by the Association of Analytical Communities[1]. The quality of drinking water was evaluated in accordance with ISO 5667.

Productive variables and data collection. Weighing was performed on an HZ50002B CGoldenwall balance. Fifteen birds per treatment were weighed at various stages, namely on days 1, 4, 7, and 10 (Pre-starter); 14, 21, and 22 (Starter); and 28, 35, and 42 (Finisher). The feed offered but not consumed was weighed daily. We evaluated: initial body weight, final body weight, daily feed intake, daily weight gain, increased weight gain, feed conversion ratio, mortality, complete blood count, and blood biochemistry. The equations were as follows:

$$\text{DFI} = \frac{F_o - F_c}{\text{Total number of animals}} \quad (1)$$

where DFI is the daily feed intake, g; F_o is the feed offered, g; and F_c is the feed not consumed, g.

$$\text{IBW} = \text{FBW} - \text{IBW} \quad (2)$$

[1] AOAC. Official methods of analysis of the association of official analytical chemists. 20th ed. Washington: AOAC Inc., 2016.



a



b

Figure 1 Experimental facilities: a – experimental pens; b – pre-starter phase

where IWG is the increased weight gain, g; IBW is the initial body weight, g; and FBW is the final body weight, g.

$$\text{FCR} = \frac{Q_f}{W_g} \quad (3)$$

where FCR is the feed conversion ratio; Q_f is the quantity of feed consumed during a period, g; and W_g is the weight gain during the same period, g.

$$\%\ \text{Mortality} = \frac{\text{Total deaths} \times 100}{\text{Total population}} \quad (4)$$

Blood and biomarkers. Chicken blood was drawn by cardiac puncture. On day 1, a pooled sample was taken from the broiler chicken without any dietary intervention as a baseline value. From day 7 onward, the blood profile was monitored weekly (Fig. 2), with processing carried out according to ISO 15189:2022 (the quality of clinical laboratories).

Statistical analysis. The data were analyzed using the Statistical Product and Service Solutions (SPSS) software, IBM SPSS version 21. The following model was used to describe the diets' effects on the productive traits:

$$Yij = \mu + Ti + eij \quad (5)$$

where μ is the overall mean; *Ti* is the treatment effect (*i* = control, *Sargassum* sp.); and *eij* is the experimental error.

Mortality data, being binomial, were analyzed separately using the Chi-square (χ^2) test to determine the significance of differences between the treatments. The differences were considered statistically significant at $p < 0.05$.



Figure 2 Blood samples

Table 1 Proximate composition of *Sargassum* sp., %

Parameter	*Sargassum* sp.
Moisture	14.17
Protein	6.99
Fat	0.42
Ash	32.13
Fiber	10.60
Calcium	4.66
Phosphorus	0.09

Table 2 Proximate composition of the diets at various stages, %

Parameter	Pre-Starter		Starter		Finisher	
	Control	*Sargassum* sp.	Control	*Sargassum* sp.	Control	*Sargassum* sp.
Moisture	9.50	10.87	9.35	10.81	11.42	11.51
Protein	19.36	20.48	19.38	20.10	19.44	18.98
Fat	7.88	7.72	10.27	10.17	9.56	10.23
Ash	9.36	8.94	6.15	8.21	5.46	7.44
Fiber	2.42	2.90	2.27	2.89	2.68	2.87
Calcium	1.60	1.61	1.19	1.19	0.90	1.08
Phosphorus	0.68	0.65	0.60	0.60	0.62	0.58

Ethical considerations. In compliance with the ethical standards, we followed the institutional and national guidelines for the care and use of laboratory animals under the directives of the Bioethics Committee for Animal Research of the Venezuelan Institute for Scientific Research[2].

RESULTS AND DISCUSSION

Proximate composition of *Sargassum* sp. Table 1 shows the proximate analysis of the brown macroalgae *Sargassum* sp. This alga has high mineral, fiber, and protein contents. Its significant nutritional value makes it an important raw material for feed formulations in all three growth phases evaluated in chickens. Various authors obtained similar bromatological results, suggesting that this alga can partially substitute imported protein and other nutrient sources used for poultry feed [2, 12, 14].

Proximate composition of the diets. In the proximate composition profiles of the diets used (Table 2), slight variations were observed between the control and *Sargassum* sp. treatments for parameters such as moisture, protein, fat, ash, fiber, calcium, and phosphorus at different stages (Pre-starter, Starter, Finisher). These diets were isocaloric and isoprotein, consistent with the literature [3, 4, 9]. The protein content in the *Sargassum* sp. diet was slightly higher in the Pre-starter phase (20.48%) compared to the control (19.36%). This difference, although small, could contribute to better early development, considering that the seaweed is a complex source of crucial nutrients, including proteins [7–9]. However, at the Finisher stage, the protein content in the *Sargassum* sp. diet was slightly lower (18.98%) compared to the control (19.44%). These variations in protein could influence the daily weight gain and feed conversion efficiency. As can be seen in Fig. 3, the *Sargassum* sp. treatment showed a lower feed conversion ratio in the Pre-starter, Starter, and Finisher stages, suggesting better feed utilization efficiency.

Regarding fiber, the *Sargassum* sp. diet exhibited slightly higher values at all stages. This increase in fiber, although modest, could have implications for the intestinal health of the birds. Dietary fiber has been shown to influence intestinal morphology and cecal microbiota, which are essential for nutrient digestion and absorption [17, 18]. The presence of fiber in seaweed can contribute to a healthier intestinal environment, which in turn optimizes the overall performance of chickens.

The fat content in the *Sargassum* sp. diet was lower than in the control in the Pre-Starter (7.72 vs. 7.88) and Starter (10.17 vs. 10.27) stages. However, in the Finisher stage, the supplemented diet had a higher fat content than the control (10.23 vs. 9.56).

Regarding minerals, differences were observed in ash, calcium, and phosphorus contents. Ash, which represents the total mineral content, was generally higher in the *Sargassum* sp. diet in the Starter (8.21 vs. 6.15%) and Finisher (7.44 vs. 5.46%) stages. This is consistent with the studies highlighting seaweed as a rich source of minerals [7–9]. The calcium content in the *Sargassum* sp. diet was slightly higher in the Finisher stage (1.08 vs. 0.90%). The phosphorus content in the supplemented diet was lower than, or equal to, that in the control. The availability of these minerals is crucial for bone development and other physiological functions in broiler chickens.

Drinking water quality. The analysis of the quality of the drinking water used in the study (Table 3)

[2] Bioethics Committee for Animal Research of the Venezuelan Institute for Scientific Research. COBIANIM 2025-02; May 13, 2025.

Table 3 Drinking water quality

Parameter	Result	Regulated value
Residual free chlorine, mg/L Cl*	0	0.3–1.0 (provisionally accepted up to 3.0)
Turbidity, NTU	1.5	5
Apparent color, Pt/Co	5	15
pH*	6.322	6.5–8.5
Total iron, mg/L Fe	0.1	0.3 (provisionally accepted up to 1.0)
Manganese, mg/L Mn	0	0.5
Nitrite, mg/L NO_2	0.02	(Nitrite + Nitrate as N) < 10 mg/L
Nitrate, mg/L NO_3*	34.53	(Nitrite + Nitrate as N) < 10 mg/L (approx. 7.85 mg/L N from nitrate)
Chloride, mg/L Cl	17.85	300
Sulfate, mg/L SO_4	23.53	500
Total dissolved solids, mg/L	247.04	1,000

* – values found out of range

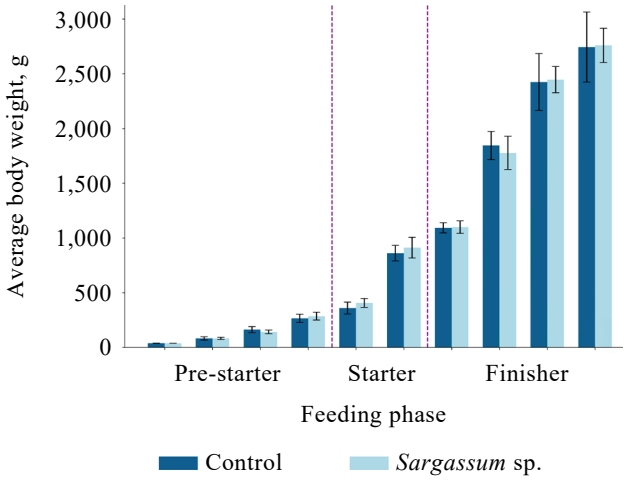


Figure 3 Changes in average body weight of broiler chickens by treatment

revealed that some values fell outside the regulated range, which is a critical factor to consider in poultry production.

Specifically, the free residual chlorine was 0 mg/L Cl, which is below the accepted range of 0.3–1.0 mg/L Cl. The absence of residual chlorine can compromise the microbiological quality of the water, since chlorine is a fundamental disinfectant for controlling the proliferation of microorganisms in poultry farm drinking water systems [19]. Poor microbiological water quality can increase the microbial load in the gastrointestinal tract of chickens, affecting their health and performance [17, 18]. The water pH (6.32) was also found to be outside the regulated range of 6.5–8.5. A slightly acidic pH, such as the one observed, can influence the palatability of the water and, consequently, the birds' water intake. Moreover, the water's pH can affect the efficacy of certain additives and overall intestinal health. For example, Mohamed *et al*. [20] demonstrated that ionized water with a slightly alkaline pH can improve the productive performance and physiological status of broiler chickens. Although we did not use ionized water, the deviation from the optimal pH could have influenced the results.

Another parameter outside the acceptable range was nitrate (34.53 mg/L NO_3), exceeding the reference value for the sum of nitrite + nitrate as N (< 10 mg/L). Elevated nitrate levels in drinking water can be harmful to avian health, affecting their performance and overall well-being. Water quality is a key component in maintaining the health, well-being, and productive performance of birds [20].

Productive parameters. Figure 3 illustrates the average body weight of the chickens over time. While a similar growth pattern was observed in both treatments, the *Sargassum* sp. treatment showed a slightly higher weight in the final stages of the study. The statistical analysis of daily weight gain in the broilers showed no significant differences ($p < 0.05$) between the control and *Sargassum* sp. treatments.

The improved weight in the experimental group is consistent with various studies that have reported *Sargassum* sp.'s positive effects on the nutritional value of feed, productive parameters, and the health of the birds [2, 3, 6, 7, 9, 11, 12].

Table 4 demonstrates the productive parameters evaluated at different stages of the study. In the Pre-starter phase, the *Sargassum* sp. treatment showed slightly higher final body weight (285.40 g) and increased weight gain (246.82 g) compared to the Control (265.80 and 227.16 g, respectively). This initial increase in yield suggests an early beneficial effect of the macroalgae. The daily feed intake was also notably higher in the *Sargassum* sp. treatment at this stage (43.41 vs. 25.11 g). Combined with greater weight gain, this translates into better efficiency. These results are consistent with those of Kumar [8], who conducted dietary supplementation with *Sargassum wightii* Greville ex J. Agardh. and observed improved feed intake and body weight gain in poultry. A particularly relevant finding in the Pre-starter phase was that the feed conversion ratio was significantly lower in the *Sargassum* sp. treatment (0.35 vs. 0.75). This indicates that the birds use feed more efficiently for growth, which is a crucial factor from an economic perspective in poultry production. These findings are consistent with those in previous studies [11, 12, 14, 16, 21], which reported a marked improvement in the feed conversion ratio.

Mortality was lower in the *Sargassum* sp. group in the Starter phase but higher in the Finisher phase, compared to the Control (3.03 vs. 6.06% and 5.30 vs. 0.00%, respectively). The Pre-starter phase demonstrated the significant decrease in mortality in the *Sargassum* sp. treatment (6.82%) compared to the Control (20.45%). This reduction in mortality is an important indicator of improved overall health and well-being of the broilers supplemented with *Sargassum* sp., especially during the most vulnerable phases of the chicks' life. Algae can be

Table 4 Productive parameters of broiler chickens at various stages

Parameter treatment	Pre-starter		Starter		Finisher	
	Control	*Sargassum* sp.	Control	*Sargassum* sp.	Control	*Sargassum* sp.
Initial body weight, g	38.64	38.58	265.80	285.40	1092.07	1099.27
Final body weight, g	265.80	285.40	1092.07	1099.27	2743.88	2759.34
Daily feed intake, g	25.11	43.41	98.95	73.75	214.90	214.68
Increased weight gain, g	227.16	246.82	826.27	813.87	1651.81	1660.08
Feed conversion ratio	0.75	0.35	0.99	0.77	1.53	1.07
Mortality, %	20.45	6.82	6.06	3.03	0.00	5.30

Table 5 Complete blood count of the control chickens

Parameter	Reference value	Days					
		7	14	21	28	35	42
Hemoglobin, g/dL	8.00–18.00	7.3*	11.6	10.4	9.7	8.0	10.4
Leucocytes, cell/μL or mm^3	4,000–40,000	29,751	90,871**	59,583**	21,450	31,949	45,117**
Segmented, %	20–50	51**	35	46	50	55**	46
Lymphocytes, %	45–75	47	62	50	46	42*	52
Eosinophils, %	0–2	1	1	2	2	1	1
Monocytes, %	2–10	1*	2	2	2	2	1*
Platelets, cells/μL or mm^3	15,000–35,000	2,000*	3,000*	3,000*	1,000*	2,000*	10,000*

* – below reference value; ** – above reference value. Values not determined

used as an alternative to antibiotics in broiler chickens to improve productive performance and reduce harmful pathogens in the gut [3–9]. The authors reported a positive effect of brown algae dietary supplementation on broiler performance and health. In another study, supplementation of broiler feed with algae such as *Sargassum* sp. improved the birds' cellular and humoral immune status, as well as their healthy intestinal microflora [2].

In the Starter and Finisher phases, the productive parameters such as the final body weight, daily feed intake, and increased weight gain were relatively similar between the two treatments. However, the feed conversion ratio in the *Sargassum* sp. group remained consistently lower than that of the Control group in the Starter phase (0.77 vs. 0.99) and in the Finisher phase (1.07 vs. 1.53). This reinforces the idea that the inclusion of *Sargassum* sp. in the diet improves feed efficiency throughout the entire production cycle, even though the differences in weight gain are not as pronounced in the later phases.

These findings align with the literature reporting positive effects of various seaweed species on broiler performance. For example, supplementation with *S. wightii* has been shown to increase weight gain and improve the feed conversion ratio [8]. Similarly, the inclusion of *Sargassum siliquastrum* (Mertens ex Turner) C. Agardh 1820 in the diet of Japanese quail has positively influenced its body weight [10]. The ability of algae to improve small intestine morphology and nutrient absorption, as observed with *Chaetomorpha linum* (O.F. Müller) Kützing, 1845 [21], resulted in improved weight gain, body weight, and feed conversion ratio. Furthermore, the use of brown seaweed meal such as *Sargassum crassifolium* J. Agardh, 1848 has been shown to positively affect growth performance, even at inclusion levels of 18% [14].

Complete blood count. The complete blood count results allowed for the evaluation of health and physiological status for both treatments throughout the study. In the Control group, hemoglobin levels were below the reference range on day 7 (7.3 g/dL), with leukocytes and platelets frequently above or below the reference values throughout the study (Table 5). Segmented neutrophils and lymphocytes also showed fluctuations outside the normal ranges on some days.

According to Table 6, hemoglobin in the *Sargassum* sp. group was also below the normal range on day 7 (6.5 g/dL). Leukocytes were above the reference range for almost the entire study and platelets were below the reference range throughout the trial. Segmented neutrophils and lymphocytes also showed variations relative to the reference values.

However, a study that evaluated the effect of dietary supplementation with *S. wightii* and *Gracilaria corticata* (J. Agardh) J. Agardh, 1852 on the blood profiles of TANUVAS Aseel chickens found these parameters within the reference ranges, namely hemoglobin, segmented neutrophils, lymphocytes, eosinophils, monocytes, and platelets [6]. Another study revealed that the addition of *Sargassum* sp., *Spirulina* sp., and *Gracilaria* sp. significantly reduced leukocytes [2]. The authors also reported that the *Sargassum* sp. treatment showed the same levels of heterophils and lymphocytes as in the control group, as well as the highest levels of monocytes among the treatments.

Blood biochemistry. Table 7 shows the blood biochemistry parameters of the control broilers. As can be seen, urea, alanine aminotransferase (ALT), aspartate aminotransferase (AST), total bilirubin, and total protein showed out-of-range values (mostly above) throughout the study. Blood glucose, creatinine, and calcium

Table 6 Complete blood count of *Sargassum* sp.-treated chickens

Parameter	Reference value	Days					
		7	14	21	28	35	42
Hemoglobin, g/dL	8.00–18.00	6.5*	9.1	9.4	9.3	8.9	9.5
Leucocytes, cell/µL or mm^3	4,000–40,000	53,788**	83,380**	64,030**	24,465	47,243**	29,836
Segmented, %	20–50	60**	61**	47	49	46	46
Lymphocytes, %	45–75	35*	36*	50	47	51	51
Eosinophils, %	0–2	2	1	1	2	2	2
Monocytes, %	2–10	3	2	2	2	1*	1*
Platelets, cells/µL or mm^3	15,000–35,000	–	2,000*	2,000*	1,000*	1,000*	1,000*

* – below reference value; ** – above reference value. Values not determined

Table 7 Blood biochemistry of the control chickens

Parameter	Reference value	Days						
		1	7	14	21	28	35	42
Blood glucose, mg/dL	200–370	244	248	321	225	195*	248	219
Urea, mg/dL	2.50–5.00	17.50**	5.70**	1.70*	3.90	11.30**	0.36*	8.10**
Creatinine, mg/dL	0.17–0.42	2.24**	0.42	0.29	0.38	0.14*	0.18	0.24
ALT, UI/L or U/L	20–50	252**	10*	138**	157**	150**	260**	321**
AST, UI/L or U/L	25–275	287**	8*	302**	169	165	270	313**
Total bilirubin, mg/dL	0.006–0.120	0.28**	0.78**	0.15**	0.69**	0.77**	0.46**	0.47**
Total protein, mg/dL	2.50–4.50	1.82*	2.59	2.06*	2.24*	2.83	2.43*	3.17
Blood calcium, mg/dL	8.00–11.00	9.96	9.47	10.33	10.59	8.07	11.97**	9.07
Cholesterol, mg/dL	87–192	249**	231**	167	142	174	141	89
Triglycerides, mg/dL	31–166	51	168**	31	102	124	67	14*

ALT – alanine aminotransferase; AST – aspartate aminotransferase; * – below reference value; ** – above reference value

Table 8 Blood biochemistry of *Sargassum* sp.-treated chickens

Parameter	Reference value	Days						
		1	7	14	21	28	35	42
Blood glucose, mg/dL	200–370	244	127*	129*	381**	262	254	381**
Urea, mg/dL	2.50–5.00	17.50**	2.6	7.70**	2.30*	12.10**	10.50**	6.80**
Creatinine, mg/dL	0.17–0.42	2.24**	0.02*	0.02*	0.40	0.21	0.45**	0.19
ALT, UI/L or U/L	20–50	252**	5*	25	125**	156**	241**	251**
AST, UI/L or U/L	25–275	287**	3*	274	175	187	222	254
Total bilirubin, mg/dL	0.006–0.12	0.28**	0.61**	2.01**	0.53**	1.76**	0.36**	0.99**
Total protein, g/dL	2.50–4.50	1.82*	0.8*	4.01	3.09	2.91	2.6	2.68
Blood calcium, mg/dL	8.00–11.00	9.96	0.99*	10.25	12.84**	10.32	10.69	10.49
Cholesterol, mg/dL	87–192	249**	211**	153	153	175	131	99
Triglycerides, mg/dL	31–166	51	175**	76	225**	199**	63	58

ALT – alanine aminotransferase; AST – aspartate aminotransferase; * – below reference value; ** – above reference value

levels fluctuated, with some values falling outside the reference ranges at several time points. Cholesterol and triglycerides showed mostly normal values, with some values falling outside the reference range.

The blood biochemistry parameters of the *Sargassum* sp.-treated broilers are presented in Table 8. As can be seen, blood glucose, urea, creatinine, ALT, and total bilirubin levels were outside the normal range, predominantly above the reference values. AST and total protein showed some deviations from the normal ranges. These results were similar to those reported in a study evaluating the supplementation with *S. wightii* and *G. corticata* in TANUVAS Aseel chickens. In particular, the authors recorded elevated uric acid and creatinine levels in all the treatments and a highly significant reduction in AST [6].

The heterophil, lymphocyte, eosinophil, and thrombocyte counts, as well as the heterophil-to-lymphocyte ratio, serum sodium, and uric acid are significant markers of physiological stress in broiler chickens subjected to crowding or feed deprivation stress [22]. It is noteworthy that blood calcium was below the reference range on day 7 (0.99 mg/dL) and above it on day 21 (12.84 mg/dL). These extreme fluctuations in calcium levels cause concern, as calcium is vital for bone health, nerve function, and muscle function in birds. Although

seaweed is rich in minerals, including calcium [7–9], the dynamics of its absorption and metabolism in the presence of *Sargassum* sp. could be complex, requiring further investigation.

Regarding lipids, cholesterol in the *Sargassum* sp. treatment was above the normal range on days 1 and 7, but then normalized. Triglycerides also showed elevated values on days 7, 21, and 28, and although peaks were observed, the overall trend toward normalization in the final stages could be a positive effect. The hypocholesterolemic effect of *Sargassum* sp. might be due to its active ingredients, such as saponins, hemicelluloses, mucilages, tannins, and pectins, which help reduce low-density lipoprotein cholesterol in the blood. In another study, the total lipid profile showed a significant reduction in total cholesterol in broiler chickens exposed to dietary supplementation with *Sargassum muticum* (Yendo) Fensholt, 1955 extract [12]. The inclusion of *S. muticum* and *Pulicaria undulata* (L.) C.A. Mey. extracts was also found to significantly decrease total plasma lipids and, at the same time, increase high-density lipoprotein cholesterol levels in broiler chickens [11].

CONCLUSIONS

The inclusion of the macroalgae *Sargassum* sp. into broiler diets demonstrates its potential as a functional additive. The proximate analysis confirmed its richness in minerals, with 32.13% ash and 10.6% fiber, positioning it as a valuable ingredient for feed formulation.

Throughout the three growth phases, the inclusion of 10% *Sargassum* sp. had a notable effect on the productive parameters. While the final body weight was not significantly different ($p > 0.05$), the supplemented diet significantly improved the feed conversion ratio and notably reduced early mortality. The improved feed conversion ratio, particularly significant in the Pre-starter phase (0.35 vs. 0.75), indicates that the broilers used the feed more efficiently. Furthermore, the significant reduction in mortality (6.82% in the *Sargassum* sp. group vs. 20.45% in the Control group) suggests a positive effect of the alga's bioactive agents on the overall well-being of the chickens, as supported by the literature.

Despite these positive results, it is important to consider the impact of drinking water quality, since out-of-range values for residual free chlorine, pH, and nitrates could have influenced the performance and health parameters of the broilers in both treatments.

While fluctuations in hematological and blood biochemistry parameters were evident in both treatments, the *Sargassum* sp. diet showed a trend toward normalizing cholesterol levels in the final stages, consistent with the hypocholesterolemic effect reported in other studies. However, extreme calcium variations were observed in the *Sargassum* sp. treatment, which warrants further investigation to understand the dynamics of this mineral's absorption and metabolism.

Finally, our findings support the feasibility of using *Sargassum* sp. as a nutritional supplement in broiler chicken feed. Its benefits in feed conversion efficiency and the reduction of early mortality highlight its potential to improve the sustainability and profitability of poultry production. However, they also suggest areas for future research, such as optimizing the dosage and gaining a deeper understanding of its physiological impact.

CONTRIBUTION

L.C. Vivas: research concept, design, literature search, experimental studies, manuscript editing. A.D. Mendoza: manuscript preparation, data acquisition, experimental studies. M.J. Casado: definition of intellectual content, literature search, manuscript editing. N.C. Pérez: research design, data analysis, statistical analysis, manuscript review. M.F. Brazón: data analysis, statistical analysis, graphics. D.S. Coll: definition of intellectual content, literature search, manuscript editing. A.J. Quintero: research design, definition of intellectual content, experimental studies, manuscript editing.

CONFLICT OF INTEREST

The authors declare the absence of any conflict of interest.

ACKNOWLEDGEMENT

The authors thank Purolomo C.A., Alibal Balanced Food C.A., REEVEX Group, the National Institute of Comprehensive Agricultural Health, the Agricultural Production Unit, Nicolino Ierrobino, the Hydrological Center C.A. for their support.

REFERENCES

1. Al-Khalaifah H, Al-Nasser AY. Evaluating the potential of *Marine algae* as sustainable ingredients in poultry feed. Agriculture. 2024;14(11):1889. https://doi.org/10.3390/agriculture14111889
2. Al-Khalaifah H, Uddin S. Assessment of *Sargassum* sp., *Spirulina* sp., and *Gracilaria* sp. as poultry feed supplements: Feasibility and environmental implications. Sustainability. 2022;14(14):8968. https://doi.org/10.3390/su14148968
3. Chavan V, Kulkarni R, Awandkar SP, Chavhan SG, Gaikwad NZ, *et al*. Effect of dietary supplementation of brown seaweed on performance of broiler chicken. Indian Journal of Animal Sciences. 2022;92(8):999–1005. https://doi.org/10.56093/ijans.v92i8.123132
4. Stokvis L, van Krimpen MM, Kwakkel RP, Bikker P. Evaluation of the nutritional value of seaweed products for broiler chickens' nutrition. Animal Feed Science and Technology. 2021;280:115061. https://doi.org/10.1016/j.anifeedsci.2021.115061

5. Alloyarova YuV, Kolotova DS, Derkach SR. Nutritional and therapeutic potential of functional components of brown seaweed: A review. Foods and Raw Materials. 2024;12(2):398–419. https://doi.org/10.21603/2308-4057-2024-2-616
6. Vijayalingam TA, Rajesh NV, Vairamuthu S, Boopathy Raja M, Sudeep Kumar NK. Effect of dietary supplementation of seaweeds on growth and blood profiles of TANUVAS Aseel chicken: Seaweed feed trails in poultry. Journal of the Hellenic Veterinary Medical Society. 2023;74(3):6085–6092. https://doi.org/10.12681/jhvms.30812
7. Vijayalingam TA, Rajesh NV. Nutritional and bioactive compounds of certain seaweeds: A livestock and poultry feed supplements. Russian Agricultural Sciences. 2023;49:223–228. https://doi.org/10.3103/S1068367423020155
8. Kumar A. Effect of *Sargassum* sp. *wightii* on growth, carcass and serum qualities of broiler chickens. Open Access Journal of Veterinary Science & Research. 2018;3(2):000156. https://doi.org/10.23880/oajvsr-16000156
9. Al-Khalaifah HS, Al-Nasser A, Surrayai T. Effects from dietary addition of *Sargassum* sp., *Spirulina* sp., or *Gracilaria* sp. powder on immune status in broiler chickens. Frontiers in Veterinary Science. 2022;9:928235. https://doi.org/10.3389/fvets.2022.928235
10. Abu Hafsa SH, Hassan AA. The effect of *Sargassum siliquastrum* supplementation on growth performance, cecal fermentation, intestine histomorphology, and immune response of Japanese quails. Animals. 2022;12(4):432. https://doi.org/10.3390/ani12040432
11. El-Fatah RAS, Abousekken MSM, Zaid AA, El-Tabaa MM, Ghazalah AA. Effect of dietary supplemention with *Sargassum muticum algae* and *Pulicaria undulate* (Rabol) on growth performance, blood parameters, immune response, manure characteristics and ammonia emissions of broilers. International Journal of Environmental Studies and Researches. 2024;3(1):28–56. https://doi.org/10.21608/ijesr.2024.346556
12. El-Fatah RAS, Abousekken MSM, Zaid AA, El-Tabaa MM, Ghazalah AA. Effect of different dietary levels of *Sargassum muticum* powder and/or extract on broilers performance and blood biochemistry. International Journal of Environmental Studies and Researches. 2023;2(4):120–138. https://doi.org/10.21608/ijesr.2023.346728
13. Dewi YL, Yuniza A, Nuraini, Sayuti K, Mahata ME. Processing of *Sargassum binderi* Seaweed for Supplementation in Poultry Diet. Journal of World's Poultry Research. 2023;13(1):103–111. https://doi.org/10.36380/jwpr.2023.11
14. Mahata ME, Rizal Y, Zurmiati, Reski S, Limbong IFS, *et al*. Impact of utilization of brown seaweed *Sargassum crassifolium* in broilers diet as a substitution of traditional feed ingredients. Journal of Animal Health and Production. 2023;11(4):404–409. https://doi.org/10.17582/journal.jahp/2023/11.4.404.409
15. Andri F, Dono ND, Sasongko H, Zuprizal Z. The effects of dietary seaweed inclusion on growth performance of broiler chickens: A systematic review and meta-analysis. F1000Research. 2020;9:1087. https://doi.org/10.12688/f1000research.25726.1
16. Mohammadigheisar M, Shouldice VL, Sands JS, Lepp D, Diarra MS, *et al*. Growth performance, breast yield, gastrointestinal ecology and plasma biochemical profile in broiler chickens fed multiple doses of a blend of red, brown and green seaweeds. British Poultry Science. 2020;61(5):590–598. https://doi.org/10.1080/00071668.2020.1774512
17. Meng W, Zou Q, Xiao Y, Ma W, Zhang J, *et al*. Growth performance and cecal microbiota of broiler chicks as affected by drinking water disinfection and/or herbal extract blend supplementation. Poultry Science. 2023;102(7):102707. https://doi.org/10.1016/j.psj.2023.102707
18. Meng W, Sui X, Xiao Y, Zou Q, Cui Y, *et al*. Regulating effects of chlorinated drinking water on cecal microbiota of broiler chicks. Poultry Science. 2023;102(12):103140. https://doi.org/10.1016/j.psj.2023.103140
19. Li Z, Liu C, Shao D, Tan C, Cao Y, *et al*. Low-concentration hypochlorous acid drinking water alleviates broiler gut microbial load while preserving overall growth performance. Toxics. 2025;13(1):48. https://doi.org/10.3390/toxics13010048
20. Mohamed A, Khalil M, Soliman F, El-Sabrout K. The effect of drinking ionized water on the productive performance, physiological status, and carcass characteristics of broiler chicks. Animals. 2025;15(2):229. https://doi.org/10.3390/ani15020229
21. Saragih HT, Fauziah IN, Saputri DA, Chasani AR. Dietary macroalgae *Chaetomorpha linum* supplementation improves morphology of small intestine and pectoral muscle, growth performance, and meat quality of broilers. Veterinary World. 2024;17(2):470–476. https://doi.org/10.14202/vetworld.2024.470-479
22. Nwaigwe C, Ihedioha J, Shoyinka S, Nwaigwe C. Evaluation of the hematological and clinical biochemical markers of stress in broiler chickens. Veterinary World. 2020;13(10):2294–2300. https://doi.org/10.14202/vetworld.2020.2294-2300

Additional information about the authors

Lorena C. Vivas ORCID 0000-0001-7757-3833
Anthony D. Mendoza ORCID 0009-0009-7792-3923
Moraiza J. Casado ORCID 0009-0007-0414-8765
Neyo C. Pérez ORCID 0000-0003-3694-273X
Marlon F. Brazón ORCID 0009-0007-0752-2695
David S. Coll ORCID 0000-0001-7276-7049
Alberto J. Quintero ORCID 0009-0007-9229-0453

Foods and Raw Materials. 2027;15(2)

ISSN 2308-4057 (Print)
ISSN 2310-9599 (Online)

Research Article
Open Access

Available online at http://jfrm.ru/en
https://doi.org/10.21603/2308-4057-2027-2-717
https://elibrary.ru/VODNSX

Elemental profile and hydrochloric acid extractability of minerals in two indigenous *Carissa carandas* types

Ankit Kumar[1,*], Rakesh Gehlot[1], Rekha Phogat[1], Abhishek Kumar[2], Kautilya Chaudhary[1], Ramesh Kumar[1]

[1] Chaudhary Charan Singh Haryana Agricultural University, Hisar, India
[2] Maharishi Markandeshwar (Deemed to be University), Mullana, India

* e-mail: ankitnagpal1995@gmail.com

Received 26.08.2025; Revised 09.10.2025; Accepted 03.02.2026; Published online 02.09.2026

Abstract:
This study addressed the research gap in the comprehensive elemental profiling and bio-accessibility assessment of various plant parts of two indigenous *Carissa carandas* (karonda) types.
Fresh fruits, leaves, bark, and roots were freeze-dried, ground, and sieved (300 µm). The samples underwent microwave-assisted digestion with sub-boiled nitric acid and hydrogen peroxide, followed by inductively coupled plasma mass spectrometry to quantify 20 elements. The list included major (P, K, Ca, Na, and Mg), minor (B, Mn, Fe, Cu, Zn, etc.), and toxic trace elements (Ni, Cd, Pb, etc.). The hydrochloric acid extractability was assessed using 0.03 N HCl incubation at 37°C for 4 h to simulate gastric conditions.
The study revealed significant tissue-specific variations in the mineral content: the leaf samples exhibited the highest levels of phosphorus (3,836.69 mg/kg) and magnesium (4,682.87 mg/kg), the fruits were rich in potassium (2,971.64 mg/kg), the bark accumulated high calcium amounts (8,823.55 mg/kg), and roots contained elevated sodium levels (2,129.18 mg/kg). The hydrochloric acid extractability also varied, with potassium and phosphorus showing high extractability in the fruit samples (80.06 and 87.51%, respectively) while magnesium and boron were more extractable in the leaves. Such toxic elements as lead (43.32 mg/kg, roots) and cadmium (1.22 mg/kg, bark) exceeded permissible limits, raising safety concerns.
C. carandas proved to be a potential source of essential minerals, particularly its leaves and fruits, which demonstrated good nutraceutical prospects. The study provides a scientific basis for targeted use of specific *C. carandas* plant parts with an outlook of *in-vivo* bioavailability examination.

Keywords: *Carissa carandas*, karonda, inductively coupled plasma mass spectrometry, mineral bio-accessibility, hydrochloric acid extractability, trace elements

Please cite this article in press as: Kumar A, Gehlot R, Phogat R, Kumar A, Chaudhary K, *et al.* Elemental profile and hydrochloric acid extractability of minerals in two indigenous *Carissa carandas* types. Foods and Raw Materials. 2027;15(2): 379–391. https://doi.org/10.21603/2308-4057-2027-2-717

INTRODUCTION

Carissa carandas L., also known as karonda and Christ thorn tree, is an evergreen shrub belonging to the *Apocynaceae* family. It grows in tropical and sub-tropical regions [1]. It is native to and commonly found throughout India, Java, Sri Lanka, Malaysia, Pakistan, and Myanmar, especially in its wild form [2]. *C. carandas* thrives on inferior and marginal lands where other fruit trees fail to grow [3]. It is cultivated primarily for its colored edible fruits, but its thorns make it an excellent hedge plant for orchards. Karonda fruits are a reservoir of essential nutrients. They are exceptionally rich in iron and calcium. Therefore, karonda fruits and foods are a valuable component of anti-anemic diet. Additionally, karonda fruits contain more ascorbic acid than apples [4]. Acidic and sweet mature fruits are popular as food. Other *C. carandas* parts are also rich in various phytocompounds, i.e., saponins, phenolics, cardiac glycosides, alkaloids, flavonoids, and triterpenoids [5].

Some elements are essential for human health in small amounts because they participate in enzymatic processes. Minor and trace elements are very important due to their essential nutritious value; however, excess intake may be harmful. Therefore, an accurate analysis of these elements in food is necessary. Inductively coupled plasma mass spectrometry (ICP-MS) provides accurate quantification of minor and trace elements in food.

Previous studies offer rather meagre information about the descriptive elemental profile of *C. carandas*

Copyright © 2026, Kumar *et al.* This is an open access article distributed under the terms of the Creative Commons Attribution 4.0 International License (https://creativecommons.org/licenses/by/4.0/), allowing third parties to copy and redistribute the material in any medium or format and to remix, transform, and build upon the material for any purpose, even commercially, provided the original work is properly cited and states its license.

fruits, leaves, bark, and roots while other berries are a popular subject of elaborated studies. For instance, Hua *et al*. [6] conducted an ICP-MS multi-element analysis on strawberries and blueberries and determined the concentration of 18 elements (B, Na, Mg, Al, P, K, Ca, Cr, Mn, Fe, Ni, Cu, Zn, Ge, As, Se, Cd, and Pb). More descriptive elemental profiles of raspberries [7, 8], wild berries [9], and other berry-type fruits have been assessed in recent years. However, these studies focus mostly on the elemental profile of berries and fail to cover other plant parts, i.e., bark, leaves, roots, stem, etc. Moreover, no comparative analysis of various plant parts with respect to elemental profile has been documented for berries, specifically for *C. carandas*.

To incorporate *C. carandas* plant into human diet, it is imperative to assess its elemental profile and hydrochloric acid (HCl) extractability. Its mineral profile may assist food scientists in developing new nutraceutical functional products.

Consequently, the goal of this research was to assess the levels of 20 elements (Li, B, Na, Mg, Al, P, K, Ca, Mn, Co, Ni, Fe, Cu, Zn, Ga, Sr, Pb, Cd, Ba, and Bi) along with their HCl extractability, i.e., bio-accessibility, in fruits, leaves, bark, and roots of two indigenous *C. carandas* types (pink and green).

STUDY OBJECTS AND METHODS

Plant material. We studied two local plant types of *Carissa carandas* L., i.e., pink and green. Fresh fruits, leaves, bark, and roots of both types were obtained from the Regional Research Station, Bawal, Chaudhary Charan Singh Haryana Agricultural University, Hisar, India. The plant parts were cleaned properly and dried in a freeze dryer to be ground into a fine powder, sieved to a uniform particle size (< 300 µm), and stored at –18°C till further experimentation.

Reagents and standards. The research featured nitric acid HNO_3 (69%; Sigma-Aldrich CHEMIE, USA), hydrogen peroxide H_2O_2 (30%) and hydrochloric acid HCl (Merck, Germany), and type I water (American Society for Testing and Materials; resistivity of 18.2 mΩ/cm at 25°C; Millipore Water Purification System).

The calibration standards for twenty elements under study (^{7}Li,^{11}B, ^{13}Na, ^{14}Mg, ^{17}Al, ^{31}P, ^{39}K, ^{40}Ca, ^{55}Mn, ^{59}Co, ^{59}Ni, ^{56}Fe, ^{64}Cu, ^{65}Zn, ^{70}Ga, ^{88}Sr, ^{107}Pb, ^{111}Cd, ^{137}Ba, and ^{209}Bi) were prepared with 0.1% HNO_3 (v/v) by adequately diluting multielement stock solutions (1,000 mg/L; Absolute Standards, Merck, Germany). Argon (purity ≥ 99.999%; Sigma Gases, New Delhi) was employed as the carrier gas.

Equipment. The multi-elemental trace analysis involved an inductively coupled plasma mass spectrometry (ICP-MS) iCAP RQ Series device (Thermo Fisher Scientific, USA) equipped with an autosampler (Autosampler ASX-560, Thermo Fisher Scientific, USA). The sample introduction system consisted of a cyclonic chamber and a concentric nebulizer. The system control relied on the Qtegra™ Instrument Control software. The samples were digested using the Anton Paar Multiwave Pro microwave digestion system. Table 1 illustrates the operational conditions.

Specification resume for ICP-MS. We placed 200 mg of each sample in microwave vials with 1 mL H_2O_2 (30%) and 4 mL sub-boiled HNO_3 (69%). The vials were left open for 20 min to prevent a sudden increase in pressure during the digestion process. The heating program consisted of three successive steps. During the first step, the temperature was rising from 25 to 100°C over 10 min. During the second step, the temperature was increasing linearly to 170°C to remain at this temperature for 30 min. The last step was a 10 min cooling phase. After opening the digestion vials, we obtained a colorless solution, clear of any particles, which signified a successful digestion. After cooling it to room temperature, we transferred the mix to 50-mL polypropylene tubes, diluted with ultrapure deionized water, and syringe-filtered it using 0.2-µm polytetrafluoroethylene membrane filters. The reagent blanks were prepared simultaneously in triplicate. The elemental analysis of the finally diluted solution in polypropylene tubes was also triplicated.

HCL extractability of minerals. We used 0.03 N HCl to extract minerals from the powdered samples. A 200-mg test sample was mixed with 10 mL of HCl (0.03 N) and incubated in an orbital shaker (100 rpm) maintained at 37°C for 4 h. The mix was then centrifuged at 5,000 rpm; the clear supernatant was dried at 100°C till 2–3 mL of extract remained. These extracts were digested in the same way as the powders. The extractable minerals in the digested samples were determined by the methods described above. To estimate the extractability, %, of each mineral component, we used the following Eq. (1):

$$\text{HCl extractablity} = \frac{\text{Mineral extractable in 0.03 N HCl}}{\text{Total mineral content}} \quad (1)$$

Table 1 Operational conditions for inductively coupled plasma mass spectrometry

Parameter	Value/setting
Nebulizer	Glass, concentric, 0.4 mL/min sample consumption
Torch vertical alignment, mm	0.2–0.5
Sampling depth, mm	15
Cooling water flow, L/min	0.59
Auxiliary gas flow rate, L/min	0.8
Dwell time, ms	50
Focus lens voltage, V	18.09
Spray chamber	Quartz, cyclonic
Radio frequency power, kW	1.54
Torch horizontal alignment, mm	0.4–1.0
Number of replicates per sample	3
Cool gas flow rate, L/min	13.9
Nebulizer gas flow rate, L/min	1.0–1.07
Sweeps/readings	10
Sample uptake rate, mL/min	0.24

RESULTS AND DISCUSSION

Carissa carandas L. is a rich source of various minerals famous for its high iron content among all fruits. In this study, we explored the mineral profiles of other karonda parts for various application prospects, i.e., nutraceuticals and pharmaceuticals. Additionally, we also assessed the hydrochloric acid (HCl) extractability of minerals to measure the bio-accessibility of these minerals in digestive systems. In Table 2, the elements are divided into major (P, K, Ca, Na, and Mg), minor (B, Mn, Fe, Cu, Zn, Li, Co, Ga, Sr, and Al), and toxic trace elements (Ni, Cd, Ba, Pb, and Bi).

Major minerals. In relation to major minerals, we observed a significant difference between various plant parts for both pink and green types of *C. carandas*. The highest phosphorus content belonged to the leaves of pink and green types as 3,836.69 ± 31.13 and 3,743.58 ± 111.36 mg/kg, respectively, with significant ($p < 0.05$) differences. The lowest value was observed in green karonda roots (1,810.87 ± 32.16 mg/kg). On the other hand, the HCl extractability of phosphorus was at its highest in pink karonda fruits (87.51 ± 2.60%) and at its lowest in pink karonda roots (55.55 ± 0.40%). The general trend for total phosphorus content and its extractability was leaf > bark > fruit > root and fruit > bark > leaf > root, respectively.

The high phosphorus content in leaves can be attributed to their role in photosynthesis and metabolic processes, which require significant amounts of phosphorus [10]. After absorption, phosphorus is loaded from the roots into the xylem and distributed into the shoots. It then accumulates in leaves during the plant growth phase until leaf senescence. Thereafter, plants remobilize phosphorus from the senescing leaves into the reproductive structures [11]. This could partly explain the higher extractability of phosphorus in *C. carandas* fruits. However, high phosphorus levels are not necessarily desirable, especially when it is in the form of phytate, which is not absorbed by humans and limits the bioavailability of dietary zinc and iron [12]. Moreover, high levels of phytic acid, such as in leaves and bark, restrict the solubilization of phosphorus: phytic acid binds to phosphorus and lowers its extractability [13].

Similarly, *C. carandas* leaves were rich in magnesium content with the highest content in green karonda leaves (4,682.87 ± 21.11 mg/kg) while the lowest content was observed in green karonda roots (1,217.67 ± 32.93 mg/kg). However, the extractability trends differed from those of phosphorus. The highest extractability of magnesium belonged to pink karonda leaves (97.72 ± 1.32%), followed by green karonda leaves (91.83 ± 0.99%), while the lowest was observed in green karonda roots (49.72 ± 0.96%). The general trend for both magnesium content and its extractability was the same, i.e., leaf > bark > fruit > root.

The high magnesium content in leaves can be attributed to its role as a central component of chlorophyll, which is vital for photosynthesis [14]. It facilitates the capture of light energy and the conversion of carbon dioxide and water into carbohydrates and oxygen, thereby playing a crucial role in plant growth and biomass accumulation. Therefore, most magnesium in plants is bound or incorporated in cellular compartments, with the highest concentrations in chloroplasts, i.e., leaves [12]. Beyond photosynthesis, magnesium acts as a co-factor for numerous enzymes involved in metabolic processes, including ATP synthesis, nucleic acid stabilization, and carbohydrate metabolism [15]. Leaf tissues are generally more permeable than bark or root tissues, allowing extracting agents to penetrate deeper, which might be responsible for the higher HCl extractability of magnesium [16].

Concerning potassium content, the highest values were observed in green and pink karonda fruits as 2,971.64 ± 24.08 and 2,855.44 ± 108.21 mg/kg, respectively. The lowest content belonged to pink karonda roots (789.06 ± 24.81 mg/kg). A similar trend was observed regarding the extractability of potassium. The highest potassium extractability was registered in pink karonda fruits (80.06 ± 2.67%), which was non-significantly followed by green karonda fruits (79.66 ± 3.09%). The lowest potassium extractability was observed in green karonda roots (30.34 ± 1.31%). The overall trend for both potassium content and its extractability was the same, i.e., fruit > leaf > bark > root.

Potassium plays vital roles in water relations, photosynthesis, and assimilating transport during fruit growth [17]. The present investigation aligns with the study conducted by Cheng *et al*. [18], who demonstrated that potassium accumulation varied significantly across different parts of apple trees during different growth stages. The increased potassium supply led to higher concentrations of potassium in all plant organs, supporting the notion that fruits naturally accumulate more potassium to support their development.

A study on strawberry fruit development indicated that potassium channels may play a critical role in fruit quality. The expression of potassium transporter genes was closely associated with fruit ripening and such quality attributes as firmness and sugar content. This correlation suggests higher potassium concentrations in fruits as compared to other plant parts. The high extractability can be explained by the fact that fruits possess specialized cellular mechanisms for potassium uptake and transport, which facilitate the movement of K^+ ions into vacuoles within fruit cells, increasing the solubility and bioavailability of potassium [19].

These channels are particularly active during the ripening process, allowing fruits to accumulate higher levels of potassium compared to leaves or roots. In addition, the chemical composition of fruits also affects potassium extractability. Fruits often contain organic acids and sugars that can form complexes with potassium, enhancing its solubility [20].

Unlike magnesium, phosphorus, and potassium, the calcium content was highest in green karonda bark (8,823.55 ± 310.98 mg/kg) while the lowest result belonged to green karonda fruits (958.80 ± 10.37 mg/kg).

Table 2 Elemental profile and hydrochloric acid extractability of *Carissa carandas* L. types, dry weight basis

Type	Part	Major minerals									
		Phosphorus		Potassium		Calcium		Sodium		Magnesium	
		Total, mg/kg	Extractability, %	Total, mg/kg	Extractability, %	Total, mg/kg	Extractability, %	Total, mg/kg	Extractability, %	Total, mg/kg	Extractability, %
Pink	Leaf	3,836.69 ± 31.13^{a}	72.36 ± 2.15^{d}	1,559.49 ± 61.69^{e}	76.56 ± 3.17^{a,b}	7,322.53 ± 46.20^{b}	28.17 ± 0.71^{g}	1,175.23 ± 11.65^{e}	72.87 ± 0.99^{a}	3,964.33 ± 153.66^{b}	97.72 ± 1.32^{a}
	Fruit	2,093.04 ± 67.92^{d}	87.51 ± 2.60^{a}	2,855.44 ± 108.21^{b}	80.06 ± 2.67^{a}	1,294.54 ± 47.84^{e}	77.06 ± 1.81^{a}	1,887.63 ± 81.67^{b}	66.71 ± 2.22^{b}	1,617.32 ± 58.31^{f}	85.63 ± 2.16^{c,d}
	Bark	3,073.42 ± 105.27^{b}	79.34 ± 0.79^{c}	1,229.81 ± 9.74^{d}	64.36 ± 1.61^{c}	7167.8 ± 264.90^{b}	49.82 ± 1.62^{c}	621.40 ± 1.12^{f}	68.50 ± 0.25^{b}	2,652.93 ± 114.78^{c}	83.53 ± 0.15^{d}
	Root	1,987.83 ± 60.92^{d}	55.55 ± 0.40^{f}	789.06 ± 24.81^{f}	47.39 ± 0.68^{d}	3,098.95 ± 97.77^{d}	46.36 ± 1.84^{d}	2,129.18 ± 94.04^{a}	59.05 ± 1.86^{e}	1,881.29 ± 53.25^{e}	59.23 ± 1.82^{e}
Green	Leaf	3,743.58 ± 111.36^{a}	63.31 ± 2.51^{e}	1,167.44 ± 52.62^{d}	73.77 ± 2.73^{b}	5,832.39 ± 205.03^{c}	36.72 ± 0.03^{e}	1,361.10 ± 47.85^{d}	62.70 ± 1.70^{c,d}	4,682.87 ± 21.11^{a}	91.83 ± 0.99^{b}
	Fruit	1,987.83 ± 86.01^{d}	83.90 ± 0.68^{b}	2,971.64 ± 24.08^{a}	79.66 ± 3.09^{a}	958.80 ± 10.37^{f}	68.74 ± 1.61^{b}	1,732.59 ± 29.67^{c}	65.73 ± 2.78^{bc}	1,939.45 ± 20.98^{e}	87.17 ± 2.91^{c}
	Bark	2,540.62 ± 29.77^{c}	71.28 ± 1.80^{d}	1,252.79 ± 46.95^{d}	77.05 ± 1.25^{a,b}	8,823.55 ± 310.98^{a}	33.83 ± 0.03^{f}	353.49 ± 4.46^{g}	59.46 ± 1.88^{e}	2,266.07 ± 40.85^{d}	87.29 ± 0.08^{c}
	Root	1,810.87 ± 32.16^{e}	60.36 ± 2.29^{e}	1,045.78 ± 25.47^{e}	30.34 ± 1.31^{e}	1,524.26 ± 38.47^{e}	48.27 ± 1.61^{c,d}	1,437.55 ± 47.94^{d}	61.18 ± 1.76^{de}	1,217.67 ± 32.93^{g}	49.72 ± 0.96^{f}
Type	Part	Toxic trace elements									
		Nickel	Cadmium		Barium		Lead		Bismuth		
		Total, mg/kg	Extractability, %	Total, mg/kg	Extractability, %	Total, mg/kg	Extractability, %	Total, mg/kg	Extractability, %	Total, mg/kg	Extractability, %
Pink	Leaf	–	–	0.52 ± 0.01^{c}	59.62 ± 1.83^{f}	39.28 ± 1.27^{b}	72.81 ± 1.84^{c}	7.10 ± 0.27^{d}	75.63 ± 1.23^{b}	0.18 ± 0.01^{e}	77.78 ± 3.01^{a}
	Fruit	–	–	0.36 ± 0.01^{e}	63.89 ± 1.27^{e}	8.94 ± 0.05^{f}	66.55 ± 0.60^{e}	5.41 ± 0.24^{g}	46.40 ± 0.46^{d}	0.29 ± 0.01^{d}	62.07 ± 0.17^{c}
	Bark	4.70 ± 0.06^{b}	36.81 ± 0.50^{a}	1.22 ± 0.05^{a}	84.43 ± 1.45^{a}	57.46 ± 2.28^{a}	68.78 ± 2.36^{d,e}	35.82 ± 0.23^{b}	33.58 ± 1.17^{f}	0.27 ± 0.01^{d}	48.15 ± 1.56^{e}
	Root	3.94 ± 0.03^{c}	22.84 ± 0.70^{b}	0.43 ± 0.01^{d}	83.72 ± 3.32^{a,b}	17.19 ± 0.62^{d}	87.03 ± 1.10^{a}	43.32 ± 0.47^{a}	37.49 ± 1.25^{e}	0.37 ± 0.01^{c}	56.76 ± 1.94^{d}
Green	Leaf	–	–	0.37 ± 0.02^{e}	86.49 ± 2.03^{a}	39.89 ± 0.15^{b}	77.86 ± 0.35^{b}	6.56 ± 0.01^{e}	73.48 ± 1.46^{b}	0.24 ± 0.01^{d,e}	79.17 ± 0.57^{a}
	Fruit	–	–	0.31 ± 0.01^{f}	67.74 ± 1.22^{d}	6.72 ± 0.10^{g}	70.68 ± 2.48^{c,d}	7.03 ± 0.05^{d}	37.84 ± 0.24^{e}	2.80 ± 0.11^{a}	7.86 ± 0.10^{f}
	Bark	5.29 ± 0.05^{a}	10.59 ± 0.14^{c}	0.71 ± 0.01^{b}	80.28 ± 2.53^{c}	35.78 ± 1.29^{c}	72.28 ± 3.13^{c}	17.18 ± 0.22^{c}	62.28 ± 1.85^{c}	0.25 ± 0.01^{d,e}	72.00 ± 2.40^{b}
	Root	1.49 ± 0.04^{d}	8.05 ± 0.21^{d}	0.42 ± 0.02^{d}	80.95 ± 0.51^{b,c}	15.32 ± 0.58^{e}	60.25 ± 0.22^{f}	5.90 ± 0.06^{f}	83.39 ± 2.93^{a}	0.57 ± 0.02^{b}	50.88 ± 2.25^{e}

Continuation of the Table 2

Type	Part	Minor minerals									
		Boron		Manganese		Iron		Copper		Zinc	
		Total, mg/kg	Extractability, %	Total, mg/kg	Extractability, %	Total, mg/kg	Extractability, %	Total, mg/kg	Extractability, %	Total, mg/kg	Extractability, %
Pink	Leaf	261.31 ± 6.76^{a}	83.52 ± 1.96^{b}	135.78 ± 3.06^{a}	91.58 ± 1.16^{a,b}	433.11 ± 4.68^{d}	34.02 ± 0.39^{d}	14.47 ± 0.63^{e}	74.92 ± 0.54^{ab}	127.50 ± 3.68^{d}	39.39 ± 0.46^{a}
	Fruit	44.59 ± 1.57^{d}	60.42 ± 0.49^{e}	41.94 ± 1.84^{c}	88.77 ± 2.56^{b}	151.11 ± 5.45^{f}	62.38 ± 1.12^{a}	31.36 ± 0.85^{b}	73.91 ± 3.13^{bc}	158.88 ± 5.16^{c}	36.22 ± 0.82^{b}
	Bark	58.98 ± 0.27^{c}	66.53 ± 0.84^{d}	132.30 ± 2.62^{a}	82.31 ± 2.89^{c}	2,945.25 ± 97.19^{a}	21.52 ± 0.31^{f}	39.05 ± 1.23^{a}	43.15 ± 0.08^{e}	194.29 ± 6.48^{a}	15.81 ± 0.26^{d}
	Root	14.02 ± 0.35^{f}	78.02 ± 3.16^{c}	38.68 ± 1.15^{c}	55.98 ± 1.16^{f}	830.03 ± 1.50^{c}	35.97 ± 0.91^{c}	21.09 ± 0.42^{d}	77.08 ± 1.46^{a}	155.84 ± 0.98^{c}	10.40 ± 0.22^{e}
Green	Leaf	226.67 ± 1.63^{b}	88.66 ± 2.22^{a}	132.08 ± 4.41^{a}	92.28 ± 1.33^{a}	438.24 ± 9.09^{d}	32.56 ± 1.03^{e}	16.27 ± 0.20^{e}	61.57 ± 1.11^{d}	133.29 ± 3.72^{d}	35.67 ± 0.90^{b}
	Fruit	40.11 ± 1.52^{d,e}	56.42 ± 0.92^{f}	32.65 ± 0.77^{d}	84.60 ± 0.75^{c}	112.89 ± 0.71	54.22 ± 0.49^{b}	20.65 ± 0.07^{d}	71.67 ± 0.78 ^{c}	131.18 ± 3.19^{d}	22.62 ± 1.26^{c}
	Bark	38.56 ± 1.56^{e}	60.55 ± 2.51^{e}	72.06 ± 0.19^{b}	78.22 ± 3.10^{d}	1,360.98 ± 52.75^{b}	18.43 ± 0.07^{g}	29.01 ± 0.10^{c}	60.55 ± 0.11^{d}	183.35 ± 5.95^{b}	9.26 ± 0.20^{f}
	Root	10.14 ± 0.06^{f}	50.24 ± 1.59^{g}	34.08 ± 0.18^{d}	61.13 ± 1.54^{e}	309.51 ± 7.53^{e}	34.87 ± 0.35^{c,d}	14.94 ± 0.50^{e}	75.85 ± 1.03^{a,b}	115.51 ± 3.02^{e}	15.37 ± 0.14^{d}
Type	Part	Lithium		Cobalt		Gallium		Strontium		Aluminum	
		Total, mg/kg	Extractability, %	Total, mg/kg	Extractability, %	Total, mg/kg	Extractability, %	Total, mg/kg	Extractability, %	Total, mg/kg	Extractability, %
Pink	Leaf	1.79 ± 0.04^{e}	90.50 ± 0.33^{a}	0.14 ± 0.01^{d}	–	0.13 ± 0.01^{e}	30.77 ± 0.33^{c}	291.62 ± 12.88^{c}	57.43 ± 0.83^{c}	274.85 ± 5.56^{e}	43.31 ± 0.78^{b}
	Fruit	0.62 ± 0.01^{f}	80.65 ± 2.84^{c}	–	–	0.06 ± 0.01^{f}	83.33 ± 2.70^{a}	51.69 ± 2.19^{g}	84.76 ± 3.44^{a}	130.00 ± 4.45^{f}	93.57 ± 2.24^{a}
	Bark	4.78 ± 0.13^{a}	55.44 ± 2.30^{f}	1.83 ± 0.04^{a}	14.75 ± 0.14^{b}	1.49 ± 0.06^{a}	6.71 ± 0.08^{h}	305.31 ± 1.38^{b}	49.07 ± 2.10^{d}	2,733.26 ± 34.49^{a}	8.53 ± 0.23^{g}
	Root	1.33 ± 0.01^{d}	71.43 ± 1.03^{d}	0.45 ± 0.01^{c}	–	0.32 ± 0.01^{c}	9.38 ± 0.21^{g}	188.25 ± 4.75^{e}	73.53 ± 3.25^{b}	568.66 ± 5.13^{c}	14.73 ± 0.49^{f}
Green	Leaf	1.29 ± 0.01^{d}	84.50 ± 1.75^{b}	0.13 ± 0.01^{d}	–	0.18 ± 0.01^{d}	22.22 ± 0.14^{d}	231.11 ± 2.50^{d}	55.96 ± 1.61^{c}	318.25 ± 9.24^{d}	40.09 ± 0.29^{c}
	Fruit	0.70 ± 0.01^{f}	71.43 ± 0.13^{d}	–	–	0.05 ± 0.01^{f}	80.00 ± 2.16^{b}	33.12 ± 1.02^{h}	81.22 ± 1.24^{a}	125.03 ± 5.07^{f}	94.32 ± 0.26^{a}
	Bark	2.13 ± 0.04^{b}	47.42 ± 1.45^{g}	0.81 ± 0.02^{b}	20.99 ± 0.45^{a}	0.56 ± 0.02^{b}	14.29 ± 0.03^{f}	370.33 ± 11.35^{a}	36.49 ± 0.86^{e}	1,092.93 ± 43.35^{b}	16.35 ± 0.60^{e}
	Root	1.20 ± 0.01^{e}	60.83 ± 0.88^{e}	0.10 ± 0.02^{e}	–	0.15 ± 0.01^{d,e}	20.00 ± 0.88^{e}	129.17 ± 0.08^{f}	71.40 ± 2.06^{b}	281.66 ± 0.76^{e}	34.99 ± 0.63^{d}

Data are represented as mean ± standard deviation, where n = 3. Different superscript letters ($^{a, b, c, d, e, f, g, h}$) represent significant difference across plant parts

However, the extractability showed some different scenario. The highest extractability of calcium was observed in pink karonda fruits (77.06 ± 1.81%) while the lowest was registered in pink karonda leaves (28.17 ± 0.71%). The overall trend for total calcium content and concerned extractability was bark > leaf > root > fruit and fruit > root > bark > leaf, respectively.

Calcium plays a crucial role in cambial activity and xylem development, which is important for structural integrity. Therefore, woody tissues, such as bark, tend to accumulate higher concentrations of minerals due to their slower turnover rates compared to more metabolically active tissues like leaves and fruits. This accumulation serves as a nutrient reserve that supports growth during critical developmental phases [21]. Regarding extractability, Hocking *et al*. [22] supported this notion, indicating that fruit tissues often contain more soluble forms of calcium, which are readily available for extraction.

The sodium content was at its maximum in the root samples. The highest sodium content belonged to pink karonda roots (2,129.18 ± 94.04 mg/kg) with the lowest extractability (59.05 ± 1.86%). The lowest sodium content was observed in green karonda bark (353.49 ± 4.46 mg/kg). The highest extractability belonged to pink karonda leaves (72.87 ± 0.99%). The overall trend for total sodium content and extractability was root > fruit > leaf > bark and leaf > fruit > bark > root, respectively.

The higher sodium content in roots can be attributed to its primary role in osmotic regulation, maintaining turgor pressure, and facilitating water uptake. The higher accumulation of sodium in roots indicates their direct contact with saline soils [23]. Despite the high sodium content in roots, their extractability is lower compared to leaves and fruits. This phenomenon can be explained by the compartmentalization of sodium ions within root cells, where they are sequestered in vacuoles to mitigate toxicity [24]. Compartmentalization serves as an important mechanism for plants to manage excess sodium, preventing it from interfering with cellular processes [25]. In contrast, the higher extractability in leaves indicates that these tissues may contain more soluble forms of sodium or less complex binding sites for this nutrient [26].

Minor minerals. In this study, the list of minor minerals included B, Mn, Fe, Cu, Zn, Li, Co, Ga, Sr, and Al. Leaves were found richer in total boron content as compared to other plant parts. The highest boron content was observed in pink karonda leaves (261.31 ± 6.76 mg/kg) while the lowest was detected in green karonda roots (10.14 ± 0.06 mg/kg). Extractability trends were also similar: the highest extractability of boron belonged to leaves, specifically in the pink karonda samples (88.66 ± 2.22%), while the lowest boron content was found in green karonda roots (50.24 ± 1.59%). The general trend for both total boron content and extractability was leaf > bark > fruit > root.

Boron plays a crucial role in the synthesis of pectin and maintaining cell wall structure in leaves, which is also essential for the proper functioning of chloroplasts. This phenomenon explains why boron accumulation is highest in leaves [26, 27]. It can be attributed to the presence of less complex binding sites in leaf tissues. This finding was in line with Ali *et al*. [28], who explained the high extractability in leaves as a result of physiological adaptations.

Similarly, leaves also demonstrated the highest manganese content, especially the pink karonda variety (135.78 ± 3.06 mg/kg), followed by pink karonda bark (132.30 ± 2.62 mg/kg) and green karonda leaves (132.08 ± 4.41 mg/kg). The lowest manganese content was in green karonda fruits (32.65 ± 0.77 mg/kg). We detected the highest extractability of manganese in green karonda leaves (92.28 ± 1.33%) and the lowest in pink karonda roots (55.98 ± 1.16%). The general trend for total manganese content and extractability was leaf > bark > fruit > root and leaf > fruit > bark > root.

Similar findings were reported by Imenšek *et al*. [12] in different plant parts of various elderberry (*Sambucus* spp.) interspecific hybrids. Marschner [29] observed a meagre distribution of manganese in plants: it accumulated primarily in photosynthetically active leaves. Bark was also found rich in manganese but could not be recommended for use because of its difficult accessibility and because bark harvesting is destructive for the plant [30]. Moreover, leaves showed the highest extractability of manganese as it exists in various chemical forms within plant tissues, with a significant proportion being water-soluble or bound to organic compounds [31]. Acidic environment can effectively release manganese from vacuolar storage, resulting in higher extractability from leaves. Iron is an antagonist to manganese extractability: high concentrations of iron in the plant restrict manganese mobility and solubility [32]. Plants often sequester excess manganese in vacuoles to mitigate potential damage in response to manganese toxicity. For example, Liu *et al*. [33] reported higher accumulation of manganese in peanut leaves (*Arachis hypogaea* L.) than in roots under the conditions of manganese toxicity.

C. carandas fruits are famous for their high iron content; however, its other parts are much higher in iron content with a lower HCl extractability. The highest iron content was observed for pink karonda bark (2,945.25 ± 97.19 mg/kg) while the lowest belonged to green karonda fruits (112.89 ± 0.71 mg/kg). The extractability trends were significantly different: the highest iron extractability was observed in fruit samples, specifically in the pink karonda variety (62.38 ± 1.12%), while the lowest belonged to green karonda bark (18.43 ± 0.07%). The general trend for total iron content and extractability was bark > root > leaf > fruit and fruit > root > leaf > bark, respectively.

Mohammadzadeh *et al*. [34] obtained similar results for Persian oak. A semi-systematic review of iron content across 1,228 plant species indicated that bark often contains substantial amounts of iron, although specific concentrations vary widely among species [35]. However, Imenšek *et al*. [12] detected more iron in blueberry roots than in bark while the lowest content was

observed in berries. This variation of iron across plant parts could be attributed to the lower solubility of iron and its cell compartmentalization in roots and bark [36]. The high extractability of iron in fruits may be due to organic acids, and iron is highly soluble in acidic environment [32].

The highest content of copper belonged to pink karonda bark (39.05 ± 1.23 mg/kg) while the lowest belonged to pink karonda leaves (14.47 ± 0.63 mg/kg), non-significantly followed by green karonda roots (14.94 ± 0.50 mg/kg). The highest extractability of copper was in pink karonda roots (77.08 ± 1.46%) while the lowest was in pink karonda bark (43.15 ± 0.08%). The general trend for total copper content and extractability was bark > fruit > leaf > root and root > fruit > leaf > bark, respectively.

Our studies were in agreement with Imenšek *et al*. [12] and Walkowiak-Tomczak *et al*. [37], where elderberry bark was found richer in copper than other plant parts. The higher concentration of copper in bark also indicates its structural role in plant system. However, wetland and metallophyte plant species tended to accumulate copper in roots [38, 39]. The high copper extractability from root may be traced to the ability of plants to sequester excess copper in vacuoles. It allows for the detoxification and storage of this micronutrient, which maintains cellular homeostasis and makes copper more available [40]. Additionally, copper ions can readily bind to cell walls and membranes, which can enhance the solubility of copper [41]. Similar findings were reported by Gul *et al*. [42] while working on *Berberis baluchistanica* Ahrendt: the total copper concentrations were higher in bark and leaves while the extractability was significantly greater in roots.

In a similar way, barks of both plant types contained high amounts of zinc and strontium. The highest concentration of zinc was observed in pink karonda bark (194.29 ± 6.48 mg/kg) and the lowest belonged to green karonda roots (115.51 ± 3.02 mg/kg). The extractability trends for zinc were somewhat different. We observed the highest extractability in pink karonda leaves (39.39 ± 0.46%) and the lowest in green karonda bark (9.26 ± 0.20%). The general trend for total zinc content and extractability was bark > fruit > root >leaf and leaf > fruit > root > bark, respectively.

Zinc deficiency are observed in those human populations that stick to diets high in phytate and low in meat [29]. Zinc shows good mobility within plant tissues and is actively transported through the phloem. Therefore, its content in plant roots does not exceed its content in other plant parts [43]. Zinc was preferentially available in leaves, nodes, and developing buds owing to its main role in photosynthesis and maintaining adequate levels for growth during critical developmental stages, which might be a cause for its higher extractability in leaves [44].

As mentioned previously, barks of both plant types also contained high amount of strontium: the highest was observed in green karonda bark (370.33 ± 11.35 mg/kg) and the lowest was detected in green karonda fruits (33.12 ± 1.02 mg/kg). The extractability trends for strontium showed converse results. The highest extractability belonged to pink karonda fruits (84.76 ± 3.44%) while the lowest one belonged to green karonda bark (36.49 ± 0.86%). The general trend for total strontium content and extractability was bark > leaf > root > fruit and fruit > root > leaf > bark, respectively.

The results of our study were in close agreement with those reported by Imenšek *et al.* [12], who found the highest strontium content in plant leaves followed by shoots and the lowest in flowers and fruits of various elderberry (Sambucus spp.) hybrids. Such results were most likely caused by the movement of strontium from roots to stem and then to the leaves. Strontium is poorly phloem-mobile: it is distributed in plants mainly through the xylem, which makes it poorly available in fruits [29]. In smaller quantities, strontium had a positive effect on metabolic bone diseases in humans [45]. On the other hand, strontium had various toxic effects on lungs and reproductive system when consumed in higher amounts, which majorly happens through leafy vegetables [46]. The higher extractability of strontium in fruits may be attributed to the presence of organic acids and the high acidic environment, which makes it more extractable and bioavailable in fruits [36].

In this research, the barks of both *C. carandas* types accumulated some minerals in a trace amount which was not found significant in terms of their nutritional value or toxicity to humans. Bark tended to accumulate higher concentrations of lithium with the highest content being observed in pink karonda bark (4.78 ± 0.13 mg/kg) and the lowest in pink karonda fruits (0.62 ± 0.01 mg/kg). On the other hand, the extractability was at its maximum in pink karonda leaves (90.50 ± 0.33%) and at its minimum in green karonda bark (47.42 ± 1.45%). The general trend for total lithium content and extractability was bark > leaf > root > fruit and leaf > fruit > root > bark, respectively.

This accumulation pattern was consistent with previous research suggesting that bark often serves as a reservoir for various minerals, including lithium, due to its structural and protective roles [47]. The high extractability in leaves may be attributed to their thinner cellular structure [48].

In a similar way, the highest content of gallium was observed in pink karonda bark (1.49 ± 0.06 mg/kg) while the lowest belonged to green karonda fruits (0.05 ± 0.01 mg/kg), non-significantly followed by pink karonda fruits (0.06 ± 0.01 mg/kg). The highest extractability of gallium was in pink karonda fruits (83.33 ± 2.70%) while the lowest was in pink karonda bark (6.71 ± 0.08%). The general trend for total gallium content and extractability was bark > root > leaf > fruit and fruit > leaf > root > bark, respectively.

According to Ha *et al*. [49] , the concentration of gallium in plants can vary significantly depending on the species and the specific cultivation conditions. For instance, couch grass and dandelions accumulated gallium

with concentrations ranging from 0.34 to 8.70 mg/kg in roots and from 0.21 to 6.75 mg/kg in leaves. Also, Shtangeeva [50] reported higher gallium content in roots than in leaves of natural plants. On the other hand, fruits tend to have higher extractability due to their composition, which often includes organic acids that enhance mineral solubility [32].

In our study, the bark samples of both plant types also contained meagre concentrations of cobalt and nickel. The highest cobalt content was observed in pink karonda bark (1.83 ± 0.04 mg/kg) while the lowest was observed in green karonda roots (0.10 ± 0.02 mg/kg). Cobalt was not detected in fruits. Similarly, nickel was not detected in leaves and fruits of both plant types. The highest contents of nickel belonged to green karonda bark (5.29 ± 0.05 mg/kg), which surpasses the generally accepted safe level of about 1 mg/kg established by the European Food Safety Authority [51]. The extractability of both minerals was much lower than for other minerals.

Certain plants can accumulate exceptionally high levels of nickel. For instance, *Brassicaceae* family, such as *Alyssum caricum* T.R. Dudley & Hub.-Mor. and *Thlaspi oxyceras* (Boiss.) B.D. Jacks., can accumulate up to 12.27 and 13.77 g/kg of nickel in their leaves, respectively [52], which was not a case in our study. We detected neither of the elements in fruits, which makes them safe for human consumption. While specific data on cobalt in plant parts has not been documented in research worldwide, certain plant species are known to accumulate cobalt under conditions similar to nickel. Generally, plants that thrive in metal-rich soils or those that have evolved mechanisms to tolerate heavy metals tend to accumulate both nickel and cobalt [53, 54].

Toxic trace elements. In this research, five elements were categorized as toxic, i.e., Cd, Al, Ba, Pb, and Bi. The highest content of aluminum was observed in pink karonda bark (2,733.26 ± 34.49 mg/kg) while the lowest was detected in green karonda fruits (125.03 ± 5.07 mg/kg), non-significantly followed by pink karonda fruits (130.00 ± 4.45 mg/kg). The highest extractability of aluminum belonged to green karonda fruits (94.32 ± 0.26%), non-significantly followed by pink karonda fruits (93.57 ± 2.24%). The lowest content was in pink karonda bark (8.53 ± 0.23%). The general trend for total aluminum content and extractability was bark > root > leaf > fruit and fruit > leaf > root > bark, respectively.

Aluminum is often found in higher concentrations in acidic soils, where it can be more soluble and readily taken up by plant roots [55]. Gallium behaves similarly in terms of mobility as it can accumulate in plant tissues alongside aluminum. Its higher extractability in fruits is attributed to the higher acidic conditions in fruit tissue that are responsible for its higher solubility [56].

In a similar way, the highest content of barium was observed in pink karonda bark (57.46 ± 2.28 mg/kg) while the lowest was detected in green karonda fruits (6.72 ± 0.10 mg/kg). The highest extractability of barium belonged to pink karonda roots (87.03 ± 1.10%) while the lowest was in green karonda roots (60.25 ± 0.22%).

Barium is often present in soils derived from parent materials rich in barium-bearing minerals, and its availability may depend on soil pH and organic matter content. The differences in extractability can also be attributed to the chemical forms of barium present in plant tissues. Barium can exist in various forms, including soluble salts and complexed forms that may affect its availability for uptake [57].

The highest content of bismuth was observed in green karonda fruits (2.80 ± 0.11 mg/kg) while the lowest belonged to pink karonda leaves (0.18 ± 0.01 mg/kg). Conversely, we detected the highest extractability of bismuth in green karonda leaves (79.17 ± 0.57%) and the lowest in green karonda fruits (7.86 ± 0.10%).

Bismuth is a heavy metal that can be absorbed by plants [58]. High bismuth content in green karonda fruits may indicate a more favorable interaction with soil conditions that promote bismuth uptake or an enhanced ability to tolerate and accumulate this metal. The high extractability observed in green karonda leaves suggests that its leaf tissues are more conducive to releasing bismuth into a soluble form, making it more accessible for uptake by organisms or during extraction processes [59].

The highest content of lead was found in pink karonda roots (43.32 ± 0.47 mg/kg), which was dramatically above the acceptable limit of approximately 0.1 mg/kg for foodstuffs[1]. The lowest amount belonged to pink karonda fruits (5.41 ± 0.24 mg/kg). However, the highest lead extractability belonged to the samples of green karonda roots (83.39 ± 2.93%) while the lowest belonged to pink karonda bark (33.58 ± 1.17%). The general trend for total lead content and extractability was root > bark > leaf > fruit and leaf > root > fruit > bark, respectively.

Lead is a non-essential heavy metal for plants, and its accumulation may result in various toxic effects in humans. A previous study on *Glycine max* L. (soybean) indicated substantial lead accumulation in roots compared to other plant parts [60]. While bark can store significant amounts of lead, its dense cellular structure may limit the solubility and availability of this metal for biological uptake or extraction processes [61].

We observed the highest content of cadmium in pink karonda bark (1.22 ± 0.05 mg/kg), which by far exceeded the maximal permissible levels of 0.05–0.1 mg/kg[2]. The lowest content belonged to the samples of green karonda fruits (0.31 ± 0.01 mg/kg). The highest extractability of cadmium was observed in green karonda leaves (86.49 ± 2.03%) while the lowest was detected in pink karonda leaves (59.62 ± 1.83%). The general trend for total cadmium content and extractability was bark > root > leaf > fruit and bark > root > leaf > fruit, respectively.

Cadmium is a toxic heavy metal that poses serious environmental and health risks [62]. The high extractability observed in green karonda leaves suggests that the structural characteristics of leaf tissues, including

[1] FAO/WHO. Joint FAO/WHO food standards programme codex committee on contaminants in foods. FAO/WHO. Rome, 2011.

[2] The same.

thinner cell walls and higher concentrations of organic acids, may facilitate this enhanced extractability. While bark can store significant amounts of cadmium, its dense cellular structure may limit the solubility and availability of this metal for biological uptake or extraction processes [63].

Multivariate analysis. The ***principal component analysis*** made it possible to explore the variation among different plant parts based on principal components (Fig. 1). The analysis successfully reduced the dimensionality of the dataset while preserving the most significant variance in their mineral composition and HCl extractability.

Regarding the total mineral content, the first two principal components (PCs) accounted for a significant portion of the variance, explaining 54.64 and 24.85%, respectively. Together, these two components captured 79.49% of the total variance. PC1 was affected by Mg, P, Mn, Fe, Li, Ga, Cd, Al, Ba, and Sr, which exhibited strong positive correlations with it. PC2 was primarily associated with B, K, and Na, which also showed positive correlations. In contrast, Mg, Fe, Al, and Ni had negative loadings, indicating an inverse relationship with PC2. This suggests that PC2 differentiated samples based on the relative proportions of alkali metals versus transition metals. Pink karonda bark, pink karonda roots, and green karonda bark had high PC1 scores, showing enrichment in heavy elements, while pink karonda leaves and green karonda leaves had high PC2 scores, dominated by alkali metals. The following correlations were strong, indicating geochemical relationships: Mg-P, Fe-Ga, Li-Fe, Cd-Al, and Ba-Sr. In contrast, Na-Ca, K-Sr, and Ni-Li exhibited inverse correlations.

Regarding HCl extractability, the first three principal components accounted for a major portion of the variance, explaining 38.89, 22.94, and 18.08%, respectively. Together, these three components captured 79.91% of the total variance. PC1 was strongly affected by Fe, Al, Ga, Zn, and P, while PC2 depended on B, Mn, Mg, Zn, and Na. The rest of the elements had a strong impact on PC3. Pink karonda fruits and green karonda fruits had high scores for PC1. Pink karonda leaves, pink karonda bark, and green karonda bark had high scores for PC2. Pink karonda roots and green karonda roots showed high scores for PC3. The test showed strong positive correlations between Mg-K, Mn-Zn, Fe-Ga, and Al-Ga while Cd-Ga, Co-Li, and Pb-Fe (–0.41) were found negatively correlated.

Hierarchical cluster analysis (HCA). To get a clearer understanding of the dataset, we conducted an unsupervised hierarchical cluster analysis of total mineral content and extractability. The hierarchical clustered heat map provides a visual representation of the correlation and clustering based on the intrinsic similarity between different groups (Fig. 2).

Regarding the total mineral content, we observed three major clusters. Cluster 1 included Mn, Mg, K, Na, and P, which showed high variability across samples, with significant changes in concentration. Cluster 2 included Pb, Bi, B, Ba, Co, Ni, and Cd with a low to moderate presence, which suggests their limited natural abundance or a lack of significant contamination in the samples. Cluster 3 included Fe, Ga, Al, Ca, Sr, Cu, Zn, and Li, which demonstrated moderate and uniform distribution. These elements likely play structural or metabolic roles and are uniformly present in biological and environmental samples.

Regarding mineral extractability, we also detected three major clusters. Cluster 1 included Na, K, and Bi, which showed high variability in extractability across the samples. Cluster 2 included Ni, Pb, Cu, Zn, Co, Fe, Ge, Al, Li, and Cd. These elements showed moderate

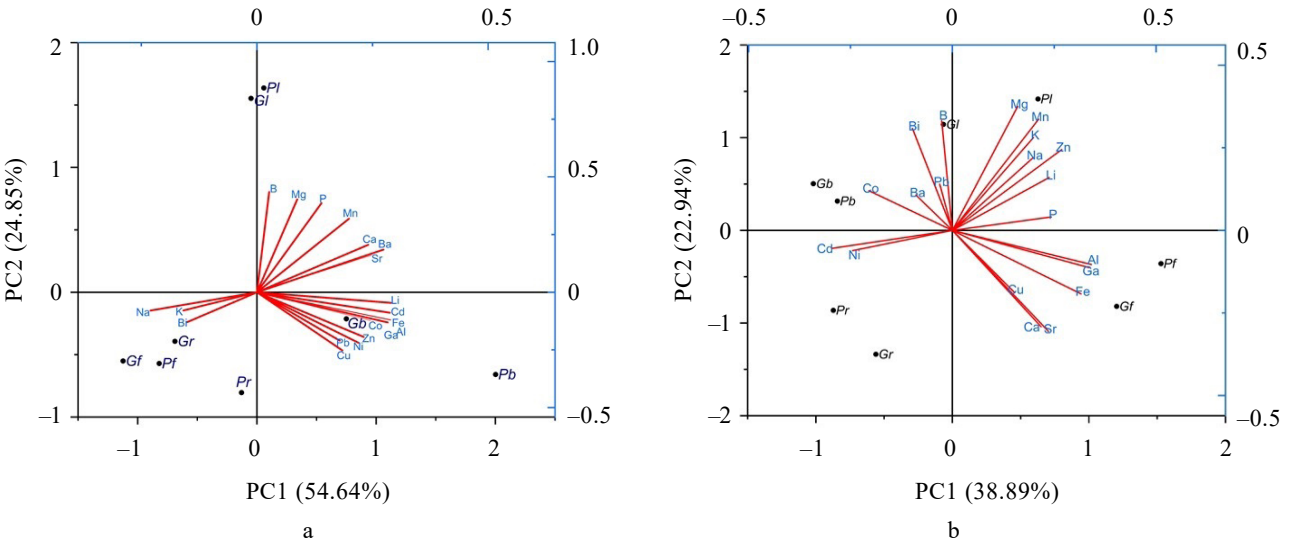


Figure 1 Principal component analysis biplots for total mineral content (a) and hydrochloric acid extractability (b) of green and pink *Carissa carandas* L. types: PC1 – Principal component 1; PC2 – Principal component 2; *Pl* – pink karonda leaves; *Pf* – pink karonda fruits; *Pb* – pink karonda bark; *Pr* – pink karonda roots; *Gl* – green karonda leaves; *Gf* – green karonda fruits; *Gb* – green karonda bark; *Gr* – green karonda roots

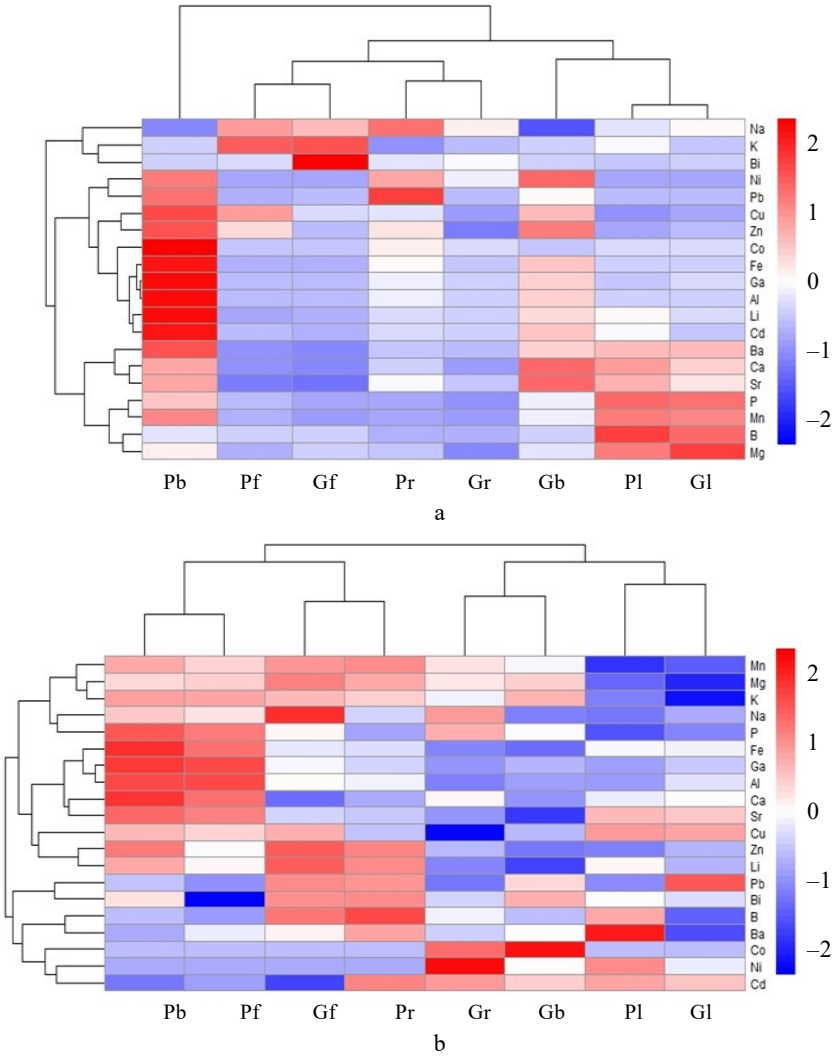


Figure 2 Non-averaged unsupervised hierarchical cluster analysis (similarity: Euclidean; linkage rule: Ward) for total mineral content (a) and hydrochloric acid extractability (b) of pink and green *Carissa carandas* L. types

and uniform extractability except for Pb. Cluster 3 included Ba, Ca, Sr, P, Mn, B, and Mg, which generally showed low to moderate extractability.

CONCLUSION

This study provided a detailed elemental analysis of different plant parts of two local types of *Carissa carandas* L. (green and pink), revealing significant variations in mineral content and hydrochloric acid extractability across tissues. Leaves were particularly rich in phosphorus and magnesium; fruits demonstrated elevated potassium levels; bark accumulated high amounts of calcium; roots showed a pronounced sodium content.

The differences in extractability suggest that the tissue-specific biochemical properties and cellular structures affected the mineral bio-accessibility, highlighting the complexity of nutrient distribution within the plant. These findings underscore the potential of *C. carandas* as a valuable source of minerals for nutraceutical and pharmaceutical applications.

Future research should focus on *in vivo* studies to further investigate the bioavailability of these minerals in human diet. Integrating advanced omics technologies, such as metabolomics and proteomics, could provide deeper insights into the underlying mechanisms that regulate mineral accumulation and extractability. Such studies will pave the way for the development of targeted functional foods and novel therapeutic agents derived from local types of *C. carandas*.

CONTRIBUTION

All the authors were equally involved in the manuscript and are equally responsible for any potential plagiarism.

CONFLICT OF INTEREST

The authors state that there is no conflict of interest.

ACKNOWLEDGEMENTS

The authors are highly grateful to the Center of Food Science and Technology, Chaudhary Charan Singh Haryana Agricultural University, Hisar, for providing assistance in this research.

REFERENCES

1. Bano Z, Begum S, Ali SS, Kiran Z, Siddiqui BS, *et al*. Phytochemicals from *Carissa carandas* with potent cytotoxic and anti-inflammatory activities. Natural Product Research. 2022;36(6):1587–1592. https://doi.org/10.1080/14786419.2021.1886101
2. Saxena D, Misra KK, Rai R. Studies on suitability of cultivars, picking dates and drying methods for the preparation of karonda (*Carissa carandus* L.) fruit powder. Indian Journal of Horticulture. 2016;73(2):267–273. http://doi.org/10.5958/0974-0112.2016.00059.1
3. Shaheen S, Jaffer M, Khan F, Hussain K, Hanif U, *et al*. Morpho-palynological assessment of medicinal flora of district Lahore, Pakistan based on LM and SEM. Microscopy Research and Technique. 2018;81:1397–1405. https://doi.org/10.1002/jemt.23096
4. Singh K, Singh SP. Karonda: A medicinal plant with immense economic potentials. AgriCos E-Newsletter 2021;2(2);83–86.
5. Bilal A, Adnan M, Mushtaq A, Blama A. A brief study of phytochemical profile and pharmacological applications of *Carissa carandas* (L.). International Journal of Chemical and Biochemical Sciences. 2015;8:92–96.
6. Hua Z, Zhen-Yu W, Xin Y, Hai-Tian Z, Ying-Chun Z, *et al*. Determination of free amino acids and 18 elements in freeze-dried strawberry and blueberry fruit using an Amino Acid Analyzer and ICP-MS with micro-wave digestion. Food Chemistry. 2014;147:189–194. https://doi.org/10.1016/j.foodchem.2013.09.118
7. Fotirić Akšić M, Nešović M, Ćirić I, Tešić Ž, Pezo L, *et al*. Chemical fruit profiles of different raspberry cultivars grown in specific norwegian agroclimatic conditions. Horticulturae. 2022;8(9):765. https://doi.org/10.3390/horticulturae8090765
8. Adamczuk N, Ośko J, Grembecka M, Konieczyński P, Migas P, *et al*. Evaluation of the content of micro- and macroelements in raspberries depending on the species, cultivar variety, and geographical environment. Nutrients. 2023;15(17):3782. https://doi.org/10.3390/nu15173782
9. Cristea G, Dehelean A, Puscas R, Covaciu FD, Hategan AR, *et al*. Characterization and differentiation of wild and cultivated berries based on isotopic and elemental profiles. Applied Sciences. 2023;13(5):2980. https://doi.org/10.3390/app13052980
10. Shen J, Yuan L, Zhang J, Li H, Bai Z, *et al*. Phosphorus dynamics: From soil to plant. Plant Physiology. 2011;156(3):997–1005. https://doi.org/10.1104/pp.111.175232
11. Veneklaas EJ, Lambers H, Bragg J, Finnegan PM, Lovelock CE, *et al*. Opportunities for improving phosphorus-use efficiency in crop plants. New Phytologist. 2012;195:306–320. https://doi.org/10.1111/j.1469-8137.2012.04190.x
12. Imenšek N, Sem V, Kolar M, Ivančič A, Kristl J. The distribution of minerals in crucial plant parts of various elderberry (*Sambucus* spp.) interspecific hybrids. Plants. 2021;10(4):653. https://doi.org/10.3390/plants10040653
13. Duhan A, Khetarpaul N, Bishnoi S. Changes in phytates and HCl extractability of calcium, phosphorus, and iron of soaked, dehulled, cooked, and sprouted pigeon pea cultivar (UPAS-120). Plant Foods for Human Nutrition. 2002;57:275–284. https://doi.org/10.1023/A:1021814919592
14. Ishfaq M, Wang Y, Yan M, Wang Z, Wu L, *et al*. Physiological essence of magnesium in plants and its widespread deficiency in the farming system of China. Frontiers in Plant Science. 2022;13:802274. https://doi.org/10.3389/fpls.2022.802274
15. Ahmed N, Zhang B, Bozdar B, Chachar S, Rai M, *et al*. The power of magnesium: Unlocking the potential for increased yield, quality, and stress tolerance of horticultural crops. Frontiers in Plant Science. 2023;14:1285512. https://doi.org/10.3389/fpls.2023.1285512
16. Bibi S, Irshad M, Ullah F, Mahmood Q, Shahzad M, *et al*. Phosphorus extractability in relation to soil properties in different fields of fruit orchards under similar ecological conditions of Pakistan. Frontiers in Ecology and Evolution. 2023;10:1077270. https://doi.org/10.3389/fevo.2022.1077270
17. Kuzin A, Solovchenko A. Essential role of potassium in apple and its implications for management of orchard fertilization. Plants. 2021;10(12):2624. https://doi.org/10.3390/plants10122624
18. Cheng L. Optimizing nitrogen and potassium management to foster apple tree growth and cropping without getting "burned". New York Fruit Quarterly. 2013;21(1):21–24.
19. Wang S, Song M, Guo J, Huang Y, Zhang F, *et al*. The potassium channel FaTPK1 plays a critical role in fruit quality formation in strawberry (*Fragaria* × *ananassa*). Plant Biotechnology Journal. 2018;16:737–748. https://doi.org/10.1111/pbi.12824
20. Razzaque AHM, Hanafi MM. Effect of potassium on growth, yield and quality of pineapple in tropical peat. Fruits. 2001;56(1):45–49.
21. Fromm J. Wood formation of trees in relation to potassium and calcium nutrition. Tree Physiology. 2010;30(9):1140–1147. https://doi.org/10.1093/treephys/tpq024

22. Hocking B, Tyerman SD, Burton RA, Gilliham M. Fruit calcium: Transport and physiology. Frontiers in Plant Science. 2016;7:569. https://doi.org/10.3389/fpls.2016.00569
23. Keisham M, Mukherjee S, Bhatla SC. Mechanisms of sodium transport in plants–progresses and challenges. International Journal of Molecular Sciences. 2018;19(3):647. https://doi.org/10.3390/ijms19030647
24. Zhao S, Zhang Q, Liu M, Zhou H, Ma C, *et al*. Regulation of plant responses to salt stress. International Journal of Molecular Sciences. 2021;22(9):4609. https://doi.org/10.3390/ijms22094609
25. Yamaguchi T, Hamamoto S, Uozumi N. Sodium transport system in plant cells. Frontiers in Plant Science. 2013;4:410. https://doi.org/10.3389/fpls.2013.00410
26. Datta S, Sinha BK, Bhattacharjee S, Seal T. Nutritional composition, mineral content, antioxidant activity and quantitative estimation of water soluble vitamins and phenolics by RP-HPLC in some lesser used wild edible plants. Heliyon. 2019;5(3):e01431. https://doi.org/10.1016/j.heliyon.2019.e01431
27. Brdar-Jokanović M. Boron toxicity and deficiency in agricultural plants. International Journal of Molecular Sciences. 2020;21(4):1424. https://doi.org/10.3390/ijms21041424
28. Ali F, Ali A, Gul H, Sharif M, Sadiq A, *et al*. Effect of boron soil application on nutrients efficiency in tobacco leaf. American Journal of Plant Sciences. 2015;6:1391–1400. http://doi.org/10.4236/ajps.2015.69139
29. Marschner P. Marschner's mineral nutrition of higher plants. 3rd ed. NY: Academic Press; 2012, 651 p. https://doi.org/10.1016/C2009-0-63043-9
30. Diviš P, Pořízka J, Vespalcov M, Matějíček A, Kaplan J. Elemental composition of fruits from different black elder (*Sambucus nigra* L.) cultivars grown in the Czech Republic. Journal of Elementology. 2015;20(3):549–557. https://doi.org/10.5601/jelem.2015.20.1.758
31. Kuang X, Wang W, Hu J, Liu W, Zeng W. Subcellular distribution and chemical forms of manganese in *Daucus carota* in relation to its tolerance. Frontiers in Plant Science. 2022;13:1–14. https://doi.org/10.3389/fpls.2022.947882
32. Oteng P, Otchere JK, Adusei S, Mensah RQ, Tei-Mensah E. Vitamin analysis, trace elements content, and their extractabilities in *Tetrapleura tetraptera*. Journal of Chemistry. 2020;2020:1608341. https://doi.org/10.1155/2020/1608341
33. Liu Y, Zhao M, Chen J, Yang S, Chen J, *et al*. Comparative transcriptome analysis reveals complex physiological response and gene regulation in peanut roots and leaves under manganese toxicity stress. International Journal of Molecular Sciences. 2023;24(2):1161. https://doi.org/10.3390/ijms24021161
34. Mohammadzadeh H, Mirzaei J, Farashiyani ME, Soheili F, Woodward S, *et al*. Variation in the nutrient contents of leaves, bark, and wood of Persian oak trees (*Quercus brantii*) affected by decline. BioResources. 2021;16(3):4704–4715. https://doi.org/10.15376/biores.16.3.4704-4715
35. Ancuceanu R, Dinu M, Hovaneţ MV, Anghel AI, Popescu CV, *et al*. A survey of plant iron content – a semi-systematic review. Nutrients. 2015;7(12):10320–10351. https://doi.org/10.3390/nu7125535
36. Page V, Feller U. Heavy metals in crop plants: Transport and redistribution processes on the whole plant level. Agronomy. 2015;5(3):447–463. https://doi.org/10.3390/agronomy5030447
37. Młynarczyk K, Walkowiak-Tomczak D, Staniek H, Kidoń M, Łysiak GP. The content of selected minerals, bioactive compounds, and the antioxidant properties of the flowers and fruit of selected cultivars and wildly growing plants of *Sambucus nigra* L. Molecules. 2020;25(4):876. https://doi.org/10.3390/molecules25040876
38. Yadav AK, Abbassi R, Kumar N, Satya S, Sreekrishnan TR, *et al*. The removal of heavy metals in wetland microcosms: Effects of bed depth, plant species, and metal mobility. Chemical Engineering Journal. 2012;211–212:501–507. https://doi.org/10.1016/j.cej.2012.09.039
39. Deng H, Ye ZH, Wong MH. Accumulation of lead, zinc, copper and cadmium by 12 wetland plant species thriving in metal-contaminated sites in China. Environmental Pollution. 2004;132(1):29–40. https://doi.org/10.1016/j.envpol.2004.03.030
40. Chen G, Li J, Han H, Du R, Wang X. Physiological and molecular mechanisms of plant responses to copper stress. International Journal of Molecular Sciences. 2022;23(21):12950. https://doi.org/10.3390/ijms232112950
41. Yruela I. Copper in plants: Acquisition, transport and interactions. Functional Plant Biology. 2009;36(5):409–430. https://doi.org/10.1071/FP08288
42. Gul Z, Akbar A, Leghari SK, Kakar AUR, Khan N, *et al*. Daily dose standardization based on essential and nonessential trace element presence in *Berberis baluchistanica* ahrendt bark, leaf, and root. BioMed Research International. 2022;2022:6811613. https://doi.org/10.1155/2022/6811613
43. Dos Santos Utmazian MN, Wenzel WW. Cadmium and zinc accumulation in willow and poplar species grown on polluted soils. Journal of Plant Nutrition and Soil Science. 2007;170(2):265–272. https://doi.org/10.1002/jpln.200622073

44. Xie R, Zhao J, Lu L, Brown P, Lin X, *et al*. Seasonal zinc storage and a strategy for its use in buds of fruit trees. Plant Physiology. 2020;183(3):1200–1212. https://doi.org/10.1104/pp.19.01563

45. Sasmaz M, Sasmaz A. The accumulation of strontium by native plants grown on Gumuskoy mining soils. Journal of Geochemical Exploration. 2017;181:236–242. https://doi.org/10.1016/j.gexplo.2017.08.001

46. Watts P, Howe P. Strontium and strontium compounds. IPCS concise international chemical assessment documents. 2010;77:1–63. https://elibrary.ru/LTZLXB

47. Kalinowska M, Hawrylak-Nowak B, Szymańska M. The influence of two lithium forms on the growth, L-ascorbic acid content and lithium accumulation in lettuce plants. Biological Trace Element Research. 2013;152:251–257. https://doi.org/10.1007/s12011-013-9606-y

48. Magalhaes JR, Wilcox GE, Rocha AN, Silva FL. Research on lithium-phytological metabolism ano recovery of hypo-lithium. Pesquisa Agropecuária Brasileira. 1990;25:1781–1787.

49. Ha NTH, Sakakibara M, Sano S, Nhuan MT. Uptake of metals and metalloids by plants growing in a lead-zinc mine area, Northern Vietnam. Journal of Hazardous Materials. 2011;186(2–3):1384–1391. https://doi.org/10.1016/j.jhazmat.2010.12.020.

50. Shtangeeva I. Temporal variability of gallium in natural plants. Toxics. 2023;11(8):675. https://doi.org/10.3390/toxics11080675

51. EFSA CONTAM Panel (EFSA Panel on Contaminants in the Food Chain). Scientific opinion on the risks to public health related to the presence of chromium in food and drinking water. EFSA Journal. 2014;12(3):3595. https://doi.org/10.2903/j.efsa.2014.3595

52. Antonkiewicz J, Jasiewicz C, Koncewicz-Baran M, Sendor R. Nickel bioaccumulation by the chosen plant species. Acta Physiologiae Plantarum. 2016;38:40. https://doi.org/10.1007/s11738-016-2062-5

53. Pishchik V, Mirskaya G, Chizhevskaya E, Chebotar V, Chakrabarty D. Nickel stress-tolerance in plant-bacterial associations. PeerJ. 2021;9:e12230. https://doi.org/10.7717/peerj.12230

54. Rue M, Paul ALD, Echevarria G, Van Der Ent A, Simonnot MO, *et al*. Uptake, translocation and accumulation of nickel and cobalt in: *Berkheya coddii*, a "metal crop" from South Africa. Metallomics. 2020;12(8):1278–1289. https://doi.org/10.1039/d0mt00099j

55. Zhao XQ, Shen RF. Aluminum–nitrogen interactions in the soil–plant system. Frontiers in Plant Science. 2018;9:807. https://doi.org/10.3389/fpls.2018.00807.

56. Ofoe R, Thomas RH, Asiedu SK, Wang-Pruski G, Fofana B, *et al*. Aluminum in plant: Benefits, toxicity and tolerance mechanisms. Frontiers in Plant Science. 2023;13:1085998. https://doi.org/10.3389/fpls.2022.1085998

57. Magalhães MOL, do Amaral Sobrinho NMB, Zonta E, Becerra AT, Lastra-Bravo XB, *et al*. Reducing conditions on barium absorption in rice plants cultured in $BaSO_4$-enriched soil. Acta Scientiarum. Agronomy. 2014;36(1):119–127. (In Portuguese) https://doi.org/10.4025/actasciagron.v36i1.17539

58. Wei C, Deng Q, Wu F, Fu Z, Xu L. Arsenic, antimony, and bismuth uptake and accumulation by plants in an old antimony mine, China. Biological Trace Element Research. 2011;144:1150–1158. https://doi.org/10.1007/s12011-011-9017-x

59. Pietrini F, Passatore L, Carloni S, Massimi L, Astolfi ML, *et al*. Bismuth exposure affects morpho-physiological performances and the ionomic profile in garden cress (*Lepidium sativum* L.) plants. Frontiers in Environmental Science. 2023;11:1221573. https://doi.org/10.3389/fenvs.2023.1221573

60. Aransiola SA, Ijah UJJ, Abioye OP. Phytoremediation of lead polluted soil by *Glycine max* L. Applied and Environmental Soil Science. 2013;2013(1):631619. https://doi.org/10.1155/2013/631619

61. Sharma P, Dubey RS. Lead toxicity in plants. Brazilian Journal of Plant Physiology. 2005;17(1):35–52. https://doi.org/10.1590/s1677-04202005000100004

62. Street JJ, Lindsay WL, Sabey BR. Solubility and plant uptake of cadmium in soils amended with cadmium and sewage sludge. Journal of Environmental Quality. 1977;6(1):72–77. https://doi.org/10.2134/jeq1977.00472425000600010016x

63. Hocaoglu-Ozyigit A, Nazli Genc B. Cadmium in plants, humans and the environment. Frontiers in Life Sciences and Related Technologies. 2020;1(1):12–21.

Additional information about the authors

Ankit Kumar ORCID 0000-0003-1267-5331
Rakesh Gehlot ORCID 0000-0002-5091-4236
Rekha Phogat ORCID 0000-0003-3462-8720
Abhishek Kumar ORCID 0000-0002-4596-0668
Kautilya Chaudhary ORCID 0000-0002-9507-6491
Ramesh Kumar ORCID 0009-0007-8002-2195

Foods and Raw Materials. 2027;15(2)

ISSN 2308-4057 (Print)
ISSN 2310-9599 (Online)

Review Article
Open Access

Available online at http://jfrm.ru/en
https://doi.org/10.21603/2308-4057-2027-2-716
https://elibrary.ru/VLODRQ

Prospects for developing sleep-related functional foods: Use of electroencephalography for objective sleep measurement

Apsorn Sattayakhom, Phanit Koomhin*, Narumol Matan**

Walailak University, Nakhon Si Thammarat, Thailand

* e-mail: phanit.ko@mail.wu.ac.th
** e-mail: nnarumol@mail.wu.ac.th

Received 23.06.2025; Revised 21.10.2025; Accepted 03.02.2026; Published online 29.09.2026

Abstract:
The development of sleep-enhancing food products can improve sleep quality. Understanding the relationship between food consumption and sleep is essential for selecting suitable ingredients for these products.
Electroencephalography is a valuable tool for identifying foods and raw materials used in sleep-promoting products, providing critical insights into their effectiveness.
This review examined the relationship between food consumption and sleep based on research from 2004 to 2024 utilizing electroencephalography tools in human and animal models. The effects of food intake on sleep were examined during the initial stage, slow-wave sleep, and the subsequent stage, rapid eye movement, with measurable parameters recorded. The intake quantity and concentration of specific foods or ingredients were analyzed in human and animal models, considering both normal sleep patterns and sleep disorder models. The analysis revealed that foods associated with sleep, as determined by electroencephalography testing, can be classified into six categories: essential oils, Chinese herbal medicines, plant and fungi extracts, tea and cocoa, probiotics and prebiotics in fermented foods, and food supplements. All the food types predominantly influenced the initial stage of sleep, specifically slow-wave sleep during non-rapid eye movement. In contrast, foods containing Chinese herbal medicines or extracts demonstrated a significant effect on the rapid eye movement stage. These findings provide valuable insights into the development of functional foods aimed at improving sleep quality.

Keywords: Sleep monitoring, slow-wave sleep, rapid eye movement sleep, sleep-enhancing food products, functional food development, sleep quality

Funding: This work was financially supported by the Research Center of Excellence in Innovation of Essential Oils and Bioactive Compounds, Walailak University, and partially supported by the National Research Council of Thailand (NRCT) and Walailak University (Grant No. N41A640166).

Please cite this article in press as: Sattayakhom A, Koomhin P, Matan N. Prospects for developing sleep-related functional foods: Use of electroencephalography for objective sleep measurement. Foods and Raw Materials. 2027;15(2):392–410. https://doi.org/10.21603/2308-4057-2027-2-716

INTRODUCTION

Health maintenance in humans encompasses various approaches, one of which is to consume foods that promote overall well-being. Numerous food products not only contribute to general health but also modulate specific physiological functions within the human body. Among these, functional foods with bioactive compounds that influence sleep have been the focus of extensive research. These compounds may facilitate sleep onset or, conversely, disrupt the sleep process by interfering with natural sleep mechanisms. The functional food market has demonstrated remarkable growth, with its global value estimated to increase from USD 119.2 billion in 2024 to USD 165.8 billion by 2029[1].

Electroencephalography (EEG) has been employed as a critical tool to investigate the relationship between food consumption and sleep. This technique measures brain wave patterns to elucidate correlations with sleep quality and is utilized in both animal and human studies.

[1] Functional food ingredients market by type (probiotics, protein & amino acids, phytochemicals & plant extracts, prebiotic, omega-3 fatty acids, carotenoids, vitamins), application, source, form, health benefits and region: global forecast to 2029. Markets and Markets. [cited 2025 Feb 10]. Available from: https://www.marketsandmarkets.com/Market-Reports/functional-food-ingredients-market-9242020.html

Copyright © 2026, Sattayakhom *et al.* This is an open access article distributed under the terms of the Creative Commons Attribution 4.0 International License (https://creativecommons.org/licenses/by/4.0/), allowing third parties to copy and redistribute the material in any medium or format and to remix, transform, and build upon the material for any purpose, even commercially, provided the original work is properly cited and states its license.

Sleep is a critical physiological function explained by several interrelated theories, including the inactivity theory, restoration theory, energy conservation theory, and brain plasticity theory [1]. According to the American Academy of Sleep Medicine, sleep is divided into two main phases: slow-wave sleep (SWS) and rapid eye movement (REM) sleep. These phases are distinguished by specific brainwave patterns, muscle activity, and eye movements. Slow-wave sleep is further divided into three stages, the first known as non-rapid eye movement [2]. Slow-frequency brainwaves, such as theta and delta waves, dominate during slow-wave sleep. In contrast, higher-frequency waves, such as alpha, beta, or gamma waves, predominate in the wake state, depending on activity levels. REM sleep is regulated by REM-on neurons, which induce this stage through superior colliculus stimulation to generate rapid eye movements, cholinergic neuron activation in the cortex to produce beta wave-dominant brain activity, and motor neuron inhibition of the medullary reticulospinal tract to induce muscle atonia. These mechanisms collectively underscore the complexity of sleep regulation and its physiological foundations [3].

In addition to EEG, electromyography (EMG) and electrooculography are standard techniques used for sleep staging. In recent years, polysomnographic devices that emphasize EEG and EMG have advanced significantly, enabling the measurement of objective sleep parameters through automatic sleep scoring algorithms [4]. In animal studies, cortical electrodes are chronically implanted and securely attached to the skull using invasive techniques for sleep monitoring [5]. In human applications, setups range from full laboratory configurations to portable devices with a limited number of electrodes, providing flexibility for various research contexts [6].

Theoretically, EEG can differentiate between the stages of slow-wave sleep: theta waves are prominent during SWS stage 1, sleep spindles and K-complexes characterize the transition to SWS stage 2, while high-voltage, slow-frequency delta waves dominate in SWS stage 3. In animal studies, the sleep stages are typically categorized into SWS, REM, and wake states. They are often analyzed using fast Fourier transform techniques to quantify brainwave activity [7].

In this review, we compiled and analyzed data on foods associated with sleep regulation to enhance their understanding and provide a foundation for their development. This review was conducted using a systematic approach, incorporating research articles published between 2004 and 2024.

STUDY OBJECTS AND METHODS

Electroencephalography is a valuable tool for identifying foods and raw materials used in sleep-promoting products, providing critical insights into their effectiveness.

Methods. The data for our systematic review were collected from the electronic databases such as Scopus, PubMed, and Google Scholar as described in Fig. 1.

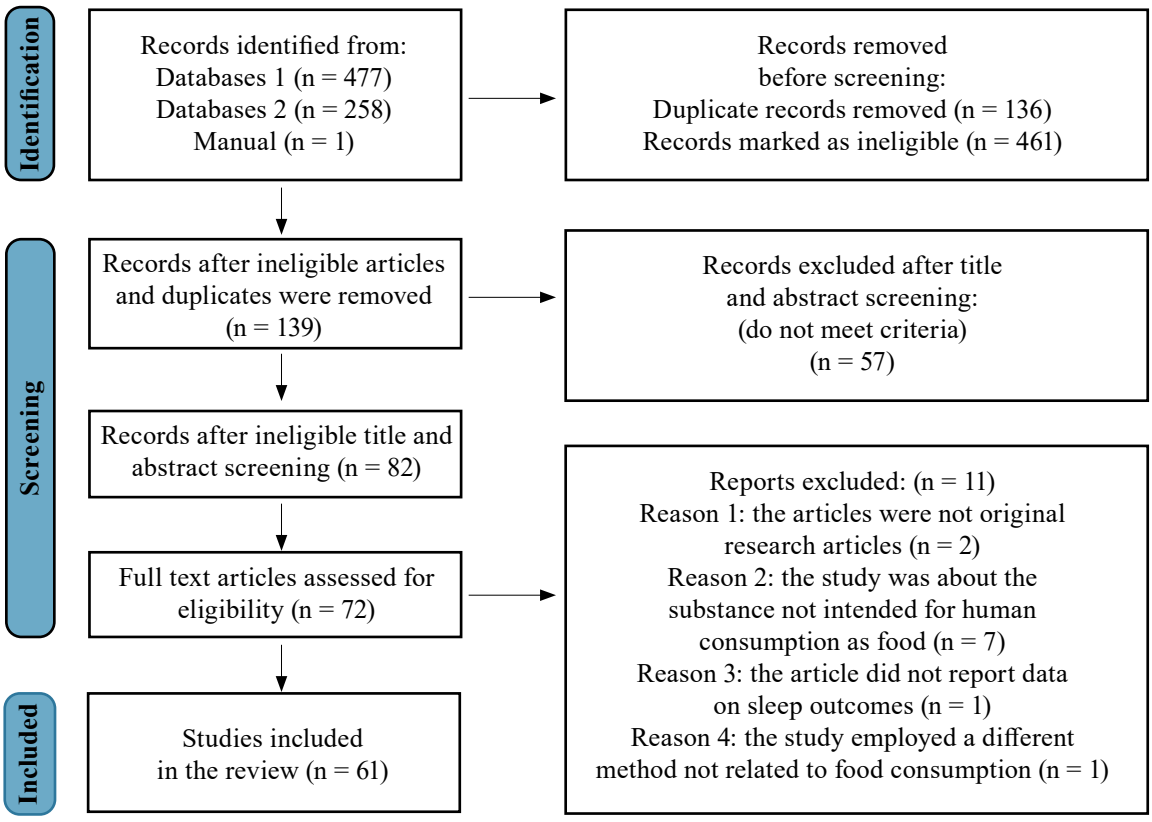


Figure 1 Workflow diagram of the study identification and selection process

Research question. The Preferred Reporting Items for Systematic Reviews and Meta-Analyses extension for systematic scoping reviews was employed as a guideline during the preparation of this review. This approach ensured transparency, rigor, and a structured methodology throughout the review process. Our primary aim was to provide an updated and comprehensive synthesis of evidence addressing the following research question: "How have sleep-related functional foods been studied using electroencephalography?"

Search strategy. To comprehensively address the research question, the study was strategically focused on sensitivity and specificity to identify literature related to food, sleep, and electroencephalography. Three electronic databases – Scopus, PubMed, and Google Scholar – were utilized, with the search conducted by two independent reviewers (A. Sattayakhom & P. Koomhin) on October 30, 2024. The search strategy was "food*" + "electroencephalogra*" + "sleep" or "food" + "electroencephalography" + "sleep". The search was limited to the articles published until 2024. After the initial acquisition, the studies were further screened. EndNote 20 (PDFNet SDK © PDFTron™ Systems Inc., 2001–2020, distributed by Clarivate Analytics (US) LLC under license) was used for importing and managing the references.

Study selection. To ensure data integrity, EndNote was employed for the identification and removal of duplicate studies. Two reviewers (A. Sattayakhom & P. Koomhin) independently checked the titles for eligibility. Then, three reviewers (A. Sattayakhom, P. Koomhin, and N. Matan) independently assessed the titles and abstracts of all the studies, applying the predetermined inclusion and exclusion criteria. Full texts of the selected studies were then retrieved and thoroughly reviewed. We included original research articles investigating the effects of functional foods on sleep, regardless of electroencephalography use. The articles excluded were those which studied substances not intended for human consumption, lacked sleep-related outcomes, or did not utilize electroencephalography. Disagreements during the selection process were resolved through discussions and mutual agreement among the three reviewers.

Data charting process. Three reviewers (A. Sattayakhom, P. Koomhin, and N. Matan) independently extracted data using a standardized form in Microsoft Excel, including the author, year, country, substance and food type, subject characteristics, study design, intervention, and outcomes. Disagreements were resolved through discussion and consensus among the reviewers. Tables summarizing the characteristics of included studies were created to present the findings of the selected studies.

RESULTS AND DISCUSSION

General findings and characteristics of the studies. A total of 61 publications were included in the review. Their analysis showed a strong regional focus in East Asia, with the Republic of Korea and Japan collectively contributing 62.30% of the total research entries. Specifically, the Republic of Korea accounted for 37.70% (23 entries), while Japan contributed 24.59% (15 entries), underscoring their substantial involvement in food and sleep research utilizing electroencephalography (EEG). The foods reported in the research papers were classified based on their purpose, origin, function, nutritive value, and functional properties. They were then grouped into six categories: essential oils, Chinese herbal medicines, plant and fungi extracts, tea and cocoa, probiotics and prebiotics fermented foods, and food supplements. Our analysis revealed that plant and fungi extracts, as well as Chinese herbal medicines, were the most frequently studied ingredients, collectively accounting for 52.46% of the total research entries, namely 29.51% (18 occurrences) for plant and 22.95% (14 occurrences) for fungi extracts. This highlights a global focus on natural and botanical products, particularly in Korea and Japan. Probiotics and prebiotics fermented foods accounted for 14.75% (9 occurrences), with Japanese research dominating in the field of traditional fermentation techniques. Essential oil compounds made up 13.11% (8 occurrences), with Thailand contributing 75.00% (6 occurrences), showcasing the country's expertise in aromatic and culinary applications. Other categories, including food supplements (9.84%) and tea and cocoa (9.84%) contributed equally to the overall study, representing a blend of niche and generalized contributions.

The studies utilized a diverse array of experimental models, with animal and human subjects accounting for 77.42 and 22.58% of the total research entries, respectively. Among the animal models, commonly used species included Institute's of Cancer Research (ICR) mice, Wistar rats, Sprague-Dawley rats, and C57BL/6N mice. These models were employed to investigate various sleep mechanisms, such as pentobarbital-induced sleep, caffeine-induced insomnia, and both acute and chronic sleep disorders. Human studies were characterized by rigorous methodologies, frequently employing double-blind, placebo-controlled, or randomized crossover designs. These studies encompassed a wide range of demographic groups, including healthy adults, individuals with poor sleep quality, and specific occupational populations. This multifaceted approach highlights the comprehensive scope of research on the effects of sleep-related food products across diverse biological and contextual settings.

Advantages of electroencephalography in analyzing food-related sleep studies. EEG has demonstrated its utility in examining the relationship between food intake and sleep. The studies included in this review predominantly consisted of animal (~ 80%) and human (~ 20%) models. The animal studies were further categorized into those involving normal animals and those with induced sleep disorders. The common inductions of sleep disorders included pentobarbital-induced sleep, caffeine-induced insomnia, and ACTH-induced (stress-induced) sleep disturbances. Animal studies offer some advantages, such as the ability to assess the toxicity of unknown substances and explore underlying mechanisms. Notable examples of such research include the studies on crude extracts of tea, cocoa, plant and fungi extracts, and herbal products (Table 1).

Table 1 Characteristics of EEG studies of food types influencing sleep function

Authors, year	Country	Substance	Subject/model	Intervention	Reference
Essential oils (8 entries)					
Cheaha *et al*., 2016	Thailand	Vetiver	Wistar rats (male; 300–350 g, 3 months old)	Vetiver essential oil inhalation for 1 h (inhalation chamber)	[30]
Koomhin *et al*., 2020	Thailand	*Michelia* × *alba* DC.	Healthy adult subjects (male and female, aged 19–25 y.o., sleep more than 6 h prior to the test day)	Inhalation of 50 µL of undiluted *Michelia* × *alba* DC. oil on a filter paper	[24]
Chandharakool *et al*., 2020	Thailand	Tangerine	Healthy adult subjects (male and female, aged 19–25 y.o., sleep more than 6 h prior to the test day)	Inhalation of 25 µL of essential oil that contains a tangerine essential oil concentration of 1:1,000 dilution (spotted on a filter paper)	[25]
Kwangjai *et al*., 2021	Thailand	*Citrus reticulata* Blanco cv. Sai-Nam-Phueng	Wistar rats (male; adult, 300–350 g)	Inhalation of 200 µL of *Citrus reticulata* Blanco on cotton wool put on saw dust in the rats' home cage inside a soundproof chamber	[26]
Ko *et al*., 2021	Taiwan	*Lavandula angustifolia* Mill.	Healthy, right-handed volunteers (mean age 22 ± 2 years)	Inhalation of *Lavandula angustifolia* Mill. essential oil repeatedly released starting from 1.5 h after bedtime to 1.5 h before the waking	[27]
Zhou *et al*., 2023	China	Anshen essential oil (tangerine peel, rose, atractylodes, lavender, etc.)	ICR mice (male; 6–8 weeks old, 25–35 g); Sprague-Dawley rats (half male and half female; female weight 150–180 g, male weight 200–220 g)/pentobarbital-induced sleep; 10 subjects with poor sleep quality or insomnia (male; aged 20–40 y.o., weight 60–75 kg, height 1.68–1.82 m, without any disease)/self-controlled experiment	The mice sniffed essential oil in an aromatherapy room for 1 h every day for 7 consecutive days; The human subjects were exposed to essential oil from 22:00 on the first night to 7:00 the next morning for 3 consecutive nights	[31]
Cheaha *et al*., 2023	Thailand	Jasmine	ICR mice (male; weighing between 25 and 45 g)	Orally administered jasmine oil (10 mL/kg body weight)	[28]
Sinthupachee *et al*., 2024	Thailand	Smoke-dried fish hydrolysates with *Litsea cubeba* (Lour.) Pers. vapor	Twelve non-smoking volunteers (six males and six females) aged 20–45 years	Oral administration: 60 µL of fish protein hydrolysates was placed directly into the subject's mouth and chewed quickly	[29]
Chinese herbal medicine (14 entries)					
Choi *et al*., 2014	Republic of Korea	*Gastrodiae rhizoma*	ICR mice (4 weeks old) and Sprague-Dawley rats (8 weeks old)/pentobarbital-induced sleep	Oral administration (25, 50, and 100 mg/kg)	[40]
Abdollahnejad *et al*., 2016	Iran	*Amygdalus communis* L. (almond)	Wistar rats (male; 250–300 g)/pentobarbital-induced sleep	Intraperitoneal injection of almond extract (100, 200, and 400 mg/kg)	[42]
Yoo *et al*., 2017	Republic of Korea	*Sinomenium acutum* (Thunb.) Rehder & E.H. Wilson	ICR mice (male; 20–25 g, 4 weeks old) and Sprague-Dawley rats (male; 300–320 g, 8 weeks old)/pentobarbital-induced sleep	Oral administration (20 and 40 mg/kg)	[35]
Woo *et al*., 2017	Republic of Korea	Decursinol angelate from *Angelica gigas* Nakai	ICR mice 20–24 g and Sprague-Dawley rats weighing 220–250 g/pentobarbital-induced sleep	Oral administration (10, 25 and 50 mg/kg)	[33]

Continuation of the Table 1

Authors, year	Country	Substance	Subject/model	Intervention	Reference
Wei *et al*., 2017	China	Stilbene glucoside from *Polygonum multiflorum* Thunb.	Kunming mice (three-week old)	Intravenous injection (10, 20, 40, and 80 mg/kg/d)	[32]
Kwon *et al*., 2017	Republic of Korea	Rosmarinic acid of *Perilla frutescens* (L.) Britton	ICR mice 20–24 g and Sprague-Dawley rats weighing 220–250 g)/pentobarbital-induced sleep	Oral administration (0.5, 1.0, and 2.0 mg/kg)	[34]
Yoon & Cho, 2018	Republic of Korea	Triphlorethol A found in seaweed (*Ecklonia cava*)	ICR mice (male, 18–22 g) and C57BL/6N mice (male, 27–30 g)/ pentobarbital-induced sleep	Oral administration (50 mg/kg)	[36]
Lin *et al*., 2019	China	*Pinelliae rhizoma praeparatum cum alumine*	SPF C57BL/6J mice 20–25 g (male; 10–12 weeks old)	Intragastric administration (9, 18, and 36 g/kg)	[37]
Yamashiro *et al*., 2020	Japan	Polyherbal formulations	Wistar rats (male; 300–450 g, 8–10 weeks old)	Intraperitoneal administration of herbal extract (15 mL/kg)	[43]
Martinez-Mota *et al*., 2021	Mexico	*Calea zacatechichi* Schltdl.	Swiss Webster mice (male; adult, 20–30 g) and Wistar rats (male; adult, 250–300 g)	Oral administration (50, 100, or 1,000 mg/kg, in a constant volume of 10.0 mL/kg for mice, and 2.0 mL/kg for rats)	[44]
Murthy *et al*., 2022	India	Ashwagandha (*Withania somnifera* (L.) Dunal)	Swiss albino mice (male; 25–30 g) and Wistar rats (both sexes; 195–225 g)/pentobarbital-induced sleep	Intraperitoneal administration of a single acute dose of test substances (5, 25, and 50 mg/kg)	[38]
Miyazaki *et al*., 2022	Japan	*Eurycoma longifolia* Jack (*Tongkat ali*)	C57BL/6N mice (male)	Oral administration: the mice had a diet mixed with extract final ratios of 0.25, 0.5, and 0.75% (w/w)	[39]
Hua *et al*., 2022	China	*Lonicerae Japonicae* Flos extract	C57BL/6J mice (male; 8–12 weeks old, weighting 20–25 g)	Intragastric administration (100 mg/kg)	[41]
Park *et al*., 2023	Republic of Korea	Ashwagandha root	ICR mice (male; 28–30 g, 6 weeks old) and Sprague-Dawley rats (male; 180–200 g, 6 weeks old)/caffeine-induced insomnia/ pentobarbital-induced sleep	Oral administration (80 mg/kg)	[14]
Plant and fungi extracts (18 entries)					
Yoon *et al*., 2014	Republic of Korea	*Ecklonia* cava ethanol extract	C57BL/6N mice (male; 27–30 g; 12 weeks old)/pentobarbital-induced sleep	Oral administration (100, 250, or 500 mg/kg)	[54]
Yamatsu *et al*., 2015	Japan	GABA and AVLE	Sixteen subjects (7 males and 9 females with PSQI scores of 6 or more, average age 36.8 ± 8.9)	Oral administration of gelatin capsules containing GABA (100 mg of GABA and 50 mg of dextrin) or AVLE (50 mg of AVLE and 100 mg of dextrin) or GABA (100 mg) and AVLE (50 mg)	[12]
Uchida *et al*., 2016	Japan	Mycelial extract of cultured *Cordyceps sinensis* extract	Sprague-Dawley rats (male; 250–300 g)	Oral administration of *Cordyceps sinensis* extract (1 g/kg)	[58]
Abdollahnejad *et al*., 2016	Iran	*Aloe vera* (L.) Burm.f. extract	Wistar rats (male; 250–300 g)/ pentobarbital-induced sleep	Intraperitoneal injection of *Aloe vera* (L.) Burm.f. aqueous extract (50, 100, and 200 mg/kg)	[42]
Kwon *et al*., 2017	Republic of Korea	*Perillae herba* ethanol extract	ICR mice and Sprague-Dawley rats/pentobarbital-induced sleep	Oral administration (12.5, 25, and 50 mg/kg)	[34]
Hong *et al*., 2018	Republic of Korea	RE, SE and their mixture	ICR mice (male, 4 weeks) and Sprague-Dawley rats (male, 8 weeks)/pentobarbital-induced sleep	Post-oral injection of RE (80, 100, 120, 140, and 160 mg/kg), SE (40, 50, 80, 100, and 120 mg/kg), and a combination of RE/SE (40, 100, and 120 mg/kg)	[50]

Continuation of the Table 1

Authors, year	Country	Substance	Subject/model	Intervention	Reference
Rahimi *et al*., 2019	Iran	Hydroalcoholic tarooneh extract (spathe of phoenix dactylifera; a hard-covering envelope of male date palm)	Wistar rats (male; 270 ± 20 g)	Intraperitoneal injection of tarooneh extract (62.5, 125, and 250 mg/kg)	[53]
Kim *et al*., 2019	Republic of Korea	Green romaine lettuce extract	ICR mice and Sprague-Dawley rats/pentobarbital-induced sleep	Oral administration (80, 100, 120, and 160 mg/kg)	[13]
Takeda *et al*., 2020	Japan	Saffron extract	Healthy Japanese adults (male and female; aged 20–64 y.o.)	Oral administration of one tablet (6.6 μg of safranal and 0.66 mg of crocin) per day	[45]
Li *et al*., 2021	Taiwan	*Hericium erinaceus* mycelium	C57BL/6 mice	Oral administration (75 and 150 mg/kg)	[56]
Li *et al*., 2021	Taiwan	*Armillaria mellea* (Fr.) P. Karst. mycelia	Sprague-Dawley rats (male; 8 weeks old, 250–300 g)	Oral administration of *Armillaria mellea* (Fr.) P. Karst. aqueous and ethanolic extract (75 and 150 mg/kg)	[55]
Kim *et al*., 2021	Republic of Korea	Quercetin-3-o-glucuronide in the ethanol extract of lotus leaf	Male ICR mice and Sprague-Dawley rats/pentobarbital-induced sleep/caffeine-induced insomnia model	Oral administration of ethanolic lotus leaf extract (150 [LLE] and 300 [HLE] mg/kg) 1 h before the analysis	[47]
Jo *et al*., 2021	Republic of Korea	Green lettuce leaf extract	Drosophila Canton-S strain, Sprague-Dawley rats, and ICR mice (male; 6 weeks old)/pentobarbital-induced sleep	Drosophila was treated with green lettuce leaf extract (0.5 and 1.0%), each concentration added to 5% sucrose and 2% agar media and exposed for nine days. In mice: oral administration (80, 120 mg/kg)	[51]
Kim *et al*., 2022	Republic of Korea	*Poria cocos* (Schw.) Wolf extract	ICR mice (male; 7 weeks old, 20–23 g) and Sprague-Dawley rats (male; 8 weeks old, weighing 180–190 g)/pentobarbital-induced sleep, caffeine-induced sleep disturbance, ACTH-induced sleep disorder	Oral administration of *Poria cocos* (Schw.) Wolf extract (10, 20, 40, 80, 160, and 320 mg/kg)	[57]
Kim *et al*., 2022	Republic of Korea	Green kiwifruit peel ethanol extract	C57BL/6N mice (male; 27–30 g)/pentobarbital-induced sleep	Oral administration of green kiwifruit peel ethanol extract (250, 500, and 1,000 mg/kg/day)	[18]
Ahn *et al*., 2022	Republic of Korea	Lotus rhizome extract	ICR mice (male; 5 weeks old, 20 ± 2 g) and Sprague-Dawley rats (male; 8 weeks old, 180 ± 20 g)/pentobarbital-induced sleep	Oral administration of lotus rhizome extract (120 or 150 mg/kg)	[46]
Kim *et al*., 2023	Republic of Korea	*Chrysanthemum* × *morifolium* var. *gracile* Hemsl. 50% ethanol extract	ICR mice (male; 32–35 g) and Sprague-Dawley rats (male; 280–300 g)/pentobarbital-induced sleep	Oral administration of *Chrysanthemum* × *morifolium* var. *gracile* Hemsl. 50% ethanol extract (50, 100, and 200 mg/kg)	[17]
Ahn *et al*., 2023	Republic of Korea	Heukharang lettuce leaf extract	ICR mice (male; 6 weeks old, 30 g) and Sprague-Dawley rats (male; 5 weeks old, 130 g)/pentobarbital-induced sleep	Oral administration of Heukharang lettuce leaf extract (50, 80, 100, and 150 mg/kg)	[49]
Tea and cocoa (6 entries)					
Panagiotou *et al*., 2019	The Netherlands	Caffeine	C57BL/6JOlaHsd mice (male; 12 weeks old)	Oral administration of 6 mL per day of caffeine containing water (0.8 mg/mL caffeine (0.08%))	[59]
Kwon *et al*., 2019	Republic of Korea	Phlorotannin (brown seaweed polyphenol) supplement	C57BL/6N (male, 27–30 g, 11 weeks old)/caffeine-induced sleep disruption	Oral administration of phlorotannin supplement (500 mg/kg)	[61]

Continuation of the Table 1

Authors, year	Country	Substance	Subject/model	Intervention	Reference
Kim *et al*., 2019	Republic of Korea	GABA and L-theanine	ICR mice (male; 4 weeks old, 18–20 g) and Sprague-Dawley rats (male; 8 weeks old, 160–180 g)/pentobarbital-induced sleep	Oral administration of GABA (60, 80, and 100 mg/kg), L-theanine (20, 30, and 40 mg/kg), or both (GABA/L-theanine) (80/20, 80/30, 100/20, and 100/30 mg/kg)	[13]
Oishi *et al*., 2020	Japan	Natural cocoa seed powder	C3 H/HeN mice (male; 5 weeks old)/chronic sleep disorders model	Dietary cocoa consumption (containing 2.0% natural cocoa)	[62]
Kim *et al*., 2023	Republic of Korea	Green tea ethanol extract and caffeine	C57BL/6N mice (11 weeks old)	Oral administration of green tea ethanol extract (1,500 mg/kg) and caffeine (25 mg/kg)	[60]
Baba *et al*., 2023	Japan	L-theanine	University students (female; aged 21.3 ± 0.5, BMI 21.6 ± 2.2)/a single-dose, four-treatment double-blind, crossover design	Oral administration of drinks containing caffeine (30 mg), theanine (50 mg), or both; caffeine and theanine were mixed in 200 mL of deionized water, adjusted to have the same taste and aroma as placebo drinks and dispensed in cans of the same shape	[22]
Probiotics and prebiotics fermented foods (9 entries)					
Miyazaki *et al*., 2014	Japan	Heat-killed *Lactobacillus brevis* SBC8803	C3H-HeN mice (male; 6 weeks old)/pentobarbital-induced sleep	Oral administration of a diet supplemented with 0.5% heat-killed SBC8803	[63]
Nakamura *et al*., 2016	Japan	Japanese sake yeast (*Saccharomyces cerevisiae* sake)	C57BL/6N strain mice (male; 23–27 g, 8 weeks old)	Oral administration of sake yeast (100, 200, and 300 mg/kg)	[15]
Monoi *et al*., 2016	Japan	Sake yeast	68 Japanese volunteers (weekday full-time employees; 35 female and 33 male; aged 38.2 ± 1.1 years, with PSQI scores > 6 (averaging 6.8 ± 0.2))	Oral administration of 4 tablets (125 mg sake yeast powder per tablet) per day for 4 days 1 h before bedtime	[66]
Yamatsu *et al*., 2015	Japan	GABA	10 Japanese volunteers (6 male and 4 female; average age: 37.7 ± 11.5 years, age range: 24–57 years; with PSQI scores of 6 or more)	Oral administration of 100 mg GABA in a gelatin capsule	[12]
Thompson *et al*., 2017	USA	Prebiotics (galactooligosaccharides and polydextrose), lactoferrin, and milk fat globule membrane	F344 rats (adult males; 40–50 g at arrival, post-natal day 24)	Oral administration of a diet supplemented with prebiotics, lactoferrin, and milk fat globule membrane for four weeks	[64]
Nakagawa *et al*., 2018	Japan	Lactic acid bacteria-containing food (900 mg of fermented products of LBH_MIKI-020, 200 mg of live lactic acid bacteria powder, 200 mg of ground lactic acid bacteria powder, and 200 mg of theanine in a daily amount)	Men and women aged 20–64 years who have a problem with everyday sleep/a placebo-controlled, double-blinded, randomized crossover study	Oral administration of 8 tablets (total 4.8 g) of the lactic acid bacteria-containing food daily	[23]
Higo-Yamamoto *et al*., 2019	Japan	Heat- killed *Lactobacillus brevis* SBC8803	C3H/HeN mice (male; 5 weeks old)	Oral administration of a diet supplemented with 0.5% heat-killed SBC8803 for 6 weeks	[65]
Nedachi *et al*., 2021	Japan	Lactic-fermented barley GABA, lafma extract, vitamin B_{12}, and vitamin B_6	Healthy middle-aged females (40–64 years after menopause with lower sleep quality)/randomized, double-blind, placebo-controlled, parallel intergroup comparison study	Oral administration, with water, 30–60 min before sleep, with no chewing, for 4 weeks (main ingredients: lactic-fermented barley GABA (120 mg), lafma extract (50 mg), 0.1% vitamin B_{12} (3 mg), and vitamin B_6 (1.5 mg))	[75]

Continuation of the Table 1

Authors, year	Country	Substance	Subject/model	Intervention	Reference
Bae *et al*., 2023	Republic of Korea	ZW, ZW-AT, ZW-EH, and ZW-FM	ICR mice (male; 5 weeks old, 25–27 g)/pentobarbital-induced sleep	Oral administration of ZW (150 and 200 mg/kg), ZW-AT (150 and 200 mg/kg), ZW-EH (150 and 200 mg/kg), and ZW-FM (50, 80, 100, 150, and 200 mg/kg)	[68]
Food supplements (6 entries)					
Minet-Ringuet *et al*., 2004	France	Dietary regimens varying in terms of the protein amount (14 versus 30%) or quality (milk protein or alpha-lactalbumin)	Wistar rats (male)	Oral administration with diet (3 regimens: P14 (140 g/kg whole milk protein), P30-WMP (300 g/kg whole milk protein), and P30-LAC (P30 + alpha-lactalbumin > 40%))	[69]
Ta *et al*., 2015	Republic of Korea	Blue mussel water extracts	ICR mice (male, 18–22 g)/pentobarbital-induced sleep	Oral administration (125, 250, 500, 1,000 and 1,500 mg/kg)	[74]
Cherasse *et al*., 2015	Japan	Zinc-containing yeast extract	C57BL/6 strain mice (male; 23–27 g, 11–13 weeks old)	Oral administration of zinc-containing yeast extract (40 and 80 mg/kg/10 mL/kg)	[72]
Halson *et al*., 2020	Australia	Tart cherry juice, high GI CHO, α-lactalbumin, adenosine-5-monophosphate, valerian, and theanine	Healthy males (age: 27.4 ± 6.2 years; weight: 83.2 ± 11.5 kg; height; 181.2 ± 6.7 cm)/double-blind, placebo-controlled cross-over experimental design	Oral administration of a dietary supplement (a combination of tart cherry juice (0, 50, 100 mL), high GI CHO (0, 25, 50 g), α-lactalbumin (0, 20, 40 g), adenosine-5-monophosphate (0, 26.5, 53 mcg), valerian (0, 750, 1,500 mg), and theanine (0, 500, 1,000 mg))	[70]
Thiagarajah *et al*., 2022	Malaysia	α-s1-casein tryptic hydrolysate and L-theanine	Human subjects (aged 37.3 ± 8.4 years)	Oral administration of a supplement containing 150 mg α-s1-casein tryptic hydrolysate and 50 mg L-theanine in the same capsule	[71]
Ye *et al*., 2023	Republic of Korea	*Glycine max* (L.) Merr. extract and genistein	Sprague-Dawley rats (8 weeks old)/pentobarbital-induced sleep	Oral administration of *Glycine max* (L.) Merr. extract (400 mg/kg) and genistein (30 mg/kg)	[73]

ICR – Institute of Cancer Research; GABA – γ-aminobutyric acid; AVLE – *Apocynum venetum* L. leaf extract; PSQI – Pittsburgh Sleep Quality Index; RE – romaine lettuce leaves extract; SE – skullcap root extract; ZW – jujube seed water extract; ZW-AT – jujube seed water extract – alcohol treated; ZW-EH – jujube seed water extract – enzyme hydrolysate; ZW-FM – jujube seed water extract – fermented product

Sleep disorder models are used to examine differences in sleep physiology and mechanisms between normal and disrupted sleep. In clinical settings, various pharmacological treatments, such as barbiturates, are prescribed to patients with sleep disorders. Therefore, identifying adjunctive therapies that enhance the efficacy of these treatments is crucial. For disorders such as caffeine-induced or stress-induced sleep disturbances, interventions tailored to the specific disorder are more effective.

Human studies involve both healthy individuals and those with poor sleep quality. While animal studies commonly employ invasive EEG and electromyography (EMG) with implanted electrodes, human studies typically rely on non-invasive methods. Quantitative sleep staging analysis is often conducted using either manual or automated scoring systems. Certain software can analyze sleep stages, such as wakefulness, slow-wave sleep (SWS) and rapid eye movement (REM), without the need for EMG data. However, some methods require EMG signals from the nuchal muscles to distinguish between wakefulness and REM sleep. Both qualitative and quantitative assessments are commonly used in human studies, with the Pittsburgh Sleep Quality Index frequently utilized for qualitative evaluation.

Sleep parameters typically measured in these studies include wakefulness, sleep latency, REM latency, wake time after sleep onset, total sleep time, time spent in bed, and sleep efficiency [7]. Noteworthily, the definitions of these parameters may vary between the studies, as presented in Table 2. Although we adopted a simplified approach to categorizing sleep parameters to facilitate screening across the studies, experimental details should be carefully considered when interpreting the results.

Table 2 Primary objective sleep outcomes

Author, year	Intervention	Species	Outcomes	References
Minet-Ringuet *et al*., 2004	Tryptophan-rich protein diet	Rats	– increased SWS	[69]
Choi *et al*., 2014	*Gastrodiae rhizoma* ethanol extract	Mice	– shortened sleep latency – increased total sleep time – decreased sleep/wake cycles	[40]
Yoon *et al*., 2014	*Ecklonia cava*	Mice	– increased SWS	[54]
Miyazaki *et al*., 2014	Dietary heat-killed *Lactobacillus brevis* SBC8803	Mice	– reduced wakefulness – increased SWS	[63]
Yamatsu *et al*., 2015	– Oral GABA – *Apocynum venetum* L. leaf extract	Human	– shortened sleep latency – increased SWS	[12]
Ta *et al*., 2015	Blue mussel water extracts	Mice	– shortened sleep latency – increased SWS – increased total sleep time	[74]
Cherasse *et al*., 2015	Zinc-containing yeast extract	Mice	– increased SWS	[72]
Yamatsu *et al*., 2015	Oral GABA	Human	– shortened sleep latency – increased SWS	[12]
Uchida *et al*., 2016	Mycelial extract of cultured *Cordyceps sinensis*	Rats	– reduced wake after sleep onset – increased SWS	[58]
Nakamura *et al*., 2016	Japanese sake yeast	Mice	– increased SWS	[15]
Monoi *et al*., 2016	Japanese sake yeast	Human	– increased delta wave power	[66]
Cheaha *et al*., 2016	Vetiver essential oil inhalation	Rats	– increased waking period – reduced SWS	[30]
Abdollahnejad *et al*., 2016	*Aloe vera* (L.) Burm.f. aqueous extract	Rats	– increased SWS – decreased REM – increased total sleeping time	[42]
Abdollahnejad *et al*., 2016	*Amygdalus communis* L. extract	Rats	– increased total sleep time – increased sleep/wake cycles	[42]
Yoo *et al*., 2017	Sinomenine	Mice	– shortened sleep latency – increased total sleep time	[35]
Woo *et al*., 2017	Decursinol angelate	Mice	– increased total sleep time – decreased sleep/wake cycles	[33]
Wei *et al*., 2017	Stilbene Glucoside (*Polygonum multiflorum* Thunb.)	Mice	– reduced wake after sleep onset – increased SWS – reduced REM – increased total sleep time	[32]
Thompson *et al*., 2017	Dietary prebiotics and bioactive milk fractions	Rats	– increased SWS	[64]
Kwon *et al*., 2017	Rosmarinic acid	Mice	– shortened sleep latency – increased total sleep time – increased number of falling asleep	[34]
Kwon *et al*., 2017	Ethanol extract of *Perillae herba*	Mice	– increased SWS – increased total sleep time – decreased sleep/wake cycles	[48]
Yoon & Cho, 2018	Triphlorethol A	Mice	– shortened sleep latency – increase total sleep time	[36]
Nakagawa *et al*., 2018	Lactic acid bacteria-containing foods	Human	– increase total sleep time	[23]
Hong *et al*., 2018	Romaine lettuce/skullcap mixture	Mice	– increased SWS – increase total sleep time	[50]
Rahimi *et al*., 2019	Hydroalcoholic tarooneh extract	Rats	– increased delta wave power – decreased alpha and beta wave power – increased total sleep time	[53]
Panagiotou *et al*., 2019	Chronic caffeine consumption	Mice	– increased SWS	[59]
Lin *et al*., 2019	*Pinelliae Rhizoma Praeparatum Cum Alumine* extract	Mice	– reduced wakefulness – increased SWS – increased REM	[37]
Kwon *et al*., 2019	A standardized phlorotannin supplement	Mice	– increased sleep latency – decreased SWS	[61]

Continuation of the Table 2

Author, year	Intervention	Species	Outcomes	References
Kim *et al*., 2019	GABA and L-theanine mixture	Mice	– shortened sleep latency – increase total sleep time	[13]
Kim *et al*., 2019	Green Romaine lettuce (*Lactuca sativa* L.)	Rats	– increased SWS – reduced REM	[52]
Higo-Yamamoto *et al*., 2019	Dietary heat-killed *Lactobacillus brevis* SBC8803	Mice	– increased SWS – reduced REM	[65]
Yamashiro *et al*., 2020	Polyherbal formulation	Rats	– reduced total sleep time	[43]
Koomhin *et al*., 2020	Michelia essential oil	Human	– reduced wakefulness	[24]
Takeda *et al*., 2020	Saffron-derived Crocin and Safranal	Human	– shortened sleep latency – increased SWS – reduced wake after sleep onset	[45]
Oishi *et al*., 2020	Dietary natural cocoa	Mice	– increased SWS	[62]
Chandharakool *et al*., 2020	Tangerine essential oil	Human	– shortened sleep latency	[25]
Halson *et al*., 2020	Nutritional intervention	Human	– shortened sleep latency	[70]
Martinez-Mota *et al*., 2021	*Calea zacatechichi* Schltdl. (Compositae)	Rats	– increased SWS	[44]
Nedachi *et al*., 2021	GABA and lafma	Human	– increased delta power	[75]
Kim *et al*., 2021	Quercetin-3-O-glucuronide in the ethanol extract of lotus leaf	Mice	– increased SWS – reduced REM – increased total sleep time	[47]
Jo *et al*., 2021	Green lettuce leaf extract	Rats	– increased SWS – reduced REM – increased total sleep time	[51]
Li *et al*., 2021	*Armillaria mellea* (Fr.) P. Karst. mycelia	Rats	– increased SWS – increased REM	[55]
Kwangjai *et al*., 2021	*Citrus reticulata* Blanco. cv. Sai-Nam-Phueng essential oil	Rats	– shortened REM sleep latency – increased REM sleep time – increased SWS and REM episodes	[26]
Li *et al.*, 2021	*Hericium erinaceus* mycelium	Mice	– increased SWS – reduced REM	[56]
Ko *et al*., 2021	Essential oil aroma (lavender aroma)	Human	– increased delta wave power	[27]
Thiagarajah *et al*., 2022	Alpha-S1-casein tryptic hydrolysate and L-theanine	Human	– increased total sleep time	[71]
Kim *et al.*, 2022	Green kiwifruit peel extract	Mice	– shortened sleep latency – increased SWS	[18]
Hua *et al*., 2022	*Lonicerae Japonicae* Flos extract	Mice	– shortened sleep latency – increased SWS – increased REM	[41]
Murthy *et al*., 2022	Hydroalcoholic extract of ashwagandha	Rats	– shortened sleep latency – increased total sleep time	[38]
Ahn *et al*., 2022	Lotus (*Nelumbo nucifera* Gaertn.) rhizome water extract	Mice	– increased SWS – increased total sleep time – increased theta and delta wave powers	[46]
Miyazaki *et al*., 2022	*Eurycoma longifolia* Jack extract	Mice	– increased SWS – increased REM – increased delta wave power – reduced wakefulness during the dark period	[39]
Kim *et al*., 2022	*Poria cocos* (Schw.) Wolf extract	Mice	– shortened sleep latency – increased SWS – increased total sleep time	[57]
Cheaha *et al*., 2023	Jasmine essential oil	Mice	– reduced wake after sleep onset – increased SWS	[28]
Ahn *et al*., 2023	Heukharang lettuce (*Lactuca sativa* L.) leaf extract	Mice	– reduced wake after sleep onset – increased SWS – increased REM – increased delta wave power – increased total sleep time	[49]

Continuation of the Table 2

Author, year	Intervention	Species	Outcomes	References
Ye *et al*., 2023	*Glycine max* (L.) Merr. extract (functional food)	Rats	– reduced awakening time – increased SWS – increased REM	[73]
Bae *et al*., 2023	Water extract from Jujube (*Zizyphus jujuba* Mill.) seeds	Mice	– shortened sleep latency – increased SWS – increased delta wave power – increased total sleep time	[68]
Kim *et al*., 2023	Green tea ethanol extract	Mice	– increased sleep latency – increased wakefulness	[60]
Baba *et al*., 2023	Theanine (non-proteinogenic amino acid found in the leaves of *Camellia sinensis* (L.) Kuntze)	Human	– reduced wake after sleep onset	[22]
Kim *et al*., 2023	*Chrysanthemum* × *morifolium* var. *gracile* Hemsl.	Mice	– increased SWS – reduced wake after sleep onset – increased delta wave power – increased total sleep time	[17]
Park *et al*., 2023	Ashwagandha (*Withania somnifera* L. Dunal) root extract	Mice and Rats	– reduced wake after sleep onset – increased SWS – increased delta wave power – increased total sleep time	[14]
Zhou *et al*., 2023	Anshen essential oil	Mice	– shortened sleep latency – increased total sleep time	[31]

SWS – slow-wave sleep; REM – rapid eye movement; GABA – γ-aminobutyric acid

The sleep-wake system is a complex, interconnected network of wake-promoting and sleep-promoting centers in the brain. Orexinergic neurons are central to regulating arousal and maintaining wakefulness, receiving input from multiple brain regions, including the brainstem, basal forebrain, prefrontal cortex, and hypothalamus [8, 9]. The ventrolateral preoptic nucleus (VLPO) plays a pivotal role in sleep induction and maintenance, with GABAergic neurons projecting to, and inhibiting, wake-promoting centers and thereby facilitating the onset of sleep [10]. According to the circadian rhythm model, the suprachiasmatic nucleus (SCN) sends signals to the VLPO indirectly during the nighttime period to initiate sleep. This sleep-promoting signal is further enhanced by melatonin released from the pineal gland, which increases the SCN's sensitivity to its own sleep-inducing signals [11]. The VLPO is inhibited by wake-promoting neurotransmitters, such as noradrenaline.

The studies examining the effects of foods and beverages on sleep parameters often focus on neurotransmitter systems [12–15], such as the GABAergic, adrenergic, glutamatergic, and serotonergic systems, as well as peripheral neural networks. The GABAergic system is frequently studied as a target. While the central nervous system is often the primary focus, the peripheral nervous system also provides valuable insights into sleep-wake physiology. GABAergic neurons play a crucial role in the mechanism of action of sedative-hypnotic drugs, such as barbiturates, which increase chloride conductance within GABAergic neurons [16].

Recent years have seen a growing interest in the development of natural sleep aids to mitigate the adverse effects of standard pharmacological treatments [17, 18]. While no single drug can perfectly replicate the physiological sleep-wake cycle, combining treatments that extend the benefits of sedative-hypnotic drugs, particularly during the SWS and REM stages, holds promising therapeutic potential. Although there is no evidence that oral γ-aminobutyric acid (GABA) supplementation crosses the blood-brain barrier, studies suggest that GABA intake can reduce stress and anxiety, promote relaxation, and stimulate the parasympathetic nervous system and enteric nervous system [19]. As such, GABA is considered a key ingredient in functional foods aimed at enhancing sleep. Several substances can increase central GABA levels by upregulating glutamic acid decarboxylase, benefiting both central and peripheral mechanisms [12, 17].

Another key neurotransmitter system involved in sleep regulation is the adrenergic system. Following prolonged wakefulness, adenosine triphosphate is metabolized into adenosine, which, at high levels, stimulates the adenosine A_{2A} receptor, promoting sleep onset in accordance with the homeostatic theory of sleep [20]. Caffeine blocks this receptor, thus increasing alertness. Consequently, compounds that stimulate this receptor represent potential targets for sleep-promoting agents [21].

The glutamatergic system remains less studied, but emerging evidence suggests that L-theanine may act as an antagonist at the α-amino-3-hydroxy-5-methyl-4-isoxazolepropionic acid receptor, potentially influencing sleep regulation [22]. Serotonergic neurotransmitters also play a role in stress responses and the maintenance of the GABAergic system, contributing to sleep rhythm regulation in some individuals. Additionally, several peripheral targets, such as the peroxisome proliferator-activated receptor alpha and the gut microbiota, have been implicated in the modulation of sleep physiology, offering further avenues for therapeutic intervention [23].

Types of foods related to sleep based on electroencephalography results. The classification of foods related to sleep is based on EEG data, which includes their purpose, origin, function, nutritive value, and functional properties. Foods are categorized into six types: essential oils, Chinese herbal medicines, plant and fungi extracts, tea and cocoa, probiotics and prebiotics from fermented foods, and food supplements.

Essential oils. Essential oils with distinct fragrances are widely used as food flavor ingredients due to their diverse properties. Their aroma often reflects the raw materials from which they are derived and thereby contributes to acceptable flavors in various food products. Numerous studies have shown that essential oils can influence human sleep by modulating alpha, beta, delta, and theta waves (Table 1). For example, *Michelia* × *alba* DC. oil reduced wakefulness and increased alpha fast activity, indicating sleep-enhancing effects [24]. Tangerine oil also reduced alpha and beta waves while increasing theta wave power, promoting relaxation and reducing sleep onset latency [25]. Orange oil, containing 75% of d-limonene, significantly increased the frequency and duration of REM sleep, while decreasing sleep onset latency and overall sleep duration [26]. Lavender oil promoted SWS by decreasing alpha wave activity and increasing delta wave activity [27]. Jasmine oil, which influences brain regions responsible for stress and anxiety, induced slow delta and beta oscillations, supporting non-rapid eye movement (NREM) sleep and suggesting its potential as a treatment for anxiety and insomnia [28]. Additionally, *Litsea cubeba* (Lour.) Pers. vapor altered brain waves differently in male and female participants, promoting relaxation in the males and causing heightened alertness in the females [29].

Essential oils extracted from various plant parts, though typically less fragrant than those from specific raw materials, can still significantly impact sleep when inhaled or ingested. For example, *Vetiveria zizanoides* (L.) Nash, an aromatic grass from tropical regions, can stimulate alertness and enhance task performance. Exposure to this oil was associated with REM sleep and a dominant parietal theta wave, with high electromyography activity during wakefulness and its near-absence during REM sleep [30]. Additionally, the key components of *Anshen* essential oil, including (+)-limonene, linalool, and ocimene, were shown to improve sleep duration and increase neurotransmitter levels, such as 5-hydroxytryptamine and GABA, in mice with induced insomnia [31].

Chinese herbal medicine. Chinese herbal medicine (CHM), which is often incorporated into traditional food dishes and herbal products (Table 1), has long been used to treat various diseases and manage insomnia. Typically made from herbs and spices, CHM is prepared as powders or water-based extracts. Recent studies using EEG techniques have provided valuable insights into the effects of CHM on sleep. While most CHM materials are traditionally sourced from Asian countries (primarily China, Republic of Korea, Japan, India, and Iran), similar active compounds from other regions are also utilized. This has supported the development of sleep-promoting products in various countries, including Mexico. Notable CHMs for insomnia include *Polygonum multiflorum* Thunb., which contains stilbene glucoside to improve sleep by reducing wakefulness and REM sleep while enhancing NREM sleep [32]; *Sinomenium acutum* (Thunb.) Rehder & E.H. Wilson, which activates the GABAergic system to improve NREM sleep [33]; and *Perilla frutescens* (L.) Britton, with rosmarinic acid that similarly boosts NREM sleep via the GABAergic system [34]. Traditional remedies such as *Angelica dahurica* (Hoffm.) Benth. & Hook.f. ex Franch. & Sav. (Bai Zhi) stimulate $GABA_A$ receptors, aiding in insomnia relief [35], while brown seaweed extract interacts with $GABA_A$ receptors to promote sleep [36]. Additionally, *Pinellia ternata* (Thunb.) Makino enhances both REM and NREM sleep, reducing wakefulness and sleep interruptions [37].

Extracts from *Withania somnifera* (L.) Dunal (ashwagandha) have shown potential for improving sleep by enhancing brainwave activity, including delta waves. They also support NREM and slow-wave sleep cycles, helping calm the mind and improve sleep quality [14, 38]. Similarly, *Eurycoma longifolia* Jack (*Tongkat ali*) has been found to improve sleep rhythms and increase delta power during NREM sleep, possibly through body temperature regulation, suggesting its potential as a natural remedy for sleep problems [39]. *Gastrodiae rhizoma* extract has also demonstrated sleep benefits by reducing sleep onset time, increasing total sleep duration, and enhancing REM sleep structure [40]. Flower-based extracts used in CHM, such as *Lonicerae Japonicae Flos* (honeysuckle), have been shown to improve sleep by reducing sleep onset time and increasing REM sleep during recovery from sleep deprivation [41]. *Aloe vera* (L.) Burm.f. extract has been reported to positively affect both REM and NREM sleep, extending total sleep time and inducing calming effects [42]. Additionally, *Amygdalus communis* L. (almond extract) enhances sleep duration and NREM sleep, while traditional herbal combinations, such as linden, mulberry, lavandin, butterfly pea, and tulsi, have been studied for their ability to reduce sleep latency and improve sleep quality [43]. Similarly, *Calea zacatechichi* Schltdl., traditionally used in Mexico, exhibits anxiolytic-like effects and promotes sleep stages associated with memory consolidation [44]. These findings highlight the potential of flower- and food-based CHMs as natural alternatives for managing sleep issues.

Plant and fungi extracts. Plant extracts, derived from fruits, roots, flowers, stems, and leaves, contain active compounds and are increasingly used as functional ingredients in food. Mushroom extracts, valued for their flavor in human diets and medicinal properties, have gained attention for improving sleep quality, particularly in oriental countries. This highlights the potential of natural ingredients in promoting better sleep and overall well-being.

Among plant extracts, saffron, derived from the flower of *Crocus sativus* Herb., has demonstrated promising effects on sleep quality by reducing sleep onset time and nighttime awakenings while increasing NREM sleep. These benefits are attributed to its active compounds, crocin and safranal, which enhance sleep quality and rhythm [45]. The ethanol extract of lotus leaf (*Nelumbo nucifera* Gaertn.), particularly quercetin-3-O-glucuronide, improves sleep by interacting with $GABA_A$ receptors, enhancing both sleep quantity and quality [46, 47]. Chrysanthemum extract and its active compound linarin have also shown potential by increasing sleep duration in animal models [17].

Promising sleep benefits are also offered by the plant extracts derived from food by-products, such as kiwifruit peel, lettuce leaves, and aloe vera [42]. Kiwifruit peel ethanol extract increases NREM sleep and reduces sleep latency in a dose-dependent manner [18]. *Perillan herba* and *Heukharang* lettuce (*Lactuca sativa* L.) extracts enhance NREM sleep by interacting with $GABA_A$-BZD receptors [48]. Additionally, GABA supplementation at a dose of 100 mg has been reported to reduce sleep onset by 5.3 min and improve sleep quality [12]. Green lettuce extract (100 mg/kg) increased total sleep time and improved NREM sleep in animal studies, with Heukharang lettuce demonstrating similar effects [49–52]. Date palm extract (125 mg/kg) has been found to improve sleep by increasing delta waves and reducing alpha and beta waves, thus contributing to deep, restful sleep [53]. Additionally, seaweed extracts, such as *Ecklonia cava* ethanol extract, induce NREM sleep without affecting REM sleep, promoting natural physiological sleep [54].

Fungi extracts have also shown promise in managing sleep disorders. *Hericium erinaceus* (honey mushroom) mycelium contains erinacine, which supports nervous system functions and improves both NREM and REM sleep, reducing anxiety and insomnia [55, 56]. *Poria cocos* (Schw.) Wolf (Bokryeong), a sclerotium fungus, enhances slow-wave sleep, reduces sleep latency, and improves sleep structure by activating $GABA_A$ receptors [57]. *Cordyceps sinensis* (Dong Chong Xia Cao) extract alleviated stress-induced sleep disturbances in rats by improving their stress adaptability and sleep restoration within hours [58]. These findings underscore the potential of plant and fungi extracts as natural remedies for improving sleep quality and offering both calming and restorative effects.

Tea and cocoa. Caffeine is one of the most commonly used stimulants in daily life. People consume caffeine through drinks such as coffee and tea. It affects sleep and our internal body clock. Chronic caffeine consumption leads to increased sleep pressure, meaning the body becomes more in need of sleep over time. However, chronic caffeine use can also make some people stay awake longer. In recent years, more people are staying awake to make up for lack of sleep (Table 1). In studies, caffeine has been shown to have different effects depending on how often it is consumed. In the short term, caffeine can make people stay awake, but when consumed long-term, it may increase the body's daily sleep-wake cycle. This means that people may sleep more during the light period and stay awake more during the dark period [59].

Green tea (*Camellia sinensis* (L.) Kuntze) also contains caffeine, like coffee. However, green tea has a relaxing effect due to an amino acid called theanine. Theanine can reduce caffeine's effects on sleep quality [22]. This suggests that drinking green tea may help improve sleep, especially in people who consume a lot of caffeinated beverages [60]. Green tea also contains GABA, an important neurotransmitter that promotes relaxation and sleep. When GABA is combined with theanine, it can improve sleep quality, as shown in studies with mice [13]. Additionally, phlorotannins, a type of polyphenol found in brown seaweed, can promote sleep by affecting the $GABA_A$ receptors. This may help relieve temporary insomnia caused by caffeine consumption [61].

Cacao beans, used in making chocolate and cocoa, are rich in phenolic compounds that may help prevent diseases related to inflammation and stress. Flavonoids in cocoa also have benefits for the brain, improving mood, memory, and learning by activating nitric oxide in blood vessels. Regular consumption of cocoa can help reduce sleep problems caused by stress without affecting sleep patterns under normal conditions [62]. In summary, both green tea and cocoa offer benefits for sleep improvement, with the ability to reduce the negative effects of caffeine and promote relaxation.

Probiotics, prebiotics, and fermented foods. Fermented foods contain probiotic bacteria, such as *Lactobacillus* species, which are commonly used as supplements to improve health, especially by supporting the immune system. Changes in the gut microbiome are linked to sleep patterns in both humans and animals (Table 1). These changes can enhance REM sleep but may also result in poorer overall sleep quality. Additionally, certain peptides from the digestion of protein and the cell walls of intestinal bacteria can enhance NREM sleep. This suggests that sleep and gut health are connected and may influence each other [63]. In a study with men and women aged 20–64, those who had trouble sleeping and took lactic acid bacteria supplements showed improvements in sleep quality. The study, which was placebo-controlled and randomized, suggests that probiotics may be a safe way to improve sleep quality for people dealing with sleep issues [23]. The gut-brain axis refers to the interaction between the brain and the intestines, and food components can influence this system through the gut microbiome. Probiotics, such as *Lactobacillus gasseri*, can interact with the gut environment and provide health benefits, including better sleep quality.

In addition, prebiotic diets, rich in prebiotics and glycoproteins, can influence the gut microbiota and promote the growth of microbial species that help reduce the impact of stress. For example, a diet rich in prebiotics can regulate the sleep and wake cycle both before

and after stress and provide stress-protective effects on daily physiology and the gut microbiota. Consumption of a prebiotic-rich diet has been shown to improve early-life NREM sleep and enhance REM sleep rebound following stress [64]. Fiber mixed with *Lactobacillus brevis* significantly helps restore wakefulness and increases NREM sleep. During the early stages of the inactive period, NREM sleep was significantly improved by the consumption of prebiotics [65].

Many fermented foods are made using probiotics. The use of yeast fermentation, such as in sake or Japanese rice wine, helps promote NREM sleep by activating receptors, which makes it a potential candidate for a supplement to improve sleep quality [15]. This is consistent with reports that drinking sake offers benefits without any adverse effects, with sake yeast supplementation being an effective and safe way to support high-quality, deep sleep [66]. In fermented foods, glucose obtained from the fermentation of starch or from high-glucose beverages contributes to facilitating sleep onset by increasing the excitability of sleep-promoting neurons in the ventrolateral preoptic nucleus. Glucose-induced excitation of the VLPO is thought to be involved in the drowsiness experienced after consuming a high-sugar meal. This new mechanism regulating VLPO neuron activity highlights the close connection between sleep and metabolism [67].

During fermentation, various plant-based raw materials provide nutrients that are beneficial for sleep, such as GABA, an amino acid found in foods such as vegetables, fruits, and fermented products [68]. GABA can be derived from sprouted brown rice, wine fermentation, or from extracts of *Apocynum venetum* L. leaves. GABA plays a crucial role in the central nervous system, significantly shortening sleep latency while increasing NREM sleep duration. It is quickly absorbed, with blood levels peaking 30 min after oral administration before gradually decreasing. The effect of GABA on sleep may be linked to its levels in the bloodstream [12].

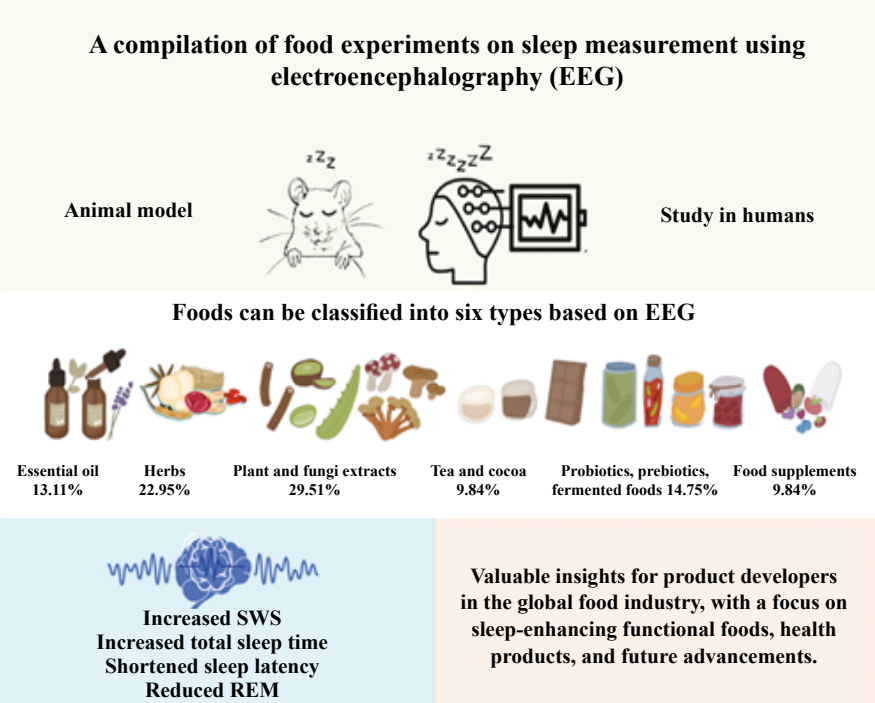
Food supplements. Food supplements are concentrated sources of nutrients, such as vitamins and minerals, or other substances that affect health. They are sold in the form of pills, tablets, capsules, or liquids with measured doses. These supplements may contain a variety of ingredients, including vitamins, minerals, amino acids, essential fatty acids, fiber, and plant or herbal extracts[2]. Some food supplements are linked to improvements in sleep (Table 1). For example, essential amino acids can improve sleep by helping to produce certain neurotransmitters. Tryptophan, a dietary protein, may assist in sleep recovery after re-feeding following a period of calorie restriction. Since tryptophan competes to cross the blood-brain barrier, increasing its levels may help improve sleep efficiency. Milk proteins, plant proteins, or alpha-lactalbumin can also help improve sleep in adults with sleep disturbances caused by nutritional problems, shift work, or fasting during Ramadan [69]. Dietary supplements containing L-theanine (655 mg) and 5′-adenylic acid (53 mcg) have been shown to significantly reduce sleep onset time and could be used to promote natural sleep [70]. A combination of alpha-s1-casein tryptic hydrolysate and L-theanine in working adults with poor sleep quality improved their sleep onset time, sleep duration (by 45 min), sleep efficiency, and daytime functioning, as well as increased their alpha brain waves [71].

Zinc-containing yeast extract (40 and 80 mg/kg) increased the total amount of NREM sleep and reduced locomotor activity in a dose-dependent manner. Zinc, as an essential trace element, has the potential to interact with various synaptic targets, including glutamate and GABA receptors, and modulate their activity [72]. Glycine is a functional food that provides many beneficial phytochemicals. Administration of glycine extract (30 mg/kg) decreased wake time and increased both REM and NREM sleep in environmental prenatal stress-stressed rats [73]. Furthermore, blue mussel (*Mytilus edulis* L.) water extracts produced a dose-dependent reduction in sleep latency and an increase in sleep duration in pentobarbital-treated mice. It decreased sleep latency and induced NREM sleep while maintaining REM sleep [74].

Future prospects of sleep product development. The development of sleep-related food products offers consumers an alternative approach to health care. By utilizing raw materials or food types supported by sleep-related data obtained through EEG, product developers can strategically select ingredients for prototype development. Sleep-inducing products provide individuals seeking improved sleep with a food-based alternative to pharmaceutical medications. The integration of EEG brainwave measurements with raw materials or food types enables the creation of functional foods. While certain foods may offer desirable taste and aroma, they may not necessarily enhance sleep functions. The combination of sensory evaluation with EEG data provides developers with the opportunity to create foods that are not only palatable but also contribute to improved sleep, thereby offering greater benefits to consumers (Fig. 2).

The use of EEG in analyzing raw materials or product types for sleep-inducing foods presents significant potential for real-world product development. EEG facilitates the analysis of brain waves and provides valuable insights into how these products may influence sleep following consumption. Based on available data, raw materials from six distinct food categories, when used within appropriate dose ranges, hold potential for developing sleep-promoting food products. The data suggests that food consumption can influence sleep, with a particular emphasis on SWS and NREM sleep over REM sleep. Several food products, including probiotics, fermented foods, tea, and cocoa, are already available and easily consumable, offering a wide range of options for consumers. In addition, raw materials that contribute to flavor, such as essential oils, can be incorporated into a variety of food products, particularly in Asian cuisines, where foods containing essential oils are commonly consumed.

[2] Food supplements. European Food Safety Authority. 2024 [cited 2024 Dec 5]. Available from: https://www.efsa.europa.eu/en/safe2eat/food-supplements



SWS – slow-wave sleep; REM – rapid eye movement

Figure 2 The role of electroencephalography in the development of sleep-related food products

According to Table 2, many foods and supplements exert a more pronounced effect on SWS than on REM sleep. The development of products that are easy to consume before bedtime, such as beverages or tablets, may help reduce beta waves and increase theta and delta waves, thus facilitating a quicker onset of sleep. While foods affecting REM sleep are less common, certain foods containing Chinese herbal medicines have demonstrated potential effects on sleep. They include *Aloe vera* aqueous extract, stilbene glucoside (*P. multiflorum*), *Pinellia rhizoma*, aluminum extract, lotus extract, *Lonicera japonica* Thunb. extract, and *E. longifolia* extract. These ingredients produce direct therapeutic effects on sleep-related conditions. Notably, these botanical ingredients contain bioactive compounds known to modulate sleep patterns through their sedative, anxiolytic, and anti-inflammatory properties, which may be particularly beneficial for individuals with insomnia or disrupted sleep.

For individuals accustomed to consuming caffeinated beverages, EEG data suggest that tea and cocoa may improve sleep quality. These foods may mitigate the stimulating effects of caffeine when consumed in controlled amounts, particularly in the evening. Therefore, the development of products in this category should focus on optimal dosages to shorten the NREM period and improve overall sleep quality. Incorporating ingredients such as theobromine from cocoa or L-theanine from tea may further enhance sleep-promoting effects by promoting relaxation and reducing sleep onset latency.

The design of sleep-related products must adhere to both international and national regulations regarding the permissible inclusion of sleep-inducing ingredients. It is essential to evaluate the safety and efficacy of these ingredients at specific dosages to ensure their suitability for marketing as food-based sleep aids. These products are a natural and accessible alternative to pharmaceutical sleep medications. This review can provide product developers with valuable insights into the potential of various ingredients tested through EEG analysis, as well as inform the development of novel sleep-related products. Future research should further explore the synergistic effects of different food components on sleep regulation, optimizing formulations that target specific sleep disorders while ensuring both safety and consumer acceptance.

CONCLUSION

The use of electroencephalography can serve as a valuable guideline in the development of sleep-related food products. Electroencephalography can measure the effects of food consumption on sleep, specifically during the slow-wave sleep stages. However, our data suggests that common foods tend to have a stronger impact on enhancing non-rapid eye movement sleep rather than rapid eye movement sleep. The observed changes in brain waves, including reductions in alpha and beta waves and increases in theta and delta waves, provide key insights into the effects of food consumption on sleep. Foods that extend the rapid eye movement stage are primarily Chinese herbal medicines, which are often more therapeutic than conventional food products. Six

sleep-related food categories identified through electroencephalography include essential oils, Chinese herbal medicines, plant and fungi extracts, tea and cocoa, probiotics and prebiotic-fermented foods, and food supplements. These products are available both as main dishes and supplements. By leveraging these insights to further develop these products, it is possible to create foods that not only taste appealing but also promote sleep-enhancing functions. This review provides valuable information for product developers in the global food industry, particularly in the functional food and health product markets, with a focus on future advancements.

CONTRIBUTION

A. Sattayakhom: conceptualization, data curation, formal analysis, investigation, methodology, resources, software, validation, visualization, writing – original draft, review and editing; P. Koomhin: conceptualization, data curation, formal analysis, investigation, funding acquisition, methodology, project administration, resources, supervision, software, validation, visualization, writing – original draft, review and editing; N. Matan: conceptualization, data curation, formal analysis, investigation, funding acquisition, methodology, project administration, resources, supervision, software, validation, visualization, writing – original draft, review and editing.

CONFLICT OF INTEREST

The authors have no conflict of interest regarding this publication.

ACKNOWLEDGEMENTS

We would like to thank Miss Pitchtida Koomhin of Sitapatr School, Nakhon Si Thammarat, Thailand, for her assistance with the hand graphics in the figure.

AI DECLARATION

During the preparation of our manuscript, the author(s) used ChatGPT and Gemini to check and polish the language and grammar. After using these tools/services, the author(s) reviewed and edited the content as needed and take full responsibility for the content of the publication.

REFERENCES

1. Brinkman JE, Reddy V, Sharma S. Physiology of Sleep. StatPearls. Treasure Island: StatPearls Publishing; 2025.
2. Berry R, Brooks R, Gamaldo C, Harding SM, Lloyd RM, *et al*. AASM Scoring Manual Updates for 2017 (Version 2.4). Journal of Clinical Sleep Medicine. 2017;13:665–666.
3. Kryger MH, Roth T, Dement WC. Principles and practice of sleep medicine. 5th ed. Philadelphia: Elsevier Health Sciences; 2010, 1766 p.
4. Van de Water ATM, Holmes A, Hurley DA. Objective measurements of sleep for non-laboratory settings as alternatives to polysomnography – a systematic review. Journal of Sleep Research. 2011;20(1pt2):183–200. https://doi.org/10.1111/j.1365-2869.2009.00814.x
5. Fisher SP, Godinho SI, Pothecary CA, Hankins MW, Foster RG, *et al*. Rapid assessment of sleep-wake behavior in mice. Journal of biological rhythms. 2012;27(1):48–58. https://doi.org/10.1177/0748730411431550
6. Park KS, Choi SH. Smart technologies toward sleep monitoring at home. Biomedical Engineering Letters. 2019;9:73–85. https://doi.org/10.1007/s13534-018-0091-2
7. Boulos MI, Jairam T, Kendzerska T, Im J, Mekhael A, *et al*. Normal polysomnography parameters in healthy adults: A systematic review and meta-analysis. The Lancet Respiratory Medicine. 2019;7(6):533–543. https://doi.org/10.1016/S2213-2600(19)30057-8
8. Hagan JJ, Leslie RA, Patel S, Evans ML, Wattam TA, *et al*. Orexin A activates locus coeruleus cell firing and increases arousal in the rat. Proceedings of the National Academy of Sciences. 1999;96(19):10911–10916. https://doi.org/10.1073/pnas.96.19.10911
9. Saito YC, Tsujino N, Abe M, Yamazaki M, Sakimura K, *et al*. Serotonergic input to orexin neurons plays a role in maintaining wakefulness and REM sleep architecture. Frontiers in Neuroscience. 2018;12:892. https://doi.org/10.3389/fnins.2018.00892
10. Arrigoni E, Fuller PM. The sleep-promoting ventrolateral preoptic nucleus: What have we learned over the past 25 years? International Journal of Molecular Sciences. 2022;23(6):2905. https://doi.org/10.3390/ijms23062905
11. Deurveilher S, Burns J, Semba K. Indirect projections from the suprachiasmatic nucleus to the ventrolateral preoptic nucleus: A dual tract-tracing study in rat. European Journal of Neuroscience. 2002;16(7):1195–1213. https://doi.org/10.1046/j.1460-9568.2002.02196.x
12. Yamatsu A, Yamashita Y, Maru I, Yang J, Tatsuzaki J, *et al*. The improvement of sleep by oral intake of GABA and *Apocynum venetum* leaf extract. Journal of Nutritional Science and Vitaminology. 2015;61(2):182–187. https://doi.org/10.3177/jnsv.61.182
13. Kim S, Jo K, Hong KB, Han SH, Suh HJ. GABA and L-theanine mixture decreases sleep latency and improves NREM sleep. Pharmaceutical Biology. 2019;57(1):64–72. https://doi.org/10.1080/13880209.2018.1557698
14. Park CW, Hong KB, Suh HJ, Ahn Y. Sleep-promoting activity of amylase-treated Ashwagandha (*Withania somnifera* L. Dunal) root extract via GABA receptors. Journal of Food and Drug Analysis. 2023;31(2):278–288. https://doi.org/10.38212/2224-6614.3456

15. Nakamura Y, Midorikawa T, Monoi N, Kimura E, Murata-Matsuno A, *et al*. Oral administration of Japanese sake yeast (*Saccharomyces cerevisiae* sake) promotes non-rapid eye movement sleep in mice via adenosine A2A receptors. Journal of Sleep Research. 2016;25(6):746–753. https://doi.org/10.1111/jsr.12434
16. Ochoa-de la Paz LD, Gulias-Cañizo R, Ruíz-Leyja ED, Sánchez-Castillo H, Parodí J. The role of GABA neurotransmitter in the human central nervous system, physiology, and pathophysiology. Revista mexicana de neurociencia. 2021;22(2):67–76. https://doi.org/10.24875/rmn.20000050
17. Kim M, Kim YJ, Lee HW, Jung JC, Oh S. *Chrysanthemum morifolium* and its bioactive substance enhanced the sleep quality in rodent models via Cl− Channel Activation. Nutrients. 2023;15(6):1309. https://doi.org/10.3390/nu15061309
18. Kim D, Yoon M, Kim S, Um MY, Cho S. Effects of green kiwifruit peel extract on sleep-wake profiles in mice: A polysomnographic study based on electroencephalogram and electromyogram recordings. Nutrients. 2022;14(22):4732. https://doi.org/10.3390/nu14224732
19. Al-Sarraf H. Transport of 14C-γ-aminobutyric acid into brain, cerebrospinal fluid and choroid plexus in neonatal and adult rats. Developmental Brain Research. 2002;139(2):121–129. https://doi.org/10.1016/S0165-3806(02)00537-0
20. Basheer R, Strecker RE, Thakkar MM, McCarley RW. Adenosine and sleep–wake regulation. Progress in neurobiology. 2004;73(6):379–396. https://doi.org/10.1016/j.pneurobio.2004.06.004
21. Satoh S, Matsumura H, Hayaishi O. Involvement of adenosine A_{2A} receptor in sleep promotion. European Journal of Pharmacology. 1998;351(2):155–162. https://doi.org/10.1016/S0014-2999(98)00302-1
22. Baba Y, Takihara T, Okamura N. Theanine maintains sleep quality in healthy young women by suppressing the increase in caffeine-induced wakefulness after sleep onset. Food and Function. 2023;14(15):7109–7116. https://doi.org/10.1039/d3fo01247f
23. Nakagawa M, Yamamoto H, Kawaji M, Miura N, Wakame K, *et al*. Effects of lactic acid bacteria-containing foods on the quality of sleep: A placebo-controlled, double-blinded, randomized crossover study. Functional Foods in Health and Disease. 2018;8(12):579–596. https://doi.org/10.31989/ffhd.v8i12.572
24. Koomhin P, Sattayakhom A, Chandharakool S, Sinlapasorn J, Suanjan S, *et al*. Michelia essential oil inhalation increases fast alpha wave activity. Scientia Pharmaceutica. 2020;88(2):23. https://doi.org/10.3390/scipharm88020023
25. Chandharakool S, Koomhin P, Sinlapasorn J, Suanjan S, Phungsai J, *et al*. Effects of tangerine essential oil on brain waves, moods, and sleep onset latency. Molecules. 2020;25(20):4865. https://doi.org/10.3390/molecules25204865
26. Kwangjai J, Cheaha D, Manor R, Sa-ih N, Samerphob N, *et al*. Modification of brain waves and sleep parameters by *Citrus reticulata* Blanco. cv. Sai-Nam-Phueng essential oil. Biomedical Journal. 2021;44(6):727–738. https://doi.org/10.1016/j.bj.2020.05.017
27. Ko LW, Su CH, Yang MH, Liu SY, Su TP. A pilot study on essential oil aroma stimulation for enhancing slow-wave EEG in sleeping brain. Scientific Reports. 2021;11:1078. https://doi.org/10.1038/s41598-020-80171-x
28. Cheaha D, Basor N, Sa-i N, Kumarnsit E, Chaikul A, *et al*. Jasmine essential oil promotes delta-beta power activities in the dorsal hippocampus under slow wave sleep promotion. Songklanakarin Journal of Science and Technology. 2023;45(1):1–10.
29. Sinthupachee A, Koomhin P, Udenigwe CC, Matan N. Active protein ingredient from smoke-dried fish hydrolysates with *Litsea cubeba* vapor for enhancing organoleptic properties, microbial safety, and brain response. ES Food & Agroforestry. 2024;18:1284. https://doi.org/10.30919/esfaf1284
30. Cheaha D, Issuriya A, Manor R, Kwangjai J, Rujiralai T, *et al*. Modification of sleep-waking and electroencephalogram induced by vetiver essential oil inhalation. Journal of Intercultural Ethnopharmacology. 2016;5(1):72–78. https://doi.org/10.5455/jice.20160208050736
31. Zhou L, Zhu LY, Zhou W, Zhou YQ, Hu PY, *et al*. Discussion on safety and related pharmacological mechanism of compound anshen essential oil in relieving sleep disorders. Chinese Pharmacological Bulletin. 2023;39(3):580–587. (In Chinese) https://doi.org/10.12360/CPB202206034
32. Wei Q, Ta G, He W, Wang W, Wu Q. Stilbene glucoside, a putative sleep promoting constituent from *Polygonum multiflorum* affects sleep homeostasis by affecting the activities of lactate dehydrogenase and salivary alpha amylase. Chemical and Pharmaceutical Bulletin. 2017;65(11):1011–1019. https://doi.org/10.1248/cpb.c17-00275
33. Woo JH, Ha TW, Kang JS, Hong JT, Oh KW. Potentiation of decursinol angelate on pentobarbital-induced sleeping behaviors *via* the activation of GABAA-ergic systems in rodents. Korean Journal of Physiology & Pharmacology. 2017;21(1):27–36. https://doi.org/10.4196/kjpp.2017.21.1.27
34. Kwon YO, Hong JT, Oh KW. Rosmarinic acid potentiates pentobarbital-induced sleep behaviors and non-rapid eye movement (NREM) sleep through the activation of $GABA_A$-ergic systems. Biomolecules & Therapeutics. 2017;25(2):105–111. https://doi.org/10.4062/biomolther.2016.035
35. Yoo JH, Ha TW, Hong JT, Oh KW. Sinomenine, an alkaloid derived from *Sinomenium acutum* potentiates pentobarbital-induced sleep behaviors and non-rapid eye movement (NREM) sleep in rodents. Biomolecules & Therapeutics. 2017;25(6):586–592. https://doi.org/10.4062/biomolther.2017.157
36. Yoon M, Cho S. Triphlorethol A, a dietary polyphenol from seaweed, decreases sleep latency and increases non-rapid eye movement sleep in mice. Marine Drugs. 2018;16(5):139. https://doi.org/10.3390/md16050139

37. Lin S, Nie B, Song K, Ye R, Yuan Z. *Pinelliae rhizoma* praeparatum cum alumine extract: Sedative and hypnotic effects in mice and component compounds. BioMed Research International. 2019;2019:6198067. https://doi.org/10.1155/2019/6198067
38. Murthy SV, Fathima SN, Mote R. Hydroalcoholic extract of *Ashwagandha* improves sleep by modulating GABA/histamine receptors and EEG slow-wave pattern in *in vitro – in vivo* experimental models. Preventive Nutrition and Food Science. 2022;27(1):108–120. https://doi.org/10.3746/pnf.2022.27.1.108
39. Miyazaki K, Itoh N, Saiki P, Kuroki Y. Supplementation with *Eurycoma longifolia* extract modulates diurnal body temperature fluctuation and sleep rhythm in mice. Journal of Nutritional Science and Vitaminology. 2022;68(4):342–347. https://doi.org/10.3177/jnsv.68.342
40. Choi JJ, Oh EH, Lee MK, Chung YB, Hong JT, *et al. Gastrodiae rhizoma* ethanol extract enhances pentobarbital-induced sleeping behaviors and rapid eye movement sleep via the activation of $GABA_A$-ergic transmission in rodents. Evidence-based Complementary and Alternative Medicine. 2014;2014:426843. https://doi.org/10.1155/2014/426843
41. Hua R, Ding Y, Liu X, Niu B, Chen X, *et al. Lonicerae Japonicae* Flos extract promotes sleep in sleep-deprived and lipopolysaccharide-challenged mice. Frontiers in Neuroscience. 2022;16:848588. https://doi.org/10.3389/fnins.2022.848588
42. Abdollahnejad F, Mosaddegh M, Nasoohi S, Mirnajafi-Zadeh J, Kamalinejad M, *et al*. Study of sedative-hypnotic effects of *Aloe vera* L. aqueous extract through behavioral evaluations and EEG recording in rats. Iranian Journal of Pharmaceutical Research. 2016;15(1):293–300.
43. Yamashiro K, Aoki M, Matsumoto N, Ikegaya Y. Polyherbal formulation enhancing cerebral slow waves in sleeping rats. Biological and Pharmaceutical Bulletin. 2020;43(9):1356–1360. https://doi.org/10.1248/bpb.b20-00285
44. Martinez-Mota L, Cruz-Tavera A, Dorantes-Barrón AM, Arrieta-Báez D, Ramírez-Salado I, *et al. Calea zacatechichi* Schltdl. (Compositae) produces anxiolytic- and antidepressant-like effects, and increases the hippocampal activity during REM sleep in rodents. Journal of Ethnopharmacology. 2021;265:113316. https://doi.org/10.1016/j.jep.2020.113316
45. Takeda R, Yamamoto K, Tokuda M, Koga J, Higaki M, *et al*. Improvement in quality of sleep by the intake of saffron–derived crocin and safranal – a randomized, double–blind, placebo–controlled, parallel–group trial–. Japanese Pharmacology and Therapeutics. 2020;48(3):497–504. (In Japanese)
46. Ahn Y, Kim S, Park C, Kim JE, Suh HJ, *et al*. Sleep-promoting activity of lotus (*Nelumbo nucifera*) rhizome water extract via $GABA_A$ receptors. Pharmaceutical Biology. 2022;60(1):1341–1348. https://doi.org/10.1080/13880209.2022.2096076
47. Kim S, Hong KB, Jo K, Suh HJ. Quercetin-3-*O*-glucuronide in the ethanol extract of lotus leaf (*Nelumbo nucifera*) enhances sleep quantity and quality in a rodent model via a GABAergic mechanism. Molecules. 2021;26(10):3023. https://doi.org/10.3390/molecules26103023
48. Kwon YO, Ha TW, Oh KW. Ethanol extract of *Perillae herba* enhances pentobarbital-induced sleep and non-rapid eye movement (NREM) sleep through $GABA_A$-ergic systems. Natural Product Sciences. 2017;23(1):53–60. https://doi.org/10.20307/nps.2017.23.1.53
49. Ahn Y, Lee HH, Kim BH, Park SJ, Kim YS, *et al*. Heukharang lettuce (*Lactuca sativa* L.) leaf extract displays sleep-promoting effects through GABAA receptor. Journal of Ethnopharmacology. 2023;314:116602. https://doi.org/10.1016/j.jep.2023.116602
50. Hong KB, Han SH, Park Y, Suh HJ, Choi HS. Romaine lettuce/skullcap mixture improves sleep behavior in vertebrate models. Biological and Pharmaceutical Bulletin. 2018;41(8):1269–1276. https://doi.org/10.1248/bpb.b18-00267
51. Jo K, Kim S, Ahn Y, Suh HJ. Effects of green lettuce leaf extract on sleep disturbance control in oxidative stress-induced invertebrate and vertebrate models. Antioxidants. 2021;10(6):970. https://doi.org/10.3390/antiox10060970
52. Kim HW, Suh HJ, Choi HS, Hong KB, Jo K. Effectiveness of the sleep enhancement by green romaine lettuce (*Lactuca sativa*) in a rodent model. Biological and Pharmaceutical Bulletin. 2019;42(10):1726–1732. https://doi.org/10.1248/bpb.b19-00454
53. Rahimi S, Alaei H, Reisi P, Zarrin B, Siahmard Z, *et al*. Hydroalcoholic Tarooneh extract (spathe of phoenix dactylifera) increased sedative-hypnotic effects and modulated electroencephalography brain waves in Anesthetized Rats. Advanced Biomedical Research. 2019;8(1):24. https://doi.org/10.4103/abr.abr_58_16
54. Yoon M, Kim JS, Jo J, Han D, Cho S. Sleep-promoting effect of *Ecklonia cava*: Ethanol extract promotes non-rapid eye movement sleep in C57BL/6N mice. Fisheries and Aquatic Sciences. 2014;17(1):19–25. https://doi.org/10.5657/FAS.2014.0019
55. Li IC, Lin TW, Lee TY, Lo Y, Jiang YM, *et al*. Oral administration of *Armillaria mellea* mycelia promotes non-rapid eye movement and rapid eye movement sleep in rats. Journal of Fungi. 2021;7(5):371. https://doi.org/10.3390/jof7050371
56. Li TJ, Lee TY, Lo Y, Lee LY, Li IC, *et al*. *Hericium erinaceus* mycelium ameliorate anxiety induced by continuous sleep disturbance *in vivo*. BMC Complementary Medicine and Therapies. 2021;21:295. https://doi.org/10.1186/s12906-021-03463-3

57. Kim H, Park I, Park K, Park S, Kim YI, *et al*. The positive effects of *Poria cocos* extract on quality of sleep in insomnia rat models. International Journal of Environmental Research and Public Health. 2022;19(11):6629. https://doi.org/10.3390/ijerph19116629
58. Uchida M, Suzuki M, Shimizu K. Mycelial extract of cultured cordyceps sinensis improves the sleep disturbance induced by placing rats on the grid suspended over water. Japanese Pharmacology and Therapeutics. 2016;44(6):881–885.
59. Panagiotou M, Meijer M, Meijer JH, Deboer T. Effects of chronic caffeine consumption on sleep and the sleep electroencephalogram in mice. Journal of Psychopharmacology. 2019;33(1):122–131. https://doi.org/10.1177/0269881118806300
60. Kim D, Kim S, Yoon M, Um MY, Cho S. Effects of chronic administration of green tea ethanol extract on sleep architecture in mice: A comparative study with a representative stimulant caffeine. Nutrients. 2023;15(4):1042. https://doi.org/10.3390/nu15041042
61. Kwon S, Yoon M, Lee J, Moon KD, Kim D, *et al*. A standardized phlorotannin supplement attenuates caffeine-induced sleep disruption in mice. Nutrients. 2019;11(3):556. https://doi.org/10.3390/nu11030556
62. Oishi K, Okauchi H, Yamamoto S, Higo-Yamamoto S. Dietary natural cocoa ameliorates disrupted circadian rhythms in locomotor activity and sleep-wake cycles in mice with chronic sleep disorders caused by psychophysiological stress. Nutrition. 2020;75–76:110751. https://doi.org/10.1016/j.nut.2020.110751
63. Miyazaki K, Itoh N, Yamamoto S, Higo-Yamamoto S, Nakakita Y, *et al*. Dietary heat-killed *Lactobacillus brevis* SBC8803 promotes voluntary wheel-running and affects sleep rhythms in mice. Life Sciences. 2014;111(1–2):47–52. https://doi.org/10.1016/j.lfs.2014.07.009
64. Thompson RS, Roller R, Mika A, Greenwood BN, Knight R, *et al*. Dietary prebiotics and bioactive milk fractions improve NREM sleep, enhance REM sleep rebound and attenuate the stress-induced decrease in diurnal temperature and gut microbial alpha diversity. Frontiers in Behavioral Neuroscience. 2016;10:240. https://doi.org/10.3389/fnbeh.2016.00240
65. Higo-Yamamoto S, Yamamoto S, Miyazaki K, Nakakita Y, Kaneda H, *et al*. Dietary heat-killed *Lactobacillus brevis* SBC8803 attenuates chronic sleep disorders induced by psychophysiological stress in mice. Journal of Nutritional Science and Vitaminology. 2019;65(2):164–170. https://doi.org/10.3177/jnsv.65.164
66. Monoi N, Matsuno A, Nagamori Y, Kimura E, Nakamura Y, *et al*. Japanese sake yeast supplementation improves the quality of sleep: A double-blind randomised controlled clinical trial. Journal of Sleep Research. 2016;25(1):116–123. https://doi.org/10.1111/jsr.12336
67. Varin C, Rancillac A, Geoffroy H, Arthaud S, Fort P, *et al*. Glucose induces slow-wave sleep by exciting the sleep-promoting neurons in the ventrolateral preoptic nucleus: A new link between sleep and metabolism. Journal of Neuroscience. 2015;35(27):9900–9911. https://doi.org/10.1523/jneurosci.0609-15.2015
68. Bae GY, Ahn Y, Hong KB, Jung EJ, Suh HJ, *et al*. Sleep-enhancing effect of water extract from jujube (*Zizyphus jujuba* Mill.) seeds fermented by *Lactobacillus brevis* L32. Foods. 2023;12(15):2864. https://doi.org/10.3390/foods12152864
69. Minet-Ringuet J, Le Ruyet PM, Tomé D, Even PC. A tryptophan-rich protein diet efficiently restores sleep after food deprivation in the rat. Behavioural Brain Research. 2004;152(2):335–340. https://doi.org/10.1016/j.bbr.2003.10.018
70. Halson SL, Shaw G, Versey N, Miller DJ, Sargent C, *et al*. Optimisation and validation of a nutritional intervention to enhance sleep quality and quantity. Nutrients. 2020;12(9):2579. https://doi.org/10.3390/nu12092579
71. Thiagarajah K, Chee HP, Sit NW. Effect of alpha-S1-casein tryptic hydrolysate and L-theanine on poor sleep quality: A double blind, randomized placebo-controlled crossover trial. Nutrients. 2022;14(3):652. https://doi.org/10.3390/nu14030652
72. Cherasse Y, Saito H, Nagata N, Aritake K, Lazarus M, *et al*. Zinc-containing yeast extract promotes nonrapid eye movement sleep in mice. Molecular Nutrition and Food Research. 2015;59(10):2087–2093. https://doi.org/10.1002/mnfr.201500082
73. Ye M, Lee S, Yu HJ, Kim KR, Park HJ, *et al*. Sedative-hypnotic effects of *Glycine max* merr. extract and its active ingredient genistein on electric-shock-induced sleep disturbances in rats. International Journal of Molecular Sciences. 2023;24(8):7043. https://doi.org/10.3390/ijms24087043
74. Ta QV, Yoon M, Yang H, Kim J, Cho S, *et al*. Effects of blue mussel (ME) water extracts on pentobarbital-induced sleep and the sleep architecture in mice. Food Science and Biotechnology. 2015;24:295–300. https://doi.org/10.1007/s10068-015-0039-6
75. Nedachi T, Haketa K, Harakawa S, Miura N, Wakame K. Effect of combining sleep-promoting food intake and electric field application on sleep in healthy participants: A pilot study. Functional Foods in Health and Disease 2021;11(12):659–672. https://doi.org/10.31989/ffhd.v11i12.861

Additional information about the authors

Apsorn Sattayakhom ORCID 0000-0003-1944-6881
Phanit Koomhin ORCID 0000-0002-1465-721X
Narumol Matan ORCID 0009-0005-3166-5325

Foods and Raw Materials. 2027;15(2)
ISSN 2308-4057 (Print)
ISSN 2310-9599 (Online)
Research Article
Open Access
Available online at http://jfrm.ru/en
https://doi.org/10.21603/2308-4057-2027-2-718
https://elibrary.ru/UNCBEA

Milk protein and peptide profiles under different heat loads: Molecular analysis

Irina A. Barkovskaya*, Polina I. Koroleva, Svetlana N. Turovskaya, Elena E. Illarionova, Vladimir V. Kondratenko, Vladimir G. Bliadze, Vladislav Yu. Yaryshev, Andrey N. Petrov

All-Russian Dairy Research Institute, Moscow, Russia

* e-mail: i_barkovskaya@vnimi.org

Received 25.01.2026; Revised 16.03.2026; Accepted 07.04.2026; Published online 29.09.2026

Abstract:
Heat treatment induces structural changes in milk proteins, thus affecting the processing suitability of milk powder. Identifying new molecular markers of heat load helps to develop rapid and efficient approaches to milk powder assessment. This study utilized molecular analysis to investigate the impact of thermal treatment on the proteome and peptidome of skim milk.
The skim milk samples were subjected to heat treatment at 70, 80, and 90°C for 30 s, while skim milk maintained at 45°C served as control. Two-dimensional electrophoresis made it possible to separate and evaluate protein structural changes. Peptide identification relied on matrix-assisted laser desorption ionization time-of-flight mass spectrometry (MALDI-TOF MS), preceded by trypsinolysis. A combination of Raman spectroscopy and principal component analysis visualized the heat-induced spectral responses to evaluate the potential of Raman spectroscopy for tracing the thermal history of milk powder.
High pasteurization temperature reduced the number of protein fractions. MALDI-TOF MS identified 30 peptides belonging to seven major milk proteins. Peptide fragments of α_{S1}-casein and β-casein were absent in the control but present in the experimental samples, indicating heat-induced protein transformation. The intermolecular interactions and disruption of the secondary structure of proteins resulted in differences in the isoelectric points. Raman spectroscopy revealed heat-induced changes in the wavenumber ranges of 900–1097, 1328–1437, and 1475–1546 cm^{-1}, attributed to the transformed carbohydrate and proteomic milk profiles. The principal component analysis made it possible to visualize the differences and identify the regions that make the highest contribution to the response.
Raman spectroscopy proved to be a reliable technique for developing and validating a rapid approach to assess the degree of heat load in milk.

Keywords: Skim milk, milk powder, heat treatment, peptide profile, milk proteins, two-dimensional electrophoresis, mass spectrometry, Raman spectroscopy

Funding: The research was part of State Assignment no. FNSS-2025-0001.

Please cite this article in press as: Barkovskaya IA, Koroleva PI, Turovskaya SN, Illarionova EE, Kondratenko VV, *et al.* Milk protein and peptide profiles under different heat loads: Molecular analysis. Foods and Raw Materials. 2027;15(2):411–424. https://doi.org/10.21603/2308-4057-2027-2-718

INTRODUCTION

Dairy production is driven by the growing global population and the increasing demand for high-quality food [1]. It is expected to grow by 22% by 2027 [2]. Dairy products have always been an integral part of the traditional Russian diet. Starting in 2015, a decade-long increase in raw milk production reached 34 million tons in 2024 [3], i.e., an increase of 13.7%. As the dairy sector keeps growing, dairy processing plants have to increase production efficiency while ensuring rapid and accurate quality control [2]. Taking into account this challenge, modern quality control must shift from conventional regulatory indicators to assessing food properties during processing and storage [4]. Milk powder is part of dairy, bakery, confectionery, and other formulations. As such, it requires a comprehensive in-depth analysis of its composition and properties. Skim milk powder is the most in-demand in the food industry. In 2024, the global production of skim milk powder amounted to 150.3 billion US dollars. With an average annual growth rate of 5.8%, it is expected

Copyright © 2026, Barkovskaya *et al.* This is an open access article distributed under the terms of the Creative Commons Attribution 4.0 International License (https://creativecommons.org/licenses/by/4.0/), allowing third parties to copy and redistribute the material in any medium or format and to remix, transform, and build upon the material for any purpose, even commercially, provided the original work is properly cited and states its license.

to exceed 260 billion US dollars by 2034[1]. In Russia, technical modernization and state support also ensure a stable increase in skim milk powder production. From January to October 2025, its volume grew by 11.8% compared to the same period in 2024 and reached 108,700 tons[2].

As a complex colloidal system of proteins, fats, carbohydrates, minerals, and vitamins, milk requires multidisciplinary analysis. The problem is that its components vary in physicochemical and structural properties, which complicates quality assessment during processing. Proteins are responsible for the allergenicity [5], functional characteristics [6], biological value [7], and technological properties of milk. Their components (α-, β-, and κ-caseins, whey proteins, immunoglobulins, and enzymes) have disparate properties [8].

Heat treatment is a mandatory process in the milk production chain as it ensures microbiological safety. The processing conditions vary greatly: sterilization, pasteurization, ultra-pasteurization, etc. As a result, the thermal exposure of the milk system components differs significantly [9]. In this regard, studying changes in milk proteins during heating is important for food safety and defines their further tech nological use [10, 11]. A rapid thermal load test means an equally rapid charting of utilization pathways.

For example, fermented dairy products require high pasteurization temperatures, and the heating mode targets protein structural changes necessary to reach the desired consistency [12]. On the contrary, cheese and cottage cheese obtained by acid-rennet coagulation need a lower degree of whey protein denaturation to obtain a curd with the necessary properties [13].

Global and domestic skim milk powder producers classify it into three main raw-material classes, depending on the whey protein nitrogen index (WPNI). This indicator is determined using the Kjeldahl method and correlates with the degree and time of thermal exposure. For instance, pre-curding processing parameters of 70°C for 15 s yield 6.00 mg WPNI/g of low-heat skim milk powder; 85°C for 60 s or 90–105°C for 30 s result in 1.51–5.99 mg WPNI/g of medium-heat skim milk powder; 90°C for 5 min or 120°C for 1–2 min produce as little as 1.50 mg WPNI/g high-heat skim milk powder [14–16].

Studies of this kind discover new heat load markers to improve the current dairy quality control procedures.

Molecular analysis methods standardize the assessment of heat load effect on dairy raw materials and help to chart further utilization pathways. They are sensitive, accurate, and comprehensive. For instance, Raman spectroscopy is fast and automated. It can be applied to complex dairy systems without special pretreatment or sample destruction.

[1] Skimmed milk powder market size and share 2025–2034. Global Market Insights. [cited 2026 Jan 20]. (In Russ.) Available from: https://www.gminsights.com/ru/industry-analysis/skimmed-milk-powder-market

[2] The production of skimmed milk powder increased by 11.8%. Milknews. [cited 2026 Jan 20]. (In Russ.) Available from: https://milknews.ru/analitika-rinka-moloka/rinok-moloka-v-Rossii/som-analitika-noyabr-2025.html

Matrix-assisted laser desorption ionization time-of-flight mass spectrometry (MALDI-TOF MS) is a multitask molecular analysis method [11]. Other similar methods include various types of electrophoresis [17, 18], IR or Raman spectroscopy for protein analysis [19], and the method of polymerase chain reaction for DNA and RNA studies [20].

Polymerase chain reaction methods are able to detect the adulteration of high-quality dairy products through the addition of cheaper raw materials, e.g., cow's milk instead of goat's or sheep's milk [21, 22]. They also detect residual amounts of pathogenic microorganisms in products that are otherwise undetectable by classical methods [23].

Computer-aided mass spectrometry assesses heat- or storage-induced changes in milk. Losito *et al.* [24] developed a method for assessing the heat treatment based on the degree of lactosylation of whey proteins. Class *et al.* [25] used high-resolution mass spectrometry and custom-designed software to identify eight peptides undergoing changes in ultra-pasteurized milk during storage. The established shelf life corresponded with the actual storage-induced changes. The main changes were observed in peptides related to α_{S1}-casein, α_{S2}-casein, β-casein, and β-lactoglobulin. The signal intensity of all these peptides increased together with ultra-pasteurization. Šebela [26] mentioned mass spectrometric approaches for assessing adulteration of milk and dairy products. Kang *et al.* [27] combined two-dimensional electrophoresis and mass spectrometry to determine the optimal processing pathway and detect markers of excessive heat load in dairy products.

Raman spectroscopy also proved effective in assessing the degree of heat load by tracing the conformational changes in milk proteins. These changes are associated with specific amide bands, namely Amide I (~ 1,650 cm^{-1}) and Amide III (~ 1,250 cm^{-1}). They serve as signal regions sensitive to thermal effect [19]. The position and shape of the amide bands tell volumes about the secondary structure of proteins and even the share of individual structural components, e.g., α-helices and β-structures. Raman spectroscopy was reported to be able to identify 10% of α-helices and a significant percentage of irregular β-structures in caseins [28]. Zhang *et al.* [29] applied Raman spectroscopy to the aggregation of whey proteins under heat load with and without pectin (0.015–0.20 wt.).

Li *et al.* [30] used a specific proteomic approach based on liquid chromatography with mass spectrometry (LC-MS/MS) to detect changes in whey protein systems heated to ≥ 90°C. Whey protein isolates demonstrated less protein oxidation compared to pure proteins (α-lactalbumin > β-lactoglobulin) and a mixed-protein whey model. Cysteine, methionine, and tryptophan residues in α-lactalbumin were found to be more susceptible to oxidation.

Meltretter *et al.* [31] studied markers of non-thermal and thermal exposure in dairy raw materials using ultra-high-performance liquid chromatography with mass spec-

trometry and multiple reaction monitoring. Lactulosyl lysine proved to be a marker of low-heat treatment while N^{ε}-carboxymethyl lysine, *N*-terminal ketoamide, and asparagine deamidation marked more intense thermal stress.

To rationally select the degree of heat treatment and identify markers for its monitoring, Lu *et al.* [32] used the proteomic method of LC-MS/MS to study lactosylated proteins subjected to various thermal modes. As a result, they detected a total of 123 lactosylated lysines in 65 proteins. Between 75 to 130°C, their number increased smoothly and moderately but soared when the temperature reached 140°C. More than half of the lysine residues were lactosylated in *κ*-casein, *β*-lactoglobulin, and *α*-lactalbumin. The fact that K_{14} lactosylated in *β*-lactoglobulin allowed the authors to tell between pasteurized and ultra-pasteurized milk: lactosylated lactotransferrin indicated medium-heat processing.

Therefore, the effect of heat load on the dairy system is a popular research topic approached using various molecular analysis methods. Yet, no immediate method exists for determining this parameter.

This study evaluated the feasibility of using Raman spectroscopy to detect changes in the proteomic profile of pasteurized skim milk under varying heat loads.

STUDY OBJECTS AND METHODS

Study objects. To assess the effect of heat load on skim milk proteins, we heated the experimental samples to 70, 80, and 90°C with a holding time of 30 s. The sample maintained at 45°C served as control (Table 1).

The experimental samples were produced using the equipment from the Shared Use Center at the All-Russian Dairy Research Institute, Moscow (Fig. 1). Raw milk (pH 6.67) was separated using an Alfa Laval laboratory separator (Alfa Laval Group, Sweden) and heated using a pilot pasteurization and cooling unit (1 L/h) designed at the All-Russian Dairy Research Institute.

The protein profile of the resulting skim milk samples was analyzed by two-dimensional electrophoresis. The peptide profile identification was performed using matrix-assisted laser desorption ionization time-of-flight mass spectrometry (MALDI-TOF MS) preceded by the trypsinolysis of protein spots. Raman spectroscopy was involved to be assessed for prospects in profiling milk powder by its thermal history.

Two-dimensional electrophoresis. Two-dimensional electrophoresis involved isoelectric focusing in ampholine buffer in line with the method described in [33]. The gels were stained with silver nitrate to visualize protein spots. The control sample was represented by a set of 14 highly purified recombinant proteins (10–200 kDa, PageRuler™ Unstained Protein Ladder #SM0661; Fermentas, USA) to determine protein molecular weights.

Peptide profiling by MALDI-TOF MS. To identify proteins, we excised individual fractions from two-dimensional electropherogram gels to grind them and subject them to trypsinolysis as in [34]. The resulting protein-containing gel fragments were incubated for 45 min in hydrolysis buffer while cooling in an ice bath. The buffer consisted of 50 mM NH_4HCO_3; 5 mM $CaCl_2$; 12.5 ng/μL trypsin (V5551; Promega, USA; activity 10,000 U/mg). After removing the supernatant and adding 5–10 μL of enzyme-free buffer, we performed hydrolysis at 37°C for 3 h, followed by enzyme inactivation with 0.1% trifluoroacetic acid solution. The peptide tests involved an Ultraflex time-of-flight mass spectrometer (Bruker, Germany) with a UV laser (336 nm) in the positive ion mode at 500–8,000 Da with trypsin autolysis for calibration.

Table 1 Samples' description

Sample	Description
C	Control: skim milk, no pasteurization, 45°C
M70	Pasteurized skim milk, 70°C, 30 s
M80	Pasteurized skim milk, 80°C, 30 s
M90	Pasteurized skim milk, 90°C, 30 s

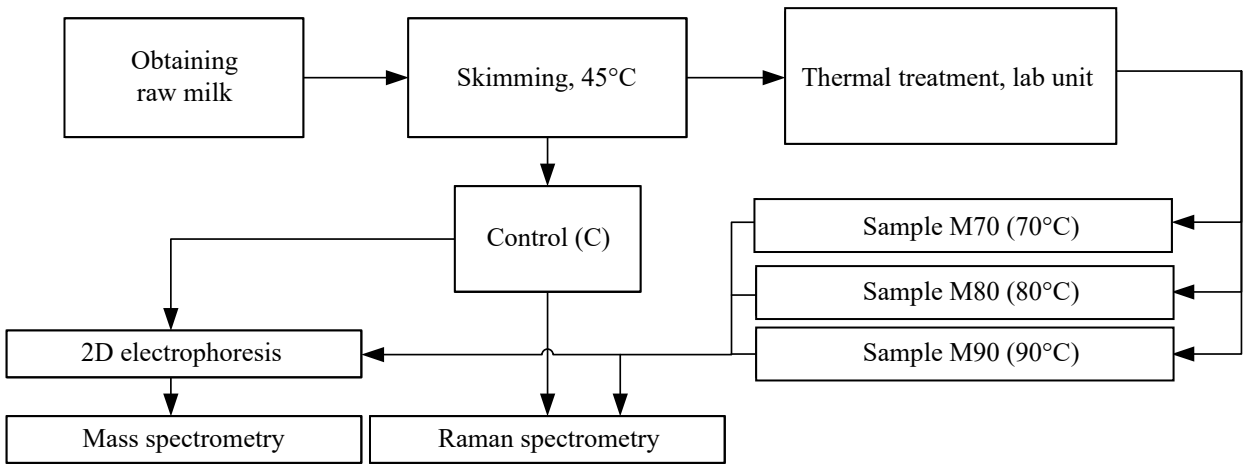


Figure 1 Experimental design

Mass spectrometry processing. The obtained tryptic peptide mass spectra were analyzed using Mascot Peptide Fingerprint (Matrix Science, USA), with an MH^+ weight determination accuracy of 0.01%. The calculations relied on the data published by the National Center for Biotechnology Information (NCBI) (https://www.ncbi.nlm.nih.gov/).

All proteomic studies were performed on the premises of the Federal Research Center for Industrial Biotechnology, Russian Academy of Sciences, Moscow.

Amino acid sequence evaluation. This part of the research involved sequences available in the UniProt database, UK, for α-lactalbumin (P00711) and lysozyme C (Q6B411). The pairwise alignment was performed using the ClustalW algorithm within Jalview (UK) with default parameters.

Raman spectroscopy. Raman spectra were obtained using an EnSpectr R785 portable Raman spectrometer (Spektr-M, Russia) at 250–2700 cm^{-1}. The measurements were triplicated at five different acquisition points for each sample. The laser wavelength was 785 nm. The resulting spectral profiles made it possible to evaluate the heat-induced spectral response of the milk system. The graphical representation and subsequent analysis relied on averaged spectra for each sample group.

Spectral data processing. The averaged spectral dataset was processed using Principal Component Analysis (Python) in Numpy, Pandas, and Sklearn. A Z-transform (standardization) assigned each feature a zero mean and a unit variance. The analysis was performed at 900–1700 cm^{-1}; the spectrum was divided into fixed-width regions. Principal component analysis served as an exploratory visualization tool for heat-induced spectral changes (MinMaxScaler, 0 to 1).

RESULTS AND DISCUSSION

Electrophoretic separation and peptide profiles. Two-dimensional electrophoresis yielded a set of protein spots of milk casein fraction and whey proteins (Fig. 2). The casein fraction included isoforms of α_{S1}-casein and β-casein, κ-casein, and heat-induced protein spots. Whey proteins included bovine serum albumin, α-lactalbumin, and β-lactoglobulin.

The casein fraction of milk proteins remained clearly visible in the electropherograms even after the heat load because caseins are more resistant to thermal treatment than whey proteins [35]. These milk proteins are characterized by a protein band and spots that appear for a specific isoform of the same molecular weight at different isoelectric points. Such distribution may be attributed to post-translational modifications or non-enzymatic changes (e.g., lactosylation) caused by storage and heating [36].

Whey proteins are heat-labile: heat-induced hydrophobicity occurs at 70–90°C, making them form insoluble coagulates or even precipitate [37]. The electropherogram fragments demonstrated a significant decrease in the color intensity in the regions related to bovine serum albumin, α-lactalbumin, and β-lactoglobulin. The most significant decrease in the number and color intensity of protein fragments belonged to sample M80 (80°C), compared to samples M70 (70°C) and M90 (90°C).

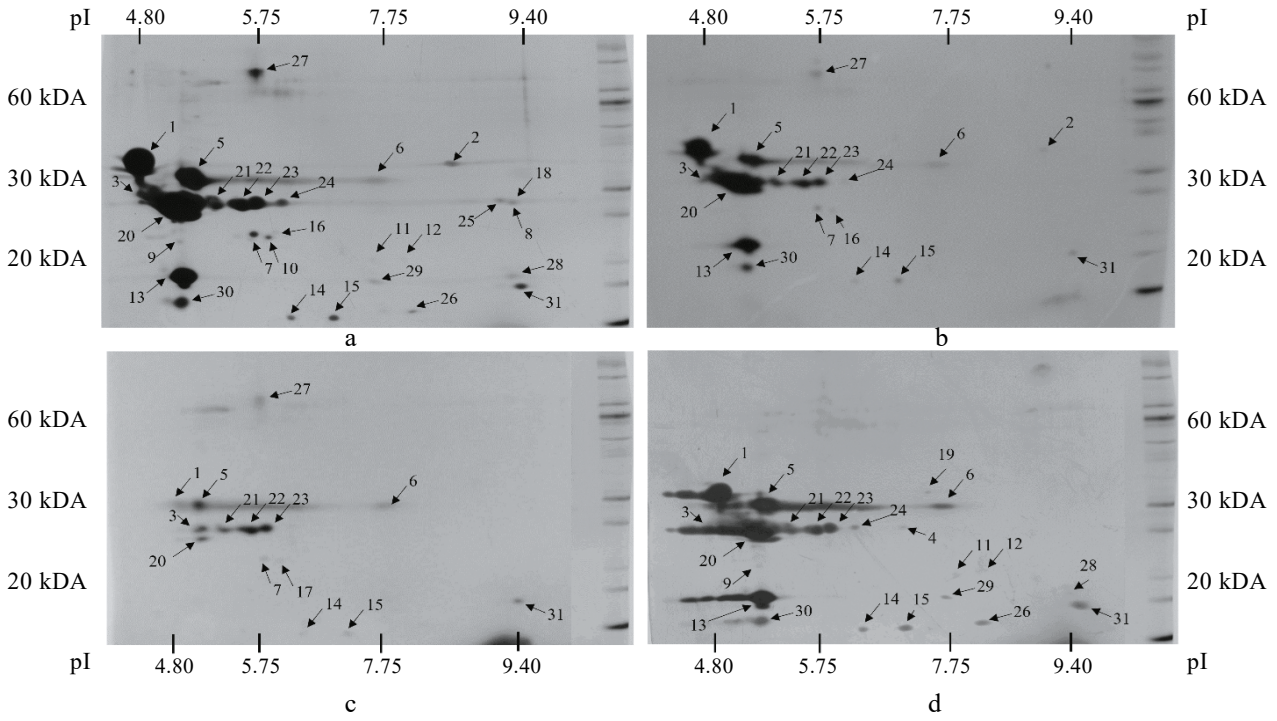


Figure 2 Two-dimensional electropherograms of skim milk samples: a – control (45°C); b – M70 (70°C); c – M80 (80°C); and d – M90 (90°C). Protein assignment was determined using MALDI-TOF MS after trypsinolysis: 1–4 – α_{S1}-casein; 5, 6 – α_{S2}-casein; 7 – β-casein (isoform X1); 8–19 – β-casein (isoform X2); 20–26 – κ-casein; 27 – bovine serum albumin; 28–30 – β-lactoglobulin; 31 – not determined

This result may be attributed to the effect of sodium dodecyl sulfate on the aggregates formed between β-lactoglobulin and κ-casein [38]. At 70–80°C, the β-lactoglobulin protein globule partially unfolds to release the thiol group and form bonds with κ-casein. The intensity of this process depends on the temperature and ionic composition of the milk matrix. In addition, heat treatment may transform non-covalent bonds between whey proteins and casein fractions into covalent ones [39, 40]. The surface of the resulting protein complex is hydrophobic and has a small number of free sulfhydryl groups, which hinders the interaction with sodium dodecyl sulfate [41]. A temperature of ≥ 90°C changes the balance of non-covalent and covalent bonds in the aggregates of β-lactoglobulin and κ-casein. This phenomenon mitigates spatial limitations during protein-reagent interactions, facilitating more efficient peptide diffusion and distribution within the polyacrylamide gel matrix [38].

Such changes in milk proteins affect the technological properties of milk powder and may ultimately limit its use as raw material. As the share of native α-lactalbumins and β-lactoglobulins goes down, the rennetability deteriorates [13]. On the other hand, the formation of β-lactoglobulin – κ-casein protein complexes can positively improve the structural characteristics of fermented milk products: curd firmness increases while syneresis decreases [42, 43].

Ichimura *et al*. [42] used the methods of scanning and transmission electron microscopy to study the quality indicators of yogurt produced from milk pasteurized at 95 and 130°C. The samples obtained from high-heat milk demonstrated a better curd structure owing to the interaction between β-lactoglobulin and κ-casein.

The capacity for acid or acid-rennet coagulation is not the only important technological property of milk. Solubility is another key indicator for milk powder. Its rate depends on the degree of transformation of the protein matrix [7]. These transformations correlate with poor solubility, emulsifying efficiency, and foamability of milk powder. Extensive milk processing increases the number of modified and aggregated forms of protein in the finished product. These forms spoil the technological properties and shorten the shelf life of milk powder. Changes in the ratio of undenatured and denatured milk proteins were reported to affect the solubility index and stability of reconstituted milk, as well as the properties of acid and rennet curd [35, 44].

The mass spectrometry of the peptide profile, performed after trypsinolysis, revealed 30 amino acid sequences belonging to seven major milk proteins: α_{S1}-casein (4); α_{S2}-casein (2); β-casein, isoform X1 (1); β-casein, isoform X2 (12); κ-casein (7); bovine serum albumin (1); β-lactoglobulin (3) (Table 2). The prevailing share of α- and β-casein fragments was consistent with the data reported in [45, 46]. These studies in the peptidomics of milk and dairy products employed high-resolution liquid chromatography with mass spectrometry profiling, which related most peptides to casein fractions. Amino acid sequences of whey proteins were less frequent. This feature of the milk system may be associated with the greater susceptibility of casein to plasmin in raw milk.

The matrix-assisted laser desorption ionization time-of-flight mass spectrometry (MALDI-TOF MS) data demonstrated the prevalene of casein peptide fragments (26 peptides) over whey protein fragments (4 peptides). This imbalance is typical of dairy systems since casein fractions constitute 80% of the total protein content in milk [47]. On the other hand, it can be explained by the properties of casein micelles, which are thermostable protein elements of the dairy system. When heated, they do not denature but undergo structural changes and mediate the appearance of new protein spots, i.e., spots do not disappear during electrophoretic separation but their forms or fragments are redistributed [8].

We identified three amino acid sequences for α_{S1}-casein in the control sample. One of them (2) had significant deviations in the isoelectric point value: the calculated value was 4.98 pH units while the experimental one was 8.8 pH units. α_{S1}-casein is characterized by phosphorylation at several amino acid residues [48]. Fraction 2 resulted from the loss of phosphate groups, which shifted the isoelectric point to the basic region, destabilizing the molecule and leading to denaturation. Sample M90 (90°C) had fragment 4, identified as α_{S1}-casein. Its isoelectric point was 6.70 pH units, which also exceeded the calculated value. This result may be associated with the appearance of new amino acid sequences caused by protein cross-linking [49].

Phosphorylation at 10–13 residues was also characteristic of α_{S2}-casein, which means that the calculated isoelectric point (8.54 pH units) did not coincide with the experimental value, as was the case for α_{S1}-casein. The main peptide fragment (fragment 5) of α_{S2}-casein occurred at the isoelectric point of 5.00 pH units because phosphorylation shifted the isoelectric point to the acidic region. Fragment 6 with the isoelectric point in the slightly alkaline region may also be due to partial loss of phosphate groups [50].

For β-casein, the fractions separated into two isoforms, and isoform X1 had only one fragment, fragment 7. Isoform X2 demonstrated several major fractions and a number of fragments. This uneven distribution is probably explained by the fact that isoform X1 belongs to β-casein A1 while isoform X2 belongs to a more common type, β-casein A2 [51]. Peptide 13 was closest to the calculated isoelectric point value (5.34 pH units) and molecular weight (24.3 kDa). The lower electrophoretic activity of other fragments can be explained by the amino acid composition of β-casein: its proline residues prevented the polypeptide chain from compact folding [37]. This factor probably destabilized β-casein molecules upon heating and caused the fractions to disappear. The smaller molecular weight fragments could be explained by the activity of plasmin, which is known to cleave β-casein into fragments while retaining its activity even after heat treatment [45]. Proteolytic cleav-

Table 2 Peptide profile of pasteurized skim milk samples: Matrix-assisted laser desorption ionization time-of-flight mass spectrometry

Fragment	Protein	NCBI code	pI, pH units		MW, kDa	MW, kDa	Peptides, units*	Sequence coverage, %*
			calc.	exp.	calc.	exp.		
1	α_{S1}-casein	NP_851372.1	4.98	4.75	24.5	36.0	8	38
2				8.80		35.0	7	33
3				4.90		30.0	5	31
4				6.70		29.5	4	26
5	α_{S2}-casein	NP_776953.1	8.54	5.00	26.0	34.0	10	45
6				7.70		34.0	3	19
7	β-casein, isoform X1	XP_010804480.3	5.53	5.70	25.2	24.5	1	8
8	β-casein, isoform X2	XP_015327157.2	5.36	9.20	24.3	29.0	4	23
9				4.95		27.0	2	7
10				5.90		24.0	5	18
11				7.70		25.0	3	12
12				7.90		23.0	3	12
13				5.00		23.0	2	15
14				6.20		13.5	1	8
15				6.70		13.5	4	18
16				5.90		27.0	5	22
17				5.90		27.0	2	15
18				9.20		29.0	1	8
19				7.50		36.0	3	12
20	κ-casein	NP_776719.1	6.30	4.95	21.2	29.0	1	5
21				5.30		29.0	7	35
22				5.50		29.0	9	37
23				5.80		29.0	9	37
24				6.00		29.0	9	37
25				9.10		29.5	7	37
26				8.00		13.5	4	30
27	Bovine serum albumin	NP_851335.1	5.82	5.50	69.3	67.0	23	42
28	β-lactoglobulin	NP_776354.2	4.93	9.20	19.8	20.0	13	72
29				7.70		7.70	1	11
30				5.00		20.0	1	8
31	n.d.	–	–	9.40	–	15.5	6	19

pI – protein's isoelectric point, pH units; calc. – calculated value; exp. – experimentally determined value (2D electrophoresis); MW – molecular weight, kDa; * – peptide profile (matrix-assisted laser desorption ionization time-of-flight mass spectrometry); n.d. – (not detected) bioinformatics processing identified the fragment as α-lactalbumin, which cannot correspond to the experimentally determined isoelectric point. NCBI – National Center for Biotechnology Information

age can also explain the appearance of fragment 19 in Sample M90 (90°C) since heat-induced unfolding of the casein micelle opens up new sections of the polypeptide chain for cleavage by plasmin.

κ-Casein demonstrated a number of peptide fragments with different isoelectric points but the same molecular weight, which exceeded the calculated one. The isoelectric point values shifted relative to the calculated value, both towards the acidic and towards the basic pH range. κ-Casein glycosylates with sialic acids; therefore, the dispersion of κ-casein fractions can be explained by the differences in glycation of amino acid residues [52, 53]. A greater number of carbohydrate molecules attached to the protein molecule shifts the isoelectric point towards the acidic region. κ-Casein can also form complexes with whey protein peptides, which appear as new fractions [37].

We identified three amino acid sequences for β-lactoglobulin, confirming the nature of the protein change upon a heat load of ≤ 80°C. Globular unfolding leads to thiol group exposure, facilitating protein-to-protein interactions via the newly accessible groups [54].

These discrepancies between the calculated and experimental isoelectric points may be due to some structural changes induced by thermal treatment, e.g., the aggregation of protein molecules, the formation of covalent cross-links during protein-to-protein interactions, etc. Such modifications of the proteomic profile affect the charge of protein substances, ultimately changing the isoelectric point [49].

Fragment 31 proved to be another feature of the mass spectrometric peptide profiling. The protein was identified as α-lactalbumin via bioinformatic processing

of the mass spectra. However, the isoelectric point of α-lactalbumin is 4.8 pH units whereas the value of the obtained fragment was 9.4 pH units. The evolutionary and structural homologue of α-lactalbumin is lysozyme C (LyzC) [55]. α-Lactalbumin consists of 142 amino acid residues while lysozyme C has 148. Their molecular masses are very close: 14.2 and 14.4 kDa, respectively. The calculated value of the isoelectric point of lysozyme C is 9.87 pH units, which is consistent with the obtained values. Probably, the error in the bioinformatics processing of the mass spectra occurred due to the similar amino acid sequences of α-lactalbumin and lysozyme C. The amino acid sequences of α-lactalbumin and lysozyme C (Fig. 3) revealed a similarity of approximately 40%, which was consistent with the data reported in [55]. The similar amino acid composition of these proteins stem from a common evolutionary ancestor of the coding genes.

The amino acid sequence demonstrated some common features, e.g., the arrangement of cysteine residues. In α-lactalbumin, they were located at positions 25, 47, 80, 92, 96, 110, 130, and 139. In lysozyme C, they were at positions 24, 48, 83, 95, 99, 113, 134, and 146. This shared feature explains the structural similarity of the proteins. However, since the conserved regions are different, the biochemical properties are different, too.

Lysozyme C is responsible for antibacterial properties. This protein exhibits hydrolytic activity against the β-1,4-glycosidic bond in the peptide glycan of the bacterial cell wall. As a result, it has an active site that consists of catalytically essential amino acids – glutamine (Glu35) and asparagine (Asn52). Lysozyme C is rich in lysine (18 residues) and arginine (17 residues), which means that its isoelectric point shifts toward the base region. At pH 6.6–6.8, the protein has a positive charge, which facilitates the binding of a negatively charged substrate [56].

α-Lactalbumin starts functioning already during lactose synthesis in the mammary gland as a regulator of the lactose synthase complex. For the protein-to-protein interaction between α-lactalbumin and galactosyltransferase to be effective, α-lactalbumin must be bound to a calcium ion. Calcium is structurally and regulatory essential as it stabilizes the native conformation of α-lactalbumin. Thus, α-lactalbumin has a calcium-binding domain that consists of Asp82, Asp84, Asp87, Glu88, and Asp81 residues, which form a Ca^{2+} coordination sphere [57].

With only 19% sequence coverage of fragment 31 (Table 2), the mass-spectrometry regions of the α-lactalbumin and lysozyme C sequences overlap. However, these proteins behave differently when separated by two-dimensional electrophoresis because lysozyme C is fortified with positively charged amino acid residues.

Table 3 illustrates the electrophoretic changes in the proteomic profile of skim milk and the identified peptide profile, thus describing the pasteurization-induced transformations in milk proteins.

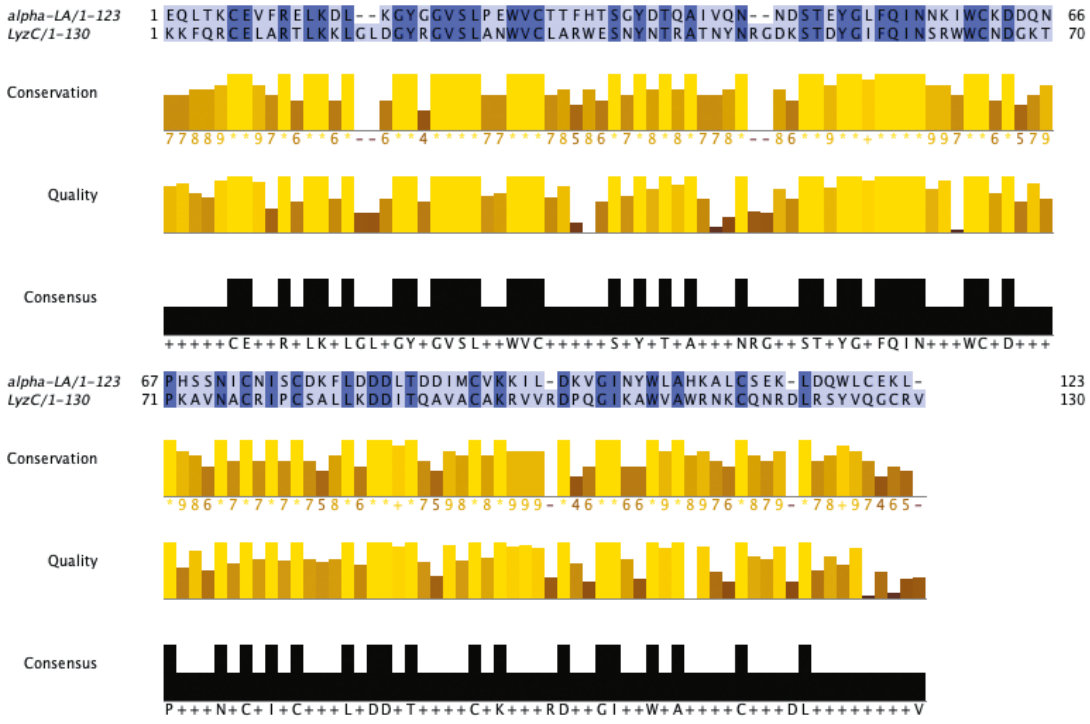


Figure 3 Amino acid sequences: α-lactalbumin vs. lysozyme. Conservation – column height indicates the degree of conservation at each position, where higher columns represent highly conserved residues; Quality – an indicator of alignment reliability at each specific position; Consensus – the consensus sequence, where letters represent identical residues while "+" indicates conservative substitutions; Numbering – labels (1, 67, 71) denote amino acid positions within the α-lactalbumin and lysozyme C sequences

Such changes indicate a whole complex of heat-induced processes: partial protein denaturation, aggregation of *β*-lactoglobulin with *κ*-casein, possible dephosphorylation of casein fractions, and the appearance of plasmin proteolysis products. Other studies [7, 8] reported similar effects: pasteurization and ultra-pasteurization reduce the proportion of soluble whey proteins in milk, inducing the formation of casein derivative fractions.

According to the mass spectrometry, the control sample (no heat load) demonstrated the most diverse peptide composition (28 protein spots).

As heat load increased, the number of peptides decreased. Sample M90 (90°C) contained some fractions that were absent from lower-heat samples M70 and M80. It even developed some completely new fragments (4 and 19), belonging to *β*-casein (isoform X2) and α_{S1}-casein, respectively. The α_{S1}-casein fragment probably separated during the heat-induced destabilization of casein micelle. In addition, casein micelles could lose phosphates, shifting the isoelectric point toward a more alkaline region [48].

Table 3 Electrophoretic profile of protein fragments in pasteurized skim milk

Fragment	Control	M70 (70°C)	M80 (80°C)	M90 (90°C)
1	+	+	+	+
2	+	+	–	–
3	+	+	+	+
4	–	–	–	+
5	+	+	+	+
6	+	+	+	+
7	+	+	+	–
8	+	–	–	–
9	+	–	–	+
10	+	–	–	–
11	+	–	–	+
12	+	–	–	+
13	+	+	–	+
14	+	+	+	+
15	+	+	+	+
16	+	+	–	–
17	–	–	+	–
18	+	–	–	–
19	–	–	–	+
20	+	+	+	+
21	+	+	+	+
22	+	+	+	+
23	+	+	+	+
24	+	+	–	+
25	+	–	–	–
26	+	–	–	+
27	+	+	+	–
28	+	–	–	+
29	+	–	–	+
30	+	+	–	+
31	+	+	+	+

The fragments with lower electrophoretic activity could be explained by the amino acid composition of *β*-casein: it includes proline residues that prevent the polypeptide chain from compact folding [37]. This factor destabilizes *β*-casein molecules during heating, and the fractions disappear. Fragments with lower molecular weight are explained by the activity of plasmin, which cleaves *β*-casein and retains its activity under heat load [45]. This factor also explains fragment 30 in sample M90 (90°C): the heat-induced change in the casein micelle's quaternary structure renders the polypeptide chain more susceptible to plasmin cleavage.

Sample M70 (70°C) was closest in protein profile to the control sample. It lost the following protein fragments: *β*-casein, isoform X2 (8, 9, 10, 11, 12, 16, 18); *κ*-casein (25, 26); *β*-lactoglobulin (28, 29). Such peptide profile of milk pasteurized at 70°C was consistent with the results reported in [58]: moderate heat loads induce the denaturation of whey proteins but cause no massive loss of soluble forms and trigger no new high-molecular forms.

Sample M80 (80°C) lacked the following fragments: α_{S1}-casein (2); *β*-casein, isoform X2 (8, 9, 10, 11, 12, 13, 16, 18); *κ*-casein (24, 25, 26); *β*-lactoglobulin (28, 29, 30). However, it had fragment 17 (*β*-casein, isoform X2). At 80°C, *β*-lactoglobulin denatured faster as evidenced by the disappearance of protein spots. Other changes involve intermolecular interactions with *κ*-casein and the formation of protein aggregates with altered electrophoretic mobility [59].

Sample M90 (90°C) demonstrated the most severe changes in the peptide profile. It lost a significant number of milk protein fragments: bovine serum albumin (27); α_{S1}-casein (2); *β*-casein, isoform X1 (7); *β*-casein, isoform X2 (8, 10); *κ*-casein (25). Paulsson & Dejmek [60] reported the disappearance of fragment 27 when they used differential scanning calorimetry to establish the protein denaturation temperature (64°C). Lysozyme C (fragment 31) is more resistant to heat load than *α*-lactalbumin. Consequently, as other fragments of whey proteins disappear under heat load, fragment 31 persists under all heat modes. Moriyama *et al.* [61] compared the structural changes in lysozyme C and *α*- lactalbumin. Lysozyme C retained a stable secondary structure at ≥ 60°C whereas *α*-lactalbumin lost its native conformation as its protein globule unfolded.

The combined two-dimensional electrophoresis and mass spectrometry yielded highly informative results in relation to milk proteomic profile transformations. However, these methods are so labor-intensive and laboratory-oriented that it limits their application as a rapid analysis of heat-induced changes in the milk matrix, making Raman spectroscopy the most likely candidate.

Spectral analysis of pasteurized milk samples. Thermal treatment induces a wide range of chemical reactions in milk, most notably protein denaturation, intermolecular cross-linking, and the Maillard reaction [62]. Raman spectroscopy is highly sensitive to subtle changes in organic molecules, which makes it a promising method for assessing the effects of heat load on milk [63]. We subjected the Raman spectrum to mathematical processing in the wave region that corresponded with milk proteins (900–1700 cm^{-1}).

It revealed several zones associated with changes in milk: 900–1097; 1328–1437; and 1475–1546 cm^{-1} (Fig. 4b).

He *et al.* [63] mentioned using the peak at ~ 1085 cm^{-1} as a marker of lactose in milk because it reflects the vibrations of C-O-H chemical bonds in disaccharide. Similarly, Vaskova & Buckova [64] referred to the band at ~ 1087 cm^{-1} in the Raman spectrum of milk to describe the vibrational vibrations of C-O-H bond in lactose. Reiner *et al.* [65] reported the spectral range of 500–1225 cm^{-1} as reflecting the changes in milk proteins, including melanoidin formation. They also associated the band at ~ 879 cm^{-1} with changes in proteins, in particular, the indole ring of tryptophan. Therefore, the spectral range of 900–1097 cm^{-1} marks lactose transformations and a weak Maillard reaction [66].

According to other studies [67, 68], the bands at ~ 1440 cm^{-1} characterize the CH_2 groups and may be used to assess heat-induced protein transformations. Similarly, Yazgan *et al.* [69] linked the spectral region of 1470–1521 cm^{-1} to the deformation of methylene groups.

The previously established changes in the proteomic profile were consistent with the changes in their spectra. The complexation of *β*-lactoglobulin and *κ*-casein alters the amide bands at 1475–1546 cm^{-1}, i.e., Amide II (~ 1553 cm^{-1}) [68]. This region characterizes the vibrations of C-O, C-C and C-O-H bonds in the amino acid residues of aspartic and glutamic amino acids, the stretching of C-N bonds in peptide groups, and the deformation of N-H bond [68]. This zone reflects alterations in the microenvironment of amino acid side chains in milk proteins, caused by denaturation and aggregation of whey proteins. The observed heat-induced decrease in intensity in this region may be associated with the unfolding of protein globules or the redistribution of hydrogen bonds, as well as protein-to-protein and protein-to-carbohydrate interactions [68]. Thus, each of the identified zones of the Raman spectrum is closely associated with protein modifications during milk heating, i.e., the carbohydrate-to-protein interactions, the rearrangement of the CH_2 groups in amino acid residues, the protein denaturation, and the interaction between whey proteins and casein. These spectral characteristics of pasteurized milk were consistent with the results we obtained by MALDI-TOF and two-dimensional electrophoresis. These results also demonstrated that increasing the heat load from 70 to 90°C led to alterations in the peptide profile and a reduction in whey protein concentration.

We performed a principal component analysis (PCA) of the spectral data to identify spectral regions potentially sensitive to heat load. Figures 5 and 6 visualize the heat-induced changes in the spectral profiles.

The PCA plotting visualizes the heat-induced variability of spectral profiles. The concentration of maximum loadings in a limited number of ranges indicates that the spectral changes are structurally determined and associated

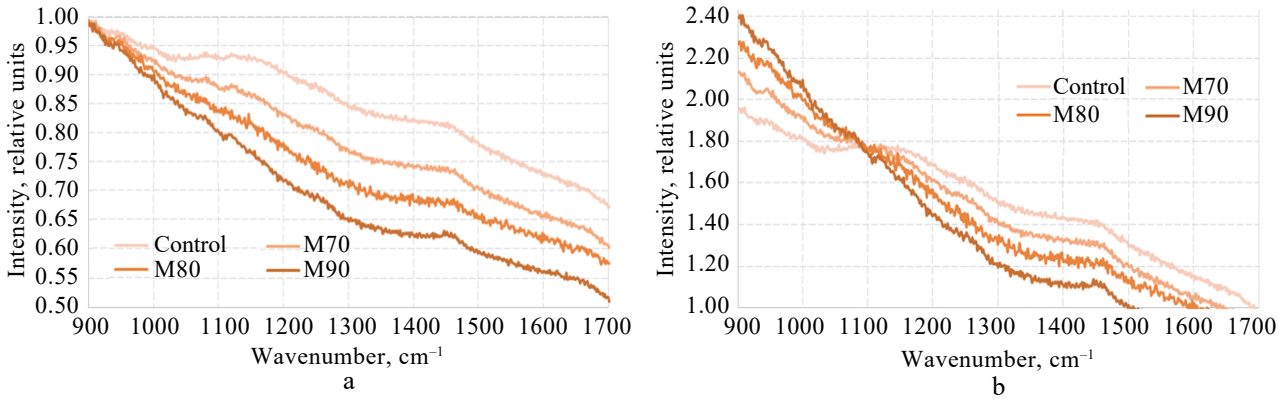


Figure 4 Raman spectra of skim milk samples: a – spectral plot after scaling (MinMaxScaler); b – spectral plot after *Z*-transformation (principal component analysis)

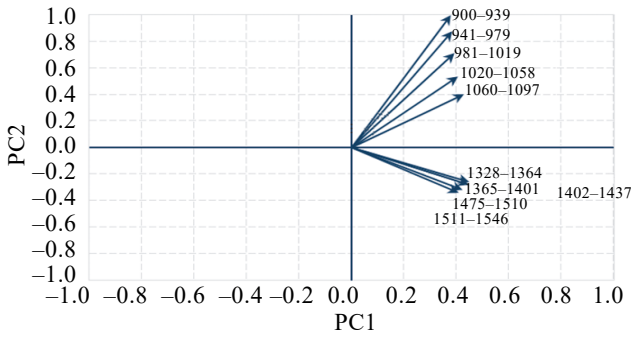


Figure 5 Raman spectral contributions to the variability of pasteurized skim milk samples

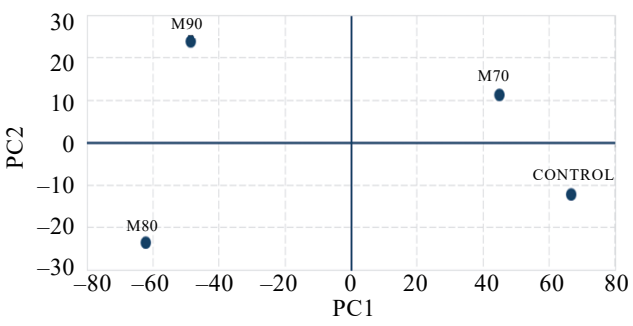


Figure 6 Discrimination of pasteurized skim milk samples based on their spectral characteristics: Principal component

with the transformations of certain chemical bonds in protein molecules and their functional groups. The high total variance of PC1 and PC2 indicates that the selected spectral features reflect heat-induced changes in the milk system.

According to the analysis of principal component loadings, the range of 900–939 cm^{-1} had the greatest contribution to data variance: PC1 = 0.378; PC2 = 1.000; load vector magnitude = 1.070. It corresponded to the fluctuations in C-O and C-O-H lactose bonds. The high loading vector magnitude value indicated the contribution of this spectral region to the variability of milk samples across the heat-load modes. In addition, it may indicate the carbohydrate profile transformation during heat treatment and the formation of Maillard reaction products, i.e., glycated regions of protein molecules.

The next significant contribution belonged to the bands at 941–979 and 981–1019 cm^{-1} with loading vector magnitudes of 0.96 and 0.81, respectively. They had positive loading values for PC1 (0.38–0.39) and PC2 (0.71–0.88). The spectral features in this region are attributed to the C-O stretching vibrations of carbohydrates. Furthermore, this spectral region may be a characteristic of protein matrix transformation detected during electrophoretic separation of milk samples. These characteristics include the redistribution of casein fraction forms and intermolecular protein interactions.

The wavenumber ranges at 1020–1058 and 1060–1097 cm^{-1} (PC1 = 0.405–0.428; loading vector magnitude = 0.59–0.67) characterize the contribution of the carbohydrate fraction to the variations in pasteurized milk samples.

The spectral regions that reflect the changes in protein molecules also make a significant contribution to the dispersion of these samples across the heat-load modes: 1328–1364; 1365–1401; 1402–1437; 1475–1510; and 1511–1546 cm^{-1} (loading vector magnitude = 0.52–0.53). These wavenumber regions characterize the deformation vibrations of CH_2 groups in amino acid side chains and the alterations in the amide bands (Amide II), which are all sensitive to the changes in the secondary structure of protein molecules.

The results of the principal component analysis were consistent with the heat-induced changes in the milk proteomic profile previously registered by two-dimensional electrophoresis and MALDI-TOF MS: whey proteins disappeared and new protein fragments appeared as a result of intermolecular protein interactions.

Thus, the mathematical processing of spectral profiles made it possible to visualize the heat-induced changes in pasteurized skim milk. Raman spectroscopy proved to be an efficient method of assessing the effects of heat load on skim milk and the feasibility of further tests.

CONCLUSION

In this research, molecular analysis methods were able to detect and identify heat-induced changes in skim milk proteomic profile. As the heat load increased from 70 to 90°C, two-dimensional electropherograms detected a significant decrease in the number of detectable protein fractions. The control sample had 28 protein spots while the skim milk sample heated to 90°C demonstrated the lowest peptide diversity but contained new fragments associated with heat-induced proteomic transformations.

The most pronounced changes occurred in whey proteins. β-Lactoglobulin fractions (20, 21) and bovine serum albumin started disappearing already at 70°C. At ≥ 80°C, we observed a complete loss of detectable fragments of α-lactalbumin and β-lactoglobulin, which indicated profound changes in the secondary structure and aggregation of proteins.

Although the casein fraction exhibited superior thermal stability, it nevertheless showed the formation of additional peptide fragments and a redistribution of isoforms. Matrix-assisted laser desorption ionization time-of-flight mass spectrometry (MALDI-TOF MS) identified 26 peptides in the casein fraction. The sample treated at 90°C revealed new amino acid sequences of β-casein (isoform X2, Fragment 30) and α_{S1}-casein (Fragment 31), which were absent from the control and the samples subjected to milder thermal treatment. The calculated and experimental isoelectric points for α_{S1}- and α_{S2}-casein fragments ranged from 4.75 to 8.80 pH units. This range indicated heat-induced partial dephosphorylation, glycosylation, and new covalent protein-to-protein complexes.

The method of Raman spectroscopy revealed heat-induced changes at 900–1097; 1328–1437; and 1475–1546 cm^{-1} associated with carbohydrate fragments, CH_2 groups of amino acid residues, and Amide II.

The principal component analysis revealed a clustering of samples based on their thermal history. The ranges characterizing the transformation of carbohydrate and protein profiles contributed most to the data dispersion: 900–939 cm^{-1} (load vector modulus = 1.07); 941–979 cm^{-1} (load vector modulus = 0.96); 1328–1364; 1365–1401; 1402–1437; 1475–1510; and 1511–1546 cm^{-1} (load vector modulus = 0.52–0.53).

The resulting molecular and spectral changes correlated with the technological transformations in milk. On the one hand, the extensive whey protein denaturation and β-lactoglobulin–κ-casein complexation adversely affect cheese-making properties and milk powder solubility. On the other hand, these changes may enable targeted modulation of curd structure in fermented dairy products.

Our study established a reliable consistency between the data obtained from two-dimensional electrophoresis, MALDI-TOF MS, and Raman spectroscopy of pasteurized milk. The heat-induced changes in the proteomic profile that were recorded during the peptide profiling found a reflection in particular spectral ranges. These correlations provide a scientifically valid platform for developing new markers of heat exposure for dairy quality control at various processing stages. These markers will establish a framework for using Raman spectroscopy to classify the thermal history of milk powder, ensuring its optimal application across different dairy production pathways.

CONTRIBUTION

All the authors were equally involved in the manuscript and are equally responsible for any potential plagiarism.

CONFLICT OF INTEREST

The authors declared no potential conflict of interest regarding the research, authorship, and / or publication of this article.

REFERENCES

1. OECD | Food and Agriculture Organization of the United Nations. OECD-FAO Agricultural Outlook 2025–2034. Paris: OECD Publishing; 2025, 166 p. https://doi.org/10.1787/601276cd-en
2. Ní Fhuaráin AM, O'Donnell CP, Luo J, Gowen AA. A review on MIR, NIR, fluorescence and Raman spectroscopy combined with chemometric modeling to predict the functional properties of raw bovine milk. ACS Food Science & Technology. 2024;4(10):2258–2271. https://doi.org/10.1021/acsfoodscitech.4c00130
3. Kartashova V. The dairy market of Russia shows growth. Animal Husbandry of Russia. 2025;(S2):2–5. (In Russ.) https://elibrary.ru/CNUOCJ
4. Khurshudyan SA, Blizkiy AM. Quality requirements for food waste. Production Quality Control. 2024;(1): 27–30.
5. Shuvarikov AS, Yurova EA, Pastukh ON. Quality indicators of cow, goat and camel milk with account of allergenicity. Izvestiya of Timiryazev Agricultural Academy. 2017;(5):115–123. (In Russ.) https://doi.org/10.26897/0021-342X-2017-5-115-123
6. Donskaya GA. Antioxidant properties of milk and dairy products: Review. Food Industry. 2020;(12):86–91. (In Russ.) https://elibrary.ru/XNCFER
7. Nunes L, Tavares GM. Thermal treatments and emerging technologies: Impacts on the structure and techno-functional properties of milk proteins. Trends in Food Science & Technology. 2019;90:88–99. https://doi.org/10.1016/j.tifs.2019.06.004
8. Čurlej J, Zajác P, Čapla J, Golian J, Benešová L, *et al*. The effect of heat treatment on cow's milk protein profiles. Foods. 2022;11(7):1023. https://doi.org/10.3390/foods11071023
9. Wang Y, Xiao R, Liu S, Wang P, Zhu Y, *et al*. The impact of thermal treatment intensity on proteins, fatty acids, macro/micro-nutrients, flavor, and heating markers of milk – a comprehensive review. International Journal of Molecular Sciences. 2024;25(16):8670. https://doi.org/10.3390/ijms25168670
10. Galstyan AG, Petrov AN, Illarionova EE, Semipyatniy VK, Turovskaya SN, *et al*. Effects of critical fluctuations of storage temperature on the quality of dry dairy product. Journal of Dairy Science. 2019;102(12):10779–10789. https://doi.org/10.3168/jds.2019-17229
11. Ebner J, Baum F, Pischetsrieder M. Identification of sixteen peptides reflecting heat and/or storage induced processes by profiling of commercial milk samples. Journal of Proteomics. 2016;147:66–75. https://doi.org/10.1016/j.jprot.2016.03.021
12. Arab M, Yousefi M, Khanniri E, Azari M, Ghasemzadeh-Mohammadi V, *et al*. A comprehensive review on yogurt syneresis: Effect of processing conditions and added additives. Journal of Food Science and Technology. 2023;60:1656–1665. https://doi.org/10.1007/s13197-022-05403-6
13. Akkerman M, Rauh VM, Christensen M, Johansen LB, Hammershøj M, *et al*. Effect of heating strategies on whey protein denaturation – revisited by liquid chromatography quadrupole time-of-flight mass spectrometry. Journal of Dairy Science. 2016;99(1):152–166. https://doi.org/10.3168/jds.2015-9924
14. Sharma A, Jana AH, Chavan RS. Functionality of milk powders and milk-based powders for end use applications – a review. Comprehensive Reviews in Food Science and Food Safety. 2012;11(5):518–528. https://doi.org/10.1111/j.1541-4337.2012.00199.x
15. Kruchinin AG, Illarionova EE, Bigaeva AV, Turovskaya SN. The role of dry milk technological properties in forming the quality of food systems. Bulletin of KSAU. 2020;(8):166–173. (In Russ.) https://doi.org/10.36718/1819-4036-2020-8-166-173
16. Bista A, Murphy EG, O'Donnell CP, O'Shea N. The effect of heat treatment on physicochemical properties of skim milk concentrate and spray-dried skim milk powder. International Journal of Dairy Technology. 2022;75(3):690–700. https://doi.org/10.1111/1471-0307.12876
17. Lindmark-Månsson H, Timgren A, Aldén G, Paulsson M. Two-dimensional gel electrophoresis of proteins and peptides in bovine milk. International Dairy Journal. 2005;15(2):111–121. https://doi.org/10.1016/j.idairyj.2004.06.010
18. Kruchinin AG, Bigaeva AV, Lazareva EG, Vafin RR, Mikhailova IYu, *et al*. Electrophoretic methods for study of protein systems. Dairy industry. 2020;(6):16–18. (In Russ.) https://doi.org/10.31515/1019-8946-2020-06-16-18

19. Barkovskaya IA, Turovskaya SN, Illarionova EE, Yaryshev VYu, Bliadze VG, *et al*. Comparison of IR and Raman spectroscopy methods for assessing structural changes in milk during heat treatment. Food Metaengineering. 2025;3(3):21–38. (In Russ.) https://doi.org/10.37442/fme.2025.3.91
20. Yurova EA, Zhizhin NA, Filchakova SA. Molecular genetic methods of analysis to identify the species affiliation of the raw material composition in food products. Vestnik of MSTU journal. 2020;23(3):214–223. https://doi.org/10.21443/1560-9278-2020-23-3-214-223
21. Khan AV, Lazareva EG, Fomenko OYu. Optimization of molecular genetic method for identification of dairy raw materials. Food Metaengineering. 2023;1(4):39–47. (In Russ.) https://doi.org/10.37442/fme.2023.4.29
22. Khan AV, Lazareva EG, Fomenko OYu. The problem of dairy products adulteration: Analysis of the state and ways of resolution. Dairy industry. 2023;(5):54–56. https://doi.org/10.21603/1019-8946-2023-5-6
23. Koval DD, Khan AV, Lazareva EG, Fomenko OYu. Isolating bacterial DNA from goat milk and its products: Comparative analysis. Food Processing: Techniques and Technology. 2025;55(2):390–399. (In Russ.) https://doi.org/10.21603/2074-9414-2025-2-2579
24. Losito I, Carbonara T, Monaci L, Palmisano F. Evaluation of the thermal history of bovine milk from the lactosylation of whey proteins: An investigation by liquid chromatography–electrospray ionization mass spectrometry. Analytical and Bioanalytical Chemistry. 2007;389:2065–2074. https://doi.org/10.1007/s00216-007-1447-0
25. Class L-C, Kuhnen G, Hanisch KL, Badekow S, Rohn S, *et al*. The shelf life of milk – A novel concept for the identification of marker peptides using multivariate analysis. Foods. 2024;13(6):831. https://doi.org/10.3390/foods13060831
26. Šebela M. Biomolecular profiling by MALDI-TOF mass spectrometry in food and beverage analyses. International Journal of Molecular Sciences. 2022;23(21):13631. https://doi.org/10.3390/ijms232113631
27. Kang W, Feng F, Zhou W, Jing M, Wang X, *et al*. Discrimination of overheated pasteurized milk using mass spectrometry-based proteomics. Journal of Chromatography B. 2024;1243:124236. https://doi.org/10.1016/j.jchromb.2024.124236
28. Panthi RR, Shibu SN, Ochalski TJ, O'Mahony JA. Raman spectra of micellar casein powders prepared with wet blending of glycomacropeptide and micellar casein concentrate. International Journal of Dairy Technology. 2023;76(2):429–435. https://doi.org/10.1111/1471-0307.12920
29. Zhang S, Zhang Z, Lin M, Vardhanabhuti B. Raman spectroscopic characterization of structural changes in heated whey protein isolate upon soluble complex formation with pectin at near neutral pH. Journal of Agricultural and Food Chemistry. 2012;60(48):12029–12035. https://doi.org/10.1021/jf303780c
30. Li C, Nielsen SB, Engholm-Keller K, Lund MN. Oxidation of whey proteins during thermal treatment characterized by a site-specific LC–MS/MS-based proteomic approach. Journal of Agricultural and Food Chemistry. 2022;70(14):4391–4406. https://doi.org/10.1021/acs.jafc.1c07946
31. Meltretter J, Wüst J, Pischetsrieder M. Modified peptides as indicators for thermal and nonthermal reactions in processed milk. Journal of Agricultural and Food Chemistry. 2014;62(45):10903–10915. https://doi.org/10.1021/jf503664y
32. Lu J, Zhu T, Dai Y, Xing L, Jinqi L, *et al*. The effect of heat treatment on the lactosylation of milk proteins. Journal of Dairy Science. 2023;106(12):8321–8330. https://doi.org/10.3168/jds.2023-23526
33. Kovalyov LI, Shishkin SS, Kovalyova MA, Ivanov AV, Vostrikova NL, *et al*. Proteomic research proteins in a sample of pork meat products. Vse o myase. 2013;(3):32–34. https://elibrary.ru/QCRSLF
34. Zvereva EA, Kovalev LI, Ivanov AV, Kovaleva MA, Zherdev AV, *et al*. Enzyme immunoassay and proteomic characterization of troponin I as a marker of mammalian muscle compounds in raw meat and some meat products. Meat Science. 2015;105:46–52.
35. Alkadur MI, Pryanichnikova NS, Yurova EA, Petrov AN. Effect of thermal treatment and pasteurization on milk powder quality. Food Processing: Techniques and Technology. 2024;54(1):275–284. (In Russ.) https://doi.org/10.21603/2074-9414-2024-2-2506
36. Runthala A, Mbye M, Ayyash M, Xu Y, Kamal-Eldin A. Caseins: Versatility of their micellar organization in relation to the functional and nutritional properties of milk. Molecules. 2023;28(5):2023. https://doi.org/10.3390/molecules28052023
37. Krishna TC, Najda A, Bains A, Tosif MM, Papliński R, *et al*. Influence of ultra-heat treatment on properties of milk proteins. Polymers. 2021;13(18):3164. https://doi.org/10.3390/polym13183164
38. Li H, Zhao T, Li H, Yu J. Effect of heat treatment on the property, structure, and aggregation of skim milk proteins. Frontiers in Nutrition. 2021;8:714869. https://doi.org/10.3389/fnut.2021.714869
39. Mohammad-Beigi H, Wijaya W, Madsen M, Hayashi Y, Li R, *et al*. Association of caseins with *β*-lactoglobulin influenced by temperature and calcium ions: A multi-parameter analysis. Food Hydrocolloids. 2023;137:108373. https://doi.org/10.1016/j.foodhyd.2022.108373

40. Zhang T, Liu Y, Cao J, Jiang L, Wang P, *et al*. Exploration of dynamic interaction between *β*-lactoglobulin and casein micelles during UHT milk process. International journal of biological macromolecules. 2024;277(Part 2):134367. https://doi.org/10.1016/j.foodhyd.2022.108373
41. Jovanovic S, Barac M, Macej O, Vucic T, Lacnjevac C. SDS-PAGE analysis of soluble proteins in reconstituted milk exposed to different heat treatments. Sensors. 2007;7(3):371–383. https://doi.org/10.3390/s7030371
42. Ichimura T, Kusaka M, Nakamura T. The effect of high-temperature heat treatment and homogenization on the microstructure of set yogurt curd networks. Journal of Dairy Research. 2023;90(3):306–311. https://doi.org/10.1017/S0022029923000523
43. Asaduzzaman M, Mahomud MS, Haque ME. Heat-induced interaction of milk proteins: Impact on yoghurt structure. International Journal of Food Science. 2021;2021:5569917. https://doi.org/10.1155/2021/5569917
44. Alkadur MI, Petrov AN, Pryanichnikova NS. Influence of the class of thermal treatment of dry milk on the structure and properties of the fermented curd. Food industry. 2024;(11):82–89. (In Russ.) https://doi.org/10.52653/PPI.2024.11.11.015
45. Wölk M, Milkovska-Stamenova S, Hoffmann R. Comprehensive profiling of the native and modified peptidomes of raw bovine milk and processed milk products. Foods. 2020;9(12):1841. https://doi.org/10.3390/foods9121841
46. Bhattacharya M, Salcedo J, Robinson RC, Henrick BM, Barile D. Peptidomic and glycomic profiling of commercial dairy products: Identification, quantification and potential bioactivities. npj Science of Food. 2019;3(1):4. https://doi.org/10.1038/s41538-019-0037-9
47. Ceballos LS, Morales ER, de la Torre Adarve G, Castro JD, Martínez LP, *et al*. Composition of goat and cow milk produced under similar conditions and analyzed by identical methodology. Journal of Food Composition and Analysis. 2009;22(4):322–329. https://doi.org/10.1016/j.jfca.2008.10.020
48. Holland JW, Gupta R, Deeth HC, Alewood PF. UHT milk contains multiple forms of α_{S1}-casein that undergo degradative changes during storage. Food Chemistry. 2012;133(3):689–696. https://doi.org/10.1016/j.foodchem.2012.01.070
49. Freire P, Zambrano A, Zamora A, Castillo M. Thermal denaturation of milk whey proteins: A comprehensive review on rapid quantification methods being studied, developed and implemented. Dairy. 2022;3(3):500–512. https://doi.org/10.3390/dairy3030036
50. McMahon DJ, Oommen BS. Casein micelle structure, functions, and interactions. In: McSweeney P, Fox P, editors. Advanced Dairy Chemistry. Boston: Springer; 2013, pp. 185–209. https://doi.org/10.1007/978-1-4614-4714-6_6
51. Caroli AM, Savino S, Bulgari O, Monti E. Detecting *β*-casein variation in bovine milk. Molecules. 2016;21(2):141. https://doi.org/10.3390/molecules21020141
52. Kang Y, Jimenez-Flores R, Richardson T. Casein genes and genetic engineering of the caseins. In: Evans JW, Hollaender A, Wilson CM, editors. Genetic Engineering of Animals. Boston: Springer; 1986, pp. 95–111. https://doi.org/10.1007/978-1-4684-5110-8_9
53. Lai EPC, Tsopmo A. Casein chemistry–structure, functions, and applications. Exploratory Foods and Foodomics. 2025;3:101099. https://doi.org/10.37349/eff.2025.101099
54. Sava N, Van der Plancken I, Claeys W, Hendrickx M. The kinetics of heat-induced structural changes of *β*-lactoglobulin. Journal of Dairy Science. 2005;88(5):1646–1653. https://doi.org/10.3168/jds.S0022-0302(05)72836-8
55. Qasba PK, Kumar S. Molecular divergence of lysozymes and *α*-lactalbumin. Critical reviews in biochemistry and molecular biology. 1997;32(4):255–306. https://doi.org/10.3109/10409239709082574
56. Davies GJ, Williams SJ. Carbohydrate-active enzymes: Sequences, shapes, contortions and cells. Biochemical Society Transactions. 2016;44(1):79–87. https://doi.org/10.1042/BST20150186
57. Barkovskaya IA, Ryabova AE, Rozhkova IV. Complex modification of whey protein profile as an approach to the creation of enriched protein ingredients. Food systems. 2025;8(2):221–230. (In Russ.) https://doi.org/10.21323/2618-9771-2025-8-2-221-230
58. Clawin-Rädecker I, Kiesner C, Schlimme E. Analysis of the acid-soluble contents of *α*-lactalbumin, *β*-lactoglobulin, serum albumin and the immunoglobulin fraction in pasteurized milk. Kieler Milchwirtschaftliche Forschungsberichte. 2000;52(4):322–334. (In German)
59. Cho Y, Singh H, Creamer LK. Heat-induced interactions of *β*-lactoglobulin A and *κ*-casein B in a model system. Journal of Dairy Research. 2003;70(1):61–71. https://doi.org/10.1017/S0022029902005642
60. Paulsson M, Dejmek P. Thermal denaturation of whey proteins in mixtures with caseins studied by differential scanning calorimetry. Journal of Dairy Science. 1990;73(3):590–600. https://doi.org/10.3168/jds.S0022-0302(90)78707-3
61. Moriyama Y, Kondo N, Takeda K. Secondary structural changes of homologous proteins, lysozyme and *α*-lactalbumin, in thermal denaturation up to 130 °C and sodium dodecyl sulfate (SDS) effects on these changes: comparison of thermal stabilities of SDS-induced helical structures in these proteins. Langmuir. 2012;28(47):16268–16273. https://doi.org/10.1021/la3035598

62. Wu J, Chen S, Van der Meeren P. Heat stability assessment of milk: A review of traditional and innovative methods. Foods. 2024;13(14):2236. https://doi.org/10.3390/foods13142236
63. He H, Sun DW, Pu H, Chen L, Lin L. Applications of Raman spectroscopic techniques for quality and safety evaluation of milk: A review of recent developments. Critical Reviews in Food Science and Nutrition. 2019;59(5):770–793. https://doi.org/10.1080/10408398.2018.1528436
64. Vaskova H, Buckova M. Measuring the lactose content in milk. MATEC Web of Conferences. 2016;76:05011. https://doi.org/10.1051/matecconf/20167605011
65. Reiner J, Protte K, Hinrichs J. Investigation of the applicability of Raman spectroscopy as online process control during consumer milk production. ChemEngineering. 2020;4(3):45. https://doi.org/10.3390/chemengineering4030045
66. Choudhary S, Arora S, Kumari A, Narwal V, Sharma V. Effect of quality of milk on Maillard reaction and protein oxidation during preparation of cow and buffalo milk *khoa*. Journal of Food Science and Technology. 2017;54:2737–2745. https://doi.org/10.1007/s13197-017-2710-9
67. Silva MG, de Paula IL, Stephani R, Edwards HGM, de Oliveira LFC. Raman spectroscopy in the quality analysis of dairy products: A literature review. Journal of Raman Spectroscopy. 2021;52(12):2444–2478. https://doi.org/10.1002/jrs.6214
68. Sibono L, Tronci S, Hedegaard MAB, Errico M, Grosso M. Raman spectroscopy coupled with multivariate statistical process control for detecting anomalies during milk coagulation. Processes. 2025;13(11):3519. https://doi.org/10.3390/pr13113519
69. Yazgan NN, Genis HE, Bulat T, Topcu A, Durna S, *et al*. Discrimination of milk species using Raman spectroscopy coupled with partial least squares discriminant analysis in raw and pasteurized milk. Journal of the Science of Food and Agriculture. 2020;100(13):4756–4765. https://doi.org/10.1002/jsfa.10534

Additional information about the authors

Irina A. Barkovskaya ORCID 0000-0003-4779-1076; eLIBRARY SPIN 9404-4365
Polina I. Koroleva ORCID 0000-0003-2802-5747; eLIBRARY SPIN 9646-9334
Svetlana N. Turovskaya ORCID 0000-0002-5875-9875; eLIBRARY SPIN 6904-5308
Elena E. Illarionova ORCID 0000-0002-9399-0984; eLIBRARY SPIN 2990-2390
Vladimir V. Kondratenko ORCID 0000-0002-0913-5644; eLIBRARY SPIN 3383-1774
Vladimir G. Bliadze ORCID 0000-0001-9300-3267; eLIBRARY SPIN 7263-6500
Vladislav Yu. Yaryshev ORCID 0009-0007-7848-4606; eLIBRARY SPIN 4906-1980
Andrey N. Petrov ORCID 0000-0001-9879-482X; eLIBRARY SPIN 2839-1773

Foods and Raw Materials. 2027;15(2)

ISSN 2308-4057 (Print)
ISSN 2310-9599 (Online)

Research Article
Open Access

Available online at http://jfrm.ru/en
https://doi.org/10.21603/2308-4057-2027-2-719
https://elibrary.ru/PSWDFT

Pulp and by-products of indigenous and non-indigenous mangoes in Uganda: Physicochemical properties

Henriettah Nakisozi, Patrick Ogwok*, Diriisa Mugampoza

Kyambogo University, Kampala, Uganda

* e-mail: ogwokp@yahoo.com

Received 26.08.2025; Revised 12.11.2025; Accepted 03.02.2026; Published online 29.09.2026

Abstract:
Mango pulp and by-products are underutilized despite their application potential in the food systems. Our study assessed the physicochemical properties of pulp and by-products of 22 mango varieties to support their added value.
We applied the methods developed by the Association of Official Analytical Chemists. The data were analyzed using descriptive statistics and non-parametric tests.
Seven varieties had total soluble solids above the Codex Alimentarius threshold of 13.5°Brix, indicating their suitability for juice processing. Non-indigenous varieties exhibited higher titratable acidity and yellowness (*b**), the traits desirable for juices and purees. Indigenous varieties had higher redness (*a**) and lower acidity, which favor fresh consumption. Among by-products, the peel had the highest crude fiber content of 10.16 ± 1.76%. The seeds recorded the highest potassium and calcium concentrations of 354.90 ± 25.10 and 437.74 ± 35.81 mg/100 g, respectively. The principal component analysis explained 87.62% of the total variation: principal component 1 (75.03%) differentiated varieties based on minerals, total soluble solids, and firmness, while principal component 2 (12.59%) accounted for differences in vitamin C and color. The principal component analysis and bootstrap hulls showed that varietal differences stemmed from the intrinsic traits rather than from the indigenous or non-indigenous classification. Kakule and Kapisa varieties appeared on the positive side of principal component 1, reflecting a higher mineral content. Apple mango and Boribo mangoes loaded positively on principal component 2 due to high vitamin C and color attributes. Kagoogwa, Takataka, and Tommy Atkins varieties clustered near the total soluble solids vector, indicating adequate soluble solids for juice processing.
Our findings confirm that indigenous mango varieties in Uganda meet the industrial quality standards.

Keywords: Mango varieties, pulp, seeds, kernel, peel, indigenous fruits, non-indigenous fruits, principal component analysis

Please cite this article in press as: Nakisozi H, Ogwok P, Mugampoza D. Pulp and by-products of indigenous and non-indigenous mangoes in Uganda: Physicochemical properties. Foods and Raw Materials. 2027;15(2):425–436. https://doi.org/10.21603/2308-4057-2027-2-719

INTRODUCTION

Mango (*Mangifera indica* L.) is a tropical fruit grown in all agroecological zones of Uganda [1]. Its genetic diversity has expanded with the introduction of non-indigenous varieties that complement locally adapted indigenous mangoes. Non-indigenous mango varieties are preferred by commercial growers for their superior agronomic traits [2]. The mango is made up of 45 to 65% pulp, 15 to 20% peel, 20 to 40% seed, and 5 to 12% kernel of the total fruit weight [3]. Mango pulp is consumed mostly fresh or transformed into a variety of products. It can be processed into juice, jam, and dried products [4]. In Uganda, mango peel, kernel, and seed are predominantly discarded, with small portions relegated to low-value applications such as animal feed and compost [1]. This limited utilization contributes to postharvest losses of up to 40% during the peak season [5]. Being a seasonal fruit, mango requires effective processing to maximize its utilization and add value to its by-products.

Physicochemical properties of mango pulp and by-products are linked to health benefits [6–8]. The pulp is high in vitamin C, which supports the immune system, collagen synthesis, and antioxidant defense [9]. Beta-carotene, violaxanthin, and lutein present in the pulp act as provitamin A, a well-known antioxidant that maintains eye health and combats oxidative damage [10]. The peel contains dietary fiber, polyphenols, and vitamins C and E that exhibit antioxidant, antimicrobial, and anti-inflammatory activities [11–13]. Polyphenols such as mangiferin, gallic acid, quercetin, and catechins are linked to free radical scavenging and other health-promoting effects [12]. Mango seed and kernel

Copyright © 2026, Nakisozi *et al.* This is an open access article distributed under the terms of the Creative Commons Attribution 4.0 International License (https://creativecommons.org/licenses/by/4.0/), allowing third parties to copy and redistribute the material in any medium or format and to remix, transform, and build upon the material for any purpose, even commercially, provided the original work is properly cited and states its license.

are important lipid sources containing oleic acids associated with cardiovascular health and improved insulin sensitivity [14]. They also provide essential minerals that promote bone health, electrolyte balance, and oxygen transport [10, 15].

Nutrient profiles of mangoes vary depending on their genotype, stage of maturity, and environmental conditions [16, 17]. Studies have shown differences in total soluble solids, acidity, and carotenoid content between the Ataulfo and Kent mango varieties [16, 18]. The oil content and fatty acid composition of mango seed and kernel differ across varieties (1). Similar patterns of variability have been observed for phenolic content, mineral composition, and bioactive profiles in the studies from Asia, Latin America, and West Africa [10]. Based on global evidence, we aimed to physicochemically characterize the pulp and by-products of common mango varieties grown in Uganda to identify nutrient-rich varieties that offer potential for added value.

STUDY OBJECTS AND METHODS

Sample collection. Twenty-two mango varieties (13 indigenous and 9 non-indigenous) were collected from the orchards in Luweero, Nakaseke, and Budaka districts of Uganda. These districts are home to most mango varieties in the country. Five mango trees per variety were selected from each location. Ten fruits were randomly picked from each tree [19]. The selection was based on visual indicators of maturity such as a flat shoulder at the stem end, fullness of cheeks, presence of bloom, and change in the peel color from dark to light green. The fruits showing any damage or infestation were excluded. The mango fruits were transported in perforated plastic crates to the Food Biosciences and Agribusiness Laboratory at the National Agricultural Research Organization. They were washed with distilled water and allowed to ripen at 28 ± 2°C with relative humidity of 85%. Ripening was monitored daily using the criteria recommended by the USA National Mango Board[1].

Sample preparation. The pulp, peel, seed, and kernel of the mangoes were separated using a clean, sharp stainless-steel knife (Victorinox, Switzerland). A portion of the pulp was homogenized using a hand-held blender (MQ5025BK, Braun, Germany). The fresh homogenate was analyzed for color, pH, titratable acidity, and total soluble solids. Other fractions of the pulp, peel, seed, and kernel were chopped into uniform pieces. These were dried in a cabinet dryer (UN55, Memmert, Germany) set at 50°C for 12 h. The samples were finely ground in a laboratory grinder (Retsch GM200, Germany), wrapped in polyethylene bags, and stored at –20°C in a freezer (Haier DW-40L508, China) prior to chemical analysis.

Quality parameters of mango pulp. ***Total soluble solids.*** A digital refractometer (RX 5000, Atago, Tokyo, Japan) was used to determine total soluble solids in mango pulp [18]. For this, a drop of the homogenate was placed on the prism of the refractometer and readings were taken. The results were obtained from three independent replicate readings per sample and expressed as °Brix.

pH. A digital pH meter (DL25, Mettler Toledo, Switzerland) was used to measure pH [20]. The pH meter was calibrated using two standard buffer solutions (pH 4.0 and 7.0) before each set of measurements. The homogenate (10 g) was mixed with 50 mL of distilled water. The mixture was stirred continuously using a magnetic stirrer until a stable pH reading was obtained. All measurements were performed in triplicate and the average value was recorded.

Titratable acidity. A 10-mL aliquot of the homogenate was titrated with 0.1 N NaOH using phenolphthalein [21]. Titration was performed until a persistent pink color was achieved. The volume of NaOH used to reach the endpoint was recorded and used to calculate the titratable acidity using the following Eq. (1):

$$C_A = \frac{V \times N \times \mathrm{MW}}{V_e} \times 100 \quad (1)$$

where C_A is the citric acid, %; V is the volume of NaOH, mL; N is the normality of NaOH (0.1 N); MW is the molecular weight of citric acid (192.12 g/mol); and V_e is the volume of mango juice (10 mL).

Vitamin C. The concentration of vitamin C was determined using the 2,6-dichloroindophenol titrimetric method [1]. The homogenized mango pulp (5 g) was diluted with 10% trichloroacetic acid to reach a final volume of 100 mL. This solution was then filtered to obtain a clear extract. The extract was titrated with a standardized 2,6-dichloroindophenol solution until a faint pink color persisted for no less than 15 s. A blank titration was performed using distilled water. The vitamin C content was expressed as mg of ascorbic acid per 100 g of the sample and calculated using the Eq. (2) below:

$$\mathrm{Vit\ C} = \frac{((A-B) \times C)}{S} \times 100 \quad (2)$$

where VitC is the vitamin C content, mg/100 mg; A is the volume of indophenol solution in the sample titration, mL; B is the volume of indophenol solution for the blank titration, mL; C is the mass of ascorbic acid equivalent to 1 mL of standard indophenol solution, mg; S is the weight of the sample, g.

Color. A colorimeter (CR-400, Minolta, Osaka, Japan) was used to measure color after calibration with a white standard tile according to the protocol of Ellong *et al.* [22]. The color parameters of the pulp were expressed as L^*, darkness/lightness (0: black; 100: white), a^* ($-a^*$: greenness, $+a^*$: redness), and b^* ($-b^*$: blueness, $+b^*$: yellowness).

Firmness. A mechanical fruit pressure tester (Model FT 327, Ravenna, Italy) with an 8-mm probe was used

[1] National mango board. Mango maturity and ripeness guide. Mango.org. [cited 2025 Feb 10]. Available from: https://www.mango.org 1

to measure firmness. At a constant rate of 2 mm/s, the probe was gently driven into the middle of the fruit and the force required to reach a depth of 10 mm was recorded in Newtons (N). Readings were taken from three different points on each fruit to determine the average firmness.

Chemical analysis of mango pulp, peel, kernel, and seed. ***Proximate composition.*** Moisture contents in mango pulp, peel, seed, and kernel were determined by drying 2 g of each sample to constant weight in a hot-air oven (Memmert UN55, Germany) following AOAC 930.04[2]. Crude ash was obtained by incinerating 2 g of the dried sample in a muffle furnace (Thermo Scientific Thermolyne 1200, USA) at 550°C according to AOAC 923.03. Crude fiber was determined using 2 g of a defatted sample through sequential acid and alkaline digestion based on AOAC 962.09[3]. Crude fat was extracted from 2 g of a sample using petroleum ether in a Soxhlet extractor (Buchi B-811, Switzerland) AOAC 920.39. Total nitrogen was measured by the Kjeldahl method using a digestion unit (DK 6, Velp Scientifica, Italy) and a distillation unit (UDK 129, Velp Scientifica, Italy). Crude protein was calculated by multiplying total nitrogen by a factor of 6.25[4]. Carbohydrate content was estimated by difference, subtracting the sum of moisture, ash, protein, fiber, and fat contents from 100%.

Mineral composition. 1 g of the sample was weighed into a porcelain crucible and placed in a muffle furnace (Thermo Scientific Thermolyne 1200, USA) set at 550°C and held at that temperature for 6 h. The residue was then dissolved in 10 mL of 1.0 M hydrochloric acid (Sigma-Aldrich, Germany). This solution was filtered through Whatman No. 42 filter paper (Cytiva, UK) into a 100-mL volumetric flask. The flask was topped up to the mark with distilled water. Sodium and potassium concentrations were determined using a flame photometer (Sherwood 410, Sherwood Scientific Ltd., UK) following Piper [23]. Magnesium, calcium, iron and zinc were measured using an atomic absorption spectrophotometer (Analyst™ 200, PerkinElmer, USA). Phosphorus was quantified colorimetrically using the molybdenum blue method at 880 nm (UV-1800 spectrophotometer, Shimadzu, Japan) as described by Horwitz & Latimer[5].

Statistical analysis. Analysis of the data was performed using SPSS (Version 22.0, IBM Corp., USA). The data were presented as mean ± standard deviation. The Shapiro-Wilk test and Levene's test were used to assess normality and homogeneity of variance, respectively. Since the data set violated normality and homogeneity assumptions, Welch's ANOVA was used to compare the mango varieties and the fruit parts. The Kruskal-Wallis test was performed to compare the differences between indigenous and non-indigenous mango varieties. The Games-Howell post-hoc test was used for pairwise comparisons. The principal component analysis was performed using XLSTAT software (Version 2022.3.1, Addinsoft, Paris, France) to explore multivariate patterns and clustering of the mango varieties based on their physicochemical traits. The statistical significance was set at $p < 0.05$.

RESULTS AND DISCUSSION

Physicochemical properties of the pulp of indigenous and non-indigenous mango varieties. ***Quality parameters of mango pulp.*** The pH, total soluble solids (TSS), titratable acidity, vitamin C content, and firmness of the mango pulp showed variation ($p < 0.05$) among the varieties, with ranges of 3.18–4.76, 8.10–16.30°Brix, 0.06–0.39%, 4.49–19.19 mg/100 mL, and 3.69–8.55 N, respectively (Table 1). The color parameters also differed ($p < 0.05$), with from 52.00 to 73.28 for L^* values, from –0.49 to 22.59 for a^*, and from 46.44 to 67.73 for b^*. Titratable acidity was higher ($p < 0.05$) in the non-indigenous mangoes than in the indigenous ones (Table 1). No significant differences ($p > 0.05$) were observed in the pH, TSS, vitamin C, and firmness between the two mango types. The non-indigenous varieties exhibited higher ($p < 0.05$) lightness (L^*) and yellowness (b^*) values, whereas the indigenous varieties had higher ($p < 0.05$) redness (a^*) values.

The differences in the pulp characteristics are largely attributed to genetic diversity and environmental conditions such as soil type, climate, and agronomic practices [1, 24]. The TSS values observed in this study were similar to previously reported ranges of 16.90 to 27°Brix in mango varieties [22, 25]. However, the Sayuni and Mabbere varieties showed low TSS values of 8.10 and 9.30°Brix, respectively, indicating low sugar accumulation at harvest maturity. These TSS values may be attributed to premature harvesting, varietal differences in carbohydrate metabolism, or slow starch–sugar conversion during ripening [26]. Similarly low TSS values were observed in late-maturing varieties which often require extended ripening periods to reach optimal sweetness [27]. In contrast, seven varieties (Kagoogwa, Apple mango, Batawi, Ssejjembe, Takataka, Kent, and Tommy Atkins) had TSS values ≥ 13.5°Brix, exceeding the Codex Alimentarius Commission fruit juice standard. This supports their suitability for juice extraction without the need for added sugar[6]. The high TSS levels, which were possibly contributed by simple sugars such as fructose and glucose, could enhance the sweetness and consumer appeal of these mangoes [24, 28].

Most varieties had pH values within the recommended range of 3.0 to 4.5 for juice production, which enhances flavor stability and microbial safety [29]. Six varieties (Table 1) fell within the ideal titratable acidity target range of 0.25 to 0.5%, making them suitable for tangy

[2] AOAC International. Official methods of analysis. 17th Ed. Gaithersburg: AOAC International; 2000.

[3] The same.

[4] The same.

[5] Horwitz W, Latimer GW. Official methods of analysis of AOAC International. 18th Ed. Maryland: AOAC International; 2005.

[6] Codex Alimentarius Commission. General standard for fruit juices and nectars (CODEX STAN 247-2005). Rome: Food and Agriculture Organization of the United Nations/World Health Organization; 2005.

Table 1 pH, total soluble solids, titratable acidity, vitamin C, firmness, and color of pulp in indigenous and non-indigenous mango varieties

Mango type	Mango variety	pH	Total soluble solids, °Brix	Titratable acidity, %	Vitamin C, mg/100 mL	Firmness, N	*L**	*a**	*b**
Indigenous	Apple mango	4.21 ± 0.00^{d}	15.10 ± 0.00^{b}	0.10 ± 0.00^{h}	8.80 ± 1.39^{e}	$4.51 \pm 0.15^{f,g}$	65.57 ± 1.58^{b}	16.68 ± 0.58^{b}	$53.86 \pm 0.52^{g,h}$
	Asante	4.35 ± 0.01^{c}	11.50 ± 0.00^{f}	0.10 ± 0.00^{h}	19.19 ± 0.01^{a}	$4.47 \pm 0.23^{f,g}$	$62.61 \pm 0.26^{c,d}$	16.12 ± 1.42^{b}	64.36 ± 0.23^{a}
	Batawi	3.65 ± 0.01^{g}	13.50 ± 0.00^{c}	0.13 ± 0.01^{g}	4.49 ± 0.10^{h}	4.17 ± 0.03^{g}	71.80 ± 0.48^{a}	2.87 ± 0.17^{j}	65.11 ± 0.10^{a}
	Bire	3.49 ± 0.00^{h}	10.10 ± 0.00^{g}	0.34 ± 0.01^{b}	$6.59 \pm 0.42^{f,g}$	3.89 ± 0.01^{g}	$64.74 \pm 0.04^{b,c}$	17.87 ± 1.06^{b}	$56.31 \pm 0.39^{e,f}$
	Boribo	4.45 ± 0.01^{b}	9.70 ± 0.00^{h}	0.06 ± 0.00^{i}	16.79 ± 0.00^{b}	3.93 ± 0.05^{g}	52.43 ± 0.57^{i}	22.59 ± 0.84^{a}	$55.32 \pm 0.19^{f,g}$
	Doodo	4.38 ± 0.02^{c}	10.70 ± 0.00^{g}	0.19 ± 0.00^{e}	13.54 ± 0.29^{c}	5.14 ± 0.08^{e}	$59.83 \pm 1.26^{e,f}$	14.58 ± 0.05^{c}	$58.58 \pm 0.28^{d,e}$
	Kagoogwa	4.05 ± 0.02^{e}	16.30 ± 0.00^{a}	0.15 ± 0.00^{f}	12.19 ± 0.20^{d}	4.62 ± 0.06^{f}	$58.29 \pm 0.62^{f,g}$	11.97 ± 0.16^{d}	$60.07 \pm 0.04^{c,d}$
	Koona	3.72 ± 0.02^{g}	11.50 ± 0.00^{f}	0.16 ± 0.01^{f}	13.39 ± 0.00^{c}	5.58 ± 0.19^{d}	$61.21 \pm 0.03^{d,e}$	5.60 ± 2.14^{g}	46.44 ± 0.46^{k}
	Mabbere	3.93 ± 0.02^{f}	9.30 ± 0.00^{h}	0.13 ± 0.01^{g}	$6.64 \pm 0.16^{f,g}$	$4.29 \pm 0.23^{f,g}$	63.80 ± 0.90^{c}	$10.23 \pm 0.12^{d,e}$	$50.47 \pm 0.15^{i,j}$
	Sayuni	3.18 ± 0.00^{i}	8.10 ± 0.00^{i}	0.32 ± 0.01^{c}	9.35 ± 0.42^{e}	8.55 ± 0.21^{a}	72.40 ± 0.83^{a}	-0.49 ± 0.42^{k}	$55.93 \pm 0.09^{f,g}$
	Ssejjembe	4.51 ± 0.01^{b}	13.70 ± 0.00^{c}	0.18 ± 0.00^{e}	11.75 ± 0.32^{d}	6.72 ± 0.07^{c}	$57.20 \pm 0.85^{g,h}$	$10.07 \pm 0.12^{d,e}$	$53.59 \pm 0.21^{g,h}$
	Takataka	4.01 ± 0.00^{e}	14.50 ± 0.01^{b}	0.17 ± 0.00^{e}	$6.82 \pm 0.01^{f,g}$	6.76 ± 0.02^{c}	$61.53 \pm 0.85^{d,e}$	13.73 ± 0.41^{c}	$48.46 \pm 0.21^{j,k}$
	Kakule	4.22 ± 0.02^{d}	11.30 ± 0.00^{f}	0.09 ± 0.01^{h}	11.99 ± 0.00^{d}	$4.33 \pm 0.02^{f,g}$	54.17 ± 0.22^{h}	14.92 ± 0.45^{c}	$52.23 \pm 0.07^{h,i}$
Non-indigenous	Duncan	3.97 ± 0.11^{f}	10.60 ± 0.01^{g}	0.17 ± 0.00^{e}	18.39 ± 0.16^{a}	4.75 ± 0.07^{f}	70.31 ± 0.51^{a}	2.53 ± 0.23^{j}	$52.43 \pm 0.12^{h,i}$
	Julie	3.32 ± 0.01^{h}	12.70 ± 0.00^{d}	0.39 ± 0.01^{a}	9.29 ± 0.16^{e}	3.85 ± 0.12^{h}	64.53 ± 1.11^{c}	7.68 ± 0.11^{f}	$58.45 \pm 0.29^{d,e}$
	Fairchild	3.92 ± 0.02^{f}	9.37 ± 0.05^{h}	0.28 ± 0.00^{c}	9.64 ± 0.11^{e}	5.11 ± 0.01^{e}	52.00 ± 0.45^{i}	15.45 ± 0.28^{c}	$55.10 \pm 0.11^{f,g}$
	Kapisa	4.60 ± 0.00^{a}	11.30 ± 0.00^{f}	0.09 ± 0.01^{h}	13.66 ± 0.00^{c}	5.25 ± 0.11^{e}	$58.14 \pm 0.01^{f,g}$	7.19 ± 0.20^{f}	$58.03 \pm 0.06^{d,e}$
	Kent	3.95 ± 0.01^{f}	13.70 ± 0.00^{c}	0.29 ± 0.01^{c}	11.40 ± 0.24^{d}	6.74 ± 0.29^{c}	73.28 ± 0.45^{a}	1.70 ± 0.65^{j}	61.29 ± 0.33^{b}
	Ponde	3.91 ± 0.01^{f}	10.10 ± 0.00^{g}	0.24 ± 0.00^{d}	18.54 ± 0.37^{a}	5.15 ± 0.08^{e}	64.14 ± 0.54^{c}	7.38 ± 0.31^{f}	$60.50 \pm 0.03^{b,c}$
	Palmer	4.76 ± 0.04^{a}	10.77 ± 0.05^{g}	0.12 ± 0.00^{g}	9.15 ± 0.03^{e}	3.69 ± 0.13^{h}	70.99 ± 0.28^{a}	5.99 ± 0.08^{g}	67.73 ± 0.14^{a}
	Seena	4.35 ± 0.01^{c}	9.30 ± 0.00^{h}	$0.11 \pm 0.01^{g,h}$	11.99 ± 0.64^{d}	7.56 ± 0.49^{b}	$63.46 \pm 0.66^{c,d}$	13.29 ± 0.43^{c}	61.52 ± 0.47^{b}
	Tommy Atkins	3.69 ± 0.01^{g}	14.30 ± 0.00^{b}	0.34 ± 0.01^{b}	4.64 ± 0.16^{h}	3.75 ± 0.01^{h}	$68.70 \pm 0.70^{a,b}$	4.38 ± 0.10^{h}	$60.16 \pm 0.15^{b,c}$
Indigenous (mean ± SD)		4.01 ± 0.40^{A}	11.95 ± 2.48^{A}	0.16 ± 0.08^{B}	11.06 ± 4.40^{A}	5.15 ± 1.40^{A}	61.97 ± 5.94^{B}	12.06 ± 6.40^{A}	55.44 ± 5.6^{B}
Non-indigenous (mean ± SD)		4.05 ± 0.45^{A}	11.35 ± 1.82^{A}	0.23 ± 0.11^{A}	11.86 ± 4.50^{A}	5.09 ± 1.34^{A}	65.06 ± 6.76^{A}	7.29 ± 4.57^{B}	59.47 ± 4.3^{A}

Values are expressed as mean ± standard deviation (SD); Lower case superscripts denote significant differences among mango varieties, while ^{A} and ^{B} denote significant differences between mango types. Values with different superscript letters in the same column are significantly different ($p < 0.05$)

products such as juices, chutneys, and jams[7]. The vitamin C content varied among the mango varieties, with many exceeding the Codex minimum of 10 mg/100 mL required for nutritional labeling[8]. These high levels suggest the potential of several varieties for use in vitamin-fortified juices. Notably, Palmer, Asante, and Kent exhibited elevated *b** values, indicating intense yellow coloration linked to carotenoid accumulation. This coloration enhances visual appeal and nutritional value in purées, juices, and complementary food[9]. The higher acidity of the non-indigenous mangoes suggests greater organic acid synthesis, which is common in commercial hybrid varieties selected for processing attributes [30]. The lower acidity of the indigenous mangoes aligns with the flavor profiles preferred for fresh consumption [31].

Proximate composition of mango pulp. The pulp of the 22 mango varieties showed variation in proximate composition (Table 2). The moisture content ranged from 45.59 to 68.43%, which is lower than 80 to 85% range commonly reported for fresh ripe mango pulp [32]. The moisture variation among the mango varieties may be attributed to the differences in harvest maturity and post-harvest handling. The fruits harvested at late maturity stages and those transported over long distances are prone to moisture loss due to continued respiration and transpiration after detachment from the tree [33]. Similar reductions in moisture during handling and temporary storage have been reported in mangoes [32–34]. The ash, fat, protein, fiber, and carbohydrate contents ranged from 2.06 to 2.63%, 0.03 to 0.47%, 0.54 to 1.50%, 3.82 to 4.78%, and 88.22 to 91.07%, respectively (Table 2). The nutritional profile of ripe mango pulp is characterized by high moisture and carbohydrate content, as well as low levels of fat, protein, and fiber [35]. No differences ($p > 0.05$) were observed between the indigenous and non-indigenous groups for moisture, ash, fat, protein, and fiber. However, the non-indigenous varieties had a higher ($p < 0.05$) carbohydrate content than the indigenous ones. The carbohydrate content of 88.22 to 91.07 g/100 g dry weight provides between 68 and 70% of the recommended daily carbohydrate intake (130 g/day) for adults [35]. Mango pulp is therefore a valuable energy source suitable for formulation of energy-dense food products, especially fruit leathers and snack bars [5].

Mineral composition of mango pulp. The mango pulp contained substantial amounts of K, Na, Ca, Mg, P, Zn, and Fe (Table 3). Potassium was the most abundant mineral ranging from 96.65 to 199.67 mg/100 g, with the highest levels found in Palmer and Kent varieties. The dominance of potassium was congruent with the

[7]Food and Agriculture Organization of the United Nations. Fruit and vegetable juice processing: Technical paper. Rome: FAO; 2005.
[8]Horwitz W, Latimer GW. Official methods of analysis…
[9]Food and Agriculture Organization… 2005.

Table 2 Proximate composition of pulp in indigenous and non-indigenous mango varieties in Uganda

Mango type	Mango variety	Moisture, % wet weight	Protein, % dry weight	Fat, % dry weight	Fiber, % dry weight	Ash, % dry weight	Carbohydrate, % dry weight
Indigenous	Apple mango	60.91 ± 0.04^{f}	1.21 ± 0.01^{c}	0.18 ± 0.01^{f}	3.82 ± 0.05^{n}	2.17 ± 0.00^{g}	91.07 ± 0.05^{a}
	Asante	60.47 ± 0.06^{g}	1.42 ± 0.01^{a}	0.04 ± 0.00^{l}	5.17 ± 0.07^{f}	2.28 ± 0.00^{e}	$89.56 \pm 0.07^{c,d}$
	Batawi	62.67 ± 0.62^{d}	1.34 ± 0.02^{b}	0.13 ± 0.00^{h}	5.54 ± 0.03^{c}	2.13 ± 0.00^{h}	$89.19 \pm 0.04^{c,d}$
	Bire	59.50 ± 0.23^{h}	1.42 ± 0.01^{a}	0.03 ± 0.00^{l}	6.22 ± 0.02^{a}	2.63 ± 0.01^{a}	88.22 ± 0.02^{d}
	Boribo	64.73 ± 0.21^{b}	1.18 ± 0.02^{d}	0.15 ± 0.00^{g}	3.86 ± 0.01^{m}	2.24 ± 0.01^{e}	$90.75 \pm 0.02^{a,b}$
	Doodo	64.17 ± 0.04^{c}	1.29 ± 0.00^{b}	0.32 ± 0.01^{c}	5.86 ± 0.01^{b}	2.17 ± 0.02^{g}	$88.56 \pm 0.02^{c,d}$
	Kagoogwa	61.92 ± 0.02^{e}	1.41 ± 0.05^{a}	0.22 ± 0.00^{e}	4.86 ± 0.07^{h}	2.12 ± 0.00^{h}	$89.76 \pm 0.09^{b,c}$
	Koona	62.92 ± 0.02^{d}	0.71 ± 0.08^{l}	0.43 ± 0.00^{b}	4.78 ± 0.96^{i}	2.13 ± 0.00^{h}	$90.25 \pm 0.96^{b,c}$
	Mabbere	62.30 ± 0.00^{e}	0.77 ± 0.01^{k}	0.07 ± 0.00^{j}	5.18 ± 0.35^{f}	2.23 ± 0.00^{e}	$90.10 \pm 0.35^{b,c}$
	Sayuni	65.73 ± 0.22^{a}	0.98 ± 0.00^{g}	0.25 ± 0.00^{d}	5.55 ± 0.33^{c}	2.22 ± 0.01^{e}	$89.09 \pm 0.33^{c,d}$
	Ssejjembe	62.03 ± 0.02^{e}	1.11 ± 0.00^{e}	0.32 ± 0.00^{c}	4.85 ± 0.09^{h}	2.27 ± 0.01^{c}	$89.82 \pm 0.09^{b,c}$
	Takataka	63.80 ± 2.99^{c}	1.18 ± 0.01^{d}	0.11 ± 0.01^{i}	4.78 ± 0.08^{i}	2.12 ± 0.00^{h}	$90.04 \pm 0.09^{b,c}$
	Kakule	62.14 ± 0.03^{e}	0.42 ± 0.00^{m}	0.16 ± 0.00^{g}	5.14 ± 0.51^{g}	2.28 ± 0.01^{c}	$90.35 \pm 0.51^{a,b}$
Non-indigenous	Duncan	68.43 ± 0.25^{a}	1.38 ± 0.01^{a}	0.26 ± 0.00^{d}	5.21 ± 0.44^{f}	2.59 ± 0.01^{b}	$88.40 \pm 0.44^{c,d}$
	Fairchild	45.59 ± 0.12^{i}	1.28 ± 0.01^{b}	0.29 ± 0.00^{d}	4.54 ± 0.03^{j}	2.27 ± 0.00^{c}	$90.79 \pm 0.03^{a,b}$
	Julie	61.55 ± 0.09^{e}	1.50 ± 0.01^{a}	0.09 ± 0.00^{k}	5.19 ± 0.05^{f}	2.21 ± 0.02^{f}	$89.38 \pm 0.05^{c,d}$
	Kapisa	61.87 ± 0.21^{e}	0.54 ± 0.01^{n}	0.05 ± 0.00^{l}	5.24 ± 0.13^{e}	2.06 ± 0.04^{i}	$90.52 \pm 0.14^{a,b}$
	Kent	61.48 ± 0.21^{e}	0.59 ± 0.00^{n}	0.08 ± 0.01^{j}	4.42 ± 0.78^{k}	2.17 ± 0.00^{g}	91.07 ± 0.78^{a}
	Palmer	62.71 ± 0.25^{d}	0.83 ± 0.00^{j}	0.47 ± 0.02^{a}	4.45 ± 0.06^{k}	2.08 ± 0.05^{i}	$90.55 \pm 0.08^{a,b}$
	Ponde	61.72 ± 0.01^{e}	0.90 ± 0.00^{h}	0.21 ± 0.01^{e}	4.85 ± 0.03^{h}	2.20 ± 0.01^{f}	$90.22 \pm 0.03^{b,c}$
	Seena	62.56 ± 1.15^{e}	1.03 ± 0.01^{b}	0.11 ± 0.01^{i}	4.82 ± 0.05^{h}	2.16 ± 0.07^{g}	$90.21 \pm 0.09^{b,c}$
	Tommy Atkins	61.55 ± 2.580^{d}	1.32 ± 0.00^{f}	0.03 ± 0.01^{l}	5.23 ± 0.11^{e}	2.52 ± 0.02^{b}	$89.30 \pm 0.11^{c,d}$
Indigenous (mean ± SD)		62.56 ± 1.74^{A}	1.11 ± 0.13^{A}	0.19 ± 0.12^{A}	5.05 ± 0.31^{A}	2.31 ± 0.69^{B}	89.75 ± 1.07^{B}
Non-indigenous (mean ± SD)		60.86 ± 6.13^{B}	1.04 ± 0.18^{B}	0.18 ± 0.14^{A}	4.88 ± 0.35^{B}	2.45 ± 0.35^{A}	90.05 ± 0.92^{A}

Values are expressed as mean ± standard deviation (SD); lower case superscript letters denote significant differences among mango varieties, while ^{A} and ^{B} denote significant differences between mango types. Values with different superscript letters in the same column are significantly different ($p < 0.05$)

Table 3 Mineral composition of pulp in indigenous and non-indigenous mango varieties in Uganda

Mango type	Mango variety	Mineral, mg/100 g						
		K	Na	Ca	Mg	P	Zn	Fe
Indigenous	Apple mango	96.65 ± 0.61^{k}	66.66 ± 0.17^{h}	25.34 ± 0.31^{d}	40.85 ± 0.10^{a}	41.47 ± 0.19^{b}	7.31 ± 0.13^{g}	0.07 ± 0.00^{j}
	Asante	114.69 ± 0.25^{j}	40.63 ± 0.57^{l}	24.15 ± 0.15^{e}	27.89 ± 0.55^{i}	33.64 ± 0.18^{c}	8.54 ± 0.09^{d}	0.02 ± 0.00^{m}
	Batawi	115.46 ± 0.49^{j}	55.60 ± 0.37^{i}	32.77 ± 0.39^{a}	26.41 ± 0.38^{j}	44.34 ± 0.05^{a}	10.39 ± 0.38^{b}	0.04 ± 0.00^{l}
	Bire	126.02 ± 1.39^{i}	44.14 ± 0.53^{k}	24.79 ± 0.31^{e}	19.32 ± 0.14^{n}	28.62 ± 0.17^{f}	6.47 ± 0.14^{i}	0.01 ± 0.00^{m}
	Boribo	161.82 ± 1.51^{e}	41.82 ± 0.54^{l}	27.99 ± 0.71^{b}	24.65 ± 0.16^{k}	29.32 ± 0.40^{e}	8.63 ± 0.27^{c}	0.05 ± 0.00^{k}
	Doodo	144.60 ± 0.24^{h}	39.39 ± 0.20^{m}	28.66 ± 0.26^{b}	35.53 ± 0.24^{c}	28.46 ± 0.30^{f}	7.49 ± 0.30^{f}	0.06 ± 0.00^{j}
	Kagoogwa	158.53 ± 1.06^{f}	45.78 ± 0.61^{k}	26.90 ± 0.64^{e}	32.43 ± 0.05^{f}	26.34 ± 0.28^{g}	6.51 ± 0.09^{i}	0.18 ± 0.00^{b}
	Koona	197.26 ± 2.31^{b}	102.88 ± 0.23^{b}	18.14 ± 0.59^{j}	25.68 ± 0.40^{j}	26.46 ± 0.09^{g}	7.70 ± 0.16^{e}	0.14 ± 0.00^{d}
	Mabbere	186.35 ± 0.91^{c}	101.58 ± 0.08^{b}	19.82 ± 0.62^{i}	29.63 ± 0.29^{g}	21.34 ± 0.16^{l}	9.77 ± 0.12^{b}	0.12 ± 0.00^{g}
	Sayuni	171.76 ± 0.57^{d}	83.91 ± 0.38^{e}	21.59 ± 0.21^{h}	14.60 ± 0.46^{o}	24.57 ± 0.21^{j}	11.51 ± 0.29^{a}	0.16 ± 0.01^{c}
	Ssejjembe	134.73 ± 0.14^{j}	93.82 ± 0.12^{d}	24.82 ± 0.15^{e}	26.56 ± 0.11^{j}	21.18 ± 0.17^{l}	7.82 ± 0.02^{e}	0.17 ± 0.01^{b}
	Takataka	189.59 ± 0.25^{b}	102.35 ± 0.16^{b}	28.03 ± 0.80^{b}	20.40 ± 0.26^{m}	23.41 ± 0.10^{k}	11.66 ± 0.16^{a}	0.13 ± 0.01^{f}
	Kakule	153.95 ± 1.06^{g}	78.46 ± 0.45^{f}	20.31 ± 0.17^{i}	30.33 ± 0.24^{g}	29.49 ± 0.09^{d}	8.13 ± 0.08^{d}	0.14 ± 0.00^{d}
Non-indigenous	Duncan	166.09 ± 0.85^{e}	32.37 ± 0.14^{n}	33.24 ± 0.60^{a}	19.00 ± 0.75^{n}	23.78 ± 0.18^{k}	6.70 ± 0.22^{h}	0.05 ± 0.00^{k}
	Julie	115.55 ± 0.45^{j}	78.20 ± 0.52^{f}	25.62 ± 0.04^{d}	33.29 ± 0.62^{e}	17.74 ± 0.14^{m}	8.59 ± 0.37^{d}	0.13 ± 0.00^{e}
	Fairchild	155.01 ± 0.37^{f}	48.91 ± 0.21^{j}	25.23 ± 0.29^{e}	36.99 ± 0.51^{b}	25.63 ± 0.38^{h}	8.30 ± 0.26^{d}	0.11 ± 0.00^{i}
	Kapisa	178.93 ± 1.19^{c}	84.63 ± 0.31^{e}	22.22 ± 0.24^{h}	34.15 ± 0.22^{d}	25.68 ± 0.32^{h}	7.28 ± 0.06^{g}	0.11 ± 0.00^{i}
	Kent	197.86 ± 0.68^{a}	113.26 ± 0.16^{a}	23.61 ± 0.52^{g}	28.69 ± 0.29^{h}	28.24 ± 0.14^{f}	10.32 ± 0.26^{b}	0.17 ± 0.00^{b}
	Ponde	151.47 ± 0.39^{g}	91.85 ± 2.75^{d}	22.65 ± 0.15^{h}	34.45 ± 0.25^{c}	25.45 ± 0.47^{i}	10.20 ± 0.16^{b}	0.32 ± 0.01^{a}
	Palmer	199.67 ± 0.70^{a}	97.83 ± 0.24^{c}	17.25 ± 0.29^{j}	26.67 ± 0.05^{j}	29.77 ± 0.20^{d}	8.62 ± 0.50^{c}	0.15 ± 0.01^{d}
	Seena	169.15 ± 0.57^{d}	98.82 ± 0.55^{c}	22.57 ± 0.30^{h}	23.37 ± 0.53^{l}	21.44 ± 0.20^{l}	7.59 ± 0.25^{f}	0.14 ± 0.01^{d}
	Tommy Atkins	114.26 ± 0.23^{j}	69.52 ± 0.48^{g}	27.74 ± 0.17^{c}	15.60 ± 0.17^{o}	13.54 ± 0.16^{n}	8.57 ± 0.36^{d}	0.12 ± 0.01^{h}
Indigenous (mean ± SD)		150.11 ± 31.55^{A}	69.00 ± 25.84^{A}	24.87 ± 4.12^{A}	27.25 ± 6.93^{A}	29.13 ± 7.05^{A}	8.61 ± 1.73^{A}	0.10 ± 0.06^{A}
Non-indigenous (mean ± SD)		160.89 ± 30.91^{A}	79.49 ± 25.71^{A}	24.46 ± 4.39^{A}	28.02 ± 7.47^{A}	23.47 ± 5.14^{B}	8.46 ± 1.22^{A}	0.14 ± 0.07^{A}

Values are expressed as means ± standard deviations (SD) on dry weight basis. Lower case superscripts denote significant differences among mango varieties, while ^{A} and ^{B} denote significant differences between mango types. Values with different superscript letters in the same column are significantly different ($p < 0.05$)

findings by Farina *et al.* [36], who reported concentrations as high as 250 mg/100 g in mangoes grown in the Mediterranean region. Potassium supports fluid balance, neuromuscular function, and cardiovascular regulation [36]. The high potassium levels in Palmer and Kent may be linked to genotypic differences in nutrient uptake efficiency and translocation capacity, as previously reported by Subedi *et al.* [37].

Sodium was the second most abundant mineral with levels between 32.37 and 113.26 mg/100 g. This differs from the results of Farina *et al.* [36], who identified phosphorus as the second most prevalent mineral in mangoes grown in the Mediterranean region. This divergence may reflect environmental and soil nutrient availability differences, since sodium accumulation increases in fruits grown under water stress or semi-arid conditions, which are typical in Central Uganda [2]. The elevated sodium levels in some varieties may reflect the effects of mineralized irrigation water or soil salinity, the conditions known to alter the ionic balance and nutrient uptake [2, 18].

The calcium content in mango pulp was similar to the levels found in tropical fruits such as papaya, guava, and pineapple [38]. Since calcium is involved in cell wall integrity and firmness retention, the varieties with high calcium levels also had higher firmness scores, as observed in Palmer mango.

No significant differences ($p > 0.05$) were observed in the levels of K, Na, Ca, Mg, Zn, and Fe between the indigenous and non-indigenous mango varieties, except for phosphorus. Zinc is a particularly important micronutrient with a recommended dietary allowance of 8 mg for adult women and 11 mg for adult men[10]. In this study, zinc levels in the mango pulp ranged from 6.47 to 11.66 mg/100 g dry weight. A typical juice serving made from 30 g of dry mango pulp (equivalent to two 250-mL servings) could provide around 1.94 to 3.50 mg of zinc. This would meet 24 to 44% of the recommended dietary allowance for women and 18 to 32% for men, highlighting mango pulp as an important dietary source of zinc. Although mango pulp contains useful amounts of minerals including K, Mg, Ca, Na, P, and Fe, these amounts are not sufficient to meet the daily requirements. Therefore, alternative foods such as legumes, green leafy vegetables, nuts and seeds, dairy products, and meat should be consumed together with mangoes in order to meet the recommended daily allowances for these minerals.

Proximate composition and visual distribution patterns for mango by-products. Fiber was the most abundant (10.16 ± 1.76%) component in the mango peel confirming its structural role and high cell wall polysaccharide density. Tommy Atkins mango had the highest fiber content (12.67 ± 0.03%) in the peel (Fig. 1). This suggests stronger skin rigidity and resistance to mechanical damage, the traits associated with longer shelf-life and transport resilience [39]. The high fiber content makes mango peel a suitable ingredient for developing functional bakery products and dietary fiber supplements aimed at improving gut health and reducing glycemic response [40].

The protein content in the mango kernel was 10.18 ± 3.39%, compared to 7.09 ± 1.64 and 2.62 ± 1.36% in the peel and seed, respectively. This confirms that kernel tissues are metabolically active and rich in storage proteins involved in seed development [41, 42]. The relatively high protein levels in the kernel indicate its potential for use in plant-based protein formulations, especially in gluten-free flour blends and infant complementary foods.

The carbohydrate content was the major component in the mango seed, ranging from 88.09 to 93.89% (Fig. 1). This makes it suitable for extraction of starch-based ingredients or use in energy-dense formulations.

[10]Diet, nutrition and the prevention of chronic diseases: Report of a joint WHO/FAO expert consultation. World Health Organization, Food and Agriculture Organization of the United Nations. Geneva: World Health Organization; 2003;(916).

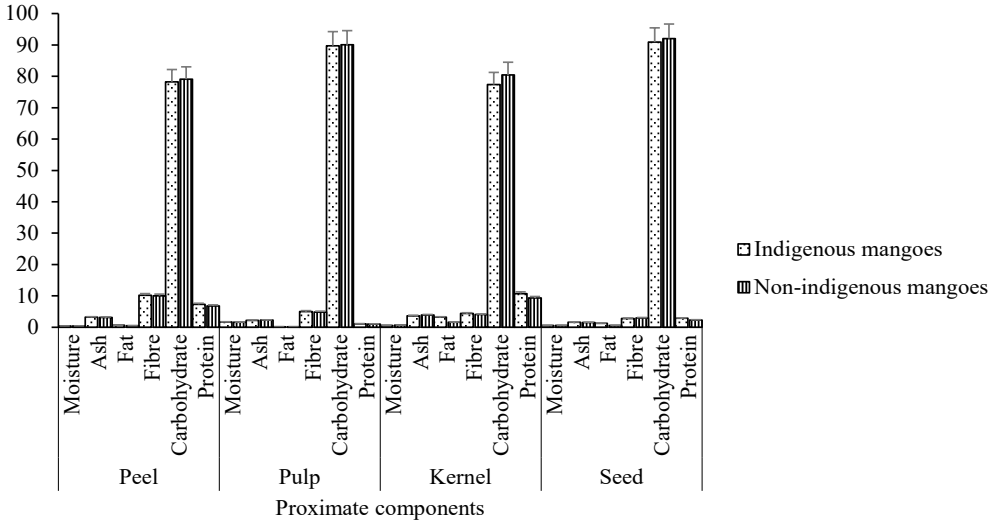


Figure 1 Proximate compositions of peel, pulp, kernel, and seed between indigenous and non-indigenous mango varieties, %

Crude fat was the highest in the kernel, ranging from 0.90 to 5.67%. This supports its use in confectionery and industrial oil extraction.

Overall, the proximate profiles demonstrate that mango by-products are valuable nutrient sources of fiber, protein, and carbohydrate. Their recovery and utilization could reduce mango processing waste and support circular bioeconomy strategies in fruit value chains. The fiber content in the mango peels was close to 8–13% reported by Berardini *et al*. [41]. A 28-g serving of Tommy Atkins dried peel provides 12% of the recommended daily fiber intake of 30 g/day[11]. Therefore, mango peel can be used as an ingredient to enhance fiber levels in food products. The protein content in the kernel was consistent with a 6–11% range reported by Soong *et al*. [42]. Kernel is richer in protein than peel or seed. The high carbohydrate levels in the mango seeds were similar to those found by Berardini *et al*. [41]. The proximate profiles of the indigenous and non-indigenous mangoes were not significantly different ($p > 0.05$). The proximate variation is more strongly influenced by variety-specific factors rather than the indigenous versus non-indigenous classification.

Mineral composition and visual distribution patterns for mango by-products. The seed had the highest concentrations of K, Ca, Mg, Na, P, and Fe, with values of 354.90 ± 25.10, 437.74 ± 35.00, 147.66 ± 32.92, 116.00 ± 3.85, 114.12 ± 3.50, and 8.46 ± 1.48 mg/100 g, respectively (Fig. 2). The mineral concentrations in the seeds were higher ($p < 0.05$) than those of in the peel and kernel. These results were consistent with the findings by Berardini *et al*. [41] and Bala *et al*. [43]. This suggests that seeds serve as storage organs for essential nutrients required during germination. This aligns with the previous reports that mineral accumulation in seeds supports enzyme activation, cellular respiration, and early seedling development[12] [41–43].

Potassium was the most abundant mineral in all by-products, particularly in the seed. This had been expected since potassium regulates osmotic balance and carbohydrate transport in developing fruit tissues. This suggests that mango seed flour could be used as a potassium fortifier in food products, especially for populations with low fruit intake.

Similarly, calcium levels were the highest in the seeds. This might be due to the role that calcium plays in maintaining cell wall stability and structural integrity.

Magnesium, an essential cofactor in enzyme activity and energy metabolism, also accumulated in the seeds. In this study, K, Ca, Mg, Na, Zn, and Fe exhibited a decreasing concentration trend from seed to peel to kernel. The concentration of phosphorus declined progressively from seed to kernel to peel, indicating a distinct pattern compared to other minerals. This divergence could be attributed to the critical role of phosphorus in seed development. In plant seeds, phosphorus is predominantly stored in the embryo in the form of inositol hexakisphosphate, also known as phytic acid [44]. In mango seeds, inositol hexakisphosphate can account for 50 to 85% of the total phosphorus content. It is primarily concentrated in the endosperm and embryo tissues, which correspond to the mango kernel [45]. In contrast, Ca, Mg, and Fe are typically involved in structural functions and are found mainly in the seed and peel [43]. These tissues tend to

[11] Diet, nutrition and the prevention…

[12] Human energy requirements: Report of a joint FAO/WHO/UNU expert consultation. Food and Agriculture Organization/World Health Organization. Rome: FAO; 2004.

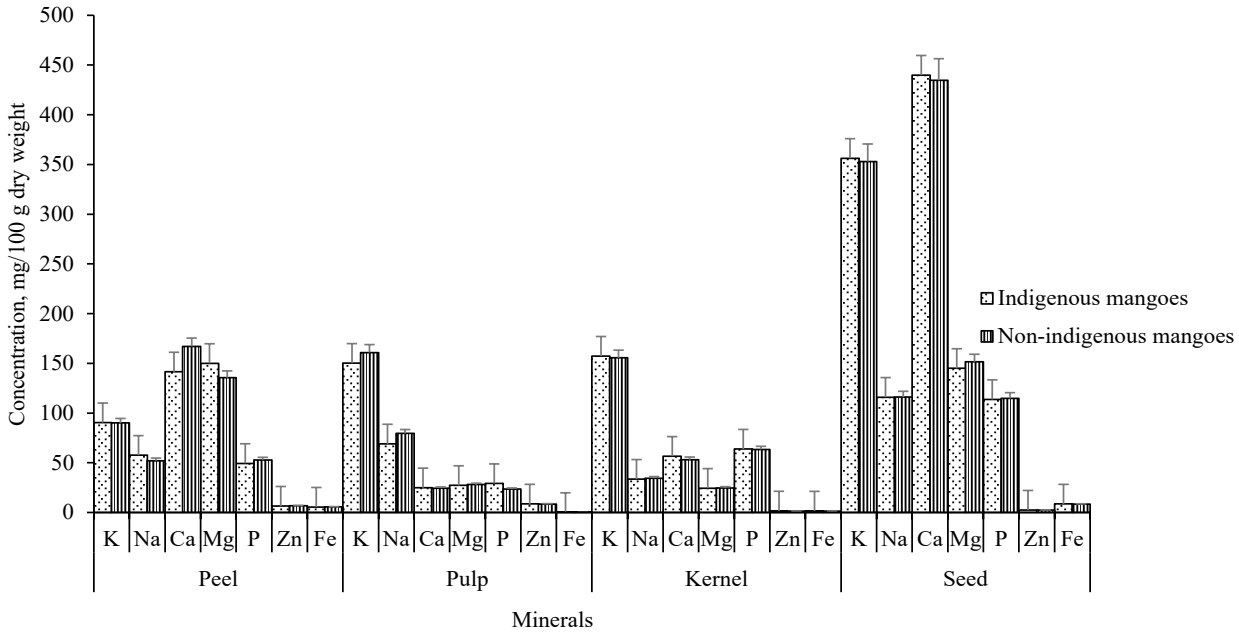
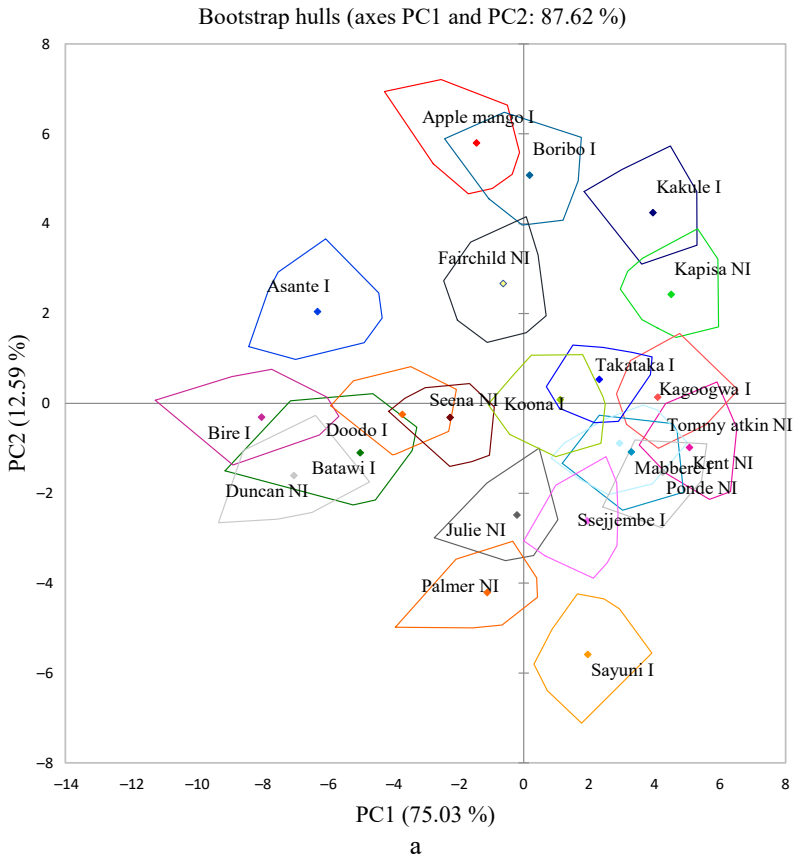
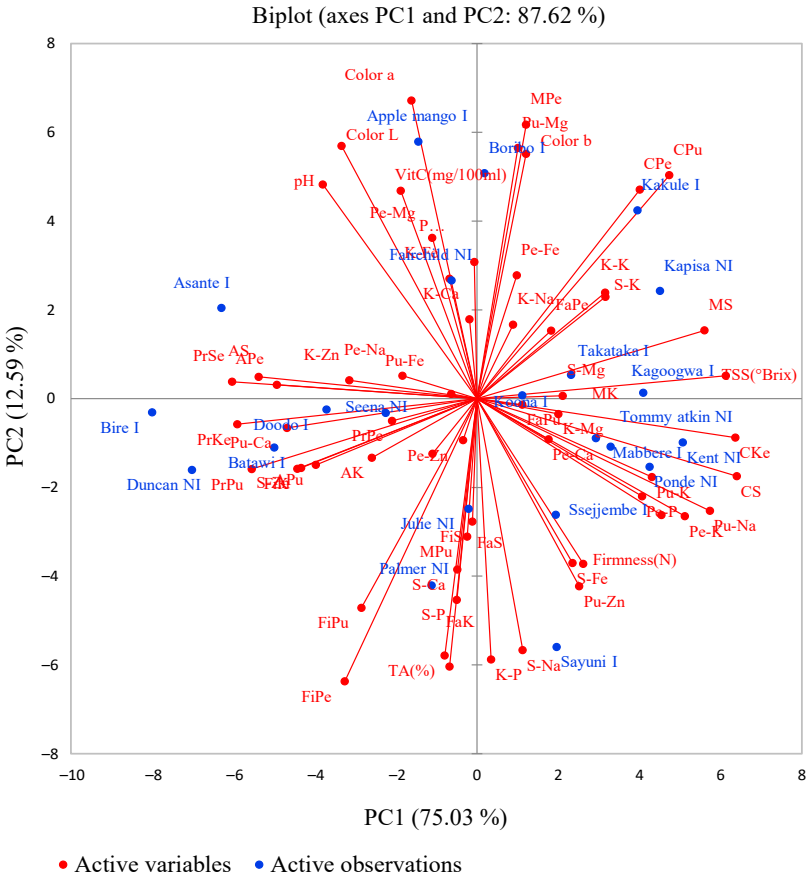


Figure 2 Mineral composition of peel, pulp, kernel, and seed between indigenous and non-indigenous mango varieties



a



b

NI – non-indigenous; I – indigenous; Fi – fiber; C – carbohydrate; Fa – fat; A – ash; M – moisture; Pr – protein; Pu – pulp; Ke – kernel; Pe – peel; S – seed

Figure 3 Principal component analysis biplot showing the distribution of indigenous and non-indigenous mango varieties based on physicochemical (a) and nutritional (b) attributes of pulp, peel, seed, and kernel

accumulate more of these minerals, which explains why the seed shows the highest levels followed by the peel, with the kernel having the lowest concentrations for most minerals [43]. Zinc concentration (6.51 mg/100 g) was the highest in the mango peels. This may reflect zinc's key role in the peel's protective functions, including membrane stabilization, antioxidant defense, and response to environmental stress [45].

Principal component analysis and bootstrap hulls interpretation. Varietal differences were driven by the mangoes' intrinsic physicochemical traits rather than by their indigenous or non-indigenous classification (Fig. 3a). The principal component analysis explained 87.62% of the total variation. Principal component (PC) 1 (75.03%) differentiated the varieties primarily on the basis of minerals, TSS, and firmness (Fig. 3b). PC2 (12.59%) captured the differences in vitamin C, color, and pH. The varieties positioned on the positive side of PC1 (Kakule and Kapisa) exhibited higher mineral concentrations, while those on the negative PC1 axis (Bire, Duncan, Doodo, and Batawi) showed lower mineral levels. Along PC2, Apple mango and Boribo loaded positively due to their high vitamin C content and strong color attributes. These patterns translate into clear processing opportunities: Kakule and Kapisa are suitable for mineral-rich and functional food products, while Apple mango and Boribo are ideal for antioxidant beverages and natural pigment extraction. The TSS-high varieties (Kagoogwa, Takataka, and Tommy Atkins) clustered near the TSS vector on PC1, indicating adequate soluble solids for juice processing. Overall, the findings provide a roadmap for aligning mango varieties with the most appropriate value-added products.

CONCLUSION

Non-indigenous mango varieties were more acidic with an intense yellow pigmentation in the pulp, which makes them ideal for juices, chutneys, and purées. Indigenous mangoes exhibited high total soluble solids giving them a more pleasant taste, which supports their suitability for fresh consumption. Mango by-products are nutritious. The seeds contained most of the important minerals. The peels were rich in fiber, while the kernels had notable amounts of protein and fats. These by-products offer opportunities for value addition through the production of fiber supplements, mineral-rich powders, and protein-enriched flours. The principal component analysis showed that the appropriate use of a mango variety depends on its natural qualities rather than the indigenous or non-indigenous grouping. This may help processors select mangoes that are best for juices, purées, and fresh eating. Overall, mango pulp and by-products offer opportunities for developing novel products that add value to the mango industry.

CONTRIBUTION

The study was conceptualized and designed by H. Nakisozi, P. Ogwok, and D. Mugampoza. H. Nakisozi contributed to data collection and sample analysis, as well as analyzed the data and wrote the manuscript draft. P. Ogwok and D. Mugampoza edited and reviewed the manuscript.

CONFLICT OF INTEREST

The authors declare no conflict of interest regarding the publication of this article.

REFERENCES

1. Nakisozi H, Ogwok P, Mugampoza D. Morphometry of mango varieties and sociodemographic factors influencing mango production in Uganda. International Journal on Food, Agriculture and Natural Resources. 2025;6(1):93–99. https://doi.org/10.46676/ij-fanres.v6i1.469
2. Akin-Idowu PE, Adebo UG, Egbekunle KO, Olagunju YO, Aderonmu OI, *et al*. Diversity of mango (*Mangifera indica* L.) cultivars based on physicochemical, nutritional, antioxidant, and phytochemical traits in South West Nigeria. International Journal of Fruit Science. 2020;20(sup2):S352–S376. https://doi.org/10.1080/15538362.2020.1735601
3. Pușcaș A, Tanislav AE, Marc RA, Mureșan V, Mureșan AE. Valorization of mango peel and seed wastes in a biologically enriched biscuit assortment. Turkish Journal of Agriculture and Forestry. 2023;47(6):1174–1181. https://doi.org/10.55730/1300-011X.3156
4. Siddiq M, Sogi DS, Roidoung S. Mango processing and processed products. In: Siddiq M, Brecht JK, Sidhu JS, editors. Handbook of mango fruit: Production, postharvest science, processing technology and nutrition. Hoboken, NJ: John Wiley & Sons, 2017, 195 p. https://doi.org/10.1002/9781119014362.ch10
5. Than TS, Htwe NN, Hlaing MT. A case study on postharvest handling practices of mango fruits in selected areas of Myanmar. International Journal of Environmental and Rural Development. 2021;12(2):189–193.
6. Lebaka VR, Wee YJ, Ye W, Korivi M. Nutritional composition and bioactive compounds in three different parts of mango fruit. International Journal of Environmental Research and Public Health. 2021;18(2):741. https://doi.org/10.3390/ijerph18020741
7. Barrón-García OY, Gaytán-Martínez M, Ramírez-Jiménez AK, Luzardo-Ocampo I, Velazquez G, *et al*. Physicochemical characterization and polyphenol oxidase inactivation of Ataulfo mango pulp pasteurized by conventional and ohmic heating processes. LWT. 2021;143:111113. https://doi.org/10.1016/j.lwt.2021.111113
8. Danyo EK, Ivantsova MN. Fruit phytochemicals: Antioxidant activity and health-promoting properties. Foods and Raw Materials. 2025;13(1):58–72. https://doi.org/10.21603/2308-4057-2025-1-623

9. Liu FX, Fu XF, Bi XF, Chen F, Liao XJ, *et al*. Physico-chemical and antioxidant properties of four mango (*Mangifera indica* L.) cultivars in China. Food Chemistry. 2013;138(1):396–405. https://doi.org/10.1016/j.foodchem.2012.09.111
10. Mwaurah PW, Kumar S, Kumar N, Panghal A, Attkan AK, *et al*. Physicochemical characteristics, bioactive compounds and industrial applications of mango kernel and its products: A review. Comprehensive Reviews in Food Science and Food Safety. 2020;19(5):2421–2446. https://doi.org/10.1111/1541-4337.12598
11. Onuh JO, Momoh G, Egwujeh S, Onuh F. Evaluation of the nutritional, phytochemical and antioxidant properties of the peels of some selected mango varieties. American Journal of Food Science and Technology. 2017;5(5):176–181. https://doi.org/10.12691/ajfst-5-5-2
12. Saroj N, Prasad K, Singh SK, Kumar V, Maurya S, *et al*. Characterization of bioactive and fruit quality compounds of promising mango genotypes grown in Himalayan plain region. PeerJ. 2023;11:e15867. https://doi.org/10.7717/peerj.15867
13. Himanshu, Kumar N, Khangwa I. Functional attributes and bio-prospects of fruit peel waste. Foods and Raw Materials. 2026;14(1):84–103. https://doi.org/10.21603/2308-4057-2026-1-660
14. Lopez-Huertas E. Health effects of oleic acid and long chain omega-3 fatty acids (EPA and DHA) enriched milks: A review of intervention studies. Pharmacological Research. 2010;61(3):200–207. https://doi.org/10.1016/j.phrs.2009.10.007
15. Gröber U, Schmidt J, Kisters K. Magnesium in prevention and therapy. Nutrients. 2015;7(9):8199–8226. https://doi.org/10.3390/nu7095388
16. Yahia EM, Ornelas-Paz JJ, Brecht JK, García-Solís P, Celis MEM. The contribution of mango fruit (*Mangifera indica* L.) to human nutrition and health. Arabian Journal of Chemistry. 2023;16:104860. https://doi.org/10.1016/j.arabjc.2023.104860
17. Maldonado-Celis ME, Yahia EM, Bedoya R, Landázuri P, Loango N, *et al*. Chemical composition of mango (*Mangifera indica* L.) fruit: Nutritional and phytochemical compounds. Frontiers in Plant Science. 2019;10:1073. https://doi.org/10.3389/fpls.2019.01073
18. Jafo Y, Nyalandu J, Bwanamdogo N. A study of some of the quality attributes of fresh mango and pineapple fruits. African Journal of Agronomy. 2019;7(1):411–427.
19. Akhter S, McDonald M, Marriott R, Jashimuddin M, Bashirul-Al-Mamun M. Morphological, nutritional and medicinal traits of wild mango (*Mangifera Sylvatica* Roxb.): Implications for increased use and options for cultivar development. Trees, Forests and People. 2021;6:100126. https://doi.org/10.1016/j.tfp.2021.100126
20. Shi S, Ma X, Xu W, Zhou Y, Wu H, *et al*. Evaluation of 28 mango genotypes for physicochemical characters, antioxidant capacity, and mineral content. Journal of Applied Botany and Food Quality. 2015;88:264–273. https://doi.org/10.5073/JABFQ.2015.088.039
21. Bora L, Singh AK, Singh CP. Characterization of mango (*Mangifera indica* L.) genotypes based on physio-chemical quality attributes. Journal of Applied and Natural Science. 2017;9(4):2199–2204. https://doi.org/10.31018/jans.v9i4.1510
22. Ellong E, Adenet S, Rochefort K. Physicochemical, nutritional, organoleptic characteristics and food applications of four mango (*Mangifera indica*) varieties. Food and Nutrition Sciences. 2015;6:242–253. https://doi.org/10.4236/fns.2015.62025
23. Piper CS. Soil and plant analysis. New Delhi: Scientific Publishers; 2019, 368 p.
24. Dutta S, Ranjan DS, De M. Characterization of the mango (*Mangifera indica* L.) fruit and fruit pulp of some indigenous mango varieties of Murshidabad district of West Bengal. International Journal of Advancement in Life Sciences Research. 2020;03(2):23–28. https://doi.org/10.31632/ijalsr.20.v03i02.003
25. Zafar TA, Sidhu JS. Composition and nutritional properties of mangoes. In: Siddiq M, Brecht JK, Sidhu JS, editors. Handbook of mango fruit: Production, postharvest science, processing technology and nutrition. NJ: Apple Academic Press; 2017, pp. 217–236. https://doi.org/10.1002/9781119014362.ch11
26. Mhaske T, Kumar S, Wani AW, Banerjee D, Saran R, *et al*. Mechanism of fruit ripening and seed development: A review. International Journal of Research in Agronomy. 2024;7(7):123–136. https://doi.org/10.33545/2618060X.2024.v7.i7b.991
27. Bhuiyan MSH, Hoque MA, Hossain MM, Zakaria M, Ahiduzzaman M. Influence of maturity stages on physico-chemical properties and shelf-life of different varieties of mangoes under ambient storage conditions. European Journal of Agriculture and Food Sciences. 2023;5(1):119–124. https://doi.org/10.24018/ejfood.2023.5.1.642
28. Ivan GD, Maicol JA, Luzneyda B, Hannia G. Agroindustrial behavior of 11 mangoes varieties (*Mangifera indica* L) present in a natural productive system of the district of San Marco de Malagana (Bolivar). 2018;15:102–108. http://doi.org/10.19026/ajfst.14.5879
29. Malainine H, Makhloufi A, Sahli A, Khadidja M. Physicochemical and microbiological quality of some commercial fruit drinks and juices in Algeria. Applied Biology in Saharan Areas. 2020;4(2):27–31.

30. Chen J, Zhu F. Characterization of physicochemical properties, fatty acids, flavor volatiles and phenolic compounds of avocado varieties. Food Chemistry. 2025;482:143533. https://doi.org/10.1016/j.foodchem.2025.143533
31. Shi W, Hou Y, Zhang Z, Yin X, Zhao X, *et al*. Determination of selenium speciation in high se-enriched edible fungus *Ganoderma lucidum* via sequential extraction. Horticulturae. 2023;9(2):161. https://doi.org/10.3390/horticulturae9020161
32. Begum ML, Ahmed M, Rahman A, Rahman H, Arfin S, *et al*. Changes of postharvest nutritional quality and antioxidant enzymes in 'Haribhanga' mango by Aloe vera gel with chitosan and coconut oil coating during ambient storage. Journal of Horticultural Research. 2023;31(2):115–126. https://doi.org/10.2478/johr-2023-0024
33. Elkhalifa AOK, Nour AEMA, Elsheikh AEO. Effect of storage on the quality attributes of concentrates of two mango (*Mangifera indica*) varieties grown in Sudan. Journal of Food Research. 2014;4(14):2069–2078. https://doi.org/10.9734/BJAST/2014/9398
34. Utami MA, Wijaya CH, Efendi D. Physicochemical characteristics and sensory profile of Gedong mango at two levels of maturity. Jurnal Teknologi dan Industri Pangan. 2020;31(2):113–126. https://doi.org/10.6066/jtip.2020.31.2.113
35. Deepa MPC, Bharati VO, Raghavan V, Udaykumar K, Orsat V. Antioxidant activity in pulp and peel of three mango varieties. Journal of Horticultural Science. 2015;10(2):199–209. https://doi.org/10.24154/jhs.v10i2.130
36. Farina V, Gentile C, Sortino G, Gianguzzi G, Palazzolo E, *et al*. Tree-ripe mango fruit: Physicochemical characterization, antioxidant properties and sensory profile of six Mediterranean-grown cultivars. Agronomy. 2020;10(6):884. https://doi.org/10.3390/agronomy10060884
37. Subedi P, Walsh K, Purdy P. Determination of optimum maturity stages of mangoes using fruit spectral signatures. Acta Horticulturae. 2013;992:515–522. https://doi.org/10.17660/ActaHortic.2013.992.64
38. Pérez-Meza NB, Ayala-Tafoya F, Vélez-de la Rocha R, López-Orona CA, Martínez-Gallardo JÁ, et al. The nutritional, mineral, and nutraceutical quality is differentially affected by the mango cultivar. Horticulturae. 2024:10(10):1082. https://doi.org/10.3390/horticulturae10101082
39. Subedi T. An assessment of mineral contents in fruits. Prithvi Academic Journal. 2023;6(1):21–31. https://orcid.org/0009-0009-9343-2809
40. Institute of Medicine (US) Panel on Micronutrients. Dietary reference intakes for vitamin A, vitamin K, arsenic, boron, chromium, copper, iodine, iron, manganese, molybdenum, nickel, silicon, vanadium, and zinc. Washington, DC: National Academies Press, 2001.
41. Berardini N, Knödler M, Schieber A, Carle R. Utilization of mango peels as a source of pectin and polyphenolics. Innovative Food Science & Emerging Technologies. 2005;6(4):442–452. https://doi.org/10.1016/j.ifset.2005.06.004
42. Soong YY, Barlow PJ, Perera CO. A cocktail of phytonutrients: Identification of polyphenols, phytosterols and tocopherols from mango (*Mangifera indica* L.) seed kernel. Institute of Food Technologists Annual Meeting. 2004.
43. Bala SM, Ameh DA, Omage JJ, Salihu A. Antinutritional factors, proximate composition and mineral elements content of the seed kernel of three Nigerian mango (*Mangifera indica* L.) varieties. Nigerian Journal of Biochemistry and Molecular Biology. 2011;26(2):81–87.
44. Thavarajah P, Thavarajah D. Inaccuracies in phytic acid measurement: Implications for mineral biofortification and bioavailability. American Journal of Plant Sciences. 2014;5(1):29–34. http://doi.org/10.4236/ajps.2014.51005
45. Camden BJ, Morel PCH, Thomas DV, Ravindran V, Bedford MR. Effectiveness of exogenous microbial phytase in improving the bioavailabilities of phosphorus and other nutrients in maize-soya-bean meal diets for broilers. Animal Science. 2016;73(2):289–297. https://doi.org/10.1017/S1357729800058264

Additional information about the authors

Nakisozi Henriettah ORCID 0000-0003-1392-8097
Ogwok Patrick ORCID 0000-0001-7312-3333
Mugampoza Diriisa ORCID 0000-0001-8382-6876

Foods and Raw Materials. 2027;15(2)

ISSN 2308-4057 (Print)
ISSN 2310-9599 (Online)

Review Article
Open Access

Available online at http://jfrm.ru/en
https://doi.org/10.21603/2308-4057-2027-2-720
https://elibrary.ru/KRUANV

Hybrid meat: A comprehensive review of composition, processing, and consumer acceptance

Nandana R, Radhalakshmi V, Linu M Salim, Jismy K J, Anooja Thomas, Jisha M S, Sajad Rehman*

Mahatma Gandhi University, Kottayam, India

* e-mail: sajadrahmanp@gmail.com

Received 15.09.2025; Revised 05.12.2025; Accepted 03.02.2026; Published online 29.09.2026

Abstract:
The increasing human population will escalate the demand for meat and alternative meat products. The term "hybrid meat" can be used to define food products that combine conventional animal meat with alternative protein sources, such as plant-based ingredients, insect protein, or cultured cells. These products are designed to reduce the environmental and ethical concerns associated with traditional meat, while retaining the desirable sensory and nutritional qualities. Our review provides a comprehensive analysis of the development, composition, processing technologies, nutritional value, environmental sustainability, consumer acceptance, safety concerns, and regulatory frameworks for hybrid meat. The incorporation of plant proteins, pulses, insect flours, and cultured cells has shown potential to improve dietary fiber, antioxidant content, and lipid profiles without significantly compromising taste or texture. Innovative technologies such as high-moisture extrusion, 3D bioprinting, and fermentation enhance the structural and functional attributes of hybrid meat products. From an environmental perspective, hybrid meat can reduce greenhouse gas emissions and resource use by lowering the total meat content. However, safety issues such as allergenicity, microbial contamination, and chemical residues require thorough monitoring. Regulatory policies are evolving globally to address these challenges, while consumer acceptance hinges on familiarity, sensory quality, and clear labelling. Numerous studies are being conducted to curb the challenges and produce hybrid meat with a specific composition and preserved flavor. As flexitarian diets gain momentum, hybrid meat emerges as a promising transition towards sustainable food systems. It bridges the gap between conventional meat and plant-based alternatives, promoting environmental sustainability.

Keywords: Hybrid meat, cultured meat, plant-based alternatives, protein, safety, sensory

Please cite this article in press as: R Nandana, V Radhalakshmi, M Salim Linu, K J Jismy, Thomas Anooja, *et al.* Hybrid meat: A comprehensive review of composition, processing, and consumer acceptance. Foods and Raw Materials. 2027;15(2):437–448. https://doi.org/10.21603/2308-4057-2027-2-720

INTRODUCTION

Meat consumption has played a pivotal role in human evolution and remains a deeply ingrained practice in cultures worldwide. From a biological standpoint, anthropological and nutritional evidence suggests that meat-eating played a crucial role in shaping the human species. According to the "expensive tissue hypothesis", high caloric density and nutrient richness of meat enabled early humans to develop larger brains by reducing the energy demands of the digestive system [1]. Meat provided essential nutrients such as vitamin B_{12}, iron, and high-quality proteins that were not readily available in plant-based foods, giving early hominins an evolutionary advantage. At the same time, the consumption of meat has been tightly interwoven with social, cultural, and symbolic meanings. Across many cultures, meat signifies wealth, power, and masculinity, being often reserved for important rituals, feasts, and social gatherings.

The growing human population is increasing the demand for meat products, and if sustainable and economical alternatives are not found, future prices may rise significantly. Scientists have been exploring alternative methods, such as man-made meat and technological developments for value-added, textured, and taste-enhancing livestock products [2]. The meat industry cannot keep up with the growing demand, so it has to come up with creative solutions to problems pertaining to sustainability, public health, and animal welfare. Furthermore, it is facing a complex regulatory environment, as well as growing competition from newly developed non-traditional meat and protein substitutes [3].

Copyright © 2026, Nandana R *et al.* This is an open access article distributed under the terms of the Creative Commons Attribution 4.0 International License (https://creativecommons.org/licenses/by/4.0/), allowing third parties to copy and redistribute the material in any medium or format and to remix, transform, and build upon the material for any purpose, even commercially, provided the original work is properly cited and states its license.

Meat production is the primary source of methane that has a limited half-life in the atmosphere compared to CO_2, but a relatively high warming potential. Even though well-managed grasslands have the potential to sequester carbon, their overall benefits are likely to be modest [4]. This explains the need for artificial meat or alternatives that can satisfy the increasing demand in the face of environmental concerns.

The emerging innovative technologies offer different varieties of meat, such as hybrid meat, vegan meat, or *in-vitro* meat. The definition of hybrid meat can vary depending on the ingredients incorporated. Hybrid meat with plant-based ingredients can be defined as hybrid meat products that combine 20–50% of plant-based and 50–80% of meat components. These products incorporate plant-based protein sourced from legumes or vegetables to replace a portion of meat. With only a few hybrid meat products available at the moment, more are expected to be developed in the future [5].

As flexible eating habits are gaining popularity, new hybrid meat products that combine plant-based and animal components are becoming more widely available [6]. With the recognizable meaty taste and texture, hybrid meat products are seen as an alternative to traditional meat products with additional dietary benefits from plants [7].

STUDY OBJECTS AND METHODS

This review aimed to summarize recent studies on hybrid meat (foods that combine components from plants and animals and are made to resemble animal-based products [8]), with a focus on raw materials, processing technologies, and consumer perception. For this, we conducted a systematic review of articles from the leading journals in food science, nutrition, and related fields published from 2012 to 2025. The journals included *Foods, Food Quality and Preference, Future Foods, International Journal of Food Science & Technology, Meat Science, Molecules, Nutrients, Science, Sustainability*, and many others. In this review, we sought to identify the key findings and future research directions for hybrid meat as a sustainable protein solution.

RESULTS AND DISCUSSION

Hybrid meat varieties. This section summarizes hybrid meat products that incorporate various ingredients providing them with distinct characteristics.

Insect-based hybrid meat. Due to the increasing demand for protein, various researchers have explored alternative protein sources to supplement or replace traditional animal proteins. Insect flours have emerged as a promising option, offering high nutritional value suitable for human consumption. For example, Talens *et al.* [9] investigated the potential of insect flour in hybrid meat products. The researchers prepared sausage samples from turkey meat partially replaced with brewer's spent grains, frozen broccoli, and mealworm (*Tenebrio molitor* L.) powder. In particular, nine different sausage formulations were developed by varying the proportions of insect flour. The ingredients were thoroughly mixed, blended, and then pasteurized before shaping and cooking the sausages. The objective was to assess the functionality and acceptability of insect flour in processed meat products. The study demonstrated that incorporating alternative protein sources such as insect flours is an effective strategy to reduce the dependence on animal protein in meat formulations. The blend with 22% of broccoli, 3% brewer's spent grains, and 10% insect flour looked the best and tasted/smelled just as good as the standard commercial product. Additionally, the study highlighted the feasibility of creating nutritionally balanced and sustainable meat alternatives through ingredient innovation.

In another study, Megido *et al.* [10] prepared four different burger patties using unflavoured ground beef, green lentils, and mealworms (*T. molitor*). One of the patties contained 45% of green lentils and 50% of insects (mealworm/lentil burger), and another one was formulated from 45% ground beef and 50% insects (mealworm/beef burger). The remaining two patties contained common burger ingredients. All the ingredients were precooked and mixed, then patties were made and cooked. The microbial analysis detected neither *Escherichia coli* nor *Clostridium perfringens* strains in the samples. The total viable counts were below the standard legal maximum for the mealworm/beef burger (5.04 log CFU/g) and mealworm lentil burger (5.28 log CFU/g). The research concluded that mealworms are safe to consume after fasting for 24 h (to remove toxins from their body) and drying. The use of the insects was accepted by the consumers.

A study conducted by Han *et al.* [11] utilized house cricket (*Acheta domesticus* L.) flour in combination with pork to produce hybrid sausages. The formulation included 42.5% of ice water, 35% lean pork, 20% pork fat, and other standard ingredients, along with cricket flour incorporated at 1, 2.5, and 5.0%. The cricket flour was prepared through lyophilization, a freeze-drying process that preserves its nutritional properties. The study aimed to evaluate the functional and sensory qualities of the resulting hybrid sausages. The researchers observed that the protein solubility and water-holding capacity of the cricket flour were influenced by such factors as pH and sodium chloride (NaCl) concentration. These variations affected the structural properties of the sausage, potentially leading to undesirable color and texture when only small amounts of cricket flour were added. Due to these challenges, further research is being carried out to enhance the lipid and protein oxidation stability in such insect-based meat formulations. This will help improve the product's quality and broaden consumer acceptance in future applications.

In Western culture, the consumption of insect-based products is gaining popularity due to their high nutritional value, including protein, vitamins, and minerals. These products also offer favorable sensory attributes such as taste and texture. Their integration into familiar food forms has further increased consumer acceptance [10].

Plant-based hybrid meat. As the increase in the dependence of animal meat for various health benefits and sensory attributes, alternative plant-based mimic meats are formulated with isolated plant proteins [12]. For example, Petrat-Melin & Dam [13] prepared burgers from 50% of plant-based ingredients (such as texturized legume protein) and 50% of meat (pork and beef, 4:1). The patties were seasoned with regular ingredients and analyzed for texture profile, cooking loss, expressible moisture, and consumer acceptance. According to the results, the most crucial characteristics for a burger were meat flavor, juiciness, spiciness, and saltiness. In summary, the hybrid burger was just as acceptable overall as a beef burger, despite having distinct qualities and being evaluated using various check-all-that-apply methods.

Sun *et al*. [14] investigated how adding hempseed meal (10, 20, 30, and 40%) affected the qualitative characteristics of chicken sausage. Their findings demonstrated that hempseed meal significantly decreased the moisture, protein, and lipid contents in chicken sausage, but increased the ash and total dietary fiber contents.

By combining chicken with pulses, Chandler & McSweeney [15] produced a hybrid meat burger and described its physical, textural, and chemical composition. At 0, 25, 50, and 75%, the chicken burger was supplemented with pulses (lentil, chickpea, and yellow pea). The samples' chemical composition, cooking qualities, and textural characteristics were examined. All the pulses led to a decrease in both moisture and lipid contents in the meat analogues. Lentils and chickpeas maintained the protein content, whereas yellow peas resulted in a reduced protein content. By decreasing the width and thickness and increasing the cooking yield, the pulses enhanced the samples' cooking qualities. At 50 and 75% replacement, the burger's textural characteristics differed considerably from those of the control burger. The study showed that pulses and chicken can be mixed only at a modest replacement level (25%) to produce a unique food product.

Stem cell-based hybrid meat. *In vitro* meat culturing, or meat cultivation, is a transformative alternative to traditional livestock production. It is designed to precisely replicate all the physical characteristics of conventional meat. This is primarily achieved by cultivating animal stem cells using advanced tissue engineering techniques. In particular, cells are proliferated in bioreactors and then guided by scaffolds to differentiate into muscle, fat, and connective tissues. The resulting product mimics the fibrous texture, juiciness, color, and overall mouthfeel found in traditional cuts of meat. The objective is to produce a sustainable and ethical protein source that is sensorially indistinguishable from its animal counterpart [16].

Kim *et al*. [17] studied the effect of adding cultured meat tissue (10, 20, and 30%) on hybrid meat's physicochemical and taste profiles. Chicken satellite cells were isolated from hindlimb muscles and suspended in growth media prepared and incubated to produce cultured meat tissues. After the dissociation of cells, the suspensions were centrifuged and the supernatant was lyophilized for storage. A pea plant protein solution and a wheat solution were used to prepare a solution for wet spinning. Imitation fiber and muscle were manufactured through wet spinning, while cellulose membrane was produced through electrospinning. The resulting hybrid cultured chicken meat was introduced to the plant-based protein solution. Each imitation fiber muscle was wrapped with an artificial muscle membrane to replicate the structure of traditional muscle. The quality of the imitated fiber muscles was thus improved, enhancing the quality of hybrid cultured chicken meat in turn. The product's sensory attributes were also improved and the method was found useful for addressing the problem of protein deficiency in plants.

Fish-based hybrid meat. Aquatic products are widely consumed due to their economic value, taste, and nutritional composition [18]. A recent study was conducted on the partial replacement of fish meat in surimi-based fish cakes with 0, 5, 10, 15, and 20% of textured vegetable protein. Fish cakes were cooked in two ways: 1) dough cylinders were placed in boiling water (100°C, 1.5 L) and cooked for 5 min; 2) dough cylinders were fried for 3 min in 1 L grapeseed oil at 180°C. Both samples were cooled to room temperature. The specific properties of fish meat contributed to a fibrous gel structure of the cake samples. Increased contents of textured vegetable protein seemed to gradually reduce the elastic property. They also decreased the fishy flavor and increased the beany flavor. Six unknown and 60 identified volatile compounds were detected in the fish cake samples. The fried fish cakes were most preferred by consumers [19].

3D printing. Bioprinting is defined as the use of biomaterials such as muscle, skin, bone, and cartilage to develop three-dimensional structures through 3D printing technology [20]. Meat substitutes can be derived from various sources, including *in vitro* cell cultures, meat by-products or waste, plants, and insects. Among these innovations, the sustainable 3D printing of meat from biological materials is referred to as bio-printed meat. This technique involves the precise layering of bioinks composed of edible materials such as proteins, lipids, insect powders, and dietary fibers. These components are blended in optimized concentrations to mimic the texture, flavor, and nutritional profile of conventional meat. Bioprinting offers a promising solution to the growing demand for sustainable and ethical meat alternatives. In addition, it allows for customizing the nutrient composition and structure, ensuring product consistency and consumer acceptance [21].

Wang *et al.* [22] prepared soft-textured meat analogues with the use of plant and animal proteins (pea protein isolate and chicken mince, respectively). In addition to the proteins, the ingredients included soy lecithin, maize starch, and beef fat. They were blended, made into a paste, and cooked before use. There were five samples with different ratios of the ingredients. The pastes were filled into syring-

es and small nugget-shaped samples were printed using a large volume extrusion 3D printer. The study found that 3D printability of the meat analogue was better with the addition of 20% chicken mince paste. The product had a good fiber texture contributed by hydrogen bonding [23].

Golovin *et al.* [24] biofabricated cellular meat constructs (30×40×3 mm) by 3D bioprinting rabbit stem cells (omentum-derived, lipogenic/myogenic differentiation) and fibroblasts within a sodium alginate/sunflower protein hydrogel. Cells demonstrated sustained viability (> 72 h) via confocal microscopy and formed tight junctions with metabolic activity, including procollagen secretion by fibroblasts and lipid accumulation by lipoblasts, as observed via transmission electron microscopy. The resulting product, comprising fibroblasts, lipocytes, myogenic cells, and hydrogel components, was confirmed safe for consumption.

Properties of hybrid meat. Hybrid meats contain plant or other alternative ingredients in addition to meat ingredients [8]. A hybrid meat burger prepared by adding pulses (yellow pea, chickpea, and lentil) at 0, 25, 50, and 75%, respectively, resulted in a decreased protein content with increasing amounts of yellow peas [15]. When added to chicken burgers, pulse flours improve the cooking yield and lessen the size reductions that occur during cooking. Adding pulses decreases the moisture content and increases the fat content in cooked meat. The inclusion of plant-based alternatives (pulses) to meat also enhances its textural properties such as hardness, cohesion, springiness, and gumminess.

Before extrusion, each protein from the plant source should be analyzed for its physicochemical characteristics, since even proteins coming from the same botanical source may have differing functions [25]. Processing parameters such as specific mechanical energy, moisture, and temperature have a significant impact on the quality of pea-based textured vegetable protein. However, because of the differences in protein subunits and the swelling (or gelling) properties of cold and hot water, pea protein-based texturized products generally have lower cutting strength and less chewiness than soy- or gluten-based products. These properties can be controlled with the use of functionality modifiers.

Compared to conventional pork and beef meats, plant-based meat analogue patties were higher in ash and crude fiber and lower in moisture, fat, and protein [26]. They also had more porous and loose structures before and after cooking, as well as lower values of lightness and redness. Their high pH (pH 7.42–7.43) might be due to the slight alkalinity of TVP.

The cutting strength of high-moisture extruded intermediates is primarily determined by their composition and water content [27]. Combining up to 40% *Alphitobius diaperinus* (Panzer, 1797) (mealworm) protein concentrate with 5–10% of soy fiber (dry matter) provided the meat analogue with a meat-like texture and 25.0–30.8% protein. The study showed that meat hybrids made of a blend of protein concentrates (soy and *A. diaperinus*) and water can develop a meat-like fiber texture by high-moisture extrusion.

A study by Han *et al.* [11] demonstrated that the pH and NaCl concentration had a substantial impact on the protein solubility and water-holding capacity of cricket flour added to the meat hybrid. However, the amount of cricket flour in the medium at the same pH and heating conditions had an impact on its gelation. Even small quantities of cricket flour can have negative effects on the color and texture of hybrid sausages and reduce their capacity to withstand oxidative storage.

Ramachandraiah studied 3D-printed hybrid meat made with insects and fish [21]. He found that the ground cricket- or grasshopper-incorporated meat had the highest protein and fiber contents, whereas the black soldier fly- or grasshopper-incorporated meat had the highest lipid content. The 3D-printed hybrid meat obtained from fish had a high nutritional value depending on the composition of the body part used.

A review by Stanišić *et al.* [28] proved that moderate levels of substitution (20–50%) in meat can preserve or enhance the product's texture, juiciness, and nutritional quality, while excessive incorporation levels frequently result in undesirable flavors, color alterations, and texture problems.

Nutritional characteristics. Hybrid meat products are engineered to retain a protein content comparable to that of traditional meat, while offering a more balanced amino acid profile. The integration of cultured animal cells ensures that essential amino acids such as lysine, leucine, and methionine are present in adequate quantities, while plant-based components (e.g., soy, pea, or lentil proteins) contribute complementary nutrients and dietary fiber. According to Curtain & Grafenauer [29], hybrid meats achieve a "complete protein" status by blending sources, which is nutritionally advantageous for populations at risk of protein insufficiency, such as vegetarians or older adults.

A key nutritional advantage of hybrid meat is its improved lipid profile. While conventional red meats are often high in saturated fats and cholesterol, hybrid products make use of unsaturated fats from plant oils such as canola, sunflower, or flaxseed. This modulation reduces the risk of cardiovascular diseases. A study by Willett *et al.* [30] demonstrated that consumers of hybrid meat products experienced improved lipid biomarkers, including reduced LDL-cholesterol levels, compared to those consuming conventional meat.

One concern often raised regarding plant-based diets is the potential deficiency in micronutrients such as vitamin B_{12}, iron, and zinc primarily found in bioavailable forms in animal products. Hybrid meat addresses this concern by enabling micronutrient fortification directly into the product formulation. Cultured meat components naturally contain heme iron and vitamin B_{12}, while plant products can be fortified with additional minerals. According to Driessen *et al.* [31], the bioavailability of iron in hybrid meat was significantly higher than in traditional plant-based alternatives due to the presence of both heme and non-heme sources.

Zhang *et al*. [32] proved that hybrid meat products contribute to good nutrition by offering health benefits and consumer appeal. Incorporating plant proteins, these products can keep protein levels similar to those in regular meat. However, at high meat substitution levels (around 40–50%), the overall protein and fat contents may decrease because plant ingredients hold more water and have fewer calories. One benefit of hybridizing proteins is a better ability to hold water and oil. This helps the product yield more, stay juicier, and have a more stable emulsion. As a result, the food becomes more enjoyable to eat. These improvements come from the way meat and plant proteins interact to form a strong, three-dimensional structure. New processing methods, such as high-moisture extrusion, high hydrostatic pressure, high-pressure homogenization, and ultrasound, are also used to improve these products. They help mix the proteins better, enhance their ability to form gels and emulsions, and break down those compounds in plant proteins which might block nutrients. This makes the final hybrid food safer, more nutritious, and better in taste and texture. Overall, these techniques not only boost the health benefits of hybrid foods but also make them more attractive in terms of taste and texture for consumers interested in sustainable diets.

Hybrid meat shows a distinct nutritional advantage by incorporating dietary fiber, a component that is almost absent in conventional meat. This additional fiber not only supports digestive health and satiety but also enhances the overall functionality of the product. For example, integrating plant-based ingredients such as legumes boosts the antioxidant capacity of hybrid meat. Studies have shown that adding red beans to turkey formulations can significantly raise the antioxidant activity, compared to pure meat samples. In addition, the soluble dietary fibers from legumes, which are rich in complex polysaccharides, provide extra benefits such as antioxidant, antiglycation, immunostimulatory, and prebiotic effects that go beyond basic nutrition [33]. Harnack *et al*. [34] reported that although conventional meat is a good source of key vitamins (e.g., B_{12} and B_3) and minerals (e.g., iron and zinc), incorporating plant ingredients can diversify and enrich the micronutrient profile of hybrid meat. Some plant-based meat alternatives contain higher levels of nutrients, such as folate, niacin, iron, phosphorus, sodium, manganese, and copper, compared to ground beef. This enhancement not only broadens the nutritional benefits but also positions hybrid meat as an attractive option for consumers seeking both balanced nutrition and innovative food products. The detailed nutrient characteristics of conventional (chicken, beef, etc.) and hybrid (with plant-based materials) meat are depicted in Table 1.

Environmental sustainability. Animal husbandry, slaughter, and transportation generate significant amounts of biological waste and pollutants in traditional meat systems. On the other hand, because cultured meat is produced in regulated conditions with reduced by-product loss, hybrid meat systems produce less organic waste. Furthermore, using plant-based ingredients adds value to those agricultural by-products (e.g., legumes or soy protein isolates) which might otherwise be wasted. The entire efficiency of the food system can be improved by this move towards circular resource usage [36].

Meat protein production uses a lot of land, water, energy, and raw materials, which makes it quite costly for the environment. The demand for full, high-quality proteins, including those derived from animals, is expected to rise globally due to the population growth estimated for 2050. The development of flexitarian eating patterns for wellness, health, and sustainability is gaining popularity. In particular, hybrid products with meat protein substitutes can lessen the effects on the environment. Proteins from vegetables (e.g., peas and chickpeas), fungi (mushrooms), and insects (e.g., cricket species and *T. molitor* larvae) have recently emerged as the most viable substitutes for meat in hybrid goods [37]. Although offering significant environmental benefits, the development of hybrid meat products involves overcoming several technological challenges. The processes must be optimized to ensure that partial substitution does not detract from the sensory and nutritional qualities of the final product.

Table 1 Nutrient profiles of conventional and hybrid meat, as sourced from [32–35]

Nutrient/Component (per 100 g serving, approximate)	Conventional meat	Hybrid meat (meat + plant)
Protein	High [33]	Slightly lower than in conventional meat, depending on substitution level [32]
Total fat	Moderate to high [33]	Potentially lower, depending on plant ingredients [32]
Dietary fiber	Negligible [35]	Significantly increased [33]
Vitamins	Present (B_{12}, B_3) [34]	Varies, with new vitamins coming from plants [33]
Minerals	Present (Fe, Zn) [34]	Varies, depending on the raw materials incorporated [33]
Antioxidant activity	Low [51]	Significantly increased with red beans [33]
Fatty acid profile	Varies based on cuts of meat [51]	Improved (e.g., lower n-6/n-3, UFA/SFA, PUFA/SFA) [33]
Anti-nutritional factors	Absent	Potentially present in raw plant proteins; reduced by processing [32]

The integration of alternative protein sources provides an innovative pathway to achieve a more resource-efficient protein supply without completely eliminating the sensory qualities that characterize meat-based dishes. Boukid *et al*. [38] suggest that hybrid meat products can play a vital role in reducing the environmental impacts of conventional meat production. By partially substituting animal proteins with alternative sources, producers can reduce resource consumption and greenhouse gas emissions without compromising the key sensory attributes. For these reasons, hybrid meat products are seen as a promising transitional strategy towards a more sustainable and health-conscious dietary future.

Consumer acceptance of hybrid meat. Concerns about environmental degradation, health safety, and the vegan movement are pushing both the industry and customers to seek meat alternatives [39]. Consumer acceptance has been studied via sensory analysis performed by trained and/or untrained participants or via surveys to obtain statistical values regarding their preference and acceptance of hybrid meat or meat alternatives.

Megido *et al*. [10] studied the consumer acceptance of insect-based alternative meat products in Western countries. In terms of overall liking, the beef burger was ranked as the best in hedonic evaluation among the four burgers, followed by the mealworm/beef burger, the mealworm/lentil burger, and the lentil burger. The level of willingness to try the same, an important factor in the study, varied depending on the age and gender of the panelists, their knowledge about, and perception of, the product, its composition, and whether they had tasted it before.

The cost of plant-based meat alternatives is still higher than that of traditional meat. According to Szenderák *et al*. [40], the consumers who were willing to pay higher prices were more likely to choose plant-based alternatives. Other factors included their dietary preferences, emotional and situational factors, familiarity with the product, environmental impacts, sensory characteristics, religious and political factors, as well as nutritional perception. As reported by Baune *et al*. [41], a meat hybrid with 30% of plant-based proteins can ultimately attract more consumers. After tasting the product (pea-based hybrid meat), almost 50% of the untrained panelists expressed a comparatively strong readiness to purchase it. The remaining 50% did not like its musty taste.

The consumer acceptance of 3D-printed and cultured alternatives is lower than that of conventional items, despite the claimed benefits such as increased sustainability, animal welfare, and healthiness [42]. In this study, the participants with a stronger affinity for meat were less inclined to use plant-based meat alternatives. No correlation was found between meat attachment and eating willingness for the other meat substitutes. The participants tended to consume all fish alternatives, except for the 3D-printed plant-based substitute. This implies that customers who consider fish to be a significant component of their diet may be willing to consume fish substitutes [43].

Consumers primarily rely on sensory factors such as taste, texture, and visual appeal to guide their preference for hybrid meat products. Items that closely resemble traditional meat in these aspects tend to be more accepted, largely because familiarity is a key driver. However, increasing the proportion of plant ingredients can disrupt the protein structure, leading to tougher, chewier textures, and off-flavors (often described as dry, beany, or bland). Moreover, noticeable color changes such as reduced redness and increased yellowness can detract from the product's appeal [32].

Safety of hybrid meat. Concerns regarding the safety of hybrid meat products arise from the integration of diverse components, each with its own set of potential hazards. These can be broadly categorized into biological, chemical, physical, and nutritional/allergenic considerations. Biological hazards in hybrid meat are mainly associated with microbial contamination and genetic instability of cultivated meat components. Every component carries microbial risks. For example, plant-based ingredients may contain pathogens such as *Clostridium* spp. and *Bacillus* spp., which may survive or re-enter products after thermal processes such as extrusion. Plant ingredients (e.g., soy, pea, wheat, rye, barley, lupin) may also contain allergens capable of triggering IgE-mediated responses, with thermal processing having uncertain effects on allergenicity. Cultivated meat faces contamination risks from bacteria (e.g., *Salmonella, Listeria, E. coli*), viruses, fungi, prions, and mycoplasma. These risks are especially pronounced during cell sourcing, media preparation, or bioreactor operations due to compromised aseptic techniques or contaminated inputs [44].

The integration of conventional meat, plant-based ingredients, and cultivated meat components in hybrid products broadens the range of potential pathogens and spoilage microorganisms. Conventional meat naturally presents microbial hazards, while plant-based ingredients may introduce additional pathogens that can survive processing [45]. Chemical additives such as flavorings, colorings, and emulsifiers are commonly used in hybrid formulations to enhance sensory attributes, and their safety must be validated at proposed usage levels. Processing techniques, including heat treatment and smoking, can cause physicochemical changes that generate reactive compounds or carcinogens. Some plant-based ingredients contain natural toxins (e.g., lectins, cyanogenic glycosides) or mycotoxins from fungal contamination, which may persist despite processing. Synthetic contaminants such as pesticide residues and residual solvents (e.g., hexane used in protein extraction) also present potential toxicological concerns.

Zandonadi *et al*. [46] proved that prion contamination in hybrid meat is a significant concern when animal-derived ingredients are involved, particularly high-risk tissues such as the brain, spinal cord, or lymphoid organs. While cultivated meat is produced in controlled environments, it carries biological hazards such as contamination from compromised sterility or

unstable cell lines. Various processing methods, such as extrusion for plant proteins, bioreactor culture for cultivated cells, or conventional meat processing, may not uniformly address all microbial threats. This necessitates a holistic food safety approach such as the Hazard Analysis and Critical Control Points, which considers cumulative or synergistic risks across components. Unintended genetic mutations in cultivated cells may result in unknown secretory products or poorly differentiated cells, potentially affecting nutritional quality or safety, including the presence of carcinogenic cell types.

Chemical hazards are also diverse and originate at different production stages. In cultivated meat, these include residues from growth media (e.g., fatal bovine serum, serum-free alternatives), veterinary drugs, or toxic substances used in cell culture (e.g., dexamethasone, indomethacin). Scaffolds and bioreactor components may degrade and release harmful by-products. Additionally, both plant-based and animal-derived materials may contain physical contaminants such as stones, metal fragments, or rubber from agricultural fields or machinery. Emerging risks include microplastics, especially from marine cell sources or lab environments, and heavy metals such as lead, mercury, or cadmium, which may leach from bioreactor systems or come from soil and plant-based ingredients. These overlapping risks highlight the need for comprehensive monitoring and regulation tailored to the complexity of hybrid meat production [46].

Beyond the microbial risks, the genetic instability of cells or cell lines is a significant concern for cultivated meat production. Continuous cell culture may lead to genetic mutations due to factors such as replication errors, environmental stress, or cell line aging. These mutations could potentially result in altered cellular functions or a reduction in nutritional value. In more serious scenarios, there is a possibility of oncogenic changes within the cells [47]. Key safety concerns in hybrid meat products primarily revolve around microbiological hazards, allergenicity, and potential for novel contaminants, which are further detailed in Table 2.

Regulatory aspects. The regulatory oversight of novel foods, such as hybrid meats, varies significantly across different regions. In the United States, a bifurcated approach is employed. The Food and Drug Administration regulates the early stages of cultivated meat production, encompassing aspects from cell sourcing all the way through cell differentiation. Conversely, the U.S. Department of Agriculture's Food Safety and Inspection Service supervises post-harvest stages, which

Table 2 Key safety concerns in hybrid meat products

Hazard category	Specific concern	Primary source	Implication	References
Biological	Microbial contamination	Conventional meat, plant-based, cultivated meat	Risk of foodborne illness from pathogens (e.g., *Salmonella*, *Escherichia coli*, *Clostridium* spp., *Bacillus* spp.) or spoilage microorganisms from diverse origins	[44]
	Microbiological risks and allergens	Insect flour-based meat, from various processes	Risk of health disorders caused by *Cronobacter*, *Bacillus*, *Staphylococcus, Clostridium, Haemophilus, Salmonella, Bacillus cereus, Vibrio,* and *Acinetobacter*	[44]
	Genetic instability/ incomplete differentiation	Cultivated meat	Risk of altered cellular functions, reduced nutritional value, or unintended (e.g., carcinogenic) cell types	[46]
Chemical	Residues from production	Cultivated meat, plant-based meat	Accumulation of growth media components, veterinary drugs, toxic chemicals, or scaffold degradation products	[45]
	Chemical additives/ by-products	All components, processing	Safety of intentionally added substances and formation of harmful compounds (e.g., carcinogens) during processing	[45]
	Natural/synthetic toxins	Plant-based, processing	Presence of mycotoxins, natural plant toxins (e.g., lectins), or residual organic solvents (e.g., hexane)	[45]
Physical	Foreign materials	All components, processing	Contamination by external objects (e.g., stones, metal shavings) or microplastics from production environment	[46]
	Heavy metals	All components, production environment	Leaching from equipment or natural presence in raw materials	[46]
Nutritional	Nutrient disparity/quality	All components, formulation	Possibility of imbalances, deficiencies (e.g., B_{12}, iron), or lower protein quality compared to conventional meat	[45]
	Bioavailability of added nutrients	Formulation	Need to assess how well added nutrients are absorbed and utilized by the body	[46]
Allergenic	Novel/known protein allergens	All components	Increased risk of allergic reactions due to diverse protein sources (e.g., soy, pea, wheat, novel cultivated proteins) and potential cross-reactivity	[44]

include critical steps such as processing, packaging, and labelling of these products. In addition, plant-based components within hybrid meats are generally regulated in a manner consistent with other conventional non-animal food products [44].

Across the Atlantic, the European Union operates under a distinct framework. Its cornerstone is the Novel Foods Regulation (EU 2015/2283), mandating a rigorous pre-market authorization process for any new food product falling under its scope. The European Food Safety Authority plays a pivotal role in this process by providing comprehensive scientific advice. To obtain authorization, detailed information is required from manufacturers, including specifics about the source organisms, confirmation of cell line identity, any genetic modifications undertaken, and conclusive evidence regarding the absence of pathogens. These varying regulatory pathways highlight the diverse strategies employed globally to ensure the safety and integrity of hybrid meat products as they enter the food supply [44].

The EU's precautionary principle often leads to a more cautious market entry. Singapore has emerged as a frontrunner, approving cultivated meat sales in 2020, with the Singapore Food Agency requiring comprehensive safety assessments. Other regions such as Israel, Australia, New Zealand, and Canada are also developing novel food regulations. The Food and Agriculture Organization and the World Health Organization have jointly published documents synthesizing information on terminology, production processes, potential hazards, and global regulatory frameworks, highlighting the key food safety issues [46].

While general principles such as the Hazard Analysis and Critical Control Points and good manufacturing practices are widely applied, specific frameworks for hybrid products are still emerging, leading to regional variations and challenges in harmonization. Labelling and nomenclature present particular hurdles, as clear communication of product origin and composition is vital for consumer trust and market acceptance [48–50]. The success of hybrid meat products in the market hinges not only on their safety but also on consumer acceptance, which is heavily influenced by transparent and trustworthy regulatory frameworks, particularly labelling [50].

Market trends. Despite the numerous product launches during the past years in various countries, few hybrid meat products have achieved a sustained market presence. This suggests a significant challenge in translating initial consumer interest into long-term loyalty. Successful examples, such as Rebel Meat and Perdue Chicken Plus, appear to have found the right target market by developing niche products that offer solutions to specific practical problems. This observation suggests that simply blending ingredients is insufficient for long-term market success. Initial novelty can quickly fade if the product fails to deliver consistent value, meet a particular consumer need, or establish a clear market niche. This implies that the hybrid meat market is not just about product innovation but also about developing sustainable business models, effective market positioning, and a deep understanding of long-term consumer needs beyond initial curiosity [8].

Furthermore, consumers' willingness to pay for hybrid meat products is a critical factor. Research suggests that consumers are generally not yet willing to pay a premium for hybrid options, especially when compared to conventional meat counterparts [49]. This price sensitivity means that manufacturers must strive to keep production costs competitive to offer hybrid products at an attractive price. Without a clear value that justifies their price and a well-defined market presence, hybrid meats may continue to face an uphill battle in gaining a significant market share against their traditional or exclusively plant-based competitors.

Challenges for hybrid meat. Despite the promising potential of hybrid meat products, a significant challenge lies in winning widespread consumer acceptance. One primary hurdle is the consumer's lack of understanding of what hybrid meat entails. Unlike clearly defined categories such as conventional meat or plant-based alternatives, hybrid products often lack a specific identity in the marketplace, leading to confusion among shoppers [8]. Another major barrier might be consumer expectations regarding the sensory attributes of hybrid products, such as taste, texture, and visual appeal. While hybrid meats aim to mimic conventional meat, any perceived deviation in these characteristics can lead to lower acceptance. Studies indicate that factors such as protein source, fat content, and even packaging can significantly influence purchasing decisions for hybrid products, often more so than for pure meat or plant-based options [49].

Zhang *et al.* [32] concluded that the development of high-quality hybrid meat products is also hampered by several complex technological challenges, particularly those concerning protein compatibility and functional performance. Combining diverse protein sources such as animal muscle, plant proteins, or even microbial proteins requires precise control over factors such as pH, temperature, and salt concentration to ensure the desired texture and cohesion of the product. Achieving a uniform and appealing structure that mimics meat can be difficult, as plant proteins may react differently during processing compared to animal proteins. This can potentially lead to altered hardness, chewiness, or discoloration. Hybrid products are frequently linked to being extensively processed or categorized as "ultra-processed foods". This viewpoint may cause consumers to feel hesitant because of unfamiliarity and a sense of unnaturalness [28].

The absence of a unified global regulatory framework for hybrid and novel protein products hampers international growth and creates uncertainty in the market for producers [49, 51]. Depending on the ingredient selection and processing, there may be changes in emulsion stability, water-holding capacity, and nutrient bioavailability (such as iron and specific amino acids).

To ensure nutritional equivalency between hybrid and traditional meats, reports advise cautious formulation and analytical verification (digestibility, micronutrient retention, etc.) [52]. Many nations lack a widely recognized regulatory definition or labelling standard for hybrid goods. This may reduce customer trust and lead to market uncertainty and lawsuit risk (e.g., whether "meat" words can be used) [53].

Future of hybrid meat. A study by Grasso [8] reported that hybrid meat products might be a simple method to reduce meat consumption without sacrificing flavor or having to develop new culinary practices, in addition to enjoying the advantages of the additional components. According to Ramachandraiah [21], 3D printing is still in its early phases, requiring further research into both printers and materials. In particular, there is a need to investigate food-safe (bioprinting) and insect-derived materials that can be used to 3D print meat analogues. The use of both plant and animal wastes and by-products from the production of meat substitutes might increase their sustainability. A survey by Megido *et al*. [10] on consumer acceptance of insect-based alternative meat products showed that 79% of the respondents were interested in consuming insects in their future. Among them, 68% would include insects in their regular diet. This suggests increasing popularity of hybrid meat incorporating insect-based products in the future.

Chandler & McSweeney [15] explored how pulses can be utilized in innovative gastronomic applications and contribute to the development of new hybrid meat products. The authors concluded that the use of pulses in hybrid meat burgers improved their cooking qualities by increasing the cooking yield, minimizing the reduction in thickness and diameter, and enhancing the fat content. Thus, the study promotes creative approaches to enhance plant protein consumption in the culinary industry.

Baune *et al*. [41] emphasized that factors such as healthiness and sustainability often score highest among intrinsic attributes, and that good communication about these benefits is pivotal for acceptance. However, challenges in the market integration of hybrid meat persist. Grasso [8] observed that very few hybrid meat products are still available in the market after initial launches, despite their favorable taste and texture in many cases. Their limited retail presence and the consumers' confusion about their categorization can impede market performance. Therefore, future market strategies need to focus on clearer branding, targeted marketing, and establishing a distinct identity for hybrid meats to ensure their sustained growth and widespread adoption.

CONCLUSION

Hybrid meat is an emerging concept in the meat industry, which involves combining traditional meat with other components to develop novel varieties for the market. These additional components can be derived from insects, plants, stem cells, or fish, so hybrid products can cater to both vegan and omnivorous preferences. Advancements in production technology have even enabled the 3D printing of hybrid meat. One notable advantage of hybrid meat is its customizable nutritional profile, which can be tailored to meet specific dietary needs.

The development of hybrid meat is driven by the escalating global demand for protein, coupled with increasing consumer awareness of the environmental impact of traditional meat production. These hybrid products offer tangible benefits in terms of sustainability (lower meat content) and health (better dietary fiber, fatty acid profiles, and antioxidant capacity). Their appeal is particularly strong among flexitarian consumers, who seek to reduce meat consumption without sacrificing familiar taste and texture. This segment, representing nearly half of the consumer base, is highly receptive to hybrid options, making them a critical target for market growth.

Some of the major challenges of hybrid meat include potential risks of microbial contamination, allergic reactions, and the presence of heavy metals, among other issues. Studies indicate that consumer acceptance of such products is likely to increase shortly. Furthermore, hybrid meat presents a promising solution for environmental sustainability. However, further research is required to fully understand the implications and potential of hybrid meat.

CONTRIBUTION

Nandana R conceptualized the research, designed the study methods, and wrote the manuscript. Sajad Rehman was involved in the conceptualization, visualization, reviewing, supervision, and editing of the manuscript. All the other authors took part in the reviewing and editing of the manuscript.

CONFLICT OF INTREST

The authors declare that there is no conflict of interest regarding this publication.

REFERENCES

1. Aiello LC, Wheeler P. The expensive-tissue hypothesis: The brain and the digestive system in human and primate evolution. Current Anthropology. 1995;36(2):199–221. https://doi.org/10.1086/204350
2. Gokirmakli C, Bayram M. Future of meat industry. MOJ Food Processing & Technology. 2017;5(1):232–238. https://doi.org/10.15406/mojfpt.2017.05.00117
3. Bonny SPF, Gardner GE, Pethick DW, Hocquette JF. What is artificial meat and what does it mean for the future of the meat industry? Journal of Integrative Agriculture. 2015;14(2):255–263. https://doi.org/10.1016/S2095-3119(14)60888-1

4. Godfray HCJ, Aveyard P, Garnett T, Hall JW, Key TJ, *et al*. Meat consumption, health, and the environment. Science. 2018;361(6399):eaam5324. https://doi.org/10.1126/science.aam5324
5. van Dijk B, Jouppila K, Sandell M, Knaapila A. No meat, lab meat, or half meat? Dutch and Finnish consumers' attitudes toward meat substitutes, cultured meat, and hybrid meat products. Food Quality and Preference. 2023;108:104886. https://doi.org/10.1016/j.foodqual.2023.104886
6. Grasso S, Jaworska S. Part meat and part plant: Are hybrid meat products fad or future? Foods. 2020;9(12):1888. https://doi.org/10.3390/foods9121888
7. Grasso S, Goksen G. The best of both worlds? Challenges and opportunities in the development of hybrid meat products from the last 3 years. LWT. 2023;173:114235. https://doi.org/10.1016/j.lwt.2022.114235
8. Grasso S. Opportunities and challenges of hybrid meat products: A viewpoint article. International Journal of Food Science & Technology. 2024;59(11):8693–8696. https://doi.org/10.1111/ijfs.17421
9. Talens C, Llorente R, Simó-Boyle L, Odriozola-Serrano I, Tueros I, *et al*. Hybrid sausages: Modelling the effect of partial meat replacement with broccoli, upcycled brewer's spent grain and insect flours. Foods. 2022;11(21):3396. https://doi.org/10.3390/foods11213396
10. Megido RC, Gierts C, Blecker C, Brostaux Y, Haubruge É, *et al*. Consumer acceptance of insect-based alternative meat products in Western countries. Food Quality and Preference. 2016;52:237–243. https://doi.org/10.1016/j.foodqual.2016.05.004
11. Han X, Li B, Puolanne E, Heinonen M. Hybrid sausages using pork and cricket flour: Texture and oxidative storage stability. Foods. 2023;12(6):1262. https://doi.org/10.3390/foods12061262
12. Chin SW, Baier SK, Stokes JR, Smyth HE. Evaluating the sensory properties of hybrid (meat and plant-based) burger patties. Journal of Texture Studies. 2024;55(1):e12819. https://doi.org/10.1111/jtxs.12819
13. Petrat-Melin B, Dam S. Textural and consumer-aided characterisation and acceptability of a hybrid meat and plant-based burger patty. Foods. 2023;12(11):2246. https://doi.org/10.3390/foods12112246
14. Sun G, Xiong Y, Feng X, Fang Z. Effects of incorporation of hempseed meal on the quality attributes of chicken sausage. Future Foods. 2022;6:100169. https://doi.org/10.1016/j.fufo.2022.100169
15. Chandler SL, McSweeney MB. Characterizing the properties of hybrid meat burgers made with pulses and chicken. International Journal of Gastronomy and Food Science. 2022;27:100492. https://doi.org/10.1016/j.ijgfs.2022.100492
16. Post MJ. Cultured meat from stem cells: Challenges and prospects. Meat Science. 2012;92(3):297–301. https://doi.org/10.1016/j.meatsci.2012.04.008
17. Kim SH, Kumari S, Kim CJ, Lee EY, Alam A, *et al*. Effect of adding cultured meat tissue on physicochemical quality and taste of hybrid cultured meat manufactured using wet-spinning. Food Science of Animal Resources. 2024;44(6):1440–1452. https://doi.org/10.5851/kosfa.2024.e104
18. Prema K, Visumathi J. Hybrid approach of CNN and SVM for shrimp freshness diagnosis in aquaculture monitoring system using IoT based learning support system. Journal of Internet Technology. 2022;23(4):801–810. https://doi.org/10.53106/160792642022072304015
19. Oh J, Park MK, Kim BR, Kwak HS. Effectiveness of textured vegetable protein incorporation for partial fish meat substitution in fish cakes. International Journal of Food Science and Technology. 2024;59(10):7080–7091. https://doi.org/10.1111/ijfs.17424
20. Zhuang P, An J, Chua CK, Tan LP. Bioprinting of 3D *in vitro* skeletal muscle models: A review. Materials & Design. 2020;193:108794. https://doi.org/10.1016/j.matdes.2020.108794
21. Ramachandraiah K. Potential development of sustainable 3D-printed meat analogues: A review. Sustainability. 2021;13(2):938. https://doi.org/10.3390/su13020938
22. Wang T, Kaur L, Furuhata Y, Aoyama H, Singh J. 3D printing of textured soft hybrid meat analogues. Foods. 2022;11(3):478. https://doi.org/10.3390/foods11030478
23. Wang T, Kaur L, Beniwal AS, Furuhata Y, Aoyama H, *et al*. Physico-chemical and textural properties of 3D printed plant-based and hybrid soft meat analogs. Plant Foods for Human Nutrition. 2023;78:375–382. https://doi.org/10.1007/s11130-023-01068-4
24. Golovin SN, Kirichenko EYu, Khanukaev MM, Logvinov AK. 3D bioprinting of hybrid cultured meat from rabbit cells and sunflower protein. Foods and Raw Materials. 2026;14(1):52–60. https://doi.org/10.21603/ 2308-4057-2026-1-659
25. Webb D, Li Y, Alavi S. Chemical and physicochemical features of common plant proteins and their extrudates for use in plant-based meat. Trends in Food Science & Technology. 2023;131:129–138. https://doi.org/10.1016/j.tifs.2022.11.006
26. Bakhsh A, Lee SJ, Lee EY, Hwang YH, Joo ST. Evaluation of rheological and sensory characteristics of plant-based meat analog with comparison to beef and pork. Food Science of Animal Resources. 2021;41(6):983–996. https://doi.org/10.5851/kosfa.2021.e50

27. Smetana S, Larki NA, Pernutz C, Franke K, Bindrich U, *et al*. Structure design of insect-based meat analogs with high-moisture extrusion. Journal of Food Engineering. 2018;229:83–85. https://doi.org/10.1016/j.jfoodeng.2017.06.035
28. Stanišić N, Delić N, Cekić B, Stojiljković N, Gogić M, *et al*. Current processing technologies and challenges in hybrid meat production. 2025;13(9):2853. https://doi.org/10.3390/pr13092853
29. Curtain F, Grafenauer S. Plant-based meat substitutes in the flexitarian age: An audit of products on supermarket shelves. Nutrients. 2019;11(11):2603. https://doi.org/10.3390/nu11112603
30. Willett W, Rockström J, Loken B, Springmann M, Lang T, *et al*. Food in the anthropocene: The EAT–Lancet commission on healthy diets from sustainable food systems. The Lancet. 2019;393(10170):447–492. https://doi.org/10.1016/S0140-6736(18)31788-4
31. Driessen C, Sexton AE, Stephens N. Twenty years of growing cultured meat: A commentary. In: Vandenbosch M, Lymbery P, editors. Cultivated meat to secure our future: Hope for animals, food security, and the environment. NY: Lantern Publishing & Media; 2023.
32. Zhang R, Farouk MM, Realini CE, Thum C. Hybridization in meat-based dual protein foods: Mechanisms, challenges, and consumer insights. Comprehensive Reviews in Food Science and Food Safety. 2025;24(4):e70216. https://doi.org/10.1111/1541-4337.70216
33. Karwowska M, Skwarek P, Solska E, Nowaczyk A, Goławski A, *et al*. Safety, sensory quality and nutritional value of hybrid meat products made from Turkey meat and red beans preserved with a bioprotective culture. Molecules. 2025;30(3):691. https://doi.org/10.3390/molecules30030691
34. Harnack L, Mork S, Valluri S, Weber C, Schmitz K, *et al*. Nutrient composition of a selection of plant-based ground beef alternative products available in the United States. Journal of the Academy of Nutrition and Dietetics. 2021;121(12):2401–2408. https://doi.org/10.1016/j.jand.2021.05.002
35. De Marchi M, Costa A, Pozza M, Goi A, Manuelian C. Detailed characterization of plant-based burgers. Scientific Reports. 2021;11:2049. https://doi.org/10.1038/s41598-021-81684-9
36. Tziva M, Negro S, Kalfagianni A, Hekkert MP. Understanding the protein transition: The rise of plant-based meat substitutes. Environmental Innovation and Societal Transitions. 2020;35:217–231. https://doi.org/10.1016/j.eist.2019.09.004
37. Câmara AKFI, Ozaki MM, de Souza Paglarini C, dos Santos M, Pollonio MAR. Hybrid meat products: Using plant, fungi, and insect sources for flexitarian diets-technological, nutritional and sensory insights. In: Can ÖP, Göksel Saraç M, Aslan Türker D, editors. Food analogues: Emerging methods and challenges. Cham: Springer; 2024, pp. 245–289. https://doi.org/10.1007/978-3-031-69872-9_10
38. Boukid F, Baune MC, Terjung N, Francis A, Smetana, S. The 'meathybrid'concept: Bridging the gap between texture, taste, sustainability and nutrition. International Journal of Food Science and Technology. 2024;59(11):8645–8655. https://doi.org/10.1111/ijfs.17425
39. Alam AN, Kim CJ, Kim SH, Kumari S, Lee SY, *et al*. Trends in hybrid cultured meat manufacturing technology to improve sensory characteristics. Food Science of Animal Resources. 2024;44(1):39–50. https://doi.org/10.5851/kosfa.2023.e76
40. Szenderák J, Fróna D, Rákos M. Consumer acceptance of plant-based meat substitutes: A narrative review. Foods. 2022;11(9):1274. https://doi.org/10.3390/foods11091274
41. Baune MC, Broucke K, Ebert S, Gibis M, Weiss J, *et al*. Meat hybrids–an assessment of sensorial aspects, consumer acceptance, and nutritional properties. Frontiers in Nutrition. 2023;10:1101479. https://doi.org/10.3389/fnut.2023.1101479
42. Bonny SP, Gardner GE, Pethick DW, Hocquette JF. Artificial meat and the future of the meat industry. Animal Production Science. 2017;57(11):2216–2223. https://doi.org/10.1071/AN17307
43. Lanz M, Hartmann C, Egan P, Siegrist M. Consumer acceptance of cultured, plant-based, 3D-printed meat and fish alternatives. Future Foods. 2024;9:100297. https://doi.org/10.1016/j.fufo.2024.100297
44. Hadi J, Brightwell G. Safety of alternative proteins: Technological, environmental and regulatory aspects of cultured meat, plant-based meat, insect protein and single-cell protein. Foods. 2021;10(6):1226. https://doi.org/10.3390/foods10061226
45. Bogueva D, McClements DJ. Safety and nutritional risks associated with plant-based meat alternatives. Sustainability. 2023;15(19):14336. https://doi.org/10.3390/su151914336
46. Zandonadi RP, Ramos MC, Elias FTS, Guimarães NS. Global insights into cultured meat: Uncovering production processes, potential hazards, regulatory frameworks, and key challenges – a scoping review. Foods. 2025;14(1):129. https://doi.org/10.3390/foods14010129
47. Bakhsh A, Kim B, Ishamri I, Choi S, Li X, *et al*. Cell-Based Meat Safety and Regulatory Approaches: A Comprehensive Review. Food Science of Animal Resources. 2025;45(1):145–164. https://doi.org/10.5851/kosfa.2024.e122

48. Young JF, Young NW. Viewpoint: Could cultivated meat's real route to mainstream markets be as hybrid food – why this makes sense? International Journal of Food Science and Technology. 2024;59(7):4446–4450. https://doi.org/10.1111/ijfs.17190
49. Salgaonkar K, Nolden AA. Exploring consumer preferences and challenges in hybrid meat products: A conjoint analysis of hotdogs. Foods. 2024;13(10):1460. https://doi.org/10.3390/foods13101460
50. Kaplan DL, McClements DJ. Hybrid alternative protein-based foods: Designing a healthier and more sustainable food supply. Frontiers in Science. 2025;3:1599300. https://doi.org/10.3389/fsci.2025.1599300
51. Covaciu FD, Feher I, Cristea G, Dehelean A. Nutritional quality and safety assessment of pork meat cuts from Romania: Fatty acids and elemental profile. Foods. 2024;13(5):804. https://doi.org/10.3390/foods13050804
52. Mercês ZC, Salvadori NM, Evangelista SM, Cochlar TB, Rios AO, *et al*. Hybrid and plant-based burgers: Trends, challenges, and physicochemical and sensory qualities. Foods. 2024;13(23):3855. https://doi.org/10.3390/foods13233855
53. Boldt LJ, Hobbs JE, Lloyd-Smith P, Yang Y. Beyond labels: Exploring consumer preferences for plant-based meat labeling policies. Applied Economic Perspectives and Policy. 2025;48(1):123–136. https://doi.org/10.1002/aepp.70013

Additional information about the authors

Nandana R ORCID 0009-0002-2486-6127
Radhalakshmi V ORCID 0000-0003-1844-1800
Linu M Salim ORCID 0009-0004-9315-8938
Jismy K J ORCID 0009-0003-2434-9987
Anooja Thomas
Jisha M S ORCID 0000-0002-1788-3802
Sajad Rehman ORCID 0009-0009-3234-2404

Foods and Raw Materials. 2027;15(2)

ISSN 2308-4057 (Print)
ISSN 2310-9599 (Online)

Research Article
Open Access

Available online at http://jfrm.ru/en
https://doi.org/10.21603/2308-4057-2027-2-722
https://elibrary.ru/FAKBDB

Antioxidative and anticataractogenic effects of *Annona muricata* leaf extracts on sodium selenite-induced cataract in rat pups

Nkechi U. Maduagwu[1], Obinna A. Ikebunwa[2,*], Chukwuebuka R. Maduagwu[3], Marachi S. Ajunwa[1], Kelechi V. Stephen[3], Nnamdi H. Nnubia[4], Stephen C. Ebiringa[5], Chigoziri A. Amugo[2], Christiana N. Chibuzo[2], Ndukwe C. Kalu[6], Mariam F. Sh. Nasralla[6], Precious C. Ugwuoke[7], Prince O. Chukwueze[6], Ujunwa G. Igboeli[8], Esther Ejimofor[9], Cynthia Yakubu[10], Kelechi I. Ezenagu[8], Chigozie C. Mbiamnozie[3], Cynthia A. Igwe[11], Ellis E. Momoh[12], Chinecherem S. Onah[2], Amazing Ikpo[13]

[1] University of Port Harcourt, Port Harcourt, Nigeria
[2] University of Nigeria, Nsukka, Nigeria
[3] Imo State University, Owerri, Nigeria
[4] Immaculate Comprehensive Secondary School, Omoku, Nigeria
[5] Nnamdi Azikiwe University, Awka, Nigeria
[6] Sechenov University, Moscow, Russia
[7] Federal Polytechnic Oko, Oko, Nigeria
[8] Nnamdi Azikiwe University, Awka, Nigeria
[9] Ebonyi State University, Abakaliki, Nigeria
[10] Africa University, Mutare, Zimbabwe
[11] School of Medical Laboratory Technicians, Nsukka, Nigeria
[12] Ambrose Alli University, Ekpoma, Nigeria
[13] Majac International School, Kaduna, Nigeria

* e-mail: Ikebunwaobinna@gmail.com

Received 02.07.2025; Revised 01.12.2025; Accepted 03.02.2026; Published online 29.09.2026

Abstract:
Oxidative stress induces lens opacity. Extracts of *Annona muricata* Linn., also known as graviola or soursop, are known for their potential anti-oxidant and curative efficacy. This study focused on the antioxidative and anticataractogenic effects of methanol and aqueous leaf extracts of *A. muricata* on sodium selenite-induced cataract in rat pups.

The study involved 55 Wistar suckling pups randomly split into 11 groups. Group 1 (normal control) received distilled water. The other groups received a single subcutaneous injection of sodium selenite (30 μmol/kg body weight) to induce oxidative stress in pups on life day 10. Additionally, Group 2 (test control, cataract-untreated) received distilled water, Group 3 (positive control) received vitamin C, Groups 4–7 received 100–250 mg/kg body weight of methanol extract, respectively, and Groups 8–11 received 100–250 mg/kg body weight of aqueous extract, respectively, for 21 days.

Compared to the test control, malondialdehyde levels were significantly lower in the treated groups, while glutathione peroxidase activity was significantly higher in the aqueous-extract groups ($p < 0.05$). No significant differences were observed in plasma catalase activity across the groups. The rat pups treated with ascorbic acid and both extracts revealed remarkable reduction in the cataractous state.

The methanol and aqueous extracts of *A. muricata* demonstrated dose-dependent antioxidative and anticataractogenic effects on cataractous rat pups, which makes graviola a promising source of new anticataract drugs.

Keywords: *Annona muricata*, graviola, soursop, cataract, lens opacity, oxidative stress, anticataract, methanol extract, aqueous extract

Please cite this article in press as: Maduagwu NU, Ikebunwa OA, Maduagwu CR, Ajunwa MS, Stephen KV, *et al.* Antioxidative and anticataractogenic effects of *Annona muricata* leaf extracts on sodium selenite-induced cataract in rat pups. Foods and Raw Materials. 2027;15(2):449–459. https://doi.org/10.21603/2308-4057-2027-2-722

Copyright © 2026, Maduagwu *et al.* This is an open access article distributed under the terms of the Creative Commons Attribution 4.0 International License (https://creativecommons.org/licenses/by/4.0/), allowing third parties to copy and redistribute the material in any medium or format and to remix, transform, and build upon the material for any purpose, even commercially, provided the original work is properly cited and states its license.

INTRODUCTION

Globally, 285 million people are visually impaired: 39 million people are totally blind while the remaining 246 million have low vision [1]. Uncorrected refractive errors are the main cause of severe and moderate visual impairments, as indicated by the World Health Organization. Approximately 80% of global visually impaired population live in Africa and Asia, especially in the rural low-income areas with insufficient and underutilized ophthalmological facilities [2, 3]. About 28,000 new cases of visual impairment are reported daily, with cataract accounting for approximately 50% [4], which makes it the leading cause of blindness worldwide [5].

Blindness directly interferes with daily routine and imposes developmental challenges in children. In adults, it compromises gainful employment, leisure, and ability for independent living, resulting in the loss of social status and self-esteem.

Currently, the only method of cataract treatment is surgical removal. Cataract surgery means that the clouded or opaque lens is replaced with an artificial lens called intraocular lens implant, which is encapsulated in the normal lens capsule [6]. Cataract surgery has an extremely high success rate. In case of posterior capsular opacification, a second surgery is required. Posterior capsular opacification is caused by ectopic growth of remaining epithelial cells in the posterior lens capsule. It obstructs the visual axis, wrinkling the capsule and causing eventual scattering of light [6].

Cataract remains a major public health problem. Targeted therapeutic treatment requires a good understanding of its formation [7] to select appropriate models for screening potential anti-cataract agents [8].

Sodium selenite-induced cataract is one of the best models for studying the fundamental mechanism of senile, or age-related, cataracts. It helps identify optimal anti-cataract agents and assess the effect of different stressors on the lens [9]. A high dose of sodium selenite induces cataract in suckling pups of rats [10], with an accompanying increase in lenticular lipid peroxidation and the formation of H_2O_2 in the aqueous humor [11].

Oxidative stress remains a major threat to lens transparency and the redox systems. Free radical-induced oxidative damage is one of the main factors that trigger the formation of age-related cataracts. The redox state plays a significant role in the development of many liver diseases. These free radicals are neutralized in the eye lens or body cells by antioxidant enzymes, vitamins, and drugs, including traditional medicines. Some traditional medicines are strong antioxidants and offer a more affordable alternative to cataract surgery [12, 13].

According to World Health Organization, over 80% of the world's population rely on herbal medicine as a remedy [14–16], which explains why traditional medicine is gaining popularity all around the world [17]. Traditional medicine provides new approaches to modern healthcare. Many modern pharmaceuticals are actually derived from plants and plant-related products. Medicinal plants are an actively developing field of research: herbal remedies require scientific rationale in order to ensure their proper use, as well as to evaluate the possibility of them being sources of new drugs. Bioassays may prove the efficacy of plant formulations while chemical analysis makes it possible to identify their active components [18–22].

Medicinal plants help against infectious diseases due to alkaloids, flavonoids, tannins, and phenolic compounds, all of which exert different physiological actions on the human body [23].

Annona muricata Linn. is commonly referred to as graviola or soursop. Its extracts are known for their potential medicinal efficacy; all its aerial parts are used as natural remedies [24].

The *Annonaceae* family includes over 130 genera and 2,300 species. *A. muricata*, also known as soursop [25, 26], contains a variety of pharmacologically active chemicals. It is farmed in tropical and subtropical regions like Southeast Asia, South America, and African rainforests. It produces edible fruit all year round, which makes it a popular traditional remedy for bacterial infections, skin conditions, respiratory disorders, fever, diabetes, high blood pressure, and cancer [27]. *A. muricata* possesses reliable antioxidant properties [28–31]. Nam *et al.* [30] reported a strong positive correlation between the antioxidant activity and the total phenolic content in *A. muricata*. Its extracts are rich in various phytochemicals, including rutin, epicatechin, ferulic acid, and *p*-coumaric acid, which makes graviola a potentially useful source of substances with antioxidant effects [30]. Muthu & Durairaj [31] described the hydroalcoholic extract of *A. muricata* leaves as a potent antioxidant nutraceutical with a radical scavenging activity strong enough to prevent human diseases caused by oxidative stress.

Cataract can be caused by age, heredity, enzyme defects, ultraviolet light exposure, trauma, diabetes, smoking, heavy metal toxicity, etc., which makes it a major cause of blindness and visual impairment [32]. Cataract surgery being the only treatment option, a synthesis of phytomedicine with conventional medicine seems to be a promising and affordable alternative. This study evaluated the antioxidative and anticataractogenic effects of methanol and aqueous extract of *A. muricata* on sodium selenite-induced cataract in Wistar suckling pups.

STUDY OBJECTS AND METHODS

Care and management of laboratory animals. The experiment featured 55 healthy Wistar suckling pups weighing between 4.7 and 12.8 g. The animals were bred in the animal house of the Department of Biochemistry, University of Port Harcourt, Rivers State, Nigeria. They were kept with their mothers to suckle, and their mothers were provided with water *ad libitum*. The animals were kept in well-ventilated cages under standard conditions of temperature and humidity. Ethical approval was obtained from the University of Port Harcourt Research Ethics Committee (Reference no. UPH/CEREMAD/REC/MM79/085). The research followed the ARRIVE guidance (Animal Research: Reporting of *In-Vivo* Experiments).

Collecting the leaves of *Annona muricata*. *Annona muricata* Linn. is locally known as graviola, or soursop in English and *shawshopu* in the Igbo language of eastern Nigeria. Fresh leaves were harvested from the field of the University of Port Harcourt, River State, between February and March 2024. The leaves were identified and authenticated as *A. muricata* (*Annonaceae* family) at the Plant Science and Biotechnology Department, University of Port Harcourt, River State, Nigeria. A voucher specimen (UPH/V/1191) of the plant was deposited in the Herbarium of Plant Science and Biotechnology, University of Port Harcourt. The leaves were washed, chopped, and air-dried at room temperature for four weeks. After that, they were ground into powder using an electric grinder (Sorex SHB-520, Korea) at the Pharmaceutical Sciences Department, University of Port Harcourt. The resulting powder was stored and used for the study.

Phytochemical screening. *Qualitative phytochemical analysis.* *Alkaloids*. The test for alkaloids followed the method developed by Sofowora [33]. Briefly, a portion (0.5 g) of the leaf powder was stirred with 5 mL of 5% HCl in a steam bath and filtered. An aliquot (1 mL) of the filtrate obtained was treated with five drops of Mayer's reagent. Another aliquot (1 mL) of the filtrate was treated with Dragendorff's reagent. The third aliquot (1 mL) was also treated with three drops of picric acid. The nature and color of the resulting precipitates were observed, noted, and recorded.

Tannins. The test for tannins was a ferric chloride test as described by Trease & Evans [34]. Another portion (0.5 g) of the leaf powder was stirred with 10 mL of distilled water and filtered. After adding three drops of 5% $FeCl_3$, we described the nature and color of the resulting precipitates.

Flavonoids. The test for flavonoids followed the protocol for the Shinoda test, as described by Trease & Evans [34]. A piece of magnesium metal was added to 5 g of leaf powder, and then 2–4 drops of concentrated hydrochloric acid were added to dissolve the powder and initiate the reaction. The nature and color of the resulting precipitates were observed, noted, and recorded.

Saponins. The presence of saponin was determined by the frothing test [3]. A portion (0.5 g) of leaf powder was placed in a test tube, which was filled with 10 mL of distilled water, shaken vigorously for 30 s, and allowed to settle for 10 min.

Cardiac glycosides. The presence of cardiac glycosides was determined by the Keller-Killiani test [33]. A portion (5 g) of the leaf powder was treated with 1 mL of $FeCl_3$ reagent. The solution and precipitates were described after adding concentrated H_2SO_4 (2–4 drops).

Phenols. The ferric chloride test involved a portion (5 g) of the leaf powder put in 5 mL of distilled water, stirred in water bath, and filtered. After adding 1–2 drops of 1% neutral $FeCl_3$ solution, the nature and color of the resultant solutions and precipitates were described. Then, sodium carbonate was added, and the observation was repeated.

Quantitative analysis of the phytochemical content. *Alkaloids*. The samples were extracted with methanol to be treated with H_2SO_4 and NaOH, and then re-extracted with chloroform. After that, we placed 20 g of the leaf powder in the macerator jar and poured in aliquot (200 mL) of absolute methanol. After 20 min of maceration and regular agitation, the mix was warmed in water bath at 40°C for about 10 min to quicken the extraction process. The mix was filled into a crucible to discard the residue. The filtrate was dried in water bath at 50°C to obtain methanol extract. Aliquot (10 mL) of H_2SO_4 was introduced into the methanol extract and stirred. The resulting mix was boiled in water bath at 60°C for about 10 min and filled into a beaker to remove the residue. After adding concentrated NaOH into the filtrate dropwise, we used litmus paper to detect when the solution became alkaline. After that, the mix was poured into the separating flask and partitioned three times with chloroform (10 mL) for exhaustive extraction of crude alkaloids. At each interval, the mix was agitated for 2–5 min. The chloroform fraction was collected into a crucible to remove the aqueous layer. After drying the chloroform fraction in water bath at 4°C, we obtained crude alkaloid and weighed the residue. The alkaloid, %, share was calculated as follows:

$$\text{Alkaloids} = \frac{\text{Weight, residue}}{\text{Weight, sample}} \times 100 \quad (1)$$

Phenolic compounds. Phenolics were extracted with distilled water and filtered through lead acetate before drying and weighing. Another portion (20 g) of the leaf powder was macerated with 200 mL of distilled water in a 250-mL capacity beaker. The mix was boiled in water bath at 50°C for 30 min and filtered while hot. 80 g of anhydrous lead acetate was packed on the clamped cylindrical glass column to serve as filtration bed; the column was clamped on retort stand. The filtrate was carefully poured into the column via capillary action while the phenolic compounds were complexed with lead acetate. After unpacking the content of the column into a crucible, we placed it into a hot oven at 50°C for the resulting dry substance to be weighed. The calculations phenolics, %, involved the following Eq. (2):

$$\text{Phenolics} = \frac{\text{Weight, residue}}{\text{Weight, sample}} \times 100 \quad (2)$$

Saponins. The saponin content was determined by the solvent extraction gravimetric method. A third portion (20 g) of the leaf powder was macerated with 200 mL of 20% methanol in a macerating jar. The mix was boiled in water bath for 20 min with continuous stirring at 50°C and filtered while hot into a crucible. The filtrate was reduced to 40 mL over water bath at about 70°C, transferred into a 250 mL separating flask (funnel), and clamped. After that, the mix was shaken vigorously with 20 mL of diethyl ether. The aqueous layer was collected;

the diethyl ether was filtered off and discarded. After adding an aliquot (60 mL) of *n*-butanol, we used 10 mL of 5% aqueous NaCl to wash the mix twice. The remaining solution evaporated at 50°C for 30 min to be placed in a hot oven. Using the weight of the crude saponins (the residue), we calculated the saponin content, %:

$$\text{Saponins} = \frac{\text{Weight, residue}}{\text{Weight, sample}} \times 100 \quad (3)$$

Preparing the leaf extracts. ***Methanol extract.*** A portion (600 g) of leaf powder was mashed in 500 mL of 70% methanol for 72 h at room temperature and air-pressure. After filtering the crude methanol extract, we allowed the filtrate to evaporate at reduced pressure (600 mmHg) using a vacuum rotary evaporator. It yielded 19.43 g of brown residue (methanol extract). After freeze-drying in a vacuum freezer dryer, the residue remained in a dried and tight container until needed for bioassay.

Aqueous extract. 2.5 L of distilled water with another portion (1,000 g) of leaf powder shaken occasionally at room temperature for 48 h. Its filtrate (aqueous extract) was dried in a vacuum rotary evaporator under 600 reduced pressure, providing 24.32 g of light green residue (aqueous extract). The residue was freeze-dried in a vacuum freeze dryer and stored in a dried and tight container until needed for bioassay.

Determining the lethal dose, 50% (LD_{50}). The test involved tree groups of four Wistar suckling pups. The extract was administered subcutaneously at doses of 200, 1,000, and 1,800 mg/kg body weight, respectively, to each group. The animals were observed over a period of 48 h for signs of acute toxicity. The number of deaths caused by the extract in each group within the time was noted and recorded. The LD_{50} was then calculated by a probit plot of the log of doses against percentage deaths (in probability units).

Evaluating the anticataract activity via ocular malondialdehyde assay. Sodium selenite (Sigma) was procured from a chemical shop; *L*-ascorbic acid was procured from a pharmacy in the University of Port Harcourt. They were administered orally to rat pups divided into 11 groups of five in each (Table 1). Group 1 (normal control) received distilled water. The other groups received a single subcutaneous injection of sodium selenite (30 µmol/kg body weight) on postpartum day ten. Additionally, Group 2 (test control, cataract-untreated) received distilled water, Group 3 (positive control) received vitamin C, Groups 4–7 received 100, 150, 200, and 250 mg/kg body weight of methanol extract, respectively, and Groups 8–11 received 100, 150, 200, and 250 mg/kg body weight of aqueous extract, respectively. The treatment continued for 21 days after the initiation of cataract. Cataract was observed when the pups first opened their eyes (16–20 days after birth).

Morphological examination of rat pup lenses. When the rat pups first opened their eyes (16–20 days after birth), their eye lenses were examined by an ophthalmologist from the Ophthalmology Department, University of Port Harcourt Teaching Hospital, to provide a morphological evaluation of any lenticular opacification. Prior to the examination, the pupils were dilated using topical ophthalmic solution containing 1.0% tropicamide with phenylephrine. One drop of the solution was instilled every 7 min for 1 h into each eye, with the animals being kept in a dark room and viewed. By photographing the lenses after pupil dilation, we graded them for the presence and severity of cataract. At the end of the experimental period, the rats were rapidly sacrificed by cervical dislocation. We removed the lenses in an intra-capsular manner under surgical microscopic magnification through an incision located 2 mm posterior to the limbus.

Sample collection. The animals were sacrificed by cervical dislocation under chloroform anesthesia. Blood samples were collected into heparin sample bottles and centrifuged at 3,500 rpm for 20 min. The plasma was collected and stored for the biochemical assays.

Biochemical assays. The superoxide dismutase activity was determined using the spectrophotometric method according to Misra & Fridovich [35]. The catalase activity was measured using the spectrophotometric method according to the method developed by Beers & Sizer [36]. To describe the plasma ascorbic acid concentration, we used the method reported by Robitaille & Hoffer [37] and Kim & Kim [38]. The glutathione peroxidase assay relied on the spectrophotometric method as in Rotruck *et al*. [39]. For the assay of ocular malondialdehyde concentration, we adopted the method suggested by Hunter *et al*. [40], as modified by Gutteridge & Wilkins [41].

Table 1 Experimental assay design

Groups	Treatment group	Details
Group 1	Normal control	Distilled water (no treatment)
Group 2	Negative (test) control	Sodium selenite + distilled water
Group 3	Positive control	Sodium selenite + vitamin C (100 mg/kg)
Group 4	Methanol extract 100 mg/kg	Sodium selenite + methanol extract (100 mg/kg)
Group 5	Methanol extract 150 mg/kg	Sodium selenite + methanol extract (150 mg/kg)
Group 6	Methanol extract 200 mg/kg	Sodium selenite + methanol extract (200 mg/kg)
Group 7	Methanol extract 250 mg/kg	Sodium selenite + methanol extract (250 mg/kg)
Group 8	Aqueous extract 100 mg/kg	Sodium selenite + aqueous extract (100 mg/kg)
Group 9	Aqueous extract 150 mg/kg	Sodium selenite + aqueous extract (150 mg/kg)
Group 10	Aqueous extract 200 mg/kg	Sodium selenite + aqueous extract (200 mg/kg)
Group 11	Aqueous extract 250 mg/kg	Sodium selenite + aqueous extract (250 mg/kg)

Sodium selenite was introduced at amount of 30 µmol/kg body weight

Histopathologic evaluation. The lenses were fixed in a solution of 10% formaldehyde for histology. The tissues were fixed, sectioned, read, and interpreted at the Anatomy Laboratory, Department of Basic Medical Sciences, University of Port Harcourt, Rivers State, Nigeria. The tissues were embedded in paraffin wax to obtain sections of 4–6 μm. The multiple sectioning of paraffin blocks made it possible to obtain lens sections with maximal anterior-posterior diameter cutting through the middle of the lens.

Statistical analysis. The data evaluation involved a statistical package for social sciences, Version 23.0. A One-way ANOVA test revealed the differences between the means and the standard deviations; the LSD test was used to compare the means. The *p*-values below 0.05 were considered significant. The LD_{50} determination relied on the probit-log analysis as described by Finney [42]. All the graphs were prepared with the Excel 2010 package.

RESULTS AND DISCUSSION

Phytochemical composition of *Annona muricata* Linn. leaf powder. Tables 2 and 3 illustrate the phytochemical composition of the *A. muricata* leaves.

The phytochemical screening of the leaf powder showed the presence of alkaloids, tannins, flavonoids, saponins, and phenolics (Tables 2 and 3). These compounds are known for their pharmacological activities. For example, papaverine is a vasodilator used to treat gastrointestinal spasms, bile ducts, and urethra [43, 44], as well as erectile dysfunction [45]. Morphine is converted to codeine, which is used as a cough suppressant, analgesic, hypnotic, and antidiarrheal agent [46]. Saponins possess a broad range of expectorant, anti-inflammatory, vasoprotective, hypocholestrolemic, hypoglycemic, antiparasitic, antioxidant, anticancer, and antiprotozoal activities [47].

Phenolics exert antioxidant, anticarcinogenic, antimutagenic, anti-inflammatory, vasodilatory, and antithrombotic activities [48]. The pharmacological range of flavonoids includes antioxidant, anti-inflammatory, antimicrobial, antitumor, anti-ulcer, and hepatoprotective effects [47]. Tannins have been reported to possess anticancer, antidiarrheal, anti-asthmatic, cardioprotective, antidiabetic, anticataractogenic, anti-inflammatory, and hepatoprotective properties [47]. Al-Sayed & El-Naga [49] reported the gastroprotective potential of ellagitannin, a tannin derivative. These pharmacological activities may be responsible for the biological effects of the *A. muricata* extracts in this study.

Indices of lethality. Within 48 h, the aqueous extract at 1,000 and 1,800 mg/kg produced 25 and 100% mortality, respectively. Figure 1 shows the probit plot of death frequency against various extract doses. This regression plot resulted in the following Eq. (4):

$$\text{Probit} = -39.8579869786464 + \\ +14.7293289928821 \times \log(\text{dose}) \quad (4)$$

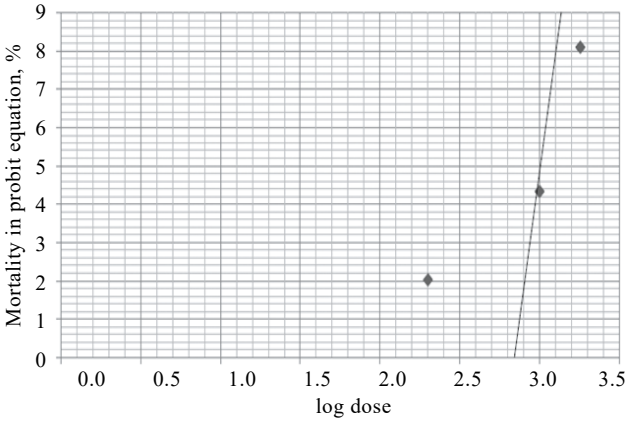
Eq. (4) provided the indices of lethality of the extract (Table 4). The oral LD_{50} of the extract was 1,110.42 mg/kg, while its LD_{01} was 771.44 mg/kg, and the zero-mortality dose was 696.85 mg/kg.

Table 2 Qualitative phytochemical tests of *Annona muricata* Linn. leaf powder

Constituent	Test	Observation	Inference
Alkaloids	Dragendorff's test	Pink coloration	Positive
	Meyer's test	Yellow precipitate	Positive
	Picric acid	Yellow precipitate	Positive
Tannins	Ferric chloride test	Brown color	Positive
Saponins	Froth test	Slightly foamy	Positive
Flavonoids	Shinoda test	Dark orange color	Positive
Cardiac glycosides	Keller-Killiani test	Greenish blue	Negative
Phenols	Ferric chloride test	A pale green color	Positive

Table 3 Quantitative phytochemical tests of *Annona muricata* Linn. leaf powder

Component	Composition, mg/g
Alkaloids	17.4 ± 0.3
Saponins	29.1 ± 0.2
Phenolic compounds	32.5 ± 1.5



The grids were left to enable easy understanding of the extrapolations

Figure 1 Death frequency probit plot for various *Annona muricata* Linn. extract doses

Table 4 Lethality indices of *Annona muricata* Linn. extract

Index	Value, mg/kg
LD_{50}	1,110.42 ± 21.30
LD_{01}	771.44 ± 15.80
Highest non-lethal dose	696.85 ± 12.30

Anti-oxidative stress activity. Table 5 and Fig. 2 show the effects of methanol and aqueous leaf extracts of *A. muricata* on plasma and ocular markers of oxidative stress in selenite-treated rats. The plasma glutathione peroxidase activity of the test control, the normal control, the positive control, and all the methanol extracts were significantly ($p < 0.05$) lower than the aqueous extracts, but not significantly different from one another.

The activity of plasma superoxide dismutase in the plasma of the test control group was significantly ($p < 0.05$) lower than those of the normal control, the methanol extracts 200 and 250 mg/kg, the aqueous extract 100, 150, and 200 mg/kg, but was not significantly different from the others.

The superoxide dismutase of the normal control and the methanol extract 250 mg/kg were significantly higher ($p < 0.05$) than the test control, the positive control, the methanol extracts 100 and 150 mg/kg, as well as the aqueous extract 250 mg/kg, but not significantly different from one another or the remaining groups. The reference treatment group was significantly lower ($p < 0.05$) than those of the normal control, the test control, and the methanol extract 250 mg/kg, but not significantly different from the others.

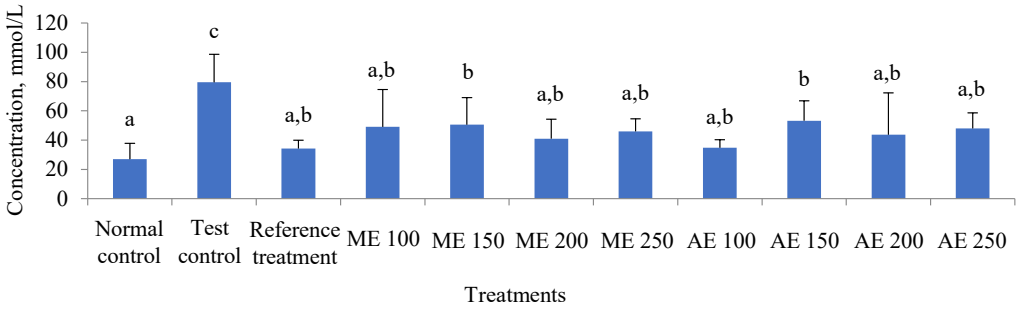
We detected no significant differences in the plasma catalase activities across the groups. The plasma ascorbic acid level of the test control group was significantly lower ($p < 0.05$) than that of the normal control, but not significantly different from the others. The plasma ascorbic acid level of the normal control was significantly higher ($p < 0.05$) than those of the test control and the aqueous extracts 100, 150, and 250 mg/kg, but not significantly different from the others. Those of the reference treatment and methanol extract 100 mg/kg were significantly higher ($p < 0.05$) than those of the aqueous extracts 150 and 250 mg/kg, but not significantly different from the others.

The plasma malondialdehyde levels of the test control group was significantly higher ($p < 0.05$) than all the other groups. That of the normal control group was significantly lower ($p < 0.05$) than the test control, the methanol extract 150 mg/kg, and the aqueous extract 150 mg/kg, but not significantly different from the others. The plasma malondialdehyde levels of the reference treatment, the methanol extract 100 mg/kg, the methanol extract 200 mg/kg, the methanol extract 250 mg/kg, the aqueous extract 100 mg/kg, the aqueous extract 200 mg/kg, and the aqueous extract 250 mg/kg were

Table 5 Effect of methanol and aqueous *Annona muricata* Linn. leaf extracts on oxidative stress markers

Groups	Treatment	Superoxide dismutase activity, $\times 10^{-2}$, U/L	Glutathione peroxidase activity, $\times 10^{-2}$, U/L	Catalase activity, $\times 10^{-8}$, U/L	Ascorbic acid concentration, mmol/L
1	Normal control	3.30 ± 0.29^{a}	6.38 ± 0.50^{a}	10.20 ± 6.39^{a}	4.30 ± 1.52^{a}
2	Negative (test) control	1.83 ± 0.60^{c}	5.93 ± 0.81^{a}	4.43 ± 2.44^{a}	$2.29 \pm 0.45^{b,c}$
3	Positive control	$2.53 \pm 0.85^{b,c,d,e}$	6.28 ± 0.54^{a}	10.10 ± 11.29^{a}	$4.20 \pm 0.89^{a,b}$
4	Methanol extract 100 mg/kg	$2.25 \pm 0.57^{b,c,e}$	5.38 ± 0.84^{a}	5.15 ± 3.41^{a}	$4.06 \pm 2.81^{a,b}$
5	Methanol extract 150 mg/kg	$2.13 \pm 0.41^{b,c}$	5.83 ± 0.15a	6.43 ± 3.55^{a}	$2.83 \pm 0.80^{a,b,c}$
6	Methanol extract 200 mg/kg	$3.20 \pm 0.28^{a,d}$	5.85 ± 1.14^{a}	10.10 ± 9.98^{a}	$3.28 \pm 1.41^{a,b,c}$
7	Methanol extract 250 mg/kg	3.45 ± 0.90^{a}	6.43 ± 0.92^{a}	6.80 ± 1.92^{a}	$3.45 \pm 0.64^{a,b,c}$
8	Aqueous extract 100 mg/kg	$2.95 \pm 0.13^{a,d,e}$	11.95 ± 1.51^{b}	2.98 ± 0.90^{a}	$2.45 \pm 0.34^{b,c}$
9	Aqueous extract 150 mg/kg	$2.80 \pm 0.28^{a,b,d,e}$	12.00 ± 0.00^{b}	8.85 ± 4.79^{a}	2.20 ± 0.36^{c}
10	Aqueous extract 200 mg/kg	$3.00 \pm 0.30^{a,d}$	12.33 ± 0.58^{b}	3.67 ± 1.05^{a}	$2.73 \pm 0.91^{a,b,c}$
11	Aqueous extract 250 mg/kg	$2.17 \pm 0.15^{b,c}$	12.33 ± 0.58^{b}	6.47 ± 0.61^{a}	2.13 ± 0.67^{c}

Values are mean ± standard deviation, n = 5 animals per group. Values on the same column with different superscript letters are significantly different at $p < 0.05$



ME – methanol extract; AE – aqueous extract; Each bar represents the mean ± SD for each group of rat pups, n = 5. Bars with the different letters are significantly different at $p < 0.05$

Figure 2 Effect of methanol and aqueous leaf extracts of *Annona muricata* Linn. on malondialdehyde concentration in rat pup lenses

not significantly different from each other, the normal control, the methanol extract 150 mg/kg, and the aqueous extract 150 mg/kg, but were significantly ($p < 0.05$) lower than the test control.

Oxidative stress occurs when the rate of production of free radicals is higher than the body's ability to counteract or detoxify their harmful effects through neutralization by antioxidants [50, 51]. Oxidative stress was implicated in the pathogenesis of cataracts in lens epithelial cells [52–54]. High tissue and blood levels of thiobarbituric acid-reactive substances (mainly malondialdehyde) are very reliable indicators of oxidative stress and lipid peroxidation [55]. In this study, the extracts improved the glutathione peroxidase (only the aqueous extract) and superoxide dismutase activities of the rat pups in the experimental groups. They also had lower malondialdehyde levels but demonstrated no significant difference in catalase activities and ascorbic acid levels, compared to the test control animals.

The levels of malondialdehyde in the treated animals clearly indicated that the extracts protected them against oxidative stress. This antioxidant protective effect may have been mediated by the saponin and phenolic compounds, e.g., flavonoids, in the leaves. These compounds are reputed to possess antioxidant properties [56–60].

Histopathological studies for ocular lens injury assessment. Figures 3–13 show photomicrographs of the ocular lenses of normal and selenite-treated rat pups on day 21 post-treatment with the extracts.

The lens of a normal control rat pup (Fig. 3) showed healthy capsule, epithelium, and lens fibers. The lens photomicrograph of a test control rat pup (Fig. 4) showed cuboidal lens epithelium, capsule, and compact fibers. The cortical lens contained eosinophilic globular degeneration. The pale and swollen fibers had two prominent clefts (artefactual). The lens photomicrograph of a cataractous rat treated with 100 mg/kg body weight of ascorbic acid (Fig. 5) showed capsule, epithelium, and lens fibers. The paleness was minimal. Figure 6 shows the photomicrograph of a cataract lens that belonged to a rat pup treated with methanol *A. muricata* extract at a dose of 100 mg/kg body weight. The lens fibers were pale, with cortical regeneration. The lens of a cataract rat pup treated with 150 mg/kg methanol *A. muricata* extract showed pale areas in the lens fiber with signs of regeneration in the cortical part (Fig. 7). The cataract lens treated with 200 mg/kg of methanol *A. muricata* extract was less pale. The photomicrograph demonstrated a resolving cataract (Fig. 8). Figure 9 shows the ciliary body, iris, and lens of a cataractous rat pup administered with 200 mg/kg of methanol *A. muricata* extract. The capsule, epithelium, and lens fibers demonstrated less paleness, indicating a resolving cataract. The lens tissue of a cataractous rat pup treated with 100 mg/kg of aqueous *A. muricata* extract (Fig. 10) showed patchy areas of pale fiber, indicating a resolving cataract. The cataract lens tissue of an experimental rat pup treated with 150 mg/kg body weight of aqueous *A. muricata* extract (Fig. 11) also showed patchy areas of paleness, with slightly swollen fibers. The result indicated the areas of healing cataract. Figure 12

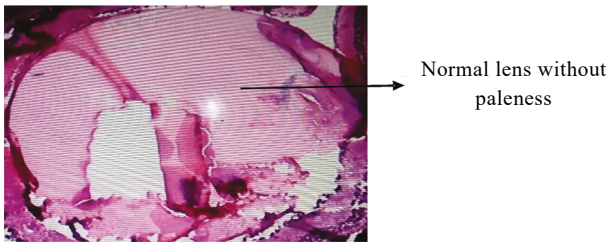


Figure 3 Normal control: Ciliary body, iris and lens (hematoxylin and eosin stain, 5× magnification)

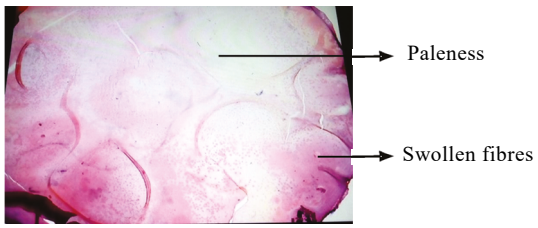


Figure 4 Negative control: Cataract lens (hematoxylin and eosin stain, 5× magnification)

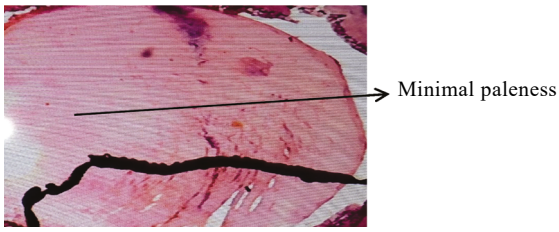


Figure 5 Positive control: Cataract lens (hematoxylin and eosin stain, 5× magnification)

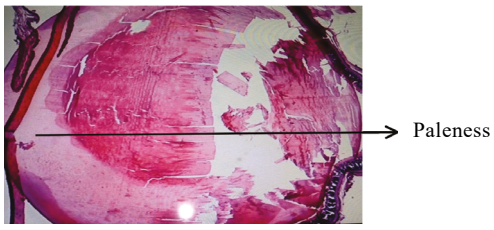


Figure 6 Methanol extract 100 mg/kg: Cataract lens (hematoxylin and eosin stain, 5× magnification)

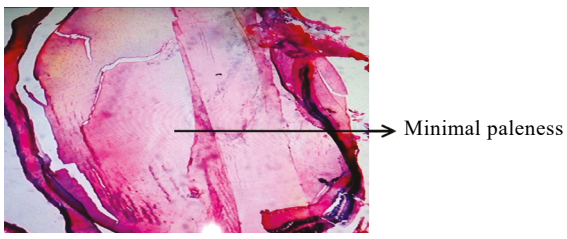


Figure 7 Methanol extract 150 mg/kg: Cataract lens (hematoxylin and eosin stain, 5× magnification)

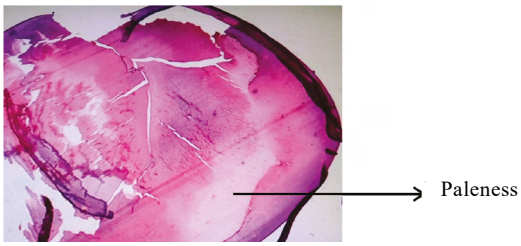


Figure 8 Methanol extract 200 mg/kg: Cataract lens (hematoxylin and eosin stain, 5× magnification)

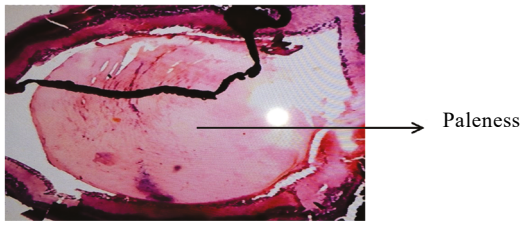


Figure 9 Methanol extract 250 mg/kg: Cataract lens (hematoxylin and eosin stain, 5× magnification)

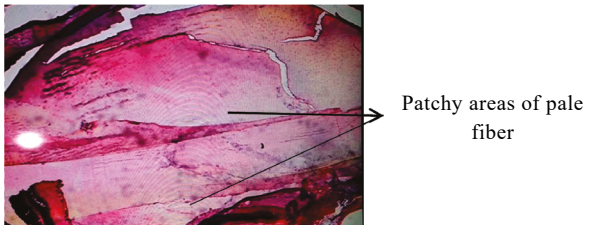


Figure 10 Aqueous extract 100 mg/kg: Cataract lens (hematoxylin and eosin stain, 5× magnification)

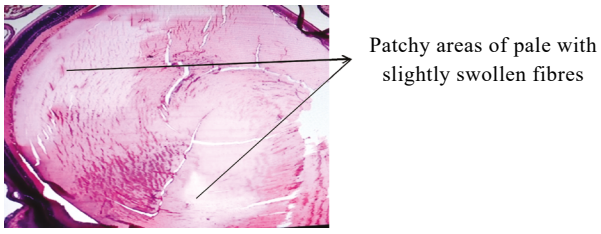


Figure 11 Aqueous extract 150 mg/kg: Cataract lens (hematoxylin and eosin stain, 5× magnification)

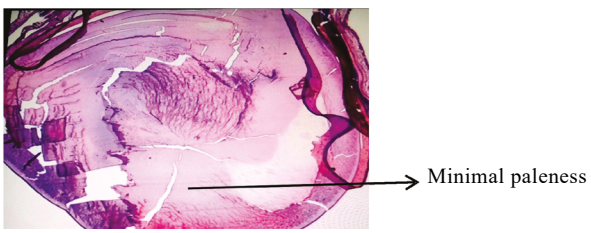


Figure 12 Aqueous extract 200 mg/kg: Cataract lens (hematoxylin and eosin stain, 5× magnification)

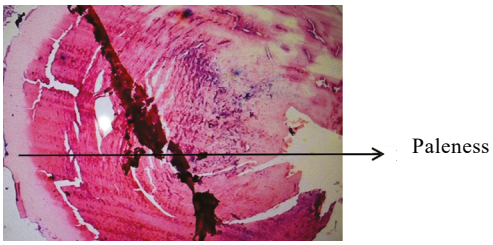


Figure 13 Aqueous extract 250 mg/kg: Cataract lens (hematoxylin and eosin stain, 5× magnification)

illustrates the lens epithelium, fiber, and capsule of an experimental rat pup administered with 200 mg/kg body weight of aqueous *A. muricata* extract. In this case, the lens showed a minimal of paleness and was very close to a healthy lens. The result indicated a resolving cataract. Figure 13 shows the capsule, epithelium, and lens fiber that belonged to a cataractous rat pulp treated with 250 mg/kg body weight of aqueous *A. muricata* extract. The area immediately beneath the lens epithelium showed paleness, but the result indicated a generally resolving cataract.

The histopathology of the ocular lens revealed remarkable reduction in the cataractous state in the rat pups treated with ascorbic acid and both extracts. The results indicated a dose-dependent regeneration. In tandem with the malondialdehyde level, this effect indicated a possible amelioration of lipid peroxidation by the extracts, which led to anticataract results.

The anticataract activity of the *A. muricata* extracts may be due to tannins, flavonoids, and phenolics, all of which are known to have antioxidant activities [47]. For instance, tannins were reported to possess reliable anticataractogenic and hepatoprotective properties [47].

CONCLUSION

The aqueous extract of *Annona muricata* Linn. leaves reduced oxidative stress in sodium selenite-induced cataract in rat pups, as indicated by reduced malondialdehyde levels and increased glutathione peroxidase activity. However, no significant differences were observed in plasma catalase activity across the experimental groups. The findings suggest that *A. muricata* leaf extracts may have antioxidative and cataract-ameliorating effects in this experimental model, although further studies are required to clarify the underlying mechanisms and therapeutic potential.

CONTRIBUTION

All the authors were involved in conducting the research and writing the manuscript. The authors declare that the work presented in this article is original and that any liability for claims relating to the content of this article will be borne by them.

CONFLICT OF INTEREST

The authors declared no conflict of interest regarding the publication of this article.

REFERENCES

1. Okoye O, Eze BI, Chuka-Okosa CM. Eliminating the barriers to uptake of cataract surgery in a resource-poor setting: A focus on direct surgical cost. Nigerian Journal of Clinical Practice. 2015;18(3):333–336. https://doi.org/10.4103/1119-3077.151768
2. Chen J, Yang C, Zheng W, Li Z, Huang Y, *et al*. Global, regional, and national epidemiology of visual impairment in working-age individuals, 1990–2019. JAMA Ophthalmology. 2024;142(1):25–32. https://doi.org/10.1001/jamaophthalmol.2023.5617
3. Wang EY, Kong X, Wolle M, Gasquet N, Ssekasanvu J, *et al*. Global trends in blindness and vision impairment resulting from corneal opacity 1984–2020: A meta-analysis. Ophthalmology. 2023;130(8):863–871. https://doi.org/10.1016/j.ophtha.2023.03.012
4. Vision Loss Expert Group of the Global Burden of Disease Study, GBD 2019 Blindness and Vision Impairment Collaborators. Global estimates on the number of people blind or visually impaired by cataract: A meta-analysis from 2000 to 2020. Eye. 2024;38:2156–2172. https://doi.org/10.1038/s41433-024-02961-1
5. Cicinelli MV, Buchan JC, Nicholson M, Varadaraj V, Khanna RC. Cataracts. The Lancet. 2023;401(10374):377–389. https://doi.org/10.1016/S0140-6736(22)01839-6
6. Lapp T, Wacker K, Heinz C, Maier P, Eberwein P, *et al*. Cataract surgery–indications, techniques, and intraocular lens selection. Deutsches Ärzteblatt International. 2023;120(21–22):377–385. https://doi.org/10.3238/arztebl.m2023.0028
7. Petrash JM. Aging and age-related diseases of the ocular lens and vitreous body. Investigative Ophthalmology & Visual Science. 2013:54:ORSF54–ORSF59. https://doi.org/10.1167/iovs.13-12940
8. Maduagwu NU, Stephen KV, Chukwunenyenwa OJ, Ekwonu CC, Amugo CA, *et al*. The ameliorative effects of methanol and aqueous leaf-extracts of *Annona muricata* Linn, against oxidative stress on the kidney in selenite-induced cataract rat model. Journal of Pharmacy & Allied Medicine. 2025;3(2):74–88. https://doi.org/10.58985/jpam.2025.v03i02.34
9. Chen H, Zhou J. Effects of sodium selenite on oxidative damage in the liver, kidney and brain in a selenite cataract rat model. Biological Trace Element Research. 2020;197:533–543. https://doi.org/10.1007/s12011-019-02000-1
10. Choi JI, Kim J, Choung SY. Polyphenol-enriched fraction of *Vaccinium uliginosum* L. protects selenite-induced cataract formation in the lens of Sprague-Dawley rat pups. Molecular Vision. 2019;25:118–128.
11. Palazzo M, Concilio M, Ambrosone L, Rinaldi M, Tranfa F, *et al*. Effects of *Laurus nobilis* eye drop on selenite-induced cataract formation and oxidative stress-related parameters in rabbits: An experimental study. Current Eye Research. 2024;49(12):1247–1252. https://doi.org/10.1080/02713683.2024.2380440
12. Gulcin İ. Antioxidants and antioxidant methods: An updated overview. Archives of Toxicology. 2020;94:651–715. https://doi.org/10.1007/s00204-020-02689-3
13. Maduagwu NU, Maduagwu CR, Okike MC, Nnubia NH, Onah DC, *et al*. Protective effects of methanol and aqueous leaf extracts of *Annona muricata* Linn on sodium selenite-induced oxidative stress on the liver in selenite cataract rat model. Research Journal of Food and Nutrition. 2025;8(1):16–32. https://doi.org/10.22259/2637-5583.0801002
14. Aware CB, Patil DN, Suryawanshi SS, Mali PR, Rane MR, *et al*. Natural bioactive products as promising therapeutics: A review of natural product-based drug development. South African Journal of Botany. 2022;151(Part B):512–528. https://doi.org/10.1016/j.sajb.2022.05.028
15. Chaachouay N, Douira A, Zidane L. Herbal medicine used in the treatment of human diseases in the Rif, Northern Morocco. Arabian Journal for Science and Engineering. 2022;47:131–153. https://doi.org/10.1007/s13369-021-05501-1
16. Isselbacher EM, Preventza O, Black JH, Augoustides JG, Beck AW, *et al*. 2022 ACC/AHA guideline for the diagnosis and management of aortic disease: A report of the American Heart Association/American college of cardiology joint committee on clinical practice guidelines. Journal of the American College of Cardiology. 2022;80(24):e223–e393. https://doi.org/10.1016/j.jacc.2022.08.004
17. Balkrishna A, Sharma N, Srivastava D, Kukreti A, Srivastava S, *et al*. Exploring the safety, efficacy, and bioactivity of herbal medicines: Bridging traditional wisdom and modern science in healthcare. Future Integrative Medicine. 2024;3(1):35–49. http://doi.org/10.14218/FIM.2023.00086
18. Chukwu CV, Omejua CG, Onyirimba CO, Uchendu IK. Anti-oxidative potential of essential oil of *Rosmarinus officinalis* in cadmium-induced neurotoxicity on the cerebellum of adult wistar rats. Tropical Journal of Natural Product Research. 2024;8(12):9564–9570. https://doi.org/10.26538/tjnpr/v8i12.31
19. Olokodana BK, Enyi OS, Chukwu CD, Bello TO, Onuchukwu IC, *et al*. Effects of aqueous extract of *Crassocephalum rubens* (Juss. ex Jacq.) on the histoarchitecture of the testis following cisplatin-induced toxicity in adult male wistar rats. Tropical Journal of Natural Product Research. 2024;8(8):8155–8159. https://doi.org/10.26538/tjnpr/v8i8.35
20. Uchendu IK, Okoroiwu HU. Evaluation of blood oxidant/antioxidant changes and testicular toxicity after subacute exposure to cadmium in albino rats: Therapeutic effect of nigella sativa seed extracts. Combinatorial Chemistry & High Throughput Screening. 2021;24(1):79–87. http://doi.org/10.2174/1386207323666200526134923
21. Amraoui A, Djerrou Z, Ali Haimoud S, Zerouki K, Elmokli S. Antihyperlipidemic and antioxidant potential of *Olea europaea* L. leaves: An experimental study *in vivo*, *in vitro* and *in silico*. Foods and Raw Materials. 2025;13(1):35–45. https://doi.org/10.21603/2308-4057-2025-1-621

22. Uchendu IK, Ikebunwa OA, Okpagu CB. Cardiorenal protective effects of extracts of bitter leaf (*Vernonia amygdalina* L.) in animal model of metabolic syndrome. Foods and Raw Materials. 2024;12(2):264–272. https://doi. org/10.21603/2308-4057-2024-2-607
23. Saboon, Chaudhari SK, Arshad S, Amjad MS, Akhtar MS. Natural compounds extracted from medicinal plants and their applications. In: Akhtar M, Swamy M, Sinniah U, editors. Natural bio-active compounds. Singapore: Springer; 2019, pp. 193–207. https://doi.org/10.1007/978-981-13-7154-7_7
24. Chan WJJ, McLachlan AJ, Hanrahan JR, Harnett JE. The safety and tolerability of *Annona muricata* leaf extract: A systematic review. Journal of Pharmacy and Pharmacology. 2020;72(1):1–6. https://doi.org/10.1111/jphp.13182
25. Ilango S, Sahoo DK, Paital B, Kathirvel K, Gabriel JI, *et al*. A review on *Annona muricata* and its anticancer activity. Cancers. 2022;14(18):4539. https://doi.org/10.3390/cancers14184539
26. Santos IL, Rodrigues AMC, Amante ER, da Silva LH. Soursop (*Annona muricata*) properties and perspectives for integral valorization. Foods. 2023;12(7):1448. https://doi.org/10.3390/foods12071448
27. Mutakin M, Fauziati R, Fadhilah FN, Zuhrotun A, Amalia R, *et al*. Pharmacological activities of soursop (*Annona muricata* Lin.). Molecules. 2022;27(4):1201. https://doi.org/10.3390/molecules27041201
28. Hasmila I, Natsir H, Soekamto NH. Phytochemical analysis and antioxidant activity of soursop leaf extract (*Annona muricata* Linn.). Journal of physics: Conference Series. 2019;1341:032027. https://doi.org/10.1088/1742-6596/1341/3/032027
29. Lee GW, Cho YH. Antioxidant activity of leaf extract from *Annona muricata*. Review of Korea Contents Association. 2016;14(3):43–46.
30. Nam JS, Park SY, Jang HL, Rhee YH. Phenolic compounds in different parts of young *Annona muricata* cultivated in Korea and their antioxidant activity. Applied Biological Chemistry. 2017;60:535–543.
31. Muthu S, Durairaj B. Evaluation of antioxidant and free radical scavenging activity of *Annona muricata*. European Journal of Experimental Biology. 2015;5(3):39–45.
32. Gupta VB, Rajagopala M, Ravishankar B. Etiopathogenesis of cataract: An appraisal. Indian Journal of Ophthalmology. 2014;62(2):103–110. https://doi.org/10.4103/0301-4738.121141
33. Sofowora A. Research on medicinal plants and traditional medicine in Africa. Journal of Integrative and Complementary Medicine. 1996;2(3):365–372. https://doi.org/10.1089/acm.1996.2.365
34. Trease GE, Evans SM. Pharmacognosy. 15th ed. London: Bailliere Tindall; 2002, 600 p.
35. Misra HP, Fridovich I. The role of superoxide anion in the auto-oxidation of epinephrine and a single assay for superoxide dismutase. Journal of Biological Chemistry. 1972;247(10):3170–3175. https://doi.org/10.1016/S0021-9258(19)45228-9
36. Beers RF, Sizer IW. A spectrophotometric method for measuring the breakdown of hydrogen peroxide by catalase. Journal of Biological Chemistry. 1952;195(1):133–140. https://doi.org/10.1016/S0021-9258(19)50881-X
37. Robitaille L, Hoffer LJ. A simple method for plasma total vitamin C analysis suitable for routine clinical laboratory use. Nutrition Journal. 2015;15:40. https://doi.org/10.1186/s12937-016-0158-9
38. Kim Y, Kim MG. HPLC-UV method for the simultaneous determinations of ascorbic acid and dehydroascorbic acid in human plasma. Translational and Clinical Pharmacology. 2016;24(1):37–42. https://doi.org/10.12793/tcp.2016.24.1.37
39. Rotruck JT, Pope AL, Ganther HE, Swanson AB, Hafeman DG, *et al*. Selenium: Biochemical role as a component of glutathione peroxidase. Science. 1973;179(4073):588–590. https://doi.org/10.1126/science.179.4073.588
40. Hunter FE, Gebicki JM, Hoffsten PE, Weinstein J, Scott A. Swelling and lysis of rat liver mitochondria induced by ferrous ions. Journal of Biological Chemistry. 1963;238(2):828–835. https://doi.org/10.1016/S0021-9258(18)81341-2
41. Gutteridge JMC, Wilkins S. Copper-dependent hydroxyl radical damage to ascorbic acid: Formation of a thiobarbituric acid-reactive product. FEBS Letters.1982;137(2):327–330. https://doi.org/10.1016/0014-5793(82)80377-3
42. Finney DJ. Probit analysis: A statistical treatment of the sigmoid response curve. Cambridge: Cambridge University Press, 1952.
43. Ashrafi S, Alam S, Sultana A, Raj A, Emon NU, *et al*. Papaverine: A miraculous alkaloid from opium and its multimedicinal application. Molecules. 2023;28(7):3149. https://doi.org/10.3390/molecules28073149
44. Simillis C. The acute abdomen. In: Watson C, Davies J, editors. Ellis and Calne's lecture notes in general surgery. Hoboken, NJ: John Wiley & Sons; 2023, pp. 289–298. https://doi.org/10.1002/9781394322008.ch29
45. Rezaiezadeh H, Ranjbar Tavakoli M, Langarizadeh MA, Saeedi Garaghani Z, Karami-Mohajeri S. Unveiling the science behind erectile dysfunction topical therapy: Investigating transdermal papaverine as a novel treatment approach. Sexual Medicine Reviews. 2024;12(4):720–730. https://doi.org/10.1093/sxmrev/qeae059
46. Ademikanra A, Olayiwola A, Oyewole O. Introduction to opioids: A review. Biomedicine and Chemical Sciences. 2023;1(4):306–311. https://doi.org/10.48112/bcs.v1i4.303
47. Kareem O, Ali T, Dar LA, Mir SA, Rashid R, *et al*. Positive health benefits of saponins from edible legumes: Phytochemistry and pharmacology. In: Masoodi MH, Rehman MU, editors. Edible plants in health and diseases. Singapore: Springer; 2022, pp. 279–298. https://doi.org/10.1007/978-981-16-4959-2_8

48. Saleem A, Akhtar MF, Sharif A, Akhtar B, Siddique R, *et al*. Anticancer, cardio-protective and anti-inflammatory potential of natural-sources-derived phenolic acids. Molecules. 2022;27(21):7286. https://doi.org/10.3390/molecules27217286
49. Al-Sayed E, El-Naga RN. Protective role of ellagitannins from *Eucalyptus citriodora* against ethanol-induced gastric ulcer in rats: Impact on oxidative stress, inflammation and calcitonin-gene related peptide. Phytomedicine. 2015;22(1): 5–15. https://doi.org/10.1016/j.phymed.2014.10.002
50. Conti V, Corbi G, Simeon V, Russomanno G, Manzo V, *et al*. Aging-related changes in oxidative stress response of human endothelial cells. Aging Clinical and Experimental Research. 2015;27:547–553. https://doi.org/10.1007/s40520-015-0357-9
51. Zhang X, Liu B, Lal K, Liu H, Tran M, *et al*. Antioxidant system and endoplasmic reticulum stress in cataracts. Cellular and Molecular Neurobiology. 2023;43(8):4041–4058. https://doi.org/10.1007/s10571-023-01427-4
52. Hu N, Jin FY, Gao MM, Liu LJ, Wang JH, *et al*. Baicalein improves Na_2SeO_3 induced cataract by enhancing the antioxidant capacity of juvenile Sprague Dawley Rat. Journal of Ethnopharmacology. 2024;320:117433. https://doi.org/10.1016/j.jep.2023.117433
53. Liu Y, Li J, Ye Z, Ma T, Li Z. Protective effects of piceatannol against selenite-induced cataract and oxidative damage in rats. Current Eye Research. 2022;47(9):1272–1278. https://doi.org/10.1080/02713683.2022.2104320
54. Li J, Huang Y, Ma T, Liu Y, Luo Y, *et al*. Carbon monoxide releasing molecule-3 alleviates oxidative stress and apoptosis in selenite-induced cataract in rats via activating Nrf2/HO-1 pathway. Current Eye Research. 2023;48(10):919–929. https://doi.org/10.1080/02713683.2023.2232569
55. Guo Z, Ma X, Zhang RX, Yan H. Oxidative stress, epigenetic regulation and pathological processes of lens epithelial cells underlying diabetic cataract. Advances in Ophthalmology Practice and Research. 2023;3(4):180–186. https://doi.org/10.1016/j.aopr.2023.10.001
56. Brindhadevi K, Chidambaram M, Kavitha R, Govindaraj R, Chinnathambi A, *et al*. Extraction, antioxidant, and anticancer activity of saponins extracted from *Curcuma angustifolia*. Applied Nanoscience. 2023;13:2063–2071. https://doi.org/10.1007/s13204-021-02096-9
57. Desta KT, Yoon H, Shin MJ, Lee S, Wang X, *et al*. Assessment of phenolic content, saponin content, and antioxidant activities in gray, red, and white adzuki bean germplasm: A multivariate analysis. The Korean Journal of Crop Science. 2023;68(3):147–166. https://doi.org/10.7740/kjcs.2023.68.3.147
58. Abu OD, Iyare HE, Ogboi KU. Antioxidant property of total saponins and tannins of *Dialium guineense* stem bark in rats hearts exposed to CCl_4. Journal of Clinical Epidemiology & Toxicology. 2022;3(3):1–4. https://doi.org/10.47363/JCET/2022(3)129
59. Vittaya L, Charoendat U, Janyong S, Ui-Eng J, Leesakul N. Comparative analyses of saponin, phenolic, and flavonoid contents in various parts of *Rhizophora mucronata* and *Rhizophora apiculata* and their growth inhibition of aquatic pathogenic bacteria. Journal of Applied Pharmaceutical Science. 2022;12(11):111–121. https://doi.org/10.7324/JAPS.2022.121113
60. Kataria A, Sharma S, Dar BN. Changes in phenolic compounds, antioxidant potential and antinutritional factors of Teff (*Eragrostis tef*) during different thermal processing methods. International Journal of Food Science and Technology. 2022;57(11):6893–6902. https://doi.org/10.1111/ijfs.15210

Additional information about the authors

Nkechi U. Maduagwu ORCID 0009-0007-9910-7017
Obinna A. Ikebunwa ORCID 0009-0006-5619-5531
Chukwuebuka R. Maduagwu ORCID 0009-0006-9669-1003
Marachi S. Ajunwa ORCID 0009-0009-4953-3768
Kelechi V. Stephen ORCID 0009-0006-1894-8790
Nnamdi H. Nnubia ORCID 0009-0007-8078-5651
Stephen C. Ebiringa ORCID 0009-0004-7131-9788
Chigoziri A. Amugo ORCID 0009-0001-1201-7024
Christiana N. Chibuzo ORCID 0009-0004-2569-0148
Ndukwe C. Kalu ORCID 0000-0003-4521-1146
Mariam F. Sh. Nasralla ORCID 0009-0007-5006-9443
Precious C. Ugwuoke ORCID 0009-0007-2364-1846
Prince O. Chukwueze ORCID 0009-0001-1615-7796
Ujunwa G. Igboeli ORCID 0009-0005-3383-4671
Esther Ejimofor ORCID 0009-0000-3778-517X
Cynthia Yakubu ORCID 0009-0004-6416-8870
Kelechi I. Ezenagu ORCID 0009-0000-9044-5852
Chigozie C. Mbiamnozie ORCID 0009-0002-2598-9137
Cynthia A. Igwe ORCID 0009-0004-3302-2924
Ellis E. Momoh ORCID 0009-0006-0159-7349
Chinecherem S. Onah ORCID 0009-0003-6035-9103
Amazing Ikpo

Foods and Raw Materials. 2027;15(2)

ISSN 2308-4057 (Print)
ISSN 2310-9599 (Online)

Research Article
Open Access

Available online at http://jfrm.ru/en
https://doi.org/10.21603/2308-4057-2027-2-723
https://elibrary.ru/GGDYNO

Genomic characterization of the *Pantoea allii* strain for biotechnological applications

Elizaveta R. Faskhutdinova[1], Natalya V. Fotina[1], Arina A. Shevel[1], Andrey V. Gordienko[2], Alexey E. Tupikin[3], Gaurav Mudgal[3], Larisa M. Aksenova[5], Lyudmila K. Asyakina[1,*]

[1] Kemerovo State University, Kemerovo, Russia
[2] Azot-Agro, Kemerovo, Russia
[3] Institute of Chemical Biology and Fundamental Medicine, Novosibirsk, Russia
[4] Chandigarh University, Mohali, India
[5] All-Russian Scientific Research Institute of Confectionery Industry, Moscow, Russia

* e-mail: alk_kem@mail.ru

Received 26.02.2026; Revised 07.05.2026; Accepted 02.06.2026; Published online 29.09.2026

Abstract:
Members of the genus *Pantoea* are known for their high ecological plasticity and diverse interactions with plants, ranging from phytopathogenic to commensal, symbiotic, and growth-promoting. Some of its strains have significant biotechnological potential due to their ability to synthesize phytohormones, siderophores, and antimicrobial secondary metabolites. In this study, we aimed to conduct whole-genome sequencing of the strain *Pantoea allii* B-14727 to identify genetic determinants associated with its antagonistic activity, competitiveness, and colonizing capacity.

The strain under study was initially identified as *Pantoea vagans* B-14727 by the 16S rRNA gene and deposited at the All-Russian Collection of Industrial Microorganisms at the Kurchatov Institute National Bioresource Center (Russia). However, based on whole-genome sequencing, its species identity was revised as *P. allii*. Its DNA was extracted with a ZymoBIOMICS DNA Miniprep Kit. Genomic sequencing was performed on the MGIseq-2000 and Polyseq One platforms, with libraries prepared by using standard NEBNext and Barcode/Ligation kits. The strain's genome was annotated using Bakta software, and its taxonomic identification was performed using GTDB-Tk and the GTDB database.

The *P. allii* B-14727 genome contained NRPS-independent siderophores (aerobactin and desferrioxamine E), terpene carotenoid clusters, RiPP peptides, and a hybrid PKS/NRPS cluster similar to the biosynthetic pathway of zeamine and its derivatives. Siderophores ensure efficient iron uptake, making the strain more competitive in conditions of iron deficiency. Carotenoids exhibit antioxidant and photoprotective functions, increasing cellular resistance to abiotic stress. The hybrid zeamine cluster contributes to the synthesis of broad-spectrum peptide antibiotics with antibacterial and fungicidal activity.

The biosynthetic systems identified in *P. allii* B-14727 indicate its pronounced adaptive and competitive potential. However, the strain's non-virulent status needs to be confirmed prior to further practical applications.

Keywords: *Pantoea*, genome, zeamine, aerobactin, desferrioxamine E, carotenoids, high-throughput sequencing

Funding: The study was funded by the Russian Science Foundation (agreement No. 25-16-20076 dated 17.04.2025) as part of the scientific project "New bacterial strains of the genus *Pantoea* to increase the resistance of cereal crops to phytopathogens" (No. 25-16-20076) and also financially supported by the Ministry of Education of Kuzbass (agreement No. 01/2025 dated 10.04.2025).

Please cite this article in press as: Faskhutdinova ER, Fotina NV, Shevel AA, Gordienko AV, Tupikin AE, *et al.* Genomic characterization of the *Pantoea allii* strain for biotechnological applications. Foods and Raw Materials. 2027;15(2):460–473. https://doi.org/10.21603/2308-4057-2027-2-723

INTRODUCTION

Pantoea is a genus of phylogenetically and ecologically diverse yellow-pigmented, rod-shaped, Gram-negative bacteria belonging to the family *Erwiniaceae* [1]. The taxonomic status of its members has been unstable, with their early isolates belonging to various genera, including *Bacillus, Enterobacter, Bacterium*, *Pseudomonas*, and *Erwinia*. This variability is associated with the limitations of phenotypic and culture-dependent approaches to distinguishing closely related enterobacteria, which resulted in several competing taxonomic interpretations. Later, as more comparative phylogenet-

Copyright © 2026, Faskhutdinova *et al.* This is an open access article distributed under the terms of the Creative Commons Attribution 4.0 International License (https://creativecommons.org/licenses/by/4.0/), allowing third parties to copy and redistribute the material in any medium or format and to remix, transform, and build upon the material for any purpose, even commercially, provided the original work is properly cited and states its license.

ic data were collected and revised, a number of previously described taxa were recognized as synonymous and therefore combined into a nomenclatural species of *Pantoea agglomerans* within the genus *Pantoea* [2].

Setting the taxonomic boundaries and using molecular genetic identification criteria have contributed to a significant revision of *Pantoea* species in recent years. Phylogenetically, *Pantoea* forms a monophyletic lineage closely related to the genera *Tatumella* and *Erwinia*. It occupies a specific position in the family *Enterobacteriaceae*, adjoining a number of evolutionarily close genera [3]. According to the modern taxonomic approach, a genus may include phenotypically similar, but genetically differentiated taxa which were previously seen as belonging to several hybridization groups. In line with this approach, the genus *Pantoea* includes about 20 species [4, 5].

Members of the genus *Pantoea* are quite common in plant-associated microbial communities. They live in plant tissues and in the rhizosphere. Their pronounced colonizing ability, high competitiveness, and significant adaptability enable them to interact with a wide variety of host plants [6]. *Pantoea* bacteria have previously been described in connection with their phytopathogenic properties, namely their ability to cause gall formation, vascular wilt, soft rots and necrotic lesions in various crops.

Phytopathogenic *Pantoea* isolates induce a wide range of plant diseases that differ in development and clinical manifestations. In some cases, pathogenesis can be triggered by a number of virulence factors. They include the type III secretion system, quorum sensing, and the synthesis of exopolysaccharides involved in adhesion, biofilm formation, and modulation of interaction with the host [7]. However, other studies have demonstrated a much broader ecological role of *Pantoea* strains. In particular, they are detected in various aquatic and terrestrial ecosystems, as well as in association with insects, animals, and humans. This indicates their ecological plasticity and ability to colonize various biotopes [8–10].

In recent decades, scientists have focused on the significant biotechnological potential of the genus *Pantoea*, primarily in sustainable crop production [11–13]. Some strains have been shown to promote growth in plants by improving their mineral nutrition. In particular, they can mobilize poorly soluble phosphates, fixate nitrogen, synthesize phytohormones (including auxins), and produce siderophores, which increase iron availability in the rhizosphere [14–17]. Furthermore, *Pantoea* bacteria can improve plant resistance to abiotic stress such as drought [18].

In biotechnology, *Pantoea* species can be used as bioinoculants and biocontrol agents. Certain strains exhibit antagonistic activity against phytopathogenic microorganisms and activate plant innate immunity. Research shows that the epiphytic colonization of plants by *Pantoea* strains can help reduce the incidence of agricultural diseases [19]. Table 1 shows the antagonistic activity of *Pantoea* species against phytopathogens.

The competitive advantages of *Pantoea* bacteria in natural ecosystems are largely due to their ability to produce a wide range of secondary metabolites with antimicrobial activity, including pantocins, herbicolins, microcins, and phenazines [33–35]. Less common metabolites include PNP-1 produced by *Pantoea ananatis* [36–38]. The *P. agglomerans* strain CPA-2 has been reported to inhibit the growth of *Penicillium* fungi in the post-harvest treatment of agricultural products [39, 40]. Thus, members of the genus *Pantoea* have high potential in bioprotection of plants and in the sustainable management of agroecosystems.

Some members of the genus *Pantoea* have demonstrated significant potential in bioremediation and purification of polluted environments due to their ability to degrade herbicides without causing toxic intermediate or end products to form [41]. However, their use is not limited to agricultural production and environmental technologies. Certain *Pantoea* strains can be used as immunomodulatory agents in adjuvant therapeutic ap-

Table 1 *Pantoea* species exhibiting antagonism against phytopathogens

Strain	Phytopathogen	Crop	Reference
Pantoea agglomerans	*Phytium* spp.	*Beta vulgaris* subsp. *vulgaris* var. *saccharifera* L.	[20]
	Pseudomonas syringae pv. *syringae*	*Hordeum vulgare* L.	[21]
	Botrytis cinerea	*Lens culinaris* Medik.	[22]
	Curtobacterium flaccumfaciens pv. *flaccumfaciens*	*Phaseolus vulgaris* L.	[23]
	Aphanomyces euteiches	*Pisum sativum* L.	[24]
	Pseudomonas syringae pv. *tomato*	*Solanum lycopersicum* L.	[25]
	Fusarium oxysporum f. sp. *conglutinans*	*Eruca vesicaria* subsp. *sativa* (Mill.) Thell.	[26]
Pantoea dispersa	*Burkholderia glumae*	*Oryza sativa* L.	[27]
	Ceratocytis fimbriata	*Pomoea batatas* L.	[28]
	Pseudomonas syringae pv. *tomato*	*Solanum lycopersicum* L.	[25]
Pantoea jilinensis	*Botrytis cinerea*	*Solanum lycopersicum* L.	[29]
Pantoea ananatis	*Xanthomonas axonopodis* pv. *vesicatoria*	*Capsicum annuum* L.	[30]
	Botrytis cinerea	*Solanum lycopersicum* L.	[31]
Pantoea vagans	*Aspergillus flavus*	*Arachis hypogaea* L., *Zea mays* L.	[32]

proaches to treat melanoma, infections, and allergies, as well as immune system dysfunctions [42–44].

Their ubiquity, ecological versatility, and relative genetic accessibility make *Pantoea* strains a convenient model system for studying the mechanisms of adaptation to various ecological niches and the manifestation of opportunistic traits. In addition, these characteristics determine their significant potential for creating commercial products for medical, agricultural, and environmental applications.

Modern molecular genetic methods, such as whole-genome sequencing, significantly expand the practical application of *Pantoea* species. Genomic analysis can identify genes responsible for biocontrol, secondary metabolite synthesis, stress resistance, and host interactions. Genomic data inform science-based selection and optimization of strains for applied purposes.

In this study, we aimed to conduct whole-genome sequencing of the *Pantoea allii* B-14727 strain to identify genetic determinants associated with its antagonistic activity, competitiveness, and colonizing ability.

STUDY OBJECTS AND METHODS

The strain used in this study was isolated from the rhizosphere of spring soft wheat at an early stage of research. It was identified by 16S rRNA sequencing and deposited at the All-Russian Collection of Industrial Microorganisms at the Kurchatov Institute National Bioresource Center (Russia) as *Pantoea vagans* B-14727. However, whole-genome sequencing identified it as *Pantoea allii*. The strain forms round, yellow colonies averaging 1.5 mm in diameter with a flat profile, smooth edges, and a glossy texture. The cells are Gram-negative bacilli with an average size of 0.809×0.469 μm. The strain promotes plant growth due to its antioxidant activity (79.29%) and its ability to produce indole-3-acetic (9.0 mg/mL) and gibberellic (346 μg/mL) acids, fix atmospheric nitrogen (840 μg/mL in the medium), solubilize (solubilization index of 333%) phosphates, potassium, and zinc, as well as to form biofilms [45].

The *P. allii* strain's antagonistic activity was assessed against *Fusarium graminearum* F-877, *Bipolaris sorokiniana* F-529, and *Botrytis cinerea* F-1006 (All-Russian Collection of Industrial Microorganisms, Kurchatov Institute National Bioresource Center). The phytopathogenic fungi were pre-cultivated on potato glucose agar (Dia-M, Russia). A 24-h culture of the strain grown in Miller's modified Luria-Bertani broth (HiMedia Laboratories, India) was submerged into Miller's modified Luria-Bertani agar-filled Petri dishes and incubated at 28 ± 2°C for 24 h. After cultivation, an agar block was cut out from the medium and placed in the well of an agar disk on another Petri dish pre-inoculated with a phytopathogen culture. The phytopathogenic fungi were inoculated by a lawn method using agar slants (0.5 McFarland) and incubated at 26 ± 2°C. The *P. allii* strain's antagonistic activity was determined by measuring the diameter of a phytopathogen growth inhibition zone around the agar block containing the strain [45].

The strain's DNA was isolated from the bacterial cells using a ZymoBIOMICS DNA Miniprep Kit (Zymo Research, USA). The amount of DNA was measured with a Nanodrop spectrophotometer (Thermo Scientific, USA) and a Qubit fluorimeter (Invitrogen, USA) at the Genomics Shared Use Center (Institute of Chemical Biology and Fundamental Medicine, Novosibirsk, Russia).

For genomic sequencing on the MGIseq platform, the bacterial DNA was fragmented by ultrasound on a Covaris S2 instrument (Covaris, USA) and treated with RNase A (Thermo Scientific, USA). DNA libraries were prepared using the NEBNext Ultra II DNA library prepkit for Illumina (New England BioLabs, USA) and NEBNext Multiplex Oligos (New England BioLabs, USA). The quality of the DNA libraries was assessed on a Qsep100 device (BiOptic, Taiwan) using a F3 Fast Cartridge kit (BiOptic, Taiwan). The number of the libraries was determined using a Qubit fluorimeter. The DNA libraries were mixed equimolarly and sequenced on MGIseq-2000 (MGI Tech, China) according to the manufacturer's protocols. A DNBSEQ-G400RS High-throughput Sequencing Set PE100 (MGI Tech, China) was used to read the library from both sides of 100 nucleotides.

The starting (non-fragmented) DNA was used for genomic sequencing on the Polyseq platform. First, adapters containing unique barcodes were ligated using a Barcode Library Preparation Kit (MGI, China). The resulting libraries were mixed equimolarly, and adapters were ligated again using a Ligation Barcode Kit (Polyseq Biotech, China). The resulting total DNA libraries were sequenced on the Polyseq One platform (Polyseq Biotech, China) at the Genomics Shared Use Center (Institute of Chemical Biology and Fundamental Medicine, Novosibirsk, Russia).

For *de novo* genome assembly and annotation, the reads obtained on Polyseq One were filtered using Fitlong v0.2.1. Genome assembly was then performed by using three different assemblers: Flye v2.9.2 [46], Minipolish v0.1.3 [47], and Raven v1.8.1. The assemblies were subjected to general contig clustering, alignment, and consensus finding by using Tricycle v0.5.4 [48]. Errors in the genomes were first corrected with Medaka v1.7.2, which uses long reads of Polyseq One. Then, the genomes were polished by Polypolish v0.5.0 [49] and POLCA v4.1.0 [50], which use short reads of MGIseq. For this, the short reads were filtered by quality (Quality value > 20) and adapter sequences were simultaneously removed by Cutadapt v5.0 [51]. Sequencing errors were corrected by using SPAdes v4.0.0 [52] in the only-error-correction mode.

Genome assembly completeness was assessed by BUSCO v5.5.0 with sets of single-copy orthologs [53]. Genome annotation was performed by Bakta v1.11.4 [54]. Genome taxonomic identification was performed by GTDB-Tk v2.4.1 with the GTDB r220.0 database [55].

Phylogenomic analysis of the strain was performed by GTDB-Tk. High phylogenetic resolution was ensured by an alignment of 120 universal bacterial proteins. A

phylogenomic tree was constructed using a reference set of over 80,000 genomes from the Genome Taxonomy Database to ensure the correct positioning of the *P. allii* strain in the global evolutionary context. Visualization was performed by Python using the Biopython library.

RESULTS AND DISCUSSION

Whole-genome analysis is an important tool in modern microbiology that provides detailed information on the genetic organization of microorganisms and their biotechnological potential. High-throughput sequencing methods enable scientists to analyze their genomic structure and identify genes associated with their metabolism, adaptation to various environmental conditions, and synthesis of bioactive compounds. Therefore, the first stage of our study involved isolating the genomic DNA of the strain under study and its sequencing on the MGIseq-2000 and Polyseq platforms.

Spectrophotometric analysis of the isolated DNA revealed its classic absorption spectrum (133 ng/μL and 4.6 μg), indicating its sufficient quality and quantity for library construction. Table 2 presents the numbers of reads and data volumes obtained from high-throughput sequencing on both platforms. The volumes of short and long reads were sufficient for assembling circular genomes [45].

Length is an important parameter for nanopore reads. We established that more than a third of the reads were longer than 10,000 nt, which is generally sufficient for assembling a circular bacterial chromosome. More than 70% of the reads had a quality of Quality value > 30. Over 1,000 errors were corrected and the genome length increased by 1,413 nucleotides (Table 3) [45].

The genome assembly quality was assessed by using the BUSCO program for the presence of single-copy orthologs. All 124 genes were found in the strain under study, indicative of the genome's high quality.

Table 2 Genomic sequencing of *Pantoea allii* B-14727 on the MGIseq-2000 and Polyseq platforms

Strain	MGIseq		Polyseq	
	Number of reads, million	Data volume, MB	Number of reads, million	Data volume, MB
Pantoea allii B-14727	6.0	602	341.7	3145

Table 3 *De novo* assembly and annotation of genomes

Indicator	B-14727
Genome before error correction	4,871,944
Genome after error correction	4,873,357
GC composition, %	53.0
Number of predicted coding sequences	4,512
rRNA clusters	7
tRNA	80
Coverage	609
The closest homologue according to the Genome Taxonomy Database	*Pantoea allii*

The phylogenomic tree (Fig. 1) had a distinct cluster organization covering a wide range of validly described species of the genus *Pantoea*, including *Pantoea ananatis, Pantoea agglomerans, Pantoea vagans, Pantoea dispersa, Pantoea eucalypti, Pantoea stewartii*, and others. Each taxon was represented by a separate branch, with closely related species forming compact phylogenetic clusters with short internal branches, indicating their recent common origin. The isolated strain B-14727 was clearly localized within the clade corresponding to the species *Pantoea allii*. It formed a common cluster with the reference strain *P. allii*, with no signs of phylogenetic divergence comparable to interspecific differences. The branch leading to strain B-14727 was minimal, indicative of high genomic identity with the type and reference representatives of this species. The absence of overlap with other species meant that the species identification was correct, with no possibility that strain B-14727 might belong to closely related but phylogenetically distinct taxa.

Therefore, the strain under study was classified as *P. allii*, with Gram-negative staining and facultative anaerobic metabolism.

The species *P. allii* has been relatively understudied compared to other species of the genus *Pantoea*, despite its potential ecological and agronomic significance. This

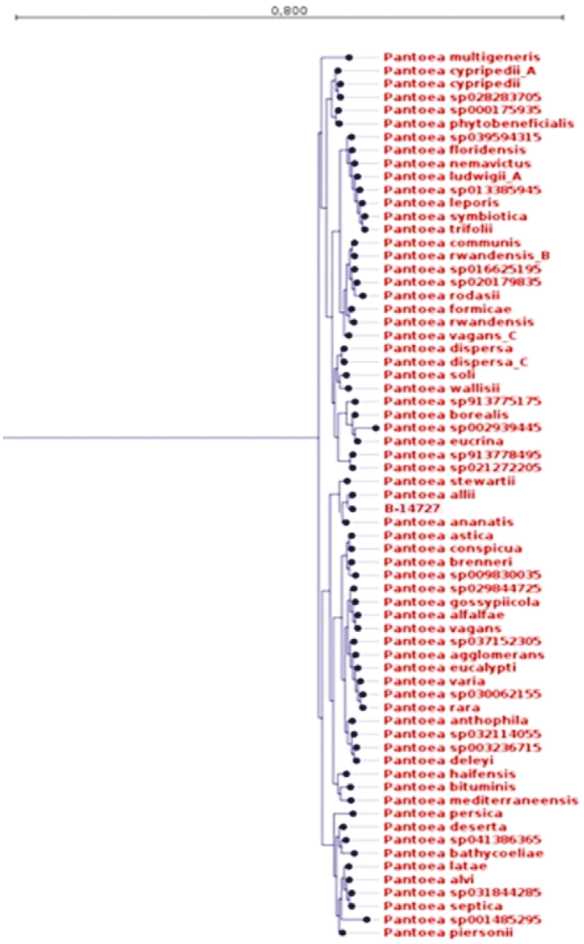


Figure 1 Phylogenomic tree for the genus *Pantoea* and strain B-14727 constructed in GTDB-Tk using 120 concatenated bacterial genes

taxon was initially described in South Africa as a phytopathogenic isolate obtained from tissues and seeds of onions (*Allium cepa* L.) affected by central rot [56]. Central rot, with leaf necrosis and internal bulb rot [57], occurs both during growth and post-harvest storage [58]. However, current data on *P. allii* are largely based on isolates obtained through targeted phytopathological studies or identified sporadically during analysis of affected plants. This limits our understanding of the species' geographic distribution and the variability of its ecological characteristics. Reports of *P. allii* isolation from rainwater indicate a possibility of its existence outside the host-pathogen system and suggest a wider range of ecological niches than previously thought [59]. To clarify the ecological role of the *P. allii* strain isolated in our study, further tests are needed to analyze its interaction with the host plant and confirm the absence of virulence.

Our next step was to study the strain's biotechnological potential. The antiSMASH platform is widely used to identify and analyze clusters of genes for secondary metabolite biosynthesis in bacterial and fungal genomes. To assess the strain's ability to synthesize antagonistic metabolites, its genomic sequences in the GenBank format were imported into antiSMASH 8.0.4. The program's built-in algorithms automatically recognized genetic clusters, classified them, and predicted potential biosynthetic products. This enabled us to identify a set of secondary metabolites potentially produced by the microorganism [60].

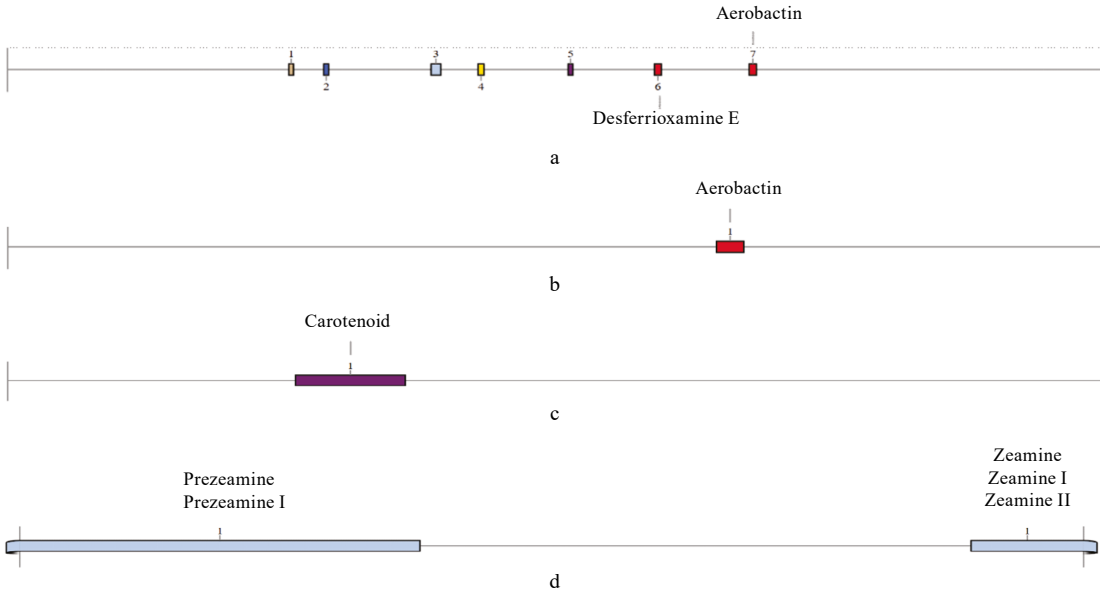
The gene clusters identified in the *Pantoea allii* B-14727 genome are presented in Fig. 2 and Table 4 [45].

The analysis of *P. allii* B-14727's genome using specialized databases (including MiBIG) identified several biosynthetic gene clusters localized on four contigs (contig_1–contig_4). These clusters are potentially responsible for the synthesis of secondary metabolites of various chemical nature (siderophores, RiPP peptides, terpenoids, NRPS, etc.) [51, 61, 62].

On contig_1, five biosynthetic gene clusters (BGCs 1–5) were identified and annotated as belonging to the hserlactone, redox-cofactor, NRPS/phosphonate, azole-containing RiPP, and terpene-precursor types. All of these BGCs showed low similarity to MiBIG reference entries (0.31–0.50), which may indicate their potential novelty or significant evolutionary divergence from previously characterized clusters. The lack of clearly comparable analogs in MiBIG and moderate homology values suggest that these BGCs are capable of mediating the biosynthesis of previously undescribed secondary metabolites or compounds with similar functions but distinct chemical structures.

A NRPS-independent siderophore biosynthesis cluster was identified on contig_1 (region 6). It exhibited high similarity (0.85) to the desferrioxamine E cluster (BGC0001572.3), previously characterized in *P. agglomerans*. The structural formula of aerobactin and desferrioxamine E is shown in Fig. 3. The cluster length was about 30.3 kb. Given its annotation and the homology level, this cluster is likely to determine the synthesis of a cyclic hydroxamate siderophore with high affinity for Fe^{3+}. Functionally, this may ensure efficient iron chelation and increase the strain's competitiveness in iron-deficiency.

Desferrioxamines belong to the class of hydroxamate siderophores. They were first discovered as metabolites of *Streptomyces* spp. In particular, it was experimentally established that *Streptomyces coelicolor* produced



The numbers refer to the predicted regions characterized in Table 4

Figure 2 Gene clusters identified in the genome of *Pantoea allii* B-14727 using antiSMASH 8.0.4: contig_1 (a); contig_2 (b); contig_3 (c); and contig_4 (d)

Table 4 *Pantoea allii* B-14727 gene clusters for the biosynthesis of secondary metabolites

Region	Type	Location on the genome, bp	Cluster length, bp	Level of similarity	Similar cluster	MiBIG database	Similarity value	Microorganism
Contig_1								
1	Hserlactone	1236095–1256727	20633	–	–	BGC0001928.2	0.46	–
2	Redox-cofactor	1389233–1411398	22166	–	–	BGC0001440.5	0.41	–
3	NRPS, phosphonate	1860921–1903830	42910	–	–	BGC0001859.4	0.36	–
4	Azole-containing-RiPP	2067374–2093638	26265	–	–	BGC0001285.5	0.31	–
5	Terpene-precursor	2463054–2483953	20900	–	–	BGC0001361.3	0.50	–
6	Nl-siderophore	2842318–2872669	30352	High	Desferrioxamine E (DFO-E)	BGC0001572.3	0.85	*Pantoea agglomerans*
7	Nl-siderophore	3258174–3290546	32373	High	Aerobactin	BGC0001499.5	0.90	*Pantoea ananatis*
Contig_2								
1	Nl-siderophore	840312–872684	32373	High	Aerobactin	BGC0001499.5	0.90	*Pantoea ananatis*
Contig_3								
1	Terpene	67528–93289	25762	High	Carotenoid	BGC0000638.3	0.89	*Pantoea ananatis*
Contig_4								
1	hglE-KS PUFA NRPS T1PKS	149575–62927	80607	High	Zeamine Zeamine I Zeamine II Prezeamine Prezeamine I	BGC0001872.3	1.27	*Xenorhabdus bovienii* SS-2004

desferrioxamine B (DFO-B) and desferrioxamine E (DFO-E) [63]. DFO-E is a macrocyclic ferrioxamine formed by three repeating fragments of 5-succinylated 1-amino-5-(hydroxyamino)pentane. Initially described in the context of antibiotic activity, it was then studied in relation to iron chelation [64]. Studies show that exogenous application of DFO-E can induce changes in secondary metabolism and stimulate morphological differentiation in various actinomycetes. Therefore, it can be considered as a signaling-metabolic factor [65].

Actinomycetes and a number of other bacteria can produce DFO-E, particularly members of the genus *Pantoea*. According to phylogenetic and genomic data, they might have horizontally acquired these biosynthetic determinants from the closely related genus *Erwinia* [66, 67]. Unlike *Pantoea* species, current literature fully describes this biosynthetic pathway in the model organism *S. coelicolor*. In the latter, DFO-E biogenesis occurs via an NRPS-independent mechanism involving the NRPS-independent siderophore synthetase DesD [68], with a sequential condensation of three monomeric units of N-hydroxy-N-succinylcadaverine [69–70].

The genetic determinants that ensure the biosynthesis and transport of aerobactin are organized into a single operon, which includes five genes: *iucABCD* and *iutA*. The genes *iucABCD* encode enzymes of the

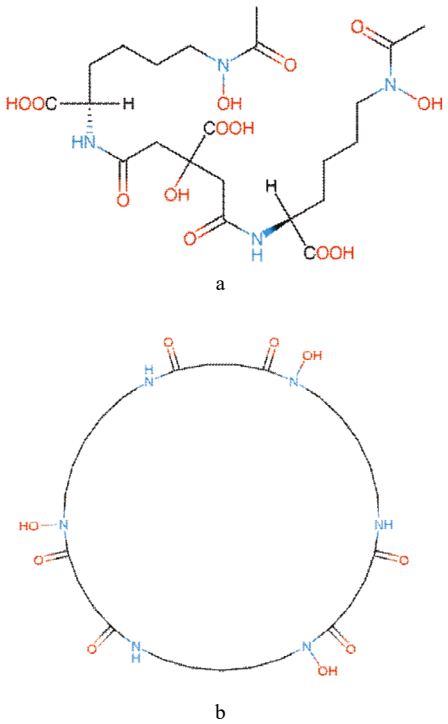


Figure 3 Structural formula of siderophores: aerobactin (a); desferrioxamine E (b)

aerobactin biosynthetic pathway, while *iutA* encodes a high-affinity outer membrane receptor that ensures the capture of the siderophore-iron complex [71, 72]. Recent comparative studies of *Pantoea* strain genomes have identified types of siderophores and the corresponding biosynthetic clusters, as well as reconstructed the probable sources of their origin. In particular, the production of aerobactin has been shown as a common feature for *P. stewartii, P. ananatis*, and *Pantoea septica*, which they obtained through a horizontal gene transfer from members of the order *Enterobacterales* [73].

According to Choi *et al.* [74], the synthesis of aerobactin and desferrioxamine E in *Pantoea ananatis* PA13 is negatively regulated by the iron-dependent global repressor Fur. These siderophores are vital for the strain's antibacterial activity against *Erwinia amylovora* and *Yersinia enterocolitica*. Furthermore, the siderophores give *P. ananatis* selective advantages in the plant-associated niche, improving its competition in local microbial communities.

In our study, a terpene biosynthetic cluster was identified in the genome of the *P. allii* B-14727 strain on contig_3. It exhibited a high degree of similarity (0.89) to the carotenoid biosynthetic cluster BGC0000638.3 described in *P. ananatis*. This homology suggests that this cluster encodes enzymatic components responsible for the synthesis of carotenoid pigments.

The structural formula of a carotenoid is shown in Fig. 4. Carotenoids are among the most diverse natural antioxidants. They are synthesized by many organisms, including animals, plants, and microorganisms. They owe their yellow-orange color to their ability to absorb light in the range of 400–550 nm [75]. Carotenoids are a class of pigment isoprenoids with pronounced antioxidant properties that protect cells against a wide range of reactive oxygen species, including H_2O_2, hydroxyl radicals, and superoxide anions [76]. They act as antioxidants by inactivating singlet oxygen ($^1O_2$) and free radicals generated during oxidative stress. A significant source of reactive oxygen species in plant tissue is a photosensitized formation of reactive oxygen derivatives upon absorption of visible light by the chlorophyll of the host plant. Pigmentation-deficient mutants have overall reduced survival compared to the wild type in the presence of H_2O_2 on nutrient-rich media [77].

Several *Erwinia* species, which are close relatives of *Pantoea*, produce yellow carotenoid pigments and possess a conserved carotenoid biosynthetic operon consisting of the genes *crtE, crtX, crtY, crtI*, and *crtB*. The *crtB* gene encodes phytoene synthase, an enzyme in the first step of carotenoid biosynthesis, and its mutations result in a nonpigmented phenotype [75]. The *P. stewartii* genome contains a conserved carotenoid biosynthetic operon found in *Erwinia* spp., where *crtE* encodes geranylgeranyl pyrophosphate synthase, *crtX* encodes 3-hydroxy-*β*-carotene glycosylase, *crtY* encodes lycopene cyclase, and *crtI* encodes phytoene dehydrogenase [78]. The *crtB* gene encodes phytoene synthase, which converts geranylgeranyl pyrophosphate to phytoene, an early step in *β*-carotene biosynthesis [79].

A number of plant-associated bacteria, including *Erwinia herbicola*, can biosynthesize carotenoids, which increase resistance to photodynamically induced oxidative stress associated with the photosynthetic activity of chlorophyll [80]. In addition, carotenoids perform a photoprotective function, reducing the damage caused by ultraviolet irradiation, primarily in the near UV range (320–400 nm) [81]. Therefore, the biosynthesis of this carotenoid in *P. allii* B-14727 can:

– protect the cells from reactive oxygen species generated in the rhizosphere and on the plant surface by photochemical reactions and the metabolism of the host plant and competing microorganisms;

– improve resistance to abiotic stresses, including UV radiation, temperature fluctuations, and osmotic pressure, which is critical for epiphytic and rhizosphere life [79, 82];

– stabilize membranes and protein complexes, including transporters and receptors involved in plant colonization and nutrient acquisition [83];

– enhance competitiveness indirectly, since antioxidant protection allows the cells to maintain metabolic activity under conditions of microbial competition and exposure to antimicrobial compounds.

A large hybrid cluster (~ 80.6 kb) was identified in the genome of the *P. allii* B-14727 strain on contig_4, which included the hglE-KS domains, PUFA-like enzymes, NRPS, and T1PKS. This cluster exhibited high similarity (1.27) to the cluster of zeamine and its derivatives (zeamine, zeamine I, zeamine II, and prezeamine)

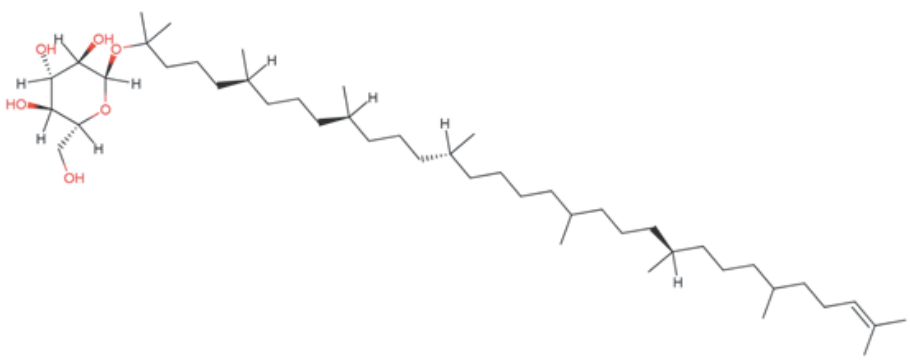


Figure 4 Structural formula of a carotenoid

(Fig. 5), previously described in *Xenorhabdus bovienii* SS-2004. The similarity value of > 1 indicated not only conservation but also a possible expansion or enhancement of the cluster's functional potential.

Zeamines are a structurally and functionally distinct group of broad-spectrum antibiotics. Their production is controlled by the LuxI/LuxR quorum sensing system, which provides the producer with increased competitiveness and ecological adaptability in microbial communities [84, 85].

Chemically, zeamines have a previously undescribed molecular scaffold comprising an atypical polyamino alcohol chain (zeamine II) linked to a polyketide moiety by an amide bond. This moiety additionally contains a valine residue in the structures of zeamine and zeamine I. Valine is thought to be part of a nonribosomal hexapeptide leader sequence, which undergoes proteolytic cleavage during post-assembly processing [86].

In *Serratia plymuthica* RVH1, zeamine is biosynthesized in a gene cluster of approximately 50 kb, which is evolutionarily conserved among different bacterial taxa [87, 88]. In addition to the genes that putatively encode postsynthetic modification enzymes (Zmn15, Zmn22) and components of the export system (Zmn20–21), this cluster includes determinants of two functionally distinct biosynthetic lineages. The first is a FAS/PKS type I system, homologous to polyunsaturated fatty acid synthases (Zmn10–14), while the second is a hybrid NRPS/PKS complex (Zmn16–19). This intricate genetic organization indicates the involvement of a previously undescribed combination of multienzyme complexes of the NRPS, PKS, and PUFA synthase types in the assembly of zeamine [86].

Zeamines exhibit high antibacterial activity against a number of clinically significant bacterial pathogens, including multidrug-resistant strains such as *Staphylococcus aureus* and *Pseudomonas aeruginosa* [89, 90]. Studies demonstrate that zeamines inhibit the growth of both Gram-positive and Gram-negative bacteria at low concentrations, indicating their pronounced antimicrobial potential. Furthermore, zeamines have promising fungicidal properties against *Peronophythora litchi* and other fungal phytopathogens [91, 92].

In our study, the *P. allii* B-14727 strain exhibited high antagonistic activity against phytopathogens (Fig. 6), which is likely due to the production of antimicrobial metabolites such as zeamines.

According to Fotina [45], the *P. allii* B-14727 strain can effectively inhibit the growth of the phytopathogenic fungi *Fusarium graminearum* F-877, *Bipolaris sorokiniana* F-529, and *Botrytis cinerea* F-1006, with inhibition zones of 8.3, 9.5, and 7.0 cm in diameter, respectively.

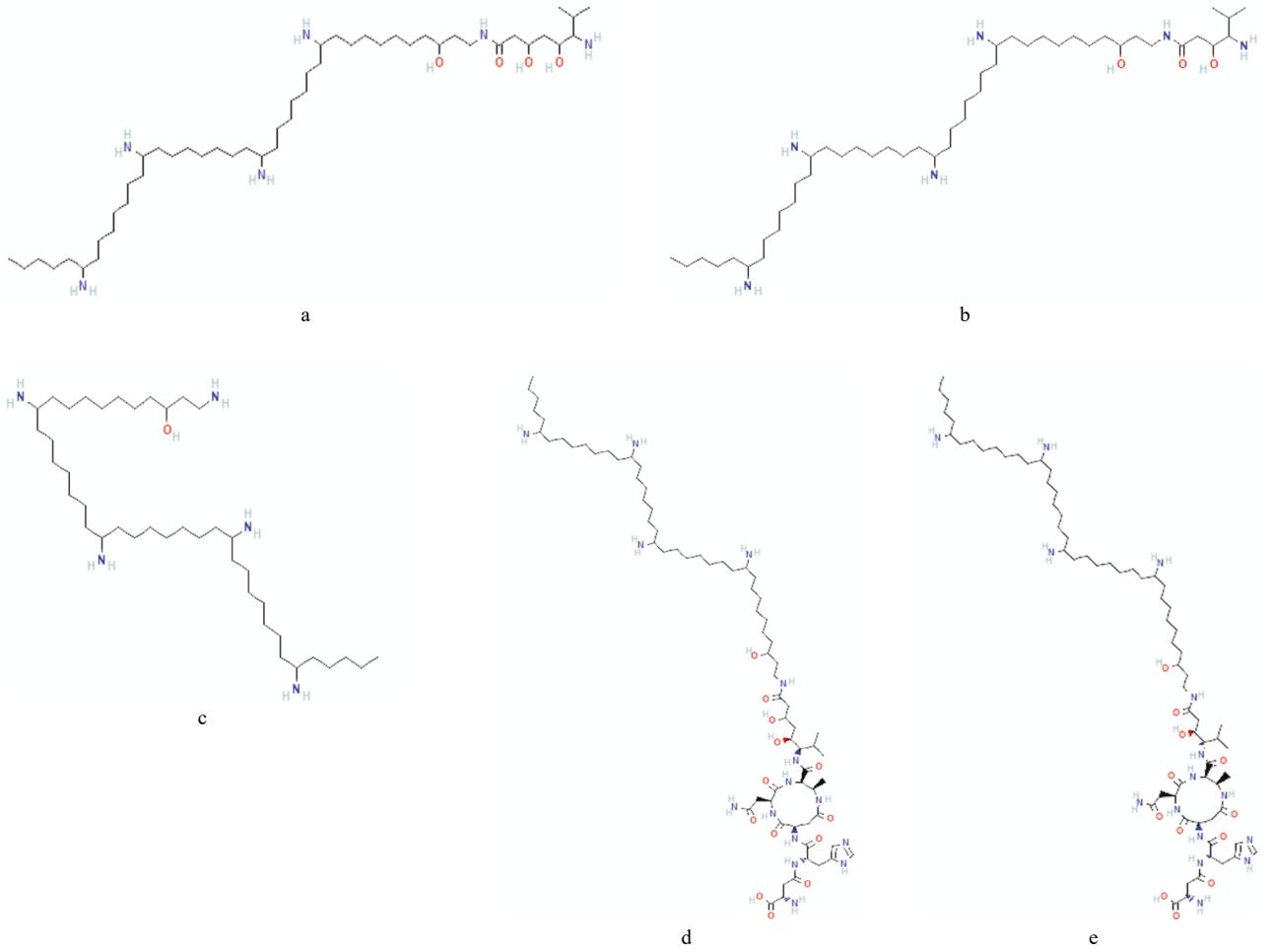


Figure 5 Structural formula of peptide antibiotics: zeamine (a); zeamine I (b); zeamine II (c); prezeamine (d); and prezeamine I (e)

Thus, the *P. allii* B-14727 genome has a diverse set of biosynthetic gene clusters, including multiple siderophore systems (desferrioxamine E and aerobactin), a carotenoid biosynthesis cluster, and a large hybrid PKS/NRPS cluster similar to the zeamine biosynthetic pathway. This combination of highly efficient iron uptake systems and a cluster of zeamine-like antibiotics indicates high adaptive and competitive potential of the strain under conditions of iron deficiency and microbial competition.

CONCLUSION

Modern molecular genetic studies have significantly revised the taxonomic boundaries of the genus *Pantoea*. Its members implement a variety of ecological strategies, ranging from phytopathogenic to mutualistic relationships with plants, as well as biocontrol. This functional variability underpins ongoing scientific interest in *Pantoea* bacteria for their use in sustainable agriculture that seeks environmentally friendly and biologically based plant protection technologies and increased productivity.

By analyzing the genome of *Pantoea allii* B-14727, we identified and classified numerous biosynthetic gene clusters potentially responsible for the synthesis of secondary metabolites of diverse chemical nature. In particular, the genome was annotated to contain clusters of NRPS-independent siderophores, including aerobactin and desferrioxamine E, a carotenoid cluster, clusters of RiPP peptides, and a large hybrid PKS/NRPS cluster similar to the zeamine biosynthetic pathway.

Highly conserved siderophore biosynthetic gene clusters appear to play a key role in high-affinity iron uptake, making the strain *P. allii* B-14727 more competitive in conditions of limited iron availability and intense intermicrobial competition. Due to its antioxidant and photoprotective properties, the carotenoid cluster potentially increases cellular resistance to abiotic stressors. The presence of a hybrid PKS/NRPS cluster of the zeamine-like type suggests the strain's ability to synthesize broad-spectrum peptide antibiotics. In addition to antibacterial activity, these antibiotics potentially exhibit fungicidal activity, further expanding the adaptive capabilities of *P. allii* B-14727 in microbial communities.

Noteworthily, the current genetic databases contain no, or very little, information on gene clusters that are directly related to canonical zeamine biosynthesis in members of the genus *Pantoea*. Therefore, the zeamine-like hybrid PKS/NRPS cluster identified in *P. allii* B-14727 in our study is a potentially novel variant of the biosynthetic pathway that needs further structural and functional validation (including comparative genomic analysis and experimental confirmation of its metabolite profile).

However, since the *Pantoea allii* species includes phytopathogenic strains, our results need to be reinterpreted. *P. allii* is associated with onion diseases, in-

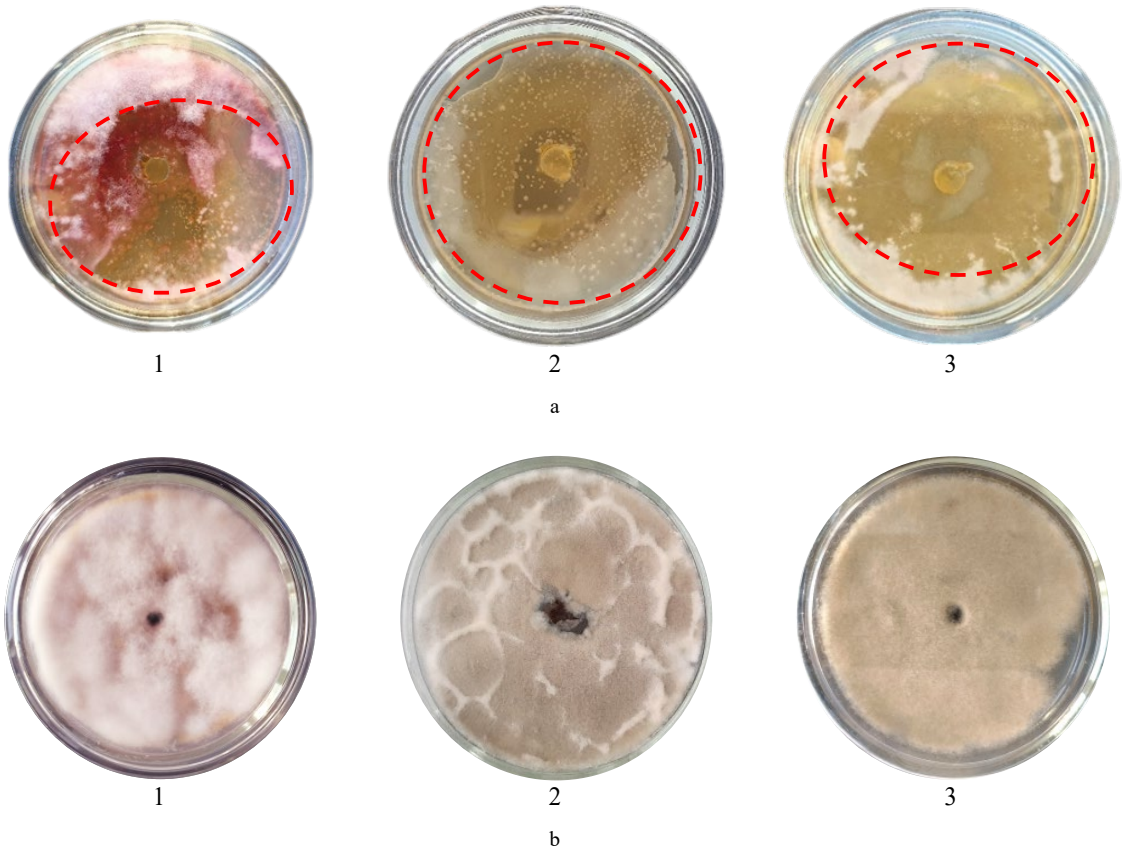


Figure 6 Antagonistic activity of *Pantoea allii* B-14727 *in vitro* against phytopathogenic fungi: treated with the test strain (a) control (b) 1 – *Fusarium graminearum* F-877; 2 – *Bipolaris sorokiniana* F-529; 3 – *Botrytis cinerea* F-1006 [45]

cluding bacterial rot and necrosis. Its pathogenicity is determined by a number of factors such as the production of toxins and enzymes that degrade cell walls and secretion systems. Notably, many of its properties that have traditionally been considered as "growth-promoting" (e.g., the synthesis of siderophores and secondary metabolites, or the ability to effectively colonize plant tissue) can also contribute to pathogenesis, providing a competitive advantage and, at the same time, infecting the host plant. Therefore, the *P. allii* B-14727 strain needs to be further analyzed for virulence.

Thus, the safety and functional role of *P. allii* B-14727 needs to be further confirmed, despite its high biosynthetic potential (e.g., for biocontrol) identified in this study. In line with modern approaches to developing microbial preparations for sustainable agriculture, further research will aim to experimentally confirm the strain's lack of virulence in model systems. Such research may involve inoculating a host plant with this strain and evaluating its impact on the plant's physiology.

CONTRIBUTION

The authors were equally involved in writing the manuscript and therefore bear equal responsibility for plagiarism.

COFLICT OF INTEREST

The authors declare no conflict of interest regarding this publication.

REFERENCES

1. Rimes-Casais FF, Pedrosa-Silva F, Venancio TM. Comparative genomic insights into the genus *Pantoea*: Genetic determinants of ecological lifestyle diversity and plant growth-promoting potential. World Journal of Microbiology and Biotechnology. 2026;42:46. https://doi.org/10.1007/s11274-025-04780-2
2. Tindall BJ. The combination *Enterobacter agglomerans* is to be cited as *Enterobacter agglomerans* (Beijerinck 1888) Ewing and Fife 1972 and the combination *Pantoea agglomerans* is to be cited as *Pantoea agglomerans* (Beijerinck 1888) Gavini *et al*. 1989. Opinion 90. Judicial Commission of the International Committee on Systematics of Prokaryotes. International Journal of Systematic and Evolutionary Microbiology. 2014;64(Pt_10):3582–3583. https://doi.org/10.1099/ijs.0.069161-0
3. Brady CL, Cleenwerck I, Venter SN, Engelbeen K, De Vos P, *et al*. Emended description of the genus *Pantoea*, description of four species from human clinical samples, *Pantoea septica* sp. nov., *Pantoea eucrina* sp. nov., *Pantoea brenneri* sp. nov. and *Pantoea conspicua* sp. nov., and transfer of *Pectobacterium cypripedii* (Hori 1911) Brenner *et al*. 1973 emend. Hauben *et al*. 1998 to the genus as *Pantoea cypripedii* comb. nov. International Journal of Systematic and Evolutionary Microbiology. 2010;60(10):2430–2440. https://doi.org/10.1099/ijs.0.017301-0
4. Brady CL, Cleenwerck I, van der Westhuizen L, Venter SN, Coutinho TA, *et al*. *Pantoea rodasii* sp. nov., *Pantoea rwandensis* sp. nov. and *Pantoea wallisii* sp. nov., isolated from *Eucalyptus*. International Journal of Systematic and Evolutionary Microbiology. 2012;62(Pt_7):1457–1464. https://doi.org/10.1099/ijs.0.069161-0
5. Brady CL, Goszczynska T, Venter SN, Cleenwerck I, De Vos P, *et al*. *Pantoea allii* sp. nov., isolated from onion plants and seed. International Journal of Systematic and Evolutionary Microbiology. 2011;61(4):932–937. https://doi.org/10.1099/ijs.0.022921-0
6. Crosby KC, Rojas M, Sharma P, Johnson MA, Mazloom R, *et al*. Genomic delineation and description of species and within-species lineages in the genus *Pantoea*. Frontiers in Microbiology. 2023;14:1254999. https://doi.org/10.3389/fmicb.2023.1254999
7. Roper MC. *Pantoea stewartii* subsp. *stewartii*: Lessons learned from a xylem-dwelling pathogen of sweet corn. Molecular Plant Pathology. 2011;12(7):628–637. https://doi.org/10.1111/j.1364-3703.2010.00698.x
8. Nadarasah G, Stavrinides J. Quantitative evaluation of the host-colonizing capabilities of the enteric bacterium *Pantoea* using plant and insect hosts. Microbiology. 2014;160(3):602–615. https://doi.org/10.1099/mic.0.073452-0
9. Völksch B, Thon S, Jacobsen ID, Gube M. Polyphasic study of plant- and clinic-associated *Pantoea agglomerans* strains reveals indistinguishable virulence potential. Infection, Genetics and Evolution. 2009;9(6):1381–1391. https://doi.org/10.1016/j.meegid.2009.09.016
10. Brady C, Cleenwerck I, Venter S, Vancanneyt M, Swings J, *et al*. Phylogeny and identification of *Pantoea* species associated with plants, humans and the natural environment based on multilocus sequence analysis (MLSA). Systematic and Applied Microbiology. 2008;31(6–8):447–460. https://doi.org/10.1016/j.syapm.2008.09.004
11. Johnson KB, Stockwell VO, Sawyer TL, Sugar D. Assessment of environmental factors influencing growth and spread of *Pantoea agglomerans* on and among blossoms of pear and apple. Phytopathology. 2000;90(11):1285–1294. https://doi.org/10.1094/PHYTO.2000.90.11.1285
12. Serazetdinova YuR, Kolpakova DE, Borodina EE, Pleshivtsev II, Gordienko AV, *et al*. Biological control of cereal crop diseases using bacteria of the genus *Pantoea*. Biosfera. 2025;17(3):153–174. (In Russ.) https://elibrary.ru/JTQYYG
13. Serazetdinova YuR, Fotina NV, Tupikin AE, Lyubimova NA, Asyakina LK. Genetic determinants of antagonistic and growth-stimulating activity of *Pantoea pleuroti*. Food Processing: Techniques and Technology. 2026;56(2):234–246. (In Russ.) https://doi.org/10.21603/2074-9414-2026-2-2645

14. Borodina EE, Gordienko AV, Pleshivtsev II, Fotina NV, Fedorova AM, *et al*. New *Pantoea* strain as antistress agent and growth stimulator in grain growing. Food Processing: Techniques and Technology. 2025;55(4):710–722. (In Russ.) https://doi.org/10.21603/2074-9414-2025-4-2606
15. Quecine MC, Araújo WL, Rossetto PB, Ferreira A, Tsui S, *et al*. Sugarcane growth promotion by the endophytic bacterium *Pantoea agglomerans* 33.1. Applied and Environmental Microbiology. 2012;78(21):7511–7518. https://doi.org/10.1128/AEM.00836-12
16. Nascimento FX, Hernandez AG, Glick BR, Rossi MJ. The extreme plant-growth-promoting properties of *Pantoea phytobeneficialis* MSR2 revealed by functional and genomic analysis. Environmental Microbiology. 2020;22(4):1341–1355. https://doi.org/10.1111/1462-2920.14946
17. Lv L, Luo J, Ahmed T, Zaki HEM, Tian Y, *et al*. Beneficial effect and potential risk of *Pantoea* on rice production. Plants. 2022;11(19):2608. https://doi.org/10.3390/plants11192608
18. Luziatelli F, Ficca AG, Cardarelli M, Melini F, Cavalieri A, *et al*. Genome sequencing of *Pantoea agglomerans* C1 provides insights into molecular and genetic mechanisms of plant growth-promotion and tolerance to heavy metals. Microorganisms. 2020;8(2):153. https://doi.org/10.3390/microorganisms8020153
19. Duchateau S, Borrego C, Verdelet S, Dorey S, Aziz A, *et al*. Growth-promoting and biocontrol features of *Pantoea ananatis* BRT175 in tomato. Biological Control. 2026;212:105949. https://doi.org/10.1016/j.biocontrol.2025.105949
20. Bardin SD, Huang HC, Liu L, Yanke LJ. Control, by microbial seed treatment, of dampingoff caused by *Pythium* sp. on canola, safflower, dry pea, and sugar beet. Canadian Journal of Plant Pathology. 2003;25(3):268–275. https://doi.org/10.1080/07060660309507079
21. Braun-Kiewnick A, Jacobsen BJ, Sands DC. Biological control of *Pseudomonas syringae* pv. *syringae*, the causal agent of basal kernel blight of barley, by antagonistic *Pantoea agglomerans*. Phytopathology. 2000;90(4):368–375. https://doi.org/10.1094/PHYTO.2000.90.4.368
22. Huang PQ, Zheng X. An improved formal total synthesis of (-)-anisomycin (ZH-531DP). Arkivoc. 2003;2:7–14. https://doi.org/10.3998/ark.5550190.0004.202
23. Hsieh TF, Huang HC, Erickson RS. Biological control of bacterial wilt of bean using a bacterial endophyte, *Pantoea agglomerans*. Journal of Phytopathology. 2005;153(10):608–614. https://doi.org/10.1111/j.1439-0434.2005.01027.x
24. Godebo AT, Germida JJ, Walley FL. Isolation, identification, and assessment of soil bacteria as biocontrol agents of pea root rot caused by *Aphanomyces euteiches*. Canadian Journal of Soil Science. 2020;100(3):206–216. https://doi.org/10.1139/cjss-2019-0133
25. Morella NM, Zhang X, Koskella B. Tomato seed-associated bacteria confer protection of seedlings against foliar disease caused by *Pseudomonas syringae*. Phytobiomes Journal. 2019;3(3):177–190. https://doi.org/10.1094/PBIOMES-01-19-0007-R
26. Liu W, Chen Z, Zhang T, Lu C, Dong D, *et al*. Application of *Pantoea agglomerans* strain Z01 to control Fusarium wilt and its effect on the quality parameters of rockets. Annals of Microbiology. 2014;64:1443–1446. https://doi.org/10.1007/s13213-013-0735-5
27. Kouzai Y, Akimoto-Tomiyama C. A seed-borne bacterium of rice, *Pantoea dispersa* BB1, protects rice from the seedling rot caused by the bacterial pathogen *Burkholderia glumae*. Life. 2022;12(6):791. https://doi.org/10.3390/life12060791
28. Jiang L, Jeong JC, Lee JS, Park JM, Yang JW, *et al*. Potential of *Pantoea dispersa* as an effective biocontrol agent for black rot in sweet potato. Scientific Reports. 2019;9:16354. https://doi.org/10.1038/s41598-019-52804-3
29. Zheng L, Zhang J, Wu X, Gu X, Wang S, *et al*. A novel biocontrol strain *Pantoea jilinensis* D25 for effective biocontrol of tomato gray mold (causative agent *Botrytis cinerea*). Biological Control. 2021;164:104766. https://doi.org/10.1016/j.biocontrol.2021.104766
30. Kang SH, Cho HS, Cheong H, Ryu CM, Kim JF, *et al*. Two bacterial entophytes eliciting both plant growth promotion and plant defense on pepper (*Capsicum annuum* L.). Journal of Microbiology and Biotechnology. 2007;17(1):96–103.
31. Enya J, Shinohara H, Yoshida S, Tsukiboshi T, Negishi H, *et al*. Culturable leaf-associated bacteria on tomato plants and their potential as biological control agents. Microbial Ecology. 2007;53:524–536. https://doi.org/10.1007/s00248-006-9085-1
32. Zhang D, Tian X, Hu T, Wang Y, Wang Y, *et al*. Biological control of *Aspergillus flavus* in peanut and maize kernel using *Pantoea vagans* BWL1. Antonie Van Leeuwenhoek. 2025;118:144. https://doi.org/10.1007/s10482-025-02154-0
33. Smits THM, Rezzonico F, Kamber T, Blom J, Goesmann A, *et al*. Metabolic versatility and antibacterial metabolite biosynthesis are distinguishing genomic features of the fire blight antagonist *Pantoea vagans* C9-1. PLoS One. 2011;6(7):e22247. https://doi.org/10.1371/journal.pone.0022247

34. Smits THM, Rezzonico F, Kamber T, Goesmann A, Ishimaru CA, *et al*. Genome sequence of the biocontrol agent *Pantoea vagans* strain C9-1. Journal of Bacteriology. 2010;192(24):6486–6487. https://doi.org/10.1128/jb.01122-10

35. Vanneste JL, Yu J, Cornish DA. Presence of genes homologous to those necessary for synthesis of microcin MccEh252 in strains of *Pantoea agglomerans*. XI International Workshop on Fire Blight. 2008;793:391–396. https://doi.org/10.17660/ActaHortic.2008.793.58

36. Halgren A, Maselko M, Azevedo M, Mills D, Armstrong D, *et al*. Genetics of germination-arrest factor (GAF) production by *Pseudomonas fluorescens* WH6: Identification of a gene cluster essential for GAF biosynthesis. Microbiology. 2013;159(Pt_1):36–45. https://doi.org/10.1099/mic.0.062166-0

37. Trippe K, McPhail K, Armstrong D, Azevedo M, Banowetz G. *Pseudomonas fluorescens* SBW25 produces furanomycin, a non-proteinogenic amino acid with selective antimicrobial properties. BMC Microbiology. 2013;13:111. https://doi.org/10.1186/1471-2180-13-111

38. Walterson AM, Smith DDN, Stavrinides J. Identification of a *Pantoea* biosynthetic cluster that directs the synthesis of an antimicrobial natural product. PLoS One. 2014;9(5):e96208. https://doi.org/10.1371/journal.pone.0096208

39. Zamani M, Tehrani AS, Ahmadzadeh M, Hosseininaveh V, Mostofy Y. Control of *Penicillium digitatum* on orange fruit combining *Pantoea agglomerans* with hot sodium bicarbonate dipping. Journal of Plant Pathology. 2009;91(2): 437–442.

40. Cañamás TP, Viñas I, Usall J, Casals C, Solsona C, *et al*. Control of postharvest diseases on citrus fruit by preharvest application of the biocontrol agent *Pantoea agglomerans* CPA-2: Part I. Study of different formulation strategies to improve survival of cells in unfavourable environmental conditions. Postharvest Biology and Technology. 2008;49(1):86–95.

41. Pileggi M, Pileggi SAV, Olchanheski LR, da Silva PAG, Munoz Gonzalez AM, *et al*. Isolation of mesotrione-degrading bacteria from aquatic environments in Brazil. Chemosphere. 2012;86(11):1127–1132. https://doi.org/10.1016/j.chemosphere.2011.12.041

42. Nakata K, Inagawa H, Soma GI. Lipopolysaccharide IP-PA1 from *Pantoea agglomerans* prevents suppression of macrophage function in stress-induced diseases. Anticancer Research. 2011;31(7):2437–2440.

43. Hebishima T, Matsumoto Y, Watanabe G, Soma GI, Kohchi C, *et al*. Oral administration of immunopotentiator from *Pantoea agglomerans* 1 (IP-PA1) improves the survival of B16 melanoma-inoculated model mice. Experimental Animals. 2011;60(2):101–109. https://doi.org/10.1538/expanim.60.101

44. Yoshida A, Kohchi C, Inagawa H, Nishizawa T, Soma GI. Improvement of allergic dermatitis via regulation of the Th1/Th2 immune system balance by macrophages activated with lipopolysaccharide derived from *Pantoea agglomerans* (IP-PA1). Anticancer Research. 2009;29(11):4867–4870.

45. Fotina NV. Search, study of properties and practical application of rhizobacteria in regulating biotic stress of wheat: Cand. Sci. Bio. Diss. Kemerovo. 2025. 174 p. (In Russ.).

46. Kolmogorov M, Yuan J, Lin Y, Pevzner P. Assembly of long error-prone reads using repeat graphs. Nature Biotechnology. 2019;37:540–546. https://doi.org/10.1038/s41587-019-0072-8

47. Wick RR, Holt KE. Benchmarking of long-read assemblers for prokaryote whole genome sequencing. F1000Research. 2019;8:2138. https://doi.org/10.12688/f1000research.21782.1

48. Wick RR, Judd LM, Cerdeira LT, Hawkey J, Méric G, *et al*. Trycycler: Consensus long-read assemblies for bacterial genomes. Genome Biology. 2021;22:266. https://doi.org/10.1186/s13059-021-02483-z

49. Wick RR, Holt KE. Polypolish: Short-read polishing of long-read bacterial genome assemblies. PLoS Computational Biology. 2022;18(1):e1009802. https://doi.org/10.1371/journal.pcbi.1009802

50. Zimin AV, Salzberg SL. The genome polishing tool POLCA makes fast and accurate corrections in genome assemblies PLoS Computational Biology. 2020;16(6):e1007981. https://doi.org/10.1371/journal.pcbi.1007981

51. Marcel M. Cutadapt removes adapter sequences from high-throughput sequencing reads. EMBnet journal. 2011;17(1):10 https://doi.org/10.14806/ej.17.1.200

52. Bankevich A, Nurk S, Antipov D, Gurevich AA, Dvorkin M, *et al*. SPAdes: A new genome assembly algorithm and its applications to single-cell sequencing. Journal of Computational Biology. 2012;19(5):455–477. https://doi.org/10.1089/cmb.2012.0021

53. Manni M, Berkeley MR, Seppey M, Zdobnov EM. BUSCO: Assessing genomic data quality and beyond. Current Protocols. 2021;1:e323. https://doi.org/10.1002/cpz1.323

54. Schwengers O, Jelonek L, Dieckmann MA, Beyvers S, Blom J, *et al*. Bakta: Rapid and standardized annotation of bacterial genomes via alignment-free sequence identification. Microbial Genomics. 2021;7(11):000685. https://doi.org/10.1099/mgen.0.000685

55. Chaumeil PA, Mussig AJ, Hugenholtz P, Parks DH. GTDB-Tk: A toolkit to classify genomes with the Genome Taxonomy Database. Bioinformatics. 2020;36(6):1925–1927. https://doi.org/10.1093/bioinformatics/btz848

56. Blin K, Shaw S, Vader L, Szenei J, Reitz ZL, *et al*. antiSMASH 8.0: Extended gene cluster detection capabilities and analyses of chemistry, enzymology, and regulation. Nucleic Acids Research. 2025;53(W1):W32–W38. https://doi.org/10.1093/nar/gkaf334

57. Brady CL, Goszczynska T, Venter SN, Cleenwerck I, De Vos P, *et al*. *Pantoea allii* sp. nov., isolated from onion plants and seed. International Journal of Systematic and Evolutionary Microbiology. 2011;61(4):932–937. https://doi.org/10.1099/ijs.0.022921-0

58. Carr EA, Zaid AM, Bonasera JM, Lorbeer JW, Beer SV. Infection of onion leaves by *Pantoea ananatis* leads to bulb infection. Plant Disease. 2013;97(12):1524–1528. https://doi.org/10.1094/PDIS-06-12-0597-RE

59. Vahling-Armstrong C, Dung JKS, Humann JL, Schroeder BK. Effects of postharvest onion curing parameters on bulb rot caused by *Pantoea agglomerans*, *Pantoea ananatis* and *Pantoea allii* in storage. Plant Pathology. 2015;65(4):536–544. https://doi.org/10.1111/ppa.12438

60. Shin GY, De Armas S, Galván GA, Siri MI, Rojas M, *et al*. Comparative genomics of *Pantoea allii* lineages and distribution of ecologically relevant traits. Microbial Genomics. 2026;12(2):001624. https://doi.org/10.1099/mgen.0.001624

61. Seel W, Baust D, Sons D, Albers M, Etzbach L, *et al*. Carotenoids are used as regulators for membrane fluidity by *Staphylococcus xylosus*. Scientific Reports. 2020;10:330. https://doi.org/10.1038/s41598-019-57006-5

62. Masschelein J, Clauwers C, Stalmans K, Nuyts K, De Borggraeve W, *et al*. The zeamine antibiotics affect the integrity of bacterial membranes. Applied and Environmental Microbiology. 2015;81(3):1139–1146. https://doi.org/10.1128/AEM.03146-14

63. Yang CC, Leong J. Production of deferriferrioxamines B and E from a ferroverdin-producing *Streptomyces* species. Journal of Bacteriology. 1982;149(1):381–383. https://doi.org/10.1128/jb.149.1.381-383.1982

64. Meiwes J, Fiedler HP, Zähner H, Konetschny-Rapp S, Jung G. Production of desferrioxamine E and new analogues by directed fermentation and feeding fermentation. Applied Microbiology and Biotechnology. 1990;32:505–510. https://doi.org/10.1007/BF00173718

65. Yamanaka K, Oikawa H, Ogawa HO, Hosono K, Shinmachi F, *et al*. Desferrioxamine E produced by *Streptomyces griseus* stimulates growth and development of *Streptomyces tanashiensis*. Microbiology. 2005;151(9):2899–2905. https://doi.org/10.1099/mic.0.28139-0

66. Smits THM, Duffy B. Genomics of iron acquisition in the plant pathogen *Erwinia amylovora*: Insights in the biosynthetic pathway of the siderophore desferrioxamine E. Archives of Microbiology. 2011;193:693–699. https://doi.org/10.1007/s00203-011-0739-0

67. Franza T, Mahé B, Expert D. *Erwinia chrysanthemi* requires a second iron transport route dependent of the siderophore achromobactin for extracellular growth and plant infection. Molecular Microbiology. 2005;55(1):261–275. https://doi.org/10.1111/j.1365-2958.2004.04383.x

68. Ronan JL, Kadi N, McMahon SA, Naismith JH, Alkhalaf LM, *et al*. Desferrioxamine biosynthesis: Diverse hydroxamate assembly by substrate-tolerant acyl transferase DesC. Philosophical Transactions of the Royal Society B. 2018;373(1748):20170068. https://doi.org/10.1098/rstb.2017.0068

69. Barona-Gómez F, Wong U, Giannakopulos AE, Derrick PJ, Challis GL. Identification of a cluster of genes that directsdesferrioxamine biosynthesis in *Streptomyces coelicolor* M145. Journal of the American Chemical Society. 2004;126(50):16282–16283. https://doi.org/10.1021/ja045774k

70. Kadi N, Oves-Costales D, Barona-Gomez F, Challis GL. A new family of ATP-dependent oligomerization-macrocyclization biocatalysts. Nature Chemical Biology. 2007;3:652–656. https://doi.org/10.1038/nchembio.2007.23

71. de Lorenzo V, Bindereif A, Paw BH, Neilands JB. Aerobactin biosynthesis and transport genes of plasmid ColV-K30 in *Escherichia coli* K-12. Journal of Bacteriology. 1986;165(2):570–578. https://doi.org/10.1128/jb.165.2.570-578.1986

72. Challis GL. A widely distributed bacterial pathway for siderophore biosynthesis independent of nonribosomal peptide synthetases. ChemBioChem. 2005;6(4):601–611. https://doi.org/10.1002/cbic.200400283

73. Wang Y, Wilks JC, Danhorn T, Ramos I, Croal L, *et al*. Phenazine-1-carboxylic acid promotes bacterial biofilm development via ferrous iron acquisition. Journal of Bacteriology. 2011;193(14):3606–3617. https://doi.org/10.1128/jb.00396-11

74. Choi O, Cho J, Kang B, Lee Y, Kim J. Negatively regulated aerobactin and desferrioxamine E by fur in *Pantoea ananatis* are required for full siderophore production and antibacterial activity, but not for virulence. Applied and Environmental Microbiology. 2022;88(6):e0240521. https://doi.org/10.1128/aem.02405-21

75. Zhang L, Yang Q, Luo X, Fang C, Zhang Q, *et al*. Knockout of *crtB* or *crtI* gene blocks the carotenoid biosynthetic pathway in *Deinococcus radiodurans* R1 and influences its resistance to oxidative DNA-damaging agents due to change of free radicals scavenging ability. Archives of Microbiology. 2007;188:411–419. https://doi.org/10.1007/s00203-007-0262-5

76. Chen CH, Han RM, Liang R, Fu LM, Wang P, *et al*. Direct observation of the *β*-carotene reaction with hydroxyl radical. The Journal of Physical Chemistry B. 2011;115(9):2082–2089. https://doi.org/10.1021/jp1100889
77. Mohammadi M, Burbank L, Roper MC. Biological role of pigment production for the bacterial phytopathogen *Pantoea stewartii* subsp. *stewartii*. Applied and Environmental Microbiology. 2012;78(19):6859–6865. https://doi.org/10.1128/AEM.01574-12
78. Sedkova N, Tao L, Rouvière PE, Cheng Q. Diversity of carotenoid synthesis gene clusters from environmental *Enterobacteriaceae* strains. Applied and Environmental Microbiology. 2005;71(12):8141–8146. https://doi.org/10.1128/AEM.71.12.8141-8146.2005
79. Sandmann G. Carotenoid biosynthesis in microorganisms and plants. European Journal of Biochemistry. 1994;223(1):7–24. https://doi.org/10.1111/j.1432-1033.1994.tb18961.x
80. Perry KL, Simonitch TA, Harrison-Lavoie KJ, Liu ST. Cloning and regulation of *Erwinia herbicola* pigment genes. Journal of Bacteriology. 1986;168(2):607–612. https://doi.org/10.1128/jb.168.2.607-612.1986
81. Umeno D, Tobias AV, Arnold FH. Diversifying carotenoid biosynthetic pathways by directed evolution. Microbiology and Molecular Biology Reviews. 2005;69(1):51–78. https://doi.org/10.1128/mmbr.69.1.51-78.2005
82. Choi O, Kang B, Lee Y, Lee Y, Kim J. *Pantoea ananatis* carotenoid production confers toxoflavin tolerance and is regulated by Hfq-controlled quorum sensing. MicrobiologyOpen. 2021;10(1):e1143. https://doi.org/10.1002/mbo3.1143
83. Kumar SV, Taylor G, Hasim S, Collier CP, Farmer AT, *et al*. Loss of carotenoids from membranes of *Pantoea* sp. YR343 results in altered lipid composition and changes in membrane biophysical properties. Biochimica et Biophysica Acta (BBA) – Biomembranes. 2019;1861(7):1338–1345. https://doi.org/10.1016/j.bbamem.2019.05.009
84. Van Houdt R, Moons P, Aertsen A, Jansen A, Vanoirbeek K, *et al*. Characterization of a *luxI*/*luxR*-type quorum sensing system and *N*-acyl-homoserine lactone-dependent regulation of exo-enzyme and antibacterial component production in *Serratia plymuthica* RVH1. Research in Microbiology. 2007;158(2):150–158. https://doi.org/10.1016/j.resmic.2006.11.008
85. Moons P, Van Houdt R, Aertsen A, Vanoirbeek K, Engelborghs Y, *et al*. Role of quorum sensing and antimicrobial component production by *Serratia plymuthica* in formation of biofilms, including mixed biofilms with *Escherichia coli*. Applied and Environmental Microbiology. 2006;72(11):7294–7300. https://doi.org/10.1128/AEM.01708-06
86. Masschelein J, Mattheus W, Gao LJ, Moons P, Van Houdt R, *et al*. A PKS/NRPS/FAS hybrid gene cluster from *Serratia plymuthica* RVH1 encoding the biosynthesis of three broad spectrum, zeamine-related antibiotics. PLoS One. 2013;8(1):e54143. https://doi.org/10.1371/journal.pone.0054143
87. Fuchs SW, Grundmann F, Kurz M, Kaiser M, Bode HB. Fabclavines: Bioactive peptide-polyketide-polyamino hybrids from *Xenorhabdus*. ChemBioChem. 2014;15(4):512–516. https://doi.org/10.1002/cbic.201300802
88. Garlant L, Koskinen P, Rouhiainen L, Laine P, Paulin L, *et al*. Genome sequence of *Dickeya solani*, a new soft rot pathogen of potato, suggests its emergence may be related to a novel combination of non-ribosomal peptide/polyketide synthetase clusters. Diversity. 2013;5(4):824–842. https://doi.org/10.3390/d5040824
89. Wu J, Zhang HB, Xu JL, Cox RJ, Simpson TJ, *et al*. ^{13}C labeling reveals multiple amination reactions in the biosynthesis of a novel polyketide polyamine antibiotic zeamine from *Dickeya zeae*. Chemical Communications. 2010;46(2):333–335. https://doi.org/10.1039/b916307g
90. Zhou J, Zhang H, Wu J, Liu Q, Xi P, *et al*. A novel multidomain polyketide synthase is essential for zeamine production and the virulence of *Dickeya zeae*. Molecular Plant-Microbe Interactions. 2011;24(10):1156–1164. https://doi.org/10.1094/MPMI-04-11-0087
91. Liao L, Cheng Y, Liu S, Zhou J, An S, *et al*. Production of novel antibiotics zeamines through optimizing *Dickeya zeae* fermentation conditions. PLoS One. 2014;9(12):e116047. https://doi.org/10.1371/journal.pone.0116047
92. Liao L, Zhou J, Wang H, He F, Liu S, *et al*. Control of litchi downy blight by zeamines produced by *Dickeya zeae*. Scientific Reports. 2015;5:15719. https://doi.org/10.1038/srep15719

Additional information about the authors

Elizaveta R. Faskhutdinova ORCID 0000-0001-9711-2145; eLIBRARY SPIN 6173-3576
Natalya V. Fotina ORCID 0000-0002-7655-0258; eLIBRARY SPIN 5500-7190
Arina A. Shevel ORCID 0009-0000-3630-2826; eLIBRARY SPIN 5159-2151
Andrey V. Gordienko eLIBRARY SPIN 4209-7793
Alexey E. Tupikin ORCID 0000-0002-8194-0322; eLIBRARY SPIN 7084-4313
Gaurav Mudgal ORCID 0000-0003-4303-4983
Larisa M. Aksenova ORCID 0009-0009-9927-3642; eLIBRARY SPIN 6604-7452
Lyudmila K. Asyakina ORCID 0000-0003-4988-8197; eLIBRARY SPIN 4479-3384

Foods and Raw Materials. 2027;15(2)

ISSN 2308-4057 (Print)
ISSN 2310-9599 (Online)

Research Article
Open Access

Available online at http://jfrm.ru/en
https://doi.org/10.21603/2308-4057-2027-2-724
https://elibrary.ru/EMMLQJ

The probiotic potential of microorganism strains: A comprehensive study

Anna S. Frolova, Anna D. Vesnina*, Anastasiya M. Fedorova, Elena V. Ostapova, Vladimir P. Yustratov, Irina S. Milentyeva

[1] Kemerovo State University, Kemerovo, Russia

* e-mail: koledockop1@mail.ru

Received 17.03.2026; Revised 14.04.2026; Accepted 02.06.2026; Published online 29.09.2026

Abstract:
Probiotics are live microorganisms that exert beneficial effects on the host by modulating the gut microbiota and synthesizing bioactive compounds. Of particular importance are metabolites involved in energy metabolism, including compounds of the tricarboxylic acid cycle and B vitamins, which act as coenzymes. This necessitates the search for strains with pronounced metabolic activity and resistance to gastrointestinal conditions. We aimed to comprehensively evaluate the *in vitro* probiotic potential of specific microbial strains for their subsequent use in dietary supplements and functional foods.

We studied the following strains: *Propionibacterium troenii* (B-6083, B-6080), *Weissella thailandensis* (B-10412), *Bifidobacterium bifidum* (AC-1779), *Bifidobacterium longum* (AC-1257), *Pediococcus acidilactici* (B-7509, B-7533), and *Enterococcus faecium* (B-4054). The commercial probiotics "Hemopropiovit" and "Bifiform" were used as the controls. The strains' antibiotic resistance was determined by the disk diffusion method, their survival in the gastrointestinal tract was measured spectrophotometrically, their antagonistic activity was analyzed by the agar diffusion method, while the compositions and contents of microbial metabolites were identified by high-performance liquid chromatography.

The strains were sensitive to antibiotics (inhibition zones > 21 mm), with the highest values recorded for B-6083 (50.6 ± 4.1 mm). High resistance to bile was demonstrated by B-7509 and B-7533 (optical density 2.288 ± 0.049 and 2.364 ± 0.028 at 0.5% bile), as well as B-4054 (optical density 1.242 ± 0.005 at 40.0% bile). The strains AC-1257, B-7509, and B-7533 showed resistance to 6.5% NaCl. The most pronounced antagonistic activity was demonstrated by B-6083 against *Escherichia coli* (inhibition zone 29.47 ± 0.50 mm) and by B-7533 against *Bacillus cereus* (23.07 ± 0.47 mm). The strains exhibited high metabolic activity such as synthesizing bioactive compounds. The highest content of vitamin B_1 was found in B-10412 (23.10 ± 0.44 mg/g), while succinic acid predominated in B-6080 (432.2 ± 8.2 mg/L). The highest total contents of amino acids were observed in B-7509 (145.2 mg/g) and B-10412 (142.1 mg/g). Some strains showed high probiotic potential by demonstrating resistance to stress factors and exhibiting high antagonistic activity.

The strains B-7509, B-7533, AC-1257, B-10412, B-4054, B-6083, and B-6080 possess significant probiotic potential and may be considered as promising components for dietary supplements and functional foods. However, further research is needed such as *in vivo* studies in rodents.

Keywords: Probiotics, probiotic potential, lactic acid bacteria, antagonistic activity, resistance to gastrointestinal stress factors, bioactive metabolites

Funding: This study was part of the state assignment on "Development of biologically active additives consisting of metabolites of plant objects in vitro to protect the population from premature aging" (project FZSR-2024-0008) and made use of the facilities of the Collective Use Center "Instrumental Methods of Analysis in Applied Biotechnology" at Kemerovo State University.

Please cite this article in press as: Frolova AS, Vesnina AD, Fedorova AM, Ostapova EV, Yustratov VP, *et al.* The probiotic potential of microorganism strains: A comprehensive study. Foods and Raw Materials. 2027;15(2):474–494. https://doi.org/10.21603/2308-4057-2027-2-724

INTRODUCTION

Probiotics are live microorganisms that provide health benefits if administered in sufficient amounts [1–4]. Their functional value is determined by their complex interactions with the gut microbiota, metabolic pathways, and immune regulatory mechanisms [5–7].

According to modern research, the gut microbiome is key to maintaining homeostasis. Particularly, it influences energy metabolism, the synthesis of bioactive compounds, and the development of the immune response [8–10]. Probiotic microorganisms are therefore an effective tool for maintaining microbial balance and preventing dysbiosis [11–15]. Modern studies of bioac-

Copyright © 2026, Frolova *et al.* This is an open access article distributed under the terms of the Creative Commons Attribution 4.0 International License (https://creativecommons.org/licenses/by/4.0/), allowing third parties to copy and redistribute the material in any medium or format and to remix, transform, and build upon the material for any purpose, even commercially, provided the original work is properly cited and states its license.

tive components in foods have confirmed the role of probiotics in modulating the gut microbiota and regulating inflammatory processes and metabolic disorders [16–18].

Lactic acid bacteria (LAB) are of particular importance among probiotic cultures. These are anaerobic, Gram-positive microorganisms that can grow in the presence of oxygen [19, 20]. Scientists began to take interest in their dietary use at the beginning of the 20th century, when a hypothesis was proposed that fermented dairy products had a positive effect on human health [21].

Currently, LAB are recognized for their role in synthesizing a wide range of compounds that ensure microbiological stability and improve the quality of food products [22, 23]. Most of their functional properties are strain-specific, which necessitates their individual analyses *in vitro* and *in vivo* [24, 25].

LAB of the genera *Lactococcus* [26], *Pediococcus* [27], *Weissella* [28], and *Enterococcus* [29] have common physiological and biochemical characteristics, as well as the capacity for lactic acid fermentation. *Lactococcus* bacteria are traditionally used as a starter culture for intensive lactose fermentation and the formation of desirable sensory characteristics [30]. *Pediococcus* and *Weissella* bacteria have a high technological value and antagonistic activity against foreign microflora due to their ability to produce bacteriocins and exopolysaccharides [27, 31]. Some bacteriocins produced by LAB hold the GRAS status. Therefore, bacteriocins prooduced by LAB are widely used in food industry and in pharmaceutical industry [32]. Although bacteria of the genus *Enterococcus* also belong to lactic acid bacteria, their use in food and probiotic systems requires strict safety control [33].

Apart from LAB, probiotic compositions can include other bacteria with similar functionalities. For example, members of the genus *Bifidobacterium* are among the most abundant symbionts in the human gut, contributing to the formation of metabolic and immune homeostasis [34]. They produce bioactive compounds that help maintain colonization resistance and reduce the risk of dysbacteriosis [35].

Bacteria of the genus *Propionibacterium* produce propionic and acetic acids, as well as B vitamins [36]. They are used in functional foods due to their metabolic activity and ability to synthesize antimicrobial compounds [37].

The functional activity of probiotic microorganisms is largely determined by the range of metabolites they synthesize. For example, their antimicrobial, anti-inflammatory, and metabolic regulatory activities are due to organic acids, short-chain fatty acids, and other bioactive compounds that they produce [38, 39]. Furthermore, probiotics actively participate in substrate and energy metabolism, creating conditions for gut homeostasis [40, 41].

Organic acids synthesized by probiotic bacteria are particularly important metabolites that regulate microbiota and metabolic processes [42]. When accumulated in large amounts, they decrease the pH and inhibit the growth of opportunistic microorganisms, contributing to the antimicrobial activity of probiotic cultures [43]. In addition, compounds such as citric and succinic acids are important intermediate metabolites involved in the tricarboxylic acid cycle, which promotes cellular respiration and energy synthesis [44–47].

Amino acids, both essential and nonessential, are equally important metabolites of probiotic bacteria [48–50]. They are involved in maintaining the body's physiological functions and metabolic interactions [51]. Amino acids perform a structural function, regulate immune responses, and act as precursors of bioactive compounds [52].

Probiotic microorganisms also participate in the metabolism of B vitamins. The gut microbiota and probiotic bacteria can synthesize vitamins B_1, B_2, B_3, B_5, B_6, B_9, and B_{12}, which act as coenzymes in key metabolic reactions [53–55]. These vitamins are involved in the metabolism of carbohydrates, fatty acids, and amino acids, as well as in mitochondrial function and cellular energy supply. Participating in cellular respiration, they regulate the Krebs cycle, which supplies the body with energy [56].

In this study, we aimed to assess *in vitro* the probiotic potential of *Lactococcus*, *Pediococcus*, *Weissella*, *Enterococcus*, *Bifidobacterium*, and *Propionibacterium* strains for their subsequent use in dietary supplements and functional foods to prevent metabolic disorders.

STUDY OBJECTS AND METHODS

The following strains were obtained from the All-Russian Collection of Industrial Microorganisms at the State Research Institute of Genetics and Selection of Industrial Microorganisms, the Kurchatov Institute National Research Center (Russia): *Propionibacterium troenii* T-127 (B-6083); *Propionibacterium troenii* T-126 (B-6080); *Weissella thailandensis* A12 (B-10412); *Bifidobacterium bifidum* E319f (AC-1779); *Bifidobacterium longum* U-4 (AC-1257); *Bifidobacterium longum* BGV-11 (AC-1742); *Lactococcus lactis subsp. cremoris* 55 K 2-2-2 (B-1689); *Lactococcus lactis subsp. cremoris* 791 7 (B-1688); *Pediococcus acidilactici* P-60 (B-7509); *Pediococcus acidilactici* P 60 (B-7533); *Enterococcus faecium* 320 D (B-5000); and *Enterococcus faecium* JDC 86 (B-4054).

The lyophilized cultures were incubated in a sterile solution of 0.9% NaCl for 30 ± 5 min and then transferred onto nutrient media. Strains B-6083, B-6080, B-10412, B-7509, B-7533, and B-5000 were inoculated onto MRS medium, g/L, composed of: 21.5 pancreatic hydrolysate of fish meal with Tween (Dia-M, Russia); 5.0 baker's yeast extract (Dia-M, Russia); 5.0 peptone (Gelatin Peptone, Spain); 20.0 glucose (Pharmstandard Leksredstva, Russia); 2.0 KH_2PO_4 (Chem-ex, Russia); 3.0 sodium acetate (Chem-ex, Russia); 2.0 ammonium citrate dibasic (Chem-ex, Russia); 0.1 $MgSO_4 \times 7H_2O$ (Chem-ex, Russia); and 0.05 $MnCl_2 \times 4H_2O$ (Chem-ex, Russia). Strains AC-1779, AC-1257, AC-1742, B-1689, B-1688, and B-4054 were inoculated onto Bifidum medium, g/L, composed of: 30.0 pancreatic casein hydrolysate (Dia-M, Russia); 5.0 baker's yeast extract; 7.5 glucose; 2.5 lactose (Chem-ex, Russia); 0.5 cysteine (Dia-M, Russia); 2.5 NaCl (REAKHIM, Russia); 0.5 $MgSO_4 \times 7H_2O$; 0.5 ascorbic acid (Dia-M, Russia); and 0.3 sodium acetate. The strains grown on the nutrient media were stored at 4 ± 1°C.

The following commercial probiotic preparations were purchased from the Edelweiss-O pharmacy (Russia) to be used as positive controls:
– Hemopropiovit (control 1), which contains *Propionibacterium freudenreichii* III85, *Bifidobacterium bifidum* 83, and *Lactococcus lactis* subsp. *cremoris* 244;
– Bifiform (control 2), which contains *Enterococcus faecium* and *Bifidobacterium longum*.

Cultural characterization. For cultural characterization, daily cultures were pre-grown on MRS or Bifidum agar nutrient media. Bacterial strain suspensions were surface-seeded onto the media with a Drygalski spatula. Their morphological characteristics were assessed after Gram staining [57] using a Micro-GRAM-NITsF reagent kit (MiniMed, Russia) and an AxioScope A1 upright microscope (Carl Zeiss AG, Germany).

The cultures were further cultivated at 37 ± 2°C to imitate the physiological conditions of the human gastrointestinal tract and identify those strains which could be adapted to *in vivo* conditions [58].

Preparation of bacterial suspensions. Microbial strains were plated on MRS or Bifidum solid nutrient media. Daily cultures were cultivated in a TV-80-1 thermostat (Ryazan Instrument-Making Plant, Russia). The microbial suspensions were adjusted to a density of 0.5 on the McFarland scale in the corresponding liquid media using a Densichek Plus densitometer (BioMerieux, France). Strains from passages 3–4 were used in further studies.

Antibiotic resistance. Antibiotic resistance of the strains was assessed by the disk diffusion method [59]. For this, 100 μL of a bacterial suspension was inoculated onto the surface of the agar medium. Then, disks were placed with azithromycin (15 μg), cephalexin (30 μg), gentamicin (120 μg), streptomycin (300 μg), and tetracycline (30 μg) (Bio-Rad, France). Disks soaked in distilled water were used as a negative control. After 24 ± 1 h of incubation, the diameters of the inhibition zones were measured and the strains were classified as resistant (< 9.9 mm), intermediate (10.0–20.9 mm), or sensitive (> 21.0 mm).

Resistance to gastrointestinal conditions. Resistance to bile, salt, and stressful pH conditions was determined spectrophotometrically at 600 nm using a Shimadzu UV-1800 spectrophotometer (Shimadzu Corporation, Japan) [60]. Resistance to bile (0.5, 20.0, and 40.0% of the medium volume) was determined as described by Kitaevskaya [61]. Resistance to elevated salt (NaCl) concentrations (2.0, 4.0, and 6.5% of the medium volume) and to stressful pH conditions (2.0, 3.0, 5.0, and 9.2) was determined as described in General Pharmacopoeia Monograph 1.7.2.0012.15, "Industrial probiotic strains and probiotic control strains". Optical density was measured relative to the nutrient medium without a microbial suspension. Samples of nutrient media inoculated with microbial suspensions were used as negative controls.

Antimicrobial activity of bacterial metabolites. Antagonistic activity of microbial metabolites was determined by the agar diffusion method as described by Davoodabadi *et al.* [62] and Pazhoohan *et al.* [63]. The strains obtained from the All-Russian Collection of Industrial Microorganisms (Russia) were used as test cultures, namely: *Escherichia coli* (B-6645); *Pseudomonas aeruginosa* (B-8243); *Bacillus cereus* (B-8076); *Enterococcus faecalis* (B-8173); *Klebsiella pneumoniae* (B-7001).

For this, 300 μL of a suspension of test cultures (0.5 McFarland turbidity) was inoculated onto a solid nutrient medium (MPA), g/L, composed of: 10.0 peptone; 11.0 meat extract (HiMedia, India); 5.0 NaCl; and 20.0 bacteriological agar (HiMedia, India). Wells with a diameter of 6–8 mm were filled with 50 μL of the culture broth with microbial metabolites, while the control well was filled with 50 μL of distilled water (negative control). A disk with an antibiotic (positive control) was placed in the center of the plate, namely: streptomycin (300 mg), cephalexin (30 μg), gentamicin (120 μg), and tetracycline (30 mg). The plates were kept at room temperature (22 ± 2°C) for 1–2 h and then incubated at 37 ± 2°C for 16–18 h. Antagonist activity was determined by measuring the inhibition zones and classified as "no activity" (< 10.9 mm), "weak" (11.0–16.9 mm), "moderate" (17.0–22.9 mm), or "high" (> 23.0 mm) [64].

To obtain microbial metabolites, a microbial suspension (10% of the medium volume) was added to centrifuge tubes (Eppendorf, Germany) containing the nutrient medium and cultivated under steady-state conditions in a TV-80-1 thermostat. The biomass was separated from the culture broth at 7,000 g in a 5430 centrifuge (Eppendorf, Germany). The culture broth was subsequently tested for antagonist activity and biocompatibility.

Microbial growth curves. Microbial growth curves were obtained to identify points of exponential growth, stationary growth, and the death phase and to study the qualitative and quantitative composition of metabolites at these points. The growth curves were obtained spectrophotometrically at 600 nm in real time using an RTS-8 Plus bioreactor (Biosan, Latvia) [65]. For this, a bacterial suspension was inoculated into liquid MRS or Bifidum media (5% of the medium volume) and cultivated under stationary conditions until the death phase was reached.

Quantitative determination of metabolites. The composition of metabolites was determined by high-performance liquid chromatography (HPLC) on a Shimadzu LC-20 Prominence chromatograph (Shimadzu Corporation, Japan) with a Shimadzu SPD20MA diode array detector and a Phenomenex Gemini 5 μm C-18,250×4.6 mm column. Water-soluble vitamins were determined according to State Standard R 55482-2013 and as described by Frolova *et al.* [66]. Organic acids were determined according to State Standard 33410-2015. Amino acids were determined by reversed-phase HPLC as described by Belashova *et al.* [67].

The microbial strains were cultivated under stationary conditions and sampled at three growth points: exponential, stationary, and death phases. The samples were analyzed for water-soluble B vitamins (B_1, B_2, B_3, B_5, B_6, and B_{12}), amino acids (tryptophan, glutamic acid,

serine, glycine, histidine, glutamine, arginine, lysine, threonine, alanine, proline, asparagine, tyrosine, methionine, valine, cysteine, cystine, leucine, isoleucine, and phenylalanine), and organic acids (oxalic, tartaric, maleic, citric, and succinic acids).

Biocompatibility of the strains. Biocompatibility was assessed by using the agar diffusion method with some modification [68]. A microbial suspension was uniformly applied to MRS or Bifidum agar media. Then, 50 μL of the culture broth was placed into wells with a diameter of 6–8 mm. The plates were kept at 22 ± 2°C for 1–2 h and then incubated at 37 ± 2°C for 16–18 h. Strain biocompatibility was assessed by measuring the growth inhibition zone: growth inhibition (> 10.0 mm; indicated as "–"); biocompatibility (< 10.0 mm with no signs of growth stimulation; indicated as "+"); and growth stimulation (< 10.0 mm with signs of growth stimulation; indicated as "++").

The assays were performed in triplicate and the results were presented as a mean and standard error.

RESULTS AND DISCUSSION

Cultural characterization. Since the strains were obtained from the All-Russian Collection of Industrial Microorganisms, their taxonomic affiliation and safety needed no confirmation. Based on Gram staining, the strains were characterized as Gram-positive bacteria.

Cultural and morphological analysis revealed that the colonies cultivated on agar nutrient media possessed genus-specific characteristics. The colonies had a rounded, convex shape, with smooth edges and a shiny white surface. The colony's diameter of 1–2 mm was consistent with the standard morphological characteristics of the strains of their genus.

Antibiotic resistance. The European Food Safety Authority and the World Health Organization emphasize in their guidelines that the strains used in the food industry should not contain transferable genes conferring resistance to clinically significant antibiotics. We tested the strains under study for their susceptibility to a range of antibiotics (Table 1).

We found that the susceptibility of microorganisms to antibiotics varied significantly between the bacterial strains and genera. The antibiotic resistance of B-10412 and B-4054 was previously described in [69]. Most of the cultures exhibited high sensitivity to the tested antibiotics, with zones of growth inhibition greater than 21 mm in diameter.

Control 1 demonstrated intermediate sensitivity to many antibiotics. The growth inhibition zones were 10.0–15.3 mm for azithromycin, cephalexin (CXN), gentamicin, and streptomycin (HLS). However, Control 1 was found to be sensitive to tetracycline (TET). In comparison, Control 2 exhibited higher sensitivity to the antibiotics, especially to azithromycin and TET.

The highest sensitivity to azithromycin was found in Strains B-6083, B-6080, B-1688, and B-1689. Their inhibition zones were 2.0–3.5 times as large as those of Control 1. Strains B-7509 and B-7533 showed smaller growth inhibition zones compared to the other strains. Yet, they were 1.4–2.0 times larger than those of Control 1, but 1.3–1.8 times smaller than those of Control 2. Thus, the cultures retained high sensitivity to macrolide antibiotics, which is consistent with a study of lactic acid bacteria by Duche *et al.* [70].

Most strains were sensitive to cephalexin, with the largest growth inhibition zones (over 50.0 mm in diameter) recorded for the genus *Propionibacterium* (B-6083, B-6080). Strains B-7509 and B-7533, however, showed significantly smaller inhibition zones, indicating their high resistance to *β*-lactam antibiotics. Given the widespread use of these drugs in veterinary medicine and animal husbandry, the identified sensitivity values can be considered a positive sign, since they demonstrate a lower risk of accumulation and transmission of antibiotic resistance genes through horizontal transfer [71].

Table 1 Effect of antibiotics on the growth of the strains assessed by the disk diffusion method

Sample	Diameter of growth inhibition zone, mm					
	Azithromycin, 15 μg	Cephalexin, 30 μg	Gentamicin, 120 μg	Streptomycin, 300 μg	Tetracycline, 30 μg	Water
B-6083	31.2 ± 0.8	55.4 ± 0.5	39.9 ± 1.0	19.3 ± 3.1	50.6 ± 4.1	0.0 ± 0.0
B-6080	35.6 ± 5.1	54.6 ± 2.5	46.4 ± 0.5	26.5 ± 1.4	45.8 ± 1.6	0.0 ± 0.0
AC-1779	15.9 ± 1.0	36.5 ± 0.5	29.4 ± 0.6	18.6 ± 1.5	19.5 ± 0.5	0.0 ± 0.0
AC-1257	11.7 ± 1.5	34.6 ± 06	23.1 ± 2.0	17.1 ± 1.0	15.4 ± 0.5	0.0 ± 0.0
AC-1742	–	–	–	–	–	–
B-1689	21.1 ± 1.0	32.5 ± 0.5	29.5 ± 8.8	29.9 ± 2.0	23.3 ± 0.8	0.0 ± 0.0
B-1688	22.5 ± 0.5	37.4 ± 0.5	22.4 ± 0.5	20.5 ± 0.5	23.5 ± 0.5	0.0 ± 0.0
B-7509	14.2 ± 0.3	10.1 ± 1.0	10.2 ± 0.3	11.4 ± 0.5	17.2 ± 0.9	0.0 ± 0.0
B-7533	19.5 ± 5.2	13.4 ± 1.5	15.1 ± 1.0	9.4 ± 0.5	26.6 ± 5.8	0.0 ± 0.0
B-5000	–	–	–	–	–	–
Control 1 (Hemopropiovit)	10.0 ± 1.0	11.7 ± 2.9	15.3 ± 5.0	15.3 ± 0.6	24.0 ± 2.6	0.0 ± 0.0
Control 2 (Bifiform)	25.7 ± 4.0	14.2 ± 0.3	23.3 ± 3.1	21.3 ± 1.5	29.3 ± 2.1	0.0 ± 0.0

"–" – indicates no growth during the test

Most studied cultures exhibited sensitivity to gentamicin. This antibiotic had the greatest inhibitory effect on Strains B-6083 and B-6080. Their growth inhibition zones were 2.6–3.0 and 1.7–2.0 times as large as those of Control 1 and Control 2, respectively. Strains B-1689, B-1688, and AC-1779 also showed larger (1.5–1.9 times) inhibition zones than those of Control 1. Strains B-7509 and B-7533 demonstrated intermediate resistance. The inhibition of Strain B-7509 was 1.5 times lower than that of Control 1, while this indicator for Strain B-7533 was close to that of Control 1. Resistance to aminoglycosides is natural due to the low permeability of cell membranes and energy metabolism. The significant sensitivity of some strains in our study may indicate the lack of pronounced natural resistance [70].

Streptomycin had the greatest inhibitory effect on Strains B-1689 and B-1688. Strains AC-1779 and AC-1257 showed intermediate resistance, while B-7533 was found highly resistant. This resistance may be associated with the presence of antibiotic resistance genes, such as *aadA*, which encode aminoglycoside enzymes and can be transmitted to other bacteria through horizontal transfer. A number of studies have shown that while adapting to streptomycin, probiotic microorganisms can develop cross-resistance to other antibiotics. This emphasizes the need to evaluate the safety of probiotic strains in terms of the possible spread of resistance genes [72].

Most strains exhibited high sensitivity to tetracycline. The largest zones of growth inhibition were observed for Strains B-6083 and B-6080, with their diameters being 1.9–2.1 and 1.5–1.7 times greater than those for Control 1 and Control 2, respectively. Strains B-1688, B-1689, and B-7533 also showed larger (1.1–1.5 times) inhibition zones than Control 1 and comparable or slightly larger zones than Control 2. In contrast, Strains AC-1779, AC-1257, and B-7509 demonstrated intermediate resistance, with their inhibition zones being smaller than those for Control 1 (1.2–1.5 times) and Control 2 (1.5–1.7 times). Bacterial resistance to this antibiotic is most often associated with the presence of specific resistance genes, such as *tet(A), tet(L), tet(K),* and *tet(M)*, which encode mechanisms for active antibiotic efflux from the cell or ribosome protection [73]. Therefore, the intermediate resistance detected in individual strains may indicate potential development of such mechanisms, which requires additional molecular genetic analysis.

Strains AC-1742 and B-5000 did not show any growth on the nutrient media. This could be due to their specific physiological requirements for cultivation conditions.

Resistance to gastrointestinal conditions. An important criterion for selecting a probiotic strain is its survivability in the gastrointestinal tract, specifically its resistance to bile, elevated salt (NaCl) concentrations, and stressful pH conditions. We assessed changes in strain biomass growth in the nutrient media supplemented with varying amounts of bile (Table 2).

The control samples demonstrated high resistance to bile. Specifically, at 0.5% bile, optical density increased 1.1–1.2 times. At higher concentrations (20.0–40.0%), optical density remained at comparable levels or decreased 1.2–1.5 times.

In most cases, adding 0.5% of bile resulted in lower culture growth compared to the control (without bile), but the degree of inhibition varied significantly between the strains. Strains B-7509 and B-7533 demonstrated the highest resistance, which remained steady and only decreased 1.1 times. Their growth was 1.3–1.5 times as high as that of Controls 1 and 2. Strain B-4054 was also resistant, with higher optical density compared to the control. Strains B-6083 and B-6080 showed a 1.9–2.8-fold decrease in growth compared to the control, indicating their sensitivity to bile at 0.5%. Strains AC-1779 and AC-1257 demonstrated higher resistance. Their

Table 2 Effect of bile on strain growth

Sample	Optical density at 600 nm			
	Control (–)	Bile 0.5 %	Bile 20.0 %	Bile 40.0 %
B-6083	1.065 ± 0.004	0.554 ± 0.325	0.335 ± 0.011	0.518 ± 0.012
B-6080	1.143 ± 0.278	0.408 ± 0.070	0.347 ± 0.005	0.461 ± 0.005
B-10412	1.271 ± 0.140	0.784 ± 0.124	0.294 ± 0.001	0.439 ± 0.015
AC-1779	0.700 ± 0.008	0.529 ± 0.053	0.341 ± 0.007	0.468 ± 0.003
AC-1257	1.357 ± 0.027	0.946 ± 0.021	0.311 ± 0.007	0.402 ± 0.002
AC-1742	–	–	–	–
B-1689	0.538 ± 0.002	0.095 ± 0.003	0.242 ± 0.001	0.420 ± 0.013
B-1688	0.491 ± 0.025	0.099 ± 0.003	0.275 ± 0.008	0.462 ± 0.010
B-7509	2.402 ± 0.007	2.288 ± 0.049	0.962 ± 0.163	0.577 ± 0.229
B-7533	2.433 ± 0.001	2.364 ± 0.028	1.362 ± 0.020	0.887 ± 0.051
B-5000	–	–	–	–
B-4054	1.560 ± 0.003	1.568 ± 0.047	0.992 ± 0.067	1.242 ± 0.005
Control 1 (Hemopropiovit)	1.491 ± 0.015	1.710 ± 0.009	1.515 ± 0.019	1.045 ± 0.168
Control 2 (Bifiform)	1.549 ± 0.006	1.625 ± 0.019	1.933 ± 0.087	1.246 ± 0.028

"–" indicates no growth during the test

growth reduced 1.3–1.4 times and was 1.2–1.5 times lower than that of Controls 1 and 2. Strains B-1688 and B-1689 were the most sensitive to bile at 0.5%. Their growth reduced 4.9–5.7 times and was 10–15 times lower than that of Controls 1 and 2.

Increasing the bile concentration to 20.0% caused a more pronounced growth inhibition in most of the cultures. Strains B-6083, B-6080, AC-1257, and B-10412 showed a 3.3–4.3-fold decrease in growth relative to the bile-free control. Their growth was 4.5–6.5 times lower compared to Controls 1 and 2. Strain AC-1779 showed a 2.1-fold decrease in optical density compared to the bile-free control. Strains B-1688 and B-1689 also demonstrated a significant decrease in growth (1.8–2.2 times). Strains B-7509, B-7533, and B-4054 were the most resistant, showing a 2.5, 1.8, and 1.6-fold decrease in growth, respectively. Although their growth was higher than that of most other strains, it was still 1.4–2.0 times lower than that of the controls.

A 40.0% concentration of bile inhibited the growth of most strains, although some cultures maintained relatively high growth rates. Strains B-6083 and B-6080 demonstrated a 2.1–2.5-fold decrease in growth compared to the initial level. Yet, their growth remained higher than that at 20.0% bile, which may indicate partial adaptation. Compared to Controls 1 and 2, their growth was 2.0–2.5 times lower. Strains AC-1779 and AC-1257 showed a 1.5–3.4-fold decrease in growth relative to the initial level. Their growth was 2.5–3.0 times lower compared to the controls. Strains 16-88 and B-1689 showed pronounced sensitivity. Despite a slight increase in growth compared to 20.0% bile, their growth remained 1.02–1.30 times lower than the initial level and 2.5–3.0 times lower compared to the controls. Strains B-7509, B-7533, and B-4054 were the most resistant, with a 4.2, 2.7, and 1.3-fold decrease in growth, respectively, compared to the bile-free control. Their growth rates were closest to those of Controls 1 and 2.

Thus, Strains B-7509 and B-7533 were the most resistant to bile at 0.5–20.0%, while B-4054 exhibited the highest resistance to bile at 40.0%. In some cases, their growth rates were 3.0–5.0 times as high as those of less resistant strains and were comparable to those of commercial probiotics.

Our results are consistent with those reported by Hu *et al.* [74]. Their study of the *Pediococcus acidilactici* strain revealed a decrease in culture viability with increasing bile salt concentrations. Some cultures maintained high growth rates even at elevated bile concentrations. This indicates the presence of adaptive resistance mechanisms that allow certain strains to overcome the inhibitory effect of bile and maintain their probiotic potential.

Bile has a pronounced antimicrobial effect, disrupting the integrity of cell membranes and causing protein denaturation. Therefore, the ability of bacteria to maintain growth under such conditions is an important indicator of their probiotic potential. Several studies have shown high survival of certain bifidobacteria strains exposed to bile salts. This survival is associated with the development of stable physiological mechanisms for adaptation to these conditions [75].

Probiotic strains must be resistant to elevated salt levels as they pass through the gastrointestinal tract. Therefore, we assessed changes in strain biomass growth in nutrient media with varying NaCl concentrations (Table 3).

At 2.0, 4.0, and 6.5% NaCl, Control 1 showed a 1.3, 1.5, and 1.1-fold decrease in optical density, respectively, compared to its initial level. Control 2 exhibited more stable growth. At 2.0 and 4.0% NaCl, its optical density decreased 1.1-fold, whereas at 6.5%, it decreased 1.5-fold. Thus, Control 2 demonstrated higher resistance to the effects of salt compared to Control 1.

The resistance of Strains B-10412 and B-4054 to NaCl was described in our previous work [69]. At 2.0% NaCl, most of the strains retained their growth, with varying changes in optical density. Strains B-7509 and B-7533 showed virtually no response to salt stress. Their optical density remained at the initial salt-free level (1.1-fold difference) and exceeded the values for Control 1 and 2 (2.1 and 1.7 times, respectively). Strains

Table 3 Effect of elevated salt levels on strain growth

Sample	Optical density at 600 nm			
	Control (–)	NaCl 2.0%	NaCl 4.0%	NaCl 6.5%
B-6083	1.065 ± 0.004	0.691 ± 0.029	0.480 ± 0.008	0.340 ± 0.008
B-6080	1.143 ± 0.278	1.030 ± 0.034	1.083 ± 0.057	0.635 ± 0.051
AC-1779	0.700 ± 0.008	0.688 ± 0.012	0.904 ± 0.057	0.713 ± 0.140
AC-1257	1.357 ± 0.027	1.394 ± 0.073	1.392 ± 0.022	1.397 ± 0.064
AC-1742	–	–	–	–
B-1689	0.538 ± 0.002	0.433 ± 0.011	0.229 ± 0.049	0.117 ± 0.004
B-1688	0.491 ± 0.025	0.675 ± 0.032	0.718 ± 0.011	0.360 ± 0.209
B7509	2.402 ± 0.007	2.412 ± 0.020	2.189 ± 0.002	1.713 ± 0.009
B7533	2.433 ± 0.001	2.419 ± 0.004	2.157 ± 0.002	0.910 ± 0.040
B-5000	–	–	–	–
Control 1 (Hemopropiovit)	1.491 ± 0.015	1.130 ± 0.168	0.962 ± 0.010	1.390 ± 0.355
Control 2 (Bifiform)	1.549 ± 0.006	1.444 ± 0.013	1.358 ± 0.012	1.057 ± 0.095

"–" – indicates no growth during the test

AC-1257 and B-6080 also demonstrated high resistance. Their optical density was comparable with the initial level (1.1-fold difference) and was 1.2–1.3 times as high as that for Control 1. Strain AC-1779 showed virtually no change in growth, but its optical density was 1.6 and 2.1 times lower than that for Control 1 and 2, respectively. Strain B-6083 had a 1.5-fold decrease in growth and was inferior to Control 1 and 2 (1.6 and 2.1 times, respectively). Strain B-1689 was the most sensitive, its optical density being 1.2 times lower than the initial level, as well as 2.6 and 3.3 times lower than the values for Control 1 and 2, respectively.

At 4.0% NaCl, most strains retained their resistance, but some had more pronounced changes. Strains B-7509 and B-7533 remained highly resistant, with a 1.1-fold decrease in optical density and higher values compared to Control 1 and 2 (2.3 and 1.6 times, respectively). Strain AC-1257 demonstrated stable growth, 1.4 times the value for Control 1. The growth of Strain B-6080 remained at the initial level and was comparable with Control 2. Strain AC-1779 showed a 1.3-fold increase in optical density over the initial level, but remained 1.5 times lower than Control 2. Strain B-6083 had a 2.2-fold decrease in growth, its optical density being 2.0 and 2.8 times lower than Control 1 and 2, respectively. The most pronounced growth inhibition was observed in Strain B-1689, with a 2.3-fold decrease and optical density being 4.2 times and almost 6.0 times lower than the values for Control 1 and 2, respectively.

At 6.5% NaCl, some of the strains showed a more pronounced decrease in growth, while others retained a relatively high resistance. Strain AC-1257 maintained high growth, its optical density remaining virtually unchanged at 1.3 times over Control 2. Strain B-7509 showed a 1.4-fold decrease, but its optical density was 1.2 and 1.6 times as high as the values for Control and 2, respectively. Strain B-7533 had a more pronounced decrease (2.7 times), but its optical density was 1.2 and 1.5 times lower than Control 2 and 1, respectively. Strain B-6080 showed a 1.8-fold decrease in growth and its optical density was 2.2 and 1.7 times lower than that of Control 1 and 2, respectively. Strain AC-1779 showed virtually no decrease in growth, but its optical density was 2.0 and 1.5 times lower than that of Control 1 and 2, respectively. Strain B-6083 demonstrated a 3.1-fold decrease in growth, with its optical density being 4.1 and 3.1 times lower than that of Control 1 and 2, respectively. Strain B-1689 was the most sensitive, with its optical density decreasing 4.6-fold, which was 11.9 and 9.0 times lower than the values for Control 1 and 2, respectively.

Thus, according to the results, Strains AC-1257, B-7509, and B-7533 demonstrated the greatest resistance to elevated salt levels and maintained high growth at 6.5% NaCl. Meanwhile, Strain B-1689 was the most sensitive to salt stress. Overall, the growth rates of several cultures under study were comparable to those for the control probiotic preparations.

Our results are consistent with the studies reporting that lactic acid bacteria can tolerate elevated concentrations of NaCl and maintain growth at 6.5% NaCl. Madushanka *et al.* [76] found that most isolates of lactic acid bacteria retained growth at NaCl concentrations of up to 6.5% due to their physiological and biochemical mechanisms of adaptation to osmotic stress. Nidamarthi *et al.* [77] demonstrated that probiotic strains were able to maintain growth at up to 6.0% NaCl, but then moderately decreased growth at higher concentrations.

Probiotic strains must maintain their viability under stressful pH conditions as they pass through the gastrointestinal tract. Therefore, we assessed their biomass growth in nutrient media with pH values of 2.0, 3.0, 5.0, and 9.2 (Table 4).

The acidic and alkaline environments had a pronounced effect on the growth of the strains under stressful pH conditions, with varying degrees of resistance.

Table 4 Effect of stressful pH conditions on strain growth

Sample	Optical density at 600 nm				
	Control (–)	pH 2.0	pH 3.0	pH 5.0	pH 9.2
B-6083	1.065 ± 0.004	0.180 ± 0.001	0.202 ± 0.008	0.173 ± 0.001	1.761 ± 0.041
B-6080	1.143 ± 0.278	0.155 ± 0.001	0.169 ± 0.007	0.154 ± 0.002	1.269 ± 0.156
B-10412	1.271 ± 0.140	0.157 ± 0.001	0.285 ± 0.135	0.113 ± 0.001	1.373 ± 0.157
AC-1779	0.700 ± 0.008	0.079 ± 0.002	0.067 ± 0.001	0.250 ± 0.005	0.328 ± 0.090
AC-1257	1.357 ± 0.027	0.077 ± 0.001	0.074 ± 0.001	0.336 ± 0.010	1.050 ± 0.034
AC-1742	–	–	–	–	–
B-1689	0.538 ± 0.002	0.075 ± 0.001	0.067 ± 0.001	0.137 ± 0.003	0.187 ± 0.009
B-1688	0.491 ± 0.025	0.072 ± 0.001	0.068 ± 0.001	0.219 ± 0.016	0.587 ± 0.046
B-7509	2.402 ± 0.007	0.178 ± 0.008	0.167 ± 0.005	2.364 ± 0.003	0.426 ± 0.021
B-7533	2.433 ± 0.001	0.187 ± 0.002	0.187 ± 0.002	2.387 ± 0.006	0.432 ± 0.021
B-5000	–	–	–	–	–
B-4054	1.560 ± 0.003	0.187 ± 0.002	0.160 ± 0.002	0.877 ± 0.067	1.959 ± 0.037
Control 1 (Hemopropiovit)	1.491 ± 0.015	0.112 ± 0.001	0.112 ± 0.003	0.987 ± 0.008	1.774 ± 0.114
Control 2 (Bifiform)	1.549 ± 0.006	0.110 ± 0.002	0.106 ± 0.006	0.692 ± 0.033	1.845 ± 0.006

"–" – indicates no growth during the test

At pH 2.0, no growth was observed of any of the strains under study compared to the control. The optical density of Strains B-6083 and B-6080 decreased 5.9 and 7.4 times, respectively. For Strain B-10412, this indicator decreased 8.1-fold. Bifidobacteria strains (AC-1779 and AC-1257) were more sensitive, with their optical density decreasing 8.9 and 17.6 times, respectively. Strains B-1689 and B-1688 showed a 7.2–7.5-fold decrease in optical density. Strains B-7509 and B-7533 also showed a significant growth decrease of 13.2 times compared to the control. For Strain B-4054, this indicator decreased 8.3 times. Commercial probiotics (Controls 1 and 2) also exhibited pronounced growth inhibition, with a 13.3–14.1 decrease in optical density.

At pH 3.0, most of the strains showed lower growth, but it was slightly higher in some cultures compared to their growth at pH 2.0. Strains B-6083 and B-6080 had 5.3 and 6.8 times lower optical density, respectively, relative to the control. For strain B-10412, this indicator was higher than at pH 2.0, but it was still 4.5 times lower than the control value. Strains AC-1779 and AC-1257 had a 10.4–18.3-fold decrease in optical density compared to the control. Strains B-1689 and B-1688 demonstrated a decrease of 7.0–7.2 times, while Strains B-7509 and B-7533 showed a decrease of 13.0–14.4 times. Strain B-4054 also had a significant decrease of 9.7 times. The commercial probiotics (Controls 1 and 2) demonstrated comparable sensitivity, with their optical density decreasing 13.3–14.6 times.

At pH 5.0, the strains demonstrated higher growth compared to their rates at pH 2.0 and 3.0. Strains B-7509 and B-7533 were very close to the control values, which indicated their high tolerance to these pH conditions. Strain B-4054 showed a moderate decrease in growth (1.8 times lower than the control). The growth of AC-1779 and AC-1257 remained 2.8–4.0 times lower than that of the control. Strains B-1689 and B-1688 showed a 2.2–3.9-fold decrease. For B-6083, B-6080, and B-10412, the growth rates remained significantly (6.2–11.2 times) lower than the control. The commercial probiotics demonstrated a 1.5–2.2-fold decrease in growth.

At an alkaline pH (9.2), a number of the strains showed increased growth compared to the control. Strains B-6083, B-10412, and B-4054 had a 1.7, 1.1, and 1.3 times increase in optical density, respectively. The growth of Strain B-6080 was close to the control. Strains AC-1779 and AC-1257 demonstrated a 2.1 and 1.3 times decrease in growth, respectively. Strains B-1689 and B-1688 also showed lower values (2.9 and 1.2 times, respectively) compared to the control. Strains B-7509 and B-7533 showed a marked decrease (5.6 times) in growth relative to the control. The commercial probiotics, on the contrary, demonstrated a 1.2-fold increase in optical density.

Thus, we found that most of the strains were sensitive to highly acidic pH values (2.0–3.0), while some cultures maintained high growth in moderately acidic (pH 5.0) and alkaline (pH 9.2) environments. Strains B-7509 and B-7533 were the most resistant at pH 5.0, while Strains B-4054 and B-6083 were the most resistant at pH 9.2. In some cases, the growth rates of the cultures were comparable to those for the commercial probiotics.

According to literature, probiotic microorganisms should remain viable after passing through the gastrointestinal tract at low pH values of 2.0–6.5 [78, 79]. Our results demonstrate that some of the cultures can maintain their viability under stressful pH conditions. This is an important indicator of their potential adaptation to the conditions in the upper gastrointestinal tract.

Our results are consistent with the studies on lactic acid bacteria exposed to neutral and alkaline pH values. Several studies have shown that lactic acid bacteria isolates can grow at pH 7.0–9.0, although their growth intensity may vary between the strains [80]. Certain cultures maintained or even increased growth at pH 9.2, indicating the presence of mechanisms for adapting to alkaline stress.

Antimicrobial activity. We assessed the antagonistic activity of the probiotic strains against the test strains of pathogenic and opportunistic microorganisms (Table 5).

Control 1 exhibited weak antagonistic activity against *Pseudomonas aeruginosa, Enterococcus faecalis*, and *Klebsiella pneumoniae* and no activity against *Escherichia coli* and *Bacillus cereus*. Control 2 demonstrated moderate activity against *K. pneumoniae,* weak activity against *E. coli, B. cereus*, and *E. faecalis*, and no activity against *P. aeruginosa*.

The resistance of Strains B-10412 and B-4054 to *E. coli* is described in our previous work [68]. Strain B-6083 exhibited the most pronounced antagonistic activity against *E. coli*. It was 2.4 times higher than the activity of Control 2 and over 2.4 times higher than that of HLS. Strains AC-1779 and AC-1257 also demonstrated high activity, 1.9 and 2.0 times higher than the values for Control 2 and HLS. Strains B-10412 [69] and B-7533 demonstrated weak activity, at the level of Control 2 and HLS. The remaining strains showed no antagonistic activity against *E. coli*.

Antagonistic activity against *P. aeruginosa* was moderate in Strain AC-1779: it was 1.4 times higher than in Control 1 but 1.2 times lower than in gentamicin. Strains AC-1257, B-7509, B-7533, and B-10412 exhibited weak activity: it was comparable to Control 1, but significantly (1.5 times or more) lower than in gentamicin. The remaining strains showed no activity against *P. aeruginosa*.

Antagonistic activity against *B. cereus* was the most pronounced in Strain B-7533, 1.5 times the value for Control 2 but almost the same (1.1-fold difference or less) as CXN. Strain B-7509 demonstrated moderate activity, 1.3 times higher than Control 2 but 1.1 lower than CXN. Strains AC-1779, AC-1257, B-10412, B-1689, B-1688, and B-4054 showed weak activity. Strains B-6083 and B-6080 were completely inactive.

Table 5 Antagonistic activity of the probiotic strains

Sample	Diameter of growth inhibition zone, mm				
	Escherichia coli	*Pseudomonas aeruginosa*	*Bacillus cereus*	*Enterococcus faecalis*	*Klebsiella pneumoniae*
B-6083	29.47 ± 0.50	0.00 ± 0.00	10.05 ± 0.20	11.16 ± 0.22	0.00 ± 0.00
B-6080	0.00 ± 0.00	0.00 ± 0.00	0.00 ± 0.00	0.00 ± 0.00	0.00 ± 0.00
B-10412	*	13.26 ± 0.27	14.55 ± 0.30	10.43 ± 0.21	15.67 ± 0.32
AC-1779	23.53 ± 0.50	17.64 ± 0.36	16.94 ± 0.33	10.82 ± 0.22	14.28 ± 0.29
AC-1257	23.60 ± 0.36	17.18 ± 0.35	13.84 ± 0.26	11.91 ± 0.24	12.09 ± 0.24
AC-1742	–	–	–	–	–
B-1689	0.00 ± 0.00	0.00 ± 0.00	12.40 ± 0.25	13.48 ± 0.27	14.04 ± 0.29
B-1688	0.00 ± 0.00	0.00 ± 0.00	12.72 ± 0.26	15.40 ± 0.31	10.58 ± 0.22
B-7509	0.00 ± 0.00	13.98 ± 0.29	20.48 ± 0.42	16.38 ± 0.33	14.94 ± 0.30
B-7533	13.23 ± 0.75	13.07 ± 0.27	23.07 ± 0.47	15.81 ± 0.32	19.16 ± 0.39
B-5000	–	–	–	–	–
B-4054	*	0.00 ± 0.00	14.05 ± 0.29	12.71 ± 0.26	15.70 ± 0.32
Control 1 (Hemopropiovit)	0.00 ± 0.00	12.65 ± 0.26	0.00 ± 0.00	9.38 ± 0.19	11.71 ± 0.24
Control 2 (Bifiform)	12.23 ± 0.34	0.00 ± 0.00	15.48 ± 0.32	11.79 ± 0.24	17.90 ± 0.36
Streptomycin, 300 mg	12.00 ± 0.32				
Gentamicin, 120 mcg		20.53 ± 0.33			
Cephalexin, 30 mcg			23.5 ± 0.38		27.6 ± 0.45
Tetracycline, 30 mg				25.5 ± 0.42	
Water	0.00 ± 0.00	0.00 ± 0.00	0.00 ± 0.00	0.00 ± 0.00	0.00 ± 0.00

"–" indicates no growth during the test; * – refers to the authors' previous publication [68]

Antagonistic activity against *E. faecalis* was the most pronounced in Strains B-7509 and B-7533, 1.7 times higher than in Control 1 and 1.3–1.4 times higher than in Control 2, but 1.6 times lower than in TET. Strains B-1688, B-1689, AC-1257, AC-1779, and B-10412 also showed weak activity, 1.1–1.6 times higher than Control 1 and about the same level as Control 2, but significantly lower (1.6–2.4 times) than TET. Strain B-6083 showed the weakest activity, while B-6080 did not exhibit any inhibitory effect at all.

Antagonistic activity against *K. pneumoniae* was the most pronounced in Strain B-7533. This strain showed moderate values, which were 1.1 times higher than those for Control 2 and 1.6 times higher than those for Control 1, yet 1.4 times lower than those for CXN. Strains B-10412 and B-4054 demonstrated weak activity, 1.3–1.4 times higher than Control 1 and at the same level as Control 2, but 1.7–1.8 times lower than the antibiotic. Strains B-7509, AC-1779, B-1689, and AC-1257 also showed weak activity, 1.1–1.3 times higher than Control 1, but 1.3 times lower than Control 2 and significantly (1.8–2.0 times) lower than CXN. Strains B-6083 and B-6080 showed no activity against *K. pneumoniae*.

Thus, the most pronounced antagonistic activity was observed in B-6083 against *E. coli*, as well as in B-7533 and B-7509 against *B. cereus, E. faecalis,* and *K. pneumoniae*. Strains AC-1779 and AC-1257 exhibited high or moderate activity against *E. coli* and *P. aeruginosa*, whereas Strains B-1689, B-1688, and B-4054 demonstrated mostly weak antagonistic activity. In some cases, the strains' activity was comparable to, or higher than, the activity of commercial probiotics.

Our results are consistent with other studies that report pronounced antimicrobial properties of probiotic microorganisms. Fijan *et al.* [81] studied the antagonistic activity of representatives of the genera *Propionibacterium*, *Bifidobacterium, Lactococcus,* and *Enterococcus* against a wide range of opportunistic bacteria, including *E. coli, P. aeruginosa, E. faecalis,* and *K. pneumoniae*. Their inhibition efficiency varied between the strains and was determined by the production of organic acids, bacteriocins, and other antimicrobial metabolites. Probiotic compositions demonstrated a more pronounced antagonistic effect compared to individual strains, with zones of inhibition of pathogen growth averaging 10.0–20.0 mm. This indicated possible synergism between different probiotic microorganisms. Individual representatives, including propionic acid bacteria, usually exhibited a more moderate inhibitory effect. Sanam *et al.* [82] studied the antagonistic activity of probiotic microorganisms against *E. coli* and *B. cereus*. They found that lactic acid bacteria isolated from mare's milk can form inhibition zones with a diameter of 29.6 mm for *B. cereus* and 31.2 mm for *E. coli*. The authors assumed that this inhibitory effect was due to the synthesis of various antimicrobial metabolites, including organic acids, diacetyl, hydrogen peroxide, and bacteriocins.

Srinu *et al.* [83] showed that the strains *Bifidobacterium bifidum* and *Bifidobacterium adolescentis* can inhibit the growth of various pathogenic bacteria, with zones of growth inhibition reaching 14.0–18.0 mm in diameter (15.0–18.0 mm for *E. coli* and 14.0–16.0 mm for *K. pneumoniae*. Probiotics of the genus *Pediococ-*

cus also exhibit antagonistic activity. Ouili *et al.* [84] found that the strains of *Pediococcus pentosaceus* isolated from fermented plant products can effectively inhibit the growth of pathogenic microorganisms (*E. coli* and *P. aeruginosa*), with zones of growth inhibition greater than 18.0 mm in diameter. Representatives of the genus *Weissella* can also produce an inhibitory effect on the growth of pathogens, both gram-positive and gram-negative, as reported by Fhoula *et al.* [85]. In particular, they exhibited pronounced antimicrobial activity against *P. aeruginosa*, *E. coli*, and *E. faecalis*, with growth inhibition zones reaching 36.0 ± 1.8, 26.0 ± 0.9, and 26.0 ± 1.0 mm in diameter, respectively.

In our study, not all of the cultures exhibited sufficient viability and probiotic potential. Particularly, Strains AC-1742 and B-5000 failed to grow on the nutrient media, possibly due to their specific physiological requirements for cultivation conditions. As a result, we were unable to assess their antagonistic activity and resistance to gastrointestinal stress and excluded them from further analysis.

Strains B-1689 and B-1688 were also excluded from further analysis because of their relatively low resistance to gastrointestinal stress factors. In particular, exposure to bile (0.5%) resulted in significant growth inhibition, with optical density decreasing fivefold compared to the control. At 6.5% NaCl, Strain B-1689 demonstrated the most pronounced decrease in growth among the cultures under study (4.6 times lower than the control). When tested for antagonistic activity, these strains showed no inhibitory effect against *E. coli* and *P. aeruginosa* and demonstrated weak activity against the other pathogen cultures. Taken together, these results indicate a relatively low probiotic potential for these strains.

Microbial growth curves. The microbial growth curves showed changes in the optical density of the strains relative to their cultivation time (Fig. 1).

The data revealed the following growth phases: a lag phase, an exponential phase, a stationary phase, and a death phase. Strains B-7509 and B-7533 began to grow after 4–6 h, indicating a short adaptation period. Strain B-10412 took longer to adapt, its active growth starting after 9 h. Strains AC-1779 and AC-1257 also had quite a long lag phase, with the first noticeable changes recorded between 4 and 6 h. Strains B-6083 and B-6080 had the longest adaptation period, staring to grow after 13 h. In contrast, Strain B-4054 and the control cultures showed growth after 3 h.

The most intense increase in cell numbers was observed between 8 and 22 h of cultivation. Strains B-7509 and B-7533 grew most rapidly, their optical density increasing 4.1-fold between 9 and 23 h. Strain B-10412 showed a slower initial increase, but its optical density increased 8.6-fold between 16 and 24 h. The *Bifidobacterium* strains showed more moderate growth. The optical density of Strains AC-1779 and AC-1257 increased 2.2 and 1.4-fold, respectively, between 15 and 23 h. The *Propionibacterium* strains took longer to start the exponential phase. Strain B-6083 showed a 2.7-fold growth between 16 and 30 h, while B-6080 showed an 8.5-fold growth between 15 and 30 h. In contrast, Strain B-4054 reached its maximum growth by the 7th h of cultivation and then stopped growing. Controls 1 and 2 also reached the stationary phase quite quickly, within 10 h of cultivation.

The stationary growth phase started after 22–24 h of cultivation for most of the cultures. The highest values were observed in Strains B-7509 and B-7533, with their optical density reaching 7.01 ± 0.15 and 6.61 ± 0.14, re-

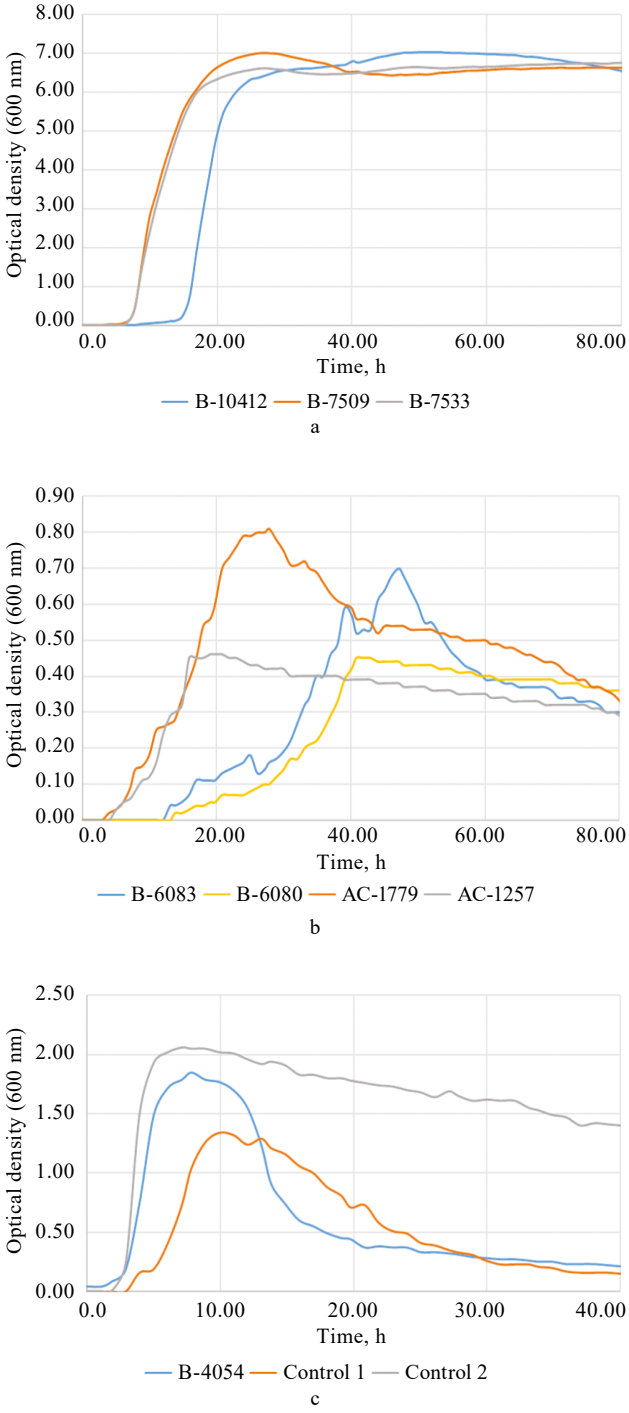


Figure 1 Growth curves for: a – Strains B-10412, B-7509, and B-7533; b – Strains B-6083, B-6080, AC-1779, and AC-1257; and c – B-4054, Controls 1 and 2

spectively, after 27 h of cultivation. Strain B-10412 reached a maximum of 7.03 ± 0.15 after 50 h. The *Bifidobacterium* strains showed significantly low values, reaching their maximum after 28 h (0.81 ± 0.02 for AC-1779) and 19 h (0.46 ± 0.01 for AC-1257), and then stabilizing or gradually decreasing. The *Propionibacterium* strains had even lower maximum values, 0.70 ± 0.01 for B-6083 (47 h) and 0.45 ± 0.01 for B-6080 (41 h). After rapid initial growth, Strain B-4054 entered the stationary phase after 15–16 h, with its values gradually decreasing 3.3-fold by the 45th h of cultivation. The control cultures entered the stationary phase earlier, with Control 1 reaching its maximum after 10 h (1.34 ± 0.03) and Control 2, after 7 h (2.06 ± 0.04).

After reaching their maximum, most cultures showed a gradual decrease in their optical density due to the depletion of nutrients and the accumulation of metabolites. The most pronounced decrease was observed in Strain B-10412 (down to 6.54 ± 0.14 by the 80th h). In contrast, Strains B-7509 and B-7533 hardly decreased at all, their optical density remaining stable throughout the entire observation period. The *Propionibacterium* and *Bifidobacterium* strains showed a more gradual decrease – 2.3-fold for B-6083 between 48 and 80 h, 2.4-fold for AC-1779 between 29 and 80 h, and 1.6-fold for AC-1257 between 22 and 80 h. The optical density of B-4054 and the control cultures decreased much earlier, after 10–15 h of cultivation.

Thus, the growth curves demonstrated that Strains B-7509, B-7533, and B-10412 exhibited the most vigorous growth and a prolonged stationary phase. Strains AC-1779, AC-1257, B-6083, and B-6080 had a longer lag phase and a moderate growth rate. Strain B-4054 and the control cultures showed intermediate growth rates.

Based on the S-shaped growth curves, we identified three time points (1 – exponential phase, 2 – maximum biomass accumulation, and 3 – death phase) at which samples were collected for metabolite analysis (Table 6).

Quantification of microbial metabolites. Table 7 shows the contents of B vitamins in the strains sampled at three time points.

The quantitative analysis of B vitamins revealed that the strains differed significantly in their ability to synthesize vitamins at different stages of growth. Riboflavin (vitamin B_2) was not detected in any of the samples.

Vitamin B_1 had the highest content in Strain B-10412, remaining high throughout the entire cultivation period. In B-6080, its accumulation showed a 6.7-fold increase compared to time point 1. Strains B-7509 and B-7533 increased their thiamine concentrations 1.2 and 3.0-fold, respectively, towards the end of cultivation (time point 3). Strain B-6083 showed a moderate increase at time point 2, followed by a decrease at time point 3. In Strains AC-1779 and AC-1257, thiamine concentrations remained relatively stable between the time points.

Vitamin B_3 had its highest concentrations in the *Bifidobacterium* strains. In AC-1779, the niacin content increased gradually throughout cultivation, while in AC-1257, it increased at time point 2 after a slight decrease. Strain B-10412 showed a noticeable (3.2-fold) decrease in niacin between time points 1 and 2, followed by a partial increase. B-6083 reached a pronounced peak in vitamin B_3 at time point 2, followed by a 2.5 decrease. Strains B-7509 and B-7533 accumulated maximum niacin contents towards the end of cultivation. Particularly, Strain B-7509 had a 2.7-fold increase compared to time point 1. Strain B-4054 showed a sharp decrease in niacin at time point 2, followed by a partial recovery by time point 3.

We found significant fluctuations in vitamin concentrations at individual time points during cultivation. Some strains showed abrupt changes in compounds between the growth phases. For example, B-6080 had a sharp increase in thiamine at time point 2, while B-7533 accumulated the vitamins between time points 1 and 3. Strains AC-1779 and AC-1257 showed more gradual changes (e.g., a gradual increase in niacin).

The contents of vitamins B_5, B_6, and B_{12} were low in all the strains, less than 0.1 mg/g. However, some cultures consistently produced trace amounts of these compounds. B-10412 showed a gradual increase in vitamin B_6, while B-6080 showed a consistent increase in vitamin B_5 throughout cultivation. Strain B-4054 had 4.5-fold increase in vitamin B_{12} between time points 1 and 3. In the *Bifidobacterium* strains, pantothenic acid (B_5) and pyridoxine (B_6) were detected at virtually all growth points, indicating high activity of the metabolic pathways.

Table 6 Time points at which samples were collected for metabolite analysis

Strain	Exponential phase, h	Maximum biomass accumulation, h	Death phase, h
B-6083	10.0 ± 1.0	24.0 ± 2.0	40.0 ± 2.0
B-6080	35.0 ± 2.0	41.0 ± 2.0	70.0 ± 2.0
B-10412	16.0 ± 1.0	48.0 ± 2.0	72.0 ± 2.0
AC-1779	16.0 ± 1.0	28.0 ± 2.0	32.0 ± 2.0
AC-1257	12.0 ± 1.0	16.0 ± 1.0	21.0 ± 2.0
B-7509	10.0 ± 1.0	26.0 ± 2.0	35.0 ± 2.0
B-7533	10.0 ± 1.0	26.0 ± 2.0	35.0 ± 2.0
B-4054	4.0 ± 0.5	8.0 ± 1.0	10.0 ± 1.0
Control 1 (Hemopropiovit)	7.0 ± 1.0	10.0 ± 1.0	20.0 ± 1.0
Control 2 (Bifiform)	3.0 ± 0.5	9.0 ± 1.0	14.0 ± 1.0

Table 7 B vitamin contents at all time points

Sample	Time point	Vitamin content, mg/g					
		B_1	B_2	B_3	B_5	B_6	B_{12}
B-6083	1	2.22 ± 0.04	n.d.	1.79 ± 0.03	0	n.d.	0.06 ± 0.01
	2	2.51 ± 0.05	n.d.	5.05 ± 0.10	0	n.d.	0.02 ± 0.01
	3	1.95 ± 0.04	n.d.	2.06 ± 0.04	0	0.02 ± 0.01	0.04 ± 0.01
B-6080	1	2.69 ± 0.05	n.d.	1.71 ± 0.03	0.07 ± 0.01	0.02 ± 0.01	0.01 ± 0.01
	2	17.97 ± 0.34	n.d.	1.39 ± 0.03	0.10 ± 0.01	0.01 ± 0.01	0.01 ± 0.01
	3	2.84 ± 0.05	n.d.	1.43 ± 0.03	0.11 ± 0.01	0.03 ± 0.01	0.03 ± 0.01
B-10412	1	23.10 ± 0.44	n.d.	12.16 ± 0.23	0.12 ± 0.01	0.02 ± 0.01	0.09 ± 0.01
	2	15.88 ± 0.30	n.d.	3.79 ± 0.07	0.10 ± 0.01	0.04 ± 0.01	0.02 ± 0.01
	3	12.32 ± 0.23	n.d.	4.31 ± 0.08	0.10 ± 0.01	0.06 ± 0.01	0.04 ± 0.01
AC-1779	1	1.63 ± 0.03	n.d.	13.54 ± 0.26	0.02 ± 0.01	0.01 ± 0.01	0.02 ± 0.01
	2	1.34 ± 0.03	n.d.	13.90 ± 0.26	0.04 ± 0.01	0.01 ± 0.01	0.02 ± 0.01
	3	2.80 ± 0.05	n.d.	14.32 ± 0.27	0.04 ± 0.01	0.02 ± 0.01	0.03 ± 0.01
AC-1257	1	1.26 ± 0.02	n.d.	14.48 ± 0.28	0.02 ± 0.01	0.02 ± 0.01	0.02 ± 0.01
	2	1.44 ± 0.03	n.d.	13.56 ± 0.26	0.03 ± 0.01	0.01 ± 0.01	0.01 ± 0.01
	3	1.25 ± 0.02	n.d.	15.82 ± 0.30	0.03 ± 0.01	0.01 ± 0.01	0.02 ± 0.01
B-7509	1	12.80 ± 0.24	n.d.	1.29 ± 0.02	0.06 ± 0.01	0.03 ± 0.01	0.05 ± 0.01
	2	–	–	–	–	–	–
	3	15.84 ± 0.30	n.d.	3.53 ± 0.07	0.06 ± 0.01	0.02 ± 0.01	n.d.
B-7533	1	4.82 ± 0.09	n.d.	2.06 ± 0.04	0.05 ± 0.01	0.01 ± 0.01	0.06 ± 0.01
	2	–	–	–	–	–	–
	3	13.75 ± 0.26	n.d.	2.64 ± 0.05	0.05 ± 0.01	0.04 ± 0.01	0.02 ± 0.01
B-4054	1	1.67 ± 0.03	n.d.	5.81 ± 0.11	0	n.d.	0.02 ± 0.01
	2	2.32 ± 0.04	n.d.	n.d.	0.02 ± 0.01	0.02 ± 0.01	0.05 ± 0.01
	3	2.29 ± 0.04	n.d.	1.51 ± 0.03	0.02 ± 0.01	0.02 ± 0.01	0.09 ± 0.01
Control 1 (Hemopropiovit)	1	3.29 ± 0.06	n.d.	1.03 ± 0.02	0.01 ± 0.01	0.02 ± 0.01	0.02 ± 0.01
	2	3.55 ± 0.07	n.d.	1.29 ± 0.02	0.02 ± 0.01	0.02 ± 0.01	0.01 ± 0.01
	3	2.92 ± 0.06	n.d.	9.70 ± 0.18	0.02 ± 0.01	0.03 ± 0.01	0.02 ± 0.01
Control 2 (Bifiform)	1	2.97 ± 0.06	n.d.	1.62 ± 0.03	0	0.02 ± 0.01	0.02 ± 0.01
	2	2.51 ± 0.05	n.d.	1.83 ± 0.03	0.02 ± 0.01	0.02 ± 0.01	0.06 ± 0.01
	3	1.46 ± 0.03	n.d.	1.23 ± 0.02	0.02 ± 0.01	0.01 ± 0.01	0.03 ± 0.01

n.d. – not detected; 0 – detected in a minimum threshold amount; "–" failed analysis; time points: 1 – exponential phase, 2 – maximum biomass accumulation, and 3 – death phase

A number of studies have confirmed the ability of probiotic microorganisms to synthesize B vitamins. These compounds play an important role in energy metabolism by acting as cofactors in enzymatic reactions associated with the formation of ATP [40, 86]. LeBlanc *et al.* [87] reported that lactic acid bacteria, as well as normal human gut microbiota, are capable of synthesizing thiamine (B_1), riboflavin (B_2), pyridoxine (B_6), folates (B_9), and cobalamin (B_{12}). Probiotic strains *Bifidobacterium longum* and *B. bifidum* secreted thiamine *in vitro*, but failed to produce folates and riboflavin, which indicates their pronounced strain specificity.

Studies also report a possible synergistic interaction between probiotics and B vitamins. For example, Sang *et al.* [88] showed that the combined administration of probiotic strains of the genus *Lactobacillus* and B vitamins in animals improved the absorption of vitamins B_1, B_3, B_5, and B_{12} by 14.5–71.2% compared to their separate use. The authors assumed that this effect was due to the positive influence of the probiotics on the gut microbiota and vitamin absorption processes, improving their bioavailability.

Our analysis revealed that different strains showed maximum vitamin accumulation at different time points. Furthermore, most of the samples did not demonstrate consistent maximum values at time point 2. This was rather a transitional phase between active growth and a subsequent decline in metabolic activity. Therefore, further research was limited to the comparison between time points 1 (exponential growth phase) and 3 (death phase).

Table 8 presents the contents of organic acids in the strain samples.

Our analysis revealed that the probiotic strains differed significantly in the spectrum and intensity of metabolite synthesis. The most pronounced differences were observed for citric and succinic acids.

The *Propionibacterium* strains showed different metabolic profiles. B-6083 synthesized tartaric, maleic, and citric acids at time point 1, with only a small amount of maleic acid remaining at point 3. B-6080 exhibited a different pattern of metabolic activity. It synthesized significant amounts of succinic and citric acids at time point 1. By time point 3, however, citric acid was

absent, while succinic acid increased 1.2-fold, reaching its maximum accumulation at the death phase.

B-10412 synthesized a wide range of organic acids. At time point 1, this strain contained significant concentrations of citric and succinic acids, along with maleic and tartaric acids. At time point 3, succinic and citric acids decreased 5.5 and 1.5 times, respectively, while tartaric acid increased 3.6 times.

The *Bifidobacterium* strains exhibited significant changes in their metabolic profiles between the time points. Strain AC-1779 showed oxalic, citric, and succinic acids at time point 1, with none of them detected at time point 3. In contrast, AC-1257 synthesized tartaric and succinic acids at time point 1, while oxalic and citric acids were detected at time point 3, with citric acid increasing 13.3-fold.

Strain B-7509 exhibited high concentrations of succinic and citric acids at time point 1, while tartaric and maleic acids were detected at time point 3. Strain B-7533 demonstrated a general increase in most organic acids by time point 3, indicating high metabolic activity during the death phase. In particular, citric acid, succinic acid, and maleic acid increased 2.1, 7.7, and 3.4 times, respectively.

Strain B-4054 had a high concentration of maleic acid at time point 1. At time point 3, maleic acid disappeared, while concentrations of citric, succinic, and tartaric acids increased 3.8, 4.8, and 9.3 times.

The control samples had high concentrations of individual organic acids. Control 1 showed significant amounts of citric, tartaric, and succinic acids at time point 1, which significantly decreased by point 3. Control 2 exhibited less diversity in its metabolic profile, with citric and succinic acids detected at point 1. At time point 3, tartaric acid remained high, while citric acid decreased.

The synthesis of organic acids is one of the key metabolic functions of probiotic microorganisms. These compounds result from the fermentation of carbohydrates and contribute to the antimicrobial properties of bacteria. The contents of organic acids depend on the strain and its cultivation conditions. Scauro *et al.* [89] reported that the probiotic strains of *Lactiplantibacillus plantarum* synthesized lactic, citric, acetic, ascorbic, malic, tartaric, and other acids. Their accumulation varied significantly between the cultures, indicating pronounced strain-specificity of their metabolism. Ye *et al.* [90] found that probiotic bacteria synthesized a number of organic acids (including succinic and tartaric) and their derivatives involved in the metabolism of the tricarboxylic acid cycle. Increased succinic acid levels are often associated with the activation of metabolic pathways of the Krebs cycle and the conversion of other organic acids during microbial growth. Mohamad *et al.* [91] considered the synthesis of organic acids as one of the main antagonistic activities of probiotic bacteria. They noted that the accumulation of organic acids in the culture medium decreased its pH and created unfavorable conditions for the growth of pathogenic and opportunistic microorganisms. Organic acids such as citric, tartaric, succinic, and others form an acidic environment and inhibit foreign microflora.

Thus, our results confirmed the pronounced strain-specific nature of organic acid synthesis. The

Table 8 Contents of organic acids in the probiotic strains

Strain	Time point	Organic acid content, mg/L				
		Oxalic	Tartaric	Maleic	Citric	Succinic
B-6083	1	n.d.	3.7 ± 0.1	0.6 ± 0.1	15.1 ± 0.3	0
	3	0	0	0.1 ± 0.1	0	0
B-6080	1	0	1.2 ± 0.1	0	25.1 ± 0.5	358.8 ± 6.8
	3	0	3.5 ± 0.1	0	0	432.2 ± 8.2
B-10412	1	0	1.0 ± 0.1	2.2 ± 0.1	59.2 ± 1.1	47.0 ± 0.9
	3	n.d.	3.6 ± 0.1	0.2 ± 0.1	39.6 ± 0.8	8.6 ± 0.2
AC-1779	1	17.7 ± 0.3	0	0	26.3 ± 0.5	8.8 ± 0.2
	3	0	0	0	0	0
AC-1257	1	0	5.8 ± 0.1	0.8 ± 0.1	2.1 ± 0.1	48.2 ± 0.9
	3	16.9 ± 0.3	0	0	27.9 ± 0.5	0
B-7509	1	4.1 ± 0.1	0.9 ± 0.1	0	42.6 ± 0.8	344.3 ± 6.6
	3	0	2.8 ± 0.1	0.9 ± 0.1	0	0
B-7533	1	2.6 ± 0.1	15.9 ± 0.3	0.5 ± 0.1	21.6 ± 0.4	5.3 ± 0.1
	3	4.3 ± 0.1	19.1 ± 0.4	1.7 ± 0.1	45.8 ± 0.9	40.9 ± 0.8
B-4054	1	n.d.	0.6 ± 0.1	52.3 ± 1.0	8.7 ± 0.2	7.0 ± 0.1
	3	11.3 ± 0.2	5.6 ± 0.1	0	32.8 ± 0.6	33.6 ± 0.6
Control 1 (Hemopropiovit)	1	5.7 ± 0.1	45.3 ± 0.9	1.5 ± 0.1	95.5 ± 1.8	278.3 ± 5.3
	3	13.7 ± 0.3	26.1 ± 0.5	0	25.0 ± 0.5	0.6 ± 0.1
Control 2 (Bifiform)	1	0	0	1.1 ± 0.1	15.3 ± 0.3	28.1 ± 0.5
	3	0.5 ± 0.1	4.4 ± 0.1	0	10.3 ± 0.2	0

n.d. – not detected; 0 – detected but in a minimum threshold amount; time points: 1 – exponential phase; 3 – death phase

strains differed not only in the range of metabolites but also in the levels of their accumulation between the time points. For some strains, maximum acid concentrations were recorded during the exponential phase, while others showed maximum values during the death phase.

In comparison with the exponential phase, the death phase (time point 3) showed the most complete and stable metabolic profile, reflecting the strain's total metabolic activity throughout the entire growth cycle. By this point, the culture had undergone the main stages of adaptation to the environmental conditions accompanied by the accumulation or conversion of metabolites. For this reason, further metabolic profiling was conducted at time point 3, the phase at which the strains most fully manifest their metabolic characteristics.

Tables 9–10 present the contents of amino acids in the probiotic strains.

Our analysis revealed significant differences in the range and contents of amino acids synthesized by the strains. The highest total amino acid content was observed in Strain B-7509, with similar values recorded in B-10412. A slightly lower content was registered in B-7533, while no amino acids were detected in B-6080 and AC-1257. A similar situation was observed for the control samples.

Strain B-10412 synthesized a broad spectrum of amino acids, with high concentrations of individual compounds. The highest levels were recorded for tryptophan, glutamic acid, glycine, and isoleucine. The strain's diverse profile also included tyrosine, cystine, arginine, phenylalanine, leucine, and other amino acids.

Strain B-7509 had the highest concentration of proline, as well as high levels of glycine, glutamic acid, isoleucine, serine, histidine, phenylalanine, alanine, and lysine. Strain B-7533 had a similar profile, with the highest contents of proline, glutamic acid, glycine, serine, histidine, isoleucine, phenylalanine, and methionine.

AC-1779 showed a moderate level of amino acid accumulation, with proline, glutamic acid, and glycine as the most prevalent compounds. Lower concentrations were detected for alanine, phenylalanine, lysine, and isoleucine.

Strain B-6083 had a relatively balanced amino acid profile. The highest concentrations were observed for proline and glycine. Moderate values were recorded for glutamic acid, isoleucine, alanine, and serine. Other amino acids were present in low concentrations.

B-4054 exhibited a relatively moderate overall content of amino acids, with some compounds accumulated in higher concentrations than others. The highest values were observed for proline, glycine, and isoleucine. Also present were tryptophan, glutamic acid, valine, alanine, and phenylalanine.

The synthesis and accumulation of free amino acids is an important metabolic characteristic of probiotic microorganisms. These compounds result from the proteolytic activity of bacteria and the hydrolysis of protein substrates during fermentation. Many lactic acid bacteria

Table 9 Contents of amino acids in the strains B-6083, B-6080, B-10412, AC-1779, and AC-1257

Amino acid	Amino acid content in samples, mg/g				
	B-6083	B-6080	B-10412	AC-1779	AC-1257
Tryptophan	1.7 ± 0.1	n.d.	32.9 ± 0.6	25.5 ± 0.5	n.d.
Glutamic	5.2 ± 0.1	n.d.	18.2 ± 0.3	11.1 ± 0.2	n.d.
Serine	3.0 ± 0.1	n.d.	1.5 ± 0.1	0.7 ± 0.1	n.d.
Glycine	12.1 ± 0.2	n.d.	13.2 ± 0.2	9.3 ± 0.2	n.d.
Histidine	1.6 ± 0.1	n.d.	4.4 ± 0.1	1.0 ± 0.1	n.d.
Glutamine	1.4 ± 0.1	n.d.	0.7 ± 0.1	1.7 ± 0.1	n.d.
Arginine	0.4 ± 0.1	n.d.	3.0 ± 0.1	0.8 ± 0.1	n.d.
Lysine	1.4 ± 0.1	n.d.	2.6 ± 0.1	3.1 ± 0.1	n.d.
Threonine	0.6 ± 0.1	n.d.	3.8 ± 0.1	0.9 ± 0.1	n.d.
Alanine	3.5 ± 0.1	n.d.	28.6 ± 0.5	1.8 ± 0.1	n.d.
Proline	13.2 ± 0.2	n.d.	5.0 ± 0.1	20.1 ± 0.4	n.d.
Asparagine	0.1 ± 0.1	n.d.	2.5 ± 0.1	0.5 ± 0.1	n.d.
Tyrosine	0.2 ± 0.1	n.d.	1.7 ± 0.1	0.8 ± 0.1	n.d.
Methionine	1.3 ± 0.1	n.d.	1.9 ± 0.1	1.6 ± 0.1	n.d.
Valine	3.1 ± 0.1	n.d.	0.9 ± 0.1	1.4 ± 0.1	n.d.
Cysteine	1.1 ± 0.1	n.d.	1.1 ± 0.1	0.7 ± 0.1	n.d.
Cystine	0.2 ± 0.1	n.d.	2.3 ± 0.1	0.4 ± 0.1	n.d.
Leucine	2.2 ± 0.1	n.d.	5.6 ± 0.1	0.5 ± 0.1	n.d.
Isoleucine	4.0 ± 0.1	n.d.	8.2 ± 0.2	1.8 ± 0.1	n.d.
Phenylalanine	2.3 ± 0.1	n.d.	3.9 ± 0.1	3.2 ± 0.1	n.d.
Total:	58.3	–	142.1	86.9	–

n.d. – not detected; "0" – detected but in a minimum threshold amount

Table 10 Contents of amino acids in the strains B-7509, B-7533, and B-4054, as well as Controls 1 and 2

Amino acid	Amino acid content in samples, mg/g				
	B-7509	B-7533	B-4054	Control 1	Control 2
Tryptophan	7.5 ± 0.1	0.9 ± 0.1	4.9 ± 0.1	n.d.	n.d.
Glutamic	17.4 ± 0.3	20.3 ± 0.4	4.0 ± 0.1	n.d.	n.d.
Serine	6.0 ± 0.1	6.2 ± 0.1	1.3 ± 0.1	n.d.	n.d.
Glycine	20.3 ± 0.4	15.3 ± 0.3	10.8 ± 0.2	n.d.	n.d.
Histidine	6.8 ± 0.1	6.8 ± 0.1	0.9 ± 0.1	n.d.	n.d.
Glutamine	4.3 ± 0.1	4.1 ± 0.1	1.6 ± 0.1	n.d.	n.d.
Arginine	2.7 ± 0.1	2.4 ± 0.1	0	n.d.	n.d.
Lysine	5.4 ± 0.1	4.7 ± 0.1	1.0 ± 0.1	n.d.	n.d.
Threonine	3.4 ± 0.1	3.4 ± 0.1	2.0 ± 0.1	n.d.	n.d.
Alanine	6.6 ± 0.1	4.5 ± 0.1	3.5 ± 0.1	n.d.	n.d.
Proline	32.0 ± 0.6	25.0 ± 0.5	15.6 ± 0.2	n.d.	n.d.
Asparagine	0.2 ± 0.1	1.3 ± 0.1	0.2 ± 0.1	n.d.	n.d.
Tyrosine	0.4 ± 0.1	0.2 ± 0.1	0.1 ± 0.1	n.d.	n.d.
Methionine	3.7 ± 0.1	3.3 ± 0.1	0.7 ± 0.1	n.d.	n.d.
Valine	6.3 ± 0.1	4.5 ± 0.1	3.4 ± 0.1	n.d.	n.d.
Cysteine	3.3 ± 0.1	2.9 ± 0.1	0.9 ± 0.1	n.d.	n.d.
Cystine	0.1 ± 0.1	0.3 ± 0.1	0.1 ± 0.1	n.d.	n.d.
Leucine	5.1 ± 0.1	3.6 ± 0.1	1.9 ± 0.1	n.d.	n.d.
Isoleucine	7.9 ± 0.1	5.8 ± 0.1	4.7 ± 0.1	n.d.	n.d.
Phenylalanine	5.7 ± 0.1	5.2 ± 0.1	2.1 ± 0.1	n.d.	n.d.
Total:	145.2	120.7	60	–	–

n.d. – not detected; "0" – detected but in a minimum threshold amount

exhibit high proteolytic activity, which breaks down proteins into peptides and free amino acids, which are involved in subsequent microbial metabolism. Ter *et al.* [92] noted that lactic acid bacteria are capable of actively hydrolyzing dietary proteins and forming a wide range of free amino acids, including proline, glycine, glutamic acid, leucine, and isoleucine. This has a significant effect on the functional properties of fermented products.

In a study of amino acid metabolism in fermented milk, Terzioğlu *et al.* [93] demonstrated that the probiotic cultures of *Lactobacillus* and *Bifidobacterium* contribute to the accumulation of alanine, glycine, proline, and glutamic acid, with their contents dependent on the composition of the microbial culture and the fermentation substrate.

Overall, our results indicate pronounced strain-specificity in the amino acid profiles of the cultures. The strains differed in the intensity of protein metabolism, which determined the formation of specific amino acid profiles. These metabolic characteristics can be used among the criteria for selecting promising cultures for further research and for developing functional products with increased amino acid contents.

Biocompatibility of the strains. Table 11 provides data on the biocompatibility of the probiotic strains with each other.

Biocompatibility analysis revealed that most interactions between the strains were neutral or stimulatory, with some strains exhibiting sensitivity to the metabolites of other microorganisms. For example, B-6083 biomass growth was inhibited by all metabolites except for AC-1779. Strain B-10412 was inhibited by AC-1779 and AC-1257, with other interactions being neutral.

Strains AC-1257, B-7509, and B-7533 exhibited mostly stimulatory effects, reflecting their high potential for co-cultivation. Notably, B-4054 was stimulated by metabolites from several strains (B-6083, AC-1779, AC-1257, and B-7509), while the remaining metabolites were neutral.

Thus, our results demonstrate that strain combinations with mostly stimulatory or neutral interactions can be used to form consortia with minimal conflicts between microorganisms. The most promising combinations are between AC-1257, B-7509, B-10412, and B-4054. Their metabolites promote each other's growth or have no negative impact on each other, ensuring the stability and efficiency of co-cultivation.

Table 11 Mutual biocompatibility of microbial metabolites

Microbial metabolites in culture broth	Strain biomass						
	B-6083	B-10412	AC-1779	AC-1257	B-7509	B-7533	B-4054
B-6083		–	++	++	+	+	++
B-10412	–		++	++	+	+	+
AC-1779	+	–		+	++	++	++
AC-1257	–	–	+		++	++	++
B-7509	–	+	++	++		+	++
B-7533	–	+	++	++	+		+
B-4054	–	+	+	+	++	++	

"+" – biocompatibility; "++" – growth stimulation; "–" – growth inhibition

CONCLUSION

Our comprehensive assessment of the probiotic strains revealed those that are sensitive to clinically significant antibiotics, resistant to gastrointestinal stress factors, and capable of high antagonistic activity against opportunistic microflora. Based on their combined properties, the most promising strains are *Pediococcus acidilactici* B-7509 and B-7533, *Bifidobacterium longum* AC-1257, *Weissella thailandensis* B-10412, and *Enterococcus faecium* B-4054.

Metabolic analysis demonstrated their ability to synthesize bioactive compounds, including B vitamins, organic acids, and amino acids. The highest amino acid content was observed in *P. acidilactici* B-7509 (145.2 mg/g) and *W. thailandensis* B-10412 (142.1 mg/g).

Biocompatibility analysis revealed mostly neutral or stimulatory interactions between the strains. The most promising combinations for probiotic consortia are between *B. longum* AC-1257, *P. acidilactici* B-7509 and B-7533, *W. thailandensis* B-10412, and *E. faecium* B-4054.

According to our results, these strains have high potential as components of dietary supplements and functional foods [94]. However, their potential use in starter cultures requires additional research to assess their safety and technological properties in accordance with regulatory requirements.

The strains' antagonistic activity and resistance to gastrointestinal factors indicate their potential effectiveness when administered orally. According to current research, probiotic metabolites can have a positive effect on lipid metabolism (reducing cholesterol and triglyceride levels) [95], carbohydrate metabolism [96], and the gut microbiota [40]. Therefore, these cultures need to be further studied as part of probiotic consortia. The next stage would be to evaluate their functional activity *in vivo* using animal models.

CONTRIBUTION

The authors were equally involved in writing this manuscript and bear equal responsibility for plagiarism.

CONFLICT OF INTEREST

The authors declare no conflict of interest regarding this publication.

REFERENCES

1. Latif A, Shehzad A, Niazi S, Zahid A, Ashraf W, *et al*. Probiotics: Mechanism of action, health benefits and their application in food industries. Frontiers in Microbiology. 2023;14:1216674. https://doi.org/10.3389/fmicb.2023.1216674
2. Dmitrieva A, Kozlova O, Atuchin V, Milentieva I, Vesnina A, *et al*. Study of the effect of baicalin from *Scutellaria baicalensis* on the gastrointestinal tract normoflora and *Helicobacter pylori*. International Journal of Molecular Sciences. 2023;24(15):11906. https://doi.org/10.3390/ijms241511906
3. Sarita B, Samadhan D, Hassan MZ, Kovaleva EG. A comprehensive review of probiotics and human health-current prospective and applications. Frontiers in Microbiology. 2025;15:1487641. https://doi.org/10.3389/fmicb.2024.1487641
4. Chandrasekaran P, Weiskirchen S, Weiskirchen R. Effects of probiotics on gut microbiota: An overview. International Journal of Molecular Sciences. 2024;25(11):6022. https://doi.org/10.3390/ijms25116022
5. Pires L, González-Paramás AM, Heleno SA, Calhelha RC. The role of gut microbiota in the etiopathogenesis of multiple chronic diseases. Antibiotics. 2024;13(5):392. https://doi.org/10.3390/antibiotics13050392
6. Wu Y, Jha R, Li A, Liu H, Zhang Z, *et al*. Probiotics (*Lactobacillus plantarum* HNU082) supplementation relieves ulcerative colitis by affecting intestinal barrier functions, immunity-related gene expression, gut microbiota, and metabolic pathways in mice. Microbiology Spectrum. 2022;10(6):e01651-22. https://doi.org/10.1128/spectrum.01651-22
7. Zhang Y, Zheng T, Ma D, Shi P, Zhang H, *et al*. Probiotics *Bifidobacterium lactis* M8 and *Lactobacillus rhamnosus* M9 prevent high blood pressure via modulating the gut microbiota composition and host metabolic products. mSystems. 2023;8:e00331-23. https://doi.org/10.1128/msystems.00331-23
8. Prosekov AYu, Vesnina AD, Lyubimova NA, Chekushkina DYu, Mikhailova ES. Consumer genomics in personalized nutrition. Food Processing: Techniques and Technology. 2025;55(2):400–415. (In Russ.) https://doi.org/10.21603/2074-9414-2025-2-2582
9. Howard EJ, Lam TKT, Duca FA. The gut microbiome: Connecting diet, glucose homeostasis, and disease. Annual Review of Medicine. 2022;73(1):469–481. https://doi.org/10.1146/annurev-med-042220-012821
10. Singh A, Alexander SG, Martin S. Gut microbiome homeostasis and the future of probiotics in cancer immunotherapy. Frontiers in Immunology. 2023;14:1114499. https://doi.org/10.3389/fimmu.2023.1114499
11. Wang X, Zhang X, Zhang P. Probiotics regulate gut microbiota: An effective method to improve immunity. Molecules. 2021;26(19):6076. https://doi.org/10.3390/molecules26196076
12. Frolova AS, Serazetdinova YuR, Milentyeva IS, Neverova OA. Studying the probiotic properties of a consortium stands of *Lactobacillus acidophilus*. XXI century: Resumes of the Past and Challenges of the Present plus. 2022;11(3):97–102. (In Russ.) https://doi.org/10.46548/21vek-2022-1159-0014

13. Mogoş GFR, Manciulea M, Enache RM, Pavelescu LA, Popescu OA, *et al*. Intestinal microbiota in early life: Latest findings regarding the role of probiotics as a treatment approach for dysbiosis. Nutrients. 2025;17(13):2071. https://doi.org/10.3390/nu17132071
14. Shen Y, Fan N, Ma SX, Cheng X, Yang X, *et al*. Gut microbiota dysbiosis: Pathogenesis, diseases, prevention, and therapy. MedComm. 2025;6(5):e70168. https://doi.org/10.1002/mco2.70168
15. Matzaras R, Nikopoulou A, Protonotariou E, Christaki E. Gut microbiota modulation and prevention of dysbiosis as an alternative approach to antimicrobial resistance: A narrative review. The Yale Journal of Biology and Medicine. 2022;95(4):479–494.
16. Le VM, Vesnina AD, Prosekov AYu, Dolganyuk VF, Larichev TA, *et al*. Effects of plant metabolites on *Aliivibrio fischeri* and test strains of gastrointestinal microbiota. Food Processing: Techniques and Technology. 2025;55(4):874–884. (In Russ.) https://doi.org/10.21603/2074-9414-2025-4-2614
17. Liu M, Chen J, Dharmasiddhi IPW, Chen S, Liu Y, *et al*. Review of the potential of probiotics in disease treatment: Mechanisms, engineering, and applications. Processes. 2024;12(2):316. https://doi.org/10.3390/pr12020316
18. Vesnina AD, Frolova AS, Chekushkina DYu, Milentyeva IS, Luzyanin SL, *et al*. Gut microbiota and its role in development of chronic disease and aging. Foods and Raw Materials. 2026;14(1):174–197. https://doi.org/10.21603/2308-4057-2026-1-668
19. Castellone V, Bancalari E, Rubert J, Gatti M, Neviani E, *et al*. Eating fermented: Health benefits of lab-fermented foods. Foods. 2021;10(11):2639. https://doi.org/10.3390/foods10112639
20. Mokoena MP, Omatola CA, Olaniran AO. Applications of lactic acid bacteria and their bacteriocins against food spoilage microorganisms and foodborne pathogens. Molecules. 2021;26(22):7055. https://doi.org/10.3390/molecules26227055
21. Burgain J, Scher J, Francius G, Borges F, Corgneau M, *et al*. Lactic acid bacteria in dairy food: Surface characterization and interactions with food matrix components. Advances in Colloid and Interface Science. 2014;213:21–35. https://doi.org/10.1016/j.cis.2014.09.005
22. Grosu-Tudor SS, Stancu MM, Pelinescu D, Zamfir M. Characterization of some bacteriocins produced by lactic acid bacteria isolated from fermented foods. World Journal of Microbiology and Biotechnology. 2014;30(9):2459–2469. https://doi.org/10.1007/s11274-014-1671-7
23. Casaburi A, Di Martino V, Ferranti P, Picariello L, Villani F. Technological properties and bacteriocins production by *Lactobacillus curvatus* 54M16 and its use as starter culture for fermented sausage manufacture. Food Control. 2016;59:31–45. https://doi.org/10.1016/j.foodcont.2015.05.016
24. Lahiri D, Nag M, Dutta B, Sarkar T, Pati S, *et al*. Bacteriocin: A natural approach for food safety and food security. Frontiers in Bioengineering and Biotechnology. 2022;10:1005918. https://doi.org/10.3389/fbioe.2022.1005918
25. Salvucci E, LeBlanc JG, Pérez G. Technological properties of lactic acid bacteria isolated from raw cereal material. LWT. 2016;70:185–191. https://doi.org/10.1016/j.lwt.2016.02.043
26. Wu F, Xie X, Du T, Jiang X, Miao W, *et al*. *Lactococcus lactis*, a bacterium with probiotic functions and pathogenicity. World Journal of Microbiology and Biotechnology. 2023;39:325. https://doi.org/10.1007/s11274-023-03771-5
27. Todorov SD, Dioso CM, Liong MT, Nero LA, Khosravi-Darani K, *et al*. Beneficial features of pediococcus: From starter cultures and inhibitory activities to probiotic benefits. World Journal of Microbiology and Biotechnology. 2023;39:4. https://doi.org/10.1007/s11274-022-03419-w
28. Fusco V, Chieffi D, Fanelli F, Montemurro M, Rizzello CG, *et al*. The *Weissella* and *Periweissella* genera: Up-to-date taxonomy, ecology, safety, biotechnological, and probiotic potential. Frontiers in Microbiology. 2023;14:1289937. https://doi.org/10.3389/fmicb.2023.1289937
29. Unban K, Klongklaew A, Kodchasee P, Pamueangmun P, Shetty K, *et al*. *Enterococci* as dominant xylose utilizing lactic acid bacteria in eri silkworm midgut and the potential use of *Enterococcus hirae* as probiotic for eri culture. Insects. 2022;13(2):136. https://doi.org/10.3390/insects13020136
30. Ge S, Han J, Sun Q, Ye Z, Zhou Q, *et al*. Optimization of cryoprotectants for improving the freeze-dried survival rate of potential probiotic *Lactococcus lactis* ZFM559 and evaluation of its storage stability. LWT. 2024;198:116052. https://doi.org/10.1016/j.lwt.2024.116052
31. Singh JK, Devi PB, Reddy GB, Jaiswal AK, Kavitake D, *et al*. Biosynthesis, classification, properties, and applications of *Weissella* bacteriocins. Frontiers in Microbiology. 2024;15:1406904. https://doi.org/10.3389/fmicb.2024.1406904
32. Zimina MI, Sukhih SA, Babich OO, Noskova SYu, Abrashina AA, *et al*. Investigating antibiotic activity of the genus *Bacillus* strains and properties of their bacteriocins in order to develop next-generation pharmaceuticals. Foods and Raw Materials. 2016;4(2):92–100. https://doi.org/10.21179/2308-4057-2016-2-92-100

33. Chung J, Otoguro M, Yanagida F, Wu H, Chang Yu, *et al*. *Enterococcus alishanensis* sp. nov., a novel lactic acid bacterium isolated from fresh coffee beans. International Journal of Systematic and Evolutionary Microbiology. 2022;72(2):005255. https://doi.org/10.1099/ijsem.0.005255

34. Gavzy SJ, Kensiski A, Lee ZL, Mongodin EF, Ma B, *et al*. *Bifidobacterium* mechanisms of immune modulation and tolerance. Gut Microbes. 2023;15(2):2291164. https://doi.org/10.1080/19490976.2023.2291164

35. Martin AJM, Serebrinsky-Duek K, Riquelme E, Saa PA, Garrido D. Microbial interactions and the homeostasis of the gut microbiome: The role of *Bifidobacterium*. Microbiome Research Reports. 2023;2:17. https://doi.org/10.20517/mrr.2023.10

36. Collograi KC, da Costa AC, Ienczak JL. Fermentation strategies to improve propionic acid production with *propionibacterium* ssp.: A review. Critical Reviews in Biotechnology. 2022;42(8):1157–1179. https://doi.org/10.1080/07388551.2021.1995695

37. Rossi F, Santonicola S, Giaccone V, Truant A, Colavita G. Dairy propionibacteria: Probiotic properties and their molecular bases. Biomolecules. 2025;15(6):886. https://doi.org/10.3390/biom15060886

38. Tegegne BA, Kebede B. Probiotics, their prophylactic and therapeutic applications in human health development: A review of the literature. Heliyon. 2022;8(6):e09725. https://doi.org/10.1016/j.heliyon.2022.e09725

39. Gryaznova MV, Burakova IYu, Smirnova YuD, Nesterova EYu, Rodionova NS, *et al*. Bacterial composition of dairy base during fermentation. Food Processing: Techniques and Technology. 2023;53(3):554–564. (In Russ.) https://doi.org/10.21603/2074-9414-2023-3-2456

40. Bermúdez-Humarán LG, Chassaing B, Langella P. Exploring the interaction and impact of probiotic and commensal bacteria on vitamins, minerals and short chain fatty acids metabolism. Microbial Cell Factories. 2024;23(1):172. https://doi.org/10.1186/s12934-024-02449-3

41. Kishilova SA, Leonova VA, Mitrova VA, Rozhkova IV. Advanced biotechnological solutions for lactic acid bacteria in dairy industry: From strain selection to probiotic products. Food Processing: Techniques and Technology. 2025;55(3):624–633. (In Russ.) https://doi.org/10.21603/2074-9414-2025-3-2596

42. Tang H, Huang W, Yao YF. The metabolites of lactic acid bacteria: Classification, biosynthesis and modulation of gut microbiota. Microbial Cell. 2023;10(3):49–62. https://doi.org/10.15698/mic2023.03.792

43. Jahedi S, Pashangeh S. Bioactivities of postbiotics in food applications: A review. Iranian Journal of Microbiology. 2025;17(3):348–357. https://doi.org/10.18502/ijm.v17i3.18816

44. Sachdeva A, Tomar T, Malik T, Bains A, Karnwal A. Exploring probiotics as a sustainable alternative to antimicrobial growth promoters: Mechanisms and benefits in animal health. Frontiers in Sustainable Food Systems. 2025;8:1523678. https://doi.org/10.3389/fsufs.2024.1523678

45. Wang R, Lou L. The central role of the citric acid cycle in energy metabolism: From metabolic intermediates to regulatory mechanisms. Biological Evidence. 2024;14(3):110–121. https://doi.org/10.5376/be.2024.14.0013

46. Kurhaluk N. Tricarboxylic acid cycle intermediates and individual ageing. Biomolecules. 2024;14(3):260. https://doi.org/10.3390/biom14030260

47. Liu X, Zhao G, Sun S, Fan C, Feng X, *et al*. Biosynthetic pathway and metabolic engineering of succinic acid. Frontiers in Bioengineering and Biotechnology. 2022;10:843887. https://doi.org/10.3389/fbioe.2022.843887

48. Abdallah A, Elemba E, Zhong Q, Sun Z. Gastrointestinal interaction between dietary amino acids and gut microbiota: With special emphasis on host nutrition. Current Protein & Peptide Science. 2020;21(8):785–798. http://doi.org/10.2174/1389203721666200212095503

49. Zhang X, Zheng Y, Liu Z, Su M, Wu Z, *et al*. Insights into characteristic metabolites and potential bioactive peptides profiles of fresh cheese fermented with three novel probiotics based metabolomics and peptidomics. Food chemistry: X. 2024;21:101147. https://doi.org/10.1016/j.fochx.2024.101147

50. Sidorova YuS, Biryulina NA, Zilova IS, Mazo VK. Amaranth grain proteins: Prospects for use in specialized food products. Problems of Nutrition. 2022;91(3):96–106. (In Russ.) https://doi.org/10.33029/0042-8833-2022-91-3-96-106

51. Rozhkova IV, Yurova EA, Leonova VA. Evaluation of the amino acid composition and content of organic acids of complex postbiotic substances obtained on the basis of metabolites of probiotic bacteria *Lacticaseibacillus paracasei* ABK and *Lactobacillus helveticus* H9. Fermentation. 2023;9(5):460. https://doi.org/10.3390/fermentation9050460

52. Gao PP, Liu HQ, Ye ZW, Zheng QW, Zou Y, *et al*. The beneficial potential of protein hydrolysates as prebiotic for probiotics and its biological activity: A review. Critical Reviews in Food Science and Nutrition. 2024;64(33):13045–13057. https://doi.org/10.1080/10408398.2023.2260467

53. Kostiuchenko O, Lushnikova I, Skibo G. The role of gut microbiota metabolites in the regeneration and protection of nervous tissue: A narrative review. Regenerative Medicine Reports. 2024;1(1):12–30. https://doi.org/10.4103/REGENMED.REGENMED-D-24-00004

54. Hossain KS, Amarasena S, Mayengbam S. B vitamins and their roles in gut health. Microorganisms. 2022;10(6):1168. https://doi.org/10.3390/microorganisms10061168

55. Vera-Santander VE, Hernández-Figueroa RH, Jiménez-Munguía MT, Mani-López E, López-Malo A. Health benefits of consuming foods with bacterial probiotics, postbiotics, and their metabolites: A review. Molecules. 2023;28(3):1230. https://doi.org/10.3390/molecules28031230

56. Vesnina A, Kozlova O, Ivanova S, Prosekov A. Citric acid cycle genes and nutrigenetics. International Journal of Molecular Sciences. 2026;27(5):2360. https://doi.org/10.3390/ijms27052360

57. Froböse NJ, Bjedov S, Schuler F, Kahl BC, Kampmeier S, *et al*. Gram staining: A comparison of two automated systems and manual staining. Journal of Clinical Microbiology. 2020;58(12):e01914–e01920. https://doi.org/10.1128/JCM.01914-20

58. Shevchenko IA. Radiotelemetric study of temperature in the gastrointestinal tract. Kazan medical journal. 1968;49(3):14–17. (In Russ.) https://doi.org/10.17816/kazmj60420

59. Guryeva VI, Bachinskaya VM, Sharapova NR. Determination of probiotic bacterial strains sensitivity to antibacterial drugs by the disc diffusion method. Vestnik of the Mari State University. Chapter «Agriculture. Economics». 2024;10(1):9–16. (In Russ.) https://doi.org/10.30914/2411-9687-2024-10-1-9-16

60. Hajbullin RG, Ahmadulina ER, Volkova LV. Effect of fermented substance of *A. lappa* L. leaf biomass on growth kinetics of *L. plantarum*. International research journal. 2022;5(119):202–206. https://doi.org/10.23670/IRJ.2022.119.5.038

61. Kitaevskaya SV. Modern trends in the selection and identification of probiotic strains of lactic acid bacteria. Bulletin of Kazan Technological University. 2012;15(17):184–188. (In Russ.) https://elibrary.ru/PGQVGP

62. Davoodabadi A, Dallal MMS, Foroushani AR, Douraghi M, Yazdi MKS, *et al*. Antibacterial activity of *Lactobacillus* spp. isolated from the feces of healthy infants against enteropathogenic bacteria. Anaerobe. 2015;34:53–58. https://doi.org/10.1016/j.anaerobe.2015.04.014

63. Pazhoohan M, Sadeghi F, Moghadami M. Antimicrobial and antiadhesive effects of *Lactobacillus* isolates of healthy human gut origin on Enterotoxigenic *Escherichia coli* (ETEC) and Enteroaggregative *Escherichia coli* (EAEC). Microbial Pathogenesis. 2020;148:104271. https://doi.org/10.1016/j.micpath.2020.104271

64. Jomehzadeh N, Javaherizadeh H, Amin M, Saki M, Al-Ouqaili MTS, *et al*. Isolation and identification of potential probiotic *Lactobacillus* species from feces of infants in southwest Iran. International Journal of Infectious Diseases. 2020;96:524–530. https://doi.org/10.1016/j.ijid.2020.05.034

65. Serazetdinova YuR, Chekushkina DYu, Borodina EE, Kolpakova DE, Minina VI, *et al*. Synergistic interaction between Azotobacter and Pseudomonas bacteria in a growth-stimulating consortium. Foods and Raw Materials. 2025;13(2):376–393. https://doi.org/10.21603/2308-4057-2025-2-651

66. Frolova AS, Fokina AD, Milentyeva IS, Asyakina LK, Proskuryakova LA, *et al*. The biological active substances of *Taraxacum officinale* and *Arctium lappa* from the Siberian federal district. International Journal of Molecular Sciences. 2024;25(6):3263. https://doi.org/10.3390/ijms25063263

67. Belashova OV, Kozlova OV, Velichkovich NS, Fokina AD, Yustratov VP, *et al*. A phytochemical study of the clover growing in Kuzbass. Foods and Raw Materials. 2024;12(1):194–206. https://doi.org/10.21603/2308-4057-2024-1-599

68. Frolova AS, Milentyeva IS, Kolpakova DE, Neverova OA, Yustratov VP, *et al*. *Lactobacilli* in probiotic consortia: Profile and prospects. Food Processing: Techniques and Technology. 2026;56(1):164–179. (In Russ.) https://doi.org/10.21603/2074-9414-2026-1-2630

69. Frolova AS, Chekushkina DYu, Loseva AI, Neverova OA, Zaushintsena AV, *et al*. Lactic acid bacteria in cheese production. Cheese- and buttermaking. 2025;(4):70–76. (In Russ.) https://doi.org/10.21603/2073-4018-2025-4-35

70. Duche RT, Singh A, Wandhare AG, Sangwan V, Sihag MK, *et al*. Antibiotic resistance in potential probiotic lactic acid bacteria of fermented foods and human origin from Nigeria. BMC Microbiology. 2023;23:142. https://doi.org/10.1186/s12866-023-02883-0

71. Liu K, Liu J, Su Y, Wang M, Long T, *et al*. IncI2 plasmid transfer and changes of intestinal microbiota in mice under *β*-lactam antibiotic pressure. BMC Veterinary Research. 2025;21:343. https://doi.org/10.1186/s12917-025-04808-7

72. Tian Q, Ye H, Zhou X, Wang J, Zhang L, *et al*. Evaluating the health risk of probiotic supplements from the perspective of antimicrobial resistance. Microbiology Spectrum. 2025;13:e00019-24. https://doi.org/10.1128/spectrum.00019-24

73. Kusunur AB, Mogilipuri SS, Moturu D, Benala M, Vaiyapuri M, *et al*. Tetracycline resistance potential of heterotrophic bacteria isolated from freshwater fin-fish aquaculture system. Journal of Applied Microbiology. 2023;134(4):lxad060. https://doi.org/10.1093/jambio/lxad060

74. Hu G, Naveed M, Shabbir MA, Sarwar A, Yousaf J, *et al*. Revolutionizing the probiotic functionality, biochemical activity, antibiotic resistance and specialty genes of *Pediococcus acidilactici* BCB1H via *in-vitro* and *in-silico* approaches. Zeitschrift für Naturforschung C. 2025;80(3–4):103–118. https://doi.org/10.1515/znc-2024-0074

75. Yang H, Xiong J, He L, Li C, Qiao S, *et al*. Stress tolerance, safety, and probiotic traits of cholesterol-decreasing *Bifidobacterium* BLH1 isolated from Guizhou red sour soup, a traditional Chinese fermented food. LWT. 2024;192:115696. https://doi.org/10.1016/j.lwt.2023.115696

76. Madushanka D, Vidanarachchi JK, Kodithuwakku S, Nayanajith GRA, Jayatilake S, *et al*. Isolation and characterization of probiotic lactic acid bacteria from fermented traditional rice for potential applications in food and livestock production. Applied Food Research. 2025;5(1):100865. https://doi.org/10.1016/j.afres.2025.100865

77. Nidamarthi PP, Poongavanam SS, Karlapudi AP. Screening and characterization of *Enterococcus faecium* as a potential probiotic: Probiotic parameters and efficacy evaluation. Biologia. 2026;81:37. https://doi.org/10.1007/s11756-025-02074-4

78. Alameri F, Tarique M, Osaili T, Obaid R, Abdalla A, *et al*. Lactic acid bacteria isolated from fresh vegetable products: Potential probiotic and postbiotic characteristics including immunomodulatory effects. Microorganisms. 2022;10(2):389. https://doi.org/10.3390/microorganisms10020389

79. Kassa G, Alemayehu D, Andualem B. Isolation, identification, and molecular characterization of probiotic bacteria from locally selected Ethiopian free range chickens gastrointestinal tract. Poultry Science. 2024;103(2):103311. https://doi.org/10.1016/j.psj.2023.103311

80. Kolech A, Alemu S, Milkessa T. Evaluation of the antimicrobial properties of potential probiotic lactic acid bacteria from raw and fermented cow milk. Scientific Reports. 2026;16:8355. https://doi.org/10.1038/s41598-026-39586-1

81. Fijan S, Kocbek P, Steyer A, Vodičar PM, Strauss M. The antimicrobial effect of various single-strain and multi-strain probiotics, dietary supplements or other beneficial microbes against common clinical wound pathogens. Microorganisms. 2022;10(12):2518. https://doi.org/10.3390/microorganisms10122518

82. Sanam MUE, Detha AIR, Rohi NK. Detection of antibacterial activity of lactic acid bacteria, isolated from Sumba mare's milk, against *Bacillus cereus*, *Staphylococcus aureus*, and *Escherichia coli*. Journal of Advanced Veterinary and Animal Research. 2022;9(1):53–58. https://doi.org/10.5455/javar.2022.i568

83. Srinu B, Devi KK, Rao TM. Study on synergistic and antimicrobial activity of certain *Bifidobacterium bifidum* strains and plant extracts against clinical isolates. The Journal of Phytopharmacology. 2024;13(4):294–297. https://doi.org/10.31254/phyto.2024.13404

84. Ouili AS, Ouattara A, Mogmenga I, Compaoré COT, Maiga Y, *et al*. *In vitro* screening for potential probiotic properties of *Pediococcus Pentosaceus* strains isolated from fermented Bambara groundnut (*Vigna subterranea* L.) grains: A legume native to West Africa. The Microbe. 2025;7:100418. https://doi.org/10.1016/j.microb.2025.100418

85. Fhoula I, Boumaiza M, Tayh G, Rehaiem A, Klibi N, *et al*. Antimicrobial activity and safety features assessment of *Weissella* spp. from environmental sources. Food Science & Nutrition. 2022;10(9):2896–2910. https://doi.org/10.1002/fsn3.2885

86. Linares DM, Gómez C, Renes E, Fresno JM, Tornadijo ME, *et al*. Lactic acid bacteria and bifidobacteria with potential to design natural biofunctional health-promoting dairy foods. Frontiers in Microbiology. 2017;8:846. https://doi.org/10.3389/fmicb.2017.00846

87. LeBlanc JG, Chain F, Martín R, Bermúdez-Humarán LG, Courau S, *et al*. Beneficial effects on host energy metabolism of short-chain fatty acids and vitamins produced by commensal and probiotic bacteria. Microbial Cell Factories. 2017;16:79. https://doi.org/10.1186/s12934-017-0691-z

88. Sang L, Yang S, Zhu Y, Zhu Z, Yang B, *et al*. The combined use of B vitamins and probiotics promotes B vitamin absorption and increases *Akkermansia* abundance. Food & Function. 2024;15(13):7017–7031. https://doi.org/10.1039/d4fo01805b

89. Scauro A, Rocchetti MT, Soccio M, la Gatta B, Liberatore MT, *et al*. Postbiotic potential of newly isolated riboflavin-overproducing *Lactiplantibacillus plantarum* strains. Probiotics and Antimicrobial Proteins. 2025:18:524–540. https://doi.org/10.1007/s12602-025-10538-x

90. Ye Z, Sun S, Chen HY, Ji C, Zhou Z. Metabolomic and bioactivity analysis of plum pulp fermented with *Lactiplantibacillus*, *Lacticaseibacillus*, and *Bifidobacterium* strains. Food Chemistry: X. 2025;30:102969. https://doi.org/10.1016/j.fochx.2025.102969

91. Mohamad NI, Manan MA, Lazim MIM, Sani NA. Antibacterial activity and organic acids formation by *Lactobacillus* sp. originated from pickled guava and papaya. Journal of Sustainability Science and Management. 2022;17(2):286–295. https://elibrary.ru/XLLFMA

92. Ter ZY, Chang LS, Babji AS, Zaini NAM, Fazry S, *et al*. A review on proteolytic fermentation of dietary protein using lactic acid bacteria for the development of novel proteolytically fermented foods. International Journal of Food Science and Technology. 2024;59(3):1213–1236. https://doi.org/10.1111/ijfs.16888

93. Terzioğlu ME, Bakirci İ. Comparison of amino acid profile, ACE inhibitory activity, and organic acid profile of cow and goat yogurts produced with *Lactobacillus acidophilus* LA-5, *Bifidobacterium animalis* subsp. lactis BB-12, and classical yogurt culture. Probiotics and Antimicrobial Proteins. 2024;16:1566–1582. https://doi.org/10.1007/s12602-023-10123-0

94. Vesnina AD, Fedorova AM, Milentyeva IS, Proskuryakova LA. Processing whey as secondary dairy raw material in functional foods. Cheese- and butter making. 2026;1:61–66. (In Russ.) https://doi.org/10.21603/2073-4018-2026-1-48

95. Wu Yu, Zhang Q, Ren Yi, Ruan Z. Effect of probiotic *Lactobacillus* on lipid profile: A systematic review and meta-analysis of randomized, controlled trials. PLoS One. 2017;12(6):e0178868. https://doi.org/10.1371/journal.pone.0178868

96. Qiu X, Wu Q, Li W, Tang K, Zhang J. Effects of *Lactobacillus* supplementation on glycemic and lipid indices in overweight or obese adults: A systematic review and meta-analysis. Clinical Nutrition. 2022;41(8):1787–1797. https://doi.org/10.1016/j.clnu.2022.06.030

Additional information about the authors

Anna S. Frolova ORCID 0000-0003-3988-8521; eLIBRARY SPIN 5194-7508
Anna D. Vesnina ORCID 0000-0002-4552-7418; eLIBRARY SPIN 9668-2838
Anastasiya M. Fedorova ORCID 0000-0002-8071-4411; eLIBRARY SPIN 4142-7468
Elena V. Ostapova ORCID 0000-0002-4704-484X; eLIBRARY SPIN 8145-8879
Vladimir P. Yustratov ORCID 0000-0002-1779-4332; eLIBRARY SPIN 3578-5617
Irina S. Milentyeva ORCID 0000-0002-3536-562X; eLIBRARY SPIN 8227-2844